

**FNR is a Regulator of *Salmonella*
Pathogenicity Island 2 in *Salmonella*
Typhimurium**

**A thesis submitted to the University of Dublin in fulfillment of the
requirements for the degree Doctor of Philosophy by**

Stefani Christine Kary

2019

**The Moyne Institute of Preventive Medicine
Department of Microbiology
Trinity College
University of Dublin**

Declaration

I hereby declare that this thesis has not previously been submitted for a degree at this or any other University and that it represents my own unaided work, except where duly acknowledged in the text.

I agree that this thesis may be lent or copied at the discretion of the librarian, Trinity College Dublin.

Stefani Christine Kary

Summary

During infection, *S. Typhimurium* employs *Salmonella* pathogenicity island (SPI)-encoded type three secretion systems (T3SS) 1 and 2 to invade and survive in host cells. However, expression of SPI-2 is seen at the epithelial border prior to host cell invasion in response to an unknown signal. A zone of relative oxygenation adjacent to the gastrointestinal tract mucosa, caused by diffusion of oxygen from the capillary network has been shown to cause priming of *Shigella* and Enterotoxigenic *E. coli* for entry into host cells through the oxygen sensing capabilities of the anaerobic metabolism regulator FNR. However, regulation of SPI-2 by FNR has not been established in *S. Typhimurium*. Here we show using a combination of RNA-seq and ChIP-seq that SPI-2 is highly expressed in an Δfnr mutant under microaerobic conditions, and that FNR is a direct repressor of SPI-2 genes. Our particular focus on FNR regulation of SPI-2 under microaerobic growth in a glycerol/trimethylamine N-oxide/fumarate minimal medium has revealed that, not only does FNR repress the expression of the SPI-2 encoded type three secretion system apparatus proteins, effectors and chaperones through direct regulation of the SPI-2 response regulator SsrB, but it is also involved in the direct repression of a great number of effectors and virulence relevant sRNAs encoded throughout the chromosome and on the *Salmonella* virulence plasmid and that growth under aerobic conditions relieved repression. Furthermore, we have shown that the accurate spatiotemporal expression of SPI-2 is integral for maintenance of bacterial fitness, provided additional evidence that oxygen is an important signalling molecule for the control of bacterial motility and demonstrated that FNR is an important regular in both intra- and extracellular environments. Our results demonstrate that *S. Typhimurium* regulates expression of virulence genes in response to changing oxygen concentrations to prepare for the harsh intracellular environment of host cells using the regulator of anaerobic metabolism FNR. Importantly, analysis of our Δfnr RNA-seq-based transcriptomic data in conjunction with previously published datasets, will provide a more complete picture of mixed regulatory interactions within the cell. We hope that the addition of this data will help in the development of the full understanding of all regulatory interactions and inputs involved in the establishment of *S. Typhimurium* infection.

Acknowledgements

First and foremost, I would like to express my sincere gratitude to my advisor Prof. Carsten Kröger for providing me with the opportunity of a lifetime, for his continuous support, patience, motivation, immense knowledge, and abundant supply of chocolate and donuts that never failed to brighten any mood. His guidance, encouragement and generosity helped me immensely throughout the time of research and writing of this thesis. I could not have imagined having a better advisor and mentor for my Ph.D.

I would also like to thank my postgraduate thesis committee Prof. Charles Dorman, Prof. Joan Geoghegan and Prof. Marta Martins, for the useful discussions, advice and help during the last three years. A huge thank you to the postdocs who taught me so much, Dr. Aoife Colgan, Dr. Aalap Mogre, and Dr. Aleksandra Miranda Caso Luengo. Without you, I would not have been able to complete this work.

Thank you to Prof. Andrew Cameron who encouraged me to pursue a Ph.D. after my M.Sc., introduced me to Carsten all those years ago, and who welcomed me back into the lab when I was visiting home. I cannot thank Dr. Keith Mackenzie enough for all of his help and encouragement and for doing an amazing job with the ChIP-seq samples. Thank you to Dr. Tzu-Chiao Chao and Dr. Nicole Hansmeier for their outstanding work that contributed immensely to this thesis. Thank you to Dr. Ciaran Finn for his insight, helpful chats and strains, and to Dr. Daniel Ryan for the beautiful anaerobic growth curves at the 11th hour. Thank you to Dr. Karsten Hokamp for computational support, and to Prof. Jay Hinton for the trip to Liverpool and helpful comments. Thank you to Prof. Alastair Fleming for his generosity with lab equipment and friendly chats when we were the last people in the department at the end of the day. Thank you to Dr. Marta Zapotoczna for all of her help discussions and our late night office rants that really helped to blow off some steam. Thank you to Aisling Towell for her help with protein purification and always providing the best of Disney music. Thank you to the members of the Dorman Lab past and present for always lending a helping hand, or incubator, or enzyme in a time of need. Thank you to Michelle and Amy for wonderful chats, laughs, and encouragement. How can I begin to thank Daniela and Niamh? You kept my spirits high, were a shoulder to cry on, and you truly kept me sane these last three years. Thank you to the rest of the folks in the Moyne past and present; Thaina, Marty, Roberto, Isa, Orquidia, Elaine, Brenda, Mohamed, Chandie, Kieran, Leanne, Joana and Orla for always lending an ear and thank you to the undergraduate students who, although trying at times, always gave us something to giggle about and especially thank you to Naoise, Vivian, and Marina who helped so much in the lab.

I cannot thank Jane enough for keeping the lab stocked, always finding what was needed and providing numerous goodies throughout the years. Thank you to Deirdre for all of the protocols, advice and lots of laughs. Thank you to Jayne and Caroline who helped keep this place organized and for help with all of my shipping debacles. I have to thank of course Stephen and Ronan for all of the wonderful conversation and for always making sure I had all the flasks a girl could dream of, and sorry about the smell from all of my experiments, MMA is really the worst. Thank you to Connie and Miriam (and Jane again!) for sharing their space in my final 6 months in the lab. Thank you to Dave and Margaret for keeping me stocked up with media and to Gerry for all of his problem solving.

Thank you to Dara & Laura who opened their home to me from my first day in Dublin, and to Joanna for helping me find an apartment so quickly! Thank you to Fitzy and his family for the wonderful Christmases that felt like a home away from home. Thank you to Niamh and all the ladies at TropicalPopical who kept me fabulous throughout this endeavour. Thank you to all my friends back home especially the dance girls and Becca for their unwavering support from afar.

Thank you to Zewdi for all of your love and faith. A special thank you to my mom and dad who always helped me keep everything organized back home, and for your support and love. And of course to Niko, who despite being a dog makes pretty good FaceTime calls.

And finally, to Mesel, for always believing in me, giving continuous love, support, laughter, help, and taking my call no matter the hour. Thank you for your patience, for waiting three years, and for never taking anything for granted.

Publications and Conferences

Publications

Kröger, C., Rothhardt, J. E., Brokatzky, D., Felsl, A., **Kary, S. C.**, Heermann, R. & Fuchs, T. M. (2018). The small RNA RssR regulates myo-inositol degradation by *Salmonella enterica*. *Scientific Reports* **8**, 17739. Nature Publishing Group. DOI:10.1038/s41598-018-35784-8

Colgan, A. M., Quinn, H. J., **Kary, S. C.**, Mitchenall, L. A., Maxwell, A., Cameron, A. D. S. & Dorman, C. J. (2018). Negative supercoiling of DNA by gyrase is inhibited in *Salmonella enterica* serovar Typhimurium during adaptation to acid stress. *Molecular Microbiology* **169**, 4499–3. DOI:10.1111/mmi.13911

Miranda-CasoLuengo, A. A., **Kary, S. C.**, Erhardt, M. & Kröger, C. (2017). Small RNA, big effect: Control of flagellin production. *Trends in Microbiology* 1–2. Elsevier Ltd. DOI:10.1016/j.tim.2017.10.003

Kary, S. C., Yoneda, J. R. K., Olshefsky, S. C., Stewart, L. A., West, S. B. & Cameron, A. D. S. (2017). The global regulatory cyclic AMP receptor protein (CRP) controls multifactorial fluoroquinolone susceptibility in *Salmonella enterica* Serovar Typhimurium. *Antimicrobial Agents and Chemotherapy* **61**, 010401–14. DOI:10.1128/AAC.01666-17

Kröger, C., **Kary, S. C.**, Schauer, K. & Cameron, A. (2016). Genetic regulation of virulence and antibiotic resistance in *Acinetobacter baumannii*. *Genes* **8**, 12–19. DOI:10.3390/genes8010012

Conferences

Kary, S. C., Colgan, A. M., Mogre, A., Hansmeier, N., MacKenzie, K. D., Chao, T. C., Hokamp, K., Dorman, C. J., Hinton, J. C. D., Cameron, A. D. S., and Kröger, C. FNR is a regulator of SPI-2 in *Salmonella* Typhimurium (2018), Oral Presentation at the Canadian Society of Microbiologists (CSM) Student Symposium Competition, Winnipeg, Manitoba, Canada.

Kary, S. C., Colgan, A. M., Mogre, A., Hansmeier, N., MacKenzie, K. D., Chao, T. C., Hokamp, K., Dorman, C. J., Hinton, J. C. D., Cameron, A. D. S., and Kröger, C. FNR is a regulator of SPI-2 in *Salmonella* Typhimurium (2018), Oral Presentation at the Dublin Academy of Pathogenomics and Infection Biology Meeting, Dublin, Ireland.

Kary, S. C., Colgan, A. M., Mogre, A., Hansmeier, N., MacKenzie, K. D., Chao, T. C., Hokamp, K., Dorman, C. J., Hinton, J. C. D., Cameron, A. D. S., and Kröger, C. FNR is a regulator of SPI-2 in *Salmonella* Typhimurium (2018) Poster Presentation at the Dublin Academy of Pathogenomics and Infection Biology Meeting, Dublin, Ireland.

Kary, S. C., Colgan, A. M., Mogre, A., Hansmeier, N., MacKenzie, K. D., Chao, T. C., Hokamp, K., Dorman, C. J., Hinton, J. C. D., Cameron, A. D. S., and Kröger, C. FNR is a regulator of SPI-2 in *Salmonella* Typhimurium (2017) Poster Presentation at the Microbiology Society Annual Conference, Edinburgh, Scotland, UK.

Table of Contents

<i>Declaration</i>	<i>I</i>
<i>Summary</i>	<i>II</i>
<i>Acknowledgements</i>	<i>III</i>
<i>Publications and Conferences</i>	<i>V</i>
<i>Table of Contents</i>	<i>VII</i>
<i>List of Figures</i>	<i>XII</i>
<i>List of Tables</i>	<i>XIV</i>
<i>List of Formulas</i>	<i>XV</i>
<i>List of Abbreviations</i>	<i>XV</i>
1 Chapter 1 General Introduction	1
1.1 Salmonella	2
1.1.1 Overview of the <i>Salmonella</i> genus	2
1.1.2 Pathogenesis of <i>S. Typhimurium</i>	4
1.1.3 Flagella.....	8
1.1.4 <i>Salmonella</i> pathogenicity islands.....	9
1.2 Metabolism in the gut	20
1.2.1 Oxygen in the gut.....	20
1.2.2 Anaerobic respiration in the gut.....	22
1.3 Regulation of the aerobic to anaerobic switch	26
1.3.1 FNR.....	26
1.3.2 Regulation of FNR.....	27
1.3.3 Mechanisms of transcriptional regulation by FNR.....	28
1.3.4 The FNR regulon	31
1.4 Aims of the Study	33
2 Chapter 2 Material & Methods	35
2.1 Chemicals and Reagents	36
2.2 General Microbiological Techniques	36
2.2.1 Media	36
2.2.2 Maintenance of Bacterial Stocks	36
2.2.3 Culture Conditions.....	36
2.2.4 Monitoring Bacterial Growth.....	37

2.2.5	Antibiotics.....	38
2.2.6	Motility Assays.....	38
2.2.7	Growth curves and kinetic gene expression assay.....	38
2.2.8	Oxygen gradient gene expression assay.....	39
2.2.9	Relative Fitness Assay.....	39
2.3	General molecular techniques.....	47
2.3.1	Isolation of chromosomal <i>S. Typhimurium</i> 4/74 DNA for use in PCR.....	47
2.3.2	Isolation of plasmid DNA.....	47
2.3.3	Polymerase chain reaction (PCR).....	47
2.3.4	Agarose gel electrophoresis.....	48
2.3.5	Restriction digestion.....	48
2.3.6	Purification of PCR products.....	48
2.3.7	Precipitation of DNA.....	49
2.3.8	Extraction of DNA from agarose gels.....	49
2.4	Preparation and transformation of competent bacteria.....	49
2.4.1	Preparation of electro-competent <i>S. Typhimurium</i> and electroporation.....	49
2.4.2	Preparation and transformation of chemically competent <i>E. coli</i>	50
2.5	Genetic manipulations.....	55
2.5.1	P22 Phage transduction.....	55
2.5.2	Removal of antibiotic resistance cassettes.....	56
2.5.3	Modular Tn7-based plasmid system.....	56
2.6	Analysis of RNA.....	58
2.6.1	Extraction of RNA from <i>S. Typhimurium</i> 4/74.....	58
2.6.2	DNase I digestion.....	59
2.6.3	Reverse transcription.....	59
2.6.4	Real-time quantitative PCR.....	59
2.6.5	Generation of Digoxigenin-labelled riboprobes.....	60
2.6.6	Northern blotting.....	61
2.6.7	cDNA preparation of RNA and RNA-seq.....	61
2.7	Analysis of proteins.....	63
2.7.1	Preparation of whole cell lysates for analysis of cellular proteins.....	63
2.7.2	Preparation of culture supernatants for analysis of secreted proteins.....	63
2.7.3	SDS polyacrylamide gel electrophoresis (SDS-PAGE).....	63
2.7.4	Coomassie staining of polyacrylamide gels.....	64
2.7.5	Western Immunoblotting.....	64
2.7.6	Proteomic analysis by mass spectrometry.....	65
2.8	Chromatin Immunoprecipitation.....	66
2.8.1	Preparation of cross-linked lysates.....	66
2.8.2	Immunoprecipitation.....	67

2.8.3	Washing the Protein-G agarose beads and elution of DNA	68
2.8.4	Reversal of cross-links and DNA extraction	68
2.9	DNA sequencing.....	70
2.9.1	Preparation of DNA libraries.....	70
2.9.2	Sequencing with Illumina MiSeq	70
2.10	Bioinformatic analysis.....	70
2.10.1	Mapping of RNA-seq data and differential expression analysis.....	70
2.10.2	ChIP-seq analysis.....	71
2.11	DNA binding analysis.....	76
2.11.1	Large scale induction of protein production	76
2.11.2	6×His-Tag protein purification	76
2.11.3	Electrophoretic mobility shift assay.....	77
2.12	Atomic force microscopy imaging.....	77
2.13	Infection of murine macrophages	78
3	Chapter 3 Transcriptional regulation in Δ<i>fnr</i>	79
3.1	Introduction	80
3.1.1	Overview of the Study	80
3.1.2	Bacterial transcriptome analysis using RNA-seq	82
3.2	Results.....	83
3.2.1	Strategy for experimental design	83
3.2.2	Reproducibility of RNA-seq data	85
3.2.3	Absence of polar effects in Δ <i>fnr</i>	87
3.2.4	Complementation of the Δ <i>fnr</i> mutant	88
3.2.5	RNA-seq determines differentially expressed genes in Δ <i>fnr</i>	92
3.2.6	SPI-2 is derepressed in Δ <i>fnr</i> under microaerobic conditions in MMA.....	99
3.2.7	Expression and secretion of effector proteins.....	104
3.2.8	Repression of motility in Δ <i>fnr</i>	107
3.2.9	Regulation of small RNAs.....	112
3.3	Discussion	118
3.3.1	SPI-2 expression in MMA	118
3.3.2	Motility and chemotaxis	119
3.3.3	Regulation of sRNAs by FNR	119
3.3.4	Comparison of FNR regulons.....	120
3.3.5	The benefits and limitations of an RNA-seq-based approach for the investigation of bacterial regulons.....	124
3.3.6	Summary	125

4	<i>Chapter 4 Promoter occupancy of FNR</i>	127
4.1	Introduction	128
4.1.1	Identification of global FNR binding through ChIP-seq	128
4.2	Results	131
4.2.1	Verification of 3×FLAG-FNR	131
4.2.2	Overview of FNR binding using ChIP-seq.....	133
4.2.3	FNR consensus binding motif.....	134
4.2.4	Verification of FNR binding.....	139
4.2.5	FNR binding to control regions	143
4.2.6	FNR binding to SPI-2 promoters	145
4.2.7	FNR binding to the <i>ydgT</i> promoter.....	149
4.2.8	Expression from SPI-2 promoters.....	149
4.3	Discussion	152
4.3.1	Low binding affinity at SPI-2	152
4.3.2	The role of <i>ydgT</i>	153
4.3.3	The benefits and limitations of ChIP-seq for investigations of in vivo protein-DNA interactions.....	153
4.3.4	Summary	156
5	<i>Chapter 5 Effects of Δfnr on virulence in macrophages and bacterial fitness</i> . 158	
5.1	Introduction	159
5.1.1	Investigation of virulence and bacterial fitness in Δfnr	159
5.2	Results	161
5.2.1	SPI-2 expression <i>in vitro</i>	161
5.2.2	Intramacrophage survival of <i>S. Typhimurium</i>	164
5.2.3	Contribution of alternative electron acceptors to growth and SPI-2 expression	169
5.2.4	Relative fitness <i>in vitro</i>	170
5.2.5	Proteomic study of Δfnr	175
5.3	Discussion	179
5.3.1	SPI-2 regulation by FNR <i>in vitro</i> and <i>in vivo</i>	179
5.3.2	Attenuation of Δfnr in murine macrophages.....	179
5.3.3	Fitness of Δfnr	180
6	<i>Chapter 6 General Discussion</i>	181
6.1	Importance of this study	182
6.1.1	Context of the study	182
6.1.2	Global analysis of FNR-mediated regulation in <i>S. Typhimurium</i>	183
6.2	Future prospects	186
6.2.1	Signals for expression of virulence.....	186

6.2.2	sRNAs, the missing link?.....	187
6.2.3	Regulation of motility.....	189
6.2.4	Differences in virulence gene expression in Δfnr based on strain.....	189
6.2.5	Limitations of our approach and existing technologies.....	190
6.3	Concluding remarks	191
	<i>References</i>	<i>193</i>
	<i>Appendix I.....</i>	<i>222</i>
	<i>Appendix II.....</i>	<i>321</i>
	<i>Appendix III.....</i>	<i>335</i>
	<i>Appendix IV.....</i>	<i>344</i>

List of Figures

Chapter 1	Page
Figure 1.1 <i>S. Typhimurium</i> must circumvent stressful conditions during infection.	7
Figure 1.2 The SPI-2 type III secretion system.	12
Figure 1.3 Regulation at <i>Salmonella</i> pathogenicity island 2 involves many transcription factors.	19
Figure 1.4 The oxygen gradient in the gut.	22
Figure 1.5 FNR activity is directly regulated by oxygen.	28
Figure 1.6 Activation of simple class I and class II FNR-dependent promoters.	30
 Chapter 2	
Figure 2.1 Experimental set-up for aerobic and microaerobic growth	37
Figure 2.2 Construction of the <i>fnr</i> ⁺ complementing strain.	57
 Chapter 3	
Figure 3.1 Workflow of general experimental procedures for investigating the regulation of SPI-2.	81
Figure 3.2 Growth of <i>S. Typhimurium</i> and isogenic mutants under microaerobic conditions in MMA.	84
Figure 3.3 High correlations of RNA-seq data from independent biological replicates.	86
Figure 3.4 Confirmation of <i>fnr</i> chromosomal deletion by RNA-seq.	88
Figure 3.5 <i>pfnr</i> overexpresses <i>fnr</i> but rescues <i>FnrS</i> expression in Δ <i>fnr</i> .	90
Figure 3.6 <i>fnr</i> ⁺ rescues <i>FnrS</i> and <i>fnr</i> expression under microaerobic & anaerobic conditions.	91
Figure 3.7 Relative gene expression across the <i>S. Typhimurium</i> chromosome and plasmids.	95
Figure 3.8 Classification of FNR-regulated genes according to COGs.	96
Figure 3.9 SPI-2 expression is highly up-regulated in the absence of FNR.	97
Figure 3.10 Low level absolute and relative expression in SPI-1, 3, 4 and 5.	98
Figure 3.11 SPI-2 apparatus and effector expression is up-regulated in Δ <i>fnr</i> under microaerobic conditions in MMA.	101
Figure 3.12 FNR blocks <i>ssaG</i> expression under low O ₂ conditions.	102
Figure 3.13 SPI-2 expression is increased in WT under aerobiosis.	103
Figure 3.14 Expression of SPI-2 effector proteins.	105
Figure 3.15 Secretion of SPI-1 and SPI-2 effector proteins.	106
Figure 3.16 Down regulation of genes at major chemotaxis and flagellar loci.	109
Figure 3.17 Chemotaxis regulatory pathways and flagellar assembly genes activated by FNR.	110
Figure 3.18 Motility is repressed and flagella are absent in Δ <i>fnr</i> .	111
Figure 3.19 Regulatory network of FNR regulated sRNAs.	116
Figure 3.20 Comparison of FNR regulons.	123

Chapter 4	Page
Figure 4.1	Workflow of chromatin immunoprecipitation sequencing to identify FNR binding sites. 130
Figure 4.2	FnrS is expressed in FNR-3×FLAG and the <i>fnrS</i> gene is bound by FNR-3×FLAG. 132
Figure 4.3	FNR ChIP peaks across 2 replicates on the 4/74 chromosome and plasmids. 136
Figure 4.4	Overview of 2 independent ChIP-seq replicates. 138
Figure 4.5	FNR binding motifs. 139
Figure 4.6	FNRD154A is active under microaerobic conditions. 141
Figure 4.7	Alignment of <i>S. Typhimurium</i> and <i>E. coli</i> FNR protein sequences. 141
Figure 4.8	(FNRD154A) ₂ is active and can be purified under aerobic conditions. 142
Figure 4.9	The genes encoding SsrA and SsrB are the most differentially expressed of SPI-2 regulators. 143
Figure 4.10	FNR binding at the P _{<i>fnr</i>} and P _{<i>fnrS</i>} promoters and a negative control. 144
Figure 4.11	FNR binding at the P _{<i>ssrB</i>} , P _{<i>ssrA</i>} and P _{<i>ssaB</i>} promoters. 147
Figure 4.12	FNR binding at the P _{<i>ydgT</i>} promoter. 150
Figure 4.13	Promoter expression from SPI-2 promoters. 151
Figure 4.14	Putative FNR binding sites overlap with TF binding at the <i>ssrB/ssrA/ssaB</i> locus. 157
 Chapter 5	
Figure 5.1	Workflow of general experimental procedures for investigating expressed proteins. 160
Figure 5.2	Growth of 4/74 and isogenic mutants in SPI-2 inducing media. 162
Figure 5.3	Aerobic and microaerobic growth and <i>ssaG</i> expression in 4/74 and isogenic mutants over time in LB, inSPI2 and NonSPI. 163
Figure 5.4	The Δ <i>fnr</i> mutant is attenuated in murine macrophages at early time points. 166
Figure 5.5	Plasmid carriage reduced intramacrophage replication and SPI-2 expression was elevated at early time points in Δ <i>fnr</i> during infection. 167
Figure 5.6	Growth in MMA prior to infection reduces bacterial uptake, but increases fold replication. 168
Figure 5.7	Growth and <i>ssaG</i> expression in MMA with and without alternative electron acceptors. 170
Figure 5.8	The Δ <i>fnr</i> mutant has reduced fitness in microaerobic MMA. 172
Figure 5.9	In SPI-2 inducing conditions the Δ <i>ssrAB</i> mutant outcompetes WT. 173
Figure 5.10	The Δ <i>fnr</i> mutant has reduced fitness and WT and the Δ <i>ssrAB</i> are the same in microaerobic LB. 174
Figure 5.11	Venn diagram representing proteins detected by mass spectrometry in WT and Δ <i>fnr</i> . 177
Figure 5.12	Classification of abundant proteins from WT and Δ <i>fnr</i> into COG categories. 178
 Chapter 6	
Figure 6.1	Model of SPI-2 repression by FNR under changing oxygen conditions. 185

List of Tables

	Page
Chapter 1	
Table 1.1 <i>Salmonella</i> pathogenicity islands 1 through 5.	18
Table 1.2 Electron acceptors used by <i>Salmonella</i> during anaerobic respiration.	24
Chapter 2	
Table 2.1 Media recipes.	41
Table 2.2 Bacterial strains used in this study.	43
Table 2.3 Plasmids used in this study.	45
Table 2.4 Table of oligonucleotides.	52
Table 2.5 Buffers and solutions for Northern blotting.	62
Table 2.6 Buffers for ChIP.	69
Table 2.7 Table of programs and online tools for bioinformatic analysis in this study.	73
Chapter 3	
Table 3.1 sRNAs down-regulated in Δfnr .	114
Table 3.2 sRNAs up-regulated in Δfnr .	115
Appendix I	
Table S1 RNA-seq data: Absolute and relative expression.	222
Appendix II	
Table S2 COG categories.	321
Table S3 COG organized DE genes.	330
Appendix III	
Table S4 ChIP-seq peaks: FNR binding.	335
Table S5 ChIP-seq peaks associated with up-regulated DE genes.	340
Table S6 ChIP-seq peaks associated with down-regulated DE genes.	341
Table S7 Letter-probability matrix of FNR binding motif (TTGATNTRSATCAA)	341
Table S8 Top 100 FNR Motif Hits.	342
Appendix IV	
Table S9 Proteomics: Proteins in WT.	344
Table S10 Proteomics: Proteins in Δfnr .	358

List of Formulas

Section	Formula	Page
2.2.9	Competitive Index	40
2.8.4	Quantity of Immunoprecipitated DNA	68
2.10.1	Transcripts per Million	71
2.11.3	Bound Ratio	77

List of Abbreviations

3'UTR	Three prime untranslated region
4/74	<i>Salmonella enterica</i> serovar Typhimurium strain 4/74
5'UTR	Five prime untranslated region
Amp	Ampicillin
APS	Ammonium persulfate
B_{max}	Maximum bound ratio
bp	Base pair
cDNA	Complementary DNA
CDS	Coding sequence
CFU	Colony forming unit
ChIP	Chromatin Immunoprecipitation
CI	Competitive index
Cm	Chloramphenicol
dH ₂ O	Distilled water
Dig	Digoxigenin
DNA	Deoxyribonucleic acid
dNTP	Deoxyribonucleotide
EDTA	Ethylenediaminetetraacetic acid
EMSA	Electrophoretic mobility shift assay
ESP	Early stationary phase
FLP	Flippase recombinase
FRT	Flippase recognition site
GFP	Green fluorescent protein
GI	Gastrointestinal
HRP	Horseradish peroxidase
IGB	Integrated Genome Browser
InSPI2	SPI-2 inducing PCN medium
iNTS	Invasive Non Typhoisaal <i>Salmonella</i>
Kan	Kanamycin
kb	Kilobase pair
K_D	Dissociation constant
LA	Lennox agar

LB	Lennox broth
LEP	Late exponential phase
LSP	Late stationary phase
MCS	Multiple cloning site
MEP	Mid exponential phase
MES	2-(N-morpholino)ethanesulfonic acid
MMA	Minimal medium A
MOPS	3-(N-morpholino)propanesulfonic acid
mRNA	Messenger RNA
NAP	Nucleoid associated protein
NonSPI2	Non-SPI-2 inducing PCN medium
nt	Nucleotide
OD ₆₀₀	Optical density at 600 nm
ORF	Open reading frame
PBS	Phosphate buffered saline
PCN	Phosphate, Carbon, Nitrogen medium
PCR	Polymerase chain reaction
PES	Polyethersulfone
PIPES	Piperazine-N,N'-bis(2-ethanesulfonic acid)
qPCR	Quantitative real-time PCR
RBS	Ribosome binding site
RNA	Ribonucleic acid
RNA-seq	High-throughput cDNA sequencing
RNAP	RNA polymerase
RNase	Ribonuclease
RNS	Reactive nitrogen species
ROS	Reactive oxygen species
rpm	Revolutions per minute
rRNA	Ribosomal RNA
RT	Reverse transcriptase/transcription
SCV	<i>Salmonella</i> containing vacuole
SDS	Sodium dodecyl sulphate
SDS-PAGE	Sodium dodecyl sulphate poly-acrylamide electrophoresis
SOB	Super optimal broth
SOC	Super optimal broth with catabolite repression
SPI	<i>Salmonella</i> Pathogenicity Island
sRNA	Small RNA
SSC	Saline-sodium citrate
STncXXX	<i>Salmonella</i> Typhimurium non-coding
Str	Streptomycin
T3SS	Type three secretion system
TAE	Tris acetate ethylenediaminetetraacetic acid
TBE	Tris borate ethylenediaminetetraacetic acid
TCA	Trichloroacetic acid
TCS	Two component system

TE	Tris Ethylenediaminetetraacetic acid
TEMED	Tetramethylethylenediamine
Tet	Tetracycline
TF	Transcription factor
TMAO	Trimethylamine <i>N</i> -oxide
TPM	Transcripts per million
tRNA	Transfer RNA
TSS	Transcription start site
UV	Ultra violet
v/v	Volume per volume
w/v	Weight per volume
WT	wild-type
X	xylose

Chapter 1

General Introduction

1.1 *Salmonella*

1.1.1 Overview of the *Salmonella* genus

Members of the genus *Salmonella* belong to the *Enterobacteriaceae* family (Ibarra & Steele-Mortimer, 2009; Rhen & Dorman, 2005). They diverged from a common ancestor with *Escherichia coli* (*E. coli*) between 100 and 150 million years ago (Fookes *et al.*, 2011; Sabbagh *et al.*, 2010). *Salmonella* are Gram-negative, rod-shaped, motile flagellates, facultative anaerobes and facultative intracellular pathogens (Fàbrega & Vila, 2013). The nomenclature of *Salmonella* is complex, contentious and still evolving. The current recommended system of nomenclature by the World Health Organization (WHO) Collaborating Centre (Issenhuth-Jeanjean *et al.*, 2014) subdivides the genus by differences in their 16S ribosomal RNA (rRNA) into two species: *Salmonella bongori* (*S. bongori*) and *Salmonella enterica* (*S. enterica*) (Popoff *et al.*, 2004). The type species, *S. enterica*, can be further divided into six subspecies, *enterica* (I), *salamae* (II), *arizonae* (IIIa), *diarizonae* (IIIb), *houtenae* (IV) and *indica* (VI), based on their genomic relatedness and biochemical properties (Reeves *et al.*, 1999). *S. enterica* subsp. *enterica* is found predominantly in mammals and contributes to the vast majority of *Salmonella* infections in humans and warm-blooded animals. *S. bongori* and the remaining *S. enterica* subspecies are commonly associated with commensalism of cold-blooded vertebrates and isolation from environmental sources, with only a limited number of human infections reported (Desai *et al.*, 2013; Fookes *et al.*, 2011; Sabbagh *et al.*, 2010). *Salmonella* is further subdivided into serovars (serotypes) based on serologic identification of O (lipopolysaccharide) and H (flagellar) antigens with over 2,500 in total, and the *enterica* subspecies encompassing over 1,500 serovars (Grimont & Weill, 2007; Issenhuth-Jeanjean *et al.*, 2014). For simplicity, the species and subspecies of *S. enterica* subsp. *enterica* serovars are commonly omitted, for example *Salmonella enterica* subsp. *enterica* sv. Typhimurium is shortened to *S. Typhimurium* (Brenner *et al.*, 2000).

S. enterica infections, or salmonellosis, result in two major clinical manifestations: gastroenteritis and enteric fever. Enteric fever, also called Typhoid fever is human host-restricted systemic febrile infection caused by *S. Typhi*. A clinically similar but, often less severe disease, Paratyphoid fever, is caused by *S. Paratyphi* A, B and C (Crump & Mintz, 2010; McClelland *et al.*, 2004). *S. Typhi* is a relatively recently evolved serovar of *Salmonella*, as its divergence from a common ancestor is estimated to be only 50,000 years

ago and it has adapted to exclusively infect humans (Kidgell *et al.*, 2002). *S. Typhi* remains relevant today as it causes an estimated 21 million infections annually, resulting in approximately 200,000 – 600,000 deaths primarily in regions with poor economic development in children, adolescents, and the elderly (Buckle *et al.*, 2012; Crump & Mintz, 2010). *S. Typhi* is spread through fecal-oral transmission via contaminated food or water. After exposure, signs and symptoms may initially be absent, as the bacteria can disseminate systemically without triggering a pro-inflammatory response or diarrheal disease. Infected individuals carry *S. Typhi* in their bloodstream and intestinal tract, and they shed bacteria in their stool. After the incubation period, some people may remain asymptomatic. Asymptomatic carriers of *S. Typhi* harbour the bacteria in their gallbladder and, as was demonstrated by the infamous case of Mary Mallon or “Typhoid Mary” in the early 1900s, go on to spread enteric fever through person-to-person transmission (Basnyat & Baker, 2015; Gonzalez-Escobedo *et al.*, 2010). Others will go on to exhibit extreme fatigue, high fever (>39°C), coughing, vomiting, headache and rapid pulse (Dougan & Baker, 2014).

Strains of non-typhoidal *Salmonella* (NTS) are the second most common causative agent of gastroenteritis after *Campylobacter* species, responsible for an estimated 93 million cases of gastroenteritis annually, as well as more than 155,000 deaths (Majowicz *et al.*, 2010; Murray *et al.*, 2015). The majority of human infections are caused by two *S. enterica* serovars, Typhimurium and Enteritidis. NTS infection begins with an inflammatory response upon invasion of host epithelial cells, with 80% of cases leading to a self-limiting gastroenteritis with symptoms including diarrhea with or without blood, abdominal cramps, nausea and fever (Dougan & Baker, 2014). NTS is typically non-fatal in healthy adults however, infants, young children, elderly people and immunocompromised patients are highly susceptible to NTS infections (Scallan *et al.*, 2011). Invasive NTS (iNTS) has recently emerged as a new pathogenic clade with a distinct genotype in sub-Saharan Africa. This emerging pathogen may have adapted to occupy an ecological and immunological niche provided by HIV, malaria, and malnutrition in Africa (Feasey *et al.*, 2012). iNTS strains of *S. Typhimurium* lead to an estimated 2 to 3 million infections and up to 700,000 deaths per year, with a mortality rate between 20-25% (Ao *et al.*, 2015; Feasey *et al.*, 2012; Gordon, 2008). Unlike Typhoidal serovars, NTS are zoonotic pathogens and have a broad spectrum of warm- and cold-blooded hosts. Thus, NTS are easily disseminated through agriculture resulting in contamination of food such as beef, poultry, eggs, and fresh produce (Stevens *et al.*, 2009). In mice, infection by *S. Typhimurium* results in a typhoid-like systemic fever similar to that of the human host-restricted serovars Typhi and Paratyphi. Therefore, *S. Typhimurium* is

used in murine systemic infections for the study of typhoid fever pathogenesis (Coburn *et al.*, 2006; Hurley *et al.*, 2014; Sabbagh *et al.*, 2010).

In this study *S. Typhimurium* strain 4/74 (GenBank accession numbers CP002487-CP002490) was used for all experiments. Strain 4/74 was originally isolated from a calf with salmonellosis in the UK, it is a virulent isolate and the parent strain of the commonly used lab strain and histidine (*hisG*) auxotroph SL1344. Strain 4/74 differs from SL1344 by only 8 single nucleotide polymorphisms (SNPs) including in *hisG* (Hoiseth & Stocker, 1981; Kröger *et al.*, 2012; Richardson *et al.*, 2011). Strain 4/74 is a prototroph for histidine production that possesses a functional histidine biosynthetic pathway that is important for replication in the vacuolar environment of certain mammalian cells including macrophages (Henry *et al.*, 2005) and is more invasive than another commonly used lab strain ATCC 14028S due to heterogeneity in expression of *Salmonella* pathogenicity island 1 (Clark *et al.*, 2011).

1.1.2 Pathogenesis of *S. Typhimurium*

Consumption of contaminated food and water is the primary route of infection for *S. Typhimurium* (Ohl & Miller, 2001; Thompson *et al.*, 2006). Following ingestion, *S. Typhimurium* must pass through the gastrointestinal (GI) tract from the mouth, through the esophagus, and through the stomach to reach the small intestine where it encounters a variety of stressful conditions meant to protect the host from infection (**Figure 1.1**). First, there is an upshift in temperature from that of the outside environment to approximately 37°C in humans. As *S. Typhimurium* reaches the stomach, it must also survive the extreme acidic pH. Response to acid shock and survival in the stomach is facilitated by the acid-tolerance response (ATR) (Álvarez-Ordóñez *et al.*, 2011; Haraga *et al.*, 2008; Ohl & Miller, 2001). The ATR is also responsible for preparing bacterial cells for the acidic intracellular environment later in infection (Foster, 1991; Foster & Hall, 1990). As *S. Typhimurium* travels through the duodenum and jejunum of the small intestine to reach the ileum, its preferred site for invasion, the bacterium encounters increased osmolarity and anaerobiosis, as well as the host intestinal microbiota (Hébrard *et al.*, 2011). To reach the intestinal epithelium, *S. Typhimurium* requires a functional motility and chemotaxis system (Jones *et al.*, 1981). While crossing the intestinal mucosal layer, the bacterium must resist the host innate immune system including such elements as bile salts and antimicrobial peptides in order to access and adhere to the underlying epithelium (Haraga *et al.*, 2008).

Once at the intestinal epithelium, *S. Typhimurium* invades epithelial cells. It preferentially targets microfold (M) cells for translocation and can induce transformation of epithelial cells into M cells to promote host colonization and invasion (Jepson & Clark, 2001; Tahoun *et al.*, 2012). M-cell-mediated uptake of *S. Typhimurium* also allows bacterial cells to invade adjacent epithelial cells from their apical and basolateral surfaces (Haraga *et al.*, 2008). Adherence of bacterial cells to the apical surface of epithelial cells is necessary for the induction of invasion associated genes (Jones *et al.*, 1981) and is accomplished by *Salmonella* surface appendages such as fimbriae and non-fimbrial adhesins (Wagner & Hensel, 2011). Following attachment, *Salmonella* Pathogenicity Island 1 (SPI-1) encoded type III secretion system (T3SS)-dependent translocation of effector proteins into the cytosol of non-phagocytic cells actively induces host cell cytoskeletal rearrangement, membrane ruffling and ultimately uptake of the bacterium into a membrane-derived vacuole (Finlay *et al.*, 1991; Lhocine *et al.*, 2015; Srikanth *et al.*, 2011). Detection of the invading bacteria by components of the host immune system and active translocation of additional bacterial effectors into epithelial cells by *S. Typhimurium* leads to a pro-inflammatory immune response, resulting in the inflammation of the gut, fluid secretion and the symptoms of gastroenteritis (Haraga *et al.*, 2008; Hurley *et al.*, 2014; Thiennimitr *et al.*, 2012). Inflammation promotes shedding of epithelial cells into the lumen of the intestine, depositing bacteria back into the lumen. Bacteria that remain in the intestinal lumen can benefit from the by-products inflammation of the intestine to use as electron acceptors for anaerobic metabolism to outcompete the resident microbiota who rely on fermentation (Thiennimitr *et al.*, 2012; Winter *et al.*, 2013). Enhanced growth in the intestinal lumen promotes transmission of *S. Typhimurium* to new hosts by the fecal–oral route (Lawley *et al.*, 2007).

S. Typhimurium cells that successfully invade host epithelial cells are enclosed in a membrane-derived vesicle termed the spacious phagosome (SP). The SP later fuses with lysosomes, acidifies and shrinks to become adherent around one or more bacteria creating the *Salmonella*-containing vacuole (SCV) (Steele-Mortimer, 2008). Maturation of the SCV and survival of bacterial cells is dependent upon proteins encoded on *Salmonella* pathogenicity island 2 (SPI-2). The SPI-2 T3SS translocates effector proteins across the phagosomal membrane to allow intracellular survival and replication. Formation of the SCV requires altering the host cell endocytic trafficking pathway to avoid normal phagosome maturation and fusion with lysosomes (Rathman *et al.*, 1997). As the SCV matures, *S. Typhimurium* encounters additional stressors including starvation of magnesium, phosphate and iron and a further reduction in pH (Hébrard *et al.*, 2011). The mature SCV migrates to

the Golgi-apparatus and simultaneously *Salmonella*-induced filaments (SIFs) are formed. SIFs are tubular filamentous structures which extend from the SCV and form complex networks throughout the cell to facilitate interactions with host organelles (Knuff & Finlay, 2017; Krieger *et al.*, 2014). *S. Typhimurium* can also proliferate in epithelial cells outside of their SCV. A significant subpopulation damages the SCV membrane, leading to escape from the SCV and extensive proliferation in the cytosol. These bacteria use SPI-1 encoded proteins to evade destruction by autophagic mechanisms of the host epithelial cell and survive to hyper-replicate in the epithelial cytosol (Knodler *et al.*, 2014).

Infection with NTS in healthy human adults, is usually limited to the intestine, however in cases of susceptible hosts and in murine infections, *S. Typhimurium* can go on to persist in the SCV of macrophages. SCVs transcytose to the basolateral membrane of epithelial cells and are subsequently engulfed by phagocytic cells, primarily macrophages. This bacterial internalization ultimately results in an intra-macrophage SCV. The intra-macrophage SCV is similar to the intra-epithelial SCV, and similar host cell pathways are triggered, allowing *S. Typhimurium* to proliferate by preventing phagosome maturation (Fàbrega & Vila, 2013). There are some differences between the SCVs of the epithelial cells and macrophages. While nutrient starvation and acidic pH is a feature of both intracellular vacuoles, the intra-macrophage is more bactericidal in nature (Hautefort *et al.*, 2008). Remodelling of the protein, carbohydrate and membrane components of the bacterial envelope confer resistance to antimicrobial peptides and reactive oxygen and nitrogen species (ROS, RNS) that can damage the bacterial cell (Haraga *et al.*, 2008). Infected macrophages can go on to cause systemic infection by disseminating through the bloodstream to organs such as the spleen and liver (Haraga *et al.*, 2008).

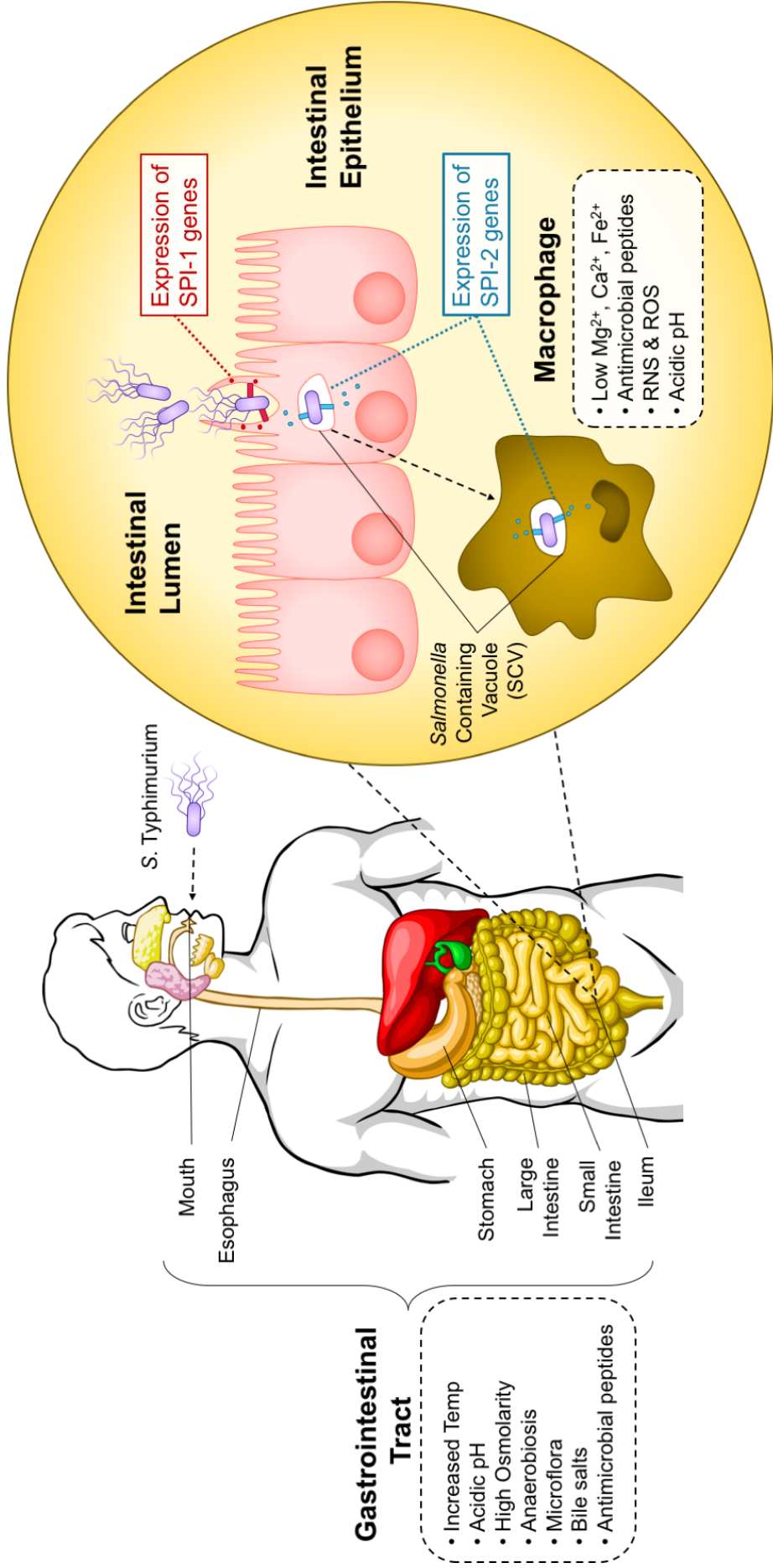


Figure 1.1 *S. Typhimurium* must circumvent stressful conditions during infection.

S. Typhimurium is ingested via contaminated food or water and passes through gastrointestinal (GI) tract from the mouth, esophagus, and stomach to the small intestine. *S. Typhimurium* encounters several deleterious stress conditions in the GI tract as part of the hosts first line of defense. Magnified panel: Environmental signals within the intestinal lumen induce expression of the *Salmonella* Pathogenicity Island 1 (SPI-1) Type 3 Secretion System (T3SS), which injects effector proteins into the host epithelial cell (in red). These effector proteins trigger intestinal inflammation and bacterial endocytosis of the bacteria and invasion of the intestinal epithelial cells. The intracellular environment of host cells provides the necessary signals for expression of the SPI-2 T3SS and effector proteins (in blue). *S. Typhimurium* survives and proliferates intracellularly within the *Salmonella* containing vacuole (SCV). In susceptible hosts, *S. Typhimurium* becomes engulfed by macrophages and survives and replicates within the SCV, leading to bacterial dissemination and systemic infection. Conditions encountered by *S. Typhimurium* within the macrophage SCV induce expression of SPI-2 genes necessary for survival and proliferation.

1.1.3 Flagella

Flagella are complex motility structures that allow rotational propulsion of bacteria and chemotaxis towards nutrients (Stecher *et al.*, 2008). *Salmonellae* are peritrichously flagellated, meaning they have multiple flagella at random positions on cell. They express between 5-10 flagella at a time (Parker & Guard-Petter, 2001; van Asten & van Dijk, 2005). The synthesis and function of the flagellar and chemotaxis systems involves over 50 genes from at least 17 operons (*flh*, *flg*, *fli*, *flj*, *mot*, *che*, *tar*, *tsr*, and *aer*) that constitute the flagellar regulon (Chilcott & Hughes, 2000). The individual flagella are composed of three distinct substructures: the basal body, a transmembrane motor, a hook that links the motor and the filament, and the filament that acts as a propeller (Aizawa, 1996). The major structural component of the filament is flagellin, a monomeric protein encoded by two different genes, *fljB* and *fliC*. *S. Typhimurium* exhibits phase variation via alternate expression of the two antigenically distinct flagellins (Bonifield & Hughes, 2003). Cytosolic delivery of flagellin by bacterial secretion systems has been shown to cause activation of the host inflammasome and subsequent pro-inflammatory cell death of infected macrophages, thus repression of flagellin in the macrophage is important for intracellular survival. Recently, a trans-acting leader mRNA was discovered to post-transcriptionally regulate *fljB* from the same operon

as a virulence protein, *mgtC_{BR}* during infection (Choi *et al.*, 2017; Miranda-CasoLuengo *et al.*, 2017). Additionally, bacteria expressing FliC-flagella were advantaged in identifying target sites on host cell surfaces and invading epithelial cells and, FliC-expressing *S. Typhimurium* outcompeted FljB-expressing bacteria for intestinal tissue colonisation in gastroenteritis and typhoid murine infection models (Horstmann *et al.*, 2017). Bacterial flagella are required for both bacterial movement and immune detection, therefore production of flagella must be tightly regulated during infection. As previously discussed, flagella play a role in *S. Typhimurium* virulence as motility is necessary for bacterial approach to the epithelial cells in the host ileum, which is a prerequisite for bacterial adhesion and invasion of host cells. Flagella also play a role in providing a competitive advantage to *S. Typhimurium* as mutations affecting flagellar assembly and chemotaxis impaired the fitness of the pathogen in the inflamed intestine, but not in the normal gut. Thus, motility allows *S. Typhimurium* to move towards high energy nutrients and utilize them for enhanced growth in the inflamed gut (Stecher *et al.*, 2008). Aflagellated *Salmonella* were deficient in their ability to upregulate the pro-inflammatory response in a murine enteritis model and caused increased epithelial apoptosis. Therefore, it can be suggested that flagella are involved in the induction of the pro-inflammatory response and inhibition of apoptosis in epithelial cells (Vijay-Kumar & Gewirtz, 2009). Recently a link has been made between SPI-2 and flagellar regulation. The study shows that SsrB, the SPI-2 response regulator, alters a transcriptional network controlling bacterial motility through an SsrB binding site upstream of *flhDC*. This repression through SsrB limits inflammasome activation during host cell infection (Ilyas *et al.*, 2018). Thus, flagella are important virulence factors for *S. Typhimurium*, as the bacterium must move toward nutrients to obtain food, and it simultaneously must evade the host immune system.

1.1.4 Salmonella pathogenicity islands

The ability of *Salmonella* to cause disease is largely dependent on the expression of genes found in the *Salmonella* pathogenicity islands (SPIs). The SPIs are large clusters of genes encoding various virulence factors with low GC content and different codon usage compared to the rest of the chromosome (Groisman & Ochman, 1997). The pathogenicity islands were acquired by horizontal gene transfer and are therefore not found in non-pathogenic relatives (Jacobsen *et al.*, 2011). To date 23 pathogenicity islands have been identified across the *Salmonella* genus (Fookes *et al.*, 2011; Hayward *et al.*, 2014; Sabbagh *et al.*, 2010), and *S. Typhimurium* carries 13 SPIs (Kröger *et al.*, 2012). However, only 5 SPIs are of particular

importance and have been clearly shown to play a role in *S. Typhimurium* virulence (Fabrega & Vila, 2013) (**Table 1.1**). Coordinated regulation of SPI encoded genes involves loci situated both within and outside the islands on the chromosome, and a virulence plasmid (Ellermeier & Slauch, 2007; Fabrega & Vila, 2013). SPI-1 and SPI-2 are the best studied pathogenicity islands, both encoding T3SSs that translocate effector molecules into host cells and are required for invasion of epithelial cells and intracellular survival, respectively (Haraga *et al.*, 2008).

1.1.4.1 *Salmonella* Pathogenicity Island-1

The SPI-1 pathogenicity island is approximately 40 kb and has been shown to be required for invasion of non-phagocytic epithelial cells, induction of intestinal inflammatory responses and diarrhea, as well as colonization of the intestine. Genes encoding the structural components of the SPI-1 T3SS and effector proteins are organised into three operons: *prg/org*, *inv/spa* and *sic/sip* (Ellermeier & Slauch, 2007). The *prg/org* and *inv/spa* operons encode a needle complex while the *sic/sip* operon encodes a translocon which embeds in the host cell membrane for translocation of effector proteins (Haraga *et al.*, 2008; Srikanth *et al.*, 2011). Upon contact with epithelial cells, *S. Typhimurium* initiates the translocation of several effector proteins in a highly co-ordinated fashion to mediate its uptake by endocytosis (Srikanth *et al.*, 2011). SopE, SopE2 and SopB are essential for invasion of *S. Typhimurium* as mutants defective in any of these effectors are incapable of inducing actin cytoskeleton rearrangements (Haraga *et al.*, 2008; Srikanth *et al.*, 2011). The effectors SipA and SipC are responsible for membrane ruffling and engulfment (Srikanth *et al.*, 2011).

Signals integrated by a multitude of SPI-1 encoded and global regulators constitute a complex regulatory network to control the expression of SPI-1. HilA (hyperinvasion locus), encoded by *hilA*, is the master regulator of SPI-1 and ultimately, all forms of regulation act via modulating its expression. Mutants of *hilA* are incapable of invasion and are phenotypically equivalent to SPI-1 mutants (Lee *et al.*, 1992). HilA binds to and activates the promoters of the needle complex operons *prg/org* and *inv/spa*. Three positive regulators, SPI-1 encoded HilC and HilD, and RtsA control the expression of *hilA* through a feed forward loop. Additionally, whether by direct regulation of *hilA* or indirect regulation via regulation of *hilC*, *hilD* or *rtsA*, SPI-1 expression is controlled by environmental cues which are sensed and integrated by two component regulatory systems such as SirA/BarA, OmpR/EnvZ and PhoP/PhoQ (Ellermeier *et al.*, 2005; Ellermeier & Slauch, 2007).

Furthermore, SPI-1 is regulated by changes in DNA supercoiling and by several global regulators including the nucleoid-associated proteins (NAPs) FIS, H-NS, IHF, Hha and HU (Baños *et al.*, 2009; Cameron *et al.*, 2011; Mangan *et al.*, 2006; 2011; Ono *et al.*, 2005; Troxell *et al.*, 2011).

1.1.4.2 *Salmonella* Pathogenicity Island-2

The SPI-2 pathogenicity island is in its entirety 40 kb however, it can be separated into two distinct sections. The first section is a 15 kb region that encodes genes necessary for anaerobic respiration using tetrathionate as a terminal electron acceptor (discussed in detail in Section 1.2.2) and other genes of unknown function. The second 25 kb region encodes the T3SS and accessory proteins. These genes have been annotated according to their function: the secretion system regulators are named *ssr*, components of the secretion system apparatus are named *ssa*, secretion system effectors are named *sse*, and secretion system chaperones are named *ssc* (Hensel, 2000). It should be noted that 2 proteins of SPI-2, *ssrA* and *ssaB*, are sometimes called *spiR* and *spiC*, respectively. However, the contemporary literature most frequently refers to them as the former, and so they shall be referred to as *ssrA* and *ssaB* in the remainder of this study. The function of the SPI-2-encoded T3SS and effectors is to mediate the survival of *S. Typhimurium* within the intracellular compartment. SPI-2 secreted effector proteins are translocated into the host cell cytoplasm across the membrane of the SCV to manipulate host cell function and to allow intracellular survival and replication (Abrahams *et al.*, 2006).

The SPI-2 T3SS is essential for the systemic phase of infection and intracellular replication of *S. Typhimurium*. It is activated within the SCV and translocates a complex set of effector proteins into the host cell cytoplasm (Kuhle & Hensel, 2004). The requirement of *S. Typhimurium* to detect the near neutral pH of the host cytosol for effector translocation to occur is debated in the literature as some groups argue that only acidification of the bacterial cytosol is required (Kenney, 2018; Yu *et al.*, 2010; 2018). Regardless, secretion occurs through a hollow needle-like filament that extends from the bacterial cell surface and a translocon pore that is formed in the host cell membrane (**Figure 1.2**). The T3SS is comprised of SsaRSTUV which form the basal body and span the inner membrane to form an export gate that is connected to two additional inner membrane proteins, SsaDJ, and an outer membrane ring, SsaC. SsaV is an essential component of the export gate and interacts in the cytoplasm with a sorting platform consisting of SsaKOQX and an ATPase SsaN. A

cytoplasmic “gatekeeper” complex comprised of SsaBLM is required for translocon protein secretion and to prevent premature secretion of effectors. After assembly of the secretion apparatus, subunits of the needle filament SsaG, inner rod protein SsaI and a molecular “ruler” protein SsaP are secreted. When the filament reaches a defined length, translocon proteins are secreted (Kuhle & Hensel, 2004; Yu *et al.*, 2018).

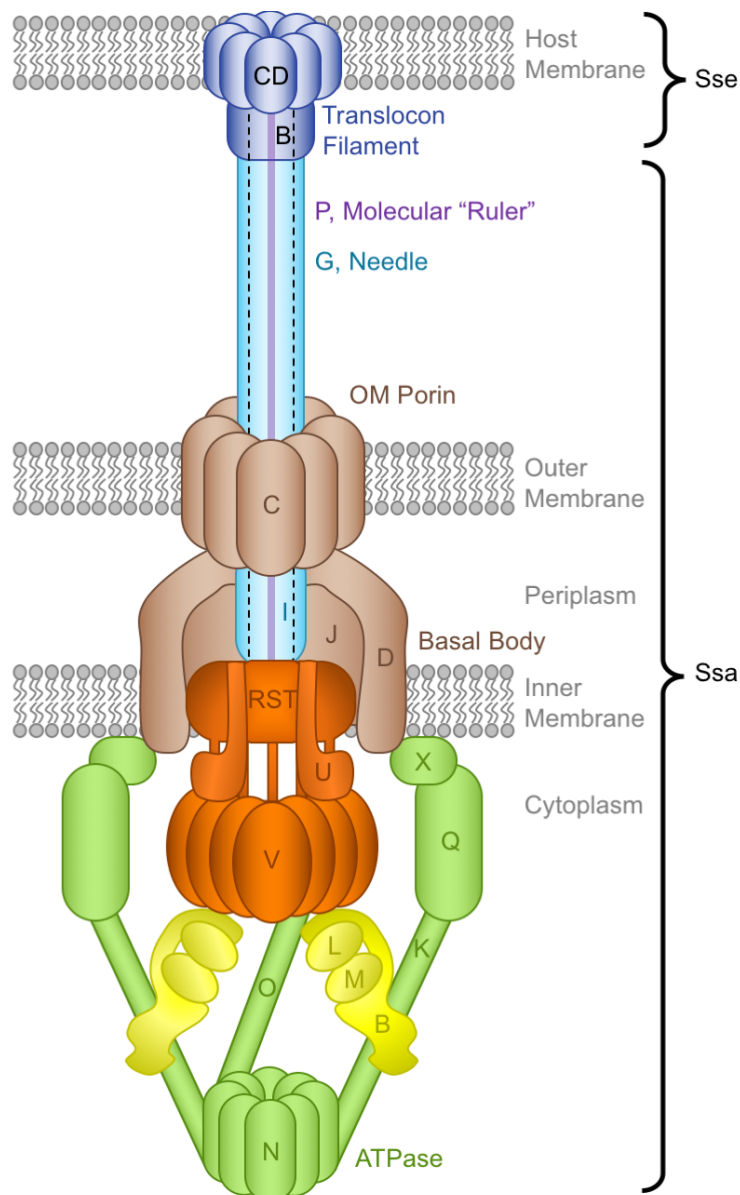


Figure 1.2 The SPI-2 type III secretion system.

Schematic drawing of the SPI-2 T3SS representing the secretion state of translocon proteins. Cytoplasmic sorting platforms are shaded in green, export gates in orange, gatekeepers in yellow, basal bodies in brown, needles and inner rods in light blue, translocon proteins in blue, and molecular “ruler” in purple. Adapted from Yu *et al.*, 2018.

SPI-2 regulation, although studied extensively, is still not completely understood and the signals for expression under certain conditions have not been elucidated. The indispensable master regulator of SPI-2, SsrA/SsrB is encoded on the island by two adjacent genes, *ssrA* and *ssrB* (Cirillo *et al.*, 1998). Transcription of *ssrA* and *ssrB* occurs from divergent promoters. The promoter of *ssrA* lies in an extremely AT rich (69.03%) intergenic region and includes 2 transcriptional start sites (TSS) where the primary (1°) TSS is located closest to the *ssrA* open reading frame (ORF), and the 2° is located upstream. The *ssrB* promoter has one TSS internal to the 3' end of the *ssrA* ORF (Feng *et al.*, 2003; Kröger *et al.*, 2012; Ochman *et al.*, 1996). SsrA/SsrB is a two-component system (TCS) where SsrA is the membrane-bound sensor kinase that phosphorylates the response regulator SsrB upon detection of an exogenous signal. SsrA is reported to respond to extracellular acidification, but no other signals have been identified (Fass & Groisman, 2009; Mulder *et al.*, 2015). Phosphorylated SsrB binds to the promoters and activates the transcription of SPI-2 encoded virulence gene operons and many effectors found outside of the gene island (Fass & Groisman, 2009; Worley *et al.*, 2000). SsrB binds to and regulates transcription from its both its own promoter and of *ssrA*. This is particularly unusual because TCSs with proteins encoded from adjacent genes are typically co-regulated resulting in a polycistronic mRNA from the same promoter. The use of separate promoters has been hypothesized to allow differential regulation of the genes according to the growth conditions, indeed in the absence of SsrA, the unphosphorylated SsrB protein controls expression of genes involved in biofilm biosynthesis (Desai *et al.*, 2016). Additionally, differential RNA-seq analysis has revealed that the *ssrB* promoter is 3.5-fold more active than the *ssrA* promoter within murine macrophages (Srikumar *et al.*, 2015). However, others have reported that a single promoter upstream of *ssrA* can drive transcription of both genes (Bustamante *et al.*, 2008; Fass & Groisman, 2009).

Many transcription factors (TFs) and NAPs have been established as regulators of SPI-2 genes as either repressors or activators in a complex regulatory network (**Figure 1.3**). The NAP H-NS is an important repressor of horizontally acquired genes and is involved in gene silencing at the *ssrAB* locus in accordance with its role in binding to AT-rich sequences (Lucchini *et al.*, 2006; Navarre *et al.*, 2006; Walther *et al.*, 2007). H-NS binding to DNA leads to the formation of a stiff nucleoprotein filament through oligomerization of H-NS monomers which silences genes by restricting access of RNA polymerase to promoters (Lim *et al.*, 2006; Liu *et al.*, 2010; Winardhi *et al.*, 2015). Repression of SPI-2 promoters can also occur through direct repression by H-NS paralogs Hha and YdgT (Silphaduang *et al.*, 2007).

H-NS can form repressive complexes on SPI-2 promoters with both YdgT and Hha that interfere with SsrB binding and transcriptional activation (Ali *et al.*, 2013; Coombes *et al.*, 2005; Silphaduang *et al.*, 2007). Hha can also repress transcription of SPI-2 genes in an H-NS-independent manner (Solórzano *et al.*, 2015). Interestingly, YdgT is required for full virulence in infected macrophages. Coombes *et al.*, postulate that the presence of YdgT might cause dampening of SPI-2 activation and the intracellular growth rate required for sustained infection and persistence, whereas the absence of YdgT ultimately leads to attenuation possibly caused by alterations in intracellular growth and/or fitness (Coombes *et al.*, 2005). Fur, a central regulator of iron utilization, causes repression of SPI-2 genes via direct binding of the *ssrB* promoter in acidic media. Within macrophages, *S. Typhimurium* lacking the Fur protein has earlier induction and ultimately higher expression of SPI-2 (Choi *et al.*, 2014). The Lrp global regulator of metabolism also plays a role in SPI-2 repression. It binds directly to a consensus motif at the *ssrA* promoter which results in down-regulation of SPI-2 genes (Baek *et al.*, 2009). The phosphorelay system RcsCDB plays a dual role in SPI-2 regulation. Microarray data has shown that the RcsCDB system normally functions as a positive regulator of SPI-2, although when highly activated, the system completely represses SPI-2 virulence (Wang *et al.*, 2007). Finally, under invasion-inducing conditions, the SPI-1 activator HilA was found to repress expression of genes encoding a SPI-2 apparatus protein, *ssaH*, and a SPI-2 effector protein, *sseL* (Thijs *et al.*, 2007).

Known signals of SPI-2 induction are acidic pH, limitation of inorganic phosphate (P_i), Mg^{2+} deprivation, high osmolarity, and the presence of antimicrobial peptides. These signals are thought to mimic the environmental cues found in the SCV (Cirillo *et al.*, 1998; Deiwick *et al.*, 1999; Löber *et al.*, 2006). Under SPI-2-inducing conditions, SsrB has a dual function in relieving the H-NS-mediated silencing of *ssrA* expression, as well as classical transcription initiation at SPI-2 genes including at the *ssaB*, *sseA*, *ssaG* and *ssaM* promoters (Walthers *et al.*, 2007; 2011). After SsrB, OmpR is arguably the most important activator of SPI-2. In the EnvZ-OmpR TCS, EnvZ is the sensor kinase and OmpR is the response regulator. OmpR has binding sites at both the *ssrA* and *ssrB* promoters, and directly activates transcription in response to low pH and osmotic stress (Feng *et al.*, 2003). Furthermore, an *ompR* mutant was severely attenuated *in vivo* (Dorman *et al.*, 1989) and the acidification of the *Salmonella* cytoplasm in the macrophage vacuole and subsequent SPI-2 T3SS effector secretion was found to be OmpR dependent (Chakraborty *et al.*, 2015). Additionally, expression of SPI-2 genes does not occur in an *ompR/envZ* mutant under SPI-2 inducing condition *in vitro* (Xu & Hensel, 2010). Another TCS involved in SPI-2 regulation is PhoQ-PhoP. Low

extracellular cation concentrations, such as those detected within the SCV, and low pH have been reported to activate the sensor kinase PhoQ, which, in turn, activates the response regulator PhoP (Choi & Groisman, 2016). Experiments have shown that PhoP controls SsrA post-transcriptionally and directly activates the *ssrB* gene by binding to its promoter (Bijlsma & Groisman, 2005). However, in the macrophage and under SPI-2 inducing conditions *phoP* mutants still express SPI-2 genes at low levels (Colgan *et al.*, 2016; Fass & Groisman, 2009), furthermore a *phoP* mutant was observed to have severely delayed SPI-2 expression in SPI-2 inducing conditions (Xu & Hensel, 2010), implying that PhoQ-PhoP activation may be necessary for full expression and correct timing of SPI-2 expression. SlyA is required for virulence and survival within macrophages so not surprisingly the *slyA* gene is highly expressed during macrophage infection, and absence of the SlyA protein renders *S. Typhimurium* extremely susceptible to oxidative stress and antimicrobial peptides (Buchmeier *et al.*, 1997; Shi *et al.*, 2004). Additionally, in SPI-2 inducing conditions a *slyA* mutant shows a 2- to 3-fold reduction and delay of SPI-2 expression *in vitro* (Xu & Hensel, 2010). Transcription of *slyA* is activated by PhoP (Norte *et al.*, 2003; Stapleton *et al.*, 2002) which promotes SlyA binding to and directly regulating expression from the *ssrA* promoter (Navarre *et al.*, 2005; Okada *et al.*, 2007). A number of these regulators work together to remove repressive HNS complexes from the *ssrA* promoter. Under inducing conditions, SlyA and HilD or in nutrient limited conditions only SlyA, displace the H-NS complex bound to the promoter upstream of *ssrA*. This allows binding of OmpR that recruits the RNA polymerase on this promoter, which induces the transcription of *ssrAB* (Banda *et al.*, 2019). HilD also mediates cross-talk between SPI-1 and SPI-2 via counter-silencing of H-NS at the *ssrB* promoter (Bustamante *et al.*, 2008; Martinez *et al.*, 2014). Xu & Hensel also observed that a *sirA* mutant had reduced SPI-2 expression (Xu & Hensel, 2010). SirA is the response regulator of the TCS SirA/BarA, which also induces expression of SPI-1 genes. SirA/BarA induction of SPI-2 gene works through HilD. A global regulatory RNA binding protein, CsrA post-transcriptionally regulates *hilD* mRNA; negative regulation of HilD is counteracted by SirA/BarA, which directly activates the expression of the sRNAs *CsrB* and *CsrC* that sequester CsrA (Martínez *et al.*, 2011).

A number of NAPs are also important for induction of SPI-2 genes. FIS is a global regulator of gene expression and chromosome structure. FIS binds directly to the promoters of *ssrA* and *ssaG* and overall expression of SPI-2 genes is downregulated in a Δfis mutant (Cameron *et al.*, 2011; Fass & Groisman, 2009; Kelly *et al.*, 2004). Additionally, low level SPI-2 expression activated by OmpR and FIS has been observed prior to epithelial invasion in the

intestinal lumen, but the signal for induction remains unclear (Brown *et al.*, 2005; Osborne & Coombes, 2011). HU and IHF are homologous histone-like proteins. Several SPI-2 genes, including the *ssrAB* genes, are downregulated in a HU double mutant, similarly loss of IHF causes a down regulation in all SPI-2 genes (Mangan *et al.*, 2006; Mangan *et al.*, 2011).

1.1.4.3 *Salmonella* Pathogenicity Islands 3 through 5

Salmonella pathogenicity islands 3 through 5 play a smaller but still important role in *Salmonella* pathogenesis. SPI-3 encodes 10 open reading frames organized into 6 operons. These include the *mgtCB* operon encoding the macrophage survival protein MgtC and the Mg²⁺ transporter MgtB. The 5' leader mRNA of *mgtC* is also involved in regulation of the *fljB* flagellin as previously discussed (Choi *et al.*, 2017; Miranda-CasoLuengo *et al.*, 2017). SPI-3 also encodes *misL* and *marT*, where MisL is a fibronectin binding protein important for oral colonization of mice and chicks, and MarT is its positive regulator (Blanc-Potard *et al.*, 2005; Tukul *et al.*, 2007). SPI-4 encodes 6 genes, *siiABCDEF*, termed the *Salmonella* intestinal infection genes which are important for interaction of *S. Typhimurium* with the host intestinal mucosa and help facilitate membrane ruffling and entry of polarized epithelial cells in conjunction with SPI-1 (Gerlach *et al.*, 2008). SPI-4 encodes a 595 kDa non-fimbrial giant adhesin, SiiE, which is secreted by a type I secretory system encoded by *siiC*, *siiD*, and *siiF* (Barlag & Hensel, 2015). SiiE mediates primary contact with host cells, allowing positioning of the SPI-1 T3SS to initiate the translocation of SPI-1 effectors (Barlag & Hensel, 2015). Expression of SPI-4 genes corresponds with that of SPI-1 genes, and the activators and repressors of SPI-1 are involved in its regulation (Main-Hester *et al.*, 2008). SPI-5 encodes SPI-1 T3SS secreted effector protein SopB which modulates host cell exocytosis and its chaperone PipC, and the SPI-2 T3SS secreted effectors PipA and PipB, thought be important in development of systemic infection and PipD a hypothetical secreted peptidase (Perrett & Zhou, 2013; Knodler *et al.*, 2002; Marcus *et al.*, 2000; Morgan *et al.*, 2004).

Overall pathogenicity islands and other horizontally acquired genes are critical for cultivating a niche for *S. Typhimurium* in the host. SPI-1, SPI-4 and SPI-5 all play a role in niche creation as they induce inflammation in the host. That niche can then be colonized with the help of anaerobic metabolism genes found on SPI-2 and a bacteriophage acquired effector, SopE which is secreted through the SPI-1 T3SS to make nitrate available for respiration (Winter *et al.*, 2013). Genes encoded on SPI-2 and SPI-3 are also important for

intracellular survival (Blanc-Potard *et al.*, 1999; Figueira & Holden, 2012). Finally, SPI-2 optimizes the niche by prolonging intestinal inflammation, and thereby making more nutrients available for this pathogen (Winter *et al.*, 2013).

Table 1.1 *Salmonella* pathogenicity islands 1 through 5^a

Pathogenicity Island	Size (kb)	Secretion System	Description
SPI-1	40	T3SS	T3SS-dependent invasion of intestinal epithelium Encodes effector proteins important for actin cytoskeleton rearrangements & membrane ruffling
SPI-2	40	T3SS	Encodes tetrathionate metabolism proteins T3SS-dependent survival within SCVs of epithelial cells and macrophages Inhibits fusions between lysosomes and SCVs Encodes effector & chaperone proteins
SPI-3	17	–	Intramacrophage survival and persistence Oral colonization of mice and chicks Trans-acting sRNA post-transcriptional repression of FliB flagellin in macrophages
SPI-4	24	T1SS	<i>Salmonella</i> intestinal infection genes mediate adhesion to epithelial cells <i>siCDF</i> encode components of a T1SS SiiE, 595 kDa non-fimbrial adhesion protein involved in oral virulence
SPI-5	6.6	–	SPI-1 T3SS effector SopB and its chaperone PipC SPI-2 T3SS effectors PipA and PipB; PipD

^aTable adapted/updated from Hurley *et al.*, 2014; Wisner *et al.*, 2012.

Figure 1.3 Regulation at *Salmonella* pathogenicity island 2 involves many transcription factors.

There are many proteins that influence expression of SPI-2 genes. Sensory kinases respond to environmental factors and in turn activate their response regulators. PhoQ-PhoP, EnvZ-OmpR, FIS, HU, IHF, SlyA and HilD cause activation and H-NS, Hha, YdgT, Lrp, HilA and Fur cause repression. The phosphorelay system RcsCDB represses SPI-2 genes when highly induced, but low induction causes activation. SsrA and SsrB the master regulators of SPI-2 are encoded upstream of the SPI-2 T3SS, effector and chaperone genes. SsrA is a sensory kinase and SsrB is a response regulator. SsrB autoregulates at its own promoter and activates the T3SS, chaperones and effector proteins on SPI-2 by relieving repression by H-NS and direct activation. HilD and SlyA also activate SPI-2 by relieving repression of H-NS.

1.2 Metabolism in the gut

1.2.1 Oxygen in the gut

When the concentration of oxygen is lower than the atmospheric concentration (~21%), the environment is referred to microaerobic or hypoxic. In bacteria, aerobic respiration occurs at oxygen concentrations above 0.5%, while anaerobic respiration occurs between 0.1 - 0.5%, and fermentation is initiated at concentrations lower than 0.1% (Unden & Bongaerts, 1997). The lumen of the ileum is a fairly anaerobic environment, and any trace amount of oxygen is readily consumed by facultative anaerobic bacteria, such as members of the *Enterobacteriaceae* family, that constitute approximately 0.1% of the microbiota (Eckburg *et al.*, 2005). The limited availability of oxygen in the lumen limits growth of *Enterobacteriaceae* populations as increasing the level of oxygen increases their relative abundance (Rigottier-Gois, 2013; Winter *et al.*, 2013). For example, under inflammatory conditions, gut luminal oxygen levels rise partly due to elevated blood flow and hemoglobin and the increase of oxygen causes a disruption in anaerobiosis which confers a selective advantage to facultative anaerobes, allowing them to out-compete anaerobes and overgrow (Rigottier-Gois, 2013; Zeng *et al.*, 2016). The ability to proliferate in the lumen is an important part of transmission in *Salmonella* infection (Santos *et al.*, 2009). *Salmonella* can survive in anaerobic environments as well by way of anaerobic respiration but will preferentially choose an aerobic environment when given the choice. Conveniently, within

the GI tract in close proximity to the mucosal surface, there is a 70 mm zone of increased oxygen concentration (Marteyn *et al.*, 2010). This creates a steep oxygen gradient from the lumen to the intestinal epithelium that is reliant on blood flow and is caused by diffusion of oxygen from the capillary network at the villi (**Figure 1.4**) (Marteyn *et al.*, 2010). Oxygen concentration also increases substantially from the tips of the villi to the crypts (Zheng *et al.*, 2015). Oxygen concentrations inside of host tissues also vary dependent on the state of infection, for example in the murine gut oxygen concentrations decreased from ~11% to 2% after *Salmonella* infection (Jennewein *et al.*, 2015). The anti-*Salmonella* activity of macrophages is also dependent on available oxygen as antimicrobial molecules such as phagocyte oxidase and nitric oxide synthase require oxygen molecules, however this leaves little free dioxygen inside of cells (Vazquez-Torres & Fang, 2001). Furthermore, low oxygen concentrations found in *Salmonella*-infected gut tissue boost *Salmonella* replication in macrophages by impairing antimicrobial activity and augmenting *Salmonella* virulence (Jennewein *et al.*, 2015). In general the tissues of the gut including intestinal epithelial cells have a lower oxygen concentration than atmospheric oxygen and are described as microaerobic or hypoxic (Zheng *et al.*, 2015; Zeitouni *et al.*, 2016). The flagella of *Salmonella* play a role in movement from the hypoxic lumen to the intestinal epithelium through the mucus layer. Chemotaxis towards host derived electron acceptors is described however, aerotaxis towards the oxygen gradient could also be involved (Marteyn *et al.*, 2010; 2011; Rivera-Chávez *et al.*, 2013; Stecher *et al.*, 2008). The anaerobic state of the lumen is due to the high rates of respiration by host and commensal cells. Therefore, pathogens like *Salmonella* must employ an alternative metabolism to survive the hypoxic environment (Cook *et al.*, 2014).

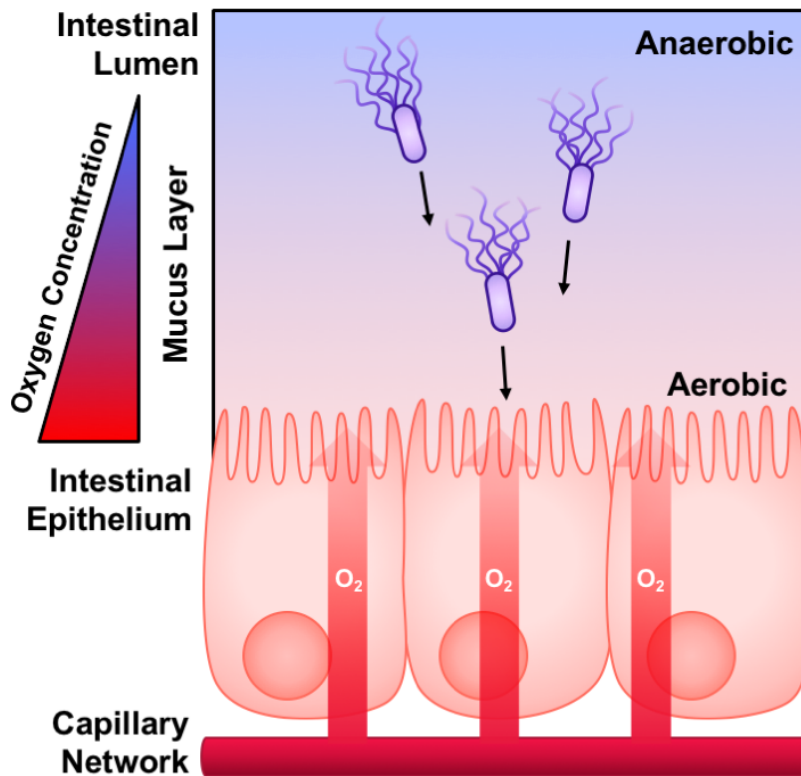


Figure 1.4 The oxygen gradient in the gut.

The intestinal lumen is an anaerobic environment (blue) however, there is a zone of relative oxygenation adjacent to the gastrointestinal tract mucosa (red), caused by diffusion of O₂ (arrows) from the capillary network at the tips of villi. Aerotaxis may occur at this site. Figure adapted from Marteyn *et al.*, 2010.

1.2.2 Anaerobic respiration in the gut

To survive in the lumen, facultative anaerobes such as *Salmonella* may employ anaerobic respiration (Rivera-Chávez & Bäumlér, 2015). Cellular respiration utilizes highly reduced electron donors such as NADH to establish an electrochemical gradient across a membrane. In aerobic respiration electrons are shuttled along the electron transport chain (ETC) from primary dehydrogenases to the terminal respiratory oxidase and the final electron acceptor oxygen and simultaneously creating a proton gradient across the cytoplasmic membrane (Ingledeew & Poole, 1984). The proton motive force drives protons down the gradient through the proton channel of ATP synthase, driving ATP synthesis from ADP and inorganic phosphate (Berg *et al.*, 2002). Simply, anaerobic respiration is respiration using terminal respiratory reductases and electron acceptors other than oxygen as the final electron acceptor

in the ETC. In organisms undergoing anaerobic respiration, oxygen is unavailable, therefore less-oxidizing substances are used as terminal electron acceptors (Neidhart, 1996). These alternative electron acceptors have smaller redox potentials than O_2 , meaning that less energy is released per oxidized molecule. Thus, anaerobic respiration is less efficient than aerobic respiration (Ingledeew & Poole, 1984; Neidhart, 1996). *S. Typhimurium* have evolved the capability to use a range of alternative electron acceptors and the expression of the terminal reductases is regulated by availability of electron acceptors (Bumann, 2009). As oxygen is the preferred electron acceptor, the presence of O_2 represses expression of the terminal reductases of anaerobic respiration. In the absence of oxygen, nitrate (NO_3^-) or nitrite (NO_2^-) are the preferred terminal electron acceptors (Richardson *et al.*, 2001). The presence of NO_3^-/NO_2^- therefore results in repression of other alternative terminal reductases, followed by the terminal electron acceptors, in order of oxidation/reduction (redox) potential: dimethyl sulfoxide (DMSO), trimethylamine N-oxide (TMAO), fumarate, and tetrathionate (**Table 1.2**). This regulatory pathway favours high ATP yields, resulting in the most efficient production of energy possible in the given environment (Cook *et al.*, 2014).

Table 1.2 Electron acceptors used by *Salmonella* during anaerobic respiration

Electron acceptor^a	Redox Couple	Redox Potential^d	Terminal respiratory enzyme	Operon^e
Nitrate	NO ₃ ⁻ /NO ₂ ⁻	+430 mV	Nitrate reductase	<i>narGHJI</i>
			Nitrate reductase	<i>narZYWV</i>
			Nitrate reductase	<i>napFDAGHBC</i>
Nitrite	NO ₂ ⁻ /NH ₄ ⁺	+350 mV	Nitrite reductase	<i>nfrABCDEFG</i>
			Nitrite reductase	<i>nirBDC</i>
DMSO	DMSO/DMS ^b	+160 mV	DMSO/TMAO reductase	<i>dmsABC</i>
TMAO	TMAO/TMA ^c	+130 mV	TMAO reductase	<i>torCAD</i>
Fumarate	fumarate/succinate	+33 mV	Fumarate reductase	<i>frdABCD</i>
Tetrathionate	S ₄ O ₆ ²⁻ / S ₂ O ₃ ²⁻	+24 mV	Tetrathionate reductase	<i>ttrBCA</i>

^aElectron acceptors are listed in descending order of their redox potential.

^bDimethyl sulfoxide/Dimethyl sulfide

^cTrimethylamine N-oxide/Trimethylamine

^dData from Thauer *et al.*, 1977

^eData from Cook *et al.*, 2014; Hensel *et al.*, 1999; Unden & Bongaerts, 1997

Terminal reductases are repressed by multiple TFs that regulate according to availability of terminal electron acceptors with the highest redox potential. Nitrate regulation is controlled by the TCSs NarXL and NarQP while oxygen regulates by the TCS ArcAB and FNR (Gilberthorpe & Poole, 2008; Stewart *et al.*, 2003).

ArcAB is the regulator of aerobic metabolism and represses the genes of aerobic metabolism under anaerobiosis (Unden & Bongaerts, 1997). FNR is the regulator of genes required for anaerobic metabolism, and it is discussed in detail in Section 1.3. Most of the genes involved in aerobic and anaerobic metabolism are regulated by more than one of the regulatory proteins, which act in many different combinations and activate or repress as necessary (Constantinidou *et al.*, 2006; Myers *et al.*, 2013). FNR and ArcA regulatory proteins play different roles under microaerobic conditions; FNR functions as an aerobic/anaerobic switch in the range of 0 to 10% air saturation, while ArcA exerts control in the 10 to 20% oxygen range. These two transcriptional regulators coordinate the hierarchical control of respiratory pathway gene expression to ensure the optimal use of oxygen in the cell environment (Tseng *et al.*, 1996) and in response to the availability of electron acceptors (Unden & Bongaerts, 1997). ArcA serves as a transcriptional regulator coordinating aerobic cellular metabolism, flagella biosynthesis, and motility in *S. Typhimurium*. Moreover, ArcA and FNR share regulation of at least 120 genes (Evans *et al.*, 2011). Recently the ArcA response regulator was found to promote intracellular survival in macrophages and neutrophils by promoting resistance to ROS, enabling *S. Typhimurium* to successfully establish a systemic infection (Pardo-Esté *et al.*, 2018).

To outgrow the resident microbiota of the gut, *Salmonella* must defend against host defenses and find nutrients. *S. Typhimurium* use virulence factors to induce intestinal inflammation (Section 1.1.2), which releases specific nutrients not usable by the microbiota (Thiennimitr *et al.*, 2012). One way in which *S. Typhimurium* can take advantage of host defenses by converting nitric oxide (NO) to NO_3^- inside macrophages. This results in a two-pronged advantage to the pathogen, as it eliminates toxic NO and provides *S. Typhimurium* with a favourable terminal electron acceptor for anaerobic respiration (Mills *et al.*, 2008). Host production of ROS and RNS creates a hostile environment in close proximity to the mucosal surface, but as these molecules diffuse towards the gut lumen they contact and oxidize organic sulfides, such as methionine, or tertiary amines, such as trimethylamine, to form S-oxides (DMSO) and N-oxides (TMAO), respectively. DMSO and TMAO can then be used by *S. Typhimurium* as terminal electron acceptors which are reduced by terminal reductases

encoded by *dmsABC* and *torCAD* (Winter *et al.*, 2010; Winter *et al.*, 2013). Additionally, when *Salmonella*-induced enteritis causes diarrhea to flush the intestines, epithelial cells shed into the lumen and become a source of membrane lipids. These lipids include phosphatidylcholine and sphingomyelin from which choline can be derived. Degradation of choline to TMA plus oxidation by ROS leads to further availability of TMAO (Winter *et al.*, 2013). Similar to the genes encoding specific virulence factors, horizontal acquisition of genes encoding metabolic functions are advantageous for surviving in the host. The genes encoding tetrathionate reductase, *ttrCBA* and their regulating TCS TtrSR, are found on SPI-2. Tetrathionate is generated when inflammation derived ROS react with endogenous thiosulphate. In contrast to the gut microbiota, *Salmonella* can use tetrathionate as a respiratory electron acceptor providing a unique advantage to the pathogen allowing for anaerobic respiration. As anaerobic respiration is more energy efficient than fermentation, *Salmonella* outcompetes strains of the microbiota in the inflamed gut (Winter *et al.*, 2010).

1.3 Regulation of the aerobic to anaerobic switch

1.3.1 FNR

Facultative anaerobic bacteria prefer an oxygenated environment however, when oxygen concentrations decrease they can reprogram their gene expression to facilitate anaerobic metabolism. That switch is regulated by an oxygen-sensing transcription factor called FNR, named for a mutant defective in "fumarate and nitrate reduction" (Lambden & Guest, 1976). FNR operates the master switch between aerobic and anaerobic metabolism by ensuring that oxygen is used in preference to alternative electron acceptors (Guest *et al.*, 1996). When *E. coli* moves from an aerobic to anaerobic environment, a third of its genes undergo transcriptional change. FNR is responsible for the regulation of half of those either directly or indirectly (Salmon *et al.*, 2003). FNR facilitates adaptation to anoxia by providing alternative pathways for energy generation and is a well-studied global transcriptional regulator in enteric bacteria (Constantinidou *et al.*, 2006; Fink *et al.*, 2007; Myers *et al.*, 2013; Wang *et al.*, 2019). FNR is a homologous protein to the cAMP receptor protein (CRP) (Shaw *et al.*, 1983), and belongs to the CRP-FNR superfamily of transcriptional regulators (Körner *et al.*, 2003). These proteins have an N-terminal sensory domain, a dimerization motif, and a C-terminal helix-turn-helix DNA-binding domain (Körner *et al.*, 2003). FNR primarily works as an activator of anaerobic metabolism genes during oxygen deprivation, however it is known to repress at a limited number of promoters (Green & Marshall, 1999).

1.3.2 Regulation of FNR

Expression of the *fnr* gene occurs under both aerobic and anaerobic conditions, and negative autoregulation and repression by glucose occurs during anaerobiosis (Mettert & Kiley, 2007a; Spiro & Guest, 1987). The concentration of FNR protein stays relatively constant regardless of the presence or absence of oxygen (Sutton *et al.*, 2004). When oxygen concentrations are as low as 0 to 5 mbar (0-0.5%) the FNR protein is active, with DNA binding capabilities (Jervis *et al.*, 2009; Sawers, 1999) (**Figure 1.5A**). Under oxygen limiting conditions, FNR binds an [4Fe-4S] cluster to four cysteine residues in the sensory domain (Green & Guest, 1993). FNR bound by [4Fe-4S] undergoes a conformational change allowing dimerization. In the presence of adequate oxygen concentrations, the [4Fe-4S] cluster is oxidized, and FNR becomes an inactive monomer (Beinert & Kiley, 1999; Green *et al.*, 2014) (**Figure 1.5B**). Importantly, FNR is highly functional over a small range of oxygen concentrations with approximately 95% activity at 0.3 μM O_2 and 50% activity at 6 μM O_2 . Surprisingly, an FNR-dependent reporter gene suggests that a chromosomally encoded FNR is 2.5% active under fully aerobic conditions (Jervis *et al.*, 2009). The functional state of FNR during the switch from aerobic to anaerobic environments is not regulated by iron content as only severely Fe^{2+} limiting conditions has any effect on FNR dependent gene expression (Niehaus *et al.*, 1991).

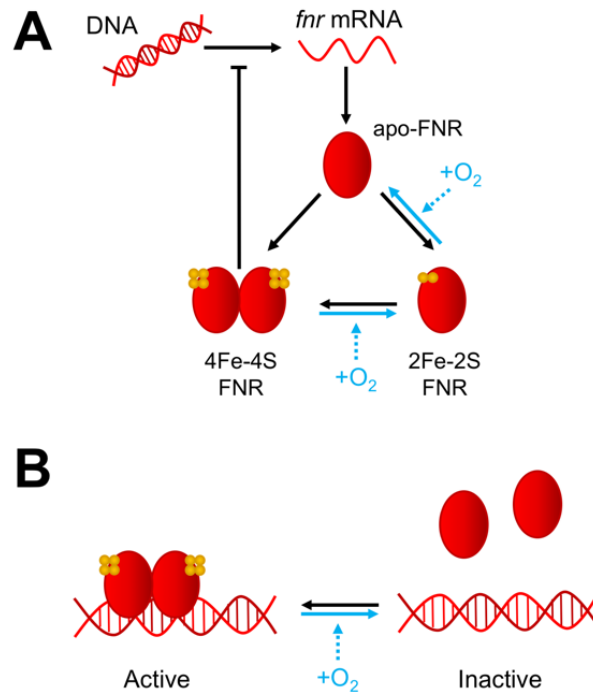


Figure 1.5 FNR activity is directly regulated by oxygen.

A. The *fnr* gene is transcribed, then translated. Cellular concentration of FNR is similar under both anaerobic and aerobic growth, but its activity is regulated directly by oxygen. Under anaerobiosis, the FNR monomer (red oval) acquires a [4Fe-4S] cluster (yellow circles) that causes a conformational change and dimerization of the protein, and it autoregulates at its own promoter. B. Under anaerobic conditions the active FNR dimer can bind to DNA causing activation and repression of many genes, however when oxygen is introduced the dimer dissociates and is no longer able to bind DNA.

1.3.3 Mechanisms of transcriptional regulation by FNR

During anaerobiosis the active FNR homodimer can bind to DNA to regulate transcription either by activation or repression. The active FNR homodimer preferably binds a specific 14 bp palindromic sequence of DNA with the consensus sequence **TTGATN₁N₂N₃N₄ATCAA** (Eiglmeier *et al.*, 1989; Gerasimova *et al.*, 2001). Interestingly, it has been shown experimentally that FNR can recognize a consensus CRP-binding site *in vivo* (Sawers *et al.*, 1997).

1.3.3.1 FNR-dependent activation

For activation to occur, FNR interacts directly with RNA polymerase (RNAP) in two ways depending on the architecture of the promoter (Blake *et al.*, 2002). FNR activates the transcription from class I and class II promoters. In class I promoters N₂ and in class II promoters N₃ of the consensus FNR site tend to be an A or T (Scott *et al.*, 2003). At class I promoters, FNR binds to a site centered at -61.5 or further upstream (-71, -82, or -92), then the activating region 1 (AR1) of the downstream subunit of the FNR homodimer directly contacts C-terminal domain of the alpha subunit (α CTD) of RNAP (**Figure 1.6A**) (Blake *et al.*, 2002; Wing *et al.*, 1995). At class II promoters, multiple interactions with RNAP are possible as FNR binds to a site centered at or near -41.5, causing the homodimer to be embedded in the polymerase. Here the α CTD makes contact with the AR1 surface of the upstream subunit of the FNR. The AR3 surface of the downstream subunit of FNR contacts σ 70 and AR2 makes contact to the N-terminal domain of the alpha subunit (α NTD), the same interaction that CRP uses with RNAP (**Figure 1.6B**) (Blake *et al.*, 2002). These direct interactions allow proper positioning of the RNAP for transcription initiation.

It has also been suggested that at some promoters FNR acts as a co-activator with other transcription factors such as CRP, NarP and NarL. A number of promoters have distinct FNR and CRP binding sites and are only activated when the conditions of both TFs are met, i.e. under anaerobiosis without glucose (Myers *et al.*, 2013). NarP and NarL are response regulators that respond to the presence of NO₃⁻ and/or NO₂⁻. The operon encoding periplasmic nitrate reductase, *napFDAGHBC*, is maximally expressed only in response to anaerobiosis and nitrate or nitrite and thus, co-activated by FNR and NarP and/or NarL (Myers *et al.*, 2013; Stewart *et al.*, 2009). Co-activation by two TFs is important for precise control of genes under specific conditions.

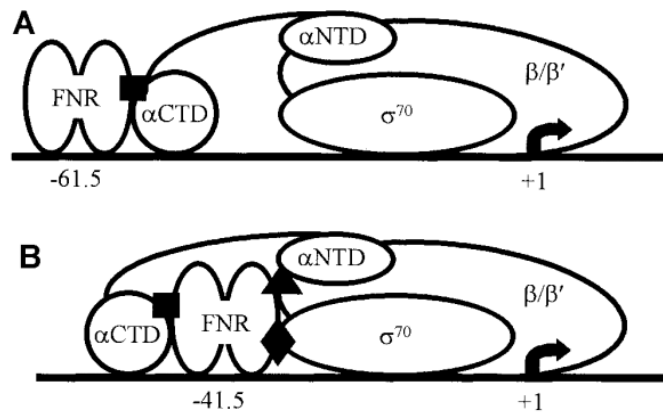


Figure 1.6 Activation of simple class I and class II FNR-dependent promoters. A. At class I promoters, FNR binds to a site centered at -61.5 or further upstream. AR1 of the downstream subunit of the FNR dimer contacts α CTD of RNAP (■). B. At class II promoters, FNR binds to a site centered at or near -41.5 and is thus embedded within RNAP. The AR1 surface of the upstream subunit of the FNR dimer contacts α CTD (■), the AR3 surface of the downstream subunit of FNR contacts σ^{70} (▲), and the AR2 surface makes contact with α NTD (◆). Figure taken from Blake *et al.*, 2002.

1.3.3.2 FNR-dependent repression

FNR-dependent repression can be complex and is not fully understood. Because FNR autoregulates at the *fnr* gene, and has 2 FNR binding sites, one centered on the *fnr* TSS ($+1.5$) and one centered farther upstream centered at -103.5 , it is an ideal candidate to examine for a repressive mechanism. Early experiments suggested both FNR binding sites needed to be present for repression of *fnr* under anaerobic conditions (Spiro & Guest, 1987) however, later *in vitro* experiments suggest the downstream binding site alone is sufficient for repression (Mettert & Kiley, 2007b). This suggests that promoter occlusion may be one way in which FNR can cause repression. However, repression by FNR at the *cydAB* (Cytochrome d terminal oxidase) promoter requires binding at both FNR binding sites, one site at the TSS and a second at -53.5 (Cotter *et al.*, 1997). Bernard *et al.* investigated repression by FNR by adding FNR consensus sites to several regions upstream of a semi-synthetic class II promoter based on that of *melR*. Binding of FNR at the -41.5 site activates expression of the promoter, however when an additional consensus site was added -85 and

-95 bp upstream, a sharp repression was observed. Similarly, a class I promoter with a binding site at -61.5 showed strong repression by FNR when a consensus site was placed at -100.5, indicating that upstream binding sites play an important role in FNR repression at some sites and that FNR can cause repression when bound in tandem spaced 44 or 53 bp apart (Barnard *et al.*, 2004). Indeed, repression of the gene encoding respiratory NADH dehydrogenase, *ndh* requires two FNR binding sites, found centered at -50.5 and -94.5 but not at the TSS. Both of binding sites appear to be required for full repression, and in a DNase footprinting assay both FNR and RNAP were able to bind simultaneously, suggesting promoter occlusion is not the mechanism for repression. Instead, FNR may jam the progression of RNAP by forming a complex and may disrupt productive RNAP interactions with other regulators (Meng *et al.*, 1997). Importantly, Williams *et al.* have shown that introducing a semi-synthetic FNR binding site to the -35 region of a promoter can simply block progress of RNAP, suggesting that a single FNR binding site is capable of causing efficient repression (Williams *et al.*, 1998). Finally, it seems that the full 14 bp palindromic binding does not need to be present for FNR binding; Several promoters only have half of the palindromic sequence at their promoters. For example, the glutamyl-tRNA reductase gene *hemA* is modestly repressed by FNR and has only a TTGAT site around -30. This half-site was protected by FNR in a DNase footprinting assay, thus suggesting that FNR can repress when only a half-site is present (Melville & Gunsalus, 1996). Additional transcriptional repression by FNR with only a half-site includes the promoters of *moeAB*, *nrdAB* and *sodA* (Constantinidou *et al.*, 2006). In summary, it appears FNR can cause repression in a multitude of ways including promoter occlusion by binding at the TSS, by blocking RNAP access by binding near the RBS, with interactions between tandem-bound FNR molecules, by jamming RNAP by forming inactive complexes and by disrupting productive RNAP interactions with other regulators.

1.3.4 The FNR regulon

The FNR regulon has previously been examined by microarray analysis in non-pathogenic *E. coli* (Constantinidou *et al.*, 2006; Grainger *et al.*, 2007; Kang *et al.*, 2005; Salmon *et al.*, 2003) and *S. Typhimurium* (Fink *et al.*, 2007) and more recently by RNA-seq in *Shigella flexneri* and Enterotoxigenic *E. coli* (ETEC) (Crofts *et al.*, 2018; Vergara-Irigaray *et al.*, 2014), and proteomic analysis in *S. Typhimurium* (Wang *et al.*, 2019). These studies find that FNR is a regulator either directly or indirectly of approximately 50% of genes that undergo transcriptional change during the switch between aerobic and anaerobic

metabolism. FNR directly regulates a subset of genes while others are affected through FNR regulation of TFs (Myers *et al.*, 2013). Also, many genes originally thought to be directly regulated by FNR but lacked FNR binding have been found to be regulated post-transcriptionally through the FNR-dependent sRNA FnrS (Durand & Storz, 2010).

Regulation of *Salmonella* gene expression is often similar to *E. coli*, and findings from a study of the *S. Typhimurium* FNR regulon were consistent with findings from *E. coli*. FNR regulates genes involved in aerobic metabolism, NO• detoxification, flagellar biosynthesis, motility, chemotaxis, and anaerobic carbon utilization under anaerobic growth found in both species. However, some genes and operons found in both species were found only to be regulated by FNR in *S. Typhimurium* include those coding for ethanolamine utilization, a universal stress protein, a ferritin-like protein, and a phosphotransacetylase. *Salmonella*-specific genes and operons regulated by FNR were all found to be activated by FNR and were of virulence and motility genes not found in *E. coli* including numerous SPI-1 encoded genes, flagellar genes *mcpAC*, *cheV*, and the virulence/motility operon *srfABC* (Fink *et al.*, 2007). Stecher *et al.* described the role of the *Salmonella* flagella in moving towards the intestinal epithelium through the mucus layer in response to readily available metabolites (Stecher *et al.*, 2008). However, Marteyn *et al.* suggest aerotaxis towards the oxygen gradient of the gut epithelium may also occur, and upregulation of motility and chemotaxis genes under anaerobic conditions fits with this model (Fink *et al.*, 2007; Marteyn *et al.*, 2011). Furthermore, the role of FNR as a positive regulator of motility and flagellar biosynthesis was confirmed by showing that Δ *fnr* is nonmotile and lacks flagella (Fink *et al.*, 2007).

FNR is essential to the enteritis model of infection, plays a weak role in typhoid fever and *fnr* mutants are attenuated in calf and chicken infections (Chaudhuri *et al.*, 2013; Rollenhagen & Bumann, 2006). The anaerobic regulator has been identified as an important regulator of virulence of other pathogens such as *Neisseria meningitides* (Bartolini *et al.*, 2006), ETEC (Crofts *et al.*, 2018), *Shigella flexneri* (Marteyn *et al.*, 2010), and in *Pseudomonas aeruginosa* by an FNR orthologue (Filiatrault *et al.*, 2006). Deletion of *fnr* in ETEC caused a significant increase in expression of all classical virulence factors, including an adhesin operon and enterotoxins, indicating FNR represses these genes under anaerobic conditions (Crofts *et al.*, 2018). Similarly, *Shigella flexneri* undergoes FNR-mediated priming for invasion by expressing extended T3SS needles while reducing effector secretion anaerobically through FNR repression of virulence gene regulators (Marteyn *et al.*, 2010).

Both groups describe a model where virulence gene expression is coordinated with pathogen proximity to the epithelium. In *Salmonella*, FNR has been shown to be positive regulator of pathogenesis. An Δfnr mutant showed a decrease in expression of invasion genes, indicating that FNR can activate the SPI-1 genes *prgKJIH*, *iagB*, *sicA*, *spaPO*, and *invJICBAEGF* and the *srfABC* virulence genes under anaerobiosis. Interestingly, the Δfnr mutant was attenuated in mice and could not survive in macrophages, although no differentially regulated SPI-2 genes were identified (Fink *et al.*, 2007).

1.4 Aims of the Study

The aim of this study is to determine the regulatory role of FNR in the expression *Salmonella* Pathogenicity Island 2 in *S. Typhimurium*.

There is increasing evidence that changes in environmental oxygen play a critical role in the timing and deployment of bacterial virulence factors, and that regulators of metabolism control the expression of genes imperative for causing infection and disease. Oxygen levels have already been shown to be important for interactions between *Salmonella* and host cells. *S. Typhimurium* grown in microaerobic environments have increased adhesive and invasive capacity compared to their aerobically grown counterparts (Lee & Falkow, 1990). Additionally, anaerobically grown *S. Typhimurium* had increased binding to murine enterocytes and intestinal mucus, and increased survival in macrophages (Singh *et al.*, 2000). FNR, the regulator of anaerobic metabolism that responds directly to oxygen concentration, has been established as an activator of genes involved in host-cell invasion such as components of the T3SS and chaperones encoded on SPI-1 (Fink *et al.*, 2007). Furthermore, FNR is required for full virulence in the murine model, and a mutant lacking this transcription factor is rapidly killed by macrophages (Fink *et al.*, 2007). The SPI-2 T3SS and an intact SCV are required for evasion of ROS in macrophages (van der Heijden *et al.*, 2015), and FNR helps to promote resistance against oxidative stress although the mechanism has not been described. Importantly, low-level invasion-independent transcriptional activity of the SPI-2 T3SS in the lumen of the gut was observed in an oral mouse model (Osborne & Coombes, 2011). Thus, FNR regulation of SPI-2 is heavily implied. Moreover, the influence of an oxygen gradient at the point of *S. Typhimurium* infection has not been considered. The effect of oxygen on invasion in *S. Typhimurium* and therefore on regulation of SPI-1 has been investigated, however SPI-2 expression and oxygen have not been linked.

Activity of FNR as a transcriptional regulator directly corresponds to the absence of oxygen, and during infection *Salmonella* encounters a steep oxygen gradient from the anaerobic lumen to a zone of relative oxygenation at the epithelial border, therefore molecular oxygen can be considered a major signal for virulence factors. We propose that direct repression of SPI-2 by FNR occurs in anaerobic and microaerobic environments, and that upon detection of increased oxygen, like at the host epithelial border, repression is lifted. Expression of SPI-2 prior to epithelial invasion could prime cells for the challenges of the intracellular environment. FNR regulation of virulence factors, especially those found within the SPIs is important as it shows the capacity of regulators of metabolism located on the core genome to evolve to regulate horizontally acquired pathogenicity genes.

The major aim of this study is to determine the regulatory role of FNR in the expression SPI-2 in *S. Typhimurium*. More specifically, we aim to determine the mechanism of SPI-2 repression by FNR, and the input for the repression. Additionally, we intend to confirm that FNR, as a regulator of anaerobic metabolism, can control SPI-2 genes in response to oxygen and alternative electron acceptors.

Chapter 2

Material & Methods

2.1 Chemicals and Reagents

Unless otherwise stated, all chemicals and reagents were purchased from Acros Organics, Agilent, Ambion, Applied Biosystems, Bioline, Fisher Scientific, Illumina, Invitrogen, New England Biolabs, Promega, Roche, Sigma-Aldrich, and Thermo Scientific.

2.2 General Microbiological Techniques

2.2.1 Media

Media recipes are shown in **Table 2.1**. All media were made using analytical grade, deionised water (Analar, BDH). Media were sterilized by autoclaving or filtration using 0.2 μm polyethersulfone (PES) membrane filters (Fisher Scientific). To prepare agar plates, Lennox agar (LA) was melted at 95°C, then cooled to 50°C before addition of appropriate antibiotics prior to pouring. Agar plates were stored at 4°C prior to use.

2.2.2 Maintenance of Bacterial Stocks

All strains and plasmids used in this study are listed in **Tables 2.2** and **2.3** respectively. Bacterial strains were prepared for long term storage by combination of overnight cultures in Lennox broth (LB, **Table 2.1**) in 30% (v/v) sterile glycerol and frozen at -80°C. When required, strains were streaked for single colonies onto LA plates with the appropriate antibiotics and grown at 30°C or 37°C. Plates were stored at 4°C and kept for a maximum of 1 week.

2.2.3 Culture Conditions

2.2.3.1 Growth in Lennox Broth

Bacterial strains were routinely grown on LA plates and incubated at 37°C. Bacterial cultures were routinely grown from single colonies in 5 mL of LB in glass test tubes at 37°C in an Innova 40 air-incubator (New Brunswick Scientific) at 200 rpm for 16 h (overnight). For further growth in LB, bacterial cultures were sub-inoculated 1:1000 in 25 mL of LB in a 250 mL Erlenmeyer flask with appropriate antibiotics and grown without agitation or with

agitation at 200 rpm at 37°C in an Innova 3100 water-bath shaker (New Brunswick Scientific).

2.2.3.2 Growth in Minimal Media

For growth in minimal media (MMA or PCN, **Table 2.1**), overnight cultures were grown as previously described. One mL of culture was harvested by centrifugation at $6,500 \times g$, washed 3 times in minimal media by centrifugation at $6,500 \times g$, and sub-inoculated 1:500 in 25 mL of minimal media in a 250 mL Erlenmeyer flask with appropriate antibiotics, and grown without agitation or with agitation at 200 rpm (**Figure 2.1**) at 37°C in an Innova 3100 water-bath shaker (New Brunswick Scientific).

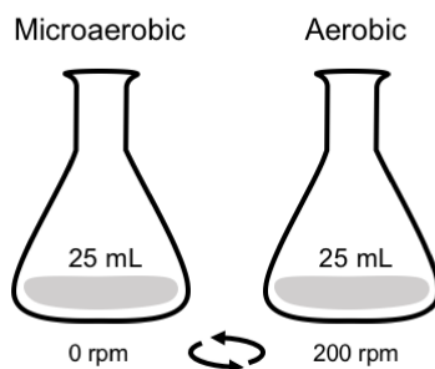


Figure 2.1 Experimental set-up for aerobic and microaerobic growth.

Cultures were grown in 25 mL of media in 250 mL and left static (0 rpm) for microaerobic growth and agitated at 200 rpm for aerobic growth. Under the “microaerobic” condition, bacteria in the initial inoculum quickly deplete the medium of oxygen below the surface, and further oxygen diffusion is limited as the flasks are not aerated.

2.2.4 Monitoring Bacterial Growth

Growth of bacterial cultures was monitored by measuring optical density at a wavelength of 600 nm (OD_{600}) with a Biomate 3S spectrophotometer (Thermo Scientific). Cultures with an OD_{600} of greater than approximately 0.5 were first diluted 10-fold in the appropriate medium before taking a measurement. To calculate viable cell counts, overnight cultures were serially diluted 10-fold in sterile PBS and plated on LA. Cell numbers were calculated as colony forming units per mL (CFU/mL).

2.2.5 Antibiotics

Antibiotic stocks were made at 1000 × concentration and stored in aliquots at -20°C. Stocks were made in dH₂O and filter sterilized with 0.2 μm PES membrane filters (Fisher Scientific), or in 70% ethanol. The following antibiotics were used in this study; Kanamycin (Kan, 50 μg/mL, dH₂O), ampicillin (Amp, 150 μg/mL, dH₂O), and chloramphenicol (Cm, 35 μg/mL, EtOH).

2.2.6 Motility Assays

Swimming motility assays were performed to measure the swimming capacity of bacterial strains under aerobic and anaerobic conditions. Swimming motility assays were performed by stab inoculation with 1 μL of 1 OD unit bacterial culture into swimming agar (**Table 2.1**) and incubated for 6 h at 37°C in an anaerobic jar with an Oxoid™ AnaeroGen™ 2.5 L Sachet (Thermo Scientific) to remove O₂ for anaerobic assays. Plates for anaerobic assays were left in anaerobic jars with an anaerobic gas sachet overnight prior to inoculation to remove any oxygen from the media. Diameter of swim colonies were measured with a ruler, and plates were photographed.

2.2.7 Growth curves and kinetic gene expression assay

2.2.7.1 Microaerobic and aerobic growth curves

Growth curves were used to measure growth rate of bacterial strains. Bacterial cultures for growth curves were inoculated as previously described (Section 2.2.3) in LB or minimal media as appropriate. Absorbance measurements (OD₆₀₀) were taken every 1 – 2 h depending on the growth rate of the culture with a Biomate 3S spectrophotometer (Thermo Scientific). Best-fit growth rate and lag time of each strain was determined using GrowthRates (Hall *et al.*, 2014).

2.2.7.2 Anaerobic growth curves

Anaerobic growth curves were performed by Daniel Ryan at The Helmholtz Institute for RNA-based Infection Research, Würzburg, Germany. Overnight cultures were grown as previously described (Section 2.2.3) and subcultured anaerobically with a 1:100 dilution into

LB media which had been kept in a Coy Anaerobic chamber with a gas mix containing 10% H₂, 5% CO₂ and 85% N₂ overnight. Bacterial cultures were grown and absorbance was measured every 20 min in a Synergy HT Microplate reader (Biotek) in the anaerobic chamber.

2.2.7.3 *Kinetic gene expression*

Gene expression was measured across growth or at OD₆₀₀ of 0.3 to determine expression of *ssaG*, *ssrA*, *ssrB*, *ssaB*, and *ydgT* at different growth phases in different media. Bacteria transformed with plasmids with transcriptional promoter fusions to *luxCDABE* (**Table 2.3**) were inoculated as previously described (Section 2.2.3) in LB or minimal media as appropriate. Absorbance measurements (OD₆₀₀) were taken every 1 – 2 h depending on the growth rate of the culture using a Biomate 3S spectrophotometer (Thermo Scientific). At the same time points, 200 µL of culture was used to measure luminescence in white-walled 96-well plates (Sarstedt) in a Synergy HT Microplate reader (Biotek). All luminescence values were normalized to the corresponding optical density (at 600 nm) of the culture.

2.2.8 *Oxygen gradient gene expression assay*

Oxygen gradient gene expression assays were used to assess the repression of SPI-2 by FNR at various oxygen concentrations. Oxygen gradient gene expression assays were carried out by mixing 2 mL liquid MMA soft agar (**Table 2.1**), cooled to 50°C, with 200 µL of overnight culture in small glass test tubes. The tubes were left to solidify at room temperature, and subsequently incubated at 37°C for 72 h. Within the test tube there is O₂ above the agar and at the surface, O₂ concentration decreases down through the agar. GFP expression was detected via a blue epi-illuminator (460 nm) using the ImageQuant LAS4000 (GE). Photos of the tubes were also taken in natural light to observe regions of turbidity indicating growth of each of the strains.

2.2.9 *Relative Fitness Assay*

Relative fitness assays were used to determine if bacterial strains with genotypic alterations such as deleted genes, would incur a fitness advantage or disadvantage in mixed populations. Strains used in these assays were used as their original versions or were transduced with the Δ SL1483::*cat* mutation as a selective marker. Strains were competed against themselves

with the selective marker to assess that there was no phenotypic disadvantage to addition of the marker. Cultures were prepared as previously described for sub-culture into minimal media, and flasks were inoculated with 10^7 cells of each strain. Inoculums were plated at 0 h and after 24 h of co-culture. CFU/mL of co-cultures was determined using the exclusion method. Briefly, co-cultures were diluted appropriately onto LA plates and LA plates containing Cm (25 $\mu\text{g/mL}$) to assess total number of colonies, and number of Cm resistant colonies. Subtraction of Cm resistant CFU from total CFU gives the number of Cm susceptible CFU. The relative fitness was determined by calculating the competitive index (C.I.) by the following formula:

$$C.I. = \frac{\ln\left(\frac{A_f}{A_i}\right)}{\ln\left(\frac{B_f}{B_i}\right)}$$

Where C.I. is competitive fitness, A and B are the population sizes of the two competitors in CFU/mL, and subscripts i and f indicate the initial and final time points in the assay, 0 h and 24 h respectively. The natural logarithm, \ln , reflects population growth (Wiser & Lenski, 2015). Relative fitness assays were performed by Stefani Kary and Naoise McGarry at Trinity College Dublin, Dublin, Ireland, and data analysis completed by Stefani Kary.

Table 2.1 Media recipes

<i>Medium</i>	<i>Reagent</i>	<i>Concentration</i>	<i>Reference</i>
Lennox Broth (LB)	Bacto-Tryptone	10 g/L	(Lennox, 1955)
	NaCl	5 g/L	
	Bacto-Yeast extract	5 g/L	
Lennox Agar (LA)	Lennox broth		(Lennox, 1955)
	Bacto-Agar	1.5% (w/v)	
Swimming Agar	Lennox broth		
	Bacto-Agar	0.3% (w/v)	
Minimal Medium A (MMA) ^{ab}	K ₂ HPO ₄	60 mM	(Constantinidou <i>et al.</i> , 2006)
	KH ₂ PO ₄	33 mM	
	(NH ₄) ₂ SO ₄	7 mM	
	Sodium citrate dihydrate	1.7 mM	
	MgSO ₄	1 mM	
	Glycerol	0.4% (v/v)	
	Fumarate	40 mM	
	TMAO	20 mM	
MMA Soft Agar	MMA		
	Bacto-Agar	1% (w/v)	
PCN (SPI-2-inducing, InSPI2)	MES (pH 5.8)	80 mM	(Löber <i>et al.</i> , 2006)
	Tricine	4 mM	
	FeCl ₃	100 µM	
	K ₂ SO ₄	376 µM	
	NaCl	50 mM	
	K ₂ HPO ₄ /KH ₂ PO ₄ (pH 5.8)	0.4 mM	
	Glucose	0.4 % (w/v)	
	NH ₄ Cl	15 mM	
	MgSO ₄	1 mM	
	CaCl ₂	0.01 mM	
	Na ₂ MoO ₄	10 nM	
	Na ₂ SeO ₃	10 nM	
	H ₃ BO ₃	4 nM	
	CoCl ₂	300 nM	
	CuSO ₄	100 nM	
MnCl ₂	800 nM		
ZnSO ₄	1 nM		

^avariations of this medium without fumarate and/or TMAO were used in some experiments, unless otherwise stated MMA refers to the medium containing both fumarate and TMAO.

^bvariations of this medium with different concentrations of K₂HPO₄ and KH₂PO₄ and pH were used for some experiments, unless otherwise stated MMA refers to the medium with the above recipe and pH of ~7.4.

Table 2.1 Media recipes (continued)

<i>Medium</i>	<i>Reagent</i>	<i>Concentration</i>	<i>Reference</i>
PCN (SPI-2-Non- inducing, NonSPI2)	PCN w/o MES & K ₂ HPO ₄ /KH ₂ PO ₄		(Löber <i>et al.</i> , 2006)
	MOPS (pH 7.4)	80 mM	
	K ₂ HPO ₄ /KH ₂ PO ₄ (pH 7.4)	25 mM	
Green Agar	Bacto-Tryptone	8 g/L	(Smith & Levine, 1967)
	NaCl	5 g/L	
	Bacto-Yeast extract	1 g/L	
	Alizarin yellow	0.625 g/L	
	Aniline blue	0.006% (w/v)	
	Glucose	0.8% (w/v)	
	Bacto-Agar	1.5% (w/v)	
Super Optimal Broth (SOB)	Bacto-Tryptone	20 g/L	(Hanahan, 1983)
	NaCl	5 g/L	
	Bacto-Yeast extract	5 g/L	
	KCl	2.5 mM	
	MgCl ₂	10 mM	
	MgSO ₄	10 mM	
SOB with Catabolite Repression (SOC)	SOB Glucose	20 mM	(Hanahan, 1983)

Table 2.2 Bacterial strains used in this study.

Strain Name	Relevant Genotype	Resistance	Original Source/Reference
<i>S. Typhimurium</i> 4/74	wild-type	St ^r ^R	Mark Stevens
	Δ <i>fnr</i> ::FRT		Jay Hinton, JH3307
	Δ <i>fnr</i> ::FRT attTn7:: <i>fnr</i> :: <i>kan</i>	Kan ^R	This Study
	Δ <i>ssrAB</i> ::FRT		Aoife Colgan
	Δ <i>fnr</i> ::FRT, Δ <i>ssrAB</i> ::FRT		OS: Aoife Colgan, <i>kan</i> removal: This Study
	Δ rpoE::cat	Cm ^R	Aoife Colgan
	Δ <i>hilA</i> ::FRT		OS: Jörg Vogal, JVS-1195, transduction, <i>kan</i> removal: This Study
	Δ <i>hilD</i> ::FRT		Aoife Colgan
	<i>hns</i> -1:: <i>kan</i>	Kan ^R	Jay Hinton, JH3863
	<i>fnr</i> -3×FLAG:: <i>kan</i>	Kan ^R	C. Kröger
	<i>steC</i> -3×FLAG:: <i>kan</i>	Kan ^R	OS: A. Westermann, transduction: This Study
	Δ <i>fnr</i> ::FRT <i>steC</i> -3×FLAG:: <i>kan</i>	Kan ^R	OS: A. Westermann, transduction: This Study
	Δ <i>ssrAB</i> ::FRT <i>steC</i> -3×FLAG:: <i>kan</i>	Kan ^R	OS: A. Westermann, transduction: This Study
	Δ <i>hilA</i> ::FRT <i>steC</i> -3×FLAG:: <i>kan</i>	Kan ^R	OS: A. Westermann, transduction: This Study
	Δ <i>hilD</i> ::FRT <i>steC</i> -3×FLAG:: <i>kan</i>	Kan ^R	OS: A. Westermann, transduction: This Study
	<i>sopE</i> -3×FLAG:: <i>kan</i>	Kan ^R	OS: A. Westermann, transduction: This Study
	Δ <i>fnr</i> ::FRT <i>sopE</i> -3×FLAG:: <i>kan</i>	Kan ^R	OS: A. Westermann, transduction: This Study
	Δ <i>ssrAB</i> ::FRT <i>sopE</i> -3×FLAG:: <i>kan</i>	Kan ^R	OS: A. Westermann, transduction: This Study
	Δ <i>hilA</i> ::FRT <i>sopE</i> -3×FLAG:: <i>kan</i>	Kan ^R	OS: A. Westermann, transduction: This Study
	Δ <i>hilD</i> ::FRT <i>sopE</i> -3×FLAG:: <i>kan</i>	Kan ^R	OS: A. Westermann, transduction: This Study
	<i>pipB2</i> -3×FLAG:: <i>kan</i>	Kan ^R	OS: O. Steele-Mortimer, transduction: This Study
	Δ <i>fnr</i> ::FRT <i>pipB2</i> -3×FLAG:: <i>kan</i>	Kan ^R	OS: O. Steele-Mortimer, transduction: This Study
	Δ <i>ssrAB</i> ::FRT <i>pipB2</i> -3×FLAG:: <i>kan</i>	Kan ^R	OS: O. Steele-Mortimer, transduction: This Study
	Δ <i>hilD</i> ::FRT <i>pipB2</i> -3×FLAG:: <i>kan</i>	Kan ^R	OS: O. Steele-Mortimer, transduction: This Study

Table 2.2 Bacterial strains used in this study (continued).

Strain Name	Relevant Genotype	Resistance	Original Source/Reference
S. Typhimurium 4/74	ASL1483::cat <i>Δfnr</i> ::FRT ASL1483::cat <i>ΔssrAB</i> ::FRT ASL1483::cat <i>Δfnr</i> ::FRT <i>ΔssrAB</i> ::FRT ASL1483::cat Φ(<i>ssaG</i> ' <i>gfp</i> ⁺)1, cat <i>Δfnr</i> ::kan Φ(<i>ssaG</i> ' <i>gfp</i> ⁺)1, cat <i>ΔssrAB</i> ::kan Φ(<i>ssaG</i> ' <i>gfp</i> ⁺)1, cat	Cm ^R Cm ^R Cm ^R Cm ^R Cm ^R Kan ^R , Cm ^R	C. Kröger OS: C. Kröger, transduction: This Study OS: C. Kröger, transduction: This Study OS: C. Kröger, transduction: This Study Jay Hinton, JH3009 OS: Jay Hinton, JH3009, C. Kröger OS: Jay Hinton, JH3009, C. Kröger
<i>E. coli</i> TOP10	F ⁻ <i>mcrA</i> Δ(<i>mrr</i> - <i>hsdRMS</i> - <i>mcrBC</i>) (φ80 <i>lacZ</i> Δ <i>M15</i> Δ <i>lacX74</i> <i>mupG</i> <i>recA1</i> <i>araD139</i> Δ(<i>ara</i> - <i>leu</i>)7697 <i>galE15</i> <i>galK16</i> <i>rpsL</i> (St ^R) <i>endA1</i> λ ⁻	St ^R	Invitrogen
<i>E. coli</i> DH5α	F ⁻ <i>endA1</i> <i>glnV44</i> <i>thi-1</i> <i>recA1</i> <i>relA1</i> <i>gyrA96</i> <i>deoR</i> <i>mupG</i> <i>purB20</i> φ80 <i>dlacZ</i> Δ <i>M15</i> Δ(<i>lacZYA</i> - <i>argF</i>) <i>UI169</i> , <i>hsdR17</i> (<i>trk</i> ⁻ <i>mK</i> ⁺), λ ⁻		Charles Dorman
<i>E. coli</i> DH5α <i>pir</i> ⁺	<i>endA1</i> <i>hsdR17</i> <i>glnV44</i> (=supE44) <i>thi-1</i> <i>recA1</i> <i>gyrA96</i> <i>relA1</i> φ80 <i>dlacZ</i> Δ(<i>lacZ</i>) <i>M15</i> Δ(<i>lacZYA</i> - <i>argF</i>) <i>UI169</i> <i>zdg-232</i> ::Tn10 <i>uidA</i> :: <i>pir</i> ⁺		Jörg Vogel
<i>E. coli</i> BL21(DE3) (PK22)	<i>fnuA2</i> [lon] <i>ompT</i> <i>gal</i> (λ <i>DE3</i>) [<i>dcn</i>] <i>ΔhsdS</i> λ <i>DE3</i> = λ <i>SBamHI</i> <i>ΔEcoRI</i> - <i>B</i> <i>int</i> ::(<i>lacI</i> :: <i>PlacUV5</i> ::T7 <i>gene1</i>) <i>i21</i> <i>Anin5</i> <i>ΔfnrΔcrp</i>		(Shan <i>et al.</i> , 2012b)

OS: Original Strain

Table 2.3 Plasmids used in this study.

Plasmid Name	Description	Resistance	Reference
pBR322	Low copy number cloning vector	Tet ^R , Amp ^R	(Bolivar <i>et al.</i> , 1977)
p <i>fnr</i>	<i>fnr</i> with 215 bp upstream cloned in pBR322	Amp ^R	This Study
p <i>fnrDI54A</i>	Oxygen insensitive <i>fnr</i> (DI54A) with native promoter cloned in pBR322	Amp ^R	This Study
p(<i>fnrDI54A</i>) ₂	Oxygen insensitive <i>fnr</i> (DI54A) ₂ from <i>E. coli</i> with 6xHis-tag in pET28a	Kan ^R	(Shan <i>et al.</i> , 2012b)
pCP20	Plasmid with yeast Flp recombinase gene, FLP, and temperature sensitive replication	Cm ^R , Amp ^R	(Cherepanov & Wackernagel, 1995)
pDIGc	Constitutive expression of GFP in bacteria	Amp ^R	(Helaine <i>et al.</i> , 2010)
pDEW201	Moderate copy number with a promoterless <i>luxCDABE</i>	Amp ^R	(Van Dyk & Rosson, 1998)
pDEW201-P _{ssaG}	P _{ssaG} cloned into pDEW201	Amp ^R	This Study
pUC18R6K-miniTn7T-PacI	Delivery plasmid for chromosomal integration at <i>attTn7</i> downstream of <i>glmS</i>	Amp ^R	(Shivak <i>et al.</i> , 2016)
pHSG415- <i>tmsABCD</i>	Replication-proficient helper plasmid with temperature-sensitive origin	Amp ^R	(Shivak <i>et al.</i> , 2016)
pCS26-Kn ^R - <i>luxCDABE</i> -PacI	Low copy number modular cloning vector with a promoterless <i>luxCDABE</i>	Kan ^R	(Shivak <i>et al.</i> , 2016)
pCS26-Kn ^R -PacI	Low copy number modular cloning vector without reporter	Kan ^R	This Study
pCS26-Kn ^R - <i>fnr</i> -PacI	<i>fnr</i> and native promoter cloned into pCS26-Kn ^R -PacI	Kan ^R	This Study
pCS26-Kn ^R - <i>fnr</i> -pUC18R6K-miniTn7T	pCS26-Kn ^R - <i>fnr</i> -PacI cloned into pUC18R6K-miniTn7T-PacI	Kan ^R , Amp ^R	This Study
pCS26-Cm ^R - <i>luxCDABE</i> -PacI	Low copy number modular cloning vector with a promoterless <i>luxCDABE</i>	Cm ^R	(Shivak <i>et al.</i> , 2016)

Table 2.3 Plasmids used in this study (continued).

<i>Plasmid Name</i>	<i>Description</i>	<i>Resistance</i>	<i>Reference</i>
pCS26-Cm ^R - <i>luxCDABE</i> -Pacl-P _{SSV41°}	P _{SSV41°} cloned into pCS26-Cm ^R - <i>luxCDABE</i> -Pacl	Cm ^R	This Study
pCS26-Cm ^R - <i>luxCDABE</i> -Pacl-P _{SSV4}	P _{SSV4} cloned into pCS26-Cm ^R - <i>luxCDABE</i> -Pacl	Cm ^R	This Study
pCS26-Cm ^R - <i>luxCDABE</i> -Pacl-P _{SSVB}	P _{SSVB} cloned into pCS26-Cm ^R - <i>luxCDABE</i> -Pacl	Cm ^R	This Study
pCS26-Cm ^R - <i>luxCDABE</i> -Pacl-P _{SSVB}	P _{SSVB} cloned into pCS26-Cm ^R - <i>luxCDABE</i> -Pacl	Cm ^R	This Study
pCS26-Cm ^R - <i>luxCDABE</i> -Pacl- <i>dbpA</i>	<i>dbpA</i> cloned into pCS26-Cm ^R - <i>luxCDABE</i> -Pacl	Cm ^R	This Study

2.3 General molecular techniques

2.3.1 Isolation of chromosomal *S. Typhimurium* 4/74 DNA for use in PCR

Overnight cultures were prepared as previously described (Section 2.2.3). 400 μ L of the culture was harvested by centrifugation at $8,000 \times g$ for 1 minute at room temperature. The cell pellet was resuspended in 200 μ L of sterile nuclease free H₂O and boiled at 100°C for 5 min, and subsequently vortexed for 30 s to ensure complete lysis. Cell debris was pelleted by centrifugation at $8,000 \times g$ for 5 min, and supernatants were added to 1 volume chloroform and vortexed for 30 s. Organic and aqueous phases of the solution were separated by centrifugation at $8,000 \times g$ for 10 min at 4°C. 75% of the aqueous layer was transferred to a new 1.5 mL tube to eliminate chloroform contamination. DNA contained in the aqueous phase was measured with the NanoDrop ND-1000 Spectrophotometer (Thermo Scientific) and the concentration was adjusted to 100 ng/mL.

2.3.2 Isolation of plasmid DNA

Plasmid DNA was extracted and purified using the GeneJet Plasmid Miniprep Kit (Thermo Scientific) according to the manufacturers' instructions except plasmids were eluted into dH₂O. For extremely low copy plasmids, such as pCS26 derivatives, up to 50 mL of culture was harvested and multiple minipreps were combined into 50 μ L of dH₂O.

2.3.3 Polymerase chain reaction (PCR)

PCR amplifications were carried out in a SimpliAmp Thermal Cycler (Applied Biosystems, Thermo Scientific). Routine PCR and colony screening were carried out using Taq polymerase (New England Biolabs) according to the manufacturers' specifications. Q5 polymerase (New England Biolabs) was used for applications requiring high fidelity amplification and RANGER Mix (Bioline) was used for products larger than 10 kbp according to the manufacturers' specifications. As a template for PCR, 100 ng chromosomal DNA, 1-10 ng of plasmid DNA, or single colony resuspended in 200 μ L of H₂O was used.

2.3.4 Agarose gel electrophoresis

Agarose gel electrophoresis was used for size separation of DNA and RNA molecules. DNA samples were mixed with DNA loading dye (40% (v/v) glycerol, 60 mM EDTA, 10 mM Tris-HCl pH 7.6, 0.25% (w/v) bromophenol blue pH 8.0, 0.25% (w/v) xylene cyanol FF, 0.25% (w/v) orange G) to a final concentration of 1 × DNA loading dye and routinely electrophoresed in a 1% to 2.5% (w/v) agarose gel in 1 × Tris Acetate Ethylenediaminetetraacetic acid (TAE) buffer at 90 V. RNA samples were mixed with RNA loading dye (0.025% (w/v) xylene cyanol FF, 0.025% (w/v) bromophenol blue, 18 mM EDTA pH 8.0, 0.025% (w/v) SDS, 95% (v/v) formamide) to a final concentration of 1 × RNA loading dye and heat denatured at 65°C for 5 min. RNA was routinely electrophoresed in a 2.5% (w/v) agarose gel in 1 × Tris Borate EDTA (TBE) buffer at 90 V. Gels were stained with SafeView Nucleic Acid Stain (NBS Biologicals) prior to visualization under ultra violet light in the ImageQuant™ LAS 4000 (GE Healthcare Life Sciences). The molecular size of electrophoresed DNA fragments was estimated by comparison with HyperLadder™ I (Bioline) or O'GeneRuler™ 1 kb DNA Ladder (Thermo Scientific).

2.3.5 Restriction digestion

All enzymes were purchased from Thermo Scientific (FastDigest enzymes), New England Biolabs, or Roche and used according to the manufacturers' specifications. Restriction digestions were carried out in a SimpliAmp Thermal Cycler (Applied Biosystems, Thermo Scientific) and digestion products were analyzed by agarose gel electrophoresis as previously described.

2.3.6 Purification of PCR products

If required for downstream applications, PCR products were purified to remove primers, enzymes, and other impurities using the Monarch® PCR & DNA Cleanup Kit (New England Biolabs) or the High Pure PCR Product Purification Kit (Roche) according to the manufacturers' specifications. In order to concentrate samples, multiple PCR reaction products were combined and spun through a single spin column.

2.3.7 Precipitation of DNA

In order to increase the concentration of low concentration DNA samples Pellet Paint® Co-Precipitant (Millipore) was used to facilitate alcohol precipitation of nucleic acids. 1 µL of Pellet Paint® and 1 volume of 3 M sodium acetate were added to the sample and mixed briefly. 2 volumes of ethanol were then added followed by briefly vortexing the sample, and a 2 min incubation at room temperature. Sample was centrifuged at 8,000 × g for 5 min and washed in 70% ethanol. DNA pellet was then resuspended in desired volume of H₂O.

2.3.8 Extraction of DNA from agarose gels

DNA digests or PCR products that required precise purification of a product of interest were electrophoresed as previously described. DNA fragments were visualized briefly under ultra violet light and the specific DNA band was excised with a scalpel. The excised DNA in agarose was weighed and dissolved in gel dissolving buffer at 55°C with occasional vortexing. Once dissolved, 3 M sodium acetate pH 5.2 was added to lower the pH of the sample to increase binding to the column membrane. Monarch® DNA Gel Extraction Kit or High Pure PCR Product Purification Kit (Roche) were used to spin column purify the DNA according to the manufactures' specifications.

2.4 Preparation and transformation of competent bacteria

2.4.1 Preparation of electro-competent S. Typhimurium and electroporation

Overnight cultures of *S. Typhimurium* were subcultured 1:100 in 50 mL LB with appropriate antibiotics and grown with agitation at 200 rpm at 30°C or 37°C to exponential phase (OD₆₀₀ 0.5). Cultures were then incubated on ice for 20 min. Cells were harvested by centrifugation at 2,880 × g at 4°C for 10 min and resuspended in 40 mL ice-cold sterile 10% (v/v) glycerol and incubated on ice for 20 min. The glycerol wash was repeated two additional times with resuspensions in 25 mL, then 10 mL of ice-cold 10% (v/v) glycerol. After a final centrifugation at 2,880 × g and 4°C, the pellet was resuspended in 300 µL of ice-cold 10% (v/v) glycerol. Cells were either stored at -80°C or immediately electroporated. 40 µL of electro-competent cells were added to 2 mm electroporation cuvettes with up to 5 µL of plasmid DNA and electroporated with the GenePulser Xcell electroporator (Biorad) at 2.5 kV, 200 Ω, 25 µF. 1 mL of SOC (**Table 2.1**) was added to cells, and the cells were recovered

at 37°C for 1 h or at 30°C for 2 h with agitation at 200 rpm. For small and high copy plasmids 150 µL of cells was plated on LA plates with appropriate antibiotics and incubated at 30°C or 37°C overnight. For large and low copy plasmids, cells were harvested by centrifugation at 6,500 × g and resuspended in 150 µL of SOC. The entire resuspension was plated on LA plates with appropriate antibiotics and incubated at 30°C or 37°C overnight.

2.4.2 Preparation and transformation of chemically competent *E. coli*

2.4.2.1 CaCl₂ chemically competent E. coli

Overnight cultures of *E. coli* were diluted 1:100 in 50 mL LB with appropriate antibiotics with agitation at 200 rpm to exponential phase (OD₆₀₀ 0.4 – 0.8). Cells were then incubated on ice for 20 min. Cells were harvested by centrifugation at 2,880 × g and 4°C and resuspended in 40 mL sterile ice-cold 100 mM CaCl₂ and incubated on ice for 20 min. Cells were harvested as before and resuspended in 10 mL sterile ice-cold 100 mM CaCl₂. Sterile glycerol was added to a final concentration of 10%, and cells were incubated on ice for an additional 20 min. Cells were either stored at -80°C in 300 µL aliquots or immediately transformed. CaCl₂ competent cells were used for the transformation of small plasmids.

2.4.2.2 PIPES chemically competent E. coli

Overnight cultures of *E. coli* were diluted 1:100 in 100 mL LB with appropriate antibiotics with agitation at 200 rpm to exponential phase (OD₆₀₀ 0.4 – 0.8). Cells were then incubated on ice for 20 min. Cells were harvested by centrifugation at 2,880 × g and 4°C and resuspended in 30 mL sterile ice-cold 100 mM MgCl₂ and incubated on ice for 20 min. Cells were harvested as before and resuspended in 30 mL sterile ice-cold PIPES buffer (60 mM CaCl₂, 10 mM PIPES pH 7.6, 15% (v/v) glycerol). Cells were harvested as before and resuspended in 5 mL PIPES buffer. Cells were either stored at -80°C in 300 µL aliquots or immediately transformed. PIPES competent cells were used for the transformation of large (>10 kb) plasmids.

2.4.2.3 Chemical transformation of E. coli

100 – 300 µL of chemically competent cells was mixed with up 20 µL of plasmid DNA or ligation mixture and incubated on ice for 20 min. The cells were then heat shocked in a 42°C

water-bath for 90 – 120 s, followed by a 2 min incubation on ice. 1 mL of SOC was added to each transformation, and cells were recovered at 37°C with agitation at 200 rpm for 1 h. Cells were harvested by centrifugation at $6,500 \times g$ and resuspended in 150 μL of SOC. The entire resuspension was plated on LA plates with appropriate antibiotics and incubated at 37°C overnight.

Table 2.4 Table of oligonucleotides

<i>Primer</i>	<i>Sequence (5' – 3')</i>	<i>Description</i>
FNR_com_F215	TTTAAAGCTTAAAGGCTATCTTTATTATG	To amplify <i>fnr</i> with 215 bp upstream, adds HindIII restriction site
FNR_com_R	TTTGTGACAGCTTTGTAACATAAAGAGTAACTC	To amplify <i>fnr</i> , adds SalI
D145A_FNR_F	*ATTAAAGGCGCTCAGGATATGA	To introduce D154A mutation to <i>fnr</i> on a plasmid
D145A_FNR_R	TTCACCGCTCATCAGACGCAT	To introduce D154A mutation to <i>fnr</i> on a plasmid
pBR_seq_4	TGCCACCTGACCCTCTAAG	Sequencing primer for pBR322
pDEW201_PssaG_F	CCGGAATTCTTACTCGCTTCGGTATGG	To amplify P _{ssaG} , adds EcoRI restriction site
pDEW201_PssaG_R	TTCCGGATCCCAATATCCCATTAATGCTTTTCC	To amplify P _{ssaG} , adds BamHI restriction site
luxC_R	CCAGTACTATCAGCGC	Verify insertion in pDEW201
qPCR_ssea_F	TCACCAAAATCCGGCTAAG	To amplify <i>ssea4</i> for qPCR
qPCR_ssea_R	GCAACGCCCTTGTGAAATAAG	To amplify <i>ssea4</i> for qPCR
qPCR_ssah_F	GCGTTAACCATAGCCTGATTTTC	To amplify <i>ssah</i> for qPCR
qPCR_ssah_R	CCAACAATAATGCCAGACATACC	To amplify <i>ssah</i> for qPCR
qPCR_fnr_F	ATTGGCAGCGGTCATCAT	To amplify <i>fnr</i> for qPCR
qPCR_fnr_R	TGACCGCAGGTTAGGCATTT	To amplify <i>fnr</i> for qPCR
hemX_RT_F	CGCCTGACGGTATGTTTCTT	To amplify <i>hemX</i> for qPCR, control
hemX_RT_R	CCCAACCAGGACGCTCTATTAC	To amplify <i>hemX</i> for qPCR, control
fnr_EMSA_F	AGGCTATCTTTTATTATG	To amplify P _{fnr} for EMSA
fnr_EMSA_R	CAAAAGCTGGCTGATACTGC	To amplify P _{fnr} for EMSA
FnrS_EMSA_F	ATAATAAGGTCAAAAGACAGGCTC	To amplify P _{FnrS} for EMSA
FnrS_EMSA_R	CAAAAAGCGCTTTTCAGACC	To amplify P _{FnrS} for EMSA
FnrS_EMSA_F	ATTAAATATAATGCCAACGGAG	To amplify P _{FnrS} for EMSA
YdgT_EMSA_F	TCCGTCAGAGAAGTAAGC	To amplify P _{YdgT} for EMSA
YdgT_EMSA_R	TATATAACCCAGTCGATGAC	To amplify P _{YdgT} for EMSA
SsrA_EMSA_F	ATTCACAATTACATTTTCAGC	To amplify P _{SsrA} for EMSA
SsrA_EMSA_R	CTGATTACTAAAGATGTTGCAG	To amplify P _{SsrA} for EMSA
SsrA2_EMSA_F	GGCTTTTACGGATGTGG	To amplify P _{SsrA} for EMSA
SsaB_EMSA_F		To amplify P _{SsaB} for EMSA

Table 2.4 Table of oligonucleotides (continued)

Primer	Sequence (5' – 3')	Description
ssaB_EMSA_R	AGAAATAGAAAAATGCTTCTGAG	To amplify P _{ssaB} for EMSA
ssrB_EMSA_F	CCGTTAATGATGATTCATGATCGTCT	To amplify P _{ssrB} for EMSA
ssrB_EMSA_R	AAATGCCGTATCGGCTGGA	To amplify P _{ssrB} for EMSA
dbpA_EMSA_F	CGATCATTTTAAATAGCCGTACC	To amplify <i>dbpA</i> for EMSA
dbpA_EMSA_R	CTCAAAGCTGAACTGGCTGAA	To amplify <i>dbpA</i> for EMSA
FnrS_P1	GCAGGTGAATGCAACGTCA	To amplify DNA template for FnrS riboprobe
FnrS_P2	GAATTAATACGACTCACTATAGCCGACTAATCTAAGTCGG	To amplify DNA template for FnrS riboprobe
5S_P1	GCGGCACTAGCGCGGTGGTC	To amplify DNA template for 5S riboprobe
5S_P2	GAATTAATACGACTCACTATAGCATGGGGAGACCCACACT	To amplify DNA template for 5S riboprobe
pZE.05	AATCATCACTTTCGGGAA	Verify insert insertion in pCS26
pCS26-For	TAGCAACACACAGAACAGCC	Amplify pCS26 without origin of replication
pCS26-Rev	ATCACTATACCAATTGAGATGGGC	Amplify pCS26 without origin of replication
pUC18R6K-checkF	ATCCGCCGTAGGAGCTTG	Verify insertion of pUC18R6K-miniTn7T
pUC18R6K-checkR	TTGGCCCTGCAAGGCCCTCG	Verify insertion of pUC18R6K-miniTn7T
lux-check60	TATATGCGCGAGCGCTTGATCC	Verify lux insertion
cm-check60	TGTGACCGTGTGCTTCTCAAATGC	Verify Cm ^R insertion
kn-check60	TACCCGTGATATTGCTGAAAGAGCTTGG	Verify Kn ^R insertion
glmSdetectFor	AACCA CCCC GTTCAGGCTGGCTA	Verify insertion downstream of <i>glmS</i>
glmSdetectRev	ACGTTGACCA CCCC GGCTAAC	Verify insertion downstream of <i>glmS</i>
fnrcom_XhoI_F	TTTCTCGAGAGTTTGTAACTAAAGAGTAACTC	To amplify <i>fnr</i> with promoter, adds XhoI site
fnrcom_BamHI_R	TTTGGATCC AA GGCTATCTTTTATTATG	To amplify <i>fnr</i> with promoter, adds BamHI site
PssrA_XhoI_F	TTTCTCGAGATTACACAATTACATTTTCAGC	To amplify primary <i>ssrA</i> TSS, adds XhoI site
PssrA2_XhoI_F	TTTCTCGAGGAATCCCTCCTCAGACATAAA	To amplify entire <i>ssrA</i> promoter, adds XhoI site
PssrA_BamHI_R	TTTGGATCCCTTTGGCACCTTGATCACTA	To amplify P _{ssrA} promoter, adds BamHI site
PssrB_XhoI_F	TTTCTCGAGGCTGGCTGATATTGAAAATGC	To amplify P _{ssrB} , adds XhoI site
PssrB_BamHI_R	TTTGGATCCCGCGTTAATGATGATTTTCATG	To amplify P _{ssrB} , adds BamHI site
PssaB_XhoI_F	TTTCTCGAGTTATCGGAAAATCCGAATGATAG	To amplify P _{ssaB} , adds XhoI site

Table 2.4 Table of oligonucleotides (continued)

<i>Primer</i>	<i>Sequence (5' – 3')</i>	<i>Description</i>
Pssab_BamHI_R	TTTGGATCCAGAAATAGAAATGCTTCTGAG	To amplify P _{pssab} , adds BamHI site
dbpA_XhoI_F	TTTCTCGAGCGATCATTTTAATAGCCGTACC	To amplify dbpA, adds XhoI site
dbpA_BamHI_R	TTTGGATCCCTCAAGCTGAACCTGGCTGAA	To amplify dbpA, adds BamHI site
sopE_check	ATCAGGAAGAGGCTCCGC	Verify insertion of 3×FLAG with Kan ^R at sopE
stcC_check	ATCTGTAGCGAATGTGCCC	Verify insertion of 3×FLAG with Kan ^R at stcC

* represents a 5' phosphorylation modification

Restrictions sites are underlined

SNPs are double underlined

2.5 Genetic manipulations

2.5.1 P22 Phage transduction

2.5.1.1 Preparation of bacteriophage lysates

Bacteriophage P22 HT 105/1 *int-201* was used to introduce desired mutations linked to antibiotic markers for all transductions. To generate P22 phage lysates, first a donor strain was subcultured 1:1000 in 10 mL of LB with appropriate antibiotics and grown to an OD₆₀₀ of 0.1. The culture was then inoculated with 20 μ L of P22 phage from wild-type 4/74 cells and incubated with agitation at 200 rpm for 4 h. All remaining bacterial cells were killed with the addition of 500 μ L of chloroform, gentle mixing, and incubation at room temperature for 10 min. Cellular debris was removed by collecting supernatants after centrifugation at $2,880 \times g$ for 20 min at room temperature. Supernatants were filtered using 0.2 μ m PES membrane filters (Fisher Scientific). Stocks of bacteriophage P22 were stored in 5 mL volumes supplemented with 10 μ L chloroform at 4°C.

2.5.1.2 Transduction by bacteriophage P22

Recipient strains were grown overnight as previously described (2.2.3.1). Transductions were performed by combination of 100 μ L of stationary phase recipient strain with 100 μ L of neat, 10^{-1} , and 10^{-2} dilutions of phage, and stationary incubation at 37°C for 1 h. Negative controls of recipient strain alone and phage alone samples were also incubated at 37°C. The entire transduction reaction was plated onto appropriate antibiotic LA plates and incubated at 37°C overnight. If possible, colonies were chosen from plates with the highest phage dilution to prevent the occurrence of double transductants. Green agar contains a low pH indicator whereby reduction in pH of lysed cells is detected by the presence of dark green colonies containing unstable pseudolysogens. To eliminate the possibility of phage contamination or the presence of pseudolysogens, pale colonies were passaged twice on green agar containing the relevant antibiotic (**Table 2.1**). Finally, a pale colony was chosen, verified by colony PCR and custom sequencing, and stored as a glycerol stock.

2.5.2 Removal of antibiotic resistance cassettes

To ensure that the presence of antibiotic resistance cassettes did not have polar effects on surrounding genes, and to facilitate additional genetic manipulations, resistance genes were removed from mutant *S. Typhimurium* strains using the pCP20 plasmid (Cherepanov & Wackernagel, 1995; Datsenko & Wanner, 2000). The pCP20 plasmid encodes the yeast FLP recombinase and has a temperature sensitive origin of replication. FLP targets FLP recombinase target sites (FRT sites) found flanking antibiotic resistance cassettes amplified from pKD3, pKD4 and pSUB11. FLP mediated site-specific recombination of FRT sites causes removal of the antibiotic resistance cassette, leaving a scar sequence of 82 – 85 nt. Finally, cells were cured of the pCP20 plasmid by passaging cells at 42°C. To ensure both the resistant cassette and pCP20 plasmid were lost, cells were streaked on LA plates, and LA plates containing appropriate antibiotics. Colonies that grew only on LA plates without antibiotics were verified by PCR and stored in glycerol stocks.

2.5.3 Modular Tn7-based plasmid system

A modular Tn7-based system (Shivak *et al.*, 2016) was used for construction of the *fnr*⁺ complementation (**Figure 2.2**). First, a kanamycin resistant pCS26 plasmid (pCS26-Kn^R-*luxCDABE*) was digested with NotI to remove the *luxCDABE* operon. The digested fragment was gel extracted and re-circularized with T4 DNA Ligase (Thermo Scientific). The new pCS26-Kn^R and a PCR amplified *fnr* with its promoter were digested with BamHI and XhoI and ligated with T4 DNA Ligase. The resulting pCS26-*fnr*-Kn^R plasmid and pUC18R6K-miniTn7T-PacI plasmid were digested with PacI and ligated with T4 DNA Ligase. The resulting pCS26-*fnr*-Kn^R-pUC18R6K-miniTn7T plasmid was electroporated into Δ *fnr* cells already containing the pHSG415-*tnsABCD* plasmid, cells were recovered at 30°C for 2 h to allow for transposition of *fnr* and plated on LA plates containing kanamycin and grown overnight at 37°C. Colonies were then streaked on kanamycin and ampicillin containing plates to ensure acquisition of *fnr* and loss of both plasmids. Colonies with growth on only kanamycin-containing LA were then verified by PCR and sequencing.

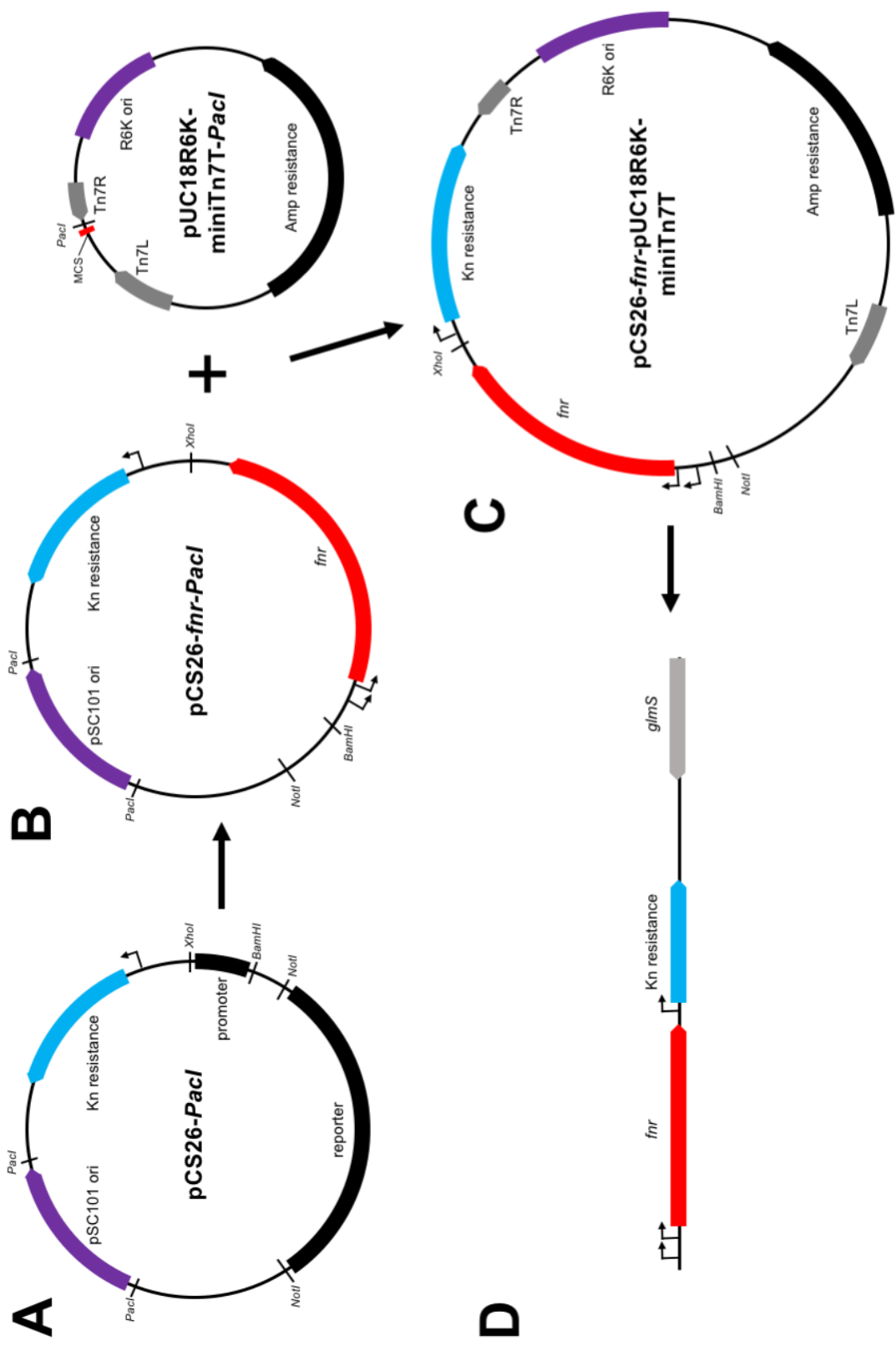


Figure 2.2 Construction of the *fnr*⁺ complementing strain.

A. A pCS26-PacI reporter plasmid with an kanamycin resistance cassette was digested with NotI, BamHI and XhoI and ligated to a XhoI and BamHI digested PCR product containing *fnr* with its native promoter to create pCS26-*fnr*-PacI. B. pCS26-*fnr*-PacI amplified to remove the pSC101 origin of replication and was SLiCE cloned into the pUC18R6K-miniTn7T-*PacI* plasmid between the Tn7L and Tn7R sites to create C. pCS26-*fnr*-pUC18R6K-miniTn7T. This plasmid was then transformed into Δ *fnr*::FRT containing the pHSG-*tnsABCD* plasmid. D. Cells were recovered at 30°C to allow transposition at the *att*::Tn7 site upstream of *glmS*. Figure adapted from Shivak *et al.*, 2016.

2.6 Analysis of RNA

2.6.1 Extraction of RNA from *S. Typhimurium* 4/74

Cultures were grown as previously described. Transcription was stopped, and RNA was stabilized by addition of 2/5 volume “stop solution” (5% phenol pH 4.3, 95% ETOH) and incubation on ice for 30 min. Cells were harvested by centrifugation at 2,880 × g and 4°C for 10 min. Pellets were either stored at -80°C or RNA was immediately extracted.

Total RNA was extracted from bacterial cultures using TRIzol[®] (Ambion) for Northern Blots and RNA sequencing (RNA-seq). For TRIzol[®] RNA extraction, extracted pellets were resuspended on ice in 1 mL TRIzol[®]. Samples were then transferred to 2 mL Heavy Phase-Lock tubes (5PRIME), 400 μL chloroform was added, samples were mixed by inversion for 10 s, and incubated at room temperature for no longer than 5 min. Aqueous and organic phases were separated by centrifugation at 20,000 × g for 15 min at room temperature. The aqueous phase was then transferred to a new 1.5 mL tube containing 300 μL isopropanol, and RNA was precipitated for 30 min at room temperature. Samples were subsequently centrifuged at 20,000 × g for 30 min at room temperature, and RNA pellets were washed with 350 μL of 70% ethanol and centrifuged for a further 10 min at 20,000 × g. The supernatant was discarded, and RNA pellets were air dried to remove residual ethanol, then resuspended in DEPC treated H₂O. Samples were intermittently vortexed and mixed at 65°C, 900 rpm on a ThermoMixer[®] (Eppendorf) for 5 minutes. RNA samples were then quantified using the NanoDrop ND-1000 Spectrophotometer (Thermo Scientific), and quality was

assessed using agarose gel electrophoresis or with the 2100 Bioanalyzer using the RNA 6000 Nano Kit (Agilent), and stored at -80°C.

Total RNA extracted using the SV Total RNA Isolation System (Promega) for RT-qPCR according to the manufactures' specifications. RNA samples were then quantified using the NanoDrop ND-1000 Spectrophotometer (Thermo Scientific), and quality was assessed using agarose gel electrophoresis, and stored at -80°C.

2.6.2 DNase I digestion

Total RNA samples were DNase I digested with the TURBO DNA-*free*TM Kit (Ambion) according to the manufacturers' instructions. DNase I digested samples were quantified with the NanoDrop ND-1000 Spectrophotometer (Thermo Scientific) and stored at -80°C.

2.6.3 Reverse transcription

Reverse transcription (RT), or cDNA synthesis, of DNase I digested total RNA was completed using the GoScriptTM Reverse Transcription System (Promega) according to the manufacturers' specifications. 400 ng of each RNA sample was processed in a 5 µL reaction volume, and following RT, was added to 100 µL of nuclease free H₂O for a final concentration of 3.33 ng/µL. For each sample a "No RT" control was also included that contained no RT enzyme to confirm the absence of genomic DNA in real-time quantitative PCR. All cDNA samples were stored at -80°C.

2.6.4 Real-time quantitative PCR

Real-time quantitative PCR (RT-qPCR) was used to quantify gene expression of *S. Typhimurium* cells. The PowerUpTM SYBRTM Green Master Mix (Applied Biosystems) was used for all RT-qPCR reactions in 20 µL volumes including 8 µL of cDNA, "No Reverse Transcriptase" RNA or genomic DNA as template. cDNA and "No Reverse Transcriptase" templates were diluted 5-fold to a final concentration of 0.67 ng/µL. Standard curves were generated with six 10-fold serial dilutions of wild-type *S. Typhimurium* 4/74 genomic DNA. RT-qPCR reactions were set up in duplicate in MicroAmp Fast Optical 96-well reaction plates (Applied Biosystems) and run on the ABI StepOnePlusTM Real-Time PCR System (Applied Biosystems). Default RT-qPCR settings were used for each run as well as for melt

curves for each new primer set. All primers used for RT-qPCR are listed in **Table 2.4**. Data analysis was done using the StepOne™ software and Prism 6 GraphPad. PCR products were quantified relative to *hemX*. The *hemX* gene encodes a putative uroporphyrinogen III C-methyltransferase and was used as a reference gene as it showed low variation in gene expression across RNA-seq transcripts from the wild-type and Δfnr mutant.

2.6.5 Generation of Digoxigenin-labelled riboprobes

Digoxigenin (DIG)-labelled single-strand RNA molecules (“riboprobes”) were generated for Northern Blotting by *in vitro* transcription using T7 RNA polymerase and the DIG Northern Starter Kit (Roche). A linear DNA template including the T7 promoter sequence (GAATTAATACGACTCACTATA) was generated through PCR with Q5 polymerase (New England Biolabs) and primers found in **Table 2.4**. DNA templates were purified through gel extraction as previously described, and 200 ng of DNA was used as template in each 20 μ L reaction (1 \times labelling mix, 1 \times transcription buffer, 40 U T7 RNA polymerase). Labelling transcription reactions were incubated at 42°C for 1 h in a SimpliAmp Thermal Cycler (Applied Biosystems, Thermo Scientific). Template DNA was removed by incubation with DNase I at 37°C for 15 min, and reactions were stopped by addition of 400 mM EDTA pH 8.0. Riboprobes were stored at -20°C.

Labelling efficiency of labelled riboprobes was tested by a dot-blot of 10-fold serial dilutions of riboprobes on a positively charged nylon membrane. Membranes were UV-crosslinked at 120 mJ (Peqlab crosslinker), rinsed with washing buffer, incubated at room temperature in 1 \times blocking buffer for 30 min, and subsequently incubated with a 1:10,000 dilution of the Anti-digoxigenin-AP, Fab fragments in 1 \times blocking buffer for 30 min. The membrane was washed two times in washing buffer, equilibrated in detection buffer for 5 min, then covered with CDP-star (Applied Biosystems). CDP-star acts as the chemiluminescent substrate, where enzymatic dephosphorylation of CDP-star by the alkaline phosphatase conjugated anti-DIG produces light which was detected using the ImageQuant™ LAS 4000 (GE Healthcare Life Sciences). All buffer and solution recipes are listed in **Table 2.5**.

2.6.6 Northern blotting

Total DNaseI treated RNA was electrophoresed through 7% acrylamide, 8.3 M urea, 1 × TBE gels. 5 µg of RNA was mixed with 2 × RNA loading dye and heat denatured at 65°C for 10 min prior to loading into gels. Gels were electrophoresed at 90 V in 1 × TBE for 1 h and 15 min. RNA-containing gels, positively charged nylon membranes (Roche), and filter paper were equilibrated in ice-cold 1 × TBE. RNA was transferred to the membrane using the Biometra Fastblot B43 semi-dry blotting apparatus at 125 mA for 30 min at 4°C. RNA was UV-crosslinked to membrane at 120 mJ (Peqlab crosslinker). The membrane was then pre-hybridized in pre-warmed DIG Easy Hyb buffer (Roche) in a rotating oven at 62°C for 1 h. Approximately 1.25 µg (5 µL) of riboprobe was boiled at 95°C for 5 min, then incubated on ice for 5 min before being added to pre-hybridization buffer. Hybridization of RNA with the riboprobe of interest was incubated in a rotating oven at 62°C overnight. Membranes were washed twice for 10 min in Stringency Wash Buffer I pre-warmed to 62°C, then washed twice for 30 min in Stringency Wash Buffer II at room temperature on a rocker. The membranes were blocked for non-specific sites with 1 × blocking buffer at room temperature for 30 min, and subsequently incubated with a 1:10,000 dilution of the Anti-digoxigenin-AP, Fab fragments in 1 × blocking buffer for 30 min. The membrane was washed two times in washing buffer for a total of 10 min, equilibrated in detection buffer for 5 min, then covered with CDP-star (Applied Biosystems). Chemiluminescence was detected as previously described using the ImageQuant™ LAS 4000 (GE Healthcare Life Sciences). To determine if RNA samples were equally loaded onto gels, membranes were re-probed as previously described with a 1:1000 diluted 5S riboprobe. All buffer and solution recipes are listed in **Table 2.5**.

2.6.7 cDNA preparation of RNA and RNA-seq

Total non-depleted RNA was sent to Vertis Biotechnologie AG (Freising Germany) for cDNA library preparation and RNA-seq.

Table 2.5 Buffers and solutions for Northern blotting

<i>Name</i>	<i>Reagent</i>	<i>Concentration</i>
RNA loading dye	xylene cyanol FF	0.025% (w/v)
	bromophenol blue	0.025% (w/v)
	EDTA pH 8.0	18 mM
	SDS	0.025% (w/v)
	formamide	95% (v/v)
20 × SSC	NaCl	3 M
	Sodium Citrate	0.3 M
Stringency wash I	SSC	2 ×
	SDS	0.1% (w/v)
	H ₂ O	
Stringency wash II	SSC	0.5 ×
	SDS	0.1% (w/v)
	H ₂ O	
Maleic acid buffer pH 7.5	Maleic acid	0.1 M
	NaCl	0.15 M
	*adjust pH with NaOH pellets	
Washing buffer	Maleic acid buffer	1 ×
	Tween-20	0.3% (v/v)
1 × Blocking buffer	Casein Blocking Solution (Roche)	1 ×
	Maleic acid buffer	1 ×
Detection buffer pH 9.5	Tris-HCl	0.1 M
	NaCl	0.1 M

2.7 Analysis of proteins

2.7.1 Preparation of whole cell lysates for analysis of cellular proteins

Cultures were grown as previously described. 1 OD₆₀₀ unit of cells were harvested for PCN and LB cultures, while MMA cultures required 5 OD₆₀₀ units. Cells were harvested by centrifugation at 4°C for 8 min at 2,880 × g. Cell pellets were washed once in 1 mL PBS then resuspended in 20 mL nuclease free H₂O and 20 mL 2 × Laemmli buffer (0.1 M Tris-HCl pH 6.8, 6% (w/v) SDS, 20% (v/v) glycerol, 10% (v/v) β-mercaptoethanol, 0.1% (w/v) bromophenol blue). Samples were boiled for 5 min at 100°C, then centrifuged for 3 min at 6,500 × g at 4°C. Supernatants were moved to new 1.5 mL tubes and stored at -20°C.

2.7.2 Preparation of culture supernatants for analysis of secreted proteins

Cultures were grown as previously described (Section 2.2.3). 10 OD₆₀₀ units of cells were harvested for PCN and LB cultures, while MMA cultures required 50 OD₆₀₀ units. Cells were centrifuged at 4°C for 40 min at 2,880 × g, and supernatants were filtered through 0.2 μm PES membrane filters (Fisher Scientific) into sterile tubes. Ice-cold trichloroacetic acid (TCA) was added to a final concentration of 10% (v/v) to precipitate proteins, and proteins were harvested by centrifugation at 4°C for 40 min at 2,880 × g. Protein pellet were washed in 1 mL ice-cold acetone, transferred to new 1.5 mL tubes and centrifuged at 4°C for 10 min at 6,500 × g. Pellets were resuspended in 20 μL nuclease free H₂O and 20 μL 2 × Laemmli buffer. Samples were boiled at 99°C for 5 min prior to storing at -20°C.

2.7.3 SDS polyacrylamide gel electrophoresis (SDS-PAGE)

SDS polyacrylamide gels (SDS-PAGE) were used for size separation of denatured proteins based on molecular weight using a discontinuous gel system. Resolving gels were made to a final concentration of 10 to 12.5% from a 40% acrylamide/bis-acrylamide (37:5:1) stock, with 0.375 M Tris-Cl (pH 8.8), 0.1% (w/v) SDS, and were polymerized by 0.1% (w/v) ammonium persulfate (APS) and 0.01% (v/v) tetramethylethylenediamine (TEMED). Once poured, resolving gels were overlaid with isopropanol until polymerization was complete. Isopropanol was removed before overlaying the resolving gel with the stacking gel. Stacking gels were comprised of 5% from a 40% acrylamide/bis-acrylamide (37:5:1) stock, with

0.082 M Tris-Cl (pH 6.8), 0.1% (w/v) SDS, and were polymerized with 0.1% (w/v) APS and 0.01% (v/v) TEMED. Samples were electrophoresed alongside the PageRuler™ Plus Prestained Protein Ladder (Thermo Scientific) to help monitor progress of the gel and estimate protein band sizes. Gels were run in 1 × running buffer (25 mM Tris, 0.19 M glycine, 0.1% (w/v) SDS) at 90 V until the dye front surpassed the stacking gel, then the voltage was increased to 180 V until the dye front reached the bottom of the gel. Gels were either analyzed by Coomassie staining or 108 immunoblotting.

2.7.4 Coomassie staining of polyacrylamide gels

SDS-PAGE gels were Coomassie stained using InstantBlue™ (Expedeon). Gels were rinsed with dH₂O then submerged in InstantBlue™ for 15 min on a rocker. Gels were then washed in dH₂O overnight and proteins were visualized using white light using the ImageQuant LAS4000 (GE).

2.7.5 Western Immunoblotting

Western immunoblotting was used to detect specific proteins from whole extracts or culture supernatants separated by size on SDS-PAGE gels. Proteins were transferred from gels to nitrocellulose membranes using a Mini Trans-Blot Electrophoretic Transfer Cell (Bio-Rad). Gels were rinsed with dH₂O then equilibrated in 1 × transfer buffer (25 mM Tris, 0.19 M glycine). Transfer “sandwiches” were assembled in gel holder cassettes in a dish containing 1 × transfer buffer as follows: a fiber pad, 3 pieces of 3 mm filter paper (Whatman), the polyacrylamide gel, a 0.45 μm PROTRAN nitrocellulose membrane (Whatman), and 3 additional pieces of 3 mm filter paper and fiber pad. Cassettes were loaded into transfer tanks with membranes towards the anode, filled with 1 × transfer buffer and an ice-pack. Proteins were transferred at 300 mA for 90 min on ice.

To verify that proteins had efficiently transferred, membranes were briefly incubated in Ponceau S solution (Sigma) until bands were visible. Membranes were imaged under white light using the ImageQuant LAS4000 (GE), then rinsed with water until staining was no longer visible.

To reduce non-specific protein binding, membranes were blocked for 90 min at room temperature in blocking buffer (5% skimmed milk powder, PBS, 0.05% Tween-20). The

primary antibodies, monoclonal anti-FLAG M2 (Sigma) and monoclonal anti-DnaK (*E. coli*, Enzo Life Sciences) derived from mice, were diluted in blocking buffer 1:10,000 and 1:30,000 respectively, and incubated with membranes at 4°C overnight on a rocker. DnaK served as a loading control for whole cell extracts and as a cell lysis control for supernatants. DnaK was used as a control for protein levels as a cytosolic control for Western blotting. This allowed us to determine if general protein levels were expressed evenly between different samples. Membranes were washed in PBST (PBS, 0.05% Tween-20) four times for a total of 40 min before incubation with the secondary antibody, anti-mouse IgG horseradish peroxidase (HRP, Santa Cruz Biotechnology), diluted 1:6,000 in blocking buffer for 90 min at room temperature on a rocker. Membranes were washed an additional 3 times in PBST for a total of 30 min and once in PBS for 15 min. ECL chemiluminescent HRP substrate (Pierce) was used to detect chemiluminescent signal. A 1:1 ratio of luminol and peroxide were mixed and used to flood the membrane. Membranes were sealed in plastic and incubated in the dark for 5 min. Light emission occurs as a by-product of the oxidation of luminol by HRP and was detected using the ImageQuant LAS4000 (GE).

2.7.6 Proteomic analysis by mass spectrometry

Protein sample preparation was done by Dr. Nicole Hansmeier and all subsequent processing and analysis as described here were completed by Dr. Tzu-Chiao Chao at the University of Regina, Regina, Saskatchewan, Canada. Cultures were grown in MMA as previously described. Protein isolation was conducted according to the manufacturers' instructions for TRIzol protein extraction (Life Technologies) with minor modifications. Approximately 10^{10} bacterial cells were harvested and washed $4 \times$ with PBS, the resulting cell pellet was resuspended in 750 μ L of TRIzol and incubated for 5 min on ice. Subsequently, 200 μ L chloroform was added and incubated for 3 min on ice. The samples were centrifuged for 15 min at $12,000 \times g$ at 4°C. The phenolic phase was transferred into a new tube and the proteins were precipitated with isopropanol. The protein pellet was collected by centrifugation at $12,000 \times g$ at 4°C and washed twice with 70% ethanol, followed by 100% ethanol incubation for 20 min before air drying. Protein pellets were resolubilized in 50 mM ammonium bicarbonate buffer containing 0.1% SDS. The resulting protein samples were reduced and alkylated with 5 mM DTT and 20 mM iodoacetamide (45 min incubation at RT each) and rebuffered into 50 mM ammonium bicarbonate buffer on filter columns (MWCO 10 kDa, Amicon, Millipore). Protein concentration of the resulting protein solution was determined by Pierce BCA protein assay kit (Thermo Fisher Scientific) and 50 μ g protein was

subsequently digested with trypsin gold (protein/enzyme ratio 50:1) according to the manufacturers' instructions (Promega). Digested proteins were acidified with 0.1% formic acid and dried. Dried digested samples were resuspended in running solution (0.1% formic acid, 3% acetonitrile) and centrifuged at $12,000 \times g$ for 10 min to remove insoluble material. The supernatant (0.5 $\mu\text{g}/\mu\text{l}$ protein) was spiked with Phos B standard (Waters) for quantitation before LC-MS analyses. Each analysis injection contained 40 fmol/ μl of Hi3 Ecoli standard (Waters).

Each sample was analyzed on a NanoAcquity system (Waters) coupled to a Synapt G2 HDMS (Waters). 0.5 μg spiked digests were loaded onto a NanoAcquity UPLC Symmetry C18 trap column (180 $\mu\text{m} \times 20$ mm, dp: 5 μm , Waters) to desalt and chromatographically focus peptides for 3 min (5 $\mu\text{L}/\text{min}$ flow rate) prior to elution onto an Acquity UPLC M-class HSS T3 analytical column (75 $\mu\text{m} \times 200$ mm, dp:1.8 μm , Waters). The separation was conducted with a 120 min gradient from 3% acetonitrile/0.1% formic acid to 45% acetonitrile/0.1% formic acid at a flow rate of 0.35 $\mu\text{L}/\text{min}$. The eluted peptides were analyzed in a Synapt G2 HDMS QToF (Waters) in positive MS^E resolution mode with a 1 s scan time. In low energy MS mode, data were collected at constant collision energy of 4 eV. High energy collision energy was ramped between 18 and 42 V. Leucine enkephaline was measured as lock mass every 30 s to maintain mass accuracy throughout the run.

The resulting raw spectral data were processed with the ProteinLynx Global Server (PLGS) v. 3.02 with Identity (Waters). Data were extracted and searched against a protein sequence database built with the UniProt *Salmonella enterica* sv. Typhimurium strain LT2 reference proteome (accessed January 2016), appended with the sequences of the Hi3 Ecoli standard (Waters) for quantitation. The following settings were used as search parameters: mass tolerance of 8 ppm, trypsin specificity, 1 missed cleavage; stable modification carbamidomethyl(C); variable modification methionine oxidation, false discovery rate: 4%.

2.8 Chromatin Immunoprecipitation

2.8.1 Preparation of cross-linked lysates

Chromatin immunoprecipitation (ChIP) was carried out as previously described (Dillon *et al.*, 2010) with some modifications. All ChIP buffer recipes are listed in **Table 2.6**. Cultures of *fnr::3 \times FLAG* were grown in MMA as previously described. 40 OD units were harvested

by room temperature centrifugation at $2,880 \times g$ for 8 min. Cells were resuspended in 50 mL of 37°C PBS. Crosslinking of protein-DNA complexes was done by slowly adding molecular grade formaldehyde (Sigma) to a final concentration of 1% with gentle mixing on a Belly Dancer[®] for 30 min. Cross-linking was stopped by addition of ice-cold glycine to a final concentration of 0.125 M, and incubation for 5 min with gentle mixing. Cross-linked cells were centrifuged at 4°C, at $2,880 \times g$ for 8 min. Cell pellets were resuspended in 600 μ L of lysis buffer and incubated on ice for 30 min. Cells were further diluted in 1.4 mL of dilution buffer before sonication. Chromatin was sonicated to achieve an average fragment length of 500 bp using the MSE Soniprep sonicator (Sanyo). Sonication was performed in 10 to 15, 30 s bursts at an amplitude of 10 μ M with 1 min of incubation on ice between bursts. A sample of sonicated chromatin was verified for sonication efficiency by agarose gel electrophoresis as previously described (Section 2.3.4). Cellular debris was removed by centrifugation of samples at 4°C, at $8,000 \times g$ for 10 min. Supernatants containing sheared chromatin were added to 1 mL of dilution buffer and stored at -80°C.

2.8.2 Immunoprecipitation

To eliminate non-specific binding of the antibody, chromatin was pre-cleared using 50 μ g of normal rabbit IgG (Santa Cruz Biotechnology). Chromatin was incubated at 4°C on a rotating wheel for 1 h, followed by addition of 100 μ L of homogeneous protein G-agarose bead suspension (Roche), and incubated as before for an additional 3 h. Beads were pelleted by centrifugation at 4°C, at $2,880 \times g$ for 4 min. Chromatin-containing supernatants were carefully transferred to new 2 mL tubes to avoid disruption of beads. The “Input” sample, 200 μ L of pre-cleared chromatin, was stored at -20°C for later analysis. The remaining pre-cleared chromatin was split into 1350 μ L aliquots for Immunoprecipitation (IP) reactions. The “Mock” IP reaction was carried out using 10 μ g of normal mouse IgG (Santa Cruz Biotechnology). Mock IP reactions were used to measure the background levels of DNA binding. The experimental IP reaction, referred to hereafter as “FLAG,” was carried out using 10 μ g of monoclonal mouse anti-FLAG M2 antibody (Sigma). Both IP reactions were incubated overnight at 4°C on a rotating wheel, followed by addition of 50 μ L of homogeneous protein G-agarose bead suspension and a further 3 h of incubation.

2.8.3 Washing the Protein-G agarose beads and elution of DNA

The protein-G agarose beads were bound to antibody-protein-DNA complexes and were carefully washed in several steps. First, beads were pelleted by centrifugation at $6,000 \times g$ at 4°C for 2 min, beads were incubated on ice for 1 min before discarding supernatants. For each wash, 750 μL of the appropriate pre-chilled wash buffer was added, followed by vortexing and centrifugation at $6,000 \times g$ at 4°C for 2 min and a 1 min incubation on ice. Beads were washed in Wash Buffer I, transferred to new 1.5 mL tubes and washed again in Wash Buffer I. Beads were then washed once in Wash Buffer II and twice in TE Buffer. Finally, beads were resuspended in 225 μL of room temperature Elution Buffer, vortexed and pelleted to elute antibody-protein-DNA complexes from the beads. The elution step was performed twice, and both eluates were combined into a new 1.5 mL tube.

2.8.4 Reversal of cross-links and DNA extraction

To reverse crosslinking, Input, Mock and FLAG samples were treated with 5ng/ μL RNase A (Sigma) and 0.3 M NaCl and incubated at 65°C for a minimum of 6 h. Samples were then treated with 9 μg of Proteinase K and incubated at 45°C for a minimum of 3 h.

DNA extraction of all samples was accomplished using standard phenol-chloroform extraction followed by ethanol precipitation. Input samples were co-precipitated with glycogen, and both Mock and FLAG samples were co-precipitated with yeast tRNA and glycogen. Input DNA was ultimately resuspended in 100 μL nuclease free H_2O and Mock and FLAG DNA was resuspended in 50 μL nuclease free H_2O at 37°C and 900 rpm on a ThermoMixer[®] (Eppendorf) for 1 h.

Input and IP DNA were diluted 1:50 and 1:5 respectively for RT-qPCR analysis as previously described (section 2.6.4). The quantity of immunoprecipitated DNA is relative to specific protein binding of that region and was calculated as a fraction of the starting amount of DNA (Input). The mock IP DNA was subtracted from the experimental IP DNA and compared to a control region which was negative for specific transcription factor binding according to the following formula:

$$\frac{\text{Experimental IP of promoter } X}{\text{Experimental Input of promoter } X} - \frac{\text{Mock IP of promoter } X}{\text{Mock Input of promoter } X}$$

Table 2.6 Buffers for ChIP

Name	Reagent	Concentration
Lysis Buffer	Tris-HCl, pH 8.1	50 mM
	EDTA	10 mM
	SDS	1% (w/v)
	Protease inhibitor tablet stock	1 ×
Dilution Buffer	Tris-HCl, pH 8.1	20 mM
	NaCl	150 mM
	EDTA	2 mM
	Triton X-100	1% (v/v)
	SDS	0.01% (w/v)
IP Wash Buffer I	Tris-HCl, pH 8.1	20 mM
	NaCl	50 mM
	EDTA	2 mM
	Triton X-100	1% (v/v)
	SDS	0.1% (w/v)
IP Wash Buffer II	Tris-HCl, pH 8.1	10 mM
	LiCl	250 mM
	EDTA	1 mM
	NP-40	1% (v/v)
	Deoxycholic acid	1% (w/v)
TE Buffer, pH 8.0	Tris	10 mM
	EDTA	1 mM
	*adjust pH with HCl	
Elution Buffer	NaHCO ₃	100 mM
	SDS	1% (w/v)

2.9 DNA sequencing

2.9.1 Preparation of DNA libraries

DNA was quantified using the Qubit™ dsDNA HS Assay Kit and a Qubit™ Fluorometer (Thermo Scientific). Sequencing libraries were constructed using the NEBNext® Ultra™ II DNA Library Prep Kit (New England Biolabs) according to the manufacturers' specifications. Libraries were prepared without additional DNA fragmentation as DNA is already fragmented through the chromatin immunoprecipitation protocol and the 400 – 500 bp size selection step was used. TruSeq® DNA Adaptors (Illumina) were ligated to DNA fragments using 6 amplification cycles for Input samples, and 10 cycles for Mock and FLAG samples according to the manufacturers' specifications. Samples verified for quality using the 2100 Bioanalyzer and High Sensitivity DNA Kit (Agilent).

2.9.2 Sequencing with Illumina MiSeq

DNA libraries were prepared for sequencing with the MiSeq Reagent Kit v3 (Illumina) and run on a MiSeq System (Illumina) according to the manufacturers' specifications. The first libraries and sequencing runs were constructed and performed by Stefani Kary, with additional replicates by Dr. Keith MacKenzie at the University of Regina, Regina, Saskatchewan, Canada.

2.10 Bioinformatic analysis

2.10.1 Mapping of RNA-seq data and differential expression analysis

Data from RNA-seq was analyzed by Karsten Hokampf and Carsten Kröger at Trinity College Dublin, Dublin, Ireland. READemption (Forstner *et al.*, 2014) was used for computational evaluation of the RNA-seq data. Reads obtained from RNA-seq experiments were mapped to the 4/74 reference genome using the Segemehl mapping software (Hoffmann *et al.*, 2009). Reads that do not map in a single chromosomal location (uniquely mapped reads) were truncated from the 3' end in stepwise manner by removing one nucleotide at a time until the read is mapped uniquely or until the read length reaches 20 nucleotides. Remaining reads were discarded. Data were normalised using the transcripts per million (TPM) method (Wagner *et al.*, 2012). This method of measuring transcript

abundance from high throughput sequencing data is closely-related to the widely used reads per kilobase per million method (RPKM) (Mortazavi *et al.*, 2008), but removes the bias, of normalisation to the total number of reads mapped in each sequencing run, that the RPKM method introduces. Instead the TPM method measures transcript abundance by calculating the number of transcripts of a particular gene by dividing the number of nucleotides mapped to that gene by the length of the gene (t_g). All of these numbers are summed to get the total number of transcripts represented by all the mapped reads (T). The transcript abundance for each gene is then calculated as number of transcripts per million transcripts according to the following formula:

$$TPM = \frac{t_g}{T} 10^6$$

A TPM value of 2 is the suggested cut-off value for determining if a gene is expressed or not (Wagner *et al.*, 2013), however a more conservative cut-off of TPM = 10 was chosen for this study based on TPM values of indicator genes which were previously shown not to be expressed under a particular condition, as previously described (Kröger *et al.*, 2013). Differential expression of genes between WT and Δfnr was calculated from TPM values.

2.10.2 ChIP-seq analysis

Data from ChIP-seq was analyzed by Aalap Mogre and myself, at Trinity College Dublin, Dublin, Ireland. Qualities of sequenced reads were assessed using FastQC (Andrews, 2010). Reads were mapped to the *S. enterica* subsp. *enterica* serovar Typhimurium str. 4/74 chromosome and plasmids combined reference sequences (chromosome: NC_016857.1, TY474p1: NC_016858.1, TY474p2: NC_017675.1, TY474p3: NC_016859.1) using the Burrows-Wheeler Aligner (Li & Durbin, 2009). SAMtools was used to sort aligned reads by the reference sequence and remove unmapped and low mapping quality reads (mapping quality < 30) (Li *et al.*, 2009). Some samples had large numbers of unmapped reads that were found to map to the *S. cerevisiae* genome. Using qPCR with primers specific to *S. cerevisiae* we identified that these came from yeast gDNA contamination in the yeast tRNA used as a co-precipitant intended to increase DNA yields in the ChIP protocol. Since this contaminant gDNA was introduced in the final stages of the experiment, they do not affect the outcome of the ChIP experiment apart from reducing the coverage of the sample. We decided to not remove duplicate reads as the coverage of some of the samples was low and

peak calling was less effective after removal of duplicate reads. Model-based analysis of ChIP-Seq 2 (MACS2) (Zhang *et al.*, 2008) was used to call FNR peaks from the sorted BAM files using the mock as control. Due to differing fragment sizes among the replicates, different mock replicates were used as control for different sample replicates: mock replicate 1 was used as control for ChIP replicate 1 (fragment size ~250 nt), mock replicate 3 was used as control for ChIP replicates 2 and 3 (fragment sizes ~300 nt). Peak lists thus generated by MACS2 were roughly annotated with the names of neighbouring genes and sRNAs using a R script (R Core Team, 2013) and are available as both Excel and .gff files. Overlaps of peaks between different samples were analysed using DiffBind (Stark & Brown, 2011). Most peaks in replicate 1 overlapped with peaks in replicate 2. This list of high confidence peaks annotated roughly using a R script are available as both Excel and .gff files. Sequences of peaks from this list were used to generate the FNR motif using MEME-ChIP (Machanick & Bailey, 2011). This resulting motif was used to find all possible motifs in the genome, bound or not according to our experiment, using Find Individual Motif Occurrences (FIMO) (Grant *et al.*, 2011). deepTools was used to create bigWig (.bw) files, for display of dense, continuous data, from sorted BAM (binary SAM files) files containing coverage information scaled to the library size and multiplied by a factor (1×10^6) for each sample that could be viewed using Integrated Genome Browser (IGB) (Nicol *et al.*, 2009) along with the .gff peak lists. All scripts used in the analysis can be accessed from GitLab (<https://gitlab.com/aalap.mogre/fnr-chip-seq>).

Table 2.7 Table of programs and online tools for bioinformatic analysis in this study

<i>Name of Program/Tool</i>	<i>Description</i>	<i>Reference or URL</i>
BLAST	Basic Local Alignment Search Tool, for local sequence alignment and identification of regions of sequence similarity.	(Altschul <i>et al.</i> , 1990)
Benchling	Online tool for <i>in silico</i> manipulation of DNA sequences.	http://benchling.com
BWA	Burrows-Wheeler Aligner, a software package for mapping low-divergent sequences against a large reference genome.	(Li & Durbin, 2009)
Cytoscape	An open source software platform for visualizing molecular interaction networks and biological pathways and integrating these networks with annotations, gene expression profiles and other state data.	www.cytoscape.org
deepTools	A suite of python tools particularly developed for the efficient analysis of high-throughput sequencing data, such as ChIP-seq.	(Ramírez <i>et al.</i> , 2016)
DiffBind	For differential binding analysis of ChIP-seq peak data.	(Stark & Brown, 2011)
FastQC	A quality control tool for high throughput sequence data.	(Andrews, 2010)
FIMO	Find Individual Motif Occurrences, for scanning for occurrences of a given motif.	(Grant <i>et al.</i> , 2011)
GenBank	The NIH genetic sequence database, an annotated collection of all publicly available DNA sequences.	(Benson <i>et al.</i> , 2012)
GrowthRates	For calculating the best-fit growth rates, the lag times and the maximum OD from growth curves.	(Hall <i>et al.</i> , 2014)
ImageJ	Densitometry analysis of EMSA, Northern blot, and Western blot signals.	(Schneider <i>et al.</i> , 2012)

Table 2.7 Table of programs and online tools for bioinformatic analysis in this study (continued)

<i>Name of Program/Tool</i>	<i>Description</i>	<i>Reference or URL</i>
Inkscape	An open source professional vector graphics editor.	www.inkscape.org
IGB	Integrated Genome Browser, for visualization of RNA-seq and ChIP-seq reads, and other genomic features.	(Nicol <i>et al.</i> , 2009)
JBrowse	Visualisation of RNA-seq reads and other genome features.	(Skinner <i>et al.</i> , 2009)
Ligation Calculator	For calculation of amount of required insert DNA for a given molar ratio for ligation reactions.	http://www.insilico.uni-duesseldorf.de/Lig_Input.html
MEME-ChIP	Multiple Em for Motif Elicitation, for ChIP a motif analysis of large DNA datasets.	(Mechanic & Bailey, 2011)
MACS2	Model-based analysis of ChIP-seq 2, for improved spatial resolution of predicted binding sites of ChIP-seq data.	(Zhang <i>et al.</i> , 2008)
Multiple Primer Analyzer	For analyzing and comparing multiple primer sequences simultaneously.	ThermoFisher
NEB Tm Calculator	For estimating the optimal annealing temperature for PCR.	https://tncalculator.neb.com/
Prism GraphPad v6.0h	Statistical analysis and graphing software.	https://www.graphpad.com/scientific-software/prism/
R	A language and environment for statistical computing.	(R Core Team, 2013)
READDemption	An RNA-Seq analysis pipeline.	(Forstner <i>et al.</i> , 2014)

Table 2.7 Table of programs and online tools for bioinformatic analysis in this study (continued)

<i>Name of Program/Tool</i>	<i>Description</i>	<i>Reference or URL</i>
SalCom	<i>S. Typhimurium</i> mRNA and sRNA expression profiles based on RNA-seq data from 20 environmental conditions.	(Kröger <i>et al.</i> , 2013)
SalComMac	<i>S. Typhimurium</i> mRNA and sRNA expression profiles based on RNA-seq data within murine macrophages.	(Srikumar <i>et al.</i> , 2015)
SalComRegulon	<i>S. Typhimurium</i> mRNA and sRNA expression profiles based on RNA-seq data from 18 regulatory systems.	(Colgan <i>et al.</i> , 2016)
Segemehl	For mapping sequencer reads to a reference genome.	(Hoffmann <i>et al.</i> , 2009)
SAMTools	Sequence Alignment/Map format and tool for implementing various utilities for post-processing alignments in the SAM format, such as indexing, variant caller and alignment viewer.	(Li <i>et al.</i> , 2009)
Venny v2.1	An interactive tool for comparing lists with Venn's diagrams	http://bioinfogp.cnb.csic.es/tools/venny/index.html

2.11 DNA binding analysis

2.11.1 Large scale induction of protein production

Overnight cultures were set up in 50 mL of LB with kanamycin of PK22 cells with the p(*fnrD154A*)₂ plasmid. Strains were subcultured 1:50 in 1 L LB with kanamycin in a 2 L baffled flask, and grown at 37°C, 200 rpm to between OD₆₀₀ 0.4-1.0. Cultures were induced with 1 mM IPTG and grown at 16°C, 200 rpm overnight. Cells were harvested by centrifugation at 8,000 × g for 10 min at 4°C. Pellets were transferred to 50 mL falcon tubes with an EDTA-free protease inhibitor tablet and stored at -20°C.

2.11.2 6×His-Tag protein purification

Bacterial pellets were thawed in an ice-water slurry, resuspended in ice-cold PBS, and lysed using a French pressure cell press at 1000 psi. Lysates were centrifuged at 15,000 × g for 20 min at 4°C. DNase was added to a final concentration of 5 µg/mL gently mixed and lysates were filtered through a 0.2 µm PES membrane filter. A 5 mL HiTrap affinity column was used with a peristaltic pump. The column was washed with dH₂O, followed by 3 to 5 column volumes of Nickel Buffer A (4 mM Tris, 0.1 M NaCl, pH 7.9). The filtered lysate was then loaded onto the column and collected for downstream analysis as the “Unbound” fraction. Nickel Buffer B (4 mM Tris, 0.1 M NaCl, 0.2 M Imidazole, pH >7.9) was diluted with Nickel Buffer A using a gradient of concentrations from 10% to 100%. The column was then washed with 10 column volumes of 10% Nickel Buffer B in Nickel Buffer A to remove further unbound protein and collected as the “Wash” fraction for downstream analysis. The protein was then eluted from the column using the gradient of Nickel Buffer B concentrations collecting each fraction. The imidazole in Nickel Buffer B competes with the 6×His-tagged (FNRD154A)₂ protein for binding to the metal-charged resin in the column, thus eluting the recombinant protein. The fractions were analyzed by SDS-PAGE and Coomassie staining as described previously. Fractions containing the (FNRD154A)₂ protein were pooled and dialyzed against PBS at 4°C overnight. Proteins were then concentrated using an Amicon® Ultra-15 Centrifugal Filter (Sigma). Protein concentration was determined using a Pierce™ BCA Protein Assay Kit (Thermo Scientific) according to the manufacturers' specifications.

2.11.3 Electrophoretic mobility shift assay

Electrophoretic mobility shift assays (EMSA) were used to investigate *in vitro* binding of FNR at promoters of interest. Varying concentrations of (FNRD154A)₂ were combined with 0.5 pmol of probe DNA (**Table 2.7**) in EMSA Binding Buffer (20 mM Tris, 50 mM NaCl, 10 mM EDTA, 4 mM DTT, 5% (v/v) glycerol, 0.5 mg/mL BSA, 1 µg/mL poly-d[I-C], pH 7.2) in a 15 µL reaction volume, and incubated at 37°C for 1 h. Binding reactions were electrophoresed using 7% acrylamide, 2% glycerol, 1 × TBE gels in 1 × TBE at 150 V for 75 min on ice and at 4°C. Gels were stained with SafeView Nucleic Acid Stain (NBS Biologicals) prior to visualization under ultra violet light in the ImageQuant™ LAS 4000 (GE Healthcare Life Sciences). The molecular size of electrophoresed DNA fragments was estimated by comparison with O'GeneRuler™ 1 kb DNA Ladder (Thermo Scientific). Band shifts were quantified using ImageJ and the bound ratio was calculated using the following formula:

$$B_R = \frac{D_b}{(D_b + D_u)}$$

Where B_R is the bound ratio, D is the band intensity of DNA in pixels, and the subscripts b and u represent the bound (DNA bound by protein) and unbound (DNA only) bands. Equilibrium DNA binding curves were fitted by nonlinear regression and the dissociation constant and maximum bound ratio, K_D and B_{max} , respectively, were determined by one site specific binding with Hill slope analysis.

2.12 Atomic force microscopy imaging

For Atomic force microscopy (AFM) analysis, 20 mL of bacterial culture grown in LB as previously described, were spotted onto coverslips (Hartenstein) and incubated at room temperature for 1 h before rinsed with ultrapure water and subsequently mounted onto glass microscope slides for immediate AFM imaging. Measurements were taken using the NanoWizard II AFM system (JPK Instruments AG). To visualize the sample, the AFM was driven in soft contact mode using silicon nitride AFM probes with a nominal force constant of 0.06 N/m (SiNi, Budget Sensors). Scan rates were set to 1 Hz and images were acquired with a resolution of 512 × 512 pixel. For each sample, topographic overview images were taken before magnification was performed. Representative images are XY tilt corrected,

polynomial fitted, and unsharpened mask filtered to remove noise using JPK data processing software (JPK Instruments AG). All images are displayed in false-color. Atomic force microscopy imaging was completed by Nicole Hansmeier at Universität Osnabrück, Osnabrück, Germany.

2.13 Infection of murine macrophages

RAW 264.7 murine macrophages were grown in Dulbecco's Modified Eagle Medium (DMEM, Sigma) with fetal bovine serum (FBS, Sigma) and seeded into 24 well plates at a concentration of 4×10^5 cells per well. Macrophages were inoculated with *S. Typhimurium* strains that had been grown overnight in LB or MMA, at a multiplicity of infection (MOI) of 10:1 in DMEM. Macrophages were left to phagocytose bacterial cells for 30 min at 37°C in 5% CO₂ before treatment with 100 µg/mL gentamycin (Sigma) for 1 h at 37°C in 5% CO₂. The macrophages were washed with sterile PBS, lysed with ice-cold nuclease free water, and plated at appropriate dilutions on LA. In the remaining wells, media was replaced with DMEM with FBS and 10 µg/mL gentamycin and incubated at 37°C in 5% CO₂ for the remainder of the infection. Cells were routinely sampled at 1 h, 4 h, 8 h, and 16 h post-infection.

Chapter 3
Transcriptional regulation in Δfnr

3.1 Introduction

3.1.1 Overview of the Study

To establish and maintain a successful infection in the host, *Salmonella* must integrate a multitude of environmental inputs by co-ordinating regulatory proteins in a complex transcriptional network (Osborne *et al.*, 2009; Yoon *et al.*, 2009). *S. Typhimurium* host cell invasion, survival and proliferation inside of host cells has been thoroughly studied (Ellermeier & Slauch, 2007; Fass & Groisman, 2009; Haraga *et al.*, 2008) however, priming of cells prior to invasion is relatively underexplored (Brown *et al.*, 2005; Osborne & Coombes, 2011). Anaerobic and microaerobic growth of *Salmonella* has long been known to increase adherence and invasion of mammalian cells (Lee & Falkow, 1990; Schiemann & Shope, 1991). More recently, the regulator of anaerobic metabolism, FNR has been shown to be important for priming cells prior to host cell invasion as a regulator of virulence in response to changing oxygen concentrations in other species including *E. coli* and *Shigella flexneri* (Crofts *et al.*, 2018; Marteyn *et al.*, 2010) and has been shown to activate SPI-1 and motility/chemotaxis genes in *S. Typhimurium* (Fink *et al.*, 2007). Fink *et al.* also showed that FNR was necessary for full virulence in murine macrophages but were unable to link FNR and SPI-2. With the observation that low-level SPI-2 expression occurs at the intestinal epithelial border prior to invasion (Brown *et al.*, 2005; Osborne & Coombes, 2011) and that an oxygen gradient is present in the same location (Marteyn *et al.*, 2010), it follows that a transcription factor (TF) that responds directly to changes in oxygen, FNR, would be the prime candidate as a regulator of SPI-2 under these conditions. To our knowledge, there have been no large-scale investigations identifying the involvement of FNR in controlling SPI-2 expression in *S. Typhimurium*.

The aim of this chapter is to investigate the global changes in gene expression in an Δfnr mutant with a focus on *Salmonella* Pathogenicity Island 2, flagella and motility in *S. Typhimurium*. We have used RNA-seq to investigate the FNR regulon under microaerobic growth in MMA, a minimal medium with a glycerol carbon source and the alternative electron acceptors fumarate and TMAO and verified these results with additional molecular techniques. A general workflow of the main experimental procedure is outlined in **Figure 3.1**.

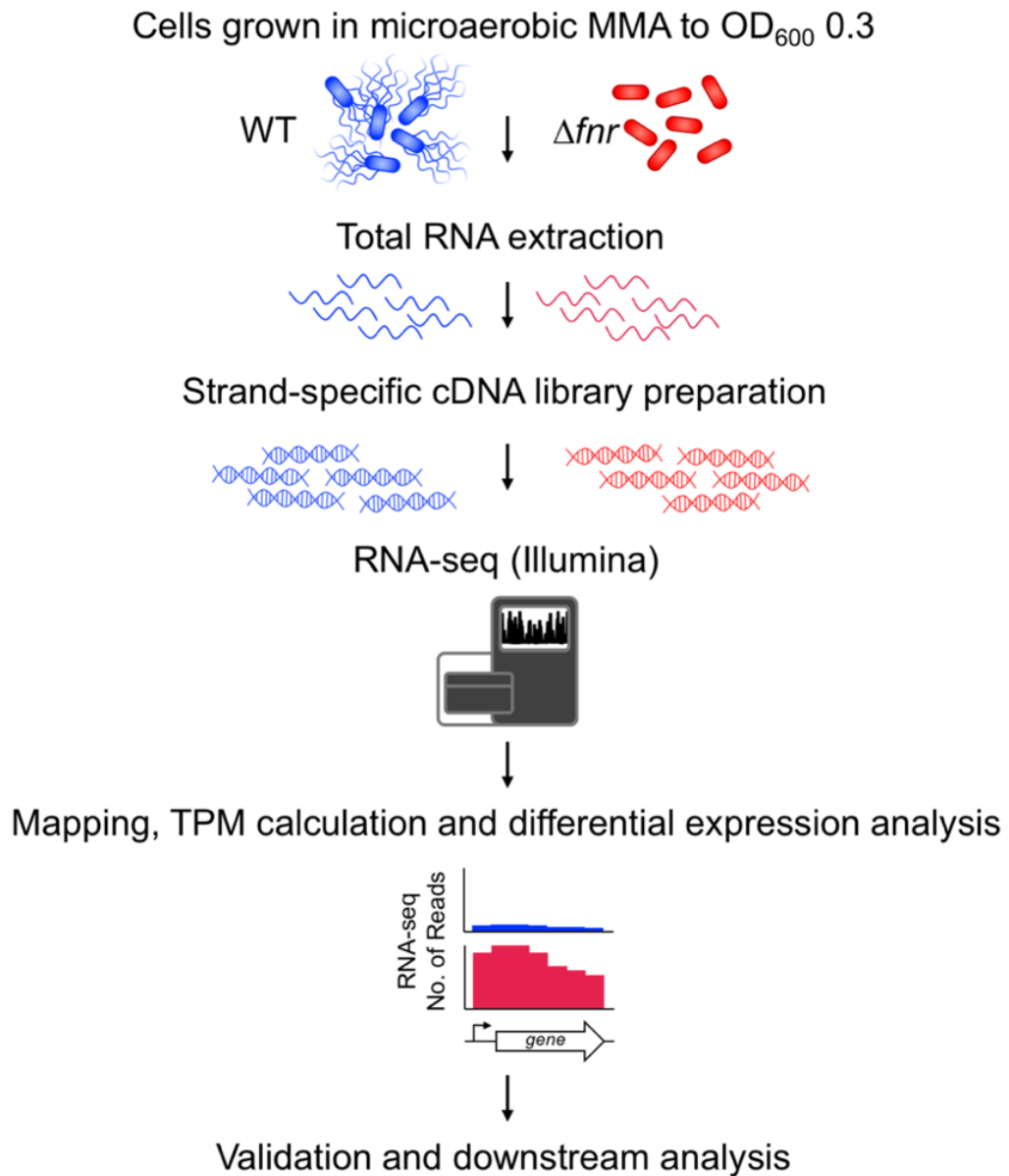


Figure 3.1 Workflow of general experimental procedures for investigating the regulation of SPI-2.

Wild-type (WT) and Δfnr cells were grown under microaerobic conditions to OD₆₀₀ 0.3 in MMA and total RNA was extracted by Dr. Aoife Colgan for replicate 1 and by me for replicate 2. cDNA library preparation and sequencing were performed by Vertis Biotechnologie AG. Mapping of sequence reads to the reference 4/74 genome and calculation of TPM values were performed by Dr. Karsten Hokamp and Dr. Carsten Kröger (Trinity College Dublin). Differential gene expression analysis, validation and downstream analyses were performed by me.

3.1.2 Bacterial transcriptome analysis using RNA-seq

RNA sequencing uses next-generation sequencing (NGS) to reveal the presence and quantity of RNA in a given condition using high-throughput sequencing of cDNA libraries. Although direct sequencing of yeast RNA on an array of nanopores has recently been demonstrated (Garalde *et al.*, 2018), cDNA sequencing or RNA-seq has been shown to generate highly reproducible and reliable data for identifying and quantifying which genes are being actively transcribed within *Salmonella* on a global scale (Colgan *et al.*, 2016; Kröger *et al.*, 2012; 2013). This technology provides a highly sensitive and dynamic method of transcriptome profiling at single nucleotide resolution (Ozsolak & Milos, 2010). The cDNA libraries used for RNA-seq in this study were generated from total RNA samples by Vertis Biotechnologie AG, Freising, Germany and RNA-seq was performed using an Illumina HiSeq 2000 platform. No methods of RNA depletion were used in this study, but analysis was limited to the sequencing reads that mapped to a single location on the chromosome (uniquely mapped reads) and reads mapping to many rRNA genes or other paralogous genes were removed. A systematic analysis of the effects of sequencing depth on discovery of rare transcripts demonstrated that sequencing of 5-10 million reads of non-rRNA fragments provides sufficient coverage of a bacterial transcriptome and is adequate to detect most expressed genes (Haas *et al.*, 2012). RNA-seq analysis pipelines and the use of TPM values to quantify gene expression (Section 2.10.1) allowed identification of differentially expressed genes in Δfnr (Forstner *et al.*, 2014; Wagner *et al.*, 2012).

The use of RNA-seq to investigate the transcriptome of Δfnr is helping to expand our knowledge of the FNR regulon and how this regulator of anaerobic metabolism can also play a role in regulation of *Salmonella* virulence-associated genes. Absolute expression values (in TPM) for every chromosomal *S. Typhimurium* 4/74 gene in Δfnr and wild-type comparator strain, sequenced in this study, are available in **Table S1** in Appendix I.

3.2 Results

3.2.1 Strategy for experimental design

Mutants in *fnr* are either unable to grow anaerobically or grow far slower than the parental strain in the presence of nonfermentable carbon sources and most terminal electron acceptors (Lambden & Guest, 1976). This presents a problem when comparing the Δfnr mutant to the WT strain, as differences are due to direct effects of FNR and of growth rate. Past studies have used glucose as a carbon source (Kang *et al.*, 2005; Salmon *et al.*, 2003), however glucose represses expression from some FNR-activated genes due to catabolite repression, (Browning *et al.*, 2005; Lambden & Guest, 1976) and replacement of glucose by a less repressing fermentable carbohydrate would decrease these effects but to an unknown extent. To alleviate these problems Fink *et al.* used MOPS buffered LB with xylose (Fink *et al.*, 2007). LB is known to induce SPI-1 expression from late exponential phase (OD₆₀₀ 1.0, LEP) to early stationary phase (OD₆₀₀ 2.0, ESP) and by oxygen shock (Kröger *et al.*, 2013), but it can be problematic in physiological studies due to intrinsic differences in complex components (Sridhar & Steele-Mortimer, 2016), and xylose is a fermentable carbon source for *Salmonella* species (Rosenberg, 1980). Constantinidou *et al.* found that using MMA with fumarate and TMAO as alternative electron acceptors and glycerol as a non-fermentable non-repressing carbon source allowed WT and an Δfnr mutant in *E. coli* to have similar growth rates (Constantinidou *et al.*, 2006). We chose to use the same medium and growth conditions, MMA and static growth, as Constantinidou *et al.* but, found that in *S. Typhimurium*, growth rates of the WT and an isogenic Δfnr mutant were not the same (**Figure 3.2A & B**). The Δfnr mutant grew significantly slower than the WT and a $\Delta ssrAB$ mutant. The growth rate of a mutant missing the *ssrAB* and *fnr* ORFs, $\Delta ssrAB/fnr$, was not significantly different than WT. In a $\Delta ssrAB$ mutant, all SPI-2 expression is turned off (Colgan *et al.*, 2016; Xu & Hensel, 2010) thus, the difference in growth between the WT and Δfnr could be due to expression of SPI-2 genes. These differences in growth and fitness will be explored further in Chapter 5. Unless otherwise indicated, samples for all subsequent experiments were taken when cultures reached an OD₆₀₀ of 0.3. A Northern blot was used to show that our microaerobic growth condition was sufficiently oxygen limited for active FNR protein to be present. WT and Δfnr cultures were grown in MMA under aerobic (aerated flasks) and microaerobic (static flasks) conditions; the FNR-dependent sRNA *FnrS* (Durand & Storz, 2010) was induced in the WT under microaerobic growth, but not aerated conditions or in Δfnr (**Figure 3.2 C**).

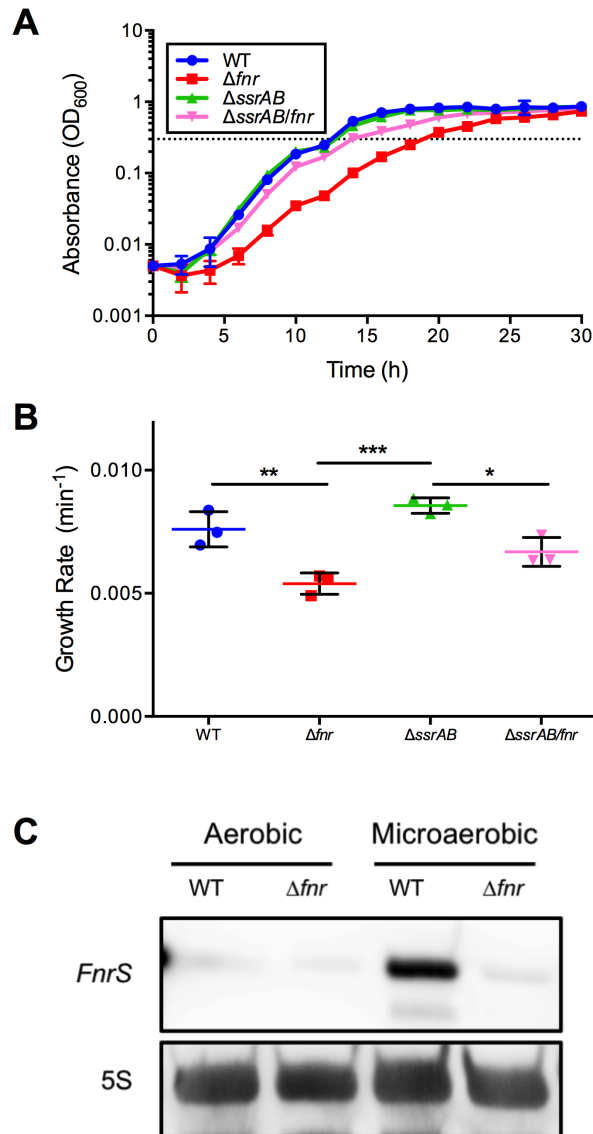


Figure 3.2 Growth of 4/74 and isogenic mutants and expression of *FnrS* under microaerobic conditions in MMA.

A. Growth curve of WT, Δfnr , $\Delta ssrAB$ and $\Delta ssrAB/fnr$. Strains were grown and sampled as previously described (Section 2.2.3.2). The dotted line indicates OD₆₀₀ 0.3, where samples were taken for all subsequent experiments. B. Best-fit growth rate determined from growth curves in A. Statistical significance was determined by an Ordinary One-Way ANOVA with Tukey's multiple comparisons test, only significant differences are labeled, * = $p \leq 0.05$, ** = $p \leq 0.01$, *** = $p \leq 0.001$, the error bars represent standard deviation. C. Northern blot showing *FnrS* expression in MMA under aerobic and microaerobic conditions. 5S RNA was probed as loading control.

3.2.2 Reproducibility of RNA-seq data

Inherent biological variability and random variation, such as that introduced during sample preparation, are features of any assay used in microbiology. Replication of experiments is necessary to identify and minimise the variation in experimental systems (Quackenbush, 2002), and to provide statistical significance for the acquired data. RNA-seq data has been previously shown to be highly reproducible, even for independent samples (Colgan *et al.*, 2016; Kröger *et al.*, 2013). The sequencing data used in this study were acquired in two separate sequencing runs using independent RNA samples. Additionally, it was important to show that our microaerobic growth condition was reproducible. It was, therefore, important to quantify the reproducibility of the results between sequencing runs to compare gene expression across both replicates. Independent biological replicates of WT and Δfnr grown to OD₆₀₀ 0.3 in microaerobic MMA were generated by Dr. Aoife Colgan and myself. The reproducibility and robust nature of the RNA-seq-based transcriptomic data set and the reproducibility of the microaerobic environment were confirmed using correlative analysis of the independent biological replicates. WT and Δfnr replicates had high values coefficient of determination or R² of 0.9209 and 0.8844, respectively (**Figure 3.3**). During downstream analyses, independently extracted RNA was used to validate many RNA-seq-based findings by northern blot and RT-qPCR.

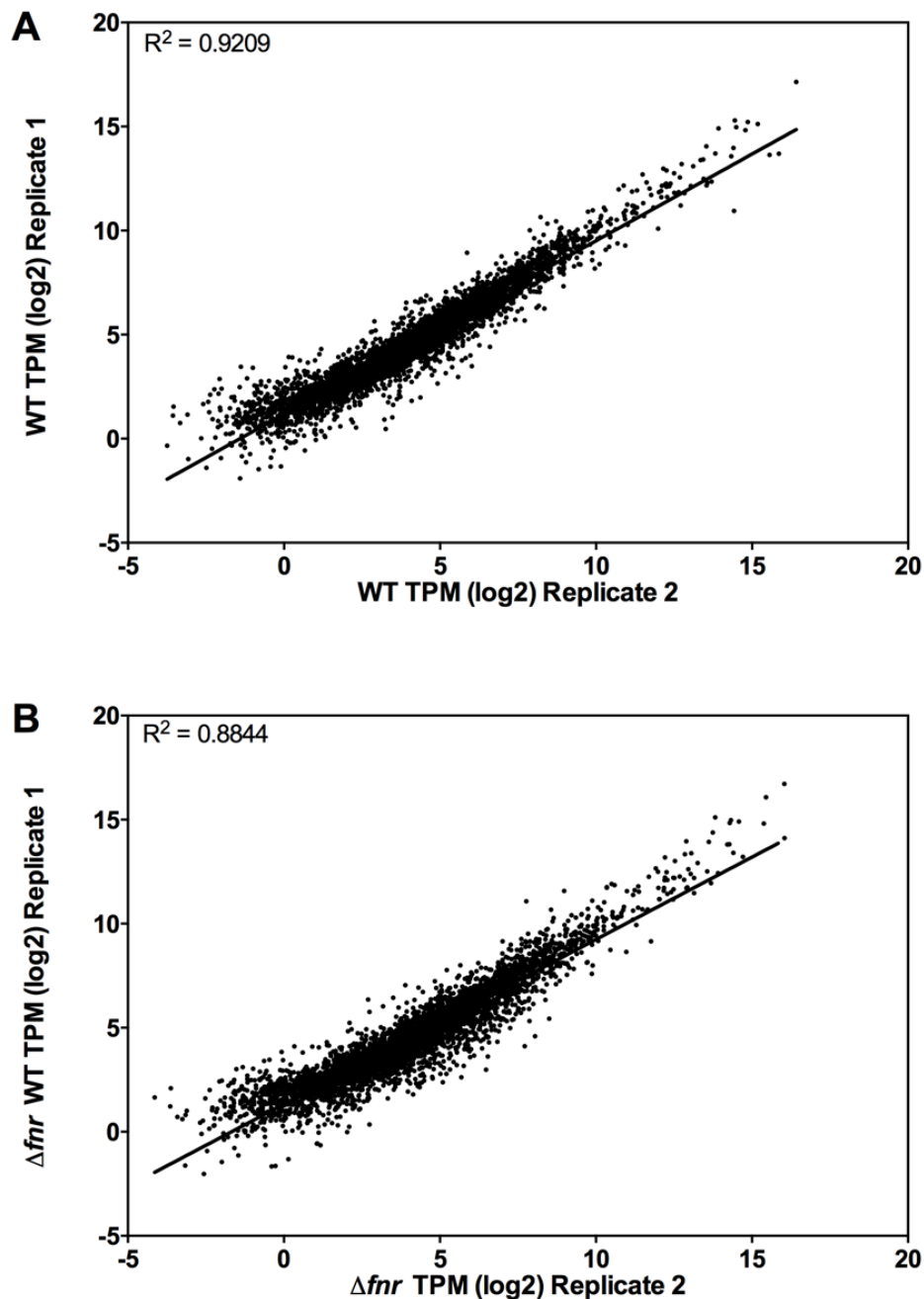


Figure 3.3 High correlation of RNA-seq data from independent biological replicates.

RNA-seq-based transcriptomic data comparing log₂ transcripts per million (TPM) values from (A) wild-type and (B) Δfnr cells grown to OD₆₀₀ 0.3 in MMA in microaerobic conditions show a high level of correlation with an independent biological replicate sequenced in a separate sequencing run. Media preparation, culture growth and RNA isolation for replicate 1 was performed by Dr. Aoife Colgan, media preparation, culture growth and RNA isolation for replicate 2 was performed by me.

3.2.3 Absence of polar effects in Δfnr

A polar mutation affects expression of downstream genes or operons and it is not desirable in a strain to be used for determining differences in gene expression. The isogenic *fnr* mutant used in this study was constructed by Dr. Aoife Colgan using the Datsenko and Wanner method of gene deletion (Datsenko & Wanner, 2000). This method involves replacing the gene of interest with an antibiotic resistance cassette by homologous recombination. The recombination event is mediated by the plasmid-encoded recombinase system of Bacteriophage λ (Murphy, 1998). The resistance cassette is amplified from a plasmid using oligonucleotides which also contain sequences homologous to the DNA on either side of the gene to be deleted. FLP recombinase target (FRT) sites flank the plasmid-encoded resistance gene to allow for removal of the antibiotic resistance gene from the resultant mutant strain using the pCP20 plasmid which encodes the yeast FLP recombinase (Cherepanov & Wackernagel, 1995). Removal of the antibiotic resistance gene leaves an 82–85 bp scar which contains an idealised ribosome binding site and a start codon to allow for expression from the downstream gene. To avoid polar effects, the mutant was transduced into a clean genetic background and then the kanamycin resistance cassette was removed. **Figure 3.4** shows RNA-seq data from the region surrounding *fnr* in the WT and Δfnr (visualised using the Integrated Genome Browser IGB) (Nicol *et al.*, 2009). In the WT, *fnr* is expressed under our growth condition, while no reads have mapped to the ORF of *fnr* in the Δfnr mutant, indicating that the deletion was successful. The genes immediately up- and downstream of *fnr* are *ogt* and *ydaA*. Expression of *ogt* was only 1.34 fold up-regulated in Δfnr , and it is expressed from its own promoter and lies upstream of the deletion, indicating the small difference is unlikely a polar effect. The *ydaA* gene is also encoded from its own promoter but, lies downstream of the *fnr* gene. Expression of *ydaA* was reduced 2.18-fold in the absence of FNR. The *ydaA* gene encodes for the universal stress protein UspE in *S. Typhimurium*, and expression of *ydaA* is highest under anaerobic shock and during anaerobic growth in WT cells (Kröger *et al.*, 2013). It is possible that the *ydaA* gene is regulated by FNR under microaerobic and/or anaerobic conditions, resulting in the decrease in *ydaA* expression in the Δfnr mutant. In *E. coli* there is a regulatory link between FNR and *ydaA* via GadX (Constantinidou *et al.*, 2006; Hodges *et al.*, 2010). There is no *gadX* orthologue in *S. Typhimurium* but, it may be possible that an alternative regulatory link exists between FNR and *ydaA* in *Salmonella*. Therefore, there were no polar effects from the deletion of the *fnr* gene. Additionally, an *fnr*⁺ complementation was created to corroborate the absence of polar effects of the Δfnr mutant.

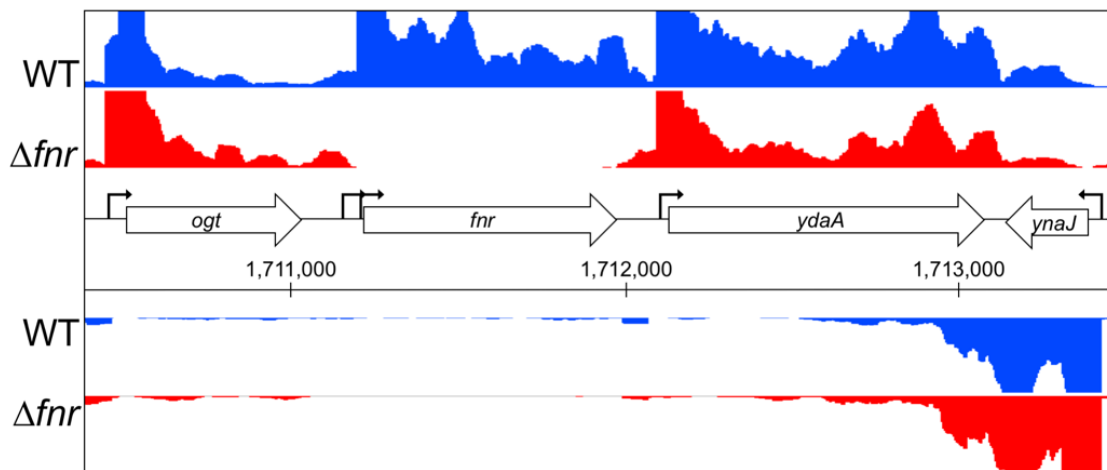


Figure 3.4 Confirmation of *fnr* chromosomal deletion by RNA-seq.

Visualization of sequenced reads in the surrounding region of the deleted *fnr* open reading frame in the mutant strain and WT, grown under microaerobic conditions in MMA, in the Integrated Genome Browser. The tracks for the WT and Δfnr mutant are blue and red, respectively. The colours of each track represent the sequencing reads which map to that locus and the height of the normalised reads is directly proportional to the level of expression at that locus, the scale is 0–100 normalized reads for each sample. The tracks demonstrate that *fnr* was expressed in the WT strain, and that no sequencing reads mapped to the deleted region in Δfnr . Neighbouring genes were generally not affected by polar mutations. White arrows with a black outline denote protein-coding genes. Black bent arrows indicate TSS. All arrows indicate the direction of transcription. The Δfnr deletion mutant was constructed by Dr. Aoife Colgan.

3.2.4 Complementation of the Δfnr mutant

Complementation of a mutant strain is important to show that any observed phenotype can be rescued and therefore, that the observed phenotype is due to the mutation in question and not a polar effect or additional unintended mutation. The Δfnr mutant was complemented both by cloning of *fnr* and its native promoter (215 nt upstream) onto the pBR322 plasmid, *pfnr*, and by introducing the same cloned fragment onto the chromosome downstream of *glmS* to create *fnr*⁺. The plasmid *pfnr* overexpressed *fnr* 36.8-fold over WT levels, but rescued *FnrS* expression to approximately normal levels in the mutant (**Figure 3.5**). However, in later experiments including motility assays and macrophage infections, *pfnr* performed poorly, therefore the chromosomal complementation was constructed (See **Figure 2.1** in section 2.5.3). The advantage of a chromosomal complementation is that there

is only a single copy of the gene, compared to plasmid complementation where multiple copies are present in the cell, even when low-copy plasmids have been used. The chromosomal complementation *fnr*⁺, expressed *fnr* to levels slightly lower but not significantly different from WT when examined by RT-qPCR, and rescued *FnrS* expression on a Northern blot. A growth curve was performed in a microplate reader under anaerobic conditions which showed *fnr*⁺ was able to restore WT growth (**Figure 3.6**).

Interestingly, Baek *et al.* discovered a 66 nt unannotated ORF, named *mia-44*, in the *fnr* promoter region beginning with a start codon 218 bp from the *fnr* start codon in *S. Typhimurium* 14028s (Baek *et al.*, 2017). After many failed attempts at cloning *fnr* with 400 bp upstream of the *fnr* start codon new oligonucleotides were designed that eliminated the putative ribosome binding site and ATG, leaving 215 bp of sequence upstream of the *fnr* start codon. A cloning attempt with the shorter sequence was immediately successful. This finding indicates that overexpression of *mia-44* may be toxic in *E. coli*, as cloning was attempted in *E. coli* TOP10.

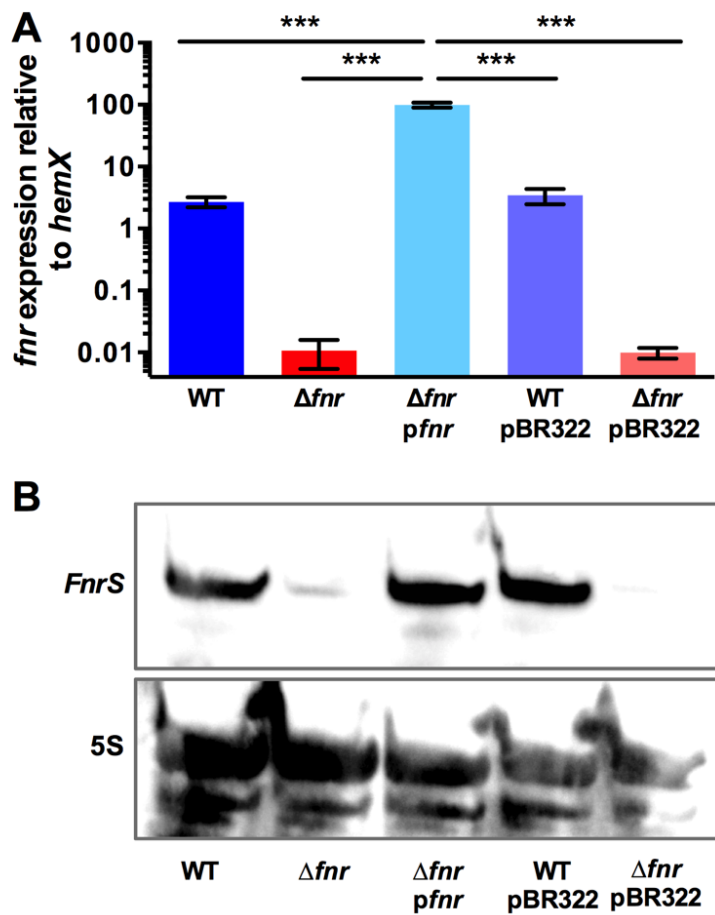


Figure 3.5 *pfnr* overexpresses *fnr* but rescues *FnrS* expression in Δfnr .

RNA was extracted from cells grown to OD_{600} 0.3 in microaerobic MMA. A. RT-qPCR data showing *fnr* expression relative to *hemX*. Statistical significance was determined by an Ordinary One-Way ANOVA with Tukey's multiple comparisons test, only significant differences are labeled, *** = $p \leq 0.001$, the error bars represent standard deviation. B. Northern blot showing *FnrS* expression is rescued by *pfnr* in the Δfnr mutant. 5S RNA was probed as loading control.

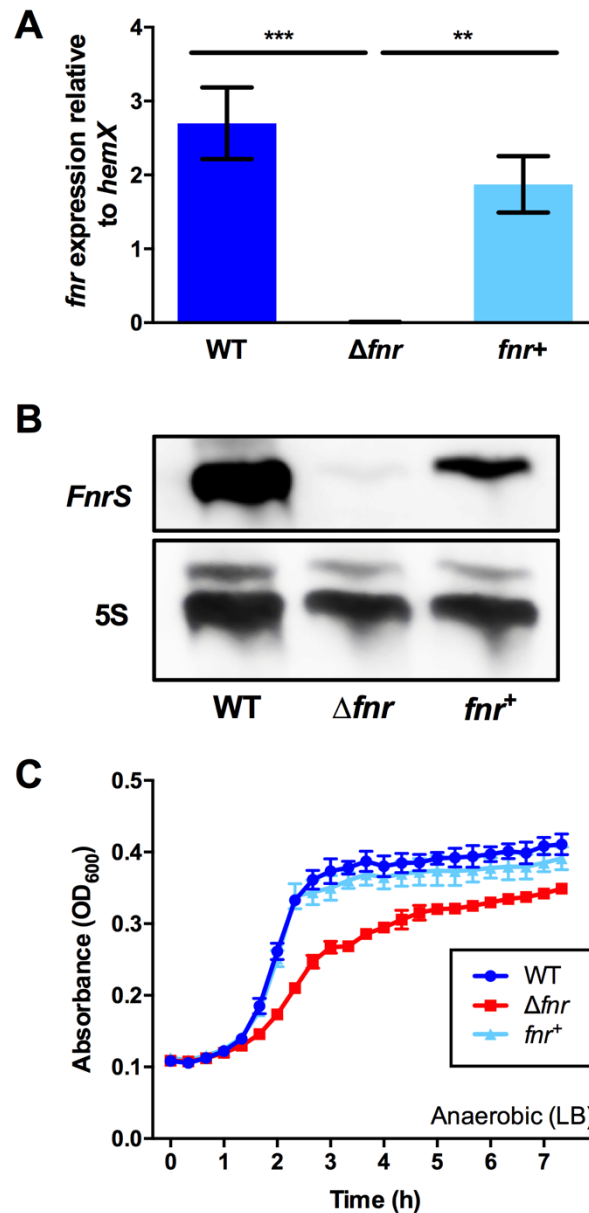


Figure 3.6 *fnr*⁺ rescues *FnrS* and *fnr* expression under microaerobic & anaerobic conditions.

RNA was extracted from cells grown to OD₆₀₀ 0.3 in microaerobic MMA for A and B. A. RT-qPCR data showing *fnr* expression is shown relative to *hemX*. Statistical significance was determined by an Ordinary One-Way ANOVA with Tukey's multiple comparisons test, only significant differences are labeled, ** = $p \leq 0.01$, *** = $p \leq 0.001$, the error bars represent standard deviation. B. Northern blot showing *FnrS* expression is partially recovered by the complementing strain *fnr*⁺ under microaerobic conditions in MMA. 5S RNA was probed as loading control. C. Growth curve showing *fnr*⁺ rescues growth rate of the mutant in LB under anaerobic conditions performed by Dr. Daniel Ryan.

3.2.5 RNA-seq determines differentially expressed genes in Δfnr

The relative expression levels during microaerobic growth of all genes found in *S. Typhimurium* 4/74 on the chromosome and its three plasmids, pColIb9, pRSF1010 and pSLT can be observed in **Figure 3.7**. The log₂ ratios of Δfnr mutant TPM over WT TPM were plotted against their location on the chromosome or plasmid. Genes which were below the 2-fold cut-off (or between log₂ of -1 to 1) were not considered to be differentially expressed (DE). DE genes in the Δfnr mutant when compared to WT were organized into clusters of orthologous groups (COGs) according to the gene list in **Table S2** in Appendix II with the addition of virulence genes, sRNAs and unknown genes (**Figure 3.8**). In total, 482 genes and sRNAs were regulated directly or indirectly by FNR under microaerobic conditions in MMA. 286 genes were activated by FNR and 196 were repressed. Not surprisingly, FNR activated many genes categorized into anaerobic metabolism. Additionally, many genes from energy production and conversion were FNR activated. Approximately 2/5 of these genes overlap with genes of anaerobic metabolism, and the majority of the remaining genes in this category encoded NADH dehydrogenase subunits. The vast majority of genes activated by FNR fell into the chemotaxis and motility, surface structures, and cell motility and secretion categories which have a high degree of redundancy. There were no genes categorized into drug analogues and resistance, protein transport, or translation, ribosomal structure and biogenesis. Many unknown genes could not be categorized as they had either unknown function, were poorly characterized or had only a general predicted function. In total 56 unknown genes were activated by FNR and 86 were repressed. The majority of genes found to be repressed by FNR did not fall into the typical COG categories; These were virulence associated genes and sRNAs. The virulence genes up-regulated in the Δfnr mutant were predominantly SPI-2 encoded or associated genes.

The most interesting feature of this data set is the up-regulation of genes encoding SPI-2 regulators, T3SS apparatus proteins, effector proteins, and chaperones (**Figure 3.9**). The 15 kb portion of the pathogenicity island with genes for tetrathionate reductase and of unknown function (Hensel, 2000) was not differentially expressed in Δfnr due to the lack of tetrathionate in the growth medium. Notably, many genes which are not encoded in SPI-2, but that are induced in SPI-2 inducing conditions (Kröger *et al.*, 2013) and many of which are effectors that are secreted through the SPI-2 T3SS were also up-regulated in the Δfnr mutant. These included effectors such as *pipB2*, *sifA*, *sifB*, *sopD2*, *sseJ*, *sseK2*, *sseL*, *steA*, and *steC*.

Also up-regulated in Δfnr were the genes from the *spv* (*Salmonella* plasmid virulence) locus found on the low-copy *Salmonella* virulence plasmid pSLT. The *spv* locus encodes the *spvABCD* operon and a positive regulator *spvR*. SpvA is an outer membrane protein that can dampen the expression of the operon, while SpvB, SpvC and SpvD are translocated into the host cell by the SPI-2 T3SS. Genes from this locus are required for full virulence in mice (Grabe *et al.*, 2016; Guiney & Fierer, 2011; Passaris *et al.*, 2018). Five PhoP-activated genes (*pag*) were up-regulated in Δfnr including the SPI-11 encoded outer membrane virulence proteins *pagC* and *pagD* which are involved in intramacrophage survival (Gunn *et al.*, 2000; Sabbagh *et al.*, 2010), the bacteriophage encoded virulence protein *pagK*, flagella-independent surface motility genes *pagM*, and inner membrane protein *pagO* (Gunn *et al.*, 2000; Park *et al.*, 2015). All of these genes are upregulated under SPI-2 inducing conditions and in macrophages (Kröger *et al.*, 2013; Srikumar *et al.*, 2015).

Genes from SPI-1, SPI-3 and SPI-4 were not DE in Δfnr and had low absolute expression in both the WT and Δfnr (**Figure 3.10A, B, & C**). The most down-regulated locus in our data set was the SPI-5 encoded gene *orfX* which was 62-fold down-regulated in Δfnr (**Figure 3.10D**). Very little is known about the specific function of *orfX* however it appears to be important for infection of chicken, pigs and calves, but not in mice (Chaudhuri *et al.*, 2013). Also encoded in SPI-5, the effector protein *pipB* was up-regulated 8.5-fold in Δfnr (**Figure 3.10D**). Similar to *orfX*, very little is known about the function of *pipB* however it is secreted via the SPI-2 T3SS (Jennings *et al.*, 2017).

DE genes which were down-regulated in Δfnr included metabolism operons that were likely upregulated in the WT because of the nutrients that were either available or missing in the growth medium. These genes included proteins for cobalamin (vitamin B₁₂) biosynthesis (*cbiFJKLMQT*) and propanediol degradation (*pduBDEGHJKMNQSV*). Previously, CRP and ArcAB were shown to regulate these operons when cells were provided a poor carbon source under aerobic conditions and anaerobic conditions (Ailion *et al.*, 1993). This data suggested that FNR may also play a role in the activation of these operons, and that since there is no added propanediol in MMA, that *S. Typhimurium* could be converting glycerol to propanediol. Interestingly, a recent proteomic study of Δfnr in SL1344 showed that under anaerobic growth in MOPS buffered LB with xylose, the propanediol utilization proteins were up-regulated (Wang *et al.*, 2019), suggesting a dual role for FNR in the regulation of propanediol utilization dependent on available nutrients. We also saw down-regulation of the glycerol metabolism operon *glpABC*, which has previously been described to be under

the indirect control of Fur, but Fur binding sites were not found in the promoter (Troxell *et al.*, 2011). Expectedly, anaerobic metabolism genes necessary for nitrate, TMAO and fumarate reduction, *narJ*, *dmsABC* and *frdABCD*, respectively were also down-regulated. Genes encoding proteins for hydrogenase maturation *hypBCDEO* and *hybABCDEFG* encoding a hydrogenase, HYD2, that is responsible for uptake of hydrogen as an electron donor during anaerobic respiration, with fumarate serving as an electron acceptor were both down regulated in the absence of FNR. NADH hydrogenase I (NDH-I) catalyzes the first step of electron transport by the oxidation of NADH and is the preferred NADH hydrogenase under oxygen limited conditions as it is “energy conserving” (Price & Driessen, 2010). NDH-I subunits are encoded by *nuoABCDEFGHIJKLMN* and were downregulated in Δfnr . Finally, two outer membrane porins (OMPs) *ompD* and *ompW* were down-regulated in the mutant. These OMPs are required for the efflux of methyl viologen, a charged quaternary ammonium compound that generates ROS under aerobic growth conditions (Gil *et al.*, 2007). *OmpW* was also down-regulated in an Δfnr mutant recent study grown under anaerobic conditions in MOPS-buffered LB with xylose (Wang *et al.*, 2019). The gene encoding *OmpW* was highly down-regulated approximately 21.5-fold. These results suggest that FNR is involved either indirectly or directly in the regulation of many different categories of genes.

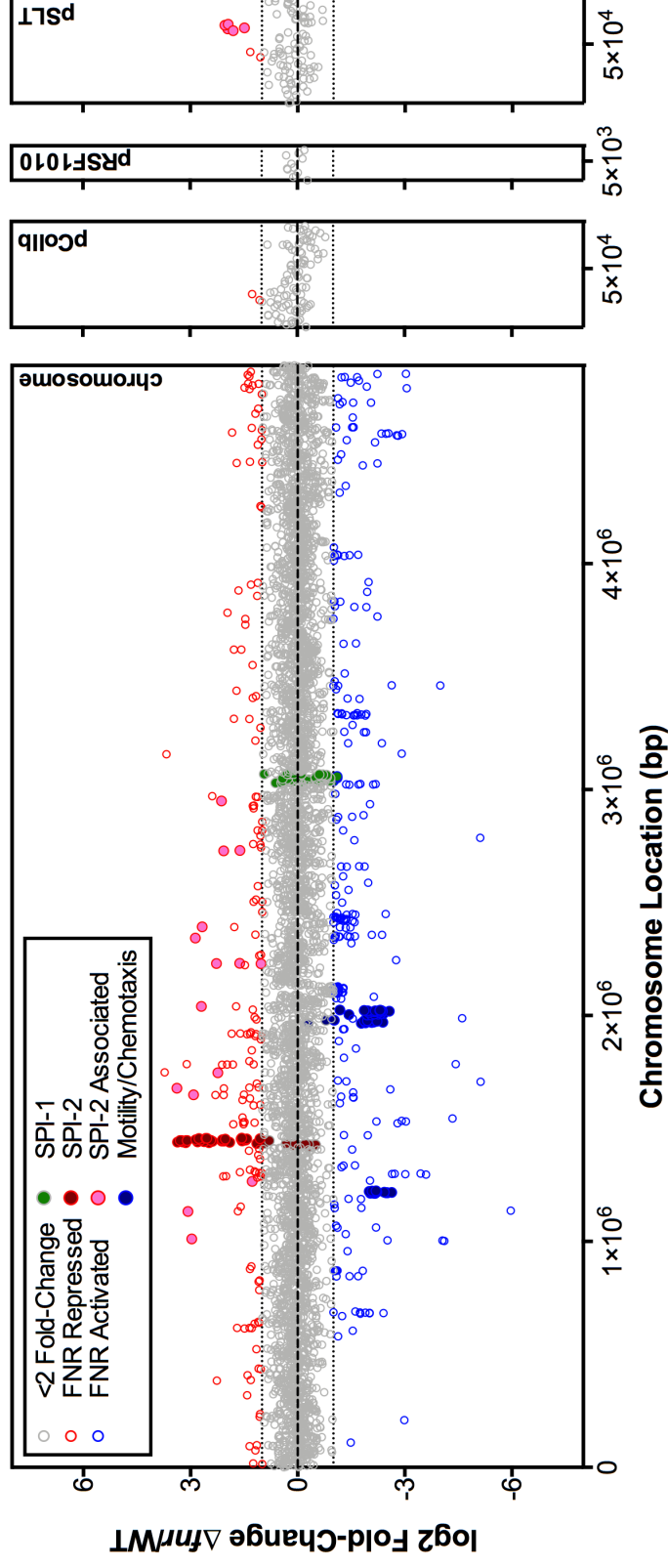


Figure 3.7 Relative gene expression across the *S. Typhimurium* chromosome and plasmids.

Comparing the transcriptome of Δfnr over WT shows genes that are activated and repressed by FNR under microaerobic conditions in MMA. The first panel shows transcripts from the chromosome followed by the three plasmids present in *S. Typhimurium* 4/74: pCollb, pRSF1010, and pSLT. Circles with a grey outline were less than 2-fold (\log_2 ratio between 1 to -1) different, circles with a red outline were upregulated in Δfnr and circles with blue outline were down-regulated in Δfnr , implying that FNR is a repressor or activator, respectively. Circles filled with green belong to SPI-1, dark red-filled circles belong to SPI-2, pink-filled circles represent SPI-2 associated genes and dark blue-filled circles belong to motility and chemotaxis genes/operons. A \log_2 value of 0 indicates no change in expression, and we used a cut-off of 1 to -1, denoted by dotted lines, to indicate differential expression.

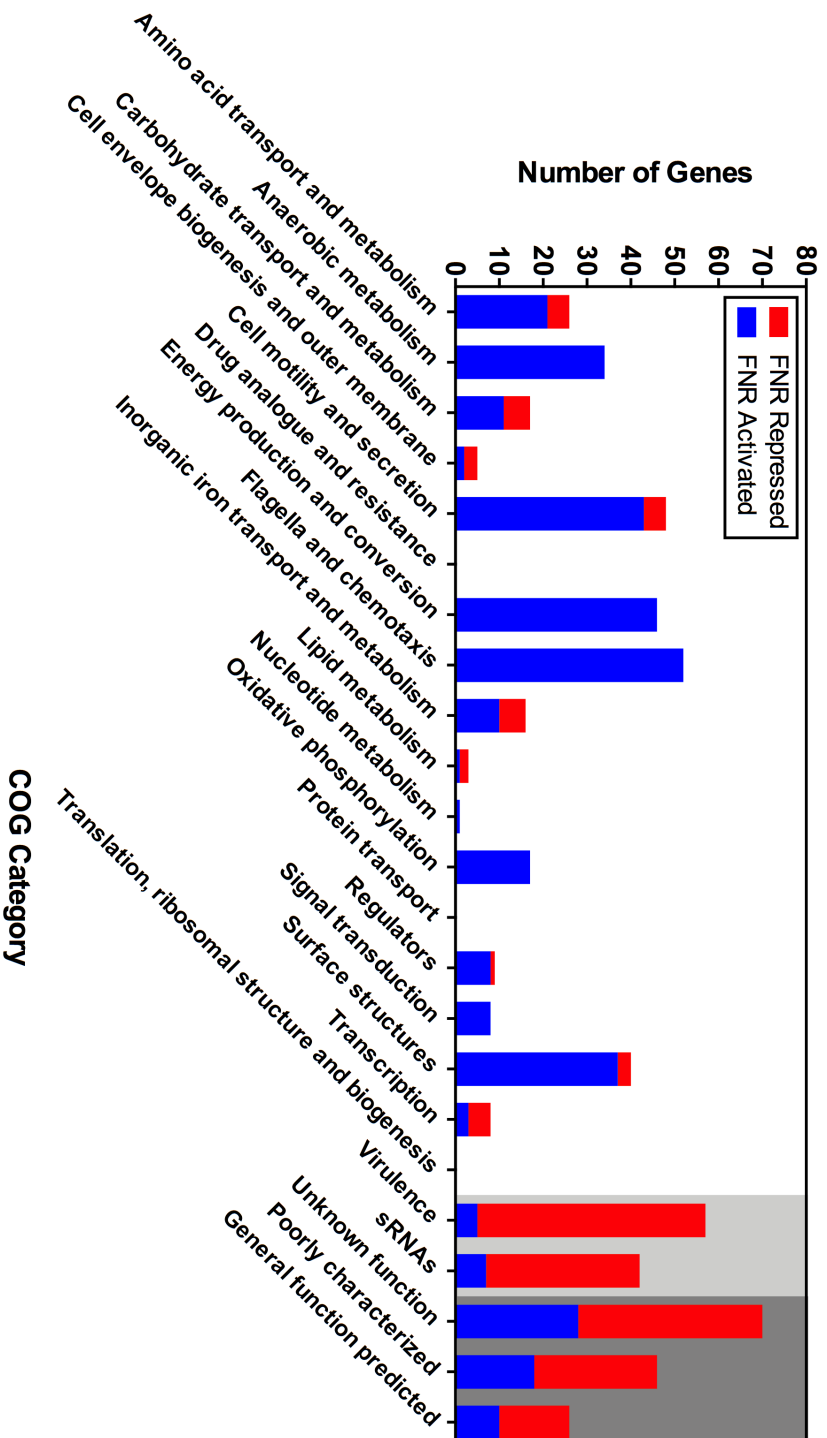


Figure 3.8 Classification of FNR-regulated genes according to COGs.

Genes which were ≥ 2 -fold differentiated were organized into COG categories according to (white panel) **Table S2** in Appendix II, (light grey panel) virulence associated genes and transcripts encoding sRNAs, and (dark grey panel) unknown categories. Red and orange bars indicate FNR repressed and activated genes, respectively. The complete list of genes in each category can be found in **Table S3** in Appendix II.

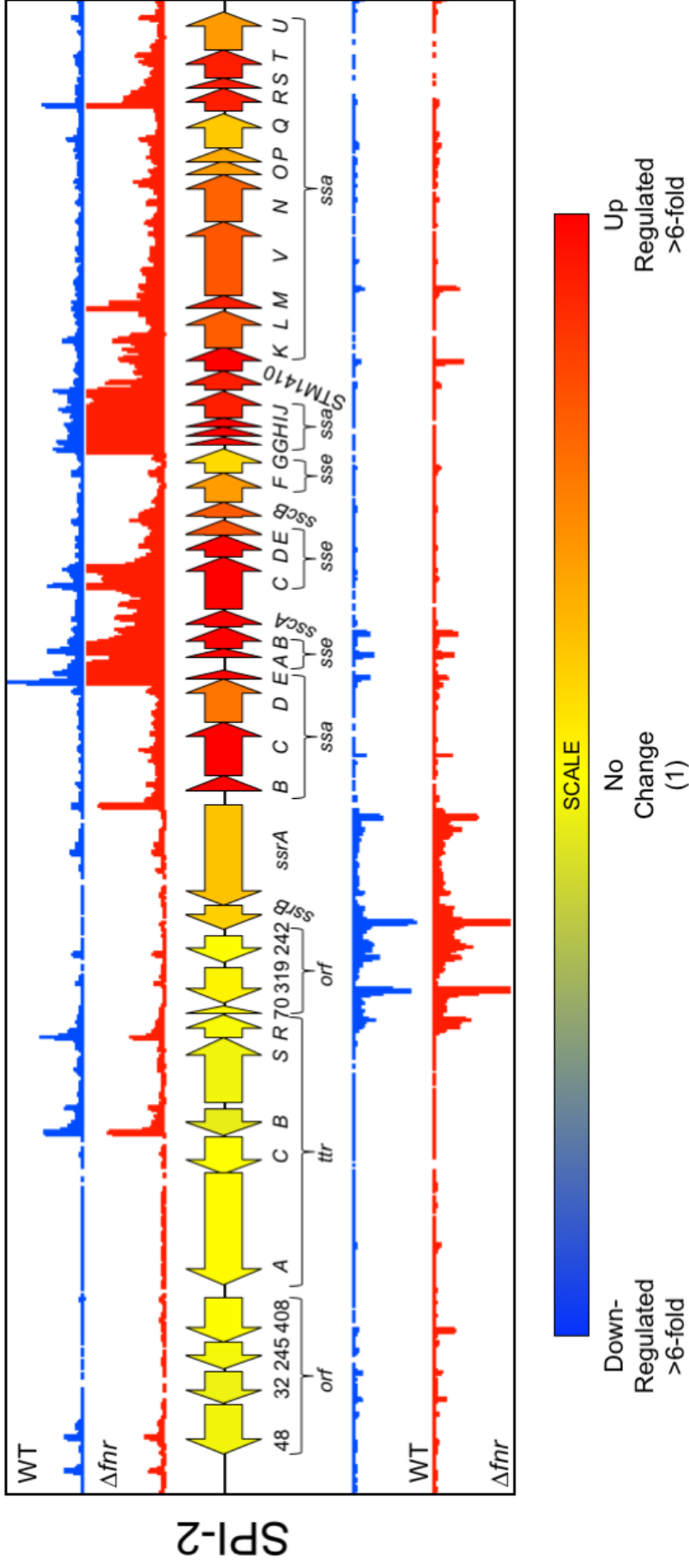


Figure 3.9 SPI-2 expression is highly up-regulated in the absence of FNR.

Visualization of relative gene expression and sequenced reads at SPI-2 in the Δfnr mutant and WT, grown under microaerobic conditions in MMA. Each arrow represents a gene and the colour represents the relative gene expression according to the scale bar. The IGB tracks for the WT and Δfnr mutant are blue and red, respectively. The colours of each track represent the sequencing reads which map to that locus and the height of the normalised reads is directly proportional to the level of expression at that locus, the scale is 0–100 normalized reads for each sample.

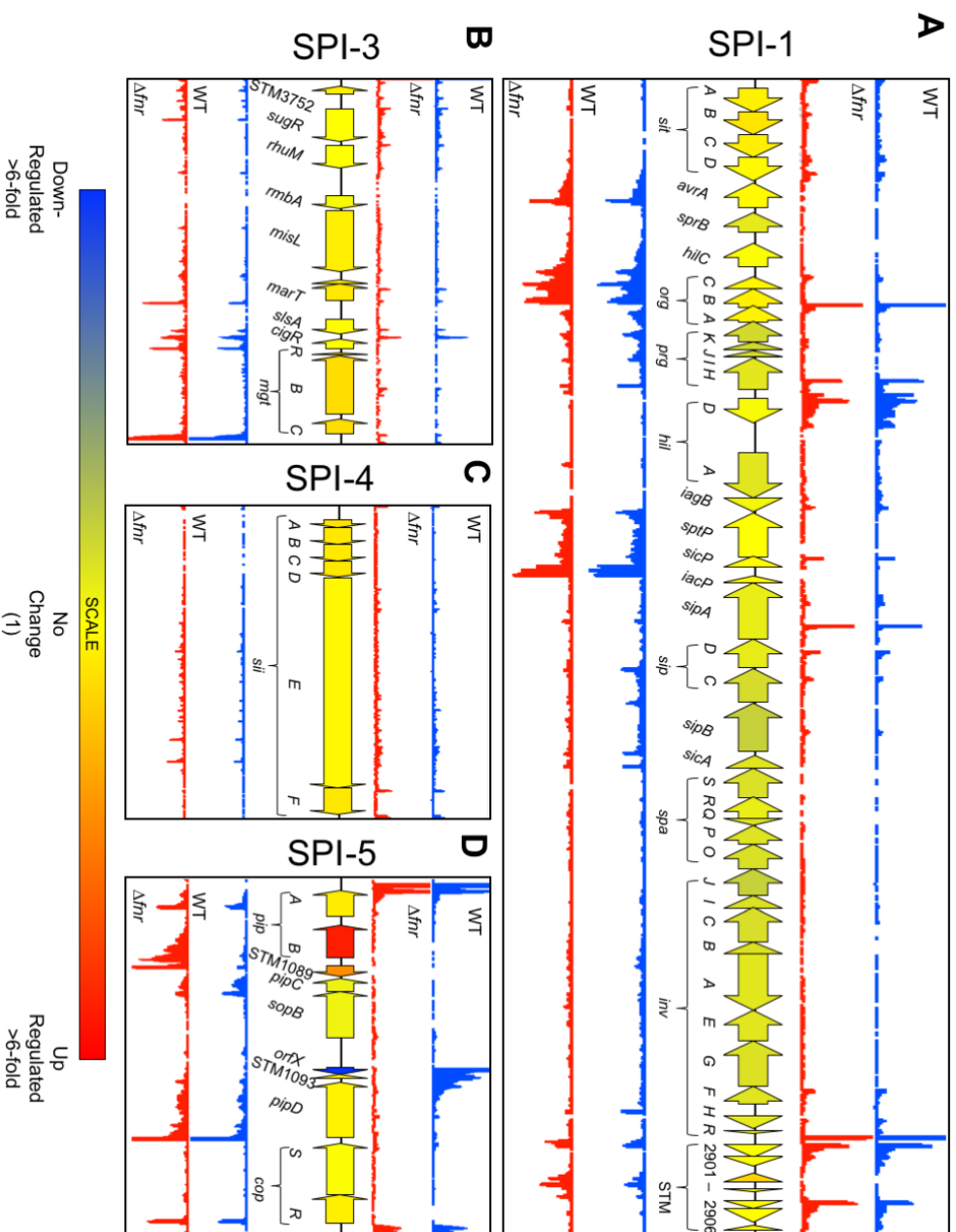


Figure 3.10 Low level absolute and relative expression in SPI-1, 3, 4 and 5.

Visualization of relative gene expression and sequenced reads at A. SPI-1, B. SPI-3, C. SPI-4 and D. SPI-5 in the *Δfnr* mutant and WT, grown under microaerobic conditions in MMA. Each arrow represents a gene and the colour represents the relative gene expression according to the scale bar. The IGB tracks for the WT and *Δfnr* mutant are blue and red, respectively. The colours of each track represent the sequencing reads which map to that locus and the height of the normalised reads is directly proportional to the level of expression at that locus and the scale is 0–100 normalized reads for each sample.

3.2.6 SPI-2 is derepressed in Δfnr under microaerobic conditions in MMA

SPI-2 genes were some of the most up-regulated genes in the Δfnr mutant according to RNA-seq. Recently, the SPI-2 protein SsaH, encoded by *ssaH*, was found to regulate the secretion of an inner rod and early substrate, SsaI, and to form a heterodimer with the chaperone protein SseA, to switch to secretion of the needle protein SsaG (Takaya *et al.*, 2019). SseA, encoded by *sseA*, is essential for SPI-2-mediated translocation of effector proteins (Coombes *et al.*, 2003). The *ssaH* and *sseA* genes were 9.6- and 9.4-fold up-regulated in Δfnr according to RNA-seq; These data were validated by RT-qPCR of independent biological replicates. Expression of *ssaH* in Δfnr showed a 3.5-fold increase over WT ($P < 0.01$) (**Figure 3.11A**), and expression of *sseA* increased 2-fold in Δfnr over WT ($P < 0.01$) (**Figure 3.11B**). Expression of *ssaH* and *sseA* in fnr^+ was not significantly different from WT, expression of *ssaH* in WT was not significantly different from the negative control *ssrAB*, and expression of *sseA* in WT was significantly higher than in $\Delta ssrAB$ (**Figure 3.11A & B**). When WT, Δfnr and $\Delta ssrAB$ were grown in microaerobic LB there was little expression of *ssaH* or *sseA*, and these values were not significantly different (**Figure 3.11C & D**). Gene expression was normalized to expression of the gene *hemX*, that has the same level of expression in WT and Δfnr in MMA FT according to RNA-seq data. These RT-qPCR data confirm that FNR represses expression of SPI-2 in WT and fnr^+ *S. Typhimurium* cells grown in MMA under microaerobic conditions.

To demonstrate the ability of FNR to block SPI-2 expression at decreasing O₂ concentrations, we developed an assay using a soft MMA agar (1% agar w/v) that creates an oxygen gradient within a test tube and strains with transcriptional fusion of the *ssaG* promoter with *gfp* (Hautefort *et al.*, 2003). Encoded by *ssaG*, SsaG proteins make up the needle structure of the SPI-2 T3SS (Diepold & Wagner, 2014). Because FNR is only active in oxygen-limited environments, cells growing at the surface of the agar would have inactive or apo-FNR proteins, while cells growing deeper in the agar experience microaerobic and anaerobic environments where FNR would form active homodimers (**Figure 3.12A**). WT, fnr^+ and $\Delta ssrAB$ cells grown in the MMA soft agar could proliferate throughout the media, while Δfnr cells could only grow near the surface due to the lack of O₂ deep in the agar and the absence of FNR in the cell preventing anaerobic respiration. The point at which Δfnr cells stopped growing is indicated with an arrow (**Figure 3.12B**). In WT and fnr^+ cells, *ssaG-gfp*⁺ was expressed only at the surface of the agar, while in Δfnr cells *ssaG-gfp*⁺ expression

was observed deeper into the agar, to the boundary of cell growth (**Figure 3.12B**). Active FNR protein homodimers in WT and *fnr*⁺ repressed SPI-2 expression in the microaerobic and anaerobic portions of the media; In Δ *fnr*, The FNR protein is absent therefore, SPI-2 was not repressed. The Δ *ssrAB* mutant was used as a negative control for *ssaG-gfp*⁺ expression, and WT transformed with the pDIGc plasmid, which expresses GFP from a strong promoter driving the expression of the ribosomal protein RpsM, was used as a positive control for GFP expression to show how deep into the media GFP fluoresces (**Figure 3.12B**).

Because cells can differ phenotypically when grown in agar versus in broth cultures, it was important to verify that SPI-2 expression was derepressed in WT cells in aerobically grown MMA broth cultures. WT, Δ *fnr* and Δ *ssrAB* strains transformed with pDEW201-P_{*ssaG*}, which express *luxCDABE* from the *ssaG* promoter, were grown in MMA to OD₆₀₀ 0.3 under aerobic and microaerobic conditions. Expression of *ssaG* was significantly higher in aerated WT samples than in static growth ($p < 0.001$): expression was 1.8 fold higher (**Figure 3.13A & B**). In the Δ *fnr* mutant, microaerobic cultures had significantly higher expression than in aerated samples ($p < 0.05$) however, they were less than 1-fold different, and there was no expression in Δ *ssrAB* under either growth condition (**Figure 3.13A & B**). Interestingly, expression of *ssaG* in aerated WT cultures was not as high when compared to aerated Δ *fnr* cultures, indicating there may be another factor involved.

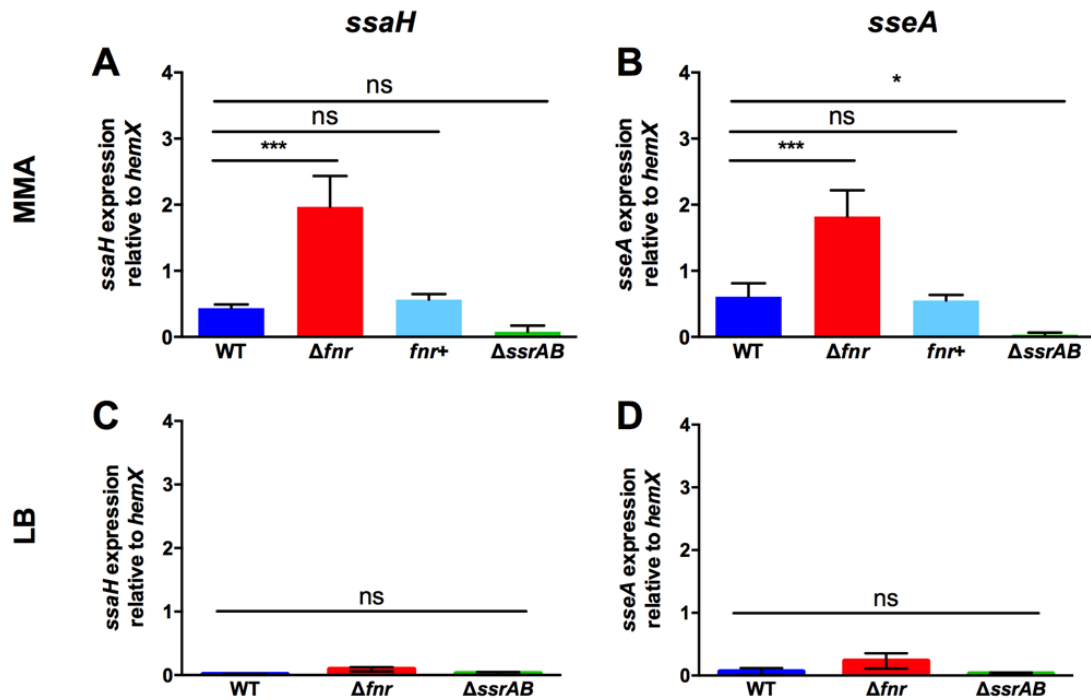


Figure 3.11 SPI-2 apparatus and effector expression is up-regulated in Δfnr under microaerobic conditions in MMA.

RT-qPCR data showing that cells grown under microaerobic conditions in MMA had A. *ssaH* and B. *sseA* expression relative to *hemX* that was significantly higher in Δfnr than WT and *fnr*⁺. RT-qPCR data showing that cells grown under microaerobic conditions in LB did not have significantly different expression relative to *hemX* of C. *ssaH* and D. *sseA*. Statistical significance determined by Ordinary one-way ANOVA with Tukey's multiple comparisons test compared to WT, ns = $p > 0.05$, * = $p \leq 0.05$, *** = $p \leq 0.001$, error bars represent standard deviation.

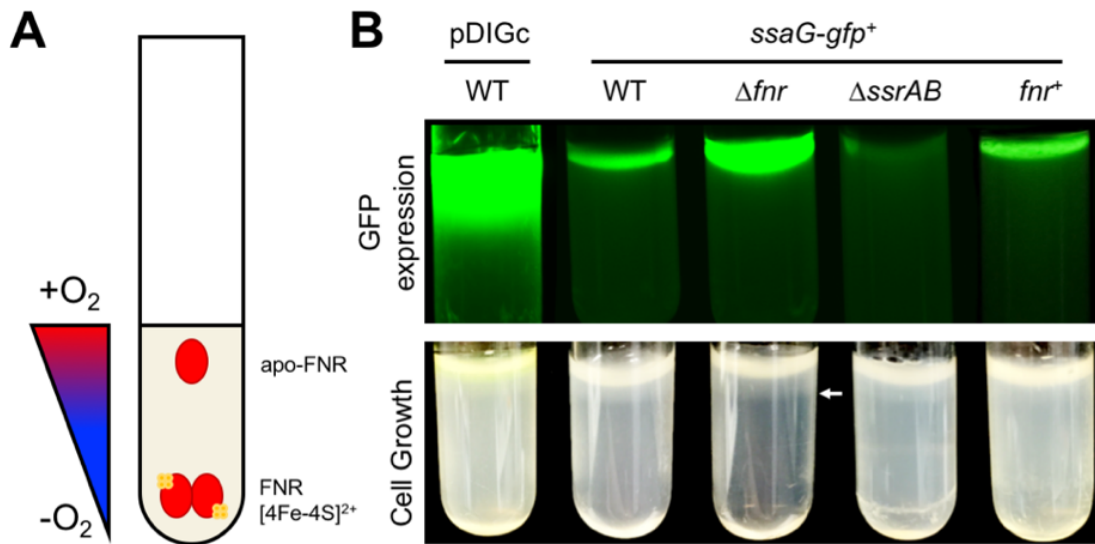


Figure 3.12 FNR blocks *ssaG* expression under low O₂ conditions.

A. Schematic explaining the presence or absence of active FNR dimers according to an oxygen gradient formed by 1% agar in MMA. B. Oxygen gradient gene expression assay demonstrating the ability of FNR to block *ssaG-gfp*⁺ expression under low O₂ concentrations after 72 h. The top panel shows GFP expression in cells grown in MMA. The bottom panel shows bacterial growth of the same cultures in the 1% agar. The white arrow indicates the point at which the Δfnr mutant can no longer grow due to low O₂ concentration.

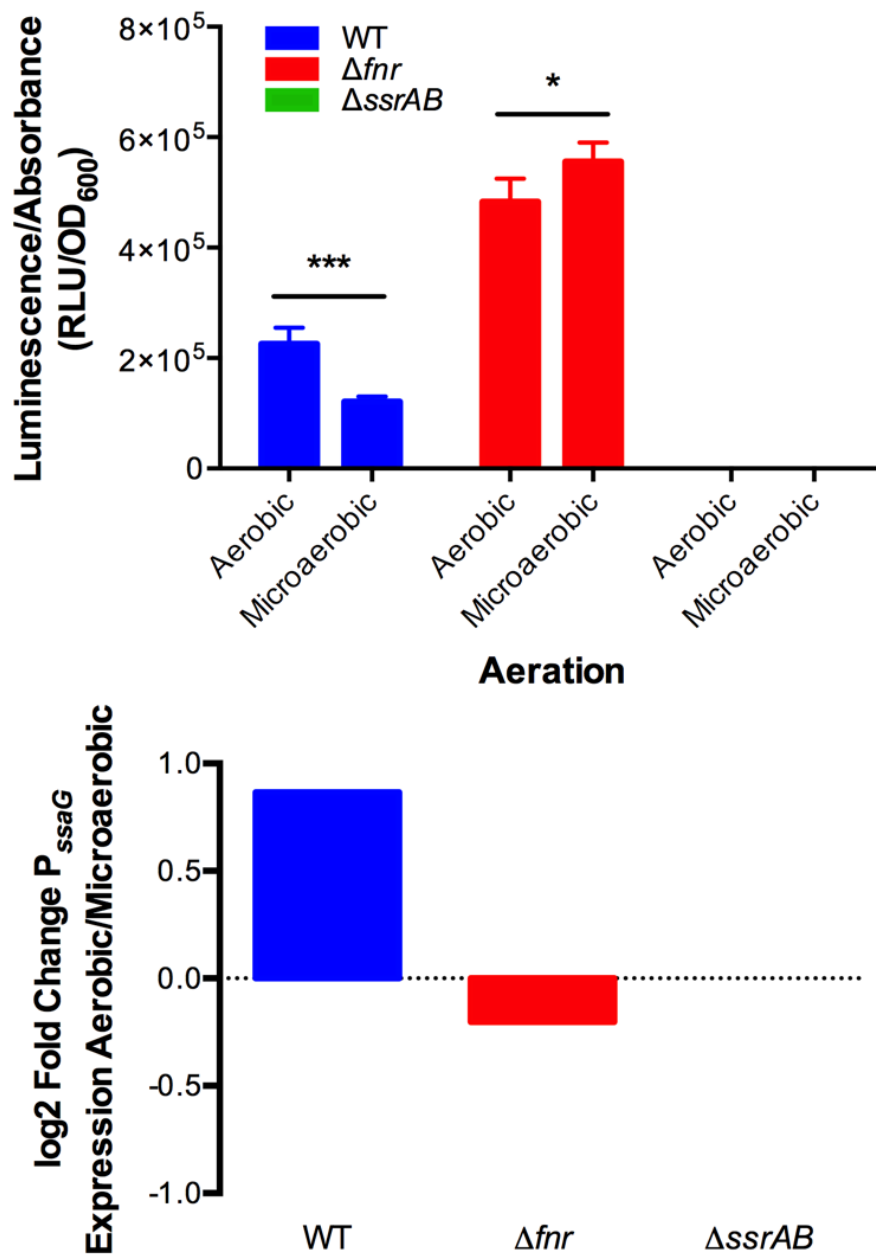


Figure 3.13 SPI-2 expression is increased in WT under aerobiosis.

Cells were grown in MMA under aerobic and microaerobic conditions to OD₆₀₀ 0.3; A. P_{ssaG} expression is shown in relative luminescence units over absorbance (RLU/OD₆₀₀) for WT, Δfnr and ΔssrAB. Statistical significance was determined between aerobic and anaerobic cultures using a two way ANOVA and Sidak's multiple comparisons test, only significant differences are shown; * = p ≤ 0.05, *** = p ≤ 0.001, error bars represent standard deviation. B. log₂ fold change in average aerobic over microaerobic P_{ssaG} expression.

3.2.7 Expression and secretion of effector proteins

The *S. Typhimurium* chromosome encodes for two type III secretion systems, T3SS-1 and T3SS-2, encoded on the pathogenicity islands SPI-1 and SPI-2, respectively. Several effector proteins are secreted through these systems into host cells. The cellular location of effectors examined by Western blot in this study are SPI-2 effectors PipB2 and SteC, and SPI-1 effector SopE. PipB2 is described as a “core” effector of SPI-2 although it is encoded outside of the SPI-2 locus (Jennings *et al.*, 2017). PipB2 is responsible for recruiting the host protein kinesin-1, a heterotetrameric, plus-end-directed microtubule motor protein, to the SCV as part of the process of *Salmonella*-induced tubule formation (Henry *et al.*, 2005; Jennings *et al.*, 2017). PipB2 is typically expressed in conjunction with SPI-2 encoded effector proteins although, it is secreted through both the T3SS-1 and T3SS-2 at different time points during infection (Baisón-Olmo *et al.*, 2012). The effector SteC is not encoded within the SPI-2 locus, but it is exclusively expressed under SPI-2 inducing conditions, inside epithelial cells and macrophages, and is secreted through T3SS-2 (Jennings *et al.*, 2017). SteC is found within the majority of intestinal serovars of *S. Typhimurium*; it is a kinase that manipulates the actin cytoskeleton by inducing assembly of the F-actin meshwork around the SCV inside of host cells (Jennings *et al.*, 2017). SopE is a guanidyl exchange factor, is translocated by the T3SS-1 upon host cell contact and promotes entry through triggering of actin-dependent ruffles (Galan & Zhou, 2000). Following host cell entry, SopE undergoes proteasomal degradation however, a subset of SopE may be important for replication in the early SCV (Vonaesch *et al.*, 2014).

Strains with 3×FLAG-tagged PipB2 and SteC proteins were grown in microaerobic MMA and aerobic SPI-2 inducing PCN (InSPI2) as a control. PipB2 levels were indistinguishable between WT, Δfnr and $hilD$ mutants in MMA, while there was no expression in $\Delta ssrAB$ (**Figure 3.14A**). Surprisingly, there was higher PipB2 expression in Δfnr when grown in aerated InSPI2, and a small amount of expression in $\Delta ssrAB$ (**Figure 3.14A**). When grown in microaerobic MMA, SteC expression was clearly higher in Δfnr than the other strains, but showed similar levels between WT, Δfnr and $\Delta hilD$ when aerobically grown in InSPI2 (**Figure 3.14B**).

T3SS delivery is a contact-dependent process characterized by the formation of a pore, or translocon, at the point of contact with the eukaryotic membrane and through which effectors are delivered into the host cell. Effector secretion into broth during *in vitro* culturing has

been observed, usually under acidic conditions which mimic the acidification of the SCV (Beuzón *et al.*, 2002). We hypothesized that effectors would not be secreted in MMA due to the neutral pH of the media. We attempted to see if SPI-2 effectors were secreted in MMA media. Whole cell lysates and culture supernatants were loaded on the same gel and probed with antibody on the same membrane. **Figure 3.15A and B** show that although there was high levels of PipB2 expression in both MMA and inSPI-2 cultures, we were unable to detect secreted protein by ponceau staining or Western blotting despite loading 50 OD units of culture supernatant. It is not clear if this was due to this protein not being secreted under these culturing conditions or if precipitation of the protein was not efficient. We did confirm, in agreement with RNA-seq data, that SPI-1 effector SopE was not expressed and therefore not secreted in microaerobic MMA (**Figure 3.15C & E**). As expected SopE was highly expressed in WT, Δfnr and $\Delta ssrAB$ and not expressed in $\Delta hilD$ in aerated LB Miller and secreted from the strains in which it was expressed (**Figure 3.15D**). To verify that there was no expression of SopE in microaerobic MMA, whole cell lysates from MMA cultures and aerated LB Miller cultures were loaded onto the same gel and probed on the same membrane for the 3×FLAG and DnaK as a control. Interestingly, $\Delta hilA$ strains with 3×FLAG-tagged *steC* and *sopE* were constructed for these experiments as controls under SPI-1 and SPI-2 inducing conditions; However, the $\Delta hilA$ strains did not increase in OD₆₀₀ over 48 h in microaerobic MMA. Therefore, $\Delta hilD$ strains were constructed and used as a substitute.

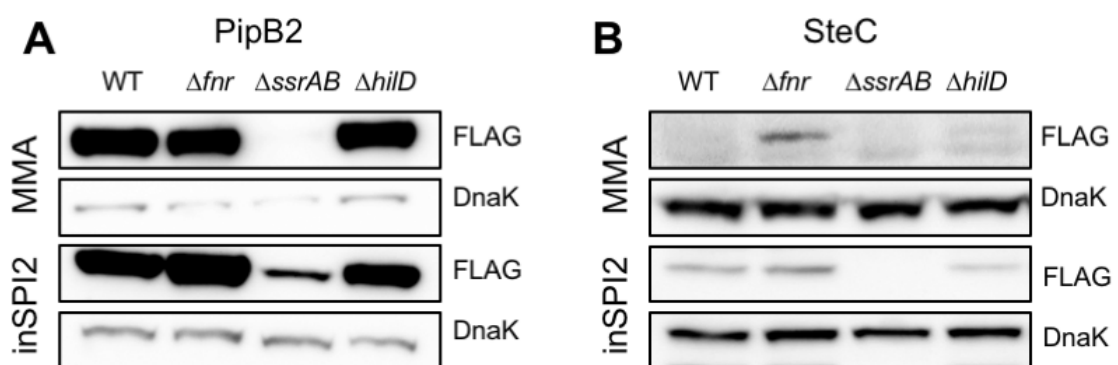


Figure 3.14 Expression of SPI-2 effector proteins.

Cells with a *A. pipB2*-3×FLAG::kan and *B. steC*-3×FLAG::kan were grown to OD₆₀₀ 0.3 in microaerobic MMA or to OD₆₀₀ 1.0 in aerated inSPI-2. 1 and 5 OD unit of lysed cells from inSPI-2 and MMA cultures, respectively, were loaded into each lane of the SDS-PAGE gel. Membranes were probed with anti-FLAG M2 and anti-DnaK antibodies.

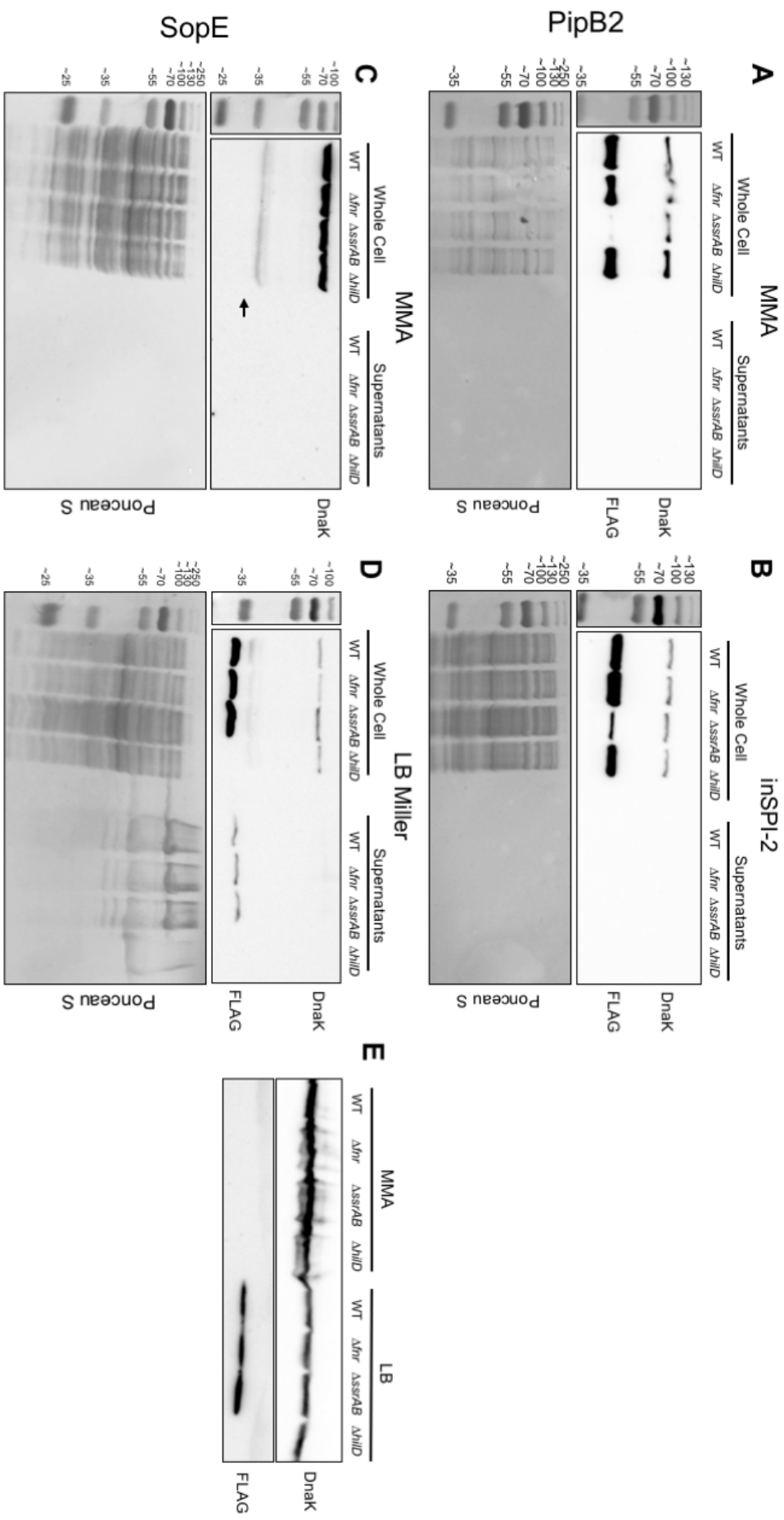


Figure 3.15 Secretion of SPI-1 and SPI-2 effector proteins.

Cells with *pipB2-3×FLAG::kan* were grown in A. MMA and B. InSPI2 media, and cells with *sopE-3×FLAG::kan* were grown in C. MMA and D. LB Miller to OD₆₀₀ 0.3 in microaerobic MMA or to OD₆₀₀ 1.0 in aerated InSPI2 and LB Miller. From MMA cultures 5 and 50 OD units were loaded for whole cell lysates and supernatants respectively; From rich media cultures 1 OD unit was loaded for whole cell lysates, and from inSPI-2 and LB Miller supernatants 50 and 10 OD units were loaded, respectively. An arrow indicates the would be location of SopE-3×FLAG in C. E. Show strains with *sopE-3×FLAG::kan* whole cell lysates only of MMA and LB Miller cultures. Membranes were probed with anti-FLAG M2 and anti-DnaK antibodies.

3.2.8 Repression of motility in Δfnr

The ability of *S. Typhimurium* to thrive in the gut is critical for transmission to new hosts. Using chemotaxis and flagella, they seek out nutrients and host cells. Flagellated subpopulations of *S. Typhimurium* accumulate proximal to the gut mucosa, the location of an oxygen gradient (Marteyn *et al.*, 2010; 2011; Stecher *et al.*, 2008). Fink *et al.* have shown under anaerobic growth conditions in MOPS-LB-X that chemotaxis, motility and flagellar genes were down-regulated (Fink *et al.*, 2007). Our RNA-seq data show that motility, chemotaxis and flagellar gene expression is also repressed in the Δfnr mutant under microaerobic conditions in MMA (**Figure 3.16**). All genes encoding proponents of the bacterial chemotaxis pathway were down-regulated ≥ 2 -fold except *cheC*, *cheD* and *cheV*. Four of the methyl-accepting chemotaxis proteins (MCPs) *aer*, *cheM*, *trg* and *tsr* were also down regulated ≥ 2 -fold in Δfnr (**Figure 3.17A**). MCPs are the receptors at the beginning of the chemotaxis signal transduction cascade that process environmental and intracellular sensory (input) signals and alter the activity of the CheAY TCS (Wuichet *et al.*, 2007). All genes encoding components of the flagellum were down-regulated ≥ 2 -fold including the motor, the C- and MS-ring of the cytoplasmic membrane, proximal and distal rods, the P- and L-rings, the hook, filament and hook-filament junction, as well as the filament cap (**Figure 3.17B**).

Therefore, strains were compared for swimming motility. Under aerobic conditions WT and Δfnr were equally motile (**Figure 3.18A**). Under anaerobic conditions, WT was motile while Δfnr exhibited limited motility. The *pfnr* and *fnr*⁺ strains complemented motility under anaerobic conditions in the mutant approximately 69% and 94%, respectively (**Figure 3.18A & B**). Thus,

the activating activity of FNR only motility only occurs under microaerobic and anaerobic conditions, as expected. The *hns-1* mutant is known to be non-motile but not deficient in growth, as H-NS is positive regulator of *flhDC* (Donato & Kawula, 1999) and was used as a negative control for swimming motility. To determine whether the reduced motility of the Δfnr strain was due to lack of flagella, WT and Δfnr cells were examined by AFM for the presence of flagella. The distinction between the WT and mutant was clear, WT cells had abundant peritrichous flagella, while Δfnr had very few flagella present (**Figure 3.18C**). The atomic force microscopy (AFM) images also allowed us to examine the cell morphology; WT and Δfnr cell were found to not be significantly different in size (**Figure 3.18D**). When cells grown microaerobically in MMA were examined using the hanging drop method, WT cells were motile while Δfnr cells exhibited only Brownian movement. Under anaerobic conditions, Δfnr had reduced motility on swimming plates and in microaerobic MMA broth.

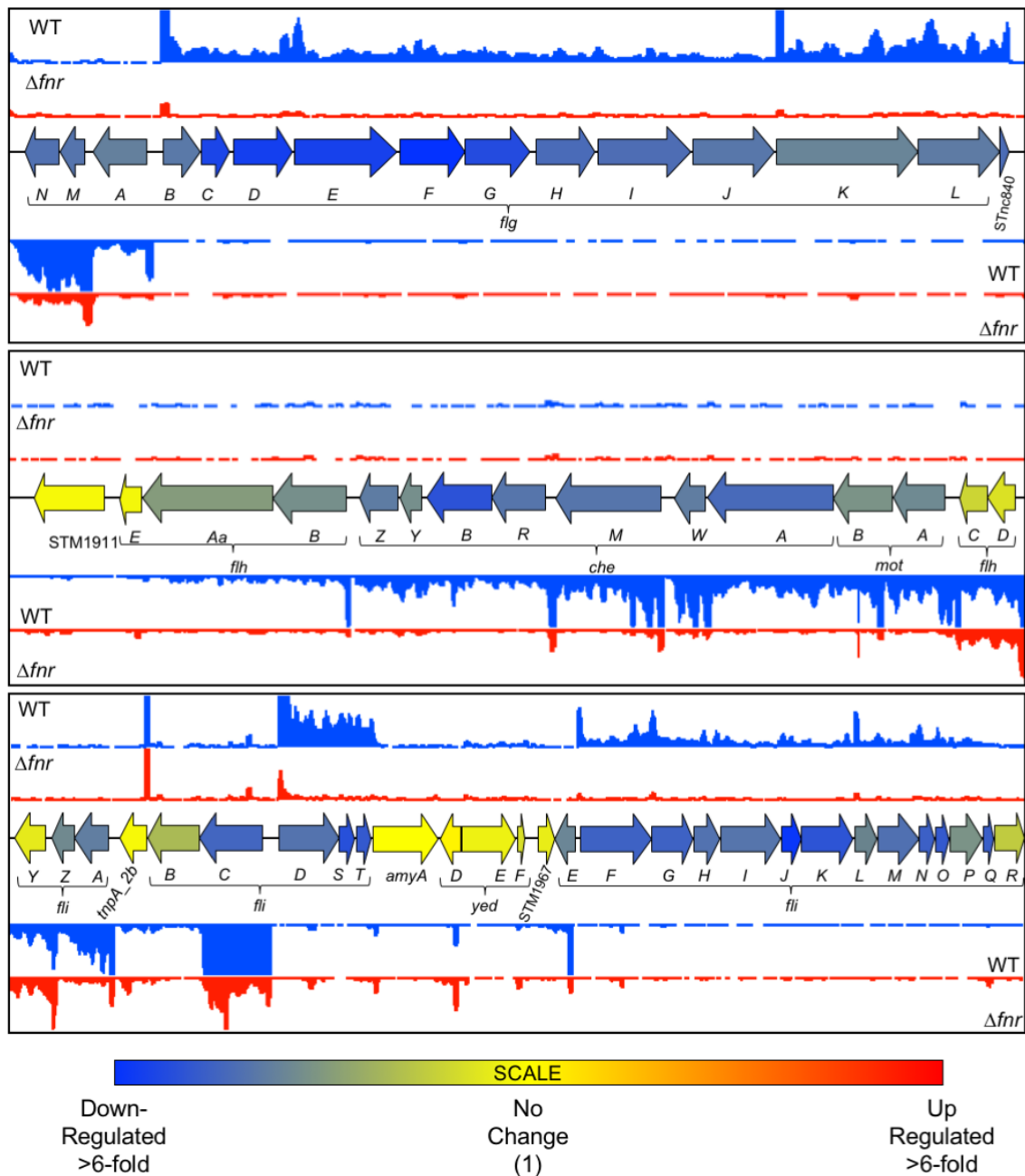


Figure 3.16 Down regulation of genes at major chemotaxis and flagellar loci.

Visualization of relative gene expression and sequenced reads at 3 chemotaxis, motility and flagellar gene loci in the Δfnr mutant and WT, grown under microaerobic conditions in MMA. Each arrow represents a gene and the colour represents the relative gene expression according to the scale bar. The IGB tracks for the WT and Δfnr mutant are blue and red, respectively. The colours of each track represent the sequencing reads which map to that locus and the height of the normalised reads is directly proportional to the level of expression at that locus.

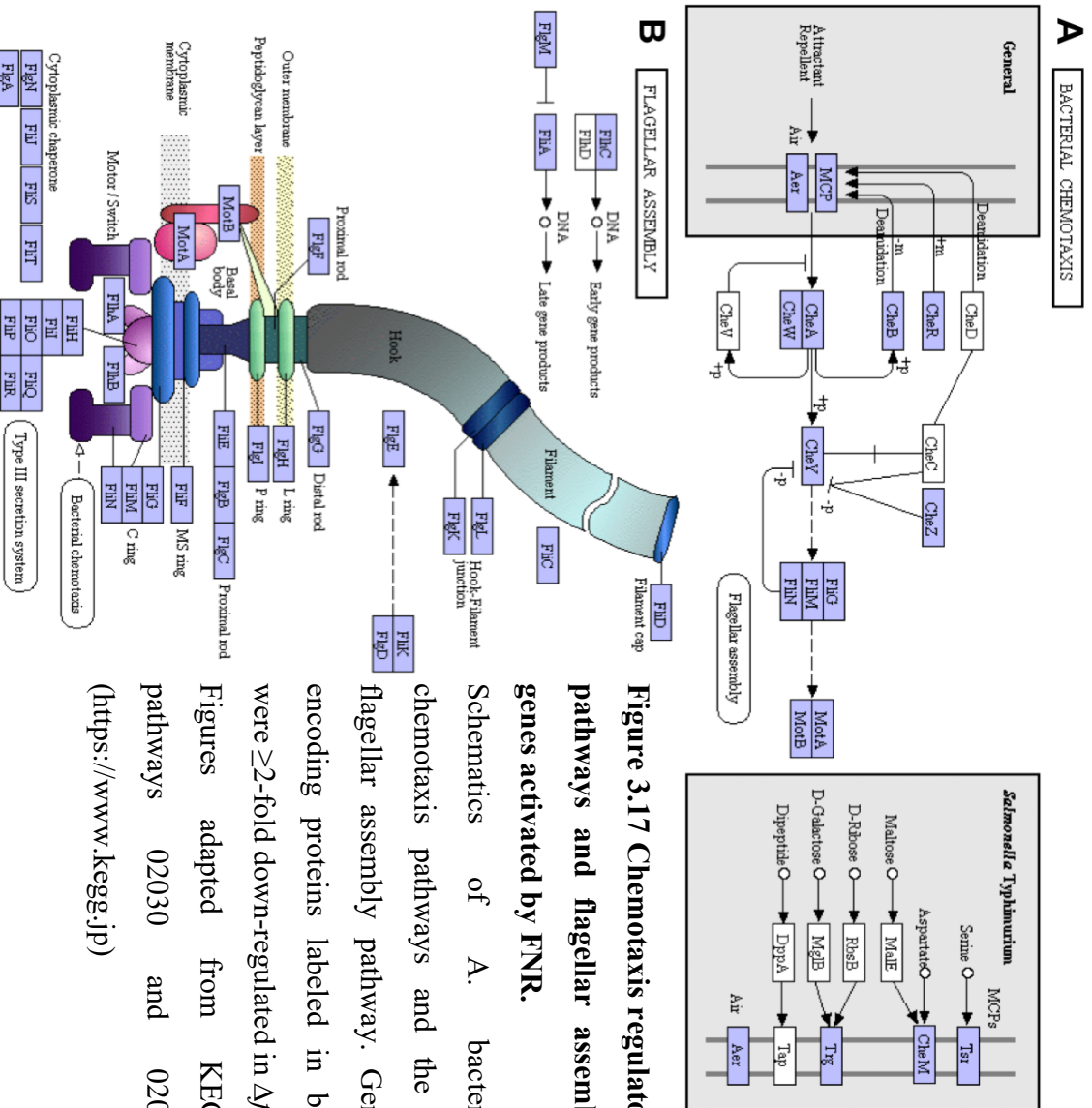


Figure 3.17 Chemotaxis regulatory pathways and flagellar assembly genes activated by FNR.

Schematics of A. bacterial chemotaxis pathways and the B. flagellar assembly pathway. Genes encoding proteins labeled in blue were ≥ 2 -fold down-regulated in *Afnr*. Figures adapted from KEGG pathways 02030 and 02040 (<https://www.kegg.jp>)

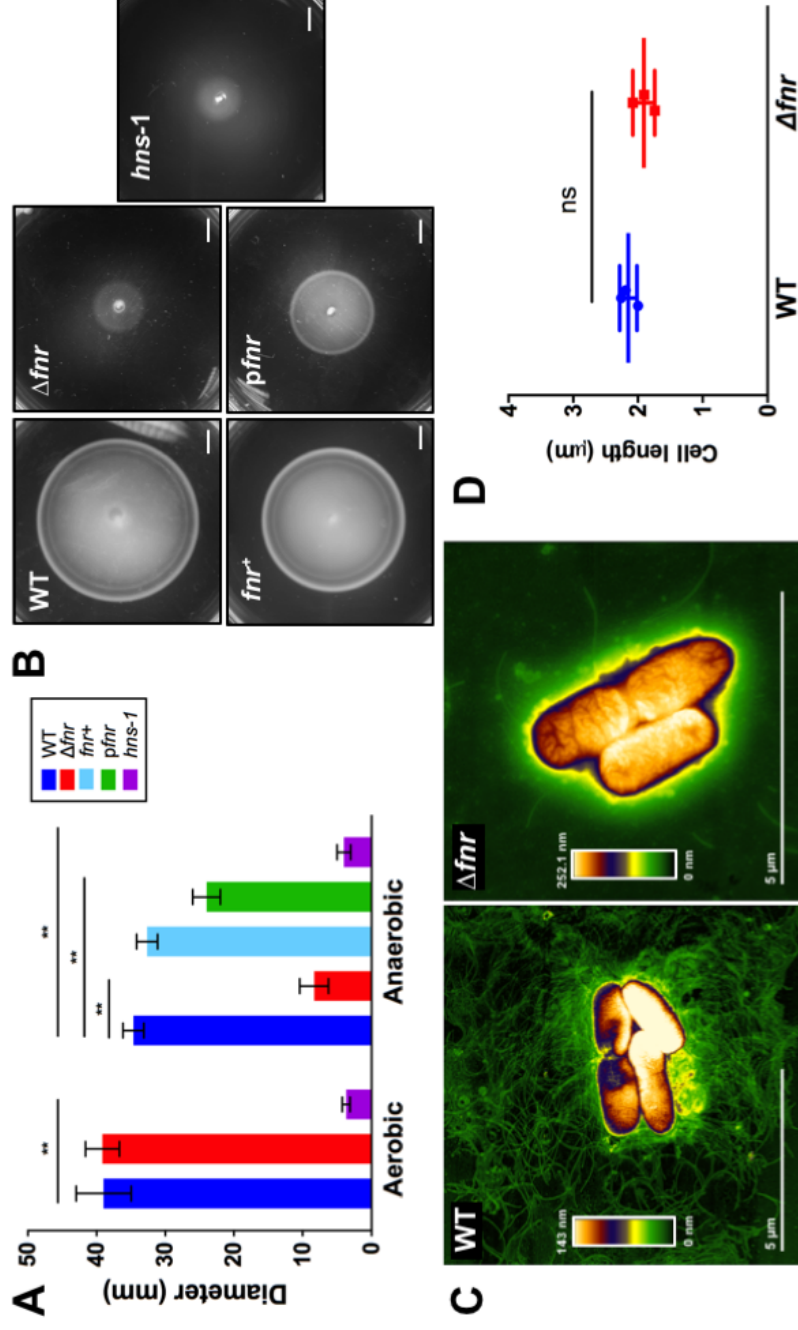


Figure 3.18 Motility is repressed and flagella are absent in Δfnr .

A. Diameters of swimming plates under aerobic and anaerobic conditions. An *hns-1* mutant was used as a negative control. Significance determined by nonparametric one-way ANOVA with Dunnett's multiple comparison test to WT of aerobiosis and anaerobiosis, respectively; only significant differences are labeled, $** = p \leq 0.01$. B. Representative photos of anaerobic swimming plates. The scale bar represents 5 mm. C. AFM images of WT and Δfnr cells taken after growth in LB to OD₆₀₀ 2.0. The scale bar represents 5 μm . D. Cell lengths in μm of WT and Δfnr cells measured from AFM images. Significance was determined by a two-tailed t test, ns = $p > 0.05$. Error bars represent standard deviation.

3.2.9 Regulation of small RNAs

Gene expression is carefully co-ordinated in response to environmental, spatial and temporal stimuli for the survival and successful infection inside the host. This must all occur without incurring fitness costs as a result of inappropriate gene expression. Gene expression is controlled at all levels from transcription initiation to translation. Post-transcriptional control of gene expression is important and often overlooked; This gene regulation is often mediated by small, regulatory non-coding RNAs (sRNAs). In our RNA-seq data set 42 sRNAs were identified as DE: 35 were up-regulated and 7 were down-regulated in the Δfnr mutant (**Table 3.1 & 3.2**).

The 7 down-regulated sRNAs from our dataset can be seen in **Table 3.1**. Not surprisingly, *FnrS*, the FNR dependent sRNA was the most down regulated, and this decrease in expression was consistent with data from cells under oxygen shock. The FNR dependency of *FnrS* had previously only been shown in *E. coli* (Boysen *et al.*, 2010; Durand & Storz, 2010); the regulation appears to be conserved in our study. Another sRNA both down regulated under oxygen shock and in Δfnr was STnc1340, an uncharacterized 82 nt sRNA. All but 1 of the down-regulated RNAs had unsuccessful transposon insertion from TraDIS data. STnc1560 is also an uncharacterized sRNA and is activated by RpoS (Lévi-Meyrueis *et al.*, 2014). Surprisingly, 2 sRNAs which were downregulated in Δfnr , STnc070 and STnc4180, are up-regulated when there is an oxygen shock (Kröger *et al.*, 2013).

Of the 35 up-regulated sRNAs in the FNR regulon, 3 have previously been reported to have a SPI-2 like pattern of expression (**Table 3.2**) (Colgan *et al.*, 2016). *IsrH_1_2*, *PinT* and STnc1480 had a high degree of correlation (>0.8) with the *ssaG* pattern of expression (Colgan *et al.*, 2016). *IsrH_1_2* is comprised of two overlapping sRNAs, *IsrH-1* and *IsrH-2*, which are 480 nt and 250 nt, respectively. *IsrH-1* shares an overlapping sequence at the 5' end of *sseL* and is expressed inversely to the SPI-2 effector, and *IsrH-2* overlaps the 3' end of *glpC*, (encoding the Glycerol-3-phosphate dehydrogenase small subunit) of the *glpABC* operon and is induced under anaerobic conditions (Padalon-Brauch *et al.*, 2008). *PinT* is a 80 nt PhoP-activated sRNA, which upon bacterial internalization temporally controls the transition from invasion (SPI-1) to intracellular survival (SPI-2) (Westermann *et al.*, 2016). STnc1480 is a 400 nt intergenic sRNA which, in a similar fashion to *ssrAB* promoters, is silenced by H-NS, and repression of the sRNA is countered by SlyA and PhoP (Colgan *et al.*, 2016). All three sRNAs are highly upregulated in SPI-2 inducing conditions

as well as in macrophage and activated by important regulators of SPI-2: SsrB, OmpR, PhoP and SlyA (Colgan *et al.*, 2016; Kröger *et al.*, 2013; Srikumar *et al.*, 2015). The most highly upregulated sRNA was *GcvB*. *GcvB* is a globally acting sRNA that regulates a post-transcriptional that influences approximately 1% of the *Salmonella* genome including the global regulator Lrp (Sharma *et al.*, 2007; 2011). Interestingly, the *GcvB* regulon overlaps with the *DapZ* regulon (Chao *et al.*, 2012), another sRNA that was up-regulated in Δfnr . These riboregulators transiently downregulate amino acid and peptide transporters, which may be important for efficient host cell invasion (Miyakoshi, 2019).

To investigate if any of the up-regulated sRNAs play an important role during *S. Typhimurium* infection, published data from a transposon-directed insertion site sequencing (TraDIS) study was interrogated. In the study, high-throughput sequencing of insertion sites of pools of *S. Typhimurium* 4/74 transposon mutants, following oral infections of chicken, pigs and calves were compared to an input inoculum (Chaudhuri *et al.*, 2013). The ratio of input to output reads was used to calculate the fitness score of each mutant. Transposon insertions that result in significant attenuation of the mutant strain were located in the three SPI2-like sRNAs as well as three others: STnc1330, STnc1920 and *tpke70* (**Table 3.2**). STnc1330 is a 141 nt sRNA regulated by RpoS and PhoPQ (Perez-Sepulveda & Hinton, 2018), STnc1920 is a 98 nt uncharacterized sRNA, and *tpke70* is predicted to regulated nitrate reductase genes *napG* and *napD* in *E. coli* (Ishchukov *et al.*, 2014).

3.2.9.1 FNR regulation of sRNAs in the context of a transcriptional network

Many sRNAs are still uncharacterized therefore, it is difficult to gain insight to their importance from a single RNA-seq experiment. For this reason, the sRNAs from our data were compared with those found in the regulons of 18 regulatory proteins in *S. Typhimurium*. Relative expression values of sRNAs found in the FNR regulon were taken from SalComRegulon, and DE sRNAs with fold-change of ≥ 2 were plotted (**Figure 3.19**). Of the 42 sRNAs found to be DE in Δfnr , only 4 were regulated by FNR alone: *tpke70*, *IsrM*, *IsrN* and STnc350. All four of these sRNAs were found to be putatively repressed. *IsrM* is important for invasion of epithelial cells, intracellular replication inside macrophages, virulence and colonisation in mice (Padalon-Brauch *et al.*, 2008). It targets the *SopA* and *HilE* mRNAs, virulence factors essential for bacterial invasion (Gong *et al.*, 2011). *IsrN* has been shown to be important for the early stages of intracellular survival (Padalon-Brauch *et al.*, 2008). As described previously, *tpke70* is also important for virulence in pigs and calves

(Chaudhuri *et al.*, 2013). STnc350 is an uncharacterized sRNA. Many of the sRNAs regulated by FNR are also regulated by other TFs including 24 sRNAs in common with Fur, 23 with RpoS, 20 with Hfq, 18 with SlyA, 16 with SsrA/B and 15 in common with both OmpR/EnvZ and HilD. This substantial overlap with important regulators of *S. Typhimurium* virulence regulators provides support that FNR is also intrinsically embedded in the complicated regulatory network controlling virulence (**Figure 3.19**).

Table 3.1 sRNAs down-regulated in Δfnr

sRNA	Strand	Start	End	$\Delta fnr/WT$	Oxygen Shock ^a	TraDIS attenuation ^b
STnc400	+	4072457	4072530	0.498	0.64	–
STnc070	+	669642	669793	0.424	2.36	–
STnc4180	-	109243	109322	0.358	1.95	–
STnc1340	-	2319956	2320037	0.353	0.18	–
STnc840	+	1224244	1224316	0.219	0.69	–
STnc1560	+	2449075	2449183	0.181	0.54	No
<i>FnrS</i>	-	1706784	1706905	0.029	0.01	–

^aData from Kröger *et al.* 2013

^bData from Chaudhuri *et al.*, 2013

Table 3.2 sRNAs up-regulated in Δfur

sRNA	Strand	Start	End	Δfur /WT	InSPI2 ^a	Macrophage ^b	SPI-2 like ^c	TraDIS attenuation ^d
<i>IsrH_1_2</i>	-	2392019	2392469	3.44	8.15	5.2	Yes	Yes
<i>PinT</i>	+	4580486	4580566	3.58	24.48	8.31	Yes	Yes ^e
STnc1480	+	1316874	1317268	2.54	28.07	11.26	Yes	Yes
STnc150	-	1282521	1282677	2.21	2.91	5.97	No	-
STnc3150	-	3273499	3273824	2.07	2.45	2.09	No	No
STnc3750	-	2503726	2503803	2.36	6.29	2.93	No	-
STnc980	-	889558	889714	2.46	1.77	2.21	No	-
<i>GcvB</i>	+	3156779	3156979	12.85	0.95	0.09	No	-
<i>IsrI</i>	-	2759018	2759265	2.38	1.63	1.66	No	-
<i>IsrM</i>	+	2927616	2927944	2.4	1	1	No	-
<i>IsrN</i>	+	2929501	2929643	2.35	1	-	No	-
<i>RprA</i>	-	1401682	1401790	2.58	0.4	0.08	No	-
<i>RyeB</i>	-	1925621	1925723	2.48	3.2	0.28	No	-
<i>RyhB-2</i>	-	1309727	1309937	2.31	0.06	85.5	No	-
<i>SraL</i>	-	4526163	4526303	2.18	13.18	0.87	No	-
<i>sRNA12</i>	-	3755045	3755125	2.78	1.37	1.39	No	-
STnc1150	+	2222979	2223134	2.79	0.98	0.54	No	-
STnc1220	-	1448718	1448790	2.75	1.68	0.29	No	-
STnc1330	+	2268274	2268414	2.05	2.3	0.58	No	Yes ^e
STnc1700	+	386381	386476	2.5	2.47	0.72	No	-
STnc1870	+	617317	617426	2.54	1.62	1	No	-
STnc1920	+	2756549	2756646	2.08	0.74	0.77	No	Yes
STnc2030	+	1784673	1784725	8.65	1	0.33	No	-
STnc3000	+	4591419	4591506	2.02	0.74	0.27	No	-
STnc310	-	3413972	3414032	2.26	1.63	0.41	No	-
STnc3120	+	4249943	4250101	2.03	1.68	0.17	No	-
STnc3210	+	17025	17111	2.38	3.52	1.42	No	-
<i>DapZ</i>	+	74847	74924	2.28	2.4	0.18	No	-
STnc3440	+	1303294	1303380	2.11	4.55	0.48	No	-
STnc350	-	3782696	3782857	3.91	1.92	0.21	No	No
STnc380	-	3906945	3907052	2.48	3.51	1.92	No	-
STnc4000	+	3619657	3619755	3.47	0.3	2.9	No	-
STnc4010	+	3729767	3729899	2.77	1	0.72	No	-
STnc890	+	14720	14783	2	1.26	0.27	No	No
<i>tpke70</i>	-	2513324	2513722	2.25	1	1	No	Yes ^e

^aData from Kröger *et al.* 2013

^bData from Srikumar *et al.*, 2014

^cData from Colgan *et al.*, 2016

^dData from Chaudhuri *et al.*, 2013

^eAttenuated in pig and calf only

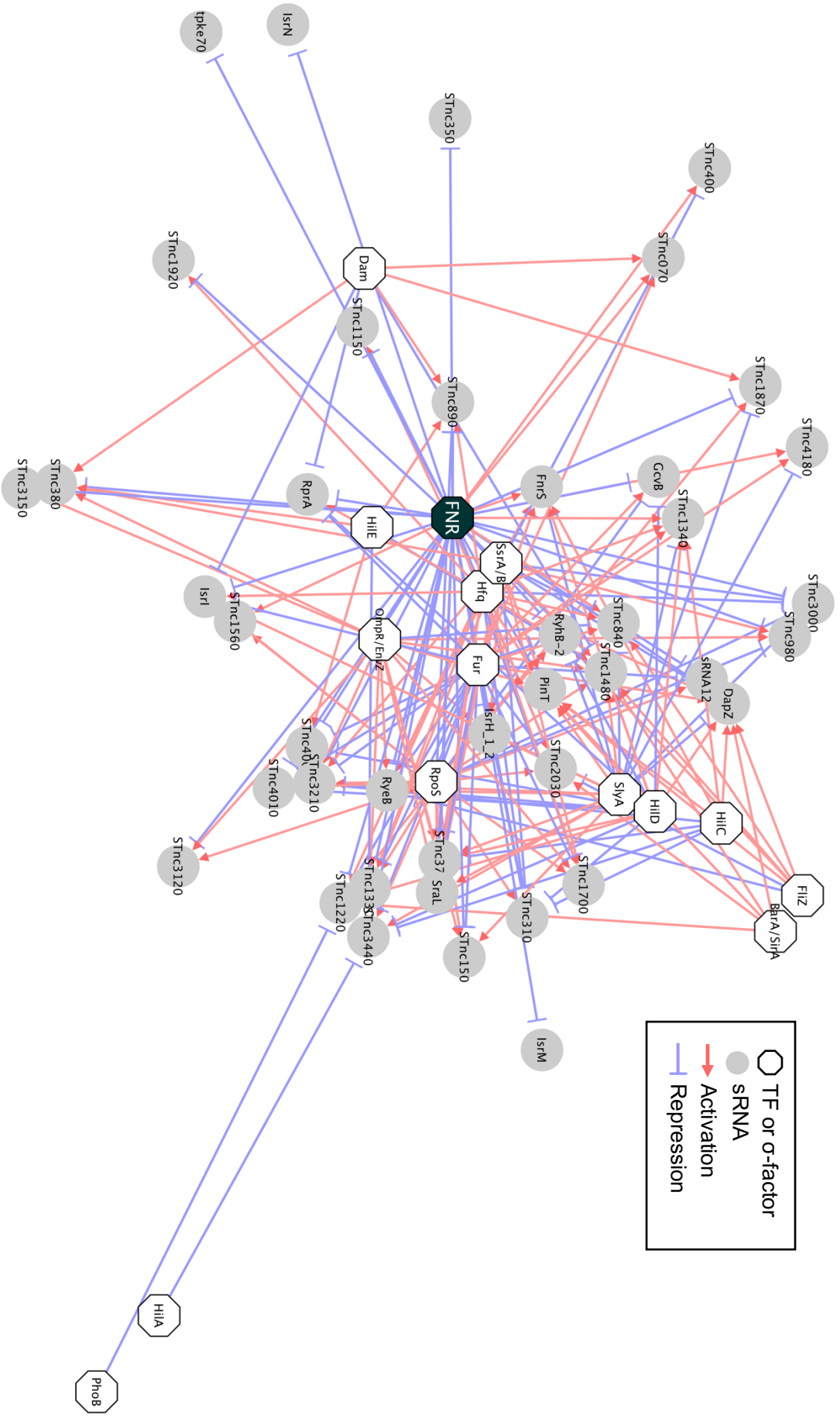


Figure 3.19 Regulatory network of FNR regulated sRNAs.

Regulatory network was generated using software from www.cytoscape.org. Regulatory interactions are based on mutant RNA-seq data from this study and Colgan *et al.*, 2016. DE sRNA genes that are down-regulated in a mutant strain lacking a TF or σ -factor (regulatory protein) are putatively activated by that regulatory protein, and the interaction is represented using a red arrow from the source node (regulatory protein) to the target node (sRNA). DE sRNA genes that are up-regulated in a mutant lacking a certain regulatory protein are putatively repressed by that regulatory protein, and the interaction is represented using a blue T-shaped line from the source to the target node. The length of each line is representative of the strength of the putative interaction: nodes representing sRNAs which show higher fold-increase or decrease in a mutant strain are located closer to that regulatory protein. Regulatory proteins are hexagonal in shape and white except FNR which is black, sRNAs are circular and grey.

3.3 Discussion

To our knowledge, the work presented here is the first large scale transcriptomic study that has been carried out in an Δfnr mutant of *S. Typhimurium* using high throughput next generation sequencing. We were able to corroborate existing data associating FNR as an activator of anaerobic metabolism, cell motility and chemotaxis, and reveal FNR as a newly identified repressor of *Salmonella* pathogenicity island 2. The use of RNA-seq rather than microarray-based technology has also allowed us to identify differentially expressed small non-coding RNAs in an Δfnr background.

3.3.1 SPI-2 expression in MMA

It was unusual to see SPI-2 expression in the MMA media as it possesses nearly the opposite signals that are typically necessary for SPI-2 induction (Deiwick *et al.*, 1999; Löber *et al.*, 2006; Xu & Hensel, 2010). The medium contains high concentrations of Mg^{2+} and P_i compared to the SPI-2 inducing media that has been used in the past, as well as neutral pH. However, we see minimal SPI-2 expression in the WT under microaerobic conditions, and those level increase nearly 2-fold when the media is aerated; in the absence of FNR we see very high induction of SPI-2 regardless of the aeration (**Figure 3.13**). This indicates that there may be another factor involved as we expected SPI-2 expression in aerated WT cultures to reach the same level of expression. However, it is unclear if OD_{600} of 0.3 in the WT and Δfnr are the same stage of growth as in microaerobic cultures therefore, a growth curve should be completed under aerated conditions in MMA. Perhaps a more informative experiment would be to grow cultures microaerobically to an OD_{600} of 0.3 and then perform an oxygen shock whilst measuring gene expression throughout. Also, it is apparent that another metabolic signal, in addition to oxygen, is important for regulation of SPI-1 or SPI-2 as expression of these genes are differentially expressed in Δfnr in different growth media (**Figure 3.9, Figure 3.10A**) (Fink *et al.*, 2007). We may also see expression of SPI-2 in microaerobic MMA, as the expression we measured is from across the gradient in the flasks as the samples taken are a mixture of the culture. It would be informative to be able to measure the concentration of oxygen precisely of our cultures. Although the measurements that have been taken were consistent over different biological replicates (**Figure 3.3**) it would be ideal to have a more homogeneous culture from which to take measurements. The oxygen gradient gene expression assay (**Figure 3.12**) could also be improved to eliminate the confounding factor of differences in density of cell growth throughout the medium.

Because of the nature of GFP, it folds more slowly under low oxygen conditions, therefore to have adequate growth in the medium the assays were left to incubate for 72 h. If the assays were redone with our luminescent pDEW201-P_{ssaG} containing strains we could likely measure P_{ssaG} expression much earlier as the *lux* operon requires less posttranslational modifications and luminescences earlier than GFP fluoresces under low oxygen conditions. This would reduce the accumulation of cells at the surface of the agar and allow us to more easily visualize which cells are expressing SPI-2. The other problem with this assay is that again we cannot measure the exact concentration of oxygen throughout the medium, but it still provides a simple visualization of expression under a gradient of oxygen concentrations.

3.3.2 Motility and chemotaxis

Although there are some major differences between the Fink *et al.* FNR regulon and the one reported here, these are almost certainly due to the difference in growth conditions between the studies, and differences between the *S. Typhimurium* strains 4/74 (used in this study) and 14028S (Clark *et al.*, 2011; Hoiseth & Stocker, 1981; Kröger *et al.*, 2012; Richardson *et al.*, 2011). Here we have grown cells in microaerobic conditions in a minimal medium (MMA) with a glycerol carbon source, whereas the Fink *et al.* study grew cells anaerobically in MOPS buffered LB with added xylose (Fink *et al.*, 2007). Core anaerobic metabolism genes were found to be DE in both studies because their expression is more dependent on the availability of oxygen than other nutrients. Interestingly, flagellar, motility and chemotaxis genes were also found to be highly down-regulated in both studies. This may indicate that for expression at these loci, the availability of oxygen is more important than other nutrients or environmental signals.

3.3.3 Regulation of sRNAs by FNR

Many of sRNAs regulated by FNR are also regulated by Fur (**Figure 3.19**). Although the functional state of FNR during aerobic/anaerobic switch is not regulated by iron content and reversible binding of Fe²⁺ under physiological conditions, and FNR does not communicate with the iron pool regulating the Fur protein (Niehaus *et al.*, 1991), they share many genes in their regulons including flagellar genes and SPI-1 genes (Colgan *et al.*, 2016). In the Colgan *et al.* study the Fur regulon was investigated under ESP growth in LB, which is closer to the growth conditions found in the Fink *et al.* microarray study (Colgan *et al.*, 2016; Fink

et al., 2007). If grown in MMA medium, it is possible that absence of Fur may result in up-regulation of SPI-2 genes, based on the similarities of the regulons.

There were 3 sRNAs upregulated in Δfnr that have been previously described as SPI-2-like as well as may other which are upregulated in SPI-2 inducing conditions and macrophages, and 6 sRNAs that have been linked to attenuation of virulence in food animals (**Table 3.2**); additionally, important virulence sRNAs *IsrM* and *IsrN* were found to be regulated by only FNR. Furthermore, *IsrM* is differentially expressed *in vivo*, with higher expression in the ileum than in the spleen (Gong *et al.*, 2011), the site where we propose FNR exerts control over virulence genes. In a recent study, deletion of *FnrS* led to increased HilD production under low aeration conditions, and *FnrS* could bind to the *hilD* mRNA 5' UTR, resulting in translational repression (Kim *et al.*, 2018). The authors discuss the importance of *FnrS* on SPI-1 expression however fail to mention the potential impact of HilD-mediated crosstalk between SPI-1 and SPI-2 (Bustamante *et al.*, 2008). Our data reveal that *FnrS* expression is dramatically decreased in Δfnr and in aerated WT cultures (**Figure 3.2C**), and SPI-2 expression is increased under these conditions (**Figure 3.13**); in the absence of *FnrS*, HilD levels may be increased, contributing to the SPI-2 induction phenotype that we have observed. These data confirm that FNR is an important regulator of sRNAs involved in virulence.

3.3.4 Comparison of FNR regulons

While comparisons to the FNR regulon in *E. coli* can be useful for widely conserved genes, *Salmonella* specific genes are obviously missed. The only existing study identifying the FNR regulon in *S. Typhimurium* through transcriptomic data was published in 2007 and was accomplished using a DNA microarray (Fink *et al.*, 2007). The drawbacks to using microarrays for transcriptomic analysis include low resolution with high background due to non-specific hybridisation between cDNA and probes (Aikawa *et al.*, 2010) and the dynamic range of microarrays is limited by the use of fluorescently-labelled DNA, detection of which can be saturated and subtle changes in gene expression may not be detected. RNA-seq allows all transcription to be studied without bias and without prior knowledge of the DNA sequences that are being transcribed, and with no limits on the dynamic range (Croucher & Thomson, 2010). The use of RNA-seq in this study as well as a different growth condition allows us to expand the existing FNR regulon to include new genes as well as not previously identified sRNAs.

In this study, the FNR regulon was examined under microaerobic conditions in MMA and analysed by RNA-seq. In **Figure 3.20** the FNR regulon as determined by this study was compared to the FNR regulon under anaerobic conditions in MOPs buffered LB with xylose as determined by microarray analysis (Fink *et al.*, 2007). Only genes with ≥ 2.5 -fold change in expression in the Δfnr mutant compared to WT were included in the comparison between the two studies. In total 75 genes were found in common in both regulons (**Figure 3.20A**). Sixty-nine genes in common were down-regulated in both studies (**Figure 3.20B**). These comprised mostly of genes which encode components of flagella biosynthesis, motility and chemotaxis regulons (discussed in more detail in Section 3.2.8) and genes involved in anaerobic systems, including *aer*, *dmsABC*, *dmsA1*, *dmsA2*, *nrdD*, *nrfA*, STM2530, and STM4305 – 4307. The *Salmonella* specific virulence proteins encoded by *srfABC* were also found to be down regulated in both studies. These SsrB-regulated factors are horizontally acquired genes and as the name would indicate, regulated by the SPI-2 encoded SsrB protein, but are expressed in SPI-1 inducing conditions and have been found to be repressed by PhoP and RcsB (Garcia-Calderon *et al.*, 2007; Worley *et al.*, 2000).

Interestingly, 3 genes found to be up-regulated in the microarray study, were down-regulated in our data set: *dcuB*, *fumB* and *nuoJ*. DcuB functions primarily as a fumarate:succinate antiporter during anaerobic fumarate respiration (Six *et al.*, 1994) and FumB is one of three fumarase isozymes participating in the TCA cycle (Woods *et al.*, 1988). These two proteins are involved in anaerobic metabolism and are induced under anaerobic conditions in *E. coli*, consistent with our data. NuoJ is part of the inner membrane component of NADH dehydrogenase I and is typically repressed by FNR (Leif *et al.*, 1995), which is consistent with data from Fink *et al.* Additionally, one gene that was down-regulated in Fink *et al.* was upregulated in our study. This was the *osmY* gene, that encodes for the periplasmic chaperone protein OsmY, that is induced under conditions of hyperosmotic stress (Yim & Villarejo, 1992). These discrepancies between the regulons indicate FNR can activate and repress expression of genes depending on the growth conditions.

Also identified in this study were 42 sRNAs which were DE in Δfnr . None of these sRNA genes could be detected by the microarray analysis. Included in this group is the sRNA *FnrS*, which is an anaerobically-inducible, FNR-dependent sRNA conserved in *E. coli* (Boysen *et al.*, 2010; Durand & Storz, 2010). Recently, *FnrS* was found to regulate SPI-1 expression by

repression of *hilD* translation (Kim *et al.*, 2018). These will be discussed further in Section 3.2.9.

Many of the genes which are only DE in the microarray-based study included genes encoding SPI-1 regulators, components of the T3SS and effector proteins. In our data set, expression of SPI-1 genes in Δfnr generally trended downward however their differential expression was less than 2.5-fold and the genes were either not or only lowly expressed in the WT and Δfnr under microaerobic growth in MMA (**Figure 3.10A**). It is unclear from the Fink *et al.* study whether SPI-1-associated genes are directly regulated by FNR or if the FNR-dependence of these genes is due to FNR-mediated down-regulation of the genes encoding FliZ and FliA, which play roles in the regulation of SPI-1 (Lucas & Lee, 2001). Another explanation may be that the disruption in anaerobic metabolism in the absence of FNR leads to induction of *hilA* via BarA/SirA, due to accumulation of fatty acid metabolites, such as acetate (Lawhon *et al.*, 2002). As mentioned previously, *FnrS* which was not identified in the Fink *et al.* study has recently been implicated in repression of *hilD* translation (Kim *et al.*, 2018), and thus may have played a role down-regulation of SPI-1 under the growth conditions in Fink *et al.* (Fink *et al.*, 2007). The differences in oxygen levels and thus in differential anaerobic metabolism gene expression may account for the variation in SPI-1 gene expression between the two studies. Another difference in the data sets were the significant number of genes encoding proteins for ethanolamine utilization in Fink *et al.* study that were not identified in our dataset. Ethanolamine is available in the host and can be used by *S. Typhimurium* as a source of carbon, nitrogen, and energy to outcompete host microbiota but, is not necessary for virulence in mice (Thiennimitr *et al.*, 2011). The lack of expression at this operon could be explained by the absence of ethanolamine in MMA, or the expression may have to do with a component of LB as *eut* genes are upregulated in LB in anaerobic growth (Kröger *et al.*, 2013).

The most striking difference between the two datasets is the increased expression of genes encoding SPI-2 regulators, components of the T3SS apparatus and effector proteins in this study (**Figure 3.7 & Figure 3.9**). These genes are not up-regulated in Δfnr in the study by Fink *et al.*, except for *sopD2* and *sseL*, which are common to both datasets (**Figure 3.20C**). In the microarray study *sopD2* and *sseL* were up-regulated in Δfnr 3.0- and 3.5-fold respectively, in this study, they were up-regulated 7.9- and 6.4-fold. These effector proteins are expressed in SPI-2 inducing conditions and in macrophages but, are not encoded within SPI-2 (Kröger *et al.*, 2013; Srikumar *et al.*, 2015). *SopD2* is important for formation of

Salmonella-induced filaments and interference with endosome to lysosome trafficking, while SseL induces late macrophage cell death (Jennings *et al.*, 2017). Fink *et al.* did not detect differential gene expression of any other of SPI-2 genes, however they found that the Δfnr mutant is attenuated for survival and replication within murine macrophages. This result would be consistent with FNR regulation of SPI-2 gene expression but was not detected under the conditions used in the microarray-based study.

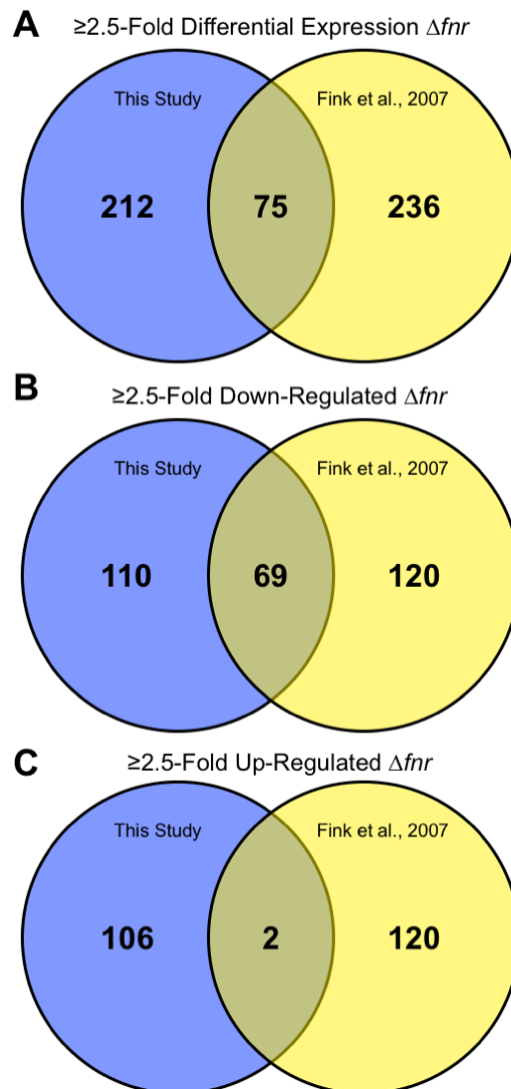


Figure 3.20 Comparison of FNR regulons.

FNR regulon under micro-aerobic conditions, as analysed by RNA-seq (this study, blue circles), compared to the FNR regulon under anaerobic conditions as determined by microarray (Fink *et al.*, 2007, yellow circles). Comparisons were made between genes that were >2.5 -fold DE in an Δfnr mutant where A. compares the entire regulon, B. compares down-regulated genes, and C. compares up-regulated genes.

3.3.5 The benefits and limitations of an RNA-seq-based approach for the investigation of bacterial regulons

RNA-seq provides convenient and precise method for studying gene expression at single nucleotide resolution. Large amounts of data can be generated rapidly and simply, relative to more laborious protocols such as DNA microarrays, RT-qPCR or transcriptional fusions. Extraction of good quality total or depleted RNA is important, and conveniently most sequencing facilities offer cDNA library preparation services to ensure consistent high-quality samples for sequencing. Sequencing technologies themselves are improving and advancing regularly, resulting in the generation of large amounts of good quality data, within a short timescale. RNA-seq technology is more accessible than ever to researchers, meaning that high throughput next generation sequencing and RNA-seq are contributing to the expansion of our knowledge base. The development of tools for bioinformatics and data handling programs permit rapid and convenient downstream analyses, allowing us to distil the important information from the massive data sets that are produced using RNA-seq. We have shown that the use of RNA-seq to determine the FNR regulon provides accurate information that agrees with what has been previously shown using transcriptional fusions and microarrays in *E. coli* and *S. Typhimurium*, but the increased sensitivity and dynamic range of RNA-seq allowed identification more subtle changes in gene expression, as well as to detect expression of non-coding sRNA species, thereby increasing our understanding of complex regulatory pathways.

However, there are some limitations to the approach used in this study. RNA is extracted from a population of bacteria for use in RNA-seq; this provides an average view of the transcriptomes of millions of cells. Additionally, our growth condition is heterogenous in nature, meaning we likely have very different expression in subpopulations throughout the oxygen gradient of the cultures. Genetically identical cells can often be phenotypically different and subpopulations of cells or outlier cells play important roles in disease outcome or antibiotic tolerance (Diard *et al.*, 2013; Helaine *et al.*, 2014). Single-cell RNA sequencing can reveal complex and rare cell populations, uncover regulatory relationships between genes. Single-cell transcriptomic analysis will allow the detection of even more subtle, and often biologically significant, changes in gene expression that could be masked at the level of whole bacterial populations (Hwang *et al.*, 2018).

RNA-seq of strains and their isogenic mutants can reveal a multitude of changes in gene expression however, it cannot distinguish between direct and indirect regulation. The complexity of bacterial regulatory networks and the interplay between different regulators means that many of the putative interactions that are detected in the absence of a TF are as a result of perturbations in regulatory cascades rather than direct control of gene expression. Therefore, it is important to combine RNA-seq with techniques which uncover direct regulation of genes such as chromatin immunoprecipitation sequencing and will be covered in detail in Chapter 4.

RNA-seq provides important clues about gene expression and regulatory interactions but important findings must be validated using additional molecular biological approaches. To provide a better understanding of the inherent complexity of biological systems, complete descriptions of biological molecular networks, including important environmental stimuli, transcription factors, regulatory proteins, sRNAs, and all other components (Golubeva *et al.*, 2012; Hébrard *et al.*, 2011). Complete descriptions of biological systems can be achieved through the integration of information from a combination of datasets, including transcriptomics, epigenomics, proteomics, global ChIP studies, and others. Great resources are available for *E. coli* including RegulonDB, EcoCyc, GenExpDB and UniProt which provide curated information on *E. coli* gene and protein expression from thousands of transcriptomic experiments (Hébrard *et al.*, 2011; The UniProt Consortium, 2017), and much information from *S. Typhimurium* is available through SalCom, SalComMac and SalComRegulon (Colgan *et al.*, 2016; Kröger *et al.*, 2013; Srikumar *et al.*, 2015). Despite decades of research, the complexities of the *E. coli* and *S. Typhimurium* genomes are only becoming realized in recent times thanks to NGS technologies. Our hope is that this transcriptomic analysis of *S. Typhimurium* FNR regulon and its role in regulation of virulence will contribute to the overall understanding of *S. Typhimurium* infection.

3.3.6 Summary

The aim of this chapter was to investigate the global changes in gene expression in an Δfnr mutant with a focus on *Salmonella* Pathogenicity Island 2, flagella and motility in *S. Typhimurium*. We have shown using a wide variety of techniques that under microaerobic conditions in MMA that the absence of the FNR protein causes SPI-2 encoded and associated genes and sRNAs to have increased expression and flagellar and motility genes to have decreased expression when compared to the WT. These results indicate that when *S.*

Typhimurium cells are exposed to oxygen (like at the epithelial border in the gut), and FNR dimers are no longer active in the cell, that SPI-2 expression increases and motility and flagellar gene expression decreases, likely in preparation for the harsh intracellular environment of host epithelial cells.

Chapter 4

Promoter occupancy of FNR

4.1 Introduction

4.1.1 Identification of global FNR binding through ChIP-seq

Transcription factors that bind to specific DNA sequences are essential for the correct regulation of gene expression and identification of the specific DNA sequences that each factor binds helps to elucidate regulatory networks within bacteria (Browning & Busby, 2004; Myers *et al.*, 2015). Traditional methods for determining the specificity of DNA-binding proteins such as electrophoretic mobility shift assays (EMSA) are important for showing direct binding but are performed under *in vitro* conditions and thus disregard any other factors which may be important for binding *in vivo*. They are also too slow and laborious to investigate an entire genome. In contrast, a high-throughput method such as chromatin immunoprecipitation sequencing (ChIP-seq) can provide global *in vivo* binding information rapidly (Stormo & Zhao, 2010). Regulatory mutants can be used to investigate bacterial regulons using RNA-seq, and the technique is able to provide candidate genes that a transcription factor is likely to regulate however, it is unable to discriminate whether regulation is direct or indirect. In Chapter 3, we identified FNR as a repressor of SPI-2 genes under microaerobic conditions in MMA, using RNA-seq, and here we used another large-scale investigative technique, ChIP-seq, to identify whether FNR repression of SPI-2 genes is direct or indirect. A general workflow of the main experimental procedure is outlined in **Figure 4.1**.

DNA-protein binding experiments, such as EMSA, were traditionally used to demonstrate that a protein could directly bind a specific fragment of DNA, but more recently ChIP has become the method of choice to provide evidence of direct protein binding *in vivo*. Originally, ChIP experiments were followed by RT-qPCR to determine protein binding within particular sequences of interest by examining enrichment of DNA from the immunoprecipitated sample, or by ChIP-chip where protein-associated DNA is hybridized to a tiling microarray to determine all DNA binding sites of a particular protein. Within the last decade, ChIP-chip has been replaced with ChIP-seq which has a much higher resolution and signal-to-noise ratio than ChIP-chip and involves the use of deep sequencing technology to determine all DNA molecules bound by DNA-associated proteins (Cai & Huang, 2012; Myers *et al.*, 2015). Sequencing-based approaches have increased sensitivity and reduced bias compared to microarray-based technology. ChIP-seq also allows for the identification of transcription factor binding site sequences at the level of the individual nucleotide and

can be used to accurately determine transcription factor binding motifs. Motif analysis can predict direct protein binding sites and provide focused data on highly likely candidate gene targets. The combination of transcriptomic data from WT and Δfnr , with FNR occupancy data obtained under the same growth conditions can associate the changes in gene expression to binding and direct regulation by FNR. To our knowledge, this study provides the first large scale investigation into DNA-protein interactions of the oxygen sensitive transcription factor FNR in *S. Typhimurium*.

The aim of this chapter is to use the global approach of ChIP-seq to identify candidate regulators of SPI-2 in the case of indirect regulation of SPI-2 through FNR or to identify FNR as a direct regulator of genes encoded on the pathogenicity island, and to verify those results with other molecular techniques.

3xFLAG-FNR strain grown in microaerobic MMA to OD₆₀₀ 0.3

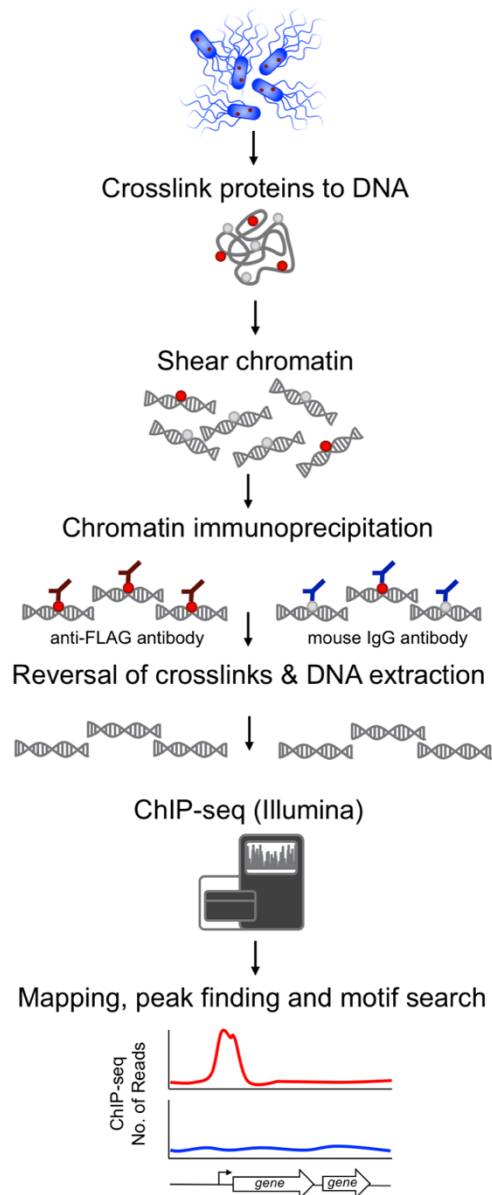


Figure 4.1 Workflow of chromatin immunoprecipitation sequencing to identify FNR binding sites.

A 3xFLAG-FNR strain was grown under microaerobic conditions to OD₆₀₀ 0.3 in MMA. Proteins were crosslinked to DNA, chromatin was sheared then immunoprecipitated by and anti-FLAG antibody to identify specific FNR binding and by a mouse IgG antibody for background non-specific binding. Crosslinks were reversed, and DNA was extracted and prepared for sequencing. Library preparation and sequencing for replicate 1 was performed by me and replicate 2 was performed by Dr. Keith MacKenzie at the University of Regina, Regina, Saskatchewan, Canada. Bioinformatic analyses were performed by Dr. Aalap Mogre at Trinity College Dublin, Dublin, Ireland.

4.2 Results

4.2.1 Verification of 3×FLAG-FNR

For ChIP-seq experiments a strain with a 3×FLAG-tagged FNR was used (originally constructed by Dr. Aoife Colgan). To ensure that the 3×FLAG-tag did not interfere with the binding capability of the FNR protein a northern blot was performed looking at expression of the FNR dependent small RNA *FnrS* (**Figure 4.2A**). There was high expression of *FnrS* in the 3×FLAG-tagged strain although slightly lower than WT levels, it was higher than in the Δfnr mutant. A preliminary ChIP-RTqPCR experiment was performed to determine enrichment of the ChIP DNA of a positive control and a negative control, the *fnrS* promoter and *hemX* respectively (**Figure 4.2B & C**). The amplified ChIP DNA was normalized to the amplified Input DNA, which was extracted prior to immunoprecipitation. Normalised ChIP-RTqPCR data from two independent biological replicate experiments and demonstrates that there is strong enrichment (approximately 16-fold) of the *fnrS* promoter region in the experimental ChIP DNA, compared to the background “Mock” ChIP DNA. The negative control gene, *hemX*, showed negligible enrichment (approximately 1-fold) in the experimental ChIP DNA sample, compared to the mock ChIP DNA sample (**Figure 4.2B**). Following subtraction of the Mock ChIP DNA, the *fnrS* promoter DNA was approximately 31-fold enriched for FNR binding, compared to the negative control region, *hemX* (**Figure 4.2C**). These data show that FNR specifically binds within the *fnrS* promoter region, FNR is a direct activator of *FnrS* transcription, and the 3×FLAG-tagged FNR can be confidently used for ChIP-seq experiments.

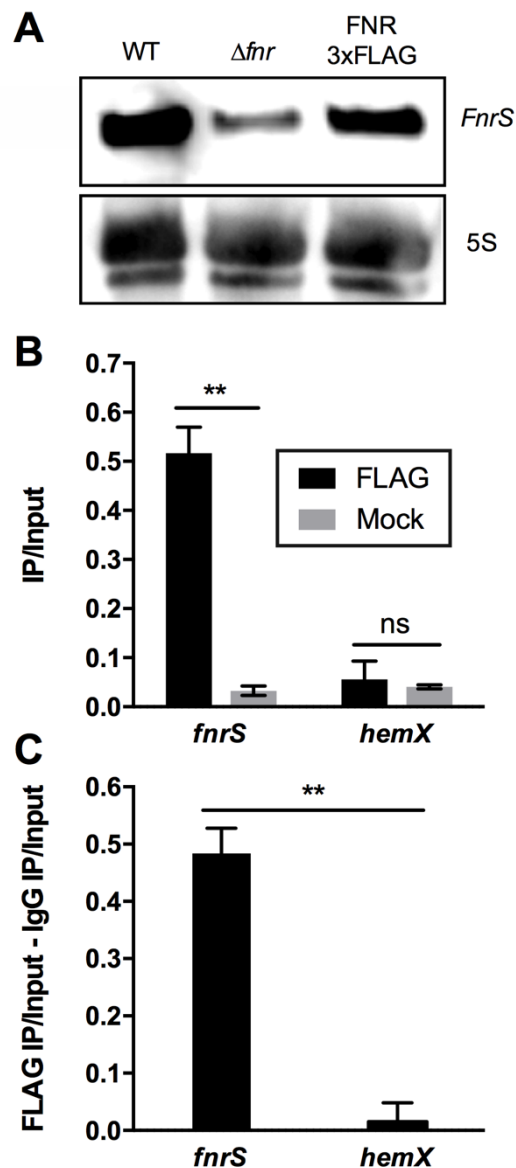


Figure 4.2 FnrS is expressed in FNR-3×FLAG and the *fnrS* gene is bound by FNR-3×FLAG.

A. Northern blot showing FnrS expression is not affected in a strain expressing FLAG-tagged FNR under microaerobic conditions in MMA. 5S rRNA was probed as loading control. B. qPCR data of a representative ChIP assay from 2 independent experiments demonstrating direct binding of FNR to the *fnrS* gene under microaerobic conditions in MMA. Experimental (FLAG) and mock ChIP DNA from *fnrS* and the negative control *hemX*, was normalised to the starting amount of DNA (IP/Input). Statistical significance determined by t-test, $\alpha = 5\%$ C. qPCR data of a representative ChIP assay from 2 independent experiments shows enrichment for FNR binding of *fnrS*, compared to the negative control region *hemX* following subtraction of background mock ChIP DNA (as described in section 2.8.4). Statistical significance determined by Unpaired two-tailed t-test, $\alpha = 5\%$. * = $P \leq 0.05$, ** = $P \leq 0.01$, *** = $P \leq 0.001$, error bars represent standard deviation.

4.2.2 Overview of FNR binding using ChIP-seq

Chromatin Immunoprecipitation is the method of choice to provide evidence for direct protein binding *in vivo*. ChIP-seq involves the use of deep sequencing technology to determine all DNA molecules bound by DNA-associated proteins (Cai & Huang, 2012). Here, we have used ChIP-seq to determine FNR binding under microaerobic conditions in MMA with a strain containing 3×FLAG-tagged FNR. **Figure 4.3** provides an overview of all the predicted FNR binding sites (blue lines and boxes) and FNR binding motifs (red lines) across the *S. Typhimurium* chromosome and two plasmids, pSLT and pColIB9 from two independent ChIP-seq experiments. There were no FNR binding sites on the pRSF1010 plasmid which was anticipated as there were no DE genes found on the plasmid (see Section 3.2.5). Binding of the global transcription factor FNR was uniform across the chromosome. Due to contamination of *S. cerevisiae* yeast genomic DNA from the tRNA used as a co-precipitant intended to increase DNA yields in the ChIP protocol the coverage of ChIP (FLAG and Mock) samples were reduced. Additionally, coverage of the FLAG 1 sample was lower than of FLAG 2 (**Figure 4.4A**) However, the coverage was sufficient to recover a similar number of peaks from both samples, and there was a large of overlap of 288 peak locations (**Figure 4.4B**).

Approximately 19% of differentially expressed genes in this study were associated with peaks from ChIP-seq (**Figure 4.4C**). As anticipated, the *fnr* promoter was bound by FNR. Also, *fnrS* was associated with FNR binding, as were promoters of *nrdD*, the anaerobic ribonucleoside-triphosphate reductase, *nirB*, the large nitrite reductase subunit, and *nuoA*, NADH dehydrogenase I chain A. The extremely downregulated SPI-5 encoded gene *orfX* and the minor curli fimbriae subunit *csgB* were also associated with FNR binding. These genes are therefore directly activated by FNR under microaerobic growth in MMA. Notable up-regulated genes with FNR binding sites included the sRNA *GcvB*, which was highly upregulated in Δfnr and controls approximately 1% of the *Salmonella* genome (Hébrard *et al.*, 2012; Sharma *et al.*, 2007; 2011), and PhoP activated genes *pagC*, *pagD* and *pagO*. FNR occupancy was also observed at the promoter of the plasmid encoded virulence gene and regulator, *spvR*. Many effector proteins which are secreted by the SPI-2 T3SS were associated with peaks including *sseK2*, *sifB*, SPI-5 encoded *pipB*, effectors important for SCV maturation *sifA*, *sseJ* and *sopD2*, and *Salmonella* translocated effectors *steA*, *steB* and *steC*. The important virulence sRNA *IsrM* was also found to be bound by FNR. Within the SPI-2 locus, specific T3SS apparatus genes associated with FNR binding included *ssaH*,

ssaI, *ssaJ* and *ssaU*, but most importantly an FNR binding peak was found near the promoter of the SPI-2 response regulator *ssrB*. Additionally, a long binding region was identified in one replicate at the *ssrA/ssaB* promoter region. These results indicate that FNR may repress SPI-2 under microaerobic conditions by direct repression of several effectors and other virulence associated genes, and especially through *ssrB*.

Approximately 81% of DE genes were not associated with FNR occupancy (**Figure 4.4C**) and, therefore, indirectly regulated by FNR under these conditions. DE genes not associated with FNR binding included the majority of flagellar and chemotaxis genes. However, *fliC* and *fliD* were associated with a peak, as well as *aer*, the gene encoding Aer the signal transducer for aerotaxis. FNR therefore, may indirectly activate certain chemotaxis and flagellar motility through direct activation of *aer*. Additionally, a recent study found that SsrB can repress *S. Typhimurium* motility through direct binding to a region upstream of *flhDC* (Ilyas *et al.*, 2018). Thus, much of the down-regulation of motility, especially of early gene products can be explained by FNR activation of *ssrB*, leading to SsrB repression of motility. Other genes which seem to be indirectly regulated by FNR include the propanediol degradation and cobalamin (vitamin B12) biosynthesis operons, SPI-1 genes *sipB* and *invJ*, and many of the T3SS apparatus and effector genes encoded within SPI-2.

Interestingly, many peaks were identified at genes not found to be DE in our study. This was also the case in an *E. coli* ChIP-seq from a previous study (Myers *et al.*, 2013). Genes of particular interest were all six SPI-4 encoded *sii* *Salmonella* intestinal invasion genes and SPI-1 encoded genes *avrA*, *sprB*, *hilC*, *prgH*, *hilD*, *hilA*, *iagB*, *sptP*, *sicP*, *invB*, *invA*, *invH*, *InvR*, STM2902, and STM2903. Regulation by FNR may be masked by other more significant factors that also regulate transcription at these loci positively or negatively. The full list of ChIP-seq peaks and ChIP peaks associated to DE genes can be found in **Tables S4, S5, and S6** in Appendix III.

4.2.3 FNR consensus binding motif

Peak sequences from ChIP-seq revealed a palindromic FNR binding motif with a length of 14 bp (**Figure 4.5**). The consensus motif was, TTGATNTRSATCAA, where A is adenine, C is cytosine, G is guanine, T is thymine, N is any nucleotide, R is a purine, and S is guanine or cytosine. This consensus motif is almost identical to the FNR consensus binding motifs found in *E. coli* (Myers *et al.*, 2013; Spiro & Guest, 1990) and similar to the previously

described *S. Typhimurium* FNR binding motif. The letter-probability matrix generated by MEME-ChIP was used to find all possible FNR binding sites in the *S. Typhimurium* chromosome using FIMO. The letter-probability matrix of the *S. Typhimurium* FNR binding motif and the top 100 FNR binding motifs found in the *S. Typhimurium* 4/74 chromosome can be found in **Tables S7** and **S8** in Appendix III. A conserved and experimentally confirmed FNR binding site can be found in the *ndh* (NADH dehydrogenase) promoter region in *E. coli*, whereby binding of FNR leads to activation (Green & Guest, 1994). We searched for this site as a positive control for our FNR motif and FIMO found an FNR binding site in the *S. Typhimurium ndh* promoter region centered around -48 from the *ndh* TSS (**Figure 4.5**). The two sites with the closest to consensus binding motifs were found in the promoters of *nirB* and *orf70* centered around -44 and -41, respectively. The large subunit of the NADH nitrite reductase is encoded by *nirB*, and FNR is known to activate at this site. Indeed, in our dataset *nirB* is down-regulated in Δfnr and a ChIP peak was observed for FNR binding at this site. Interestingly, *orf70* is a gene found in the non-T3SS section of SPI-2. A BLAST search revealed that *orf70* shares 99% identity with a fumarase encoding gene, *fumD* (Kronen & Berg, 2015). Under our growth condition, *orf70* was not differentially expressed but the promoter region was enriched in ChIP-seq. As expected, the *fnr* and *fnrS* promoter regions contained FNR binding motifs at +1 and -42, respectively.

Although there was enrichment for FNR binding across most of SPI-2 in our FLAG 2 sample and peaks called in both replicates at the *ssrB* promoter, no full 14 bp motifs were detected. However, when half of the consensus motif was used as a search query many putative sites were detected in the SPI-2 promoters. FNR half-sites have previously been confirmed to be sufficient for FNR binding and regulation (Constantinidou *et al.*, 2006; Melville & Gunsalus, 1996). The most likely candidate half sites for the *ssrB* and *ssrA/ssrB* promoter regions, based on their location are shown (**Figure 4.5**). Interestingly, both a full FNR binding motif and a half binding motif were found at the promoter of *ydgT*. As previously described, YdgT is a known repressor of SPI-2 (Coombes *et al.*, 2005). Again, the *ydgT* gene was not found to be differentially expressed in our data set, however, an enrichment for FNR binding was found in the ChIP data. These half-sites represent putative binding sites for FNR which may explain regulation of SPI-2 under microaerobic conditions.

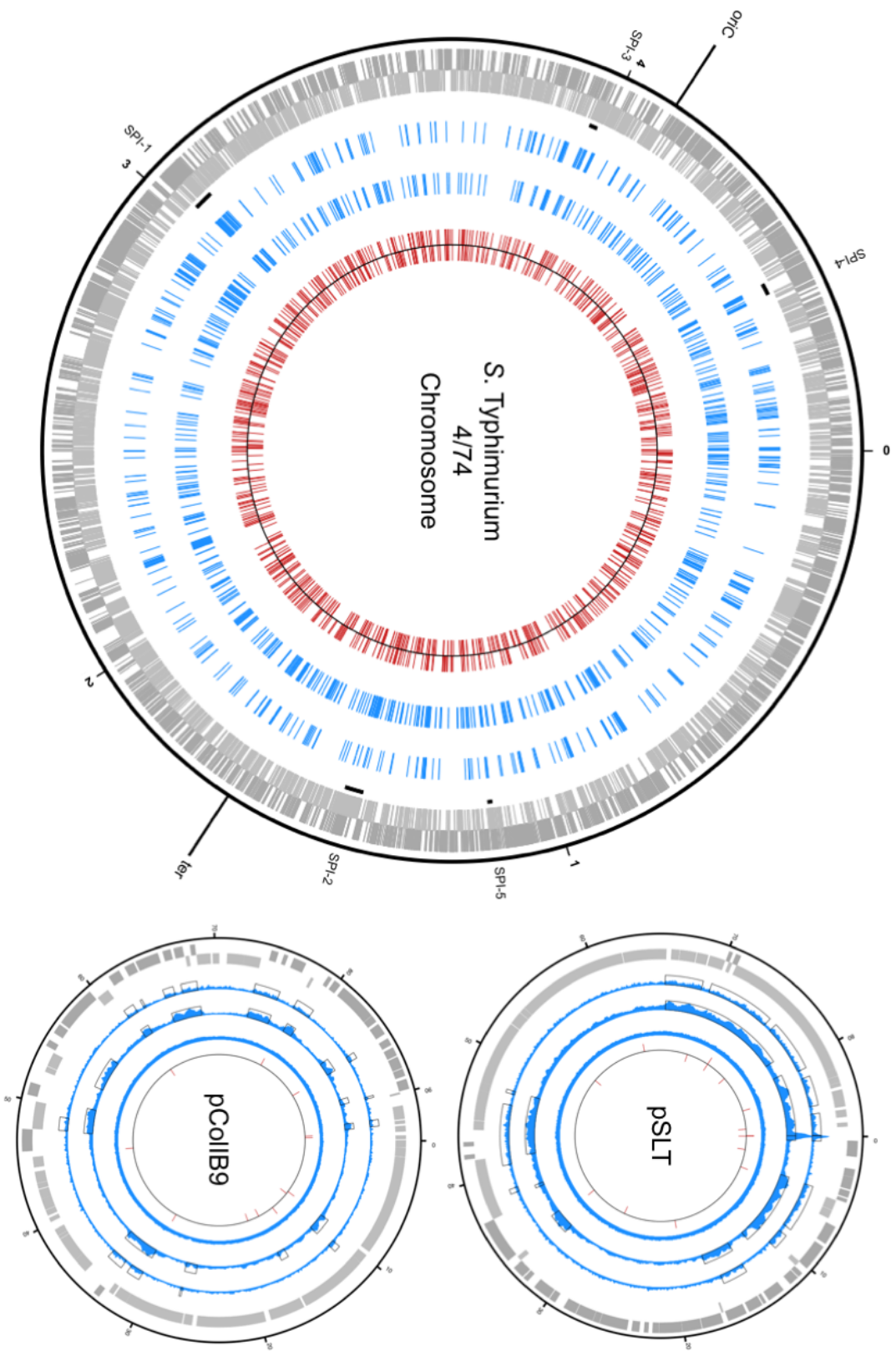


Figure 4.3 FNR ChIP peaks across 2 replicates on the 4/74 chromosome and plasmids.

Peaks representing putative FNR binding sites were determined by MACS2 across two independent replicates on the *S. Typhimurium* chromosome and pSLT and pColIB9 plasmids. From outside to inside: coordinates are denoted, on the chromosome SPIs 1 through 5 are labeled; plus strand genes are dark grey; minus strand genes are light grey; replicate 1 peaks are blue, represented by lines on the chromosome and coverage trace for the plasmids; replicate 2 peaks are blue; on plasmids only, mock coverage trace is in blue; FIMO predicted FNR binding sites based on the consensus motif on plus strand are in red; and the minus strand in red. There were no peaks on the pRSF1010 plasmid.

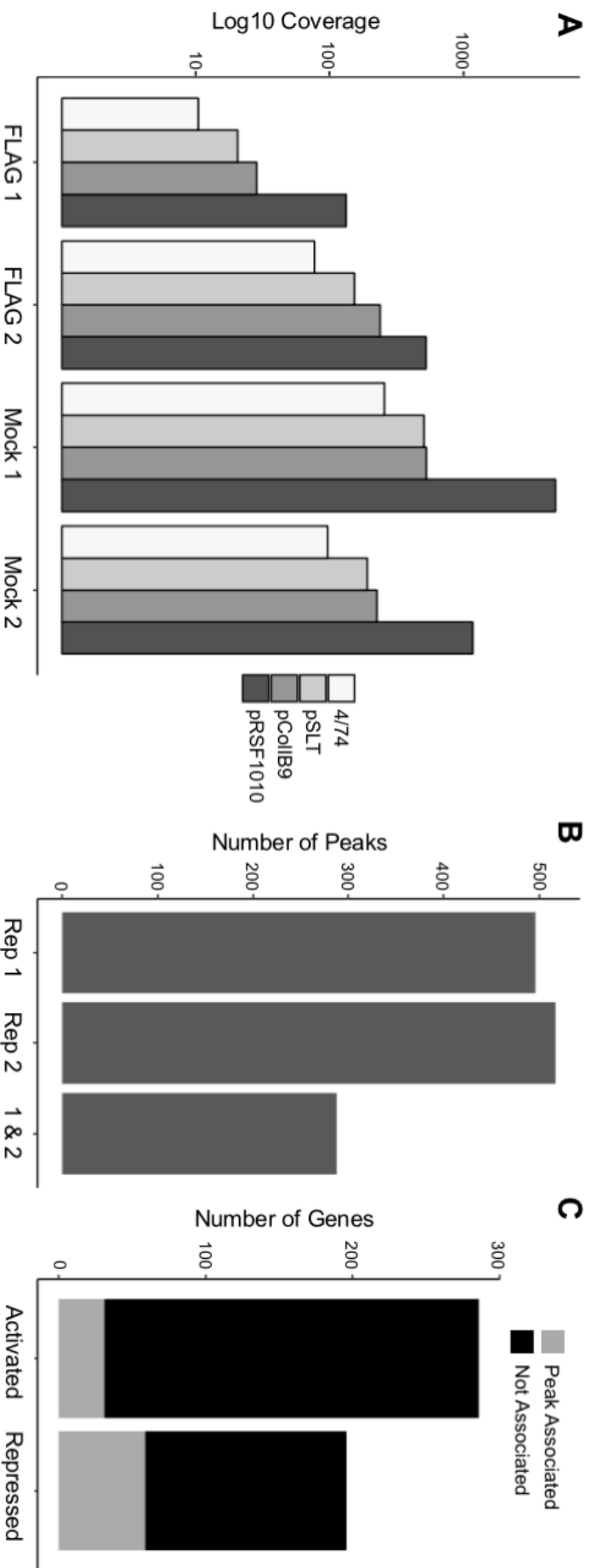


Figure 4.4 Overview of two independent ChIP-seq replicates.

A. Sequencing coverage for each ChIP FLAG and mock replicates divided between the 4/74 chromosome and plasmids. B. Total number of peaks found in each of the ChIP FLAG replicates 1 and 2 and the number of peaks that were common between the two replicates. C. Number of differentially expressed genes in *Afm* from transcriptomic data associated with peaks from ChIP-seq analysis.

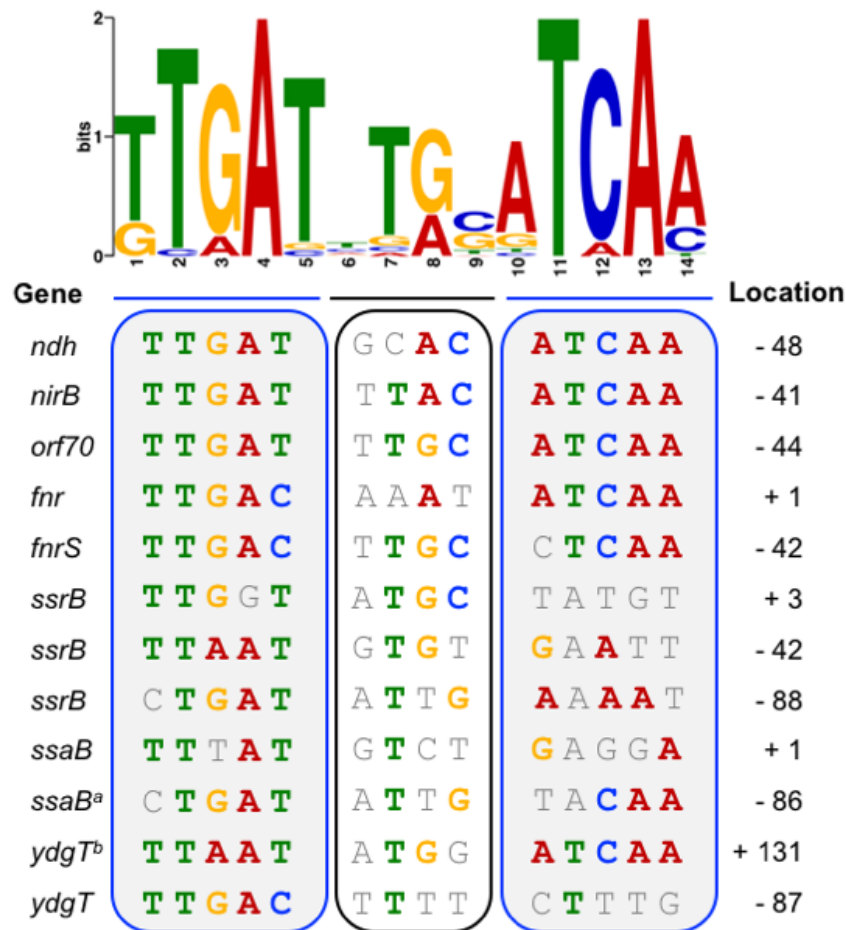


Figure 4.5 FNR binding motifs.

FNR position weight matrix was constructed from the FNR ChIP-seq peak sequences from 288 peaks common to 2 independent ChIP-seq replicates. The height (y-axis) of the letters represents the degree of conservation at that position within the aligned sequence set (in bits), with perfect conservation being 2 bits. The x-axis shows the position of each base (1–14) starting at the 5' end of the motif. Under the consensus motif, a sample of full motifs and half sites were found using the 14 bp and 7 bp of the MEME-ChIP generated motif matrix in FIMO, respectively. Only statistically significant binding sites with $p < 0.0001$ for full motifs and < 0.01 for half sites were interrogated. ^aThis half motif overlaps the 2° *ssrA* TSS. ^bThis motif is found overlapping a TSS of an antisense transcript found in the *ydgT* promoter region.

4.2.4 Verification of FNR binding

To verify putative FNR binding sites binding experiments, such as electrophoretic mobility shift assays (EMSA), have been used to demonstrate that a protein can directly bind a specific fragment of DNA. However, the native FNR protein cannot be easily used for *in*

in vitro experiments, as atmospheric oxygen levels render the protein inactive (Beinert & Kiley, 1999; Green *et al.*, 2014); therefore, a modified FNR must be used. Bates *et al.* originally showed that a mutation resulting in a switch from aspartic acid to alanine at position 154 (D154A) in the dimerization domain of the FNR monomer, resulted in a mutant FNR protein which could be purified as a dimer at atmospheric oxygen levels in *E. coli* (Bates *et al.*, 1995). We introduced the same mutation into our plasmid-borne *S. Typhimurium fnr* to create *pfnrD154A*. The WT and Δfnr mutant were transformed with both *pfnr* and *pfnrD154A*, grown in MMA under aerobic and microaerobic conditions, and *FnrS* expression was used to determine the activity of the FNR or FNRD154A protein. We saw similar levels of *FnrS* expression in cells with an FNR or FNR154A protein under microaerobic conditions, while there was a very limited expression of *FnrS* under aerobic conditions in *pfnr* cells, expression of *FnrS* was near WT microaerobic levels in the presence of FNRD154A (**Figure 4.6**). The expression in *pfnr* under aerobic conditions might be explained by the high copy number of the plasmid. Shan *et al.* were able to construct a more oxygen tolerant FNR variant by covalently linking two FNRD154A monomers in *E. coli* (Shan *et al.*, 2012a). (FNRD154A)₂ recognizes an FNR-dependent promoter under aerobic conditions and maintains its promoter specificity and conformational stability (Shan *et al.*, 2012a). Conveniently, the FNR protein is extremely well conserved at the amino acid level with the *Enterobacteriaceae* family. The amino acid sequences of FNR in *S. Typhimurium* and *E. coli* share 99.2% identity and 99.6% similarity (**Figure 4.7**). Serine (S) and asparagine (N) are neutral polar amino acids, and this substitution has no effect. Alanine (A) is a small non-reactive amino acid, a change to glutamine (Q) is significant as glutamine is much larger and polar neutral amino acid (Betts & Russell, 2003) however, the 2 amino acid differences are found near the C-terminus outside of the DNA binding region. Dr. Aixin Yan from the Shan *et al.* study provided us with a plasmid containing the (FNRD154A)₂ protein; this was used for subsequent binding experiments. To test that the *E. coli* (FNRD154A)₂ protein was active under aerobic conditions, Δfnr was transformed with the plasmids, and we carried out the same experiment using *FnrS* expression to determine activity of the protein. **Figure 4.8A** shows that Δfnr cells containing p(*fnrD154A*)₂ had higher expression of *FnrS* under aerobic than microaerobic conditions. Subsequently, we His-tag purified the protein as a dimer (**Figure 4.8B**) and concentrated the sample (**Figure 4.8C**) for use in EMSA. The same protein was recently used with success in an EMSA analysis on DNA promoters from SL1344 (Wang *et al.*, 2019).

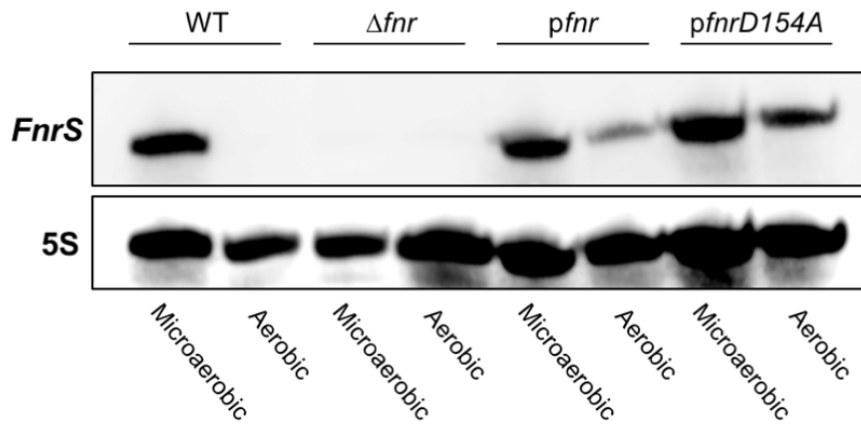


Figure 4.6 FNRD154A is active under aerobic conditions.

Northern blot showing *FnrS* was expressed under aerobic conditions in an Δfnr mutant expressing the FNRD154A protein from the pBR322 plasmid.

<i>S.</i>	1	MIPEKRIIRRIQSGGCAIHCQDCSISQLCIPFTLNEHELDQLDNI IERKK	50
<i>E.</i>	1	MIPEKRIIRRIQSGGCAIHCQDCSISQLCIPFTLNEHELDQLDNI IERKK	50
<i>S.</i>	51	PIQKGQTLFKAGDELKSLYAIRSGTIKSYTITEQGDEQITGFHLAGDLVG	100
<i>E.</i>	51	PIQKGQTLFKAGDELKSLYAIRSGTIKSYTITEQGDEQITGFHLAGDLVG	100
<i>S.</i>	101	FDAIGSGHHPSFAQALETSMVCEIPFETLDDLSGKMPNLRQMMRLMSGE	150
<i>E.</i>	101	FDAIGSGHHPSFAQALETSMVCEIPFETLDDLSGKMPNLRQMMRLMSGE	150
<i>S.</i>	151	<u>IKGDQDMILLLSKKNAEERLAAFIYNLSRRFAQRGFSPREFRLTMTRGDI</u>	200
<i>E.</i>	151	<u>IKGDQDMILLLSKKNAEERLAAFIYNLSRRFAQRGFSPREFRLTMTRGDI</u>	200
<i>S.</i>	201	GNYLGLTVETISRLLGRFQKSGMLAVKGYITIEN S DALA A LAGHTRNVA	250
<i>E.</i>	201	GNYLGLTVETISRLLGRFQKSGMLAVKGYITIEN N DALA Q LAGHTRNVA	250

Figure 4.7 Alignment of *S. Typhimurium* and *E. coli* FNR protein sequences.

FNR amino acid (aa) sequences of *S. Typhimurium* 4/74 (*S.*) and *E. coli* K-12 MG1655 (*E.*) were aligned using the BLOSUM62 matrix with a gap penalty of 10 and extend penalty of 0.5. The sequences are both 250 aa in length and have 99.2% identity and 99.6% similarity. The 4 cysteine residues important for binding 4Fe-4S clusters are underlined, the dimerization region is underlined with a dash line, the DNA binding region is in bold. Identical aa are connected with a |, differences in amino acids are labeled in red with a : and blue with a . indicating changes in aa which are strongly similar and weakly similar in their properties, respectively.

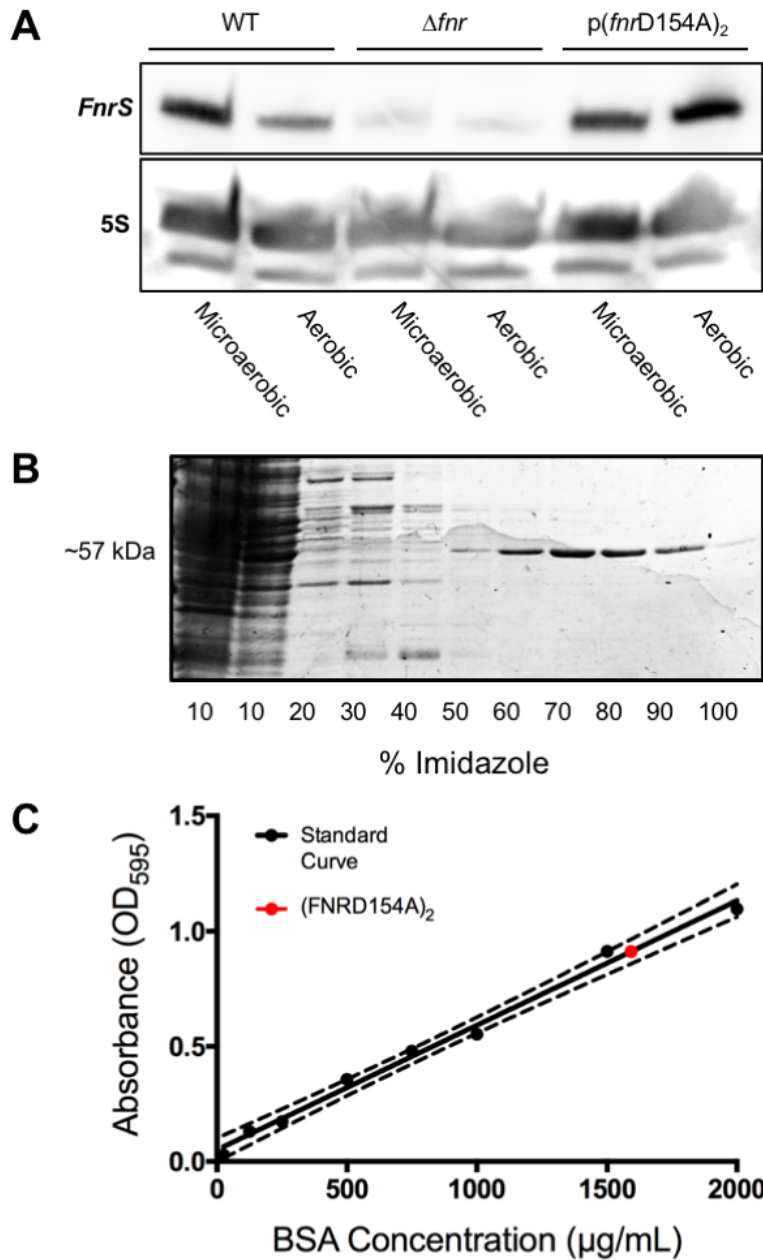


Figure 4.8 (FNRD154A)₂ is active and can be purified under aerobic conditions.

A. Northern blot showing *FnrS* was expressed under aerobic conditions in an Δfnr mutant expressing the *E. coli* (FNRD154A)₂ protein. B. Coomassie stained SDS-PAGE of protein fractions from His-Tag purification of (FNRD154A)₂ showing that the protein was isolated in its dimeric form (Approximately 57 kDa with 6His-Tag). C. BCA assay of (FNRD154A)₂ sample after purification and concentration of protein samples, the dotted lines represent a 95% confidence interval of the linear regression of the standard curve.

4.2.5 FNR binding to control regions

Based on the expression of SPI-2 regulators, either SsrA and/or SsrB were the most likely candidates to explain the increased SPI-2 expression seen in Δfnr grown in MMA under microaerobic conditions, as they were the most differentially expressed of SPI-2 regulators in Δfnr (Figure 4.9). ChIP-seq data also revealed enrichment for FNR binding in 2 independent replicates and motif analysis uncovered 3 potential FNR half-sites at the *ssrB* promoter. Peaks at the *ssrA/ssaB* promoter region were only identified in the second replicate. To verify these findings, we used electrophoretic mobility shift assays. First, as positive controls, the *fnr* and *fnrS* promoters were assayed. A site down stream of *fnrS* in the ORF of *dbpA* was chosen as a negative control as there was no FNR binding as determined by ChIP-seq and FNR would be unlikely to bind at the 3' end of an ORF that did not contain a TSS. The peaks called in ChIP-seq analysis and the coverage trace is shown in Figure 4.10 A & B and is accompanied by a schematic showing the location of sequence used for the EMSAs. As expected, P_{fnr} and P_{fnrS} EMSAs showed a band shift with a dissociation constant (K_D) of approximately 9.3×10^{-7} M and 1.5×10^{-6} M confirming that (FNRD154A)₂ binds to the *fnr* and *fnrS* promoters (Figure 4.10 C, D, F & G). The smaller the K_D , the more tightly bound the ligand (in this case DNA) is, or the higher the affinity between DNA and protein. The B_{max} is the maximum ratio of bound to unbound DNA; (FNRD154A)₂ bound to 84.9% and 92.9% of P_{fnr} and P_{fnrS} , respectively. (FNRD154A)₂ did not bind to *dbpA* DNA (Figure 4.10 E & H).

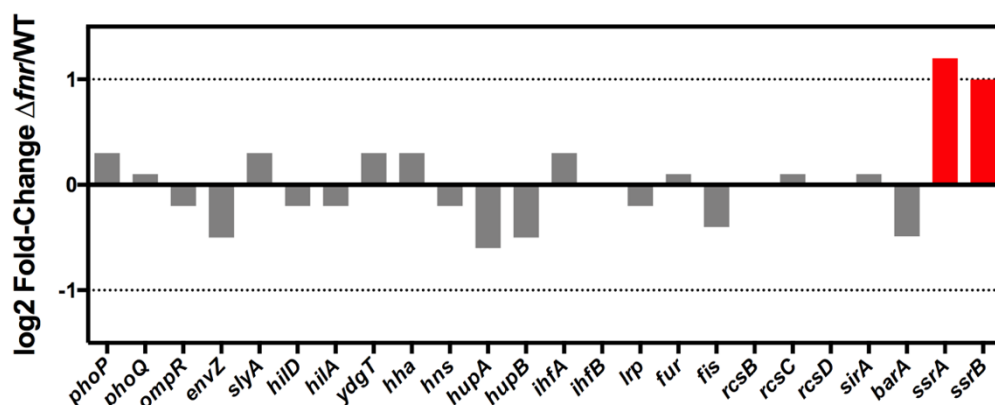


Figure 4.9 The genes encoding SsrA and SsrB are the most differentially expressed of SPI-2 regulators.

RNA-seq data showing log₂ fold-change of important SPI-2 regulators. All regulators in grey were not differentially expressed (>-1 and < 1) in Δfnr . The *ssrA* and *ssrB* genes (in red) had the highest fold-change of all regulators with known involvement in SPI-2 regulation.

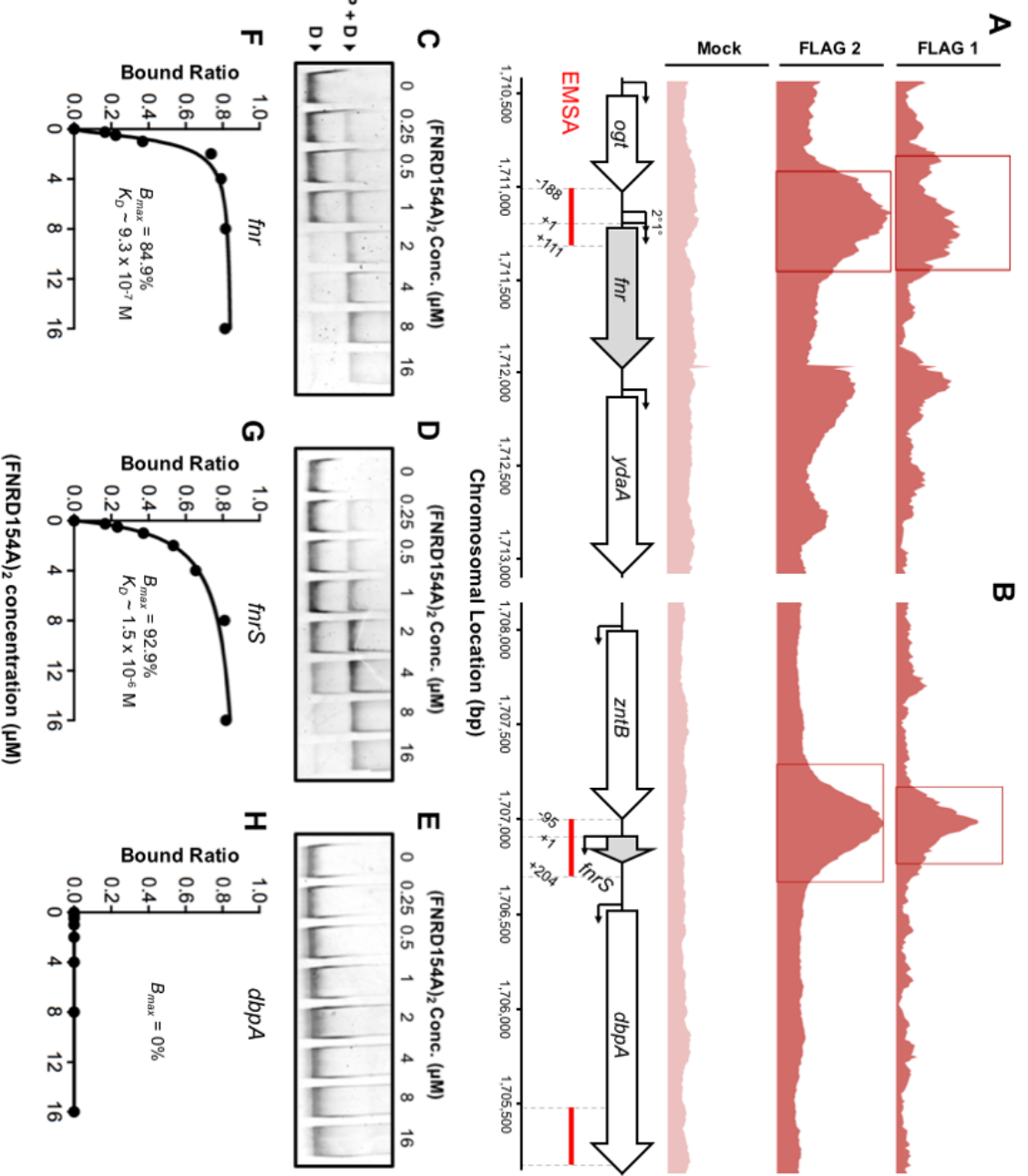


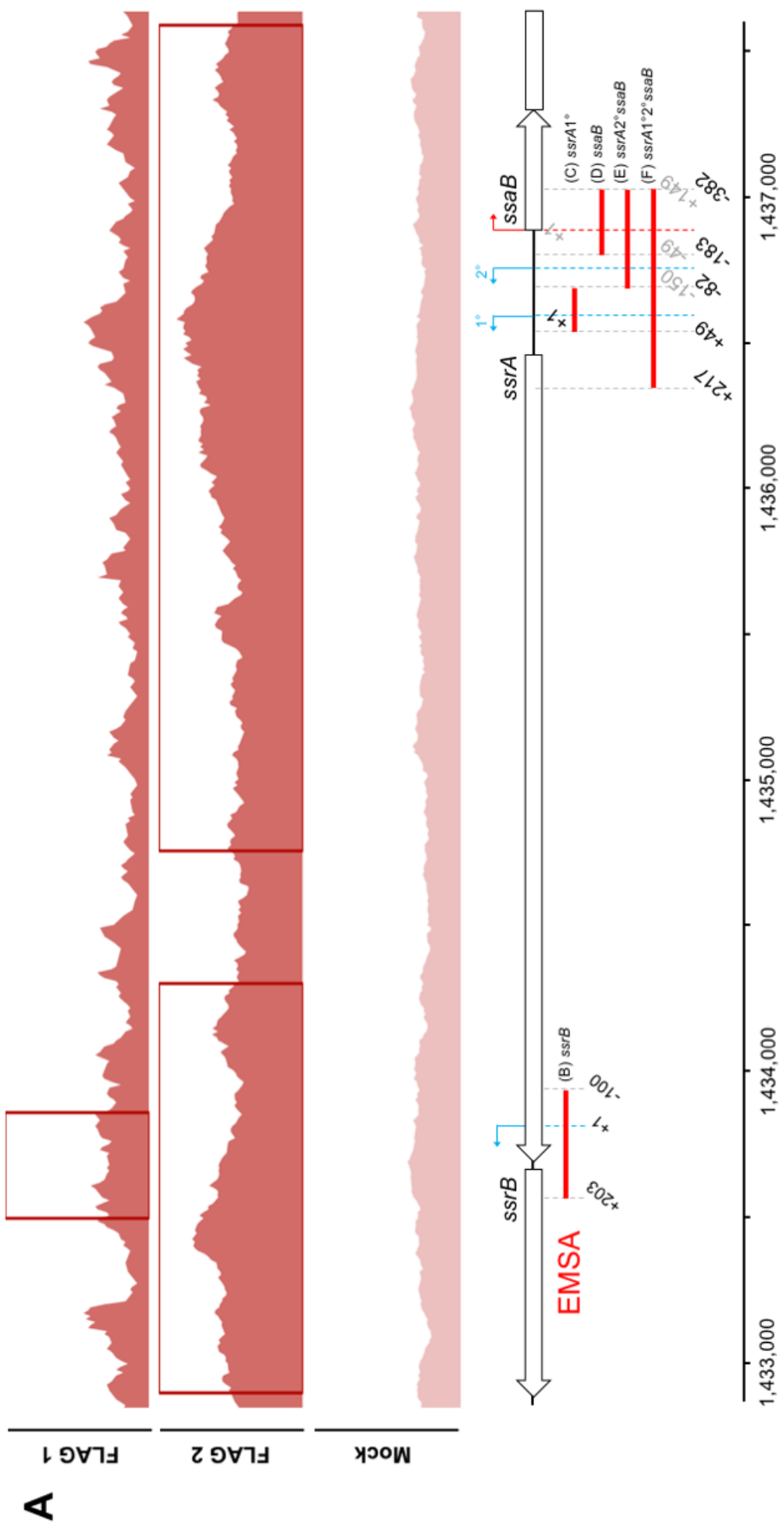
Figure 4.10 FNR binding at the P_{fnr} and P_{fnrS} promoters and a negative control.

A, B. ChIP-seq coverage (y-axis) for FLAG 1 and 2 replicates in red and Mock in light red. Boxes indicate putative FNR binding sites called by MACS2. Schematic shows location of *fnr* and *fnrS* as grey arrows and surrounding genes including *dbpA* as white as arrows and shows the location (red lines) of the sequence used for EMSA relative to the respective TSSs (black bent arrows). C – E. Representative EMSAs using purified (FNRD154A)₂ with the P_{fnr} and P_{fnrS} promoters and *dbpA*, respectively; “P + D” is protein bound to DNA, and “D” is unbound DNA. F – H. Equilibrium DNA binding curves for the P_{fnr} and P_{fnrS} promoters and *dbpA*, respectively; fitted by nonlinear regression and K_D and B_{max} were determined by one site specific binding with Hill slope analysis. Promoters P_{fnr} and P_{fnrS} were used as positive controls, and *dbpA* as a negative control for EMSAs.

4.2.6 FNR binding to SPI-2 promoters

Next, we investigated the promoters of *ssrB*, *ssrA* and *ssaB*. The P_{ssrB} is comprised of the intergenic region between *ssrB* and *ssrA* ORFs and extends to overlap a portion of the 3' end of *ssrA* (**Figure 4.11A**). (FNR154A)₂ had a weaker binding affinity to P_{ssrB} than positive controls ($K_D \sim 2.1 \times 10^{-6}$ M, **Figure 4.11B & G**). The intergenic region between the *ssrA* and *ssaB* genes is extremely AT rich (69.0% AT content) compared to the rest of the chromosome (47.8% AT content) (Papanikolaou *et al.*, 2009) and contains two TSSs for *ssrA* and one for *ssaB* (**Figure 4.11A**) and the *ssrA* mRNA is transcribed from the 1° TSS. (FNR154A)₂ was unable to cause a band shift in the region surrounding (49 bp downstream and 82 bp upstream) the 1° TSS of *ssrA*; the unbound probe appears to reduce in intensity at 16 μ M of (FNR154A)₂ however, there is no clear shifted band (**Figure 4.11C & H**). (FNR154A)₂ had a stronger binding affinity to the *ssaB* promoter ($K_D \sim 1.3 \times 10^{-6}$ M) than to P_{ssrB} , but nearly the same affinity when the DNA probe was extended to also include the 2° *ssrA* TSS ($K_D \sim 2.0 \times 10^{-6}$ M) (**Figure 4.11D, E, I, & J**). EMSA with the entire intergenic region between *ssrA* and *ssaB*, $P_{ssrA1^\circ 2^\circ ssaB}$, showed a higher binding affinity than any of the smaller fragments ($K_D \sim 6.2 \times 10^{-7}$ M) as DNA started shifting at a lower concentration of (FNR154A)₂ however, similarly to the P_{ssrA1° EMSA, the binding at 16 μ M becomes unclear; this larger DNA probe contains the P_{ssrA1° sequence, and so this result indicates there may be non-specific binding at the highest concentration of (FNR154A)₂ used in these assays (**Figure 4.11 F & K**). Non-specific binding by FNR at this site could be due to the extremely high AT concentration found at this locus. A higher concentration of the

(FNRD154A)₂ protein may be required shift a higher proportion of the DNA of these promoters, as 16 μM of the protein resulted in B_{max} values below 50% (**Figure 4.11G–K**). These results indicate that FNR binds with low affinity to P_{ssrB} and P_{ssaB} likely due to the presence of FNR half sites at these locations, and FNR may also bind non-specifically in near the P_{ssrA} due to the high AT content of this region (~69%) and high AT content of the FNR consensus binding motif (~64%).



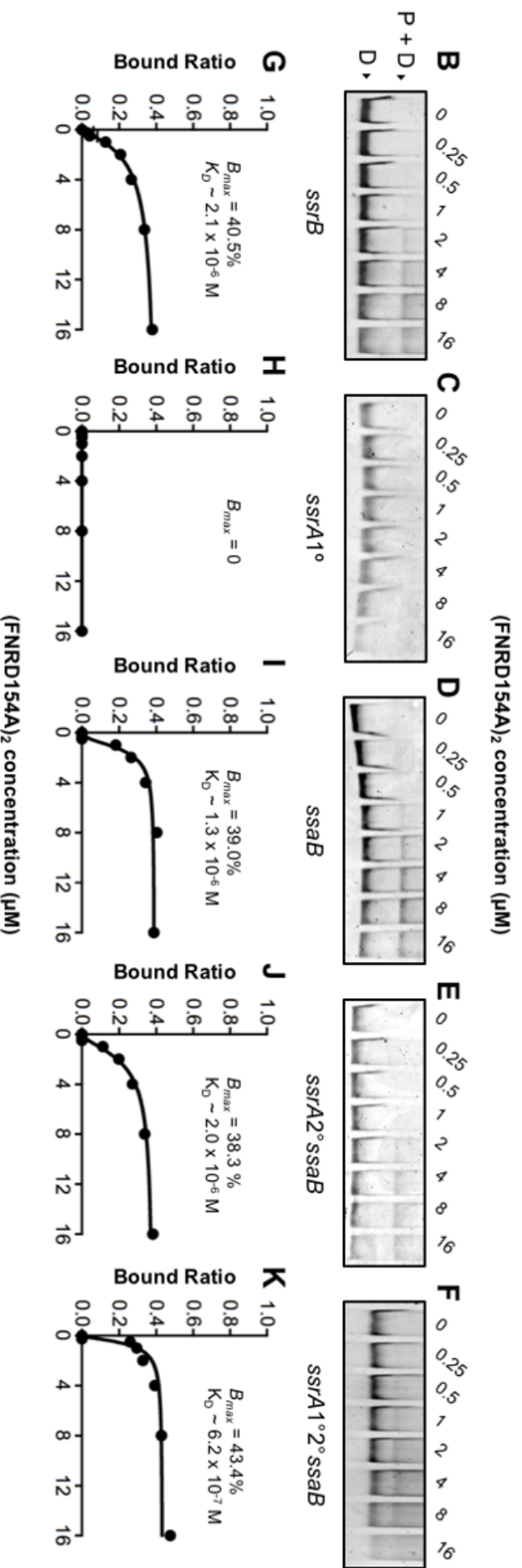


Figure 4.11 FNR binding at the P_{ssrB}, P_{ssrA} and P_{ssAB} promoters.

A. ChIP-seq coverage (y-axis) for FLAG 1 and 2 replicates in red and Mock in light red. Boxes indicate putative FNR binding sites called by MACS2. Schematic shows location of the *ssrB*, *ssrA* and *ssAB* genes in white as arrows, and shows the location (red lines) of the sequence used for EMSA relative to the respective TSSs (blue and red bent arrows); in the *ssrA/ssAB* intergenic region of the schematic, grey numbers are bp relative to the *ssAB* TSS and black numbers are bp relative to the *ssrA* 1° TSS. B – F. Representative EMSAs using purified (FNRD154A)₂ with the P_{ssrB}, P_{ssrA} 1°, P_{ssAB}, P_{ssrA} 2° and P_{ssrA} 1° 2° promoters, respectively; “P + D” is protein bound to DNA, and “D” is unbound DNA. G – K. Equilibrium DNA binding curves for the P_{ssrB}, P_{ssrA} 1°, P_{ssAB}, P_{ssrA} 2° and P_{ssrA} 1° 2° promoters, respectively; fitted by nonlinear regression and K_D and B_{max} were determined by one site specific binding with Hill slope analysis.

4.2.7 FNR binding to the *ydgT* promoter

Finally, we examined binding at the *ydgT* promoter region. As previously discussed, YdgT is a known repressor of SPI-2. Although there was little difference in expression of *ydgT* between WT and Δfnr (**Figure 4.9**), ChIP-seq showed binding near the P_{ydgT} . However, the peaks have the highest coverage at the TSS of an unannotated antisense transcript found in the *ydgT* promoter region (**Figure 4.12A**). The EMSA sequence does contain 5 bp of the 14 bp binding motif found at the antisense TSS at the edge of the DNA probe as well as the half motif centered at -87 from the *ydgT* TSS. While binding of (FNRD154A)₂ caused a shift beginning at 0.25 μ M, higher concentrations do not reveal a clear shifted band (**Figure 4.12B & C**); this could be due to transient binding at the partial antisense TSS. More experimentation is required to elucidate the binding affinities specifically for each of the antisense TSS and the P_{ydgT} half-site. Nevertheless, *ydgT* was not differentially expressed in Δfnr , indicating it likely does not play a role in FNR control over SPI-2 expression under these conditions.

4.2.8 Expression from SPI-2 promoters

To investigate the effect of Δfnr on individual promoters, the promoters of *ssrB*, *ssrA* (partial promoter, P_{ssrA1° , and full promoter) and *ssaB* and a negative control sequence from *dbpA* were cloned into the pCS26-*luxCDABE* low copy plasmid. **Figure 4.13A** shows the locations of promoter sequences taken from *ssrB*, *ssrA* and *ssaB* promoter regions relative to the TSS; the *ssrA* locations are shown relative to the primary TSS. Expression from P_{ssrB} was significantly higher (approximately 1.8-fold) in Δfnr than WT which was consistent with RNA-seq data; P_{ssrB} expression in WT was also significantly higher than in $\Delta ssrAB$ (**Figure 4.13B**). Neither P_{ssrA1° or P_{ssrA} expression was significantly different in any strain (**Figure 4.13C & D**). The result from P_{ssrA1° is consistent with our data showing that FNR is unlikely to cause repression at this location however, the expression from the full *ssrA* promoter was very low. We had expected to see higher expression, especially in the Δfnr mutant. The strains carrying this plasmid were also grown in SPI-2 inducing PCN medium as a control and showed the same low expression therefore, thus there is an unknown problem with this plasmid. As anticipated, expression from P_{ssaB} was significantly higher (approximately 18-fold) in Δfnr than WT (**Figure 4.13E**). There was no expression detected in the *dbpA* negative control (**Figure 4.13F**). These results, especially the invariable

expression from P_{ssrA1}° , highlight *ssrB* as the major target for FNR for regulation of SPI-2 expression.

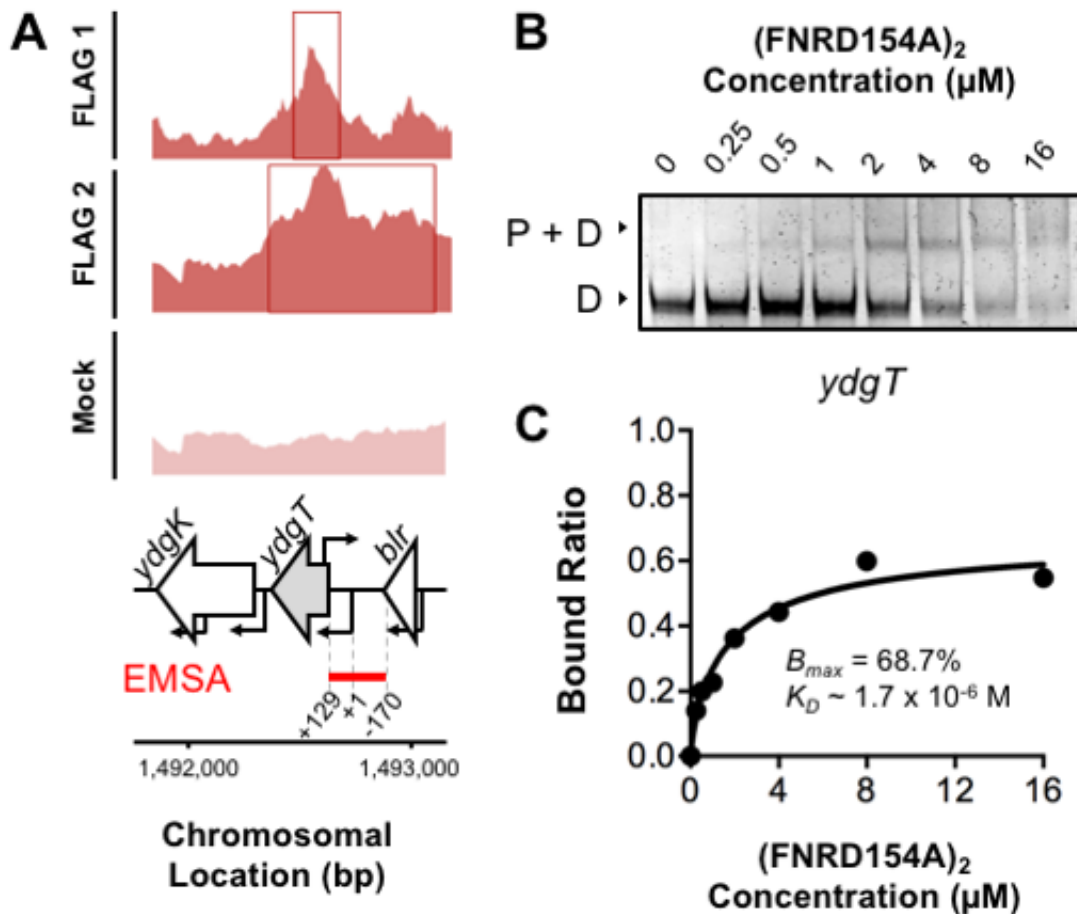


Figure 4.12 FNR binding at the P_{ydgT} promoter.

A. ChIP-seq coverage (y-axis) for FLAG 1 and 2 replicates in red and Mock in light red. Boxes indicate putative FNR binding sites called by MACS2. Schematic shows location of the *ydgT* gene in grey and surrounding genes in white as arrows and shows the location (red line) of the sequence used for EMSA relative to the *ydgT* TSS (black bent arrow). B. Representative EMSA using purified (FNRD154A)₂ with the P_{ydgT} probe; “P + D” is protein bound to DNA, and “D” is unbound DNA. C. Equilibrium DNA binding curve fitted by nonlinear regression and K_D and B_{max} determined by one site specific binding with Hill slope analysis.

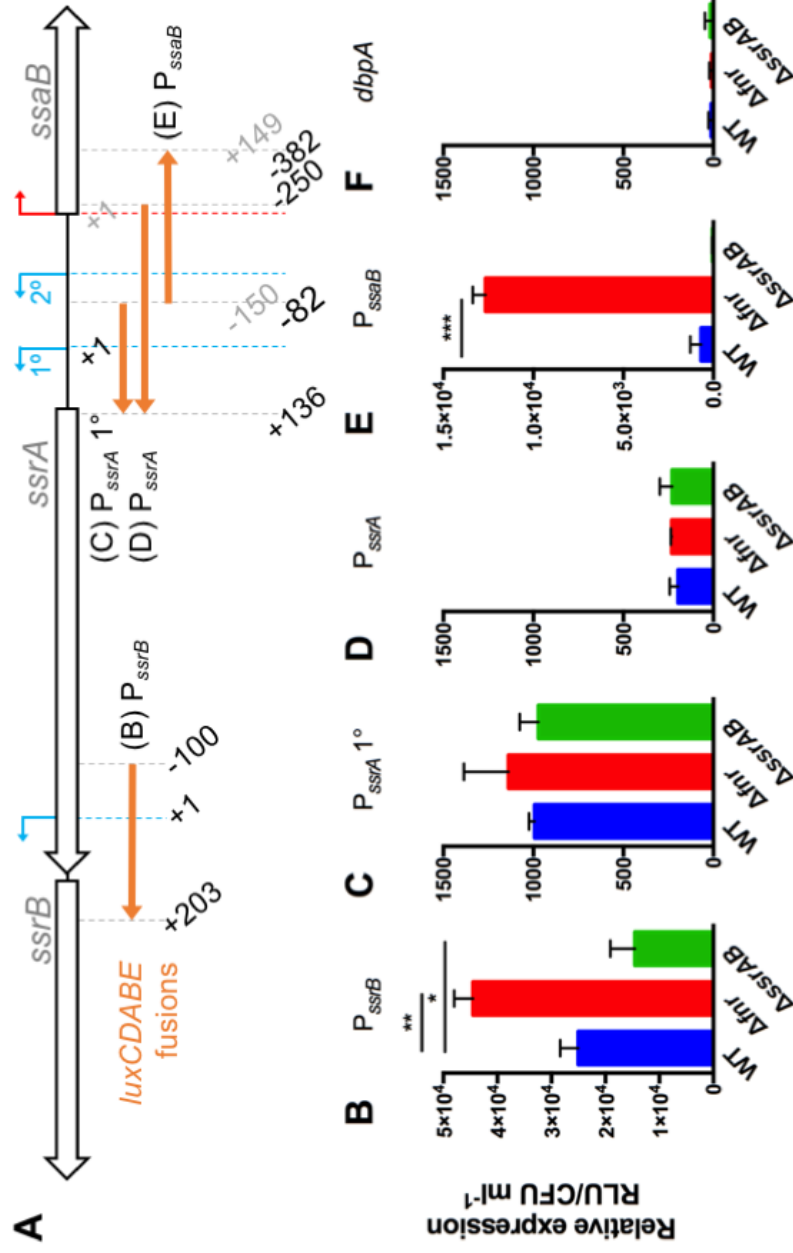


Figure 4.13 Promoter expression from SPI-2 promoters.

A. Schematic showing the locations of promoter sequences cloned into the pCS26-*luxCDABE* plasmid (orange arrows); in the *ssrA/ssaB* intergenic region grey numbers are bp relative to the *ssrA* TSS and black numbers are bp relative to the *ssrA* 1° TSS. Relative promoter expression of the *B. ssrB* promoter, C. truncated *ssrA* promoter, D. full *ssrA* promoter, E. *ssaB* promoter, and F. a section of the *dbpA* gene (as in Figure 4.10) as a negative “no promoter” control. Significance determined by nonparametric one-way ANOVA with Dunnett’s multiple comparison test to WT for each promoter; only significant differences are labeled, * = p \leq 0.05, ** = p \leq 0.01, *** = p \leq 0.001, error bars represent standard deviation.

4.3 Discussion

To our knowledge, the work presented here is the first large scale DNA-protein binding study that has been carried out for the FNR protein in *S. Typhimurium* using high throughput next generation sequencing. The use of ChIP-seq has allowed us to identify 288 putative FNR binding sites across the entire *S. Typhimurium* chromosome and plasmids. We were able to validate through ChIP-seq and EMSA that FNR acts as a direct repressor of *Salmonella* pathogenicity island 2 through direct repression of the response regulator *ssrB* and the apparatus gene *ssaB*. Consequently, FNR indirectly represses the remainder of SPI-2 genes through the repression of *ssrB*. ChIP-seq also revealed FNR binding sites at SPI-2 associated genes encoded outside of the island, which could be validated in the future.

4.3.1 Low binding affinity at SPI-2

ChIP-seq revealed occupancy of FNR in long binding regions at SPI-2 promoters, and in a low coverage sample, binding was difficult to distinguish from background (**Figure 4.11A**). However, we were able to show that FNR binds to these sequences, albeit weakly, *in vitro* using EMSA (**Figure 4.11 B–K**). The weak binding affinity found at these sites is likely due to the presence of FNR half-sites as opposed to full binding motifs (**Figure 4.5**). The quality of the binding site in a given promoter may govern the degree of anoxia required to induce that promoter (Spiro & Guest, 1990). Additionally, because our microaerobic growth condition is heterogeneous, there are likely different subpopulations of cells in the flask where binding occurs (at the bottom), and another where it cannot occur due to higher oxygen concentrations (at the surface). An experiment that would provide insight to binding of FNR to SPI-2 promoters is DNase I footprinting. DNase I footprinting is advantageous because it determines the boundaries of a transcription factor binding site and is informative for evaluating or optimizing binding motif analysis (Myers *et al.*, 2015). Although, the drawback is that DNase I footprinting is performed *in vitro*. Weak binding or failure to observe binding *in vitro* does not rule out binding *in vivo* and could signify an interesting regulatory mechanism. For example, some binding events require cooperative interactions with other TFs (Lee & Groisman, 2012; Melville & Gunsalus, 1996; Park *et al.*, 2013) and may require specific cellular conditions that are difficult to replicate *in vitro* (Myers *et al.*, 2015).

4.3.2 *The role of ydgT*

Although *ydgT* was not differentially expressed in the Δfnr mutant, FNR was found to bind at this promoter (**Figure 4.12**). Motif analysis revealed a full binding motif as well as a half motif in the *ydgT* promoter region. While FNR may regulate *ydgT* through binding at the half motif, the full FNR motif is positioned at the TSS of an unannotated antisense transcript in the *ydgT* promoter region, and not in a position relative to the *ydgT* TSS that is compatible with either activation or repression of the gene. Further investigation into this antisense transcript is required but, we can speculate that it is directly regulated by FNR due to the presence of the near consensus FNR binding motif and up-regulation in Δfnr , and its position relative to *ydgT* makes it a prime candidate as a cis-acting sRNA which may post-transcriptionally repress *ydgT* under aerobic conditions.

4.3.3 *The benefits and limitations of ChIP-seq for investigations of in vivo protein-DNA interactions*

ChIP-seq technology is becoming more accessible to researchers and producing more large-scale *in vivo* DNA-protein interaction studies which contribute to the expansion of our knowledge base. The development of tools to analyze ChIP-seq data in bacteria is an evolving pipeline and, as such, new approaches and algorithms are being introduced frequently. These bioinformatic tools allow us to distil the important information from the massive data sets that are produced using ChIP-seq. We have shown that the use of ChIP-seq provides accurate information that agrees with existing FNR binding and motif data from *E. coli*, and here in combination with RNA-seq has helped to determine the direct and indirect control exerted by the FNR regulon, particularly as it relates to SPI-2 expression.

Like other high throughput sequencing techniques such as RNA-seq, ChIP-seq also comes with limitations. As discussed in Chapter 3, examination of populations of cells gives an average view of gene regulatory events. Currently there are no studies using single-cell ChIP-seq in bacteria or eukaryotic cells (Nakato & Shirahige, 2017), and bacteria present an even larger barrier to single-cell ChIP as the small size of individual bacterial cells means they contain far less DNA and protein than eukaryotic cells. DNA sequencing coverage is a major limitation of single-cell ChIP-seq, as the analysis requires large amounts of starting material (Nakato & Shirahige, 2017).

DNA sequencing coverage can also pose a problem to existing ChIP-seq methods. In this study, the first replicate had lower sequencing coverage than replicate 2 (**Figure 4.4A**). This made peak calling more difficult, especially in the low copy replicate and in regions where FNR is suspected to bind but, at lower affinity due to the quality of FNR binding sites present (**Figure 4.5**). Peak calling algorithms, such as MACS2 (used in this study) are important because they remove the subjective bias from visual peak calling and provide a statistical basis for determining areas of enrichment (Myers *et al.*, 2015), but had problems identifying peaks in the lower coverage sample, especially in AT rich regions where FNR occupancy occurred as a long binding region. The ChIP protocol used for this study was originally designed for use with ChIP-chip and not sequencing (Dillon & Dorman, 2010). Yeast tRNA is used in the protocol as a co-precipitant intended to increase DNA yields during immunoprecipitation. However, some samples had large numbers of reads which did not map to the *S. Typhimurium* genome but, were found to map to the *S. cerevisiae* genome. Dr. Aoife Colgan who was performing similar ChIP experiments during the analysis of ChIP data in this study, used qPCR with primers specific to *S. cerevisiae* and identified that the reads came from yeast gDNA contamination in the tRNA. Since this contaminant gDNA was introduced in the final stages of the experiment, they do not affect the outcome of the ChIP experiment apart from reducing the coverage of the sample. Therefore, if the FNR-ChIP were to be repeated, eliminating yeast tRNA as a co-precipitant is advised.

Successful chromatin immunoprecipitation requires that proteins be crosslinked with DNA to trap interactions inside actively growing cells. Formaldehyde fixation is the method of choice as it allows captures of weaker and transient protein-DNA interactions (Davis *et al.*, 2011; Myers *et al.*, 2015; Schmidt *et al.*, 2009). However, more recent studies have shown that variation in ChIP signal can be attributed to cross-linking efficiency and that extended cross-linking time may introduce false positives (Baranello *et al.*, 2016; Myers *et al.*, 2013). It may be desirable to repeat the ChIP experiment in this study and reduce cross-linking time to help eliminate any binding artifacts. However, when considering FNR binding at SPI-2 promoters, we were able to show that FNR is able to bind *in vitro* to these sequences using EMSA (**Figure 4.11**).

Correlation of FNR ChIP-seq peaks with transcriptomic data showed that the minority of FNR-regulated operons could be attributed to direct FNR binding, the same as in *E. coli* (Myers *et al.*, 2013). Conversely, FNR bound some promoters, such as at SPI-1 and SPI-4

without regulating expression. These genes likely require additional regulatory input by other condition-specific transcription factors, especially given the fact it has been shown that FNR leads to differential expression of SPI-1 genes in MOPS buffered LB with xylose (Fink *et al.*, 2007; Wang *et al.*, 2019). Nuanced regulation by multiple transcription factors may allow *S. Typhimurium* to respond rapidly to environmental changes and confer an advantage in the gut which fluctuates in availability of nutrients and oxygen concentration. However, binding of a TF to a specific DNA sequence does not necessarily result in control of gene expression of nearby genes (Stormo & Zhao, 2010). Many FNR binding sites are also occupied by nucleoid associated proteins (NAPs) such as H-NS, IHF and Fis in *E. coli*, which restrict access of FNR to the genome (Myers *et al.*, 2013). This is important for this study as many NAPs also occupy the AT rich promoter regions of SPI-2 genes (**Figure 4.14**). However, SPI-2 repression by TFs such as H-NS appears not to occur in MMA under microaerobic or aerobic conditions (**Figure 3.14**), further experimentation is required to determine exactly which transcription factors bind to SPI-2 promoters under these growth conditions.

An additional control which may add confidence to our results would be to perform ChIP with either a control strain lacking FNR (Δfnr) or containing an untagged version of FNR to reveal any non-specific enrichment due to aberrant binding of the monoclonal anti-FLAG M2 antibody used in this study, thus allowing removal of any false positive areas of enrichment (Myers *et al.*, 2015). Furthermore, studies using two biological replicates have shown to be sufficient for identification of highly enriched DNA binding locations (Myers *et al.*, 2013; Park *et al.*, 2013) however, three biological replicates can aid in identifying less enriched regions and also provide greater statistical power (Myers *et al.*, 2015). Mutational analysis of putative FNR binding sites could also give greater insight into binding at SPI-2 promoters. The rearrangement of half motifs followed by either ChIP-RTqPCR or EMSA could determine if loss of the FNR motif abolished FNR binding.

Nevertheless, the combination of transcriptomic analysis, occupancy data and DNA-protein binding analysis of the *S. Typhimurium* FNR regulon and its role in regulation of virulence through direct repression of *ssrB* and SPI-2 effectors presented here, will contribute to the overall understanding of *S. Typhimurium* infection.

4.3.4 Summary

The aim of this chapter was to use the global approach of ChIP-seq to identify candidate regulators of SPI-2 under microaerobic conditions. Here we have shown that FNR binds weakly to SPI-2 promoters, particularly to the promoters of *ssrB* and *ssaB*. This may partially explain the repression of SPI-2 genes in WT under microaerobic conditions in MMA as SsrB is a necessary activator of all SPI-2 genes including those encoded outside of the genomic island. We have also shown that FNR binds strongly at the *FnrS* promoter under these conditions, and we know from transcriptomic data that *FnrS* expression is drastically decreased when FNR is absent. In a recent study, deletion of *FnrS* led to increased HilD production under low aeration conditions, and *FnrS* could bind to the *hilD* mRNA 5' UTR, resulting in translational repression (Kim *et al.*, 2018). As HilD is an important activator of SPI-2 and thus FNR could indirectly repress HilD through *FnrS* post-transcriptional repression. Overall, oxygen is an important signalling molecule for low level induction of SPI-2 genes and this induction works directly and possibly indirectly through FNR.

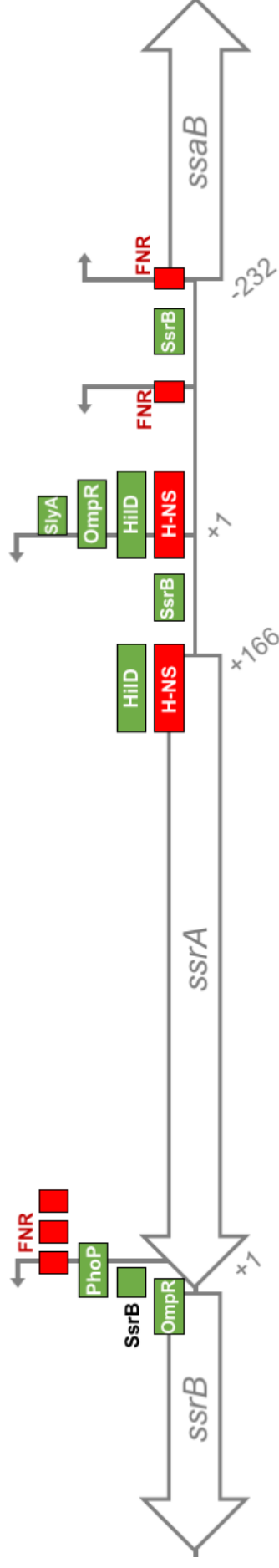


Figure 4.14 Putative FNR binding sites overlap with TF binding at the *ssrB/ssrA/ssrA/ssrB* locus.

Putative binding sites are FNR half-sites (Figure 4.9) present in locations where there was a positive band shift (Figure 4.11) SPI-2 encoded genes are represented by white arrows, TSSs are represented by bent black arrows, and transcription factor binding sites are represented by boxes filled according to the binding sites legend. Activation sites are green and repression sites are red. Numbers represent bp in the *ssrA/ssrA* intergenic region and are relative to the *ssrA* 1^o TSS. Schematic including putative FNR binding sites adapted from Banda et al., 2018.

Chapter 5
**Effects of Δfnr on virulence in macrophages and
bacterial fitness**

5.1 Introduction

5.1.1 Investigation of virulence and bacterial fitness in Δfnr

Virulence factors enhance the fitness of a pathogen under specific conditions such as in the host and genes involved in metabolism can provide a niche for bacteria during infection which allows them to out compete resident microbiota (Thiennimitr *et al.*, 2012; Winter *et al.*, 2013). After entering the gastrointestinal tract on the way to the site of infection, *S. Typhimurium* encounters a remarkable diversity in environmental conditions between the stomach, small intestine and large intestine. Moreover, even within the small intestine, there are differences in the microenvironments of the lumen, mucous layer and epithelial surface. Surviving passage through the vastly different environments encountered in the host is accomplished through appropriate coordination of virulence gene expression in response to environmental cues at different stages of infection. Both under and over-expression of virulence factors can be detrimental to bacterial fitness (Coombes *et al.*, 2005). Through previous work and this study, it is clear that FNR is an important regulator of virulence in *S. Typhimurium* (Fink *et al.*, 2007; Wang *et al.*, 2019). Here we investigate the effect of the *fnr* mutation in different media to attempt to elucidate what signals besides oxygen might be important for SPI-2 regulation in an Δfnr mutant. We also wanted to investigate the role of FNR during macrophage infection, as previous studies have revealed that Δfnr mutants are attenuated *in vivo*. Additionally, we looked at the relative bacterial fitness of Δfnr compared to WT and other isogenic mutant of strain 4/74 under different conditions in an attempt to tease apart if SPI-2 expression was a burden to cell fitness. Finally, we used a proteomic approach (**Figure 5.1**) to investigate the energetics of WT and Δfnr during growth in microaerobic MMA.

The aim of this chapter is to investigate the role of FNR during intracellular replication in murine macrophages and to investigate the bacterial fitness of the Δfnr mutant in MMA and other *in vitro* growth conditions.

Cells grown in microaerobic MMA to OD₆₀₀ 0.3

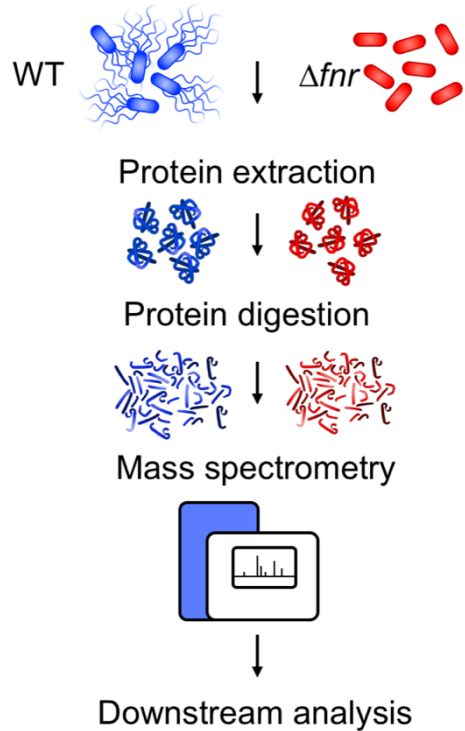


Figure 5.1 Workflow of general experimental procedures for investigating expressed proteins.

Wild-type (WT), Δfnr strains were grown under microaerobic conditions to OD₆₀₀ 0.3 in MMA and protein was extracted. Protein was digested and prepared for processing by mass spectrometry. Protein sample preparation was done by Dr. Nicole Hansmeier and all subsequent processing and analysis was completed by Dr. Tzu-Chiao Chao at the University of Regina, Regina, Saskatchewan, Canada. Downstream analysis was performed by Dr. Tzu-Chiao Chao and me.

5.2 Results

5.2.1 SPI-2 expression *in vitro*

Although SPI-2 expression has not previously been directly linked to FNR, previous studies have shown that an Δfnr mutant is attenuated during infection. The mutant was recently shown to be attenuated in a *C. elegans* infection model (Wang *et al.*, 2019), and FNR was found to be essential during an enteritis model of infection and to play a weak role during a typhoid model of infection in BALB/c mice (Rollenhagen & Bumann, 2006). Fink *et al.* have also shown that the Δfnr mutant was 100% attenuated after both oral and intraperitoneal infection of C57BL/6 mice, and that the mutant was attenuated in an *ex vivo* infection of peritoneal macrophages from C57BL/6 mice (Fink *et al.*, 2007). They have also shown that Δfnr was attenuated in mice and macrophages deficient in production of reactive nitrogen species (RNS) but not in mice and macrophages deficient in production of reactive oxygen species (ROS). They explain that the reason for attenuation of the mutant is due to the inability of the Δfnr mutant to mount a defense against ROS. However, during growth in PCN SPI-2 inducing medium (InSPI2), we observed that the Δfnr mutant had reduced growth rate compared to WT (**Figure 5.2**), similar to what we had previously seen in MMA (**Figure 3.2**), except that in InSPI2 WT growth was also slowed when compared to strains deficient in SPI-2 expression, $\Delta ssaG$ and $\Delta ssaG/fnr$. Also, PipB2 and SteC were slightly higher in Δfnr than WT in InSPI2 at OD₆₀₀ 1.0 (**Figure 3.15**). Curiously, these cultures were all grown under aerated conditions therefore, we would not expect FNR to have an effect. We reasoned that intracellular and growth attenuation of Δfnr may have to do with unrestrained expression of SPI-2 due to a lack of repression by FNR—a phenotype that can be observed in Δhns mutants where the absence of the NAP leads to uncontrolled expression of SPIs and a loss in fitness (Ali *et al.*, 2014; Lucchini *et al.*, 2006; Martinez *et al.*, 2014; Navarre *et al.*, 2006; Sturm *et al.*, 2011). WT, Δfnr and $\Delta ssaG$ strains transformed with pDEW201-P_{ssaG}, which expresses *luxCDABE* from the *ssaG* promoter, were grown in LB, InSPI2 and Non-Inducing PCN (NonSPI2) under aerobic and microaerobic conditions and growth and *ssaG* expression were measured until stationary phase was reached (**Figure 5.3**). Throughout these assays, $\Delta ssaG$ pDEW201-P_{ssaG} was used as a negative control for SPI-2 expression. There was little to no *ssaG* expression in any strain in LB regardless of oxygen concentration (**Figure 5.3A & D**) which is consistent with previously published data (Fink *et al.*, 2007; Wang *et al.*, 2019). Aerobic growth in InSPI2 showed that *ssaG* expression was marginally higher in WT than Δfnr , and there was no expression in $\Delta ssaG$

(**Figure 5.3B**). Surprisingly, expression of *ssaG* in microaerobic InSPI2 was much higher in WT than Δfnr during late exponential to early stationary phase (**Figure 5.3E**). This suggests that under *in vitro* microaerobic SPI-2 inducing conditions FNR is involved in activating SPI-2 genes, the opposite of what we have previously observed in MMA. This suggests that FNR may play a dual role in the control of SPI-2 which is dependent on environmental signals other than oxygen. Cells were also grown in NonSPI2 as a control, and regardless of aeration, there was minimal *ssaG* expression in both WT and Δfnr from lag phase to early exponential (**Figure 5.3C & F**), which could be partially explained by low level SPI-2 expression carry over from overnight growth in LB (Kröger *et al.*, 2013; Rice *et al.*, 2015).

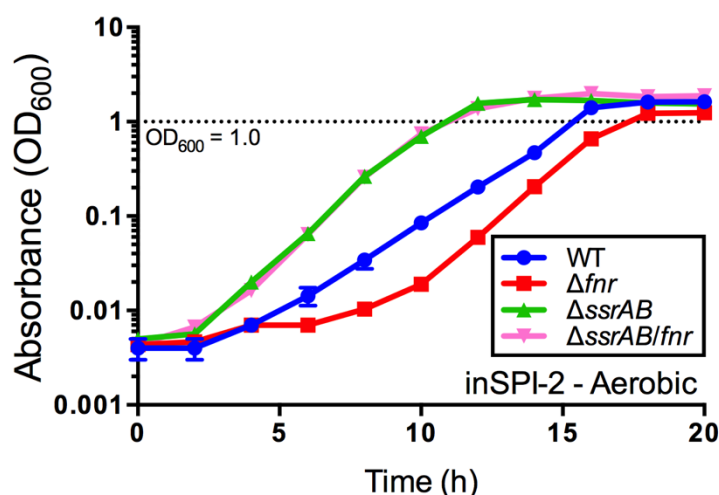


Figure 5.2 Growth of 4/74 and isogenic mutants in SPI-2 inducing media (InSPI2).

Growth curve of WT, Δfnr , $\Delta ssrAB$ and $\Delta ssrAB/fnr$ in aerobic InSPI2. Strains were grown as described in Section 2.2.3.2. The dotted line indicates OD₆₀₀ 1.0.

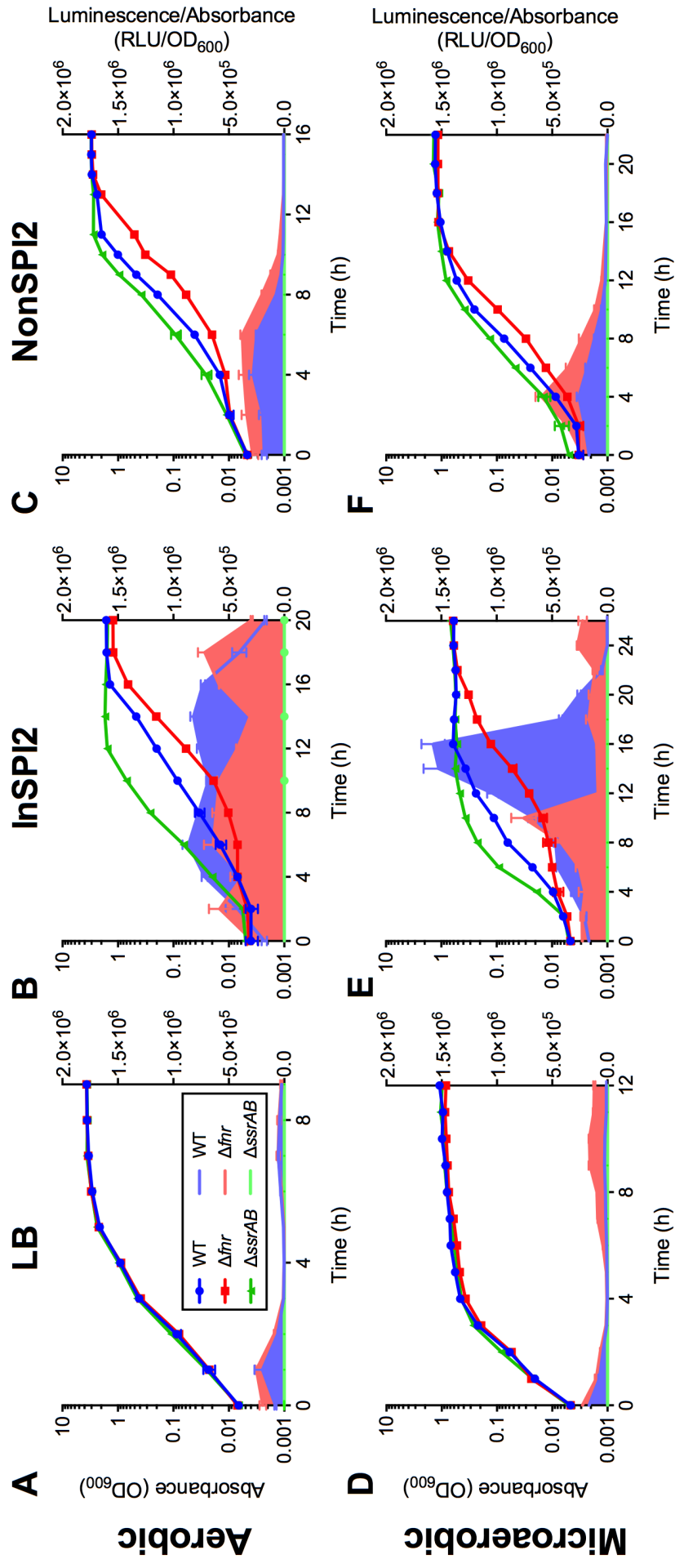


Figure 5.3 Aerobic and microaerobic growth and *ssaG* expression in 4/74 and isogenic mutants over time in LB, inSPI2 and NonSPI2.

Cultures were grown as previously described (Sections 2.2.3.1 and 2.2.3.2) and sampled every 1 to 2 h depending on the growth rate of the culture. Samples were measured for optical density (600 nm) and luminescence (RLU). Aerobic cultures were grown in A. LB, B. InSPI2 and C. NonSPI2 and microaerobic cultures were grown in D. LB, E. InSPI2, and F. NonSPI2. For all graphs, optical density is represented by connected points (bright colours) and correspond to values on the left y-axis and *ssaG* expression is represented by filled areas (light colours) and correspond to values on the right y-axis. Error bars represent standard deviation.

5.2.2 Intramacrophage survival of *S. Typhimurium*

As previously described, Δfnr has been found to be attenuated in mice, murine macrophages and in *C. elegans* (Fink *et al.*, 2007; Rollenhagen & Bumann, 2006; Wang *et al.*, 2019). In this study we infected RAW 264.7 murine macrophages at a multiplicity of infection of 10:1 with *S. Typhimurium* 4/74 and isogenic mutants. The $\Delta rpoE$ mutant was used as a negative control for intramacrophage replication for all infection experiments (Helaine *et al.*, 2010). Bacterial uptake between strains was not significantly different at 1 h post infection (**Figure 5.4A & C**), Δfnr was attenuated at 4 h and 8 h post infection, and WT and fnr^+ were not significantly different (**Figure 5.4 B & D**). Interestingly, there were fewer total CFU/mL in the Δfnr mutant at 16 h post infection, but the fold replication for WT and Δfnr was not significantly different (**Figure 5.4D**). This was interesting when compared to the result obtained by Fink *et al.*, as they saw attenuation of the mutant to 20 h post infection (Fink *et al.*, 2007). However, they used primary murine macrophages and the *S. Typhimurium* strain 14028s while we used RAW 264.7 murine macrophages and strain 4/74. These differences may account for the differences seen here.

Next, we measured intramacrophage *ssaG* expression from cells infected with WT and Δfnr cells transformed with the pDEW201-P_{*ssaG*} plasmid (**Figure 5.5**). While cells harbouring plasmids were taken up by macrophages at the same level as non-transformed cells and showed similar levels of replication at 4 h post infection (**Figure 5.5A**), replication of the pDEW201-P_{*ssaG*}-harbouring cells was significantly lower at 8 and 16 h post infection (**Figure 5.5A & B**). The WT strain with the pDEW201 empty vector had significantly lower replication only at 16 h post infection, and not nearly to the extent of the pDEW201-P_{*ssaG*} harbouring cells (**Figure 5.5B**). This is due to the inherent fitness cost associated with maintaining plasmids and high levels of luminescent proteins in the cell (Knodler *et al.*, 2005). While there was very little detectable signal due to low cell concentration at 1 and 4 h post infection, Δfnr had significantly higher *ssaG* expression at 8 h post infection. Interestingly, although there were the most cells present at 16 post infection, there was very little signal detected (**Figure 5.5C**). These results indicate that at 8 h post infection, while Δfnr is attenuated, there is also increased SPI-2 expression. Interestingly, this does not agree with *in vitro* results where SPI-2 was more highly expressed in WT cells (**Figure 5.3**). Possibly, over expression of SPI-2 in murine macrophages is energetically disadvantageous for cells.

Finally, we were interested to see what effect growth of cells in microaerobic MMA prior to infection would have on intramacrophage survival. Firstly, the macrophage uptake of WT and Δfnr were approximately 22- and 15-fold lower, respectively in cells grown in microaerobic MMA (**Figure 5.6A & C**). Cells grown in MMA were unable to reach the number of CFU/mL attained by those grown in LB by 16 h post infection (**Figure 5.6A**), however the Δfnr mutant was attenuated (**Figure 5.6B & E**). Interestingly, although starting from smaller numbers, the fold replication of MMA grown cells was significantly higher in WT and was similar in Δfnr by 16 h post infection (**Figure 5.6D**). Although macrophages phagocytose bacterial cells, up-regulated SPI-1 probably increases the number of infected cells (Drecktrah *et al.*, 2005). The most substantial difference between the LB and MMA grown cells is that LB grown cells have increased SPI-1 expression, which we have seen was at similar levels in WT and Δfnr from Western blots of SopE (**Figure 3.16**). Additionally, cells are stressed after growth in a minimal medium as compared to a rich growth medium such as LB which may have initially impaired their ability to replicate *in vivo*. Overall, we see that the Δfnr is attenuated *in vivo* which could be attributed to previously reported inability to protect against ROS (Fink *et al.*, 2007) but also over-expression of SPI-2 resulting in a reduction of fitness.

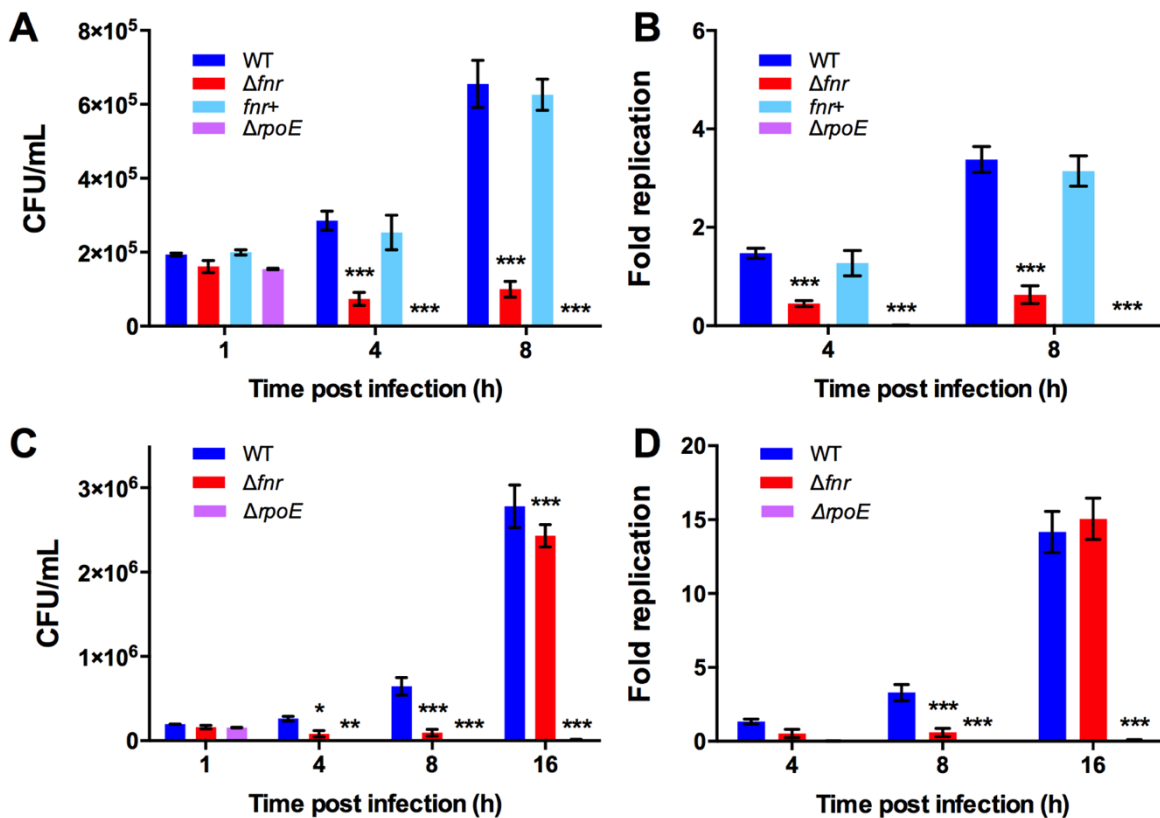


Figure 5.4 The Δfnr mutant is attenuated in murine macrophages at early time points. Survival of WT, Δfnr , fnr^+ and $\Delta rpoE$ up to 8 h post infection. A. Total viable cells post infection and B. the number of viable cells expressed as fold replication over 1 h post infection. Survival of WT, Δfnr and $\Delta rpoE$ up to 16 h post infection. C. Total viable cells post infection and D. the number of viable cells expressed as fold replication over 1 h post infection. RAW 264.7 macrophages were infection with stationary phase *S. Typhimurium* cells with an MOI of 10:1. Statistical significance determined by Two-way ANOVA with Dunnett's multiple comparisons test to WT; Only statistically significant differences are shown; * = $p \leq 0.05$, ** = $p \leq 0.01$, and *** = $p \leq 0.001$; Error bars represent standard deviation.

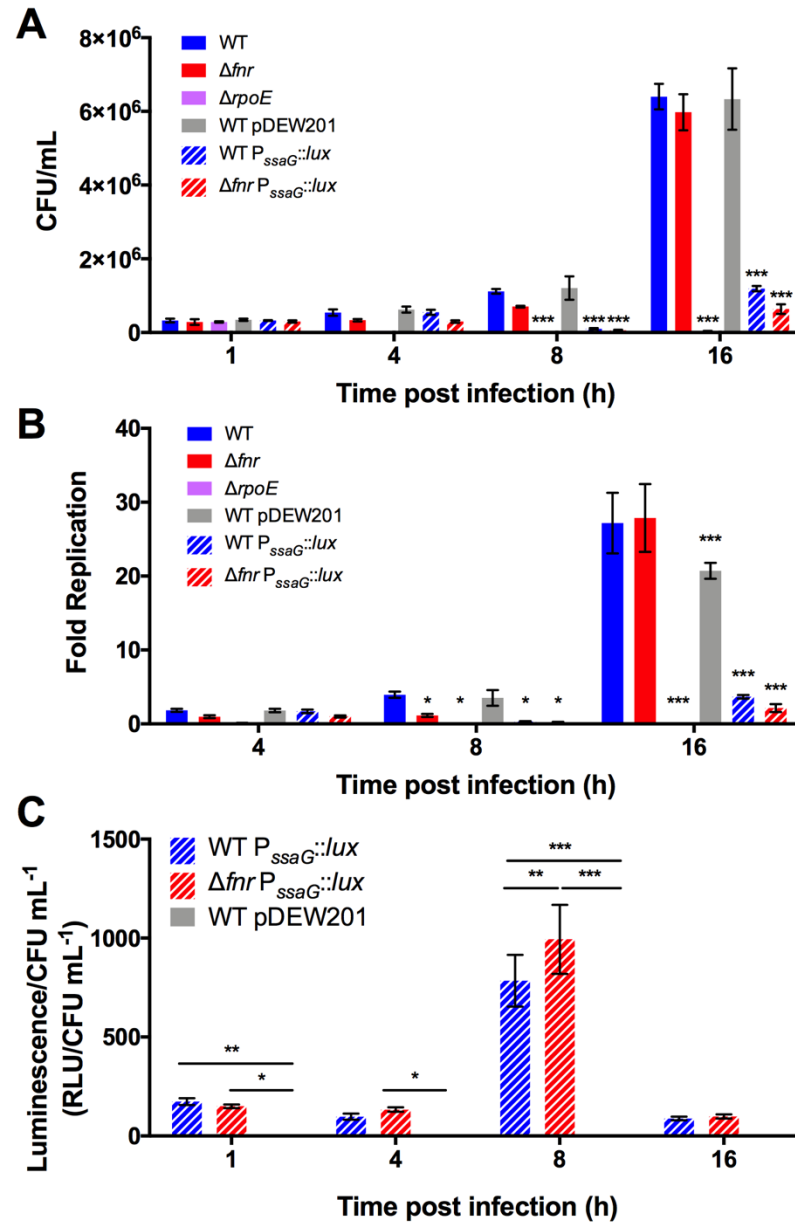


Figure 5.5 Plasmid carriage reduced intramacrophage replication and SPI-2 expression was elevated at early time points in Δfnr during infection.

Survival of WT, Δfnr , $\Delta rpoE$, WT pDEW201, WT $P_{ssaG}::lux$ and $\Delta fnr P_{ssaG}::lux$ up to 16 h post infection. A. Total viable cells post infection and B. the number of viable cells expressed as fold replication over 1 h post infection. C. Intramacrophage expression of *ssaG*. Statistical significance determined for A & B by Two-way ANOVA with Dunnett's multiple comparison's test to WT, and for C by Two-way ANOVA with Tukey's multiple comparisons test; Only statistically significant differences are shown; * = $p \leq 0.05$, ** = $p \leq 0.01$, and *** = $p \leq 0.001$; Error bars represent standard deviation.

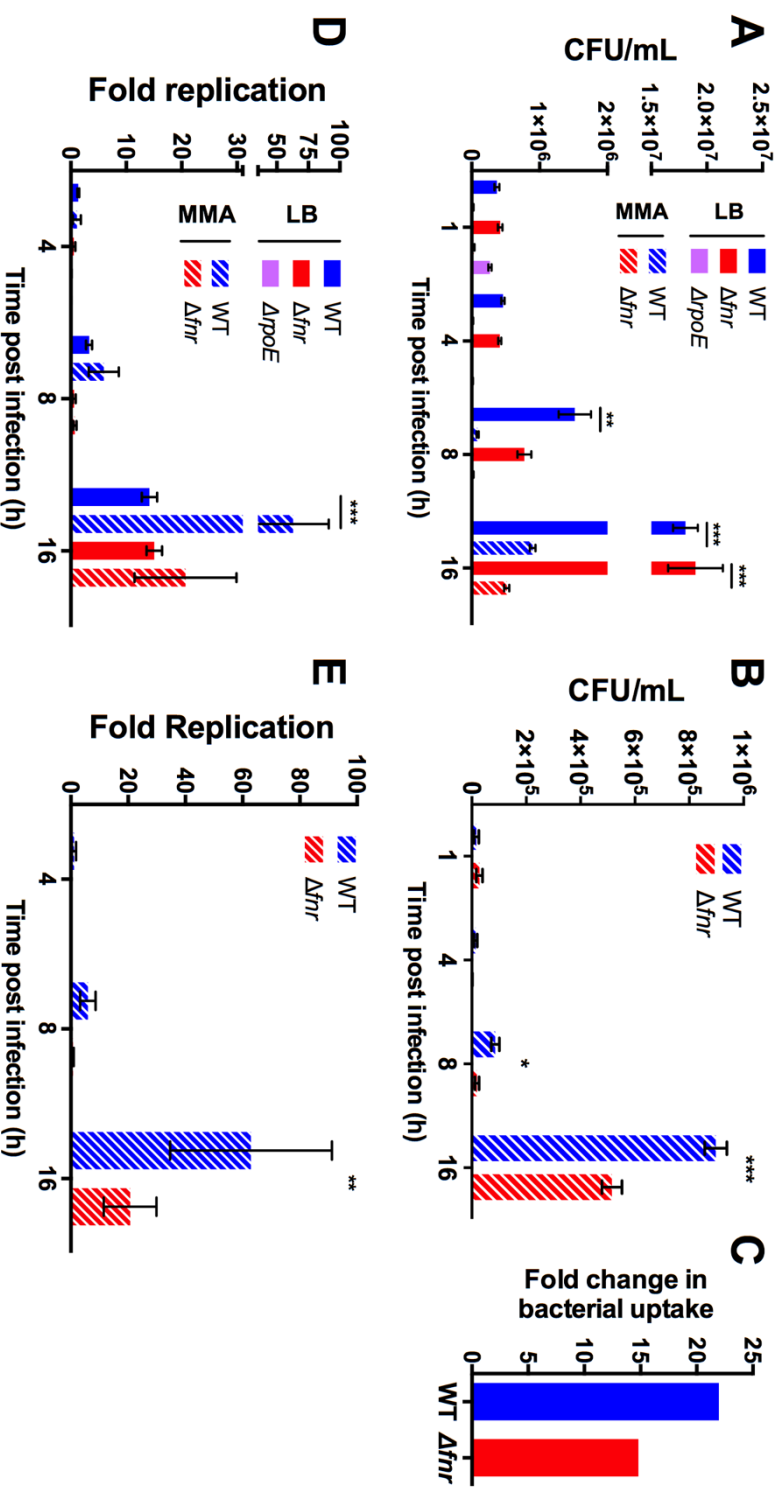


Figure 5.6 Growth in MMA prior to infection reduces bacterial uptake but increases fold replication in WT.

Survival of WT, Δfnr , $\Delta rpoE$ up to 16 h post infection when inoculum was grown in LB compared to MMA. A. Total viable cells post infection, B. Total viable cells post infection, MMA inoculum only, C. fold change in bacterial uptake in WT and Δfnr from cells grown in LB compared to MMA, D. the number of viable cells expressed as fold replication over 1 h post infection, E. the number of viable cells expressed as fold replication over 1 h post infection, MMA inoculum only. Statistical significance determined by Two-way ANOVA with Sidak's multiple comparisons test; Only statistically significant differences are shown; * = $p \leq 0.05$, ** = $p \leq 0.01$, and *** = $p \leq 0.001$; Error bars represent standard deviation.

5.2.3 Contribution of alternative electron acceptors to growth and SPI-2 expression

In this study we primarily examined expression of SPI-2 when cells reached an OD₆₀₀ of 0.3. To determine if expression was present throughout growth, kinetic gene expression assays were conducted over 28 h. Cells were transformed with pDEW201-P_{ssaG}, a low copy plasmid that produces luciferase upon activation of the *ssaG* promoter. Throughout these assays, Δ *ssrAB* pDEW201-P_{ssaG} was used as a negative control for SPI-2 expression. When grown under microaerobic conditions in MMA, *ssaG* expression in Δ *fnr* was >2-fold higher than WT over 28 h, with the highest expression ($>1 \times 10^6$ RLU) at 6 h, decreasing to approximately 5.5×10^5 RLU in mid-exponential growth, and the lowest in stationary phase, 3.5×10^5 RLU (**Figure 5.7A**). The growth of WT and Δ *ssrAB* was the same, while Δ *fnr* grew considerably slower (**Figure 5.7A**). To test whether addition of alternative electron acceptors had an influence on SPI-2 expression we grew cells in MMA without fumarate and TMAO (MMA⁻), with only fumarate (MMA^{+F}), and only TMAO (MMA^{+T}). In MMA⁻, *ssaG* expression in WT was comparable when grown in MMA, however, in Δ *fnr*, *ssaG* expression remained higher than WT but less than 5×10^5 RLU for 28 h (**Figure 5.7B**), and the lack of electron acceptors slowed the growth of all strains. When supplemented with only fumarate (MMA^{+F}), cells had similar growth to that of MMA, however *ssaG* expression in Δ *fnr* remained much lower (**Figure 5.7C**). Growth in MMA^{+T} yielded increased expression of *ssaG* in WT and a small increase in Δ *fnr* compared to MMA, with the highest expression for both strains in early exponential phase (**Figure 5.7D**). However, when grown in MMA^{+T} all strains grew slower than in MMA. The MMA experiments showed that expression of SPI-2 in Δ *fnr* is aided by addition of TMAO as an alternative electron acceptor, while fumarate may act as an electron acceptor and as an additional carbon source. Overall, the growth of Δ *fnr* was always slower in MMA regardless of the addition of alternative electron acceptors, which is correlated with increased SPI-2 expression.

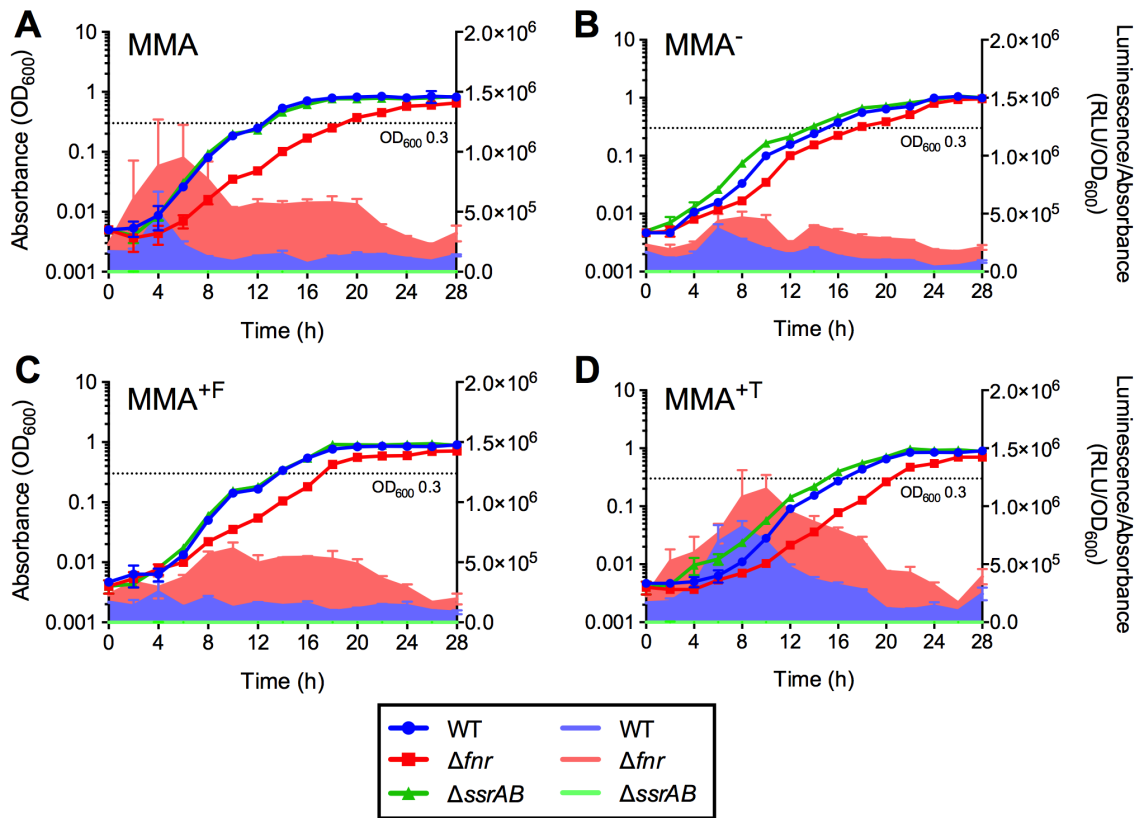


Figure 5.7 Growth and *ssaG* expression in MMA with and without alternative electron acceptors.

Cultures were grown as previously described (Section 2.2.3.2) and sampled every 1 to 2 h depending on the growth rate of the culture. Samples were measured for growth and luminescence. Cultures were grown in A. MMA with both electron acceptors fumarate and TMAO, B. MMA without alternative electron acceptors, C. MMA with only fumarate added and D. MMA with only TMAO added. For all graphs growth is shown by connected points (bright colours) and correspond to values on the left y-axis and *ssaG* expression is shown by filled areas (light colours) and correspond to values on the right y-axis. Error bars represent standard deviation.

5.2.4 Relative fitness *in vitro*

The correct spatial and temporal programming for gene expression is necessary to avoid incurring fitness costs. This is especially important during pathogenesis, when *S. Typhimurium* encounters a series of stressful environments and must out-compete the host microbiota to establish successful infection. By removal of specific regulatory proteins gene expression is altered under certain growth conditions. In the following experiments isogenic mutants of *S. Typhimurium* 4/74 were grown in co-culture to determine which strain

possessed a fitness advantage. The strains WT, Δfnr , $\Delta ssrAB$ and $\Delta ssrAB/fnr$ were transduced with a chloramphenicol resistance cassette (Cm^R) replacing the SL1483 gene, a transposase pseudogene which was unlikely to cause a reduction in fitness by removal. These strains will be referred to as WT- Cm^R , Δfnr - Cm^R , $\Delta ssrAB$ - Cm^R and $\Delta ssrAB/fnr$ - Cm^R for brevity. The competitive index (CI) was determined as described in Section 2.2.9, but briefly a CI of 1 indicates there was no difference between strains, while a CI above 1 indicates a fitness advantage and below 1 a disadvantage. Strains were competed against themselves (e.g. WT versus WT- Cm^R) to determine if the introduction of the $\Delta SL1483::Cm^R$ was detrimental to fitness. In the graphs below the y-axis shows the \log_2 CI value, but data points are labeled with non-log adjusted average CI values.

First, we compete Δfnr against each of $\Delta ssrAB$, WT and $\Delta fnr/ssrAB$ in microaerobic MMA and the introduction of $\Delta SL1483::Cm^R$ did not seem to be detrimental to strains under this condition (**Figure 5.8**). As expected, due to the serious growth defect in Δfnr in microaerobic MMA it was outcompeted by all strains. In Δfnr versus $\Delta fnr/ssrAB$ we see that the abolishment of SPI-2 expression resulted in a fitness advantage to $\Delta fnr/ssrAB$, suggesting that the expression of SPI-2 is detrimental under these growth conditions (**Figure 5.8C**). Next we performed a competition between WT and $\Delta ssrAB$ in SPI-2 inducing media. Unfortunately, under these conditions the $\Delta SL1483::Cm^R$ mutation in WT was detrimental to fitness (**Figure 5.9**). However, we could still gain insight from the WT versus $\Delta ssrAB$ - Cm^R , as the mutation had no effect on the fitness of $\Delta ssrAB$ under these conditions. Here we see a similar result as the Δfnr versus $\Delta fnr/ssrAB$ MMA competition, where the WT strain expressing SPI-2 was outcompeted by the non-expressing $\Delta ssrAB$ strain (**Figure 5.9**). Finally, we performed competitions in microaerobic LB, a condition in which there is little SPI-2 expression and no growth defects between the mutants (**Figure 5.3D**). Interestingly, the WT and $\Delta ssrAB$ both outcompeted Δfnr (**Figure 5.10A & B**). This is likely due to the ability of WT and $\Delta ssrAB$ to express anaerobic metabolism genes, however $\Delta fnr/ssrAB$, also outcompeted Δfnr (**Figure 5.10C**), suggesting that the small amount of SPI-2 expression seen at late stationary phase may be sufficient to cause a detriment to fitness of Δfnr in microaerobic LB. When we competed WT against $\Delta ssrAB$, neither strain was more fit (**Figure 5.10D**). These results provide insight into the energetic burden caused by expression of SPI-2 genes. Previously it has been shown that expression of SPI-1 genes imposed a growth penalty *in vitro* (Sturm *et al.*, 2011), and in an Δhns mutant, deletion of SPI-1 particularly, and SPI-2 to a lesser extent restored growth (Ali *et al.*, 2014). These data

suggest that expression of SPI-2 can also impose a fitness disadvantage under *in vitro* conditions where it is not necessary for expression of the virulence genes.

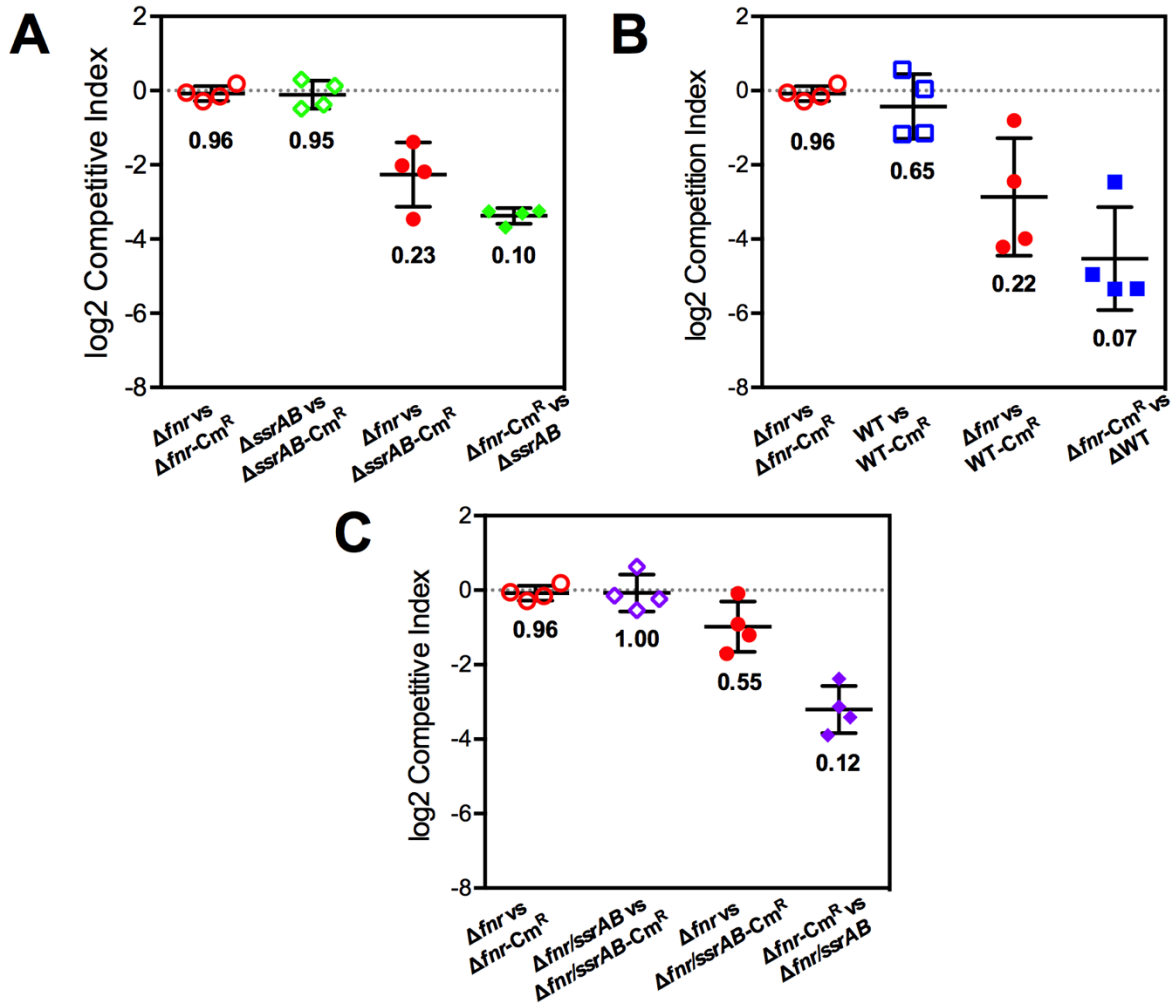


Figure 5.8 The Δfnr mutant has reduced fitness in microaerobic MMA.

Relative fitness assays showing *in vitro* co-culture competitions in microaerobic MMA between A. Δfnr and $\Delta ssrAB$, B. Δfnr and WT, and C. Δfnr and $\Delta fnr/ssrAB$. The y-axis shows log₂ transformed competitive indices, and each competition is labeled with the CI (non-log transformed). The dotted grey line indicates a CI of 1, where there is no difference between strains. Error bars represent standard deviation.

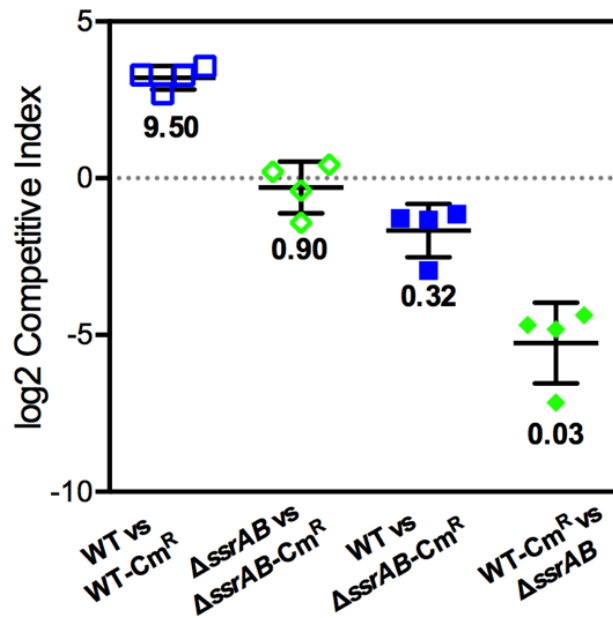


Figure 5.9 In SPI-2 inducing conditions the $\Delta ssrAB$ mutant outcompetes WT.

Relative fitness assays showing *in vitro* co-culture competition in aerobic inSPI2 between WT $\Delta fnr/ssrAB$. The y-axis shows log₂ transformed competitive indices, and each competition is labeled with the CI (non-log transformed). The dotted grey line indicates a CI of 1, where there is no difference between strains. Error bars represent standard deviation.

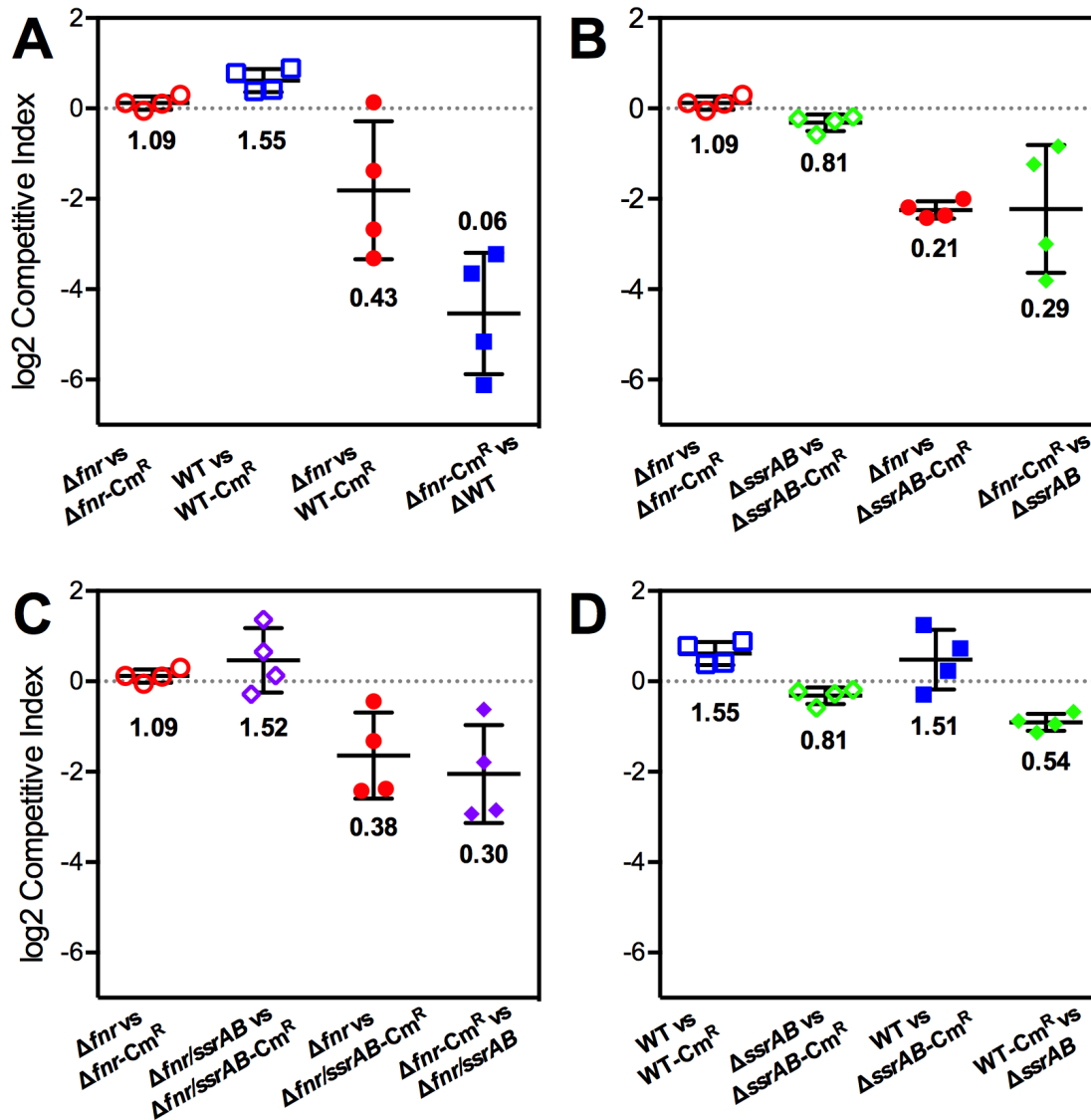


Figure 5.10 The Δfnr mutant has reduced fitness and WT and the $\Delta ssrAB$ are equally “fit” in microaerobic LB.

Relative fitness assays showing *in vitro* co-culture competitions in aerobic LB between A. Δfnr and WT, B. Δfnr and $\Delta ssrAB$, C. Δfnr and $\Delta fnr/ssrAB$, and D. WT vs $\Delta ssrAB$. The y-axis shows log₂ transformed competitive indices, and each competition is labeled with the CI (non-log transformed). The dotted grey line indicates a CI of 1, where there is no difference between strains. Error bars represent standard deviation.

5.2.5 Proteomic study of Δfnr

The Δfnr mutant has been studied primarily from a transcriptomic point of view. Only one very recent study has attempted to elucidate the FNR regulon at a proteomic level (Wang *et al.*, 2019), however they have grown cells in anaerobic MOPS buffered LB with xylose, a medium shown not to allow expression of SPI-2 in Δfnr (Fink *et al.*, 2007). In this study, we have used mass spectrometry to investigate the energy metabolism of WT and Δfnr in microaerobic MMA and to identify abundant proteins which may occur only in the mutant. In the WT, 841 proteins were detected and in the Δfnr , mutant 617 proteins were detected, and 524 proteins were common between the two (**Figure 5.11**). All detected proteins and absolute and relative quantities can be found in **Tables S9** and **S10** in Appendix IV.

The proteomic data identify abundant proteins found in the cytoplasm, however, proteins missing from the data set are not necessarily absent from cells, instead their abundance may be too low to be detected. Detected proteins included highly abundant proteins such as ribosomal subunits (Rpl, Rpm, Rps), RNA polymerase subunits (RpoA, RpoB, RpoC, and RpoZ), sigma factor RpoE. RpoE is a sigma factor typically associated with membrane stress but has been shown to be involved in upregulation of genes when transiting from aerobic to microaerobic environments in *E. coli*, which might explain its presence here (Partridge *et al.*, 2007). RpoD was only found in the Δfnr mutant, however this is likely due to an issue in relative abundance of proteins in the WT. Proteins detected in both WT and Δfnr also included a wide variety of nucleotide and amino acid biosynthesis proteins, which was expected as minimal media does not provide these nutrients. Nucleoid associated proteins and transcriptional regulators are highly abundant proteins in the cell cytoplasm (Cai & Inouye, 2002; Dillon & Dorman, 2010). Found in both the WT and Δfnr proteomes were proteins including H-NS, both IHF subunits, HU alpha subunit, LRP, Dps and OmpR. Curiously, the HU beta subunit and CRP were only found in the WT. Indeed, *hupB* and *crp* were downregulated 0.73 and 0.80-fold in Δfnr respectively according to RNA-seq data, therefore their abundance may have been too low to be detected. Fis was not present in either strain which is likely due to the poor nutrient content of the minimal medium. Although cells were taken at an OD₆₀₀ of 0.3, in MMA FT, cells would not be considered to be at early exponential growth. WT and Δfnr cultures inoculated at a starting OD₆₀₀ of 0.005 take approximately 12 h and 20 h to reach OD₆₀₀ 0.3 respectively. This may explain the presence of Dps and absence of Fis. This finding is contradictory with the literature which finds that Fis is required for *ssaG* expression or full SPI-2 expression in *S. Typhimurium* (Fass &

Groisman, 2009; Lim *et al.*, 2006) as there is highly induced expression of *ssaG* and 37 other SPI-2 encoded genes and effectors in this condition. Other highly abundant proteins found in both WT and Δfnr included outer membrane proteins (OmpA, OmpC, OmpD, OmpF, OmpS, and OmpX), and chaperonin proteins GroEL/GroES, and DnaK. FNR was not detected in WT cells, and ArcA and ArcB were not at detectable concentrations in either strain.

We categorized the detected proteins into clusters of orthologous groups (COGs) according to the COGs as defined at <http://www.ncbi.nlm.nih.gov/COG> (Figure 5.12). They are presented as percentage of detected protein. In general, the growth of both the WT and Δfnr were comparable to stationary phase cultures even though samples were taken at OD₆₀₀ 0.3, and the *fnr* mutation did not seem to have any major effects when compared to WT. Energy production and conversion, cell wall and to a lesser extent post-translational modification were the most differentially detected protein categories. Under energy metabolism, as expected anaerobic proteins were produced less in Δfnr . This includes expected candidates, such as fumarate reductase, pyruvate lyase, but also a number of propanediol utilization genes, which are expressed in the intestine (Faber *et al.*, 2017; Jakobson & Tullman-Ercek, 2016). Interestingly, the Wang *et al.*, study found that FNR directly repressed propanediol degradation (Wang *et al.*, 2019) however, our results suggest that it indirectly activates these genes thus resulting in increased protein in the WT. This suggests that FNR plays a dual role in the regulation of propanediol degradation depending on available nutrients. The slower growth of the mutant may be due to decreased anaerobic metabolism proteins as Δfnr struggles to produce energy efficiently. Slower growth of the mutant may also be due to the increased proportion of chaperones and proteases, since this can result in depleted protein synthesis under energy deficiency. Although, the *fnr* mutation generates an energy shortage under these conditions the WT is also already disadvantaged due to the poor growth conditions provided by MMA and low oxygen concentration, so the effects in Δfnr are moderate.

While this proteomics study provides valuable information into the energetics of the Δfnr mutant compared to WT, because of the number and abundance of metabolic proteins we were unable to detect many SPI-2 encoded proteins. We were able to detect the highly expressed SPI-2 effector proteins SseA and SifB in the Δfnr mutant and not the WT. Transcriptomic data previously revealed that *sseA* and *sifB* were upregulated 9.4-fold and 7.5-fold above WT, respectively. The presence of abundant SseA and SifB effector proteins

potentially indicates that the remaining upregulated genes identified by RNA-seq may also be translated and present in Δfnr cells. Many of the other most highly upregulated SPI-2 genes are SPI-2 T3SS apparatus proteins and would likely be localized at the cell envelope, meaning they would be excluded from the cytoplasmic preparation for this experiment. In addition to SPI-2 effectors, SopB, a SPI-5 encoded, SPI-1 regulated effector was also detected in only the Δfnr mutant. However, there is no difference in transcription of *sopB* between the WT and Δfnr mutant, and the absolute expression was low.

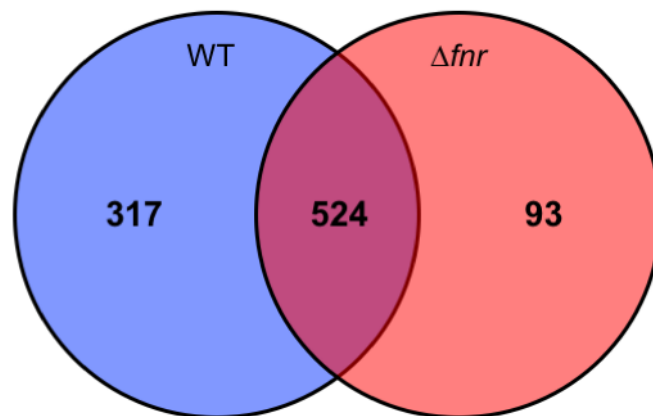


Figure 5.11 Venn diagram representing proteins detected by mass spectrometry in WT and Δfnr .

The blue circle represents the total number of proteins detected in the WT and the red circle represents the total number of proteins detected in the Δfnr mutant. The overlapping region indicates the number of proteins that were the same between both samples.

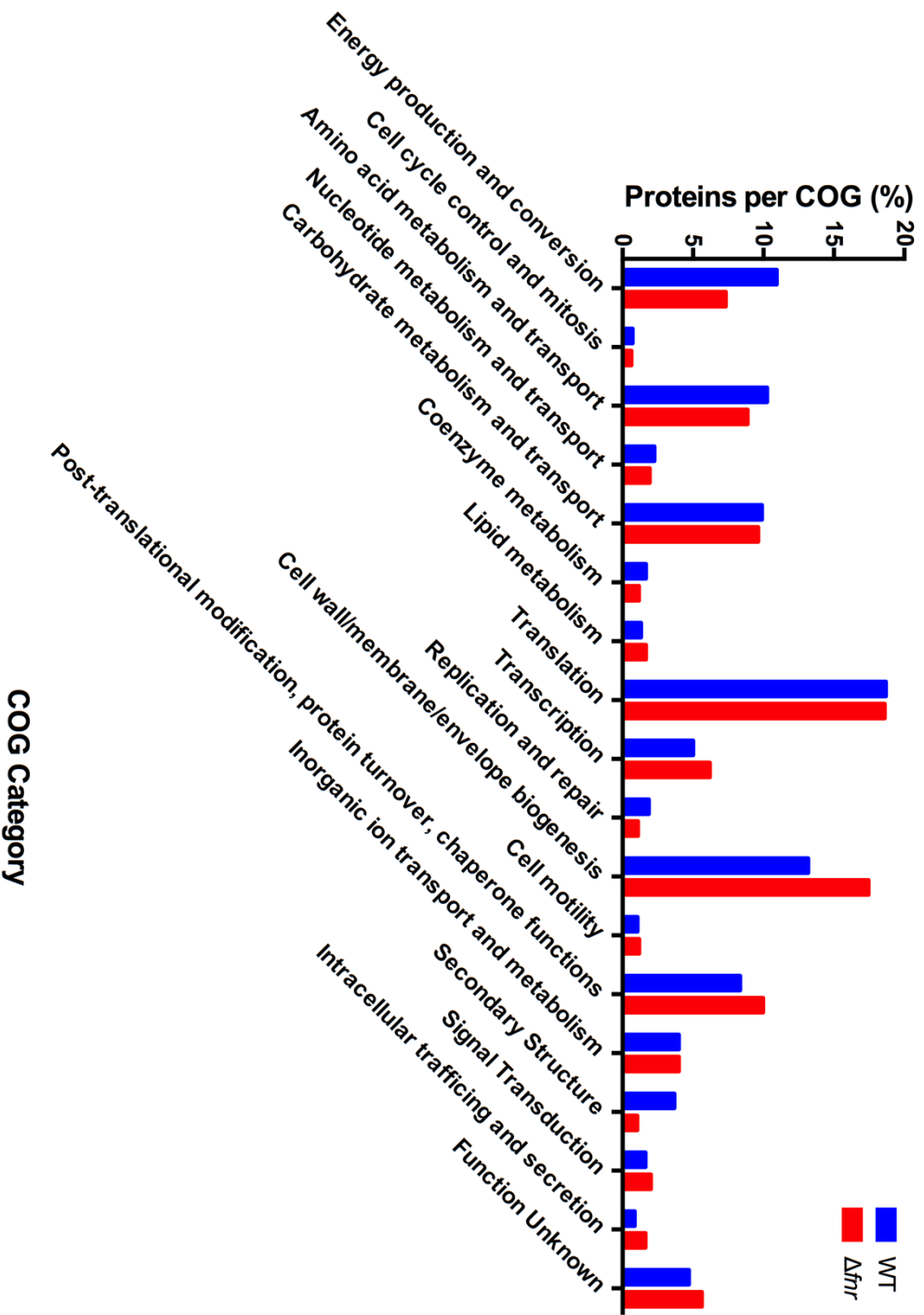


Figure 5.12 Classification of abundant proteins from WT and Δfir into COG categories.

Proteins detected in WT and Δfir cells were sorted into COG categories as defined by <http://www.ncbi.nlm.nih.gov/COG>. This graph represents the percentage of detected proteins which fit into each COG category.

5.3 Discussion

5.3.1 SPI-2 regulation by FNR *in vitro* and *in vivo*

We have shown that in microaerobic MMA SPI-2 is directly repressed by FNR in response to changes in oxygen concentration. Evidently, the addition of alternative electron acceptors fumarate and TMAO enhance that expression (**Figure 5.7**). Previous studies show that SPI-2 expression is not regulated by FNR in MOPS buffered LB with xylose under anaerobic conditions (Fink *et al.*, 2007; Wang *et al.*, 2019), and we see minimal expression of SPI-2 in microaerobic LB (**Figure 5.3D**). Surprisingly, in microaerobic InSPI2 media, FNR acted as an activator of SPI-2. This suggests that FNR may play a dual role in the regulation of SPI-2 in accordance with exogenous environmental signals besides oxygen. However, when we measured SPI-2 expression in infected macrophages, SPI-2 expression was significantly higher in Δfnr (**Figure 5.5C**). This exposes a fundamental difference between *in vitro* and *in vivo* conditions. Further work is certainly required to elucidate the role of FNR *in vivo*, and to eliminate the problems of plasmid carriage and expression vectors it would be favourable to use a technique such as dual RNA-seq (Westermann & Vogel, 2018).

5.3.2 Attenuation of Δfnr in murine macrophages

Findings from Fink *et al.* and in this study suggest that FNR is important inside the phagosome of murine macrophages (Fink *et al.*, 2007). While this environment is not completely anaerobic, we have shown that FNR is active under low oxygen conditions, not only anaerobiosis, *in vitro*. Additionally, in *E. coli*, expression of FNR activated operons such as *frd* and *dms* are expressed at up to 10% O₂ saturation (Shalel Levanon *et al.*, 2005; Tseng *et al.*, 1996). The partial pressure of oxygen (pO_2) of the macrophage phagosome of *ex vivo* murine macrophages has also been observed at levels as high as 79.8 ± 1.6 to 32.6 ± 1.7 μ M, depending on the density of the macrophages (James *et al.*, 1995). Furthermore, the production of reactive oxygen species (ROS) and oxygen consumption by macrophages and phagocytosed *S. Typhimurium* are expected to further decrease the pO_2 in the phagosome. Moreover, the pO_2 inside *ex vivo* macrophages almost certainly different from the pO_2 of *in vivo* macrophages (Atkuri *et al.*, 2005). A decrease in oxygen concentration in the murine gut from ~11% to ~2% upon infection with *S. Typhimurium* has been observed, and hypoxia enhanced SPI-2 transcription, translocation of SPI-2-encoded virulence proteins and intramacrophage replication *in vivo* (Jennewein *et al.*, 2015). More investigation into the

exact oxygen concentrations of macrophages both *ex vivo* and *in vivo* is required to elucidate the exact mechanism of FNR inside of host cells.

Despite the lack of information concerning the exact oxygen concentrations and mechanisms of intramacrophage FNR activity, it is certain that SPI-2 is necessary for the survival and intracellular replication of *S. Typhimurium*. YdgT has been previously identified as a repressor of SPI-2 expression, and negative control over this virulence system is central to systemic pathogenesis because *ydgT* mutants overexpressing virulence genes are ultimately attenuated during infection (Coombes *et al.*, 2005). As we have shown earlier, FNR binds to the promoter of *ydgT* and to a probable cis-acting sRNA. Potentially, FNR is able to indirectly modulate SPI-2 expression *in vivo* through control of YdgT. Another possibility of FNR influence on macrophage survival is through regulation of ethanolamine genes. In the Fink *et al.* study, FNR activated ethanolamine utilization genes (Fink *et al.*, 2007). A recent study found that EutH, an ethanolamine permease, is required for ethanolamine utilization at low pH and vacuole adaptation during macrophage infection (Anderson *et al.*, 2018). Thus, FNR activation of *eutH* during infection may also explain the attenuation of Δfnr in macrophages.

5.3.3 Fitness of Δfnr

While the proteomics investigation in this study provides valuable information into the energetics of the Δfnr mutant compared to WT and helps us to understand the growth defects in Δfnr , because of the number and abundance of metabolic proteins in both WT and Δfnr we were unable to detect many SPI-2 encoded proteins. A more recent proteomics study used the approach of fractionation of proteins by SDS-PAGE prior to in-gel protein digestion and mass spectrometry which allowed them to identify more than just the most abundant protein in the cell (Wang *et al.*, 2019). Another useful approach might be to use two-dimensional difference gel electrophoresis (2D DIGE) to recognize differentially expressed proteins prior to identification by mass spectrometry in order to specifically look at those proteins with the most difference between samples (Joshi & Patil, 2017; Marouga *et al.*, 2005). This would add another layer of information to our data sets and help identify where there may be post-translational differences in regulation from what is seen in transcriptomic data.

Chapter 6

General Discussion

6.1 Importance of this study

6.1.1 Context of the study

Salmonella enterica is a medically important zoonotic pathogen that causes a range of diseases from gastroenteritis to Typhoid fever. Non-host adapted serovars of *Salmonella enterica*, such as *S. Typhimurium*, are considered successful pathogens as these serovars can colonize a wide range of hosts, survive a series of stressful events during the infection process, find nutritionally compatible niches inside the host, avoid, subvert, and/or evade the host innate and adaptive immune responses, replicate using resources found in the host, exit and transmit to new hosts and, in susceptible hosts, disseminate and cause systemic infection (Fabrega & Vila, 2013) (**Figure 1.1**).

S. Typhimurium establishes infection through the integration of a multitude of environmental signals through regulatory molecules including transcription factors and small RNAs. This allows the coordination of gene expression at the transcriptional and post-transcriptional levels in a precise spatiotemporal manner. The careful coordination of gene expression by regulatory molecules ensures that *S. Typhimurium* expresses only the genes and proteins necessary for survival and proliferation under each specific environmental condition, while avoiding loss of bacterial fitness due to inappropriate or wasteful gene expression (Groisman & Mouslim, 2006; Sengupta & Bhadauria, 2014). An understanding of the complex signals, regulatory inputs and pathways that result in the transcriptional activation or repression of virulence-associated genes provides insight into the steps necessary to establish an infection. Many studies have focussed on the signals which control the expression of virulence factors through transcriptional regulators particularly as they relate to the intracellular environment or media which mimic intracellular conditions *in vitro* (Colgan *et al.*, 2016; Cirillo *et al.*, 1998; Fass & Groisman, 2009; Hébrard *et al.*, 2011; Knuff & Finlay, 2017; Kröger *et al.*, 2013; Lee *et al.*, 1999; Löber *et al.*, 2006; Martínez *et al.*, 2011; Srikumar *et al.*, 2015; Xu & Hensel, 2010; Yoon *et al.*, 2009) (**Figure 1.3**). But no studies have determined the signals or regulation which lead to low level SPI-2 gene expression prior to invasion of epithelial cells (Osborne & Coombes, 2011). There is increasing evidence that changes in environmental oxygen play a critical role in the timing and deployment of bacterial virulence factors, and that regulators of metabolism control the expression of genes imperative for causing infection and disease (Crofts *et al.*, 2018;

Marteyn *et al.*, 2010). The transcription factor FNR is a global regulator of anaerobic metabolism and responds directly to oxygen concentration (**Figure 1.4**). FNR has been established as a regulator of genes involved in host-cell invasion such as components of the T3SS and chaperones encoded on SPI-1 (Fink *et al.*, 2007; Wang *et al.*, 2019). Furthermore, FNR is required for full virulence in the murine model, and a mutant lacking this transcription factor is rapidly killed by macrophages (Fink *et al.*, 2007; Rollenhagen & Bumann, 2006). The SPI-2 T3SS and an intact SCV are required for evasion of ROS in macrophages (van der Heijden *et al.*, 2015), and FNR helps to promote resistance against oxidative stress although the mechanism has not been described (Fink *et al.*, 2007).

In this study, we used an RNA-seq-based transcriptomic approach combined with ChIP-seq to expand the regulon of FNR, under microaerobic conditions in a glycerol/trimethylamine N-oxide/fumarate minimal medium (MMA) (Constantinidou *et al.*, 2006), in *S. Typhimurium*. The use of this medium and RNA-seq has allowed identification of SPI-2 and other virulence-associated genes and sRNAs as targets for FNR gene regulation. RNA-seq provides an unbiased picture of all genes which are being actively transcribed, with no requirement for previous knowledge of the sequence which is being transcribed (Croucher & Thomson, 2010; Ozsolak & Milos, 2010), while ChIP-seq enabled mapping of FNR binding sites in a global and high-throughput fashion (Bonocora & Wade, 2015; Galagan *et al.*, 2012; Myers *et al.*, 2015). We also investigated the role of FNR in murine macrophages and the relative bacterial fitness of the Δfnr mutant.

6.1.2 Global analysis of FNR-mediated regulation in *S. Typhimurium*

To our knowledge, the work presented here is the first large scale study to combine transcriptomic and global protein-DNA binding that has been carried out in an Δfnr mutant of *S. Typhimurium* using high throughput next generation sequencing. In total, 482 genes and sRNAs were regulated directly or indirectly by FNR under microaerobic conditions in MMA. 286 genes were activated by FNR and 196 were repressed (**Figure 3.7**). We were able to corroborate existing data associating FNR as an activator of anaerobic metabolism (**Figure 3.8**), cell motility and chemotaxis (**Figure 3.17, 3.18 & 3.19**), and reveal FNR as a newly identified repressor of *Salmonella* pathogenicity island 2 (**Figure 3.9 & 4.11**). The use of RNA-seq rather than microarray-based technology has also allowed us to identify 42 differentially expressed small non-coding RNAs in an Δfnr background (**Table 3.1, 3.2, & Figure 3.20**). ChIP-seq allowed identification of 288 putative FNR binding sites across the

entire *S. Typhimurium* chromosome and plasmids under microaerobic growth conditions in MMA (**Figure 4.4B**). Approximately 19% of differentially expressed genes in this study were associated with peaks from ChIP-seq (**Figure 4.4C**). We were able to validate through ChIP-seq and EMSA that FNR acts as a direct repressor of *Salmonella* pathogenicity island 2 through direct repression of the response regulator *ssrB* and the apparatus gene *ssaB*. Consequently, FNR indirectly represses the remainder of SPI-2 genes through the repression of *ssrB*. ChIP-seq also revealed FNR binding sites at SPI-2 associated genes encoded outside of the island, which could be validated in the future.

Under oxygenated conditions, we see moderate levels of SPI-2 expression in WT and Δfnr (**Figure 3.13 & 3.14**). Furthermore, it is apparent that an additional metabolic signal, other than oxygen, is important for regulation of SPI-1 or SPI-2, as expression of these loci in Δfnr is different dependent on growth media and conditions (**Figure 3.9, 3.10A, 5.3, 5.5C**) (Fink *et al.*, 2007; Wang *et al.*, 2019). However, this was not the case for expression of motility and chemotaxis genes, which are universally down-regulated in Δfnr regardless of media composition (**Figure 3.17 & 3.19**) (Fink *et al.*, 2007). What this study highlights, is that the control of virulence expression is more complex and nuanced than originally conceived, and expression can vary dependant on numerous environmental factors which are integrated by multiple transcriptional and post-transcriptional regulators, many of which have not yet been identified.

In the context of *S. Typhimurium* infection, oxygen has previously been shown to be an important signalling molecule, but primarily for adhesion, invasion and SPI-1 expression (Ernst *et al.*, 1990; Lee & Falkow, 1990; Schiemann & Shope, 1991; Fink *et al.*, 2007). Our results show that the SPI-2 priming of *S. Typhimurium* cells *in vivo* (Brown *et al.*, 2005, Osborne & Coombes, 2011) could be a result of cells detecting oxygen at the epithelial border of the intestine through a mechanism involving FNR. Here we describe how can FNR act directly as a transcriptional repressor at SPI-2 promoters, especially *ssrB* and *ssaB*, to cause repression under oxygen-limited conditions, and for that repression to be lifted when oxygen concentrations are increased and allow expression of SPI-2 encoded and associated genes (**Figure 6.1**).

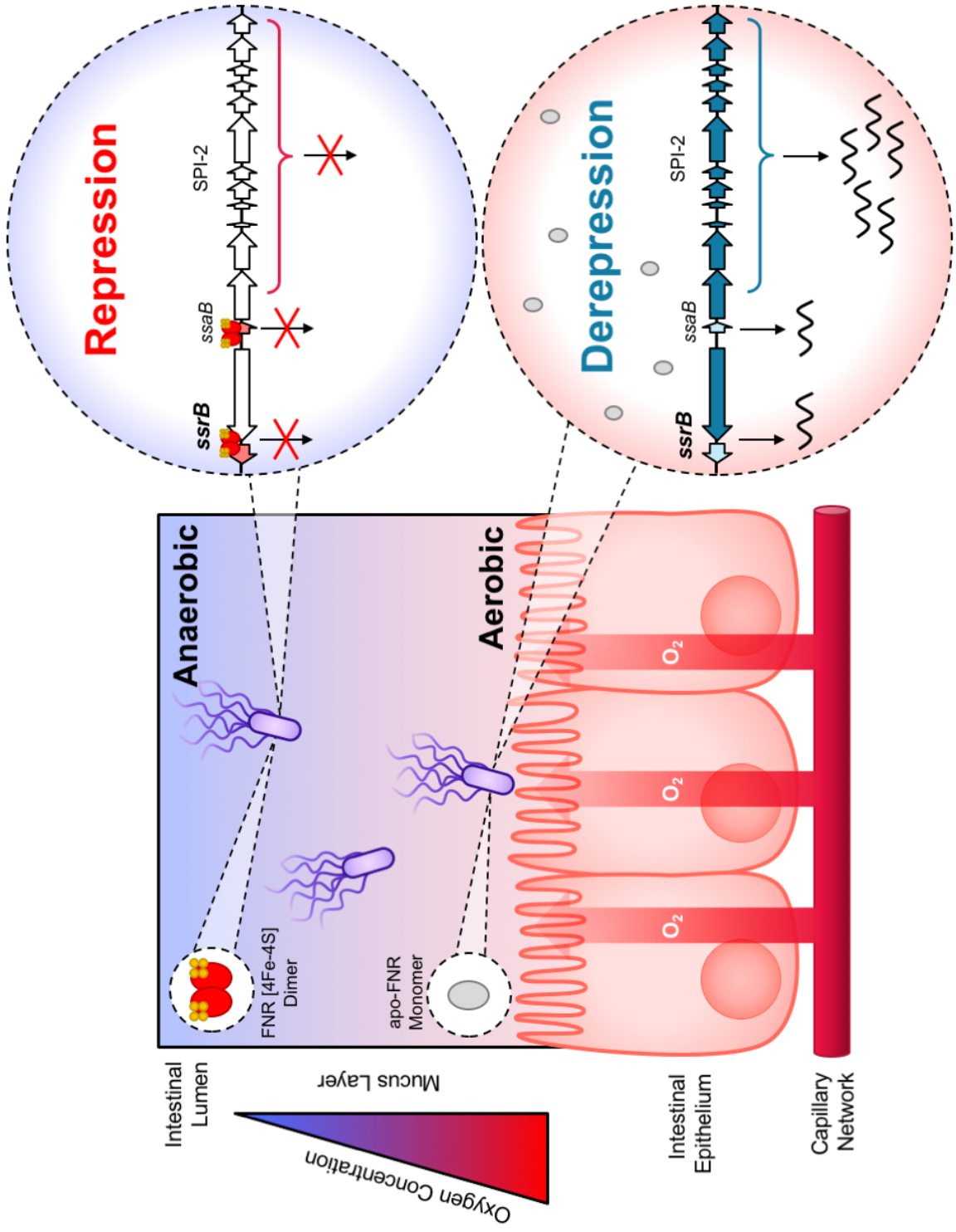


Figure 6.1 Model of SPI-2 repression by FNR under changing oxygen conditions.

The intestinal lumen is an anaerobic environment (blue) however, there is a zone of relative oxygenation adjacent to the gastrointestinal tract mucosa (red), caused by diffusion of O₂ (arrows) from the capillary network at the tips of villi. Under anaerobic and microaerobic conditions the active FNR dimer can bind to DNA, however when sufficient oxygen is detected by iron-sulphur clusters bound to FNR, the dimer dissociates to form apo-FNR and is no longer able to bind DNA. Under low oxygen conditions FNR binds directly to and represses expression from the promoter of the SPI-2 response regulator *ssrB*, *ssaB* and promoters of SPI-2 genes. Under aerobic conditions the virulence genes are derepressed allowing preemptive synthesis of important virulence factors in preparation for the harsh intracellular environment of host cells.

6.2 Future prospects

There are many possibilities for the development of this work in the future. The long term aim for this study is that the data presented here will contribute to the complete description of molecular biological networks within *S. Typhimurium*. Below, several avenues for future research are discussed using this work as a starting point.

6.2.1 Signals for expression of virulence

As previously discussed, it is unclear what component in MMA allows for SPI-2 expression as the medium does not incorporate signals which have typically been required for SPI-2 expression (Deiwick *et al.*, 1999; Löber *et al.*, 2006; Xu & Hensel, 2010). However, it may be in part due to the presence of alternative electron acceptors such as fumarate and TMAO (**Figure 5.7**). We identified a near consensus FNR binding motif in the promoter region of a potential class I fumarase homologue *orf70* (*fumD*) also encoded within SPI-2 (**Figure 4.5**). This mesaconase/fumarase enzyme has not been studied in *S. Typhimurium*, however the location of *orf70* would suggest that mesaconate or fumarate may be important signalling molecules for SPI-2 (Kronen & Berg, 2015). Further investigation into other alternative electron acceptors, such as tetrathionate, nitrate or thiosulphate, as signals for virulence regulation is also warranted. These molecules are found in the gut in response to bacteria-induced inflammation (Thiennimitr *et al.*, 2012; Winter *et al.*, 2010; 2013) and interestingly, it has been demonstrated that FNR is involved in regulation of tetrathionate and nitrate

metabolism (Prince-Carter et al., 2001). Moreover, the genes encoding tetrathionate respiration proteins, *ttrRSBCA*, are encoded within SPI-2 (Hensel et al., 1999). Tetrathionate also shares another link with FNR as the molecule supports B12-dependent anaerobic growth of *S. Typhimurium* on ethanolamine or 1,2-propanediol (Price-Carter et al., 2001). Fink et al., showed that FNR activates expression of ethanolamine utilization genes and a recent study found that EutH, an ethanolamine permease, is required for ethanolamine utilization at low pH and vacuole adaptation during macrophage infection (Anderson et al., 2018; Fink et al., 2007). Thus, FNR activation of *eutH* during infection may also explain attenuation of Δ *fnr* in macrophages. In another recent study, propanediol degradation proteins were up-regulated in Δ *fnr* under anaerobic growth in MOPS buffered LB with xylose (Wang et al., 2019), and our study revealed that the *pdu* and *cbi* operons were down-regulated in Δ *fnr*, and Pdu proteins were more abundant in WT. These links between the metabolism of molecules commonly found in the gut and virulence should certainly be investigated further.

6.2.2 sRNAs, the missing link?

Through our transcriptomic investigation we found that there were multiple virulence-associated sRNAs which were differentially expressed in Δ *fnr* (Table 3.1, 3.2, & Figure 3.20). Previously, sRNAs had been overlooked in large-scale investigations into the regulatory pathways involved in controlling gene expression in bacteria (Altuvia & Wagner, 2000). The discovery of vast numbers of sRNAs, with diverse mechanisms of action and physiological functions, in many studied bacterial species, highlight the integral role played by sRNAs in bacterial gene regulation, usually at the post-transcriptional level (Kröger et al., 2013; Ryan et al., 2017; Vogel, 2009). While more work is still required to determine the roles of the majority of sRNAs in *S. Typhimurium*, there are a few specific links with FNR which warrant more investigation.

The largest sRNA regulon belongs to *GcvB*, a sRNA which controls expression of ~1% of the *S. Typhimurium* genome (Hébrard et al., 2012; Sharma et al., 2007; 2011). Notably, in our data set *GcvB* was the most highly upregulated transcript (approximately 13-fold) in Δ *fnr* (Table 3.2). While the role of *GcvB* seems to be involved primarily in the downregulation of amino acid and peptide transporters (Sharma et al., 2011), these processes have recently been suggested to be important for efficient host cell invasion (Miyakoshi, 2019). Additionally, *GcvB* negatively regulates the global regulator Lrp (Sharma et al., 2011). This is of particular interest as Lrp is a known repressor of SPI-2. It binds directly to a consensus

motif at the *ssrA* promoter which results in down-regulation of SPI-2 genes (Baek *et al.*, 2009). Thus, there may be additional control of SPI-2 through a regulatory pathway where under low oxygen conditions FNR represses *GcvB*, which then allows repression of SPI-2 through Lrp, and conversely under aerobic conditions, repression of *GcvB* is lifted causing a downregulation in *lrp* mRNA and expression of SPI-2.

Another potential link of FNR to virulence genes expression through an sRNA exists within *FnrS*. In our study, *fnrS* was the most down regulated (approximately 35-fold) sRNA in Δfnr (**Table 3.1**). In a recent study, deletion of *FnrS* led to increased HilD production under low aeration conditions, and *FnrS* could bind to the *hilD* mRNA 5' UTR, resulting in translational repression (Kim *et al.*, 2018). The authors discuss the importance of *FnrS* on SPI-1 expression however fail to mention the potential impact of HilD-mediated crosstalk between SPI-1 and SPI-2 (Bustamante *et al.*, 2008). Our data reveal that *FnrS* expression is dramatically decreased in Δfnr and in aerated WT cultures (**Figure 3.2C**), and SPI-2 expression is increased under these conditions (**Figure 3.14**). Thus, in the absence of *FnrS*, HilD levels may be increased, contributing to the SPI-2 induction phenotype that we have observed.

When we examined the binding of FNR at the *ydgT* promoter region, ChIP-seq data showed a putative binding site near the P_{*ydgT*}. However, the peaks had the highest coverage at the TSS of an unannotated antisense transcript found in the *ydgT* promoter region (**Figure 4.12A**). A motif search also revealed a near consensus FNR binding motif at the 5' end of the antisense transcript (**Figure 4.5**). Further investigation into this antisense transcript is required but, we can speculate that it is directly regulated by FNR due to the presence of the near consensus FNR binding motif and up-regulation in Δfnr , and its position relative to *ydgT* makes it a prime candidate as a cis-acting sRNA which may post-transcriptionally repress *ydgT* under aerobic conditions.

There were no SPI-1 like RNAs found in the FNR regulon under microaerobic conditions in MMA. This is not surprising as SPI-1 genes in general were not highly expressed under these conditions (**Figure 3.10A**). The Fink *et al.* and Wang *et al.* studies used conditions conducive to SPI-1 expression however their approaches to FNR regulon identification left them unable to detect sRNAs (Fink *et al.*, 2007; Wang *et al.*, 2019). However, if the growth conditions used in the aforementioned studies were used and the regulon were assessed by RNA-seq, it is possible that SPI-1 like sRNAs may emerge as targets for FNR control.

6.2.3 Regulation of motility

It has been demonstrated that under very different growth conditions, FNR was an activator of motility and chemotaxis under low oxygen and anaerobic conditions (**Figure 3.17, 3.18 & 3.19**) (Fink *et al.*, 2007). However, we have shown that the regulation by FNR is indirect for genes with the exception of *fliC*, *fliD*, and *aer*, the gene encoding Aer the signal transducer for aerotaxis. Interestingly, a recent study demonstrated that SsrB can repress *S. Typhimurium* motility through direct binding to a region upstream of *flhDC* (Ilyas *et al.*, 2018). Thus, much of the down-regulation of motility, especially of early gene products can be explained by FNR activation of *ssrB*, leading to SsrB repression of motility. This link makes sense as FNR is intracellularly active, possibly leading to increased expression of *ssrB*, and thus down regulation of flagella which, has been observed in macrophage as a mechanism to hide from host defenses (**Figure 5.4, 5.6**) (Ibarra & Steele-Mortimer, 2009). Information on the intracellular role of FNR is lacking, and further investigation of this and of a possible link through SsrB to flagellar regulation is required.

6.2.4 Differences in virulence gene expression in Δ *fnr* based on strain

During the preparation of this thesis, a new study emerged with the goal of investigating the FNR regulon through a proteomics approach (Wang *et al.*, 2019). The same growth conditions as the Fink *et al.* study were used (anaerobic growth in MOPS buffered LB with xylose), but surprisingly Wang *et al.*, found contrasting results (Fink *et al.*, 2007; Wang *et al.*, 2019). In the microarray study SPI-1 was activated by FNR while in the proteomic study SPI-1 was found to be repressed by FNR. These results were explained by the difference in strain used in the studies. In the microarray study *S. Typhimurium* strain 14028S was used while strain SL1344 was used for the proteomic study. Interestingly, SL1344 is more invasive than 14028S due to heterogeneity in expression of *Salmonella* pathogenicity island 1 and the absence of the SPI-1 effector SopE in 14028S (Clark *et al.*, 2011). While the growth condition in our study is quite different, we found that expression of SPI-1 was minimally activated by FNR, in agreement with the Fink *et al.* study (Fink *et al.*, 2007). In this study we have used strain 4/74, a strain which harbours *sopE* and differs from SL1344 by only 8 SNPs. Therefore, there may be another difference between the Fink *et al.* and Wang *et al.* studies which has not been accounted for. Strain 4/74 is a prototroph for histidine production that possesses a functional histidine biosynthetic pathway missing from SL1344

that is important for replication in the vacuolar environment of certain mammalian cells including macrophages (Henry *et al.*, 2005) which may help to explain differences in SPI-2 expression but not SPI-1. Clearly more work is needed on elucidating the specific difference between commonly used lab strains of *S. Typhimurium* especially as it pertains to mechanisms of virulence.

6.2.5 Limitations of our approach and existing technologies

As previously discussed, there are some limitations to the approach used in this study. Samples for RNA- and ChIP-seq are taken from a population of bacteria, which provide an average view of the transcriptomes of millions of cells. Genetically identical cells can often be phenotypically different and subpopulations of cells or outlier cells play important roles in disease outcome or antibiotic tolerance (Diard *et al.*, 2013; Helaine *et al.*, 2014). Additionally, our growth condition is heterogenous in nature, meaning we likely have very different expression in subpopulations throughout the oxygen gradient of the cultures. Single-cell RNA sequencing can reveal complex and rare cell populations, uncover regulatory relationships between genes and single-cell transcriptomic analysis will allow the detection of even more subtle, and often biologically significant, changes in gene expression that could be masked at the level of whole bacterial populations (Hwang *et al.*, 2018). For ChIP-seq, there are currently no studies using single-cell ChIP-seq in bacteria or eukaryotic cells (Nakato & Shirahige, 2017) and bacteria present an even larger barrier to single-cell ChIP as the small size of individual bacterial cells means they contain far less DNA and protein than eukaryotic cells. DNA sequencing coverage is a major limitation of single-cell ChIP-seq, as the analysis requires large amounts of starting material (Nakato & Shirahige 2017).

Additionally, to provide proof of principle it would be ideal to sequence RNA extracted from an *in vivo* infection where we specifically look at transcription of cells in the gut lumen and at the epithelial border prior to host cell invasion, however, this is not yet possible. Recombinase-based *in vivo* expression technology (RIVET) is a sensitive reporter of gene expression which involves the construction of a transcriptional fusion to a site-specific recombinase, which mediates the loss of a selectable genetic marker. This technique was fundamental for finding SPI-2 expression at the epithelial border (Brown *et al.*, 2005) however, it can only detect expression of individual genes. Nonetheless, other interesting experiments can be done while new technologies and technique develop which could be very

informative. The plasmids that were constructed in this study for examining promoters of SPI-2 genes (**Figure 4.13**) were constructed on a pCS26 plasmid which can be incorporated onto the chromosome in the same method used to build our *fnr*⁺ complementation strain (**Figure 2.1**) (Shivak *et al.*, 2016). In this way, we could measure kinetic *in vivo* expression from SPI-2 promoters with the problems associated with plasmid carriage. We are also interested in performing *in vivo* competitive fitness assays in mice with WT, Δfnr and with strain constructed with an oxygen insensitive FNR. These assays would help to further elucidate the role of FNR in *Salmonella* virulence and determine if Δfnr mutant is attenuated in various tissues of the gut and to see what effect an oxygen insensitive FNR has on virulence.

Furthermore, as can be observed from the Colgan *et al.* study, the targets of transcription factors may change depending on the growth condition, indeed the HilD regulon changes depending on the growth condition (Colgan *et al.*, 2016). Similarly, we see that the growth condition in the Fink *et al.* study is extremely different, and thus yielded a different FNR regulon from the current study (Fink *et al.*, 2007). Therefore, it is important to investigate regulons of TFs under more than one condition, especially in reference to TFs who play a role in virulence. Westermann *et al.* have recently shown that dual-RNA-seq can give important insight into the *ex vivo* transcriptome (Westermann *et al.*, 2016), and the group have recently made advances in toward cell type-specific *in vivo* dual-RNA-Seq (Frönicke *et al.*, 2018) which will be very useful techniques for precisely understanding *in vivo* transcriptional regulation and expression in the future.

6.3 Concluding remarks

Overall, we have used a combination of NGS techniques to expand the scope of the FNR regulon in *S. Typhimurium* and have established FNR as a direct repressor of SPI-2. This study demonstrates that oxygen is an important environmental signal and plays a critical role in the timing and deployment of *S. Typhimurium* virulence factors, and that FNR as a regulator of anaerobic metabolism, can also control the expression of genes critical for causing infection and disease. We have also shown that it is imperative to investigate bacterial regulons under a multitude of conditions to encompass the full capacity of a transcriptional regulator. Our particular focus on FNR regulation of SPI-2 under microaerobic conditions has revealed that, not only does FNR repress the expression of the SPI-2 encoded type three secretion system apparatus proteins, effectors and chaperones through direct regulation of the SPI-2 response regulator SsrB, but it also involved in the

direct repression of a great number of effectors and virulence relevant sRNAs encoded throughout the chromosome and on the *Salmonella* virulence plasmid. Furthermore, aerobic conditions relieved repression allowing for expression of virulence factors likely in preparation for the harsh intracellular environment of host cells (**Figure 6.1**). Moreover, we have provided additional evidence that oxygen is an important signalling molecule for the control of bacterial motility and that FNR is an important regulator in both intra- and extracellular environments. Additionally, we have shown that the accurate spatiotemporal expression of SPI-2 is integral for maintenance of bacterial fitness. Importantly, analysis of our Δfnr RNA-seq-based transcriptomic data in conjunction with previously published datasets (Colgan *et al.*, 2016), will provide a more complete picture of mixed regulatory interactions within the cell. We hope that the addition of this data will help in the development of the full picture of all regulatory interactions and inputs involved in establishment of *S. Typhimurium* infection.

References

- Abrahams, G. L., Müller, P. & Hensel, M. (2006).** Functional dissection of SseF, a type III effector protein involved in positioning the *Salmonella*-containing vacuole. *Traffic* **7**, 950–965.
- Aikawa, C., Maruyama, F. & Nakagawa, I. (2010).** The dawning era of comprehensive transcriptome analysis in cellular microbiology. *Front Microbiol* **1**, 1–10.
- Ailion, M., Bobik, T. A. & Roth, J. R. (1993).** Two global regulatory systems (Crp and Arc) control the cobalamin/propanediol regulon of *Salmonella* Typhimurium. *J Bacteriol* **175**, 7200–7208.
- Aizawa, S. I. (1996).** Flagellar assembly in *Salmonella* Typhimurium. *Mol Microbiol* **19**, 1–5.
- Ali, S. S., Soo, J., Rao, C., Leung, A. S., Ngai, D. H.-M., Ensminger, A. W. & Navarre, W. W. (2014).** Silencing by H-NS potentiated the evolution of *Salmonella*. *PLoS Pathog* **10**, e1004500–22.
- Ali, S. S., Whitney, J. C., Stevenson, J., Robinson, H., Howell, P. L. & Navarre, W. W. (2013).** structural insights into the regulation of foreign genes in *Salmonella* by the Hha/H-NS complex. *J Biol Chem* **288**, 13356–13369.
- Altschul, S. F., Gish, W., Miller, W., Myers, E. W. & Lipman, D. J. (1990).** Basic local alignment search tool. *J Mol Biol* **215**, 403–410.
- Altuvia, S. & Wagner, E. G. (2000).** Switching on and off with RNA. *PNAS* **97**, 9824–9826.
- Anderson, C. J., Satkovich, J., Köseoglu, V. K., Agaisse, H. & Kendall, M. M. (2018).** The ethanolamine permease EutH promotes vacuole adaptation of *Salmonella enterica* and *Listeria monocytogenes* during macrophage infection. *Infect Immun* **86**, 7195–12.
- Andrews, S. (2010).** *FastQC: a quality control tool for high throughput sequence data.*
- Ao, T. T., Feasey, N. A., Gordon, M. A., Keddy, K. H., Angulo, F. J. & Crump, J. A. (2015).** Global burden of invasive nontyphoidal *Salmonella* disease, 2010¹. *Emerging Infect Dis* **21**, 941–949.
- Atkuri, K. R., Herzenberg, L. A. & Herzenberg, L. A. (2005).** Culturing at atmospheric oxygen levels impacts lymphocyte function. *PNAS* **102**, 3756–3759.
- Álvarez-Ordóñez, A., Begley, M., Prieto, M., Messens, W., López, M., Bernardo, A. & Hill, C. (2011).** *Salmonella* spp. survival strategies within the host gastrointestinal tract. *Microbiology* **157**, 3268–3281.

- Baek, C. H., Wang, S., Roland, K. L. & Curtiss, R. (2009).** Leucine-responsive regulatory protein (Lrp) acts as a virulence repressor in *Salmonella enterica* serovar Typhimurium. *J Bacteriol* **191**, 1278–1292.
- Baek, J., Lee, J., Yoon, K. & Lee, H. (2017).** Identification of unannotated small genes in *Salmonella*. *G3* **7**, 983–989.
- Baisón-Olmo, F., Cardenal-Muñoz, E. & Ramos-Morales, F. (2012).** PipB2 is a substrate of the *Salmonella* pathogenicity island 1-encoded type III secretion system. *Biochemical and Biophysical Research Communications* **423**, 240–246.
- Banda, M. M., Zavala-Alvarado, C., Pérez-Morales, D. & Bustamante, V. H. (2019).** SlyA and HilD counteract H-NS-mediated repression on the *ssrAB* virulence operon of *Salmonella* Typhimurium and thus promote its activation by OmpR. *J Bacteriol* 1–45.
- Baños, R. C., Vivero, A., Aznar, S., García, J., Pons, M., Madrid, C. & Juárez, A. (2009).** Differential regulation of horizontally acquired and core genome genes by the bacterial modulator H-NS. *PLoS Genet* **5**, e1000513–8.
- Baranello, L., Kouzine, F., Sanford, S. & Levens, D. (2016).** ChIP bias as a function of cross-linking time. *Chromosome Res* **24**, 175–181.
- Barlag, B. & Hensel, M. (2015).** The giant adhesin SiiE of *Salmonella enterica*. *Molecules* **20**, 1134–1150.
- Barnard, A., Wolfe, A. & Busby, S. (2004).** Regulation at complex bacterial promoters: how bacteria use different promoter organizations to produce different regulatory outcomes. *Curr Opin Microbiol* **7**, 102–108.
- Bartolini, E., Frigimelica, E., Giovinazzi, S., Galli, G., Shaik, Y., Genco, C., Welsch, J. A., Granoff, D. M., Grandi, G. & Grifantini, R. (2006).** Role of FNR and FNR-regulated, sugar fermentation genes in *Neisseria meningitidis* infection. *Mol Microbiol* **60**, 963–972.
- Basnyat, B. & Baker, S. (2015).** Typhoid carriage in the gallbladder. *The Lancet*.
- Bates, D. M., Lazazzera, B. A. & Kiley, P. J. (1995).** Characterization of FNR* mutant proteins indicates two distinct mechanisms for altering oxygen regulation of the *Escherichia coli* transcription factor FNR. *J Bacteriol* **177**, 3972–3978.
- Beinert, H. & Kiley, P. J. (1999).** Fe-S proteins in sensing and regulatory functions. *Curr Opin Chem Biol* **3**, 152–157.
- Benson, D. A., Cavanaugh, M., Clark, K., Karsch-Mizrachi, I., Lipman, D. J., Ostell, J. & Sayers, E. W. (2012).** GenBank. *Nucleic Acids Res* **41**, D36–D42.
- Berg, J. M., Tymoczko, J. L. & Stryer, L. (2002).** A proton gradient powers the synthesis of ATP. In *Biochemistry 5th edition*, W H Freeman.

- Betts, M. J. & Russell, R. B. (2003).** *Amino Acid Properties and Consequences of Substitutions*. Chichester, UK: John Wiley & Sons, Ltd.
- Beuzón, C. R., Salcedo, S. P. & Holden, D. W. (2002).** Growth and killing of a *Salmonella enterica* serovar Typhimurium *sifA* mutant strain in the cytosol of different host cell lines. *Microbiology* **148**, 2705–2715.
- Bijlsma, J. J. E. & Groisman, E. A. (2005).** The PhoP/PhoQ system controls the intramacrophage type three secretion system of *Salmonella enterica*. *Mol Microbiol* **57**, 85–96.
- Blake, T., Barnard, A., Busby, S. J. W. & Green, J. (2002).** Transcription activation by FNR: Evidence for a functional activating region 2 **184**, 5855–5861.
- Blanc-Potard, A. B., Labesse, G., Figueroa-Bossi, N. & Bossi, L. (2005).** Mutation at the ‘exit gate’ of the *Salmonella* gyrase a subunit suppresses a defect in the gyrase b subunit. *J Bacteriol* **187**, 6841–6844.
- Blanc-Potard, A. B., Solomon, F., Kayser, J. & Groisman, E. A. (1999).** The SPI-3 pathogenicity island of *Salmonella enterica*. *J Bacteriol* **181**, 998–1004.
- Bolivar, F., Rodriguez, R. L., Greene, P. J., Betlach, M. C., Heyneker, H. L., Boyer, H. W., Crosa, J. H. & Falkow, S. (1977).** Construction and characterization of new cloning vehicle. II. A multipurpose cloning system. *Gene* **2**, 95–113.
- Bonifield, H. R. & Hughes, K. T. (2003).** Flagellar phase variation in *Salmonella enterica* is mediated by a posttranscriptional control mechanism. *J Bacteriol* **185**, 3567–3574.
- Bonocora, R. P. & Wade, J. T. (2015).** ChIP-Seq for genome-scale analysis of bacterial DNA-binding proteins. In *Bacterial Regulatory RNA*, Methods in Molecular Biology, pp. 327–340. Edited by V. Arluison & C. Valverde. New York, NY: Springer New York.
- Boysen, A., Møller-Jensen, J., Kallipolitis, B., Valentin-Hansen, P. & Overgaard, M. (2010).** Translational regulation of gene expression by an anaerobically induced small non-coding RNA in *Escherichia coli*. *J Biol Chem* **285**, 10690–10702.
- Brenner, F. W., Villar, R. G., Angulo, F. J., Tauxe, R. & Swaminathan, B. (2000).** *Salmonella* nomenclature. *Journal of Clinical Microbiology* **38**, 2465–2467.
- Brown, N. F., Vallance, B. A., Coombes, B. K., Valdez, Y., Coburn, B. A. & Finlay, B. B. (2005).** *Salmonella* pathogenicity island 2 is expressed prior to penetrating the intestine. *PLoS Pathog* **1**, e32–7.
- Browning, D. F. & Busby, S. J. W. (2004).** The regulation of bacterial transcription initiation. *Nat Rev Microbiol* **2**, 57–65.

- Browning, D. F., Grainger, D. C., Beatty, C. M., Wolfe, A. J., Cole, J. A. & Busby, S. J. W. (2005).** Integration of three signals at the *Escherichia coli nrf* promoter: a role for Fis protein in catabolite repression. *Mol Microbiol* **57**, 496–510.
- Buchmeier, N., Bossie, S., Chen, C. Y., Fang, F. C., Guiney, D. G. & Libby, S. J. (1997).** SlyA, a transcriptional regulator of *Salmonella typhimurium*, is required for resistance to oxidative stress and is expressed in the intracellular environment of macrophages. *Infect Immun* **65**, 3725–3730.
- Buckle, G. C., Walker, C. L. F. & Black, R. E. (2012).** Typhoid fever and paratyphoid fever: Systematic review to estimate global morbidity and mortality for 2010. *J Glob Health* **2**, 010401.
- Bumann, D. (2009).** System-level analysis of *Salmonella* metabolism during infection. *Curr Opin Microbiol* **12**, 559–567.
- Bustamante, V. H., Martínez, L. C., Santana, F. J., Knodler, L. A., Steele-Mortimer, O. & Puente, J. L. (2008).** HilD-mediated transcriptional cross-talk between SPI-1 and SPI-2. *PNAS* **105**, 14591–14596.
- Cai, S. J. & Inouye, M. (2002).** EnvZ-OmpR interaction and osmoregulation in *Escherichia coli*. *J Biol Chem* **277**, 24155–24161.
- Cai, Y.-H. & Huang, H. (2012).** Advances in the study of protein–DNA interaction. *Amino Acids* **43**, 1141–1146.
- Cameron, A. D. S., Stoebel, D. M. & Dorman, C. J. (2011).** DNA supercoiling is differentially regulated by environmental factors and FIS in *Escherichia coli* and *Salmonella enterica*. *Mol Microbiol* **80**, 85–101.
- Chakraborty, S., Mizusaki, H. & Kenney, L. J. (2015).** A FRET-based DNA biosensor tracks OmpR-dependent acidification of *Salmonella* during macrophage infection. *PLoS Biol* **13**, e1002116.
- Chao, Y., Papenfort, K., Reinhardt, R., Sharma, C. M. & Vogel, J. O. R. (2012).** An atlas of Hfq-bound transcripts reveals 3 prime UTRs as a genomic reservoir of regulatory small RNAs. *EMBO J* **31**, 4005–4019.
- Chaudhuri, R. R., Morgan, E., Peters, S. E., Pleasance, S. J., Hudson, D. L., Davies, H. M., Wang, J., van Diemen, P. M., Buckley, A. M. & other authors. (2013).** Comprehensive assignment of roles for *Salmonella Typhimurium* genes in intestinal colonization of food-producing animals. *PLoS Genet* **9**, e1003456.
- Cherepanov, P. P. & Wackernagel, W. (1995).** Gene disruption in *Escherichia coli*: Tc^R and Km^R cassettes with the option of Flp-catalyzed excision of the antibiotic-resistance determinant. *Gene* **158**, 9–14.

- Chilcott, G. S. & Hughes, K. T. (2000).** Coupling of flagellar gene expression to flagellar assembly in *Salmonella enterica* serovar Typhimurium and *Escherichia coli*. *Microbiol Mol Biol R* **64**, 694–708.
- Choi, E., Kim, H., Lee, H., Nam, D., Choi, J. & Shin, D. (2014).** The iron-sensing fur regulator controls expression timing and levels of *Salmonella* pathogenicity island 2 genes in the course of environmental acidification. *Infect Immun* **82**, 2203–2210.
- Choi, E., Han, Y., Cho, Y.-J., Nam, D. & Lee, E.-J. (2017).** A trans-acting leader RNA from a *Salmonella* virulence gene. *PNAS*. **114**, 10232–10237.
- Choi, J. & Groisman, E. A. (2016).** Acidic pH sensing in the bacterial cytoplasm is required for *Salmonella* virulence. *Mol Microbiol* **101**, 1024–1038.
- Cirillo, D. M., Valdivia, R. H., Monack, D. M. & Falkow, S. (1998).** Macrophage-dependent induction of the *Salmonella* pathogenicity island 2 type III secretion system and its role in intracellular survival. *Mol Microbiol* **30**, 175–188.
- Clark, L., Perrett, C. A., Malt, L., Harward, C., Humphrey, S., Jepson, K. A., Martinez-Argudo, I., Carney, L. J., La Ragione, R. M. & other authors. (2011).** Differences in *Salmonella enterica* serovar Typhimurium strain invasiveness are associated with heterogeneity in SPI-1 gene expression. *Microbiology* **157**, 2072–2083.
- Coburn, B., Grassl, G. A. & Finlay, B. B. (2006).** *Salmonella*, the host and disease: a brief review. *Immunol Cell Biol* **85**, 112–118.
- Colgan, A. M., Kröger, C., Diard, M., Hardt, W.-D., Puente, J. L., Sivasankaran, S. K., Hokamp, K., Hinton, J. C. D. (2016).** The impact of 18 ancestral and horizontally-acquired regulatory proteins upon the transcriptome and sRNA landscape of *Salmonella enterica* serovar Typhimurium. *PLoS Genet* **12**, 1–42.
- Constantinidou, C., Hobman, J. L., Griffiths, L., Patel, M. D., Penn, C. W., Cole, J. A. & Overton, T. W. (2006).** A reassessment of the FNR regulon and transcriptomic analysis of the effects of nitrate, nitrite, NarXL, and NarQP as *Escherichia coli* K12 adapts from aerobic to anaerobic growth. *J Biol Chem* **281**, 4802–4815.
- Cook, G. M., Greening, C., Hards, K. & Berney, M. (2014).** *Energetics of Pathogenic Bacteria and Opportunities for Drug Development*. In *Advances in Bacterial Pathogen Biology*, 1st edn. Elsevier Ltd.
- Coombes, B. K., Brown, N. F., Kujat-Choy, S., Vallance, B. A. & Finlay, B. B. (2003).** SseA is required for translocation of *Salmonella* pathogenicity island-2 effectors into host cells. *Microbes and Infection* **5**, 561–570.

- Coombes, B. K., Wickham, M. E., Lowden, M. J., Brown, N. F. & Finlay, B. B. (2005).** Negative regulation of *Salmonella* pathogenicity island 2 is required for contextual control of virulence during typhoid. *PNAS* **102**, 17460–17465.
- Cotter, P. A., Melville, S. B., Albrecht, J. A. & Gunsalus, R. P. (1997).** Aerobic regulation of cytochrome d oxidase (*cydAB*) operon expression in *Escherichia coli*: roles of Fnr and ArcA in repression and activation. *Mol Microbiol* **25**, 605–615.
- Crofts, A. A., Giovanetti, S. M., Rubin, E. J., Poly, F. M., Gutiérrez, R. L., Talaat, K. R., Porter, C. K., Riddle, M. S., DeNearing, B. & other authors. (2018).** Enterotoxigenic *E. coli* virulence gene regulation in human infections. *PNAS* **12**, 201808982–9.
- Croucher, N. J. & Thomson, N. R. (2010).** Studying bacterial transcriptomes using RNA-seq. *Curr Opin Microbiol* **13**, 619–624.
- Crump, J. A. & Mintz, E. D. (2010).** Global trends in Typhoid and Paratyphoid Fever. *Clin Infect Dis* **50**, 241–246.
- Datsenko, K. A. & Wanner, B. L. (2000).** One-step inactivation of chromosomal genes in *Escherichia coli* K-12 using PCR products. *PNAS* **97**, 6640–6645.
- Davis, S. E., Mooney, R. A., Kanin, E. I., Grass, J., Landick, R. & Ansari, A. Z. (2011).** Chapter 20 - Mapping *E. coli* RNA Polymerase and Associated Transcription Factors and Identifying Promoters Genome-Wide. In *High-Density Sequencing Applications in Microbial Molecular Genetics*, 1st edn. Elsevier Inc.
- Deiwick, J., Nikolaus, T., Erdogan, S. & Hensel, M. (1999).** Environmental regulation of *Salmonella* pathogenicity island 2 gene expression. *Mol Microbiol* **31**, 1759–1773.
- Desai, P. T., Porwollik, S., Long, F., Cheng, P., Wollam, A., Clifton, S. W., Weinstock, G. M. & McClelland, M. (2013).** Evolutionary Genomics of *Salmonella enterica* Subspecies. *mBio* **4**, e00579–12.
- Desai, S. K., Winardhi, R. S., Periasamy, S., Dykas, M. M. & Elife, Y. J. (2016).** The horizontally-acquired response regulator SsrB drives a *Salmonella* lifestyle switch by relieving biofilm silencing. *eLIFE* **5**, e10747.
- Diard, M., Garcia, V., Maier, L., Remus-Emsermann, M. N. P., Regoes, R. R., Ackermann, M. & Hardt, W.-D. (2013).** Stabilization of cooperative virulence by the expression of an avirulent phenotype. *Nature* **494**, 353–356.
- Diepold, A. & Wagner, S. (2014).** Assembly of the bacterial type III secretion machinery. *FEMS Microbiol Rev* **38**, 802–822.

- Dillon, S. C., Cameron, A. D. S., Hokamp, K., Lucchini, S., Hinton, J. C. D. & Dorman, C. J. (2010).** Genome-wide analysis of the H-NS and Sfh regulatory networks in *Salmonella* Typhimurium identifies a plasmid-encoded transcription silencing mechanism. *Mol Microbiol* **76**, 1250–1265.
- Dillon, S. C. & Dorman, C. J. (2010).** Bacterial nucleoid-associated proteins, nucleoid structure and gene expression. *Nat Rev Microbiol* **8**, 185–195.
- Donato, G. M. & Kawula, T. H. (1999).** Phenotypic analysis of random *hns* mutations differentiate DNA-binding activity from properties of *fimA* promoter inversion modulation and bacterial motility. *J Bacteriol* **181**, 941–948.
- Dorman, C. J., Chatfield, S., Higgins, C. F., Hayward, C. & Dougan, G. (1989).** Characterization of porin and *ompR* mutants of a virulent strain of *Salmonella* Typhimurium: *ompR* mutants are attenuated *in vivo*. *Infect Immun* **57**, 2136–2140.
- Dougan, G. & Baker, S. (2014).** *Salmonella enterica* serovar Typhi and the pathogenesis of Typhoid fever. *Annu Rev Microbiol* **68**, 317–336.
- Drecktrah, D., Knodler, L. A., Ireland, R. & Steele-Mortimer, O. (2005).** The mechanism of *Salmonella* entry determines the vacuolar environment and intracellular gene expression. *Traffic* **7**, 39–51.
- Durand, S. & Storz, G. (2010).** Reprogramming of anaerobic metabolism by the *FnrS* small RNA. *Mol Microbiol* **75**, 1215–1231.
- Eckburg, P. B., Bik, E. M., Bernstein, C. N., Purdom, E., Dethlefsen, L., Sargent, M., Gill, S. R., Nelson, K. E. & Relman, D. A. (2005).** Diversity of the human intestinal microbial flora. *Science* **308**, 1635–1638.
- Eiglmeier, K., Honoré, N., Iuchi, S., Lin, E. C. & Cole, S. T. (1989).** Molecular genetic analysis of FNR-dependent promoters. *Mol Microbiol* **3**, 869–878.
- Ellermeier, C. D., Ellermeier, J. R. & Slauch, J. M. (2005).** HilD, HilC and RtsA constitute a feed forward loop that controls expression of the SPI1 type three secretion system regulator *hilA* in *Salmonella enterica* serovar Typhimurium. *Mol Microbiol* **57**, 691–705.
- Ellermeier, J. R. & Slauch, J. M. (2007).** Adaptation to the host environment: regulation of the SPI-1 type III secretion system in *Salmonella enterica* serovar Typhimurium. *Curr Opin Microbiol* **10**, 24–29.
- Ernst, R. K., D. M. Dombroski, and J. M. Merrick. (1990).** Anaerobiosis, type-1 fimbriae, and growth phase are factors that affect invasion of Hep-2 cells by *Salmonella* typhimurium. *Infect Immun* **58**,2014-2016.

- Evans, M. R., Fink, R. C., Vazquez-Torres, A., Porwollik, S., Jones-Carson, J., McClelland, M. & Hassan, H. M. (2011). Analysis of the ArcA regulon in anaerobically grown *Salmonella enterica* sv. Typhimurium. *BMC Microbiology* **11**, 58.
- Faber, F., Thiennimitr, P., Spiga, L., Byndloss, M. X., Litvak, Y., Lawhon, S., Andrews-Polymenis, H. L., Winter, S. E. & Bäumlér, A. J. (2017). Respiration of microbiota-derived 1,2-propanediol drives *Salmonella* expansion during colitis. *PLoS Pathog* **13**, e1006129.
- Fabrega, A. & Vila, J. (2013). *Salmonella enterica* serovar Typhimurium skills to succeed in the host: virulence and regulation. *Clin Microbiol Rev* **26**, 308–341.
- Fass, E. & Groisman, E. A. (2009). Control of *Salmonella* pathogenicity island-2 gene expression. *Curr Opin Microbiol* **12**, 199–204.
- Fàbrega, A. & Vila, J. (2013). *Salmonella enterica* serovar Typhimurium skills to succeed in the host: virulence and regulation. *Clin Microbiol Rev* **26**, 308–341. American Society for Microbiology.
- Feasey, N. A., Dougan, G., Kingsley, R. A., Heyderman, R. S. & Gordon, M. A. (2012). Invasive non-typhoidal *Salmonella* disease: an emerging and neglected tropical disease in Africa. *The Lancet* **379**, 2489–2499.
- Feng, X., Oropeza, R. & Kenney, L. J. (2003). Dual regulation by phospho-OmpR of *ssrA/B* gene expression in *Salmonella* pathogenicity island 2. *Mol Microbiol* **48**, 1131–1143.
- Figueira, R. & Holden, D. W. (2012). Functions of the *Salmonella* pathogenicity island 2 (SPI-2) type III secretion system effectors. *Microbiology* **158**, 1147–1161.
- Filiatrault, M. J., Picardo, K. F., Ngai, H., Passador, L. & Iglewski, B. H. (2006). Identification of *Pseudomonas aeruginosa* genes involved in virulence and anaerobic growth. *Infect Immun* **74**, 4237–4245.
- Fink, R. C., Evans, M. R., Porwollik, S., Vazquez-Torres, A., Jones-Carson, J., Troxell, B., Libby, S. J., McClelland, M. & Hassan, H. M. (2007). FNR is a global regulator of virulence and anaerobic metabolism in *Salmonella enterica* serovar Typhimurium (ATCC 14028s). *J Bacteriol* **189**, 2262–2273.
- Finlay, B. B., Ruschkowski, S. & Dedhar, S. (1991). Cytoskeletal rearrangements accompanying *Salmonella* entry into epithelial cells. *J Cell Sci* **99** (Pt 2), 283–296.
- Fookes, M., Schroeder, G. N., Langridge, G. C., Blondel, C. J., Mammina, C., Connor, T. R., Seth-Smith, H., Vernikos, G. S., Robinson, K. S. & other authors. (2011). *Salmonella bongori* provides insights into the evolution of the *Salmonellae*. *PLoS Pathog* **7**, e1002191.

- Forstner, K. U., Vogel, J., Sharma, C.. (2014).** READemption—a tool for the computational analysis of deep-sequencing-based transcriptome data. *academicoupcom*
- Foster, J. W. & Hall, H. K. (1990).** Adaptive acidification tolerance response of *Salmonella* Typhimurium. *J Bacteriol* **172**, 771–778.
- Foster, J. (1991).** *Salmonella* acid shock proteins are required for the adaptive acid tolerance response. *J Bacteriol* **173**, 6896–6902.
- Frönicke, L., Bronner, D. N., Byndloss, M. X., McLaughlin, B., Bäumlner, A. J. & Westermann, A. J. (2018).** *Toward Cell Type-Specific in vivo Dual RNA-Seq*. In *High-Density Sequencing Applications in Microbial Molecular Genetics*, 1st edn. Elsevier Inc.
- Galagan, J., Lyubetskaya, A. & Gomes, A. (2012).** ChIP-Seq and the Complexity of Bacterial Transcriptional Regulation. In *Systems Biology, Current Topics in Microbiology and Immunology*, pp. 43–68. Berlin, Heidelberg: Springer Berlin Heidelberg.
- Galan, J. E. & Zhou, D. (2000).** Striking a balance: modulation of the actin cytoskeleton by *Salmonella*. *PNAS* **97**, 8754–8761.
- Garalde, D. R., Snell, E. A., Jachimowicz, D., Sipos, B., Lloyd, J. H., Bruce, M., Pantic, N., Admassu, T., James, P. & other authors. (2018).** Highly parallel direct RNA sequencing on an array of nanopores. *Nature Methods* **15**, 201–206.
- Garcia-Calderon, C. B., Casadesus, J. & Ramos-Morales, F. (2007).** Rcs and PhoPQ regulatory overlap in the control of *Salmonella enterica* Virulence. *J Bacteriol* **189**, 6635–6644.
- Gerasimova, A. V., Rodionov, D. A., Mironov, A. A. & Gelfand, M. S. (2001).** Computer analysis of regulatory signals in bacterial genomes. FNR binding sites. *Molecular Biology* **35**, 853–861.
- Gerlach, R. G., Cláudio, N., Rohde, M., Jäckel, D., Wagner, C. & Hensel, M. (2008).** Cooperation of *Salmonella* pathogenicity islands 1 and 4 is required to breach epithelial barriers. *Cell Microbiol* **10**, 2364–2376.
- Gil, F., Ipinza, F., Fuentes, J., Fumeron, R., Villarreal, J. M., Aspée, A., Mora, G. C., Vásquez, C. C. & Saavedra, C. (2007).** The *ompW* (porin) gene mediates methyl viologen (paraquat) efflux in *Salmonella enterica* serovar Typhimurium. *Research in Microbiology* **158**, 529–536.
- Gilberthorpe, N. J. & Poole, R. K. (2008).** Nitric oxide homeostasis in *Salmonella* Typhimurium: roles of respiratory nitrate reductase and flavohemoglobin. *J Biol Chem* **283**, 11146–11154.

- Golubeva, Y. A., Sadik, A. Y., Ellermeier, J. R. & Slauch, J. M. (2012).** Integrating global regulatory input into the *Salmonella* pathogenicity island 1 type III secretion system. *Genetics* **190**, 79–90.
- Gong, H., Vu, G.-P., Bai, Y., Chan, E., Wu, R., Yang, E., Liu, F. & Lu, S. (2011).** A *Salmonella* small non-coding RNA facilitates bacterial invasion and intracellular replication by modulating the expression of virulence factors. *PLoS Pathog* **7**, e1002120–16.
- Gonzalez-Escobedo, G., Marshall, J. M. & Gunn, J. S. (2010).** Chronic and acute infection of the gall bladder by *Salmonella* Typhi: understanding the carrier state. *Nat Rev Microbiol* **9**, 9–14.
- Gordon, M. A. (2008).** *Salmonella* infections in immunocompromised adults. *J Infect* **56**, 413–422.
- Grabe, G. J., Zhang, Y., Przydacz, M., Rolhion, N., Yang, Y., Pruneda, J. N., Komander, D., Holden, D. W. & Hare, S. A. (2016).** The *Salmonella* effector SpvD is a cysteine hydrolase with a serovar-specific polymorphism influencing catalytic activity, suppression of immune responses, and bacterial virulence. *J Biol Chem* **291**, 25853–25863.
- Grainger, D. C., Aiba, H., Hurd, D., Browning, D. F. & Busby, S. J. W. (2007).** Transcription factor distribution in *Escherichia coli*: studies with FNR protein. *Nucleic Acids Res* **35**, 269–278.
- Grant, C. E., Bailey, T. L. & Noble, W. S. (2011).** FIMO: scanning for occurrences of a given motif. *Bioinformatics* **27**, 1017–1018.
- Green, J. & Guest, J. R. (1993).** Activation of FNR-dependent transcription by iron: an *in vitro* switch for FNR. *FEMS Microbiology Letters* **113**, 219–222.
- Green, J. & Guest, J. R. (1994).** Regulation of transcription at the *ndh* promoter of *Escherichia coli* by FNR and novel factors. *Mol Microbiol* **12**, 433–444.
- Green, J. & Marshall, F. A. (1999).** Identification of a surface of FNR overlapping activating region 1 that is required for repression of gene expression. *J Biol Chem* **274**, 10244–10248.
- Green, J., Rolfe, M. D. & Smith, L. J. (2014).** Transcriptional regulation of bacterial virulence gene expression by molecular oxygen and nitric oxide. *Virulence* **5**, 794–809.
- Grimont, P. & Weill, F. (2007).** Antigenic formulae of the *Salmonella* serovars. *WHO Collaborating Centre for Reference and Research on Salmonella*. Institut Pasteur, Paris.
- Groisman, E. A. & Ochman, H. (1997).** How *Salmonella* became a pathogen. *Trends in Microbiology* **5**, 343–349.

- Groisman, E. A. & Mouslim, C. (2006).** Sensing by bacterial regulatory systems in host and non-host environments. *Nat Rev Microbiol* **4**, 705–709.
- Guest, J. R., Green, J., Irvine, A. S. & Spiro, S. (1996).** Chapter 16 – The FNR modulon and FNR-regulated gene expression. In *Regulation of Gene Expression in Escherichia coli*, pp. 317–342.
- Guiney, D. G. & Fierer, J. (2011).** The role of the *spv* genes in *Salmonella* pathogenesis. *Front Microbiol* **2**, 1–10.
- Gunn, J. S., Ryan, S. S., Van Velkinburgh, J. C., Ernst, R. K. & Miller, S. I. (2000).** Genetic and functional analysis of a PmrA-PmrB-regulated locus necessary for lipopolysaccharide modification, antimicrobial peptide resistance, and oral virulence of *Salmonella enterica* serovar typhimurium. *Infect Immun* **68**, 6139–6146.
- Haas, B. J., Chin, M., Nusbaum, C., Birren, B. W. & Livny, J. (2012).** How deep is deep enough for RNA-Seq profiling of bacterial transcriptomes? *BMC Genomics* **13**, 734.
- Hall, B. G., Acar, H., Nandipati, A. & Barlow, M. (2014).** Growth Rates Made Easy. *Mol Biol Evol* **31**, 232–238.
- Hanahan, D. (1983).** Studies on transformation of *Escherichia coli* with plasmids. *J Mol Biol* **166**, 557–580.
- Haraga, A., Ohlson, M. B. & Miller, S. I. (2008).** *Salmonellae* interplay with host cells. *Nat Rev Microbiol* **6**, 53–66.
- Hautefort, I., Thompson, A., Eriksson-Ygberg, S., Parker, M. L., Lucchini, S., Danino, V., Bongaerts, R. J. M., Ahmad, N., Rhen, M. & Hinton, J. C. D. (2008).** During infection of epithelial cells *Salmonella enterica* serovar Typhimurium undergoes a time-dependent transcriptional adaptation that results in simultaneous expression of three type 3 secretion systems. *Cell Microbiol* **10**, 958–984.
- Hautefort, I., Proença, M. J. & Hinton, J. C. D. (2003).** Single-copy green fluorescent protein gene fusions allow accurate measurement of *Salmonella* gene expression *in vitro* and during infection of mammalian cells. *Appl Environ Microb* **69**, 7480–7491.
- Hayward, M. R., AbuOun, M., La Ragione, R. M., Tchórzewska, M. A., Cooley, W. A., Everest, D. J., Petrovska, L., Jansen, V. A. A. & Woodward, M. J. (2014).** SPI-23 of *S. Derby*: Role in adherence and invasion of porcine tissues. *PLoS ONE* **9**, e107857–8.
- Helaine, S., Cheverton, A. M., Watson, K. G., Faure, L. M., Matthews, S. A. & Holden, D. W. (2014).** Internalization of *Salmonella* by macrophages induces formation of nonreplicating persisters. *Science* **343**, 204–208.

- Helaine, S., Thompson, J. A., Watson, K. G., Liu, M., Boyle, C. & Holden, D. W. (2010).** Dynamics of intracellular bacterial replication at the single cell level. *PNAS* **107**, 3746–3751.
- Henry, T., García-del Portillo, F. & Gorvel, J. P. (2005).** Identification of *Salmonella* functions critical for bacterial cell division within eukaryotic cells. *Mol Microbiol* **56**, 252–267.
- Hensel, M., Hinsley, A. P., Nikolaus, T., Sawers, G. & Berks, B. C. (1999).** The genetic basis of tetrathionate respiration in *Salmonella typhimurium*. *Mol Microbiol* **32**, 275–287.
- Hensel, M. (2000).** *Salmonella* Pathogenicity Island 2. *Mol Microbiol* **36**, 1015–1023.
- Hébrard, M., Kröger, C., Sivasankaran, S. K., Händler, K. & Hinton, J. C. D. (2011).** The challenge of relating gene expression to the virulence of *Salmonella enterica* serovar Typhimurium. *Curr Opin Biotechnol* **22**, 200–210.
- Hébrard, M., Kröger, C., Srikumar, S., Colgan, A., Händler, K. & Hinton, J. C. D. (2012).** sRNAs and the virulence of *Salmonella enterica* serovar Typhimurium. *RNA Biology* **9**, 437–445.
- Hodges, A. P., Dai, D., Xiang, Z., Woolf, P., Xi, C. & He, Y. (2010).** Bayesian Network Expansion Identifies New ROS and Biofilm Regulators. *PLoS ONE* **5**, e9513–9.
- Hoffmann, S., Otto, C., Kurtz, S., Sharma, C. M., Khaitovich, P., Vogel, J., Stadler, P. F. & Hackermüller, J. (2009).** Fast mapping of short sequences with mismatches, insertions and deletions using index structures. *PLoS Comput Biol* **5**, e1000502–10.
- Hoiseth, S. K. & Stocker, B. A. (1981).** Aromatic-dependent *Salmonella* Typhimurium are non-virulent and effective as live vaccines. *Nature* **291**, 238–239.
- Horstmann, J. A., Zschieschang, E., Truschel, T., de Diego, J., Lunelli, M., Rohde, M., May, T., Strowig, T., Stradal, T. & other authors. (2017).** Flagellin phase-dependent swimming on epithelial cell surfaces contributes to productive *Salmonella* gut colonisation. *Cell Microbiol* **19**, e12739–43.
- Hurley, D., McCusker, M. P., Fanning, S. & Martins, M. (2014).** *Salmonella*-host interactions – modulation of the host innate immune system. *Front Immunol* **5**, 481.
- Hwang, B., Lee, J. H. & Bang, D. (2018).** Single-cell RNA sequencing technologies and bioinformatics pipelines. *Exp Mol Med* **50**, 1–14.
- Ibarra, J. A. & Steele-Mortimer, O. (2009).** *Salmonella*—the ultimate insider. *Salmonella* virulence factors that modulate intracellular survival. *Cell Microbiol* **11**, 1579–1586.

- Ilyas, B., Mulder, D. T., Little, D. J., Elhenawy, W., Banda, M. M., Pérez-Morales, D., Tsai, C. N., Chau, N. Y. E., Bustamante, V. H. & Coombes, B. K. (2018). Regulatory evolution drives evasion of host inflammasomes by *Salmonella* Typhimurium. *Cell Rep* **25**, 825–832.
- Ingledeu, W. J. & Poole, R. K. (1984). The respiratory chains of *Escherichia coli*. *Microbiol Rev* **48**, 222–271.
- Ishchukov, I., Wu, Y., Van Puyvelde, S., Vanderleyden, J. & Marchal, K. (2014). Inferring the relation between transcriptional and posttranscriptional regulation from expression compendia. *BMC Microbiology* **14**, 1–14.
- Issenhuth-Jeanjean, S., Roggentin, P., Mikoleit, M., Guibourdenche, M., de Pinna, E., Nair, S., Fields, P. I. & Weill, F.-X. (2014). Supplement 2008-2010 (no. 48) to the White-Kauffmann-Le Minor scheme. *Res Microbiol* **165**, 526–530.
- Jacobsen, A., Hendriksen, R. S., Aaresturp, F. M., Ussery, D. W. & Friis, C. (2011). The *Salmonella enterica* Pan-genome. *Microb Ecol* **62**, 487–504.
- Jakobson, C. M. & Tullman-Ercek, D. (2016). Dumpster diving in the gut: Bacterial microcompartments as part of a host-associated lifestyle. *PLoS Pathog* **12**, e1005558.
- James, P. E., Grinberg, O. Y., cellular, G. M. J. O.1995. (1995). Intraphagosomal oxygen in stimulated macrophages. *J Cell Physiol* **163**, 241–247.
- Jennewein, J., Matuszak, J., Walter, S., Felmy, B., Gendera, K., Schatz, V., Nowotny, M., Liebsch, G., Hensel, M. & other authors. (2015). Low-oxygen tensions found in *Salmonella*-infected gut tissue boost *Salmonella* replication in macrophages by impairing antimicrobial activity and augmenting *Salmonella* virulence. *Cell Microbiol* **17**, 1833–1847.
- Jennings, E., Thurston, T. L. M. & Holden, D. W. (2017). *Salmonella* SPI-2 type III secretion system effectors: Molecular mechanisms and physiological consequences. *Cell Host Microbe* **22**, 217–231.
- Jepson, M. A. & Clark, M. A. (2001). The role of M cells in *Salmonella* infection. *Microbes and Infection* **3**, 1183–1190.
- Jervis, A. J., Crack, J. C., White, G., Artymiuk, P. J., Cheesman, M. R., Thomson, A. J., Le Brun, N. E. & Green, J. (2009). The O₂ sensitivity of the transcription factor FNR is controlled by Ser24 modulating the kinetics of [4Fe-4S] to [2Fe-2S] conversion. *PNAS* **106**, 4659–4664.
- Jones, G. W., Richardson, L. A. & Uhlman, D. (1981). The invasion of HeLa cells by *Salmonella* Typhimurium: reversible and irreversible bacterial attachment and the role of bacterial motility. *J Gen Microbiol* **127**, 351–360.

- Joshi, K. & Patil, D. (2017).** Proteomics. In *Innovative Approaches in Drug Discovery*, pp. 273–294. Elsevier.
- Kang, Y., Weber, K. D., Qiu, Y., Kiley, P. J. & Blattner, F. R. (2005).** Genome-wide expression analysis indicates that FNR of *Escherichia coli* K-12 regulates a large number of genes of unknown function. *J Bacteriol* **187**, 1135–1160.
- Kelly, A., Goldberg, M. D., Carroll, R. K., Danino, V., Hinton, J. C. D. & Dorman, C. J. (2004).** A global role for Fis in the transcriptional control of metabolism and type III secretion in *Salmonella enterica* serovar Typhimurium. *Microbiology* **150**, 2037–2053.
- Kenney, L. J. (2018).** The role of acid stress in *Salmonella* pathogenesis. *Curr Opin Microbiol* **47**, 45–51.
- Kidgell, C., Reichard, U., Wain, J., Linz, B., Torpdahl, M., Dougan, G. & Achtman, M. (2002).** *Salmonella* Typhi, the causative agent of Typhoid fever, is approximately 50,000 years old. *Infect Genet Evol* **2**, 39–45.
- Kim, K., Golubeva, Y. A., Vanderpool, C. K. & Slauch, J. M. (2018).** Oxygen-dependent regulation of SPI1 type three secretion system by small RNAs in *Salmonella enterica* serovar Typhimurium. *Mol Microbiol* **147**, e1058–49.
- Knodler, L. A., Bestor, A., Ma, C., Hansen-Wester, I., Hensel, M., Vallance, B. A. & Steele-Mortimer, O. (2005).** Cloning vectors and fluorescent proteins can significantly inhibit *Salmonella enterica* virulence in both epithelial cells and macrophages: implications for bacterial pathogenesis studies. *Infect Immun* **73**, 7027–7031.
- Knodler, L. A., Celli, J., Hardt, W.-D., Vallance, B. A., Yip, C. & Finlay, B. B. (2002).** *Salmonella* effectors within a single pathogenicity island are differentially expressed and translocated by separate type III secretion systems. *Mol Microbiol* **43**, 1089–1103.
- Knodler, L. A., Nair, V. & Steele-Mortimer, O. (2014).** Quantitative assessment of cytosolic *Salmonella* in epithelial cells. *PLoS ONE* **9**, e84681.
- Knuff, K. & Finlay, B. B. (2017).** What the SIF is happening—The role of intracellular *Salmonella*-induced filaments **7**, 3235–3238.
- Körner, H., Sofia, H. J. & Zumft, W. G. (2003).** Phylogeny of the bacterial superfamily of Crp-Fnr transcription regulators: exploiting the metabolic spectrum by controlling alternative gene programs. *FEMS Microbiology Reviews* **27**, 559–592.
- Krieger, V., Liebl, D., Zhang, Y., Rajashekar, R., Chlanda, P., Giesker, K., Chikkaballi, D. & Hensel, M. (2014).** Reorganization of the endosomal system in *Salmonella*-infected cells: the ultrastructure of *Salmonella*-induced tubular compartments. *PLoS Pathog* **10**, e1004374.

- Kronen, M. & Berg, I. A. (2015).** Menaconase/fumarase FumD in *Escherichia coli* O157:H7 and promiscuity of *Escherichia coli* class I fumarases FumA and FumB. *PLoS ONE* **10**, e0145098–18.
- Kröger, C., Colgan, A., Srikumar, S., Händler, K., Sivasankaran, S. K., Hammarlöf, D. L., Canals, R., Grissom, J. E., Conway, T. & other authors. (2013).** An infection-relevant transcriptomic compendium for *Salmonella enterica* serovar Typhimurium. *Cell Host Microbe* **14**, 683–695.
- Kröger, C., Dillon, S. C., Cameron, A. D. S., Papenfort, K., Sivasankaran, S. K., Hokamp, K., Chao, Y., Sittka, A., Hébrard, M. & other authors. (2012).** The transcriptional landscape and small RNAs of *Salmonella enterica* serovar Typhimurium. *PNAS* **109**, e1277–86.
- Kuhle, V. & Hensel, M. (2004).** Cellular microbiology of intracellular *Salmonella enterica*: functions of the type III secretion system encoded by *Salmonella* pathogenicity island 2. *CMLS, Cell Mol Life Sci* **61**, 2812–2826.
- Lambden, P. R. & Guest, J. R. (1976).** Mutants of *Escherichia coli* K12 unable to use fumarate as an anaerobic electron acceptor. *J Gen Microbiol* **97**, 145–160.
- Lawhon, S. D., Maurer, R., Suyemoto, M. & Altier, C. (2002).** Intestinal short-chain fatty acids alter *Salmonella typhimurium* invasion gene expression and virulence through BarA/SirA. *Mol Microbiol* **46**, 1451–1464.
- Lawley, T. D., Bouley, D. M., Hoy, Y. E., Gerke, C., Relman, D. A. & Monack, D. M. (2007).** Host transmission of *Salmonella enterica* serovar Typhimurium is controlled by virulence factors and indigenous intestinal microbiota. *Infect Immun* **76**, 403–416.
- Lee, A. K., Detweiler, C. S. & Falkow, S. (1999).** OmpR regulates the two-component system SsrA-SsrB in *Salmonella* pathogenicity island 2. *J Bacteriol* **182**, 771–781.
- Lee, C. A. & Falkow, S. (1990).** The ability of *Salmonella* to enter mammalian cells is affected by bacterial growth state. *PNAS* **87**, 4304–4308.
- Lee, C. A., Jones, B. D. & Falkow, S. (1992).** Identification of a *Salmonella typhimurium* invasion locus by selection for hyperinvasive mutants. *PNAS* **89**, 1847–1851.
- Lee, E.-J. & Groisman, E. A. (2012).** Control of a *Salmonella* virulence locus by an ATP-sensing leader messenger RNA. *Nature* **486**, 271–275.
- Leif, H., Sled, V. D., Ohnishi, T., Weiss, H. & Friedrich, T. (1995).** Isolation and characterization of the proton-translocating NADH:ubiquinone oxidoreductase from *Escherichia coli*. *Eur J Biochem* **230**, 538–548.
- Lennox, E. S. (1955).** Transduction of linked genetic characters of the host by bacteriophage P1. *Virology* **1**, 190–206.

- Lévi-Meyrueis, C., Monteil, V., Sismeiro, O., Dillies, M.-A., Monot, M., Jagla, B., Coppée, J.-Y., Dupuy, B. & Norel, F. (2014). Expanding the RpoS/ σ S-network by RNA sequencing and identification of σ S-controlled small RNAs in *Salmonella*. *PLoS ONE* **9**, e96918–12 (R. Manganelli, Ed.).
- Lhocine, N., Arena, E. T., Bomme, P., Ubelmann, F., Prévost, M.-C., Robine, S. & Sansonetti, P. J. (2015). Apical invasion of intestinal epithelial cells by *Salmonella* Typhimurium requires villin to remodel the brush border actin cytoskeleton **17**, 164–177.
- Li, H. & Durbin, R. (2009). Fast and accurate short read alignment with Burrows-Wheeler transform. *Bioinformatics* **25**, 1754–1760.
- Li, H., Handsaker, B., Wysoker, A., Fennell, T., Ruan, J., Homer, N., Marth, G., Abecasis, G., Durbin, R. 1000 Genome Project Data Processing Subgroup. (2009). The sequence alignment/map format and SAMtools. *Bioinformatics* **25**, 2078–2079.
- Lim, S., Kim, B., Choi, H.-S., Lee, Y. & Ryu, S. (2006). Fis is required for proper regulation of *ssaG* expression in *Salmonella enterica* serovar Typhimurium. *Microb Pathog* **41**, 33–42.
- Liu, Y., Chen, H., Kenney, L. J. & Yan, J. (2010). A divalent switch drives H-NS/DNA-binding conformations between stiffening and bridging modes. *Genes Dev* **24**, 339–344.
- Löber, S., Jäckel, D., Kaiser, N. & Hensel, M. (2006). Regulation of *Salmonella* pathogenicity island 2 genes by independent environmental signals. *Int J Med Microbiol* **296**, 435–447.
- Lucas, R. L. & Lee, C. A. (2001). Roles of *hilC* and *hilD* in regulation of *hilA* expression in *Salmonella enterica* serovar Typhimurium. *J Bacteriol* **183**, 2733–2745.
- Lucchini, S., Rowley, G., Goldberg, M. D., Hurd, D., Harrison, M. & Hinton, J. C. D. (2006). H-NS mediates the silencing of laterally acquired genes in bacteria. *PLoS Pathog* **2**, e81.
- Machanick, P. & Bailey, T. L. (2011). MEME-ChIP: motif analysis of large DNA datasets. *Bioinformatics* **27**, 1696–1697.
- Main-Hester, K. L., Colpitts, K. M., Thomas, G. A., Fang, F. C. & Libby, S. J. (2008). Coordinate regulation of *Salmonella* pathogenicity island 1 (SPI1) and SPI4 in *Salmonella enterica* serovar Typhimurium. *Infect Immun* **76**, 1024–1035.
- Majowicz, S. E., Musto, J., Scallan, E., Angulo, F. J., Kirk, M., O'Brien, S. J., Jones, T. F., Fazil, A., Hoekstra, R. M. International Collaboration on Enteric Disease 'Burden of Illness' Studies. (2010). The global burden of nontyphoidal *Salmonella* gastroenteritis. *Clin Infect Dis* **50**, 882–889.

- Mangan, M. W., Lucchini, S., Ó Cróinín, T., Fitzgerald, S., Hinton, J. C. D. & Dorman, C. J. (2011).** Nucleoid-associated protein HU controls three regulons that coordinate virulence, response to stress and general physiology in *Salmonella enterica* serovar Typhimurium. *Microbiology* **157**, 1075–1087.
- Mangan, M. W., Lucchini, S., Danino, V., Ó Cróinín, T., Hinton, J. C. D. & Dorman, C. J. (2006).** The integration host factor (IHF) integrates stationary-phase and virulence gene expression in *Salmonella enterica* serovar Typhimurium. *Mol Microbiol* **59**, 1831–1847.
- Marcus, S. L., Brumell, J. H., Pfeifer, C. G. & Finlay, B. B. (2000).** *Salmonella* pathogenicity islands: big virulence in small packages. *Microbes and Infection* **2**, 145–156.
- Marouga, R., David, S. & Hawkins, E. (2005).** The development of the DIGE system: 2D fluorescence difference gel analysis technology. *Anal Bioanal Chem* **382**, 669–678.
- Marteyn, B., Scorza, F. B., Sansonetti, P. J. & Tang, C. (2011).** Breathing life into pathogens: the influence of oxygen on bacterial virulence and host responses in the gastrointestinal tract. *Cell Microbiol* **13**, 171–176.
- Marteyn, B., West, N. P., Browning, D. F., Cole, J. A., Shaw, J. G., Palm, F., Mounier, J., Prévost, M.-C., Sansonetti, P. & Tang, C. M. (2010).** Modulation of *Shigella* virulence in response to available oxygen *in vivo*. *Nature* **465**, 355–358.
- Martinez, L. C., Banda, M. M., Fernandez-Mora, M., Santana, F. J. & Bustamante, V. H. (2014).** HilD induces expression of *Salmonella* pathogenicity island 2 genes by displacing the global negative regulator H-NS from *ssrAB*. *J Bacteriol* **196**, 3746–3755.
- Martínez, L. C., Yakhnin, H., Camacho, M. I., Georgellis, D., Babitzke, P., Puente, J. L. & Bustamante, V. H. (2011).** Integration of a complex regulatory cascade involving the SirA/BarA and Csr global regulatory systems that controls expression of the *Salmonella* SPI-1 and SPI-2 virulence regulons through HilD **80**, 1637–1656.
- McClelland, M., Sanderson, K. E., Clifton, S. W., Latreille, P., Porwollik, S., Sabo, A., Meyer, R., Bieri, T., Ozersky, P. & other authors. (2004).** Comparison of genome degradation in Paratyphi A and Typhi, human-restricted serovars of *Salmonella enterica* that cause typhoid. *Nat Genet* **36**, 1268–1274.
- Melville, S. B. & Gunsalus, R. P. (1996).** Isolation of an oxygen-sensitive FNR protein of *Escherichia coli*: interaction at activator and repressor sites of FNR-controlled genes. *PNAS* **93**, 1226–1231.
- Meng, W., Green, J. & Guest, J. R. (1997).** FNR-dependent repression of *ndh* gene expression requires two upstream FNR-binding sites. *Microbiology* **143**, 1521–1532.

- Mettert, E. L. & Kiley, P. J. (2007a).** Contributions of [4Fe-4S]-FNR and Integration Host Factor to *fnr* Transcriptional Regulation. *J Bacteriol* **189**, 3036–3043.
- Mettert, E. L. & Kiley, P. J. (2007b).** Contributions of [4Fe-4S]-FNR and Integration Host Factor to *fnr* Transcriptional Regulation. *J Bacteriol* **189**, 3036–3043.
- Mills, P. C., Rowley, G., Spiro, S., Hinton, J. C. D. & Richardson, D. J. (2008).** A combination of cytochrome c nitrite reductase (NrfA) and flavorubredoxin (NorV) protects *Salmonella enterica* serovar Typhimurium against killing by NO in anoxic environments. *Microbiology* **154**, 1218–1228.
- Miranda-CasoLuengo, A. A., Kary, S. C., Erhardt, M. & Kröger, C. (2017).** Small RNA, big effect: Control of flagellin production. *Trends in Microbiology* 1–2.
- Miyakoshi, M. (2019).** RNA-mediated crosstalk between bacterial core genome and foreign genetic elements. In *DNA Traffic in the Environment*, pp. 77–94.
- Morgan, E., Campbell, J. D., Rowe, S. C., Bispham, J., Stevens, M. P., Bowen, A. J., Barrow, P. A., Maskell, D. J. & Wallis, T. S. (2004).** Identification of host-specific colonization factors of *Salmonella enterica* serovar Typhimurium. *Mol Microbiol* **54**, 994–1010.
- Mortazavi, A., Williams, B. A., McCue, K., Schaeffer, L. & Wold, B. (2008).** Mapping and quantifying mammalian transcriptomes by RNA-Seq. *Nature Publishing Group* **5**, 621–628.
- Mulder, D. T., McPhee, J. B., Reid-Yu, S. A., Stogios, P. J., Savchenko, A. & Coombes, B. K. (2015).** Multiple histidines in the periplasmic domain of the *Salmonella enterica* sensor kinase SsrA enhance signaling in response to extracellular acidification. *Mol Microbiol* **95**, 678–691.
- Murphy, K. C. (1998).** Use of bacteriophage λ recombination functions to promote gene replacement in *Escherichia coli*. *J Bacteriol* **180**, 2063–2071.
- Murray, P. R., Rosenthal, K. S. & Pfaller, M. A. (2015).** *Medical Microbiology*.
- Myers, K. S., Park, D. M., Beauchene, N. A. & Kiley, P. J. (2015).** Defining bacterial regulons using ChIP-seq. *Methods* **86**, 80–88.
- Myers, K. S., Yan, H., Ong, I. M., Chung, D., Liang, K., Tran, F., Keleş, S., Landick, R. & Kiley, P. J. (2013).** Genome-scale analysis of *Escherichia coli* FNR reveals complex features of transcription factor binding **9**, e1003565–24.
- Nakato, R. & Shirahige, K. (2017).** Recent advances in ChIP-seq analysis: from quality management to whole-genome annotation. *Brief Bioinformatics* **18**, 279–290.
- Navarre, W. W., Halsey, T. A., Walthers, D., Frye, J., McClelland, M., Potter, J. L., Kenney, L. J., Gunn, J. S., Fang, F. C. & Libby, S. J. (2005).** Co-regulation of

- Salmonella enterica* genes required for virulence and resistance to antimicrobial peptides by SlyA and PhoP/PhoQ. *Mol Microbiol* **56**, 492–508.
- Navarre, W. W., Porwollik, S., Wang, Y., McClelland, M., Rosen, H., Libby, S. J. & Fang, F. C. (2006).** Selective silencing of foreign DNA with low GC content by the H-NS protein in *Salmonella*. *Science* **313**, 236–238.
- Neidhart, F. C. E. (1996).** *Escherichia coli and Salmonella*, 2nd edn. Oxford, UK: Blackwell Science Ltd.
- Nicol, J. W., Helt, G. A., Blanchard, S. G., Raja, A. & Loraine, A. E. (2009).** The Integrated Genome Browser: free software for distribution and exploration of genome-scale datasets. *Bioinformatics* **25**, 2730–2731.
- Niehaus, F., Hantke, K. & Unden, G. (1991).** Iron content and FNR-dependent gene regulation in *Escherichia coli*. *FEMS Microbiology Letters* **68**, 319–323.
- Norte, V. A., Stapleton, M. R. & Green, J. (2003).** PhoP-responsive expression of the *Salmonella enterica* serovar Typhimurium *slyA* Gene. *J Bacteriol* **185**, 3508–3514.
- Ochman, H., Soncini, F. C., Solomon, F. & Groisman, E. A. (1996).** Identification of a pathogenicity island required for *Salmonella* survival in host cells. *PNAS* **93**, 7800–7804. National Academy of Sciences.
- Ohl, M. E. & Miller, S. I. (2001).** *Salmonella*: a model for bacterial pathogenesis. *Annu Rev Med* **52**, 259–274.
- Okada, N., Oi, Y., Takeda-Shitaka, M., Kanou, K., Umeyama, H., Haneda, T., Miki, T., Hosoya, S. & Danbara, H. (2007).** Identification of amino acid residues of *Salmonella* SlyA that are critical for transcriptional regulation. *Microbiology* **153**, 548–560.
- Ono, S., Goldberg, M. D., Olsson, T., Esposito, D., Hinton, J. C. D. & Ladbury, J. E. (2005).** H-NS is a part of a thermally controlled mechanism for bacterial gene regulation. *Biochem J* **391**, 203.
- Osborne, S. E. & Coombes, B. K. (2011).** Transcriptional priming of *Salmonella* pathogenicity island-2 precedes cellular invasion. *PLoS ONE* **6**, e21648–8. Public Library of Science.
- Osborne, S. E., Walthers, D., Tomljenovic, A. M., Mulder, D. T., Silphaduang, U., Duong, N., Lowden, M. J., Wickham, M. E., Waller, R. F. & other authors. (2009).** Pathogenic adaptation of intracellular bacteria by rewiring a cis-regulatory input function. *PNAS* **106**, 3982–3987. National Academy of Sciences.
- Ozsolak, F. & Milos, P. M. (2010).** RNA sequencing: advances, challenges and opportunities. *Nature Rev* **12**, 87–98.

- Padalon-Brauch, G., Hershberg, R., Elgrably-Weiss, M., Baruch, K., Rosenshine, I., Margalit, H. & Altuvia, S. (2008).** Small RNAs encoded within genetic islands of *Salmonella typhimurium* show host-induced expression and role in virulence. *Nucleic Acids Res* **36**, 1913–1927.
- Papanikolaou, N., Trachana, K., Theodosiou, T., Promponas, V. J. & Iliopoulos, I. (2009).** Gene socialization: gene order, GC content and gene silencing in *Salmonella*. *BMC Genomics* **10**, 597.
- Pardo-Esté, C., Hidalgo, A. A., Aguirre, C., Briones, A. C., Cabezas, C. E., Castro-Severyn, J., Fuentes, J. A., Opazo, C. M., Riedel, C. A. & other authors. (2018).** The ArcAB two-component regulatory system promotes resistance to reactive oxygen species and systemic infection by *Salmonella Typhimurium*. *PLoS ONE* **13**, e0203497–20
- Park, D. M., Akhtar, M. S., Ansari, A. Z., Landick, R. & Kiley, P. J. (2013).** The bacterial response regulator ArcA uses a diverse binding site architecture to regulate carbon oxidation globally. *PLoS Genet* **9**, e1003839.
- Park, S.-Y., Pontes, M. H. & Groisman, E. A. (2015).** Flagella-independent surface motility in *Salmonella enterica* serovar Typhimurium. *PNAS* **112**, 1850–1855.
- Parker, C. T. & Guard-Petter, J. (2001).** Contribution of flagella and invasion proteins to pathogenesis of *Salmonella enterica* serovar enteritidis in chicks. *FEMS Microbiology Letters* **204**, 287–291.
- Partridge, J. D., Sanguinetti, G., Dibden, D. P., Roberts, R. E., Poole, R. K. & Green, J. (2007).** Transition of *Escherichia coli* from aerobic to micro-aerobic conditions involves fast and slow reacting regulatory components. *J Biol Chem* **282**, 11230–11237.
- Passaris, I., Cambré, A., Govers, S. K. & Aertsen, A. (2018).** Bimodal expression of the *Salmonella Typhimurium spv* operon. *Genetics* **210**, 621–635.
- Perez-Sepulveda, B. M. & Hinton, J. C. D. (2018).** Functional transcriptomics for bacterial gene detectives. *Microbiology Spectrum* **6**, 1–13.
- Perrett, C. A. & Zhou, D. (2013).** *Salmonella* type III effector SopB modulates host cell exocytosis. *Emerg Microbes Infect* **2**, e32.
- Popoff, M. Y., Bockemühl, J. & Gheesling, L. L. (2004).** Supplement 2002 (no. 46) to the Kauffmann–White scheme. *Research in Microbiology* **155**, 568–570.
- Price, C. E. & Driessen, A. J. M. (2010).** Conserved negative charges in the transmembrane segments of subunit K of the NADH:Ubiquinone oxidoreductase determine its dependence on YidC for membrane insertion. *J Biol Chem* **285**, 3575–3581.

- Price-Carter, M., Tingey, J., Bobik, T. A. & Roth, J. R. (2001).** The alternative electron acceptor tetrathionate supports B12-dependent anaerobic growth of *Salmonella enterica* serovar Typhimurium on ethanolamine or 1,2-propanediol. *J Bacteriol* **183**, 2463–2475.
- Quackenbush, J. (2002).** Microarray data normalization and transformation. *Nat Genet* **32**, 496–501.
- R Core Team. (2013).** R: A language and environment for statistical computing. Vienna, Austria: R Foundation for Statistical Computing.
- Ramírez, F., Ryan, D. P., Grüning, B., Bhardwaj, V., Kilpert, F., Richter, A. S., Heyne, S., Dündar, F. & Manke, T. (2016).** deepTools2: a next generation web server for deep-sequencing data analysis. *Nucleic Acids Res* **44**, W160–W165.
- Rathman, M., Barker, L. P. & Falkow, S. (1997).** The unique trafficking pattern of *Salmonella* typhimurium-containing phagosomes in murine macrophages is independent of the mechanism of bacterial entry. *Infect Immun* **65**, 1475–1485.
- Reeves, M. W., Evins, G. M., clinical, A. H. J. O.1989. (1999).** Clonal nature of *Salmonella typhi* and its genetic relatedness to other *Salmonellae* as shown by multilocus enzyme electrophoresis, and proposal of *Salmonella bongori* comb. nov. *J Bacteriol.* **27**, 313–320
- Rhen, M. & Dorman, C. J. (2005).** Hierarchical gene regulators adapt *Salmonella enterica* to its host milieu. *Int J Med Microbiol* **294**, 487–502.
- Rice, C. J., Ramachandran, V. K., Shearer, N. & Thompson, A. (2015).** Transcriptional and post-transcriptional modulation of SPI1 and SPI2 expression by ppGpp, RpoS and DksA in *Salmonella enterica* sv Typhimurium. *PLoS ONE* **10**, e0127523.
- Richardson, D. J., Berks, B. C., Russell, D. A., Spiro, S. & Taylor, C. J. (2001).** Functional, biochemical and genetic diversity of prokaryotic nitrate reductases. *CMLS, Cell Mol Life Sci* **58**, 165–178.
- Richardson, E. J., Limaye, B., Inamdar, H., Datta, A., Manjari, K. S., Pullinger, G. D., Thomson, N. R., Joshi, R. R., Watson, M. & Stevens, M. P. (2011).** Genome sequences of *Salmonella enterica* serovar Typhimurium, Choleraesuis, Dublin, and Gallinarum strains of well-defined virulence in food-producing animals. *J Bacteriol* **193**, 3162–3163.
- Rigottier-Gois, L. (2013).** Dysbiosis in inflammatory bowel diseases: the oxygen hypothesis. *The ISME Journal* **7**, 1256–1261.
- Rivera-Chávez, F. & Bäuml, A. J. (2015).** The pyromaniac inside you: *Salmonella* metabolism in the host gut. *Annu Rev Microbiol* **69**, 31–48.

- Rivera-Chávez, F., Winter, S. E., Lopez, C. A., Xavier, M. N., Winter, M. G., Nuccio, S.-P., Russell, J. M., Laughlin, R. C., Lawhon, S. D. & other authors. (2013). *Salmonella* uses energy taxis to benefit from intestinal inflammation. *PLoS Pathog* **9**, e1003267.
- Rollenhagen, C. & Bumann, D. (2006). *Salmonella enterica* highly expressed genes are disease specific. *Infect Immun* **74**, 1649–1660.
- Rosenberg, S. L. (1980). Fermentation of pentose sugars to ethanol and other neutral products by microorganisms. *Enzyme and Microbial Technology* **2**, 185–193.
- Ryan, D., Mukherjee, M. & Suar, M. (2017). The expanding targetome of small RNAs in *Salmonella* Typhimurium. *Biochimie* 1–38.
- Sabbagh, S. C., Forest, C. G., Lepage, C., Leclerc, J.-M. & Daigle, F. (2010). So similar, yet so different: uncovering distinctive features in the genomes of *Salmonella enterica* serovars Typhimurium and Typhi. *FEMS Microbiology Letters* **305**, 1–13.
- Salmon, K., Hung, S.-P., Mekjian, K., Baldi, P., Hatfield, G. W. & Gunsalus, R. P. (2003). Global gene expression profiling in *Escherichia coli* K12. The effects of oxygen availability and FNR. *J Biol Chem* **278**, 29837–29855.
- Santos, R. L., Raffatellu, M., Bevins, C. L., Adams, L. G., Tükel, Ç., Tsolis, R. M. & Bäumlér, A. J. (2009). Life in the inflamed intestine, *Salmonella* style. *Trends in Microbiology* **17**, 498–506.
- Sawers, G. (1999). The aerobic/anaerobic interface. *Curr Opin Microbiol* **2**, 181–187.
- Sawers, G., Kaiser, M., Sirko, A. & Freundlich, M. (1997). Transcriptional activation by FNR and CRP: reciprocity of binding-site recognition. *Mol Microbiol* **23**, 835–845.
- Scallan, E., Hoekstra, R. M., Angulo, F. J., Tauxe, R. V., Widdowson, M.-A., Roy, S. L., Jones, J. L. & Griffin, P. M. (2011). Foodborne illness acquired in the United States—Major pathogens. *Emerging Infect Dis* **17**, 7–15.
- Schiemann, D. A. & Shope, S. R. (1991). Anaerobic growth of *Salmonella* typhimurium results in increased uptake by Henle 407 epithelial and mouse peritoneal cells *in vitro* and repression of a major outer membrane protein. *Infect Immun* **59**, 437–440.
- Schmidt, D., Wilson, M. D., Spyrou, C., Brown, G. D., Hadfield, J. & Odom, D. T. (2009). ChIP-seq: using high-throughput sequencing to discover protein-DNA interactions. *Methods* **48**, 240–248.
- Schneider, C. A., Rasband, W. S. & Eliceiri, K. W. (2012). NIH Image to ImageJ: 25 years of image analysis. *Nat Meth* **9**, 671–675.
- Scott, C., Partridge, J. D., Stephenson, J. R. & Green, J. (2003). DNA target sequence and FNR-dependent gene expression. *FEBS Lett* **541**, 97–101.

- Sengupta, A. & Bhadauria, S. (2014).** Exploration of multi-objective tradeoff during high level synthesis using bacterial chemotaxis and dispersal. *Procedia - Procedia Computer Science* **35**, 63–72.
- Shalel Levanon, S., San, K.-Y. & Bennett, G. N. (2005).** Effect of oxygen on the *Escherichia coli* ArcA and FNR regulation systems and metabolic responses. *Biotechnol Bioeng* **89**, 556–564.
- Shan, Y., Lai, Y. & Yan, A. (2012a).** Metabolic reprogramming under microaerobic and anaerobic conditions in bacteria. In *Reprogramming Microbial Metabolic Pathways*, Subcellular Biochemistry, pp. 159–179. Edited by X. Wang, J. Chen & P. Quinn. Dordrecht: Springer Netherlands.
- Shan, Y., Pan, Q., Liu, J., Huang, F., Sun, H., Nishino, K. & Yan, A. (2012b).** Covalently linking the *Escherichia coli* global anaerobic regulator FNR in tandem allows it to function as an oxygen stable dimer. *Biochemical and Biophysical Research Communications* **419**, 43–48.
- Sharma, C. M., Darfeuille, F., Plantinga, T. H. & Vogel, J. (2007).** A small RNA regulates multiple ABC transporter mRNAs by targeting C/A-rich elements inside and upstream of ribosome-binding sites. *Genes & Development* **21**, 2804–2817.
- Sharma, C. M., Papenfort, K., Pernitzsch, S. R., Mollenkopf, H.-J., Hinton, J. C. D. & Vogel, J. (2011).** Pervasive post-transcriptional control of genes involved in amino acid metabolism by the Hfq-dependent GcvB small RNA. *Mol Microbiol* **81**, 1144–1165.
- Shaw, D. J., Rice, D. W. & Guest, J. R. (1983).** Homology between CAP and Fnr, a regulator of anaerobic respiration in *Escherichia coli*. **166**, 241–247.
- Shi, Y., Latifi, T., Cromie, M. J. & Groisman, E. A. (2004).** Transcriptional control of the antimicrobial peptide resistance *ugtL* gene by the *Salmonella* PhoP and SlyA regulatory proteins. *J Biol Chem* **279**, 38618–38625.
- Shivak, D. J., MacKenzie, K. D., Watson, N. L., Pasternak, J. A., Jones, B. D., Wang, Y., DeVinney, R., Wilson, H. L., Surette, M. G. & White, A. P. (2016).** A modular, Tn 7-based system for making bioluminescent or fluorescent *Salmonella* and *Escherichia coli* strains. *Appl Environ Microb* **82**, 4931–4943.
- Silphaduang, U., Mascarenhas, M., Karmali, M. & Coombes, B. K. (2007).** Repression of intracellular virulence factors in *Salmonella* by the Hha and YdgT nucleoid-associated proteins. *J Bacteriol* **189**, 3669–3673.
- Singh, R. D., Khullar, M. & Ganguly, N. K. (2000).** Role of anaerobiosis in virulence of *Salmonella* Typhimurium. *Mol Cell Biochem* **215**, 39–46.

- Six, S., Andrews, S. C., Unden, G. & Guest, J. R. (1994).** *Escherichia coli* possesses two homologous anaerobic C4-dicarboxylate membrane transporters (DcuA and DcuB) distinct from the aerobic dicarboxylate transport system (Dct). *J Bacteriol* **176**, 6470–6478.
- Skinner, M. E., Uzilov, A. V., Stein, L. D., Mungall, C. J. & Holmes, I. H. (2009).** JBrowse: A next-generation genome browser. *Genome Research* **19**, 1630–1638.
- Smith, H. O. & Levine, M. (1967).** A phage P22 gene controlling integration of prophage. *Virology* **31**, 207–216.
- Solórzano, C., Srikumar, S., Canals, R., Juárez, A., Paytubi, S. & Madrid, C. (2015).** Hha has a defined regulatory role that is not dependent upon H-NS or StpA **6**, 13356–13314.
- Spiro, S. & Guest, J. R. (1987).** Regulation and over-expression of the *fnr* gene of *Escherichia coli*. *Microbiology* **133**, 3279–3288.
- Spiro, S. & Guest, J. R. (1990).** FNR and its role in oxygen-regulated gene expression in *Escherichia coli*. *FEMS Microbiology Reviews* **6**, 399–428.
- Sridhar, S. & Steele-Mortimer, O. (2016).** Inherent variability of growth media impacts the ability of *Salmonella* Typhimurium to interact with host cells. *PLoS ONE* **11**, e0157043–14.
- Srikanth, C. V., Mercado-Lubo, R., Hallstrom, K. & McCormick, B. A. (2011).** *Salmonella* effector proteins and host-cell responses. *CMLS, Cell Mol Life Sci* **68**, 3687–3697.
- Srikumar, S., Kröger, C., Hébrard, M., Colgan, A., Owen, S. V., Sivasankaran, S. K., Cameron, A. D. S., Hokamp, K. & Hinton, J. C. D. (2015).** RNA-seq brings new insights to the intra-macrophage transcriptome of *Salmonella* Typhimurium. *PLoS Pathog* **11**, e1005262–26.
- Stapleton, M. R., Norte, V. A., Read, R. C. & Green, J. (2002).** Interaction of the *Salmonella* Typhimurium transcription and virulence factor SlyA with target DNA and identification of members of the SlyA regulon. *J Biol Chem* **277**, 17630–17637.
- Stark, R. & Brown, G. (2011).** DiffBind: differential binding analysis of ChIP-Seq peak data. *bioconductorstatistiku-dortmundde*.
- Stecher, B., Barthel, M., Schlumberger, M. C., Haberli, L., Rabsch, W., Kremer, M. & Hardt, W.-D. (2008).** Motility allows *S. Typhimurium* to benefit from the mucosal defence. *Cell Microbiol* **10**, 1166–1180.
- Steele-Mortimer, O. (2008).** The *Salmonella*-containing vacuole—Moving with the times **11**, 38–45.

- Stevens, M. P., Humphrey, T. J. & Maskell, D. J. (2009).** Molecular insights into farm animal and zoonotic *Salmonella* infections. *Phil Trans R Soc B* **364**, 2709–2723.
- Stewart, V., Bledsoe, P. J., Chen, L.-L. & Cai, A. (2009).** Catabolite repression control of *napF* (periplasmic nitrate reductase) operon expression in *Escherichia coli* K-12. *J Bacteriol* **191**, 996–1005.
- Stewart, V., Chen, L.-L. & Wu, H.-C. (2003).** Response to culture aeration mediated by the nitrate and nitrite sensor NarQ of *Escherichia coli* K-12. *Mol Microbiol* **50**, 1391–1399. John Wiley & Sons, Ltd (10.1111).
- Stormo, G. D. & Zhao, Y. (2010).** Determining the specificity of protein–DNA interactions. *Nature Rev Genet* **11**, 751–760.
- Sturm, A., Heinemann, M., Arnoldini, M., Benecke, A., Ackermann, M., Benz, M., Dormann, J. & Hardt, W.-D. (2011).** The cost of virulence: retarded growth of *Salmonella* Typhimurium cells expressing type III secretion system 1. *PLoS Pathog* **7**, e1002143.
- Sutton, V. R., Stubna, A., Patschkowski, T., Münck, E., Beinert, H. & Kiley, P. J. (2004).** Superoxide destroys the [2Fe-2S] 2^+ cluster of FNR from *Escherichia coli*. *Biochemistry* **43**, 791–798.
- Tahoun, A., Mahajan, S., Paxton, E., Malterer, G., Donaldson, D. S., Wang, D., Tan, A., Gillespie, T. L., O’Shea, M. & other authors. (2012).** *Salmonella* transforms follicle-associated epithelial cells into M cells to promote intestinal invasion. *Cell Host Microbe* **12**, 645–656.
- Takaya, A., Takeda, H., Tashiro, S., Kawashima, H. & Yamamoto, T. (2019).** Chaperone-mediated secretion switching from early to middle substrates in the type III secretion system encoded by *Salmonella* pathogenicity island 2. *J Biol Chem* **294**, 3783–3793.
- Thauer, R. K., Jungermann, K. & Decker, K. (1977).** Energy conservation in chemotrophic anaerobic bacteria. *Bacteriol Rev* **41**, 100–180.
- The UniProt Consortium. (2017).** UniProt: the universal protein knowledgebase. *Nucleic Acids Res* **45**, D158–D169.
- Thiennimitr, P., Winter, S. E., Winter, M. G., Xavier, M. N., Tolstikov, V., Huseby, D. L., Sterzenbach, T., Tsolis, R. M., Roth, J. R. & Bäumler, A. J. (2011).** Intestinal inflammation allows *Salmonella* to use ethanolamine to compete with the microbiota. *PNAS* **108**, 17480–17485.
- Thiennimitr, P., Winter, S. E. & Bäumler, A. J. (2012).** *Salmonella*, the host and its microbiota **15**, 108–114.

- Thijs, I. M. V., De Keersmaecker, S. C. J., Fadda, A., Engelen, K., Zhao, H., McClelland, M., Marchal, K. & Vanderleyden, J. (2007).** Delineation of the *Salmonella enterica* serovar Typhimurium HilA regulon through genome-wide location and transcript analysis. *J Bacteriol* **189**, 4587–4596.
- Thompson, A., Rowley, G., Alston, M., Danino, V. & Hinton, J. C. (2006).** *Salmonella* transcriptomics: relating regulons, stimulons and regulatory networks to the process of infection. *Curr Opin Microbiol* **9**, 109–116.
- Troxell, B., Fink, R. C., Porwollik, S., McClelland, M. & Hassan, H. M. (2011).** The Fur regulon in anaerobically grown *Salmonella enterica* sv. Typhimurium: identification of new Fur targets. *BMC Microbiology* **11**, 236. BioMed Central Ltd.
- Tseng, C. P., Albrecht, J. & Gunsalus, R. P. (1996).** Effect of microaerophilic cell growth conditions on expression of the aerobic (*cyoABCDE* and *cydAB*) and anaerobic (*narGHJI*, *frdABCD*, and *dmsABC*) respiratory pathway genes in *Escherichia coli*. *J Bacteriol* **178**, 1094–1098.
- Tukel, C., Akcelik, M., de Jong, M. F., Simsek, O., Tsolis, R. M. & Bäumlner, A. J. (2007).** MarT Activates Expression of the MisL Autotransporter Protein of *Salmonella enterica* Serotype Typhimurium. *J Bacteriol* **189**, 3922–3926.
- Uden, G. & Bongaerts, J. (1997).** Alternative respiratory pathways of *Escherichia coli*: energetics and transcriptional regulation in response to electron acceptors. *Biochim Biophys Acta* **1320**, 217–234.
- van Asten, A. J. A. M. & van Dijk, J. E. (2005).** Distribution of ‘classic’ virulence factors among *Salmonella* spp. *FEMS Immunol Med Microbiol* **44**, 251–259.
- van der Heijden, J., Bosman, E. S., Reynolds, L. A. & Finlay, B. B. (2015).** Direct measurement of oxidative and nitrosative stress dynamics in *Salmonella* inside macrophages. *PNAS* **112**, 560–565.
- Van Dyk, T. K. & Rosson, R. A. (1998).** *Photobacterium luminescens luxCDABE* promoter probe vectors. In *Bioluminescence Methods and Protocols*, pp. 85–95. New Jersey: Humana Press.
- Vazquez-Torres, A & Fang, F. C. (2001).** Oxygen-dependent anti-*Salmonella* activity of macrophages. *Trends Microbiol* **9**, 29–33.
- Vergara-Irigaray, M., Fookes, M. C., Thomson, N. R. & Tang, C. M. (2014).** RNA-seq analysis of the influence of anaerobiosis and FNR on *Shigella flexneri*. *BMC Genomics* **15**, 438–22.
- Vijay-Kumar, M. & Gewirtz, A. T. (2009).** Flagellin: key target of mucosal innate immunity. *Mucosal Immunol* **2**, 197–205.

- Vogel, J. (2009).** A rough guide to the non-coding RNA world of *Salmonella*. *Mol Microbiol* **71**, 1–11.
- Vonaesch, P., Sellin, M. E., Cardini, S., Singh, V., Barthel, M. & Hardt, W.-D. (2014).** The *Salmonella* Typhimurium effector protein SopE transiently localizes to the early SCV and contributes to intracellular replication. *Cell Microbiol* **16**, 1723–1735.
- Wagner, C. & Hensel, M. (2011).** Adhesive mechanisms of *Salmonella enterica*. In *Bacterial Adhesion*, Advances in Experimental Medicine and Biology, pp. 17–34. Edited by D. Linke & A. Goldman. Dordrecht: Springer Netherlands.
- Wagner, G. P., Kin, K. & Lynch, V. J. (2012).** Measurement of mRNA abundance using RNA-seq data: RPKM measure is inconsistent among samples. *Theory Biosci* **131**, 281–285.
- Wagner, G. P., Kin, K. & Lynch, V. J. (2013).** A model based criterion for gene expression calls using RNA-seq data. *Theory Biosci* **132**, 159–164.
- Walthers, D., Carroll, R. K., Navarre, W. W., Libby, S. J., Fang, F. C. & Kenney, L. J. (2007).** The response regulator SsrB activates expression of diverse *Salmonella* pathogenicity island 2 promoters and counters silencing by the nucleoid-associated protein H-NS. *Mol Microbiol* **65**, 477–493.
- Walthers, D., Li, Y., Liu, Y., Anand, G., Yan, J. & Kenney, L. J. (2011).** *Salmonella enterica* response regulator SsrB relieves H-NS silencing by displacing H-NS bound in polymerization mode and directly activates transcription. *Journal of Biol Chem* **286**, 1895–1902.
- Wang, Q., Zhao, Y., McClelland, M. & Harshey, R. M. (2007).** The RcsCDB signaling system and swarming motility in *Salmonella enterica* serovar Typhimurium: Dual regulation of flagellar and SPI-2 virulence genes. *J Bacteriol* **189**, 8447–8457.
- Wang, Z., Sun, J., Tian, M., Xu, Z., Liu, Y., Fu, J., Yan, A. & Liu, X. (2019).** Proteomic analysis of FNR-regulated anaerobiosis in *Salmonella* Typhimurium. *J Am Soc Mass Spectrom*.
- Westermann, A. J., Förstner, K. U., Amman, F., Barquist, L., Chao, Y., Schulte, L. N., Müller, L., Reinhardt, R., Stadler, P. F. & Vogel, J. (2016).** Dual RNA-seq unveils noncoding RNA functions in host–pathogen interactions. *Nature* **529**, 496–501.
- Westermann, A. J. & Vogel, J. (2018).** Host-pathogen transcriptomics by dual RNA-seq. In *Bacterial Regulatory RNA*, Methods in Molecular Biology, pp. 59–75. Edited by V. Arluison & C. Valverde. New York, NY: Springer New York.

- Williams, S. M., Wing, H. J. & Busby, S. J. (1998).** Repression of transcription initiation by *Escherichia coli* FNR protein: repression by FNR can be simple. *FEMS Microbiology Letters* **163**, 203–208.
- Winardhi, R. S., Yan, J. & Kenney, L. J. (2015).** H-NS regulates gene expression and compacts the nucleoid: Insights from single-molecule experiments. *Biophysj* **109**, 1321–1329.
- Wing, H. J., Williams, S. M. & Busby, S. J. (1995).** Spacing requirements for transcription activation by *Escherichia coli* FNR protein. *J Bacteriol* **177**, 6704–6710.
- Winter, S. E., Lopez, C. A. & Bäuml, A. J. (2013).** The dynamics of gut-associated microbial communities during inflammation. *EMBO Rep* **14**, 319–327.
- Winter, S. E., Thiennimitr, P., Winter, M. G., Butler, B. P., Huseby, D. L., Crawford, R. W., Russell, J. M., Bevins, C. L., Adams, L. G. & other authors. (2010).** Gut inflammation provides a respiratory electron acceptor for *Salmonella*. *Nature* **467**, 426–429.
- Wiser, M. J. & Lenski, R. E. (2015).** A comparison of methods to measure fitness in *Escherichia coli*. *PLoS ONE* **10**, e0126210–11.
- Wisner, A., Desin, T., White, A., Potter, A. & Kster, W. (2012).** The *Salmonella* pathogenicity island-1 and -2 encoded type III secretion systems. In *Salmonella - A Diversified Superbug*. InTechOpen.
- Woods, S. A., Schwartzbach, S. D. & Guest, J. R. (1988).** Two biochemically distinct classes of fumarase in *Escherichia coli*. *Biochim Biophys Acta* **954**, 14–26.
- Worley, M. J., Ching, K. H. & Heffron, F. (2000).** *Salmonella* SsrB activates a global regulon of horizontally acquired genes. *Mol Microbiol* **36**, 749–761.
- Wuichet, K., Alexander, R. P. & Zhulin, I. B. (2007).** Comparative genomic and protein sequence analyses of a complex system controlling bacterial chemotaxis. In *Two-Component Signaling Systems, Part A*, Methods in Enzymology, pp. 3–31.
- Xu, X. & Hensel, M. (2010).** Systematic analysis of the SsrAB virulon of *Salmonella enterica*. *Infect. Immun.* **78**, 49–58.
- Yim, H. H. & Villarejo, M. (1992).** *osmY*, a new hyperosmotically inducible gene, encodes a periplasmic protein in *Escherichia coli*. *J Bacteriol* **174**, 3637–3644.
- Yoon, H., McDermott, J. E., Porwollik, S., McClelland, M. & Heffron, F. (2009).** Coordinated regulation of virulence during systemic infection of *Salmonella enterica* Serovar Typhimurium. *PLoS Pathog* **5**, e1000306–16.

- Yu, X.-J., Grabe, G. J., Liu, M., Mota, L. J. & Holden, D. W. (2018).** SsaV Interacts with SsaL to control the translocon-to-effector switch in the *Salmonella* SPI-2 type three secretion system. *mBio* **9**, 379–16.
- Yu, X.-J., McGourty, K., Liu, M., Unsworth, K. E. & Holden, D. W. (2010).** pH sensing by intracellular *Salmonella* induces effector translocation. *Science* **328**, 1040–1043.
- Zeitouni, N. E., Chotikatum, S., Köckritz-Blickwede, von, M. & Naim, H. Y. (2016).** The impact of hypoxia on intestinal epithelial cell functions: consequences for invasion by bacterial pathogens. *Mol Cell Pediatr* **14**, 1–9.
- Zeng, M. Y., Inohara, N. & ez, G. N. N. (2016).** Mechanisms of inflammation-driven bacterial dysbiosis in the gut. *Nature* **10**, 18–26.
- Zhang, Y., Liu, T., Meyer, C. A., Eeckhoute, J., Johnson, D. S., Bernstein, B. E., Nusbaum, C., Myers, R. M., Brown, M. & other authors. (2008).** Model-based analysis of ChIP-Seq (MACS). *Genome Biol* **9**, R137.
- Zheng, L., Kelly, C. J. & Colgan, S. P. (2015).** Physiologic hypoxia and oxygen homeostasis in the healthy intestine. A Review in the Theme: Cellular Responses to Hypoxia. *American Journal of Physiology-Cell Physiology* **309**, C350–C360.

Appendix I

Table S1. RNA-seq data: Absolute and relative expression.

<i>Name</i>	Δfnr TPM	WT TPM	$\Delta fnr/WT$	<i>Chr^a</i>	<i>Start</i>	<i>End</i>	<i>Strand</i>
<i>repY</i>	440	520	0.85	ST4-74_pCollb	378	467	+
<i>repZ</i>	41	49	0.85	ST4-74_pCollb	455	1486	+
<i>yacA</i>	88	72	1.23	ST4-74_pCollb	2395	2664	+
<i>yacB</i>	24	19	1.24	ST4-74_pCollb	2661	2942	+
<i>yacC</i>	31	28	1.12	ST4-74_pCollb	2982	3830	+
<i>yadA</i>	69	63	1.08	ST4-74_pCollb	3971	4420	+
<i>yaeA</i>	274	189	1.45	ST4-74_pCollb	4555	4788	+
<i>yaeB</i>	19	19	1.03	ST4-74_pCollb	4897	5166	-
<i>yafA</i>	29	30	0.99	ST4-74_pCollb	5163	5657	-
<i>yafB</i>	39	35	1.11	ST4-74_pCollb	5713	6315	-
<i>yagA</i>	23	24	0.95	ST4-74_pCollb	6669	8015	+
<i>cib</i>	38	27	1.38	ST4-74_pCollb	8294	10174	+
<i>imm</i>	75	43	1.76	ST4-74_pCollb	10192	10539	-
<i>ybaA</i>	44	25	1.77	ST4-74_pCollb	10658	10977	+
<i>ybbA</i>	4	3	1.52	ST4-74_pCollb	11076	11759	+
<i>ybfA</i>	12	13	0.95	ST4-74_pCollb	12400	12852	+
<i>resA</i>	5	5	1.02	ST4-74_pCollb	12854	13639	+
SLP2_0018	14	14	1.05	ST4-74_pCollb	13893	14096	+
<i>parA</i>	34	37	0.92	ST4-74_pCollb	14223	14855	+
SLP2_0020	44	39	1.15	ST4-74_pCollb	14855	15229	+
<i>stbA</i>	53	52	1.01	ST4-74_pCollb	15468	16442	+
<i>stbB</i>	29	31	0.95	ST4-74_pCollb	16446	16838	+
<i>impC</i>	36	43	0.84	ST4-74_pCollb	16979	17101	-
<i>yccA</i>	8	6	1.34	ST4-74_pCollb	17236	17481	+
<i>yccB</i>	9	6	1.56	ST4-74_pCollb	17495	18421	+
<i>ycdA</i>	3	4	0.81	ST4-74_pCollb	18418	18730	+
<i>ycdB</i>	3	2	1.24	ST4-74_pCollb	18806	19489	+
<i>yceA</i>	2	1	1.48	ST4-74_pCollb	19490	19711	+
<i>yceB</i>	2	2	0.77	ST4-74_pCollb	19725	20159	+
<i>ycfA</i>	4	4	1.19	ST4-74_pCollb	20205	20981	+
<i>ycgA</i>	8	9	0.88	ST4-74_pCollb	20956	21426	+
<i>ycgB</i>	4	2	1.68	ST4-74_pCollb	21399	21824	+
<i>ycgC</i>	8	4	1.99	ST4-74_pCollb	21871	22293	+
<i>ychA</i>	5	6	0.93	ST4-74_pCollb	22606	22898	+
<i>ssb</i>	6	3	2.09	ST4-74_pCollb	23250	23777	+
<i>ycjA</i>	6	4	1.45	ST4-74_pCollb	24121	26085	+
<i>psiB</i>	10	9	1.09	ST4-74_pCollb	26140	26574	+
<i>psiA</i>	10	8	1.29	ST4-74_pCollb	26625	27290	+
SLP2_0039	9	7	1.24	ST4-74_pCollb	27290	27883	+
<i>yddA</i>	62	66	0.93	ST4-74_pCollb	27955	28425	+
<i>ard</i>	8	3	2.41	ST4-74_pCollb	28331	28846	+
<i>ydfA</i>	4	2	1.69	ST4-74_pCollb	29575	30009	+
<i>ydfB</i>	4	4	1.02	ST4-74_pCollb	30103	30369	+
<i>ydgA</i>	305	195	1.57	ST4-74_pCollb	30311	31360	+
<i>ydhA</i>	6	6	1.03	ST4-74_pCollb	32007	32342	+
<i>ydiA</i>	8	6	1.37	ST4-74_pCollb	32467	33315	+

<i>Name</i>	Δfnr TPM	WT TPM	$\Delta fnr/WT$	<i>Chr</i> ^a	<i>Start</i>	<i>End</i>	<i>Strand</i>
SLP2_0047A	219	203	1.08	ST4-74_pCollb	33401	33736	-
<i>nikA</i>	39	46	0.84	ST4-74_pCollb	33969	34301	+
<i>nikB</i>	14	15	0.91	ST4-74_pCollb	34312	37011	+
<i>trbC</i>	13	10	1.27	ST4-74_pCollb	37048	39339	-
<i>trbB</i>	12	9	1.27	ST4-74_pCollb	39332	40402	-
<i>trbA</i>	8	7	1.18	ST4-74_pCollb	40421	41629	-
<i>pndC</i>	3086	3748	0.82	ST4-74_pCollb	41782	42066	+
<i>pndA</i>	5309	6352	0.84	ST4-74_pCollb	41942	42073	+
SLP2_0054A	14106	14363	0.98	ST4-74_pCollb	42696	42992	+
<i>exc</i>	426	425	1.00	ST4-74_pCollb	43906	44568	-
<i>traY</i>	15	13	1.22	ST4-74_pCollb	44633	46864	-
<i>traX</i>	7	6	1.03	ST4-74_pCollb	46892	47476	-
<i>traW</i>	4	4	0.97	ST4-74_pCollb	47505	48707	-
<i>traV</i>	7	7	1.04	ST4-74_pCollb	48674	49288	-
<i>traU</i>	8	7	1.12	ST4-74_pCollb	49288	52332	-
<i>traT</i>	6	5	1.14	ST4-74_pCollb	52422	53222	-
<i>traS</i>	3	3	1.12	ST4-74_pCollb	53206	53394	-
<i>traR</i>	13	17	0.77	ST4-74_pCollb	53458	53862	-
<i>traQ</i>	7	8	0.88	ST4-74_pCollb	53913	54440	-
<i>traP</i>	16	17	0.91	ST4-74_pCollb	54440	55144	-
<i>traO</i>	9	10	0.93	ST4-74_pCollb	55144	56433	-
<i>traN</i>	6	7	0.87	ST4-74_pCollb	56436	57419	-
<i>traM</i>	6	7	0.87	ST4-74_pCollb	57430	58122	-
<i>traL</i>	5	8	0.67	ST4-74_pCollb	58119	58466	-
<i>sogL</i>	6	6	1.02	ST4-74_pCollb	58484	62251	-
<i>nuc</i>	5	7	0.67	ST4-74_pCollb	62341	62892	-
<i>traK</i>	6	10	0.60	ST4-74_pCollb	62907	63197	-
<i>traJ</i>	5	6	0.92	ST4-74_pCollb	63194	64342	-
<i>traI</i>	5	5	0.95	ST4-74_pCollb	64339	65157	-
<i>traH</i>	8	8	1.04	ST4-74_pCollb	65154	65612	-
<i>traG</i>	9	8	1.11	ST4-74_pCollb	66007	66591	-
<i>traF</i>	21	29	0.71	ST4-74_pCollb	66651	67853	-
<i>traE</i>	13	17	0.77	ST4-74_pCollb	67938	68762	-
<i>rci</i>	15	13	1.19	ST4-74_pCollb	68913	70067	-
<i>shfB</i>	8	6	1.33	ST4-74_pCollb	70132	70383	+
<i>shfB</i>	39	22	1.79	ST4-74_pCollb	70385	70630	-
<i>shfC</i>	21	17	1.22	ST4-74_pCollb	70653	71006	+
<i>pilV</i>	10	10	0.97	ST4-74_pCollb	71003	72295	-
<i>pilU</i>	5	5	0.95	ST4-74_pCollb	72295	72951	-
<i>pilT</i>	8	11	0.77	ST4-74_pCollb	72936	73496	-
<i>pilS</i>	22	27	0.83	ST4-74_pCollb	73506	74120	-
<i>pilR</i>	9	10	0.90	ST4-74_pCollb	74138	75235	-
<i>pilQ</i>	7	9	0.84	ST4-74_pCollb	75248	76801	-
<i>pilP</i>	6	10	0.58	ST4-74_pCollb	76812	77264	-
<i>pilO</i>	6	8	0.75	ST4-74_pCollb	77251	78546	-
<i>pilN</i>	6	8	0.79	ST4-74_pCollb	78539	80221	-
<i>pilM</i>	4	7	0.64	ST4-74_pCollb	80235	80672	-
<i>pilL</i>	5	7	0.82	ST4-74_pCollb	80672	81739	-
<i>pilK</i>	4	4	0.94	ST4-74_pCollb	81773	82363	-
<i>pilJ</i>	2	2	0.70	ST4-74_pCollb	82413	82865	-
<i>pilI</i>	6	7	0.89	ST4-74_pCollb	82908	83162	-

<i>Name</i>	Δ_{fnr} TPM	WT TPM	Δ_{fnr}/WT	<i>Chr</i> ^a	<i>Start</i>	<i>End</i>	<i>Strand</i>
<i>trcD</i>	34	36	0.95	ST4-74_pCollb	83430	83996	-
<i>traC</i>	38	35	1.08	ST4-74_pCollb	84010	84693	-
<i>traB</i>	27	22	1.19	ST4-74_pCollb	84947	85480	-
<i>traA</i>	41	47	0.86	ST4-74_pCollb	85922	86209	-
<i>sullI</i>	332	402	0.83	ST4-74_pRSF1010	30	842	-
SLP3_0002	1171	1080	1.08	ST4-74_pRSF1010	854	1075	-
<i>repC</i>	17	17	1.03	ST4-74_pRSF1010	1153	1998	-
<i>repA</i>	29	29	0.99	ST4-74_pRSF1010	1991	2827	-
SLP3_0005	133	109	1.21	ST4-74_pRSF1010	2860	3063	-
SLP3_0006	271	221	1.23	ST4-74_pRSF1010	3068	3277	-
<i>mobA</i>	14	13	1.07	ST4-74_pRSF1010	3341	5467	-
<i>mobB</i>	17	16	1.13	ST4-74_pRSF1010	4309	4719	-
<i>mobC</i>	66	73	0.91	ST4-74_pRSF1010	5666	5947	+
SLP3_0012	71	57	1.25	ST4-74_pRSF1010	6504	7040	+
<i>strB</i>	102	104	0.98	ST4-74_pRSF1010	7018	7860	-
<i>aph(3'')</i> -	219	250	0.87	ST4-74_pRSF1010	7854	8654	-
<i>finO</i>	33	28	1.19	ST4-74_pSLT	21	584	-
<i>traX</i>	9	8	1.15	ST4-74_pSLT	639	1334	-
<i>traI</i>	8	7	1.03	ST4-74_pSLT	1399	6657	-
<i>trbH</i>	8	8	1.04	ST4-74_pSLT	6654	7373	-
<i>traD</i>	7	6	1.22	ST4-74_pSLT	7373	9535	-
<i>traT</i>	312	373	0.84	ST4-74_pSLT	9912	10643	-
<i>traS</i>	521	488	1.07	ST4-74_pSLT	10679	11173	-
<i>traG</i>	85	68	1.26	ST4-74_pSLT	11189	14011	-
<i>traH</i>	6	6	0.90	ST4-74_pSLT	14008	15390	-
<i>trbB</i>	6	4	1.75	ST4-74_pSLT	15380	15928	-
<i>traQ</i>	14	12	1.14	ST4-74_pSLT	15915	16208	-
<i>traF</i>	7	5	1.31	ST4-74_pSLT	16422	17171	-
<i>trbE</i>	9	8	1.14	ST4-74_pSLT	17183	17398	-
<i>traN</i>	6	6	1.04	ST4-74_pSLT	17409	19235	-
<i>trbC</i>	4	3	1.18	ST4-74_pSLT	19688	20326	-
PSLT093	6	8	0.79	ST4-74_pSLT	20311	20619	-
<i>traU</i>	5	5	0.89	ST4-74_pSLT	20638	21630	-
<i>traW</i>	2	3	0.73	ST4-74_pSLT	21627	22259	-
<i>trbI</i>	4	3	1.31	ST4-74_pSLT	22256	22642	-
<i>traC</i>	5	3	1.45	ST4-74_pSLT	22617	25265	-
PSLT087	9	8	1.16	ST4-74_pSLT	25661	26128	-
<i>traR</i>	2	1	1.81	ST4-74_pSLT	26121	26342	-
<i>traV</i>	5	6	0.90	ST4-74_pSLT	26477	26992	-
<i>trbD</i>	6	7	0.79	ST4-74_pSLT	26989	27234	-
<i>traP</i>	6	7	0.94	ST4-74_pSLT	27212	27808	-
<i>traB</i>	6	4	1.28	ST4-74_pSLT	27798	29219	-
<i>traK</i>	4	5	0.80	ST4-74_pSLT	29219	29959	-
<i>traE</i>	3	4	0.90	ST4-74_pSLT	29946	30512	-
<i>traL</i>	7	10	0.67	ST4-74_pSLT	30534	30845	-
<i>traA</i>	16	22	0.73	ST4-74_pSLT	30860	31222	-
<i>traY</i>	101	83	1.22	ST4-74_pSLT	31264	31584	-
<i>traJ</i>	8	6	1.33	ST4-74_pSLT	31585	32271	-
<i>traM</i>	36	26	1.39	ST4-74_pSLT	32464	32844	-
<i>finP</i>	49	49	0.99	ST4-74_pSLT	33259	33729	+
<i>psiA</i>	3	2	1.66	ST4-74_pSLT	35368	36105	-
<i>psiB</i>	12	13	0.93	ST4-74_pSLT	36102	36536	-

<i>Name</i>	Δ <i>fnr</i> TPM	WT TPM	Δ <i>fnr</i> /WT	Chr ^a	Start	End	Strand
PSLT068	3	2	1.17	ST4-74_pSLT	36576	38573	-
PSLT067	4	3	1.61	ST4-74_pSLT	38642	38884	-
<i>ssbB</i>	2	1	2.07	ST4-74_pSLT	38939	39457	-
PSLT064	24	18	1.34	ST4-74_pSLT	40158	40481	-
PSLT063	3	4	0.78	ST4-74_pSLT	40717	41151	-
PSLT062	5	5	1.05	ST4-74_pSLT	41218	41652	-
SLP1_0044A	4	3	1.58	ST4-74_pSLT	41666	42115	-
PSLT061	2	1	1.39	ST4-74_pSLT	42148	42885	-
SLP1_0047	4	2	1.92	ST4-74_pSLT	42984	43397	-
PSLT060	2	1	2.51	ST4-74_pSLT	43453	43674	-
PSLT059	3	2	1.44	ST4-74_pSLT	43674	44354	-
PSLT057	4	5	0.90	ST4-74_pSLT	44736	45092	-
PSLT056	5	4	1.19	ST4-74_pSLT	45085	45555	-
<i>samA</i>	25	25	1.02	ST4-74_pSLT	46066	46488	+
<i>samB</i>	7	5	1.42	ST4-74_pSLT	46488	47762	+
<i>parB</i>	63	66	0.96	ST4-74_pSLT	47844	48821	-
<i>parA</i>	53	54	0.97	ST4-74_pSLT	48818	50023	-
<i>samB</i>	151	142	1.06	ST4-74_pSLT	50438	51379	+
PSLT049	11	12	0.88	ST4-74_pSLT	52553	52969	-
<i>tlpA</i>	10	13	0.82	ST4-74_pSLT	53055	54170	-
PSLT047	62	43	1.43	ST4-74_pSLT	54429	54917	+
PSLT046	534	374	1.43	ST4-74_pSLT	55572	56312	+
<i>rlgA</i>	249	245	1.01	ST4-74_pSLT	56519	57079	+
<i>rlgA</i>	42	48	0.86	ST4-74_pSLT	57063	58727	+
PSLT043	44	49	0.91	ST4-74_pSLT	58660	59685	+
PSLT042	5	4	1.21	ST4-74_pSLT	59874	60869	-
<i>spvR</i>	12	3	3.50	ST4-74_pSLT	61520	62413	+
<i>spvA</i>	51	13	3.88	ST4-74_pSLT	62925	63692	+
<i>spvB</i>	28	10	2.81	ST4-74_pSLT	63874	65649	+
<i>spvC</i>	34	8	4.11	ST4-74_pSLT	66047	66655	+
<i>spvD</i>	24	6	3.88	ST4-74_pSLT	66916	67566	+
PSLT036	43	52	0.82	ST4-74_pSLT	67693	67956	-
PSLT035	1046	1203	0.87	ST4-74_pSLT	68174	68524	+
PSLT034	1	2	0.77	ST4-74_pSLT	68591	69151	-
SLP1_0073A	2	2	0.89	ST4-74_pSLT	69028	69687	-
PSLT033	3	5	0.62	ST4-74_pSLT	69880	70365	-
PSLT032	17	16	1.05	ST4-74_pSLT	71034	71585	-
<i>rsdB</i>	19	18	1.04	ST4-74_pSLT	71594	72376	-
PSLT030	16	17	0.91	ST4-74_pSLT	72411	72932	-
PSLT029	20	23	0.87	ST4-74_pSLT	72929	73219	-
<i>ccdB</i>	29	37	0.79	ST4-74_pSLT	73221	73526	-
<i>ccdA</i>	72	79	0.90	ST4-74_pSLT	73528	73746	-
PSLT026	186	183	1.02	ST4-74_pSLT	74422	74943	+
PSLT025	28	18	1.50	ST4-74_pSLT	75427	75723	+
<i>repA2</i>	112	101	1.11	ST4-74_pSLT	76217	77206	+
PSLT020	32	28	1.14	ST4-74_pSLT	78078	78287	-
<i>pefB</i>	7	11	0.62	ST4-74_pSLT	79178	79480	+
<i>pefA</i>	5	6	0.90	ST4-74_pSLT	79755	80273	+
<i>pefC</i>	4	3	1.09	ST4-74_pSLT	80612	82909	+
<i>pefD</i>	3	4	0.78	ST4-74_pSLT	82902	83594	+

<i>Name</i>	Δ <i>fnr</i> TPM	WT TPM	Δ <i>fnr</i> /WT	<i>Chr</i> ^a	<i>Start</i>	<i>End</i>	<i>Strand</i>
<i>orf5</i>	9	8	1.22	ST4-74_pSLT	83648	84166	+
<i>orf6</i>	151	124	1.22	ST4-74_pSLT	84419	85294	+
<i>pef1</i>	44	36	1.21	ST4-74_pSLT	85726	85938	+
<i>orf7</i>	8	5	1.75	ST4-74_pSLT	85923	86273	+
<i>srgA</i>	12	8	1.56	ST4-74_pSLT	86518	87171	+
<i>srgB</i>	5	5	1.10	ST4-74_pSLT	87304	88203	+
<i>rcK</i>	13	11	1.17	ST4-74_pSLT	88293	88850	+
<i>srgC</i>	33	22	1.54	ST4-74_pSLT	89117	89875	+
PSLT007	10	8	1.23	ST4-74_pSLT	89972	90112	-
<i>repA</i>	72	78	0.92	ST4-74_pSLT	91053	91934	-
<i>tap</i>	283	306	0.93	ST4-74_pSLT	91915	91992	-
<i>repA3</i>	5625	4088	1.38	ST4-74_pSLT	91997	92119	-
<i>repC</i>	825	742	1.11	ST4-74_pSLT	92242	92487	-
PSLT002	35	30	1.17	ST4-74_pSLT	92687	93130	-
PSLT001	36	35	1.03	ST4-74_pSLT	93464	93748	-
<i>thrL</i>	5855	4483	1.31	ST4-74	169	255	+
<i>thrA</i>	50	51	0.99	ST4-74	337	2799	+
<i>thrB</i>	72	57	1.26	ST4-74	2801	3730	+
<i>thrC</i>	63	65	0.97	ST4-74	3734	5020	+
<i>yaaA</i>	32	32	0.99	ST4-74	5114	5887	-
<i>yaaJ</i>	36	23	1.58	ST4-74	5966	7396	-
<i>talB</i>	105	126	0.84	ST4-74	7665	8618	+
<i>mog</i>	33	30	1.09	ST4-74	8729	9319	+
<i>yaaH</i>	7	9	0.74	ST4-74	9376	9942	-
<i>htgA</i>	3	2	1.21	ST4-74	10092	10805	-
<i>yaaI</i>	11	8	1.36	ST4-74	10841	11245	-
<i>dnaK</i>	102	105	0.98	ST4-74	11593	13509	+
<i>tpke11</i>	80	68	1.18	ST4-74	13507	13591	+
<i>dnaJ</i>	61	49	1.24	ST4-74	13595	14734	+
STnc890	402	201	2.00	ST4-74	14720	14783	+
STM0014	9	7	1.32	ST4-74	15014	15961	+
STM0015	6	4	1.44	ST4-74	16088	16432	+
STnc3200	15	9	1.69	ST4-74	16445	16493	-
STM0016	1	2	0.78	ST4-74	16493	17026	-
STnc3210	89	37	2.38	ST4-74	17025	17111	+
STM0017	1	1	1.24	ST4-74	17043	17486	-
<i>chiA</i>	5	5	1.10	ST4-74	18083	19966	+
STM0019	4	3	1.35	ST4-74	20058	23054	+
STM0020	8	8	0.99	ST4-74	23335	24039	+
<i>bcfA</i>	5	4	1.40	ST4-74	24469	25011	+
<i>bcfB</i>	1	1	1.44	ST4-74	25112	25798	+
<i>bcfC</i>	4	4	0.92	ST4-74	25803	28424	+
<i>bcfD</i>	3	2	1.30	ST4-74	28425	29432	+
<i>bcfE</i>	1	1	1.01	ST4-74	29433	29978	+
<i>bcfF</i>	2	1	1.28	ST4-74	29994	30512	+
<i>bcfG</i>	2	3	0.91	ST4-74	30505	31209	+
<i>bcfH</i>	10	11	0.94	ST4-74	31274	32119	+
SL1344_0029	9	7	1.39	ST4-74	32116	32445	+
STM0029	1	1	1.13	ST4-74	32545	32994	-
STM0030	4	3	1.25	ST4-74	33364	34368	+
STM0031	2	2	0.84	ST4-74	34376	34816	-

<i>Name</i>	Δfnr TPM	WT TPM	$\Delta fnr/WT$	Chr ^a	Start	End	Strand
STM0032	6	5	1.27	ST4-74	35339	37057	+
STM0033	12	12	1.06	ST4-74	37103	38674	-
STM0034	4	3	1.18	ST4-74	38773	39534	-
STM0035	8	7	1.21	ST4-74	40131	41624	+
STnc1010	53	52	1.03	ST4-74	41629	41708	+
STM0036	5	5	0.96	ST4-74	41723	42913	+
STM0037	3	2	1.25	ST4-74	42932	44185	+
STM0038	13	9	1.44	ST4-74	44312	46027	+
<i>nhaA</i>	54	49	1.11	ST4-74	46190	47356	+
<i>nhaR</i>	31	30	1.05	ST4-74	47418	48317	+
STM0041	4	4	1.00	ST4-74	48372	50411	-
STM0042	3	4	0.88	ST4-74	50451	51824	-
<i>rpsT</i>	2329	2073	1.12	ST4-74	52280	52543	-
<i>yaaY</i>	43	33	1.29	ST4-74	52649	52864	+
<i>ribF</i>	35	41	0.85	ST4-74	52872	53810	+
<i>ileS</i>	29	36	0.81	ST4-74	53855	56689	+
<i>lspA</i>	65	69	0.94	ST4-74	56689	57189	+
<i>fkpB</i>	27	37	0.72	ST4-74	57344	57793	+
<i>ispH</i>	24	30	0.78	ST4-74	57796	58746	+
STM0050	12	14	0.85	ST4-74	58946	60148	+
<i>rihC</i>	10	13	0.76	ST4-74	60164	61084	+
<i>citB2</i>	6	6	0.89	ST4-74	61106	61792	-
<i>citA2</i>	16	11	1.47	ST4-74	61794	63413	-
STnc3220	102	76	1.35	ST4-74	61807	62034	+
STM0054	3	3	1.24	ST4-74	63548	64849	-
STM0055	2	2	1.00	ST4-74	64862	66637	-
<i>oadG</i>	2	2	1.01	ST4-74	66654	66893	-
STnc4160	131	254	0.51	ST4-74	66912	67051	-
STnc3090	48	37	1.29	ST4-74	66916	67048	+
STM0057	4	4	0.93	ST4-74	67052	68392	-
<i>citC2</i>	3	4	0.79	ST4-74	68637	69683	+
<i>citD2</i>	4	4	1.17	ST4-74	69713	70006	+
<i>citE2</i>	2	3	0.73	ST4-74	70003	70872	+
<i>citF2</i>	5	5	0.87	ST4-74	70883	72403	+
<i>citX2</i>	2	3	0.72	ST4-74	72403	72954	+
<i>citG2</i>	4	3	1.46	ST4-74	72947	73840	+
<i>dapB</i>	219	276	0.79	ST4-74	74020	74841	+
<i>DapZ</i>	3249	2929	1.11	ST4-74	74847	74924	+
STnc3230	194	85	2.28	ST4-74	74894	75015	-
STM0065	4	4	1.05	ST4-74	75091	75438	+
<i>carA</i>	78	121	0.64	ST4-74	75883	77031	+
<i>carB</i>	30	59	0.52	ST4-74	77050	80277	+
<i>caiF</i>	134	160	0.84	ST4-74	80551	80946	+
<i>caiE</i>	3	3	1.20	ST4-74	81023	81619	-
<i>caiD</i>	2	2	0.93	ST4-74	81728	82513	-
<i>caiC</i>	4	3	1.46	ST4-74	82567	84120	-
<i>caiB</i>	3	4	0.82	ST4-74	84183	85454	-
<i>caiA</i>	7	8	0.87	ST4-74	85512	86654	-
<i>caiT</i>	2	3	0.66	ST4-74	86689	88206	-
<i>fixA</i>	3	4	0.78	ST4-74	88687	89457	+
<i>fixB</i>	2	2	0.76	ST4-74	89473	90414	+

<i>Name</i>	Δfur TPM	WT TPM	$\Delta fur/WT$	Chr ^a	Start	End	Strand
<i>fixC</i>	2	2	0.97	ST4-74	90464	91750	+
<i>fixX</i>	3	3	0.93	ST4-74	91747	92034	+
<i>yaaU</i>	10	9	1.12	ST4-74	92181	93521	+
STM0080	90	35	2.55	ST4-74	93610	93840	+
STM0081	85	52	1.61	ST4-74	94134	94550	+
STnc470	1034	633	1.63	ST4-74	94653	94741	-
STM0082	82	70	1.17	ST4-74	94774	95064	-
STnc4170	100	104	0.97	ST4-74	95102	95188	+
SL1344_0083A	50	33	1.50	ST4-74	95134	95226	-
STM0084	5	5	1.01	ST4-74	95962	97851	+
SL1344_0085	16	7	2.22	ST4-74	98056	98121	-
<i>yabF</i>	30	17	1.78	ST4-74	98258	98788	+
<i>kefC</i>	12	9	1.30	ST4-74	98781	100643	+
<i>folA</i>	43	37	1.16	ST4-74	100842	101321	+
STnc3240	34	23	1.44	ST4-74	101322	101483	-
<i>apaH</i>	37	27	1.41	ST4-74	101427	102275	-
<i>apaG</i>	24	33	0.73	ST4-74	102286	102663	-
<i>ksgA</i>	46	44	1.05	ST4-74	102666	103487	-
<i>pdxAa</i>	114	80	1.42	ST4-74	103484	104473	-
<i>surA</i>	79	87	0.90	ST4-74	104473	105759	-
<i>imp</i>	63	66	0.96	ST4-74	105813	108173	-
<i>djlA</i>	40	39	1.04	ST4-74	108427	109239	+
STnc4180	10	27	0.36	ST4-74	109243	109322	-
<i>rhuA</i>	11	12	0.94	ST4-74	109334	109993	-
<i>hepA</i>	6	7	0.87	ST4-74	110005	112911	-
<i>polB</i>	10	7	1.28	ST4-74	113085	115436	-
STM0098	18	16	1.11	ST4-74	115480	116100	-
SL1344_0099A	10	11	0.92	ST4-74	116195	116254	-
STM0100	6	5	1.10	ST4-74	116819	117238	+
<i>araD</i>	13	19	0.70	ST4-74	117244	117939	-
<i>araA</i>	3	3	1.02	ST4-74	118080	119582	-
<i>araB</i>	2	1	1.32	ST4-74	119593	121302	-
<i>araC</i>	10	15	0.69	ST4-74	121643	122488	+
<i>yabI</i>	21	18	1.18	ST4-74	122607	123374	+
<i>thiQ</i>	11	12	0.88	ST4-74	123413	124120	-
<i>thiP</i>	22	21	1.01	ST4-74	124104	125714	-
<i>tbpA</i>	26	26	0.97	ST4-74	125690	126673	-
<i>SroA</i>	517	666	0.78	ST4-74	126713	126802	-
<i>yabN</i>	4	5	0.85	ST4-74	126851	128509	-
<i>SgrS</i>	318	226	1.41	ST4-74	128577	128808	+
<i>sgrT</i>	0	0	-	ST4-74	128602	128724	+
<i>leuD</i>	31	35	0.90	ST4-74	129060	129665	-
<i>leuC</i>	15	22	0.69	ST4-74	129676	131076	-
<i>leuB</i>	19	25	0.74	ST4-74	131079	132170	-
<i>leuA</i>	20	28	0.73	ST4-74	132170	133741	-
<i>leuL</i>	8772	13911	0.63	ST4-74	133829	133915	-
<i>leuO</i>	5	4	1.45	ST4-74	134572	135516	+
<i>ilvI</i>	24	32	0.75	ST4-74	135901	137562	+
<i>ilvH</i>	42	51	0.82	ST4-74	137565	138056	+
STnc1500	119	121	0.99	ST4-74	138100	138274	-
<i>fruR</i>	46	59	0.78	ST4-74	138340	139344	+

<i>Name</i>	Δfnr TPM	WT TPM	$\Delta fnr/WT$	Chr ^a	Start	End	Strand
<i>mraZ</i>	235	184	1.28	ST4-74	139950	140408	+
<i>mraW</i>	119	83	1.44	ST4-74	140410	141351	+
<i>ftsL</i>	158	126	1.26	ST4-74	141348	141713	+
<i>ftsI</i>	290	205	1.42	ST4-74	141729	143495	+
<i>murE</i>	36	36	1.01	ST4-74	143482	144969	+
<i>murF</i>	32	30	1.09	ST4-74	144966	146324	+
<i>mraY</i>	54	48	1.11	ST4-74	146318	147400	+
<i>murD</i>	48	44	1.09	ST4-74	147403	148719	+
<i>ftsW</i>	45	44	1.03	ST4-74	148806	149963	+
<i>murG</i>	36	39	0.94	ST4-74	149960	151027	+
<i>murC</i>	37	38	0.96	ST4-74	151146	152621	+
<i>ddl</i>	74	78	0.95	ST4-74	152614	153534	+
<i>ftsQ</i>	82	77	1.07	ST4-74	153536	154366	+
<i>ftsA</i>	78	76	1.03	ST4-74	154363	155625	+
<i>ftsZ</i>	73	85	0.86	ST4-74	155686	156837	+
<i>lpxC</i>	222	262	0.85	ST4-74	156938	157855	+
<i>yacA</i>	28	31	0.90	ST4-74	158203	158631	+
<i>secA</i>	25	30	0.81	ST4-74	158693	161398	+
<i>mutT</i>	17	13	1.26	ST4-74	161550	161945	+
<i>yacG</i>	27	29	0.93	ST4-74	162267	162458	-
<i>yacF</i>	18	19	0.93	ST4-74	162468	163211	-
<i>coaE</i>	35	39	0.91	ST4-74	163211	163831	-
<i>guaC</i>	74	72	1.03	ST4-74	164057	165100	+
<i>pilC</i>	2	1	1.34	ST4-74	165131	166333	-
<i>pilB</i>	1	1	1.27	ST4-74	166323	167708	-
<i>pilA</i>	3	2	1.12	ST4-74	167718	168155	-
<i>nadC</i>	7	8	0.87	ST4-74	168377	169123	-
<i>ampD</i>	29	28	1.03	ST4-74	169358	169921	+
<i>ampE</i>	26	28	0.93	ST4-74	169918	170772	+
STM0148	7	6	1.14	ST4-74	170864	171814	-
STM0149	6	6	0.98	ST4-74	171814	173220	-
<i>aroP</i>	69	100	0.69	ST4-74	173384	174757	-
<i>pdhR</i>	64	78	0.82	ST4-74	175320	176084	+
<i>tp2</i>	4	5	0.82	ST4-74	176086	176242	-
<i>aceE</i>	35	54	0.64	ST4-74	176244	178907	+
<i>aceF</i>	29	45	0.65	ST4-74	178922	180811	+
<i>lpdA</i>	86	106	0.81	ST4-74	181011	182435	+
STM0155	2	3	0.79	ST4-74	182724	183008	+
STM0156	2	2	1.20	ST4-74	183046	183837	-
<i>yacH</i>	3	2	1.33	ST4-74	183850	185464	-
<i>acnB</i>	42	48	0.87	ST4-74	185853	188450	+
STM0159	118	75	1.57	ST4-74	188511	189353	-
<i>yacL</i>	74	68	1.08	ST4-74	189599	189961	+
<i>kdgT</i>	5	5	0.96	ST4-74	190196	191149	+
STM0162	4	4	0.99	ST4-74	191146	192417	+
<i>pdxAb</i>	33	33	1.01	ST4-74	192407	193390	+
STM0164	32	36	0.89	ST4-74	193400	194167	+
<i>speD</i>	27	29	0.94	ST4-74	194197	194991	-
<i>speE</i>	20	24	0.85	ST4-74	195012	195872	-
<i>yacC</i>	118	100	1.18	ST4-74	195979	196326	-
<i>cueO</i>	10	14	0.70	ST4-74	196528	198138	+

<i>Name</i>	Δ <i>fnr</i> TPM	WT TPM	Δ <i>fnr</i> /WT	<i>Chr</i> ^a	<i>Start</i>	<i>End</i>	<i>Strand</i>
<i>gcd</i>	27	14	1.92	ST4-74	198216	200606	-
<i>hpt</i>	61	61	1.00	ST4-74	200812	201348	+
<i>yadF</i>	140	115	1.21	ST4-74	201406	202068	-
<i>yadG</i>	11	10	1.03	ST4-74	202177	203103	+
<i>yadH</i>	13	12	1.06	ST4-74	203100	203870	+
<i>stiH</i>	3	3	1.16	ST4-74	203987	205066	-
<i>stiC</i>	1	1	1.38	ST4-74	205075	207621	-
<i>stiB</i>	1	1	0.90	ST4-74	207648	208331	-
<i>stiA</i>	2	2	1.25	ST4-74	208379	208918	-
<i>yadI</i>	9	68	0.13	ST4-74	209289	209729	+
<i>yadE</i>	21	20	1.01	ST4-74	209791	211020	+
STnc4190	28	36	0.79	ST4-74	209868	209971	-
<i>panD</i>	151	172	0.88	ST4-74	211027	211407	-
<i>panC</i>	11	21	0.51	ST4-74	211502	212356	-
<i>panB</i>	14	21	0.65	ST4-74	212482	213273	-
<i>folK</i>	9	9	0.96	ST4-74	213394	213873	-
<i>pcnB</i>	33	36	0.92	ST4-74	213870	215288	-
<i>yadB</i>	10	11	0.99	ST4-74	215429	216370	-
<i>dksA</i>	337	356	0.95	ST4-74	216394	216849	-
<i>sfsA</i>	75	44	1.70	ST4-74	217026	217730	-
<i>ligT</i>	56	47	1.19	ST4-74	217747	218277	-
<i>hrpB</i>	16	16	0.97	ST4-74	218305	220779	+
<i>mrcB</i>	33	37	0.88	ST4-74	220920	223442	+
STnc3250	88	48	1.81	ST4-74	223451	223676	-
<i>fhuA</i>	34	16	2.10	ST4-74	223735	225924	+
<i>fhuC</i>	6	4	1.52	ST4-74	225973	226770	+
<i>fhuD</i>	10	5	1.86	ST4-74	226770	227660	+
<i>fhuB</i>	9	5	1.65	ST4-74	227657	229714	+
<i>stfA</i>	3	2	1.17	ST4-74	230653	231213	+
<i>stfC</i>	3	3	1.01	ST4-74	231299	233956	+
<i>stfD</i>	1	0	1.42	ST4-74	233974	234726	+
<i>stfE</i>	3	3	0.99	ST4-74	234790	235257	+
<i>stfF</i>	2	2	1.06	ST4-74	235254	235730	+
<i>stfG</i>	3	1	2.08	ST4-74	235730	236260	+
STM0201	15	10	1.47	ST4-74	236260	237099	+
STnc1510	79	56	1.41	ST4-74	237091	237187	+
<i>hemL</i>	34	35	0.96	ST4-74	237207	238487	-
<i>clcA</i>	30	24	1.24	ST4-74	238657	240078	+
<i>yadR</i>	229	267	0.86	ST4-74	240160	240504	+
<i>yadS</i>	10	10	1.00	ST4-74	240605	241228	-
<i>btuF</i>	8	10	0.81	ST4-74	241265	242065	-
<i>mtn</i>	30	32	0.93	ST4-74	242058	242756	-
<i>dgt</i>	22	18	1.22	ST4-74	243051	244358	+
<i>htrA</i>	30	38	0.79	ST4-74	244488	245915	+
STnc3100	91	86	1.06	ST4-74	245838	245954	+
<i>cdaR</i>	16	11	1.43	ST4-74	246068	247225	+
<i>yaeH</i>	364	526	0.69	ST4-74	247314	247700	-
STM0212	49	34	1.42	ST4-74	248223	249248	+
STnc3110	159	107	1.48	ST4-74	249153	249274	+
<i>dapD</i>	129	180	0.71	ST4-74	249285	250109	-
<i>glnD</i>	8	10	0.85	ST4-74	250139	252811	-

<i>Name</i>	Δ <i>fnr</i> TPM	WT TPM	Δ <i>fnr</i> /WT	Chr ^a	Start	End	Strand
<i>map</i>	54	53	1.02	ST4-74	253048	253842	-
<i>t44</i>	465	619	0.75	ST4-74	254126	254264	+
<i>rpsB</i>	251	345	0.73	ST4-74	254293	255018	+
<i>tsf</i>	174	234	0.74	ST4-74	255276	256127	+
<i>pyrH</i>	39	51	0.76	ST4-74	256272	256997	+
<i>frr</i>	185	172	1.07	ST4-74	257144	257701	+
<i>sRNA1</i>	228	325	0.70	ST4-74	257725	257790	+
<i>dxr</i>	18	18	0.97	ST4-74	257842	259038	+
STnc920	257	281	0.92	ST4-74	259116	259164	+
<i>uppS</i>	57	67	0.85	ST4-74	259351	260109	+
<i>cdsA</i>	63	67	0.94	ST4-74	260122	260979	+
<i>yaeL</i>	103	105	0.98	ST4-74	260991	262343	+
<i>yaeT</i>	98	109	0.90	ST4-74	262375	264789	+
<i>hlpA</i>	202	200	1.01	ST4-74	264912	265397	+
<i>lpxD</i>	128	151	0.85	ST4-74	265401	266426	+
<i>fabZ</i>	99	109	0.91	ST4-74	266532	266987	+
<i>lpxA</i>	62	71	0.88	ST4-74	266991	267779	+
<i>lpxB</i>	19	24	0.80	ST4-74	267779	268927	+
<i>rnhB</i>	24	29	0.83	ST4-74	268924	269520	+
<i>dnaE</i>	26	32	0.82	ST4-74	269544	273026	+
<i>accA</i>	41	52	0.79	ST4-74	273039	273998	+
STM0233	8	7	1.12	ST4-74	274178	275941	+
<i>ldcC</i>	16	13	1.20	ST4-74	276017	278158	+
<i>yaeR</i>	28	20	1.42	ST4-74	278214	278603	+
<i>mesJ</i>	10	10	1.05	ST4-74	278747	279958	+
<i>rof</i>	205	197	1.04	ST4-74	280042	280296	-
<i>yaeP</i>	577	493	1.17	ST4-74	280289	280507	-
<i>yaeQ</i>	23	21	1.08	ST4-74	280687	281232	+
<i>yaeJ</i>	70	50	1.38	ST4-74	281229	281651	+
<i>cutF</i>	37	28	1.31	ST4-74	281683	282384	+
<i>proS</i>	24	30	0.81	ST4-74	282458	284176	-
<i>yaeB</i>	15	17	0.86	ST4-74	284287	284994	-
<i>rcsF</i>	67	75	0.90	ST4-74	284991	285395	-
<i>metQ</i>	167	227	0.74	ST4-74	285514	286329	-
<i>yaeE</i>	101	135	0.75	ST4-74	286368	287021	-
<i>abc</i>	86	94	0.92	ST4-74	287014	288045	-
<i>yaeD</i>	35	31	1.14	ST4-74	288235	288801	+
<i>dkgB</i>	11	9	1.15	ST4-74	295060	295863	+
<i>yafC</i>	6	5	1.14	ST4-74	295884	296798	-
STM0257	5	5	1.11	ST4-74	296903	298078	+
<i>yafD</i>	38	43	0.89	ST4-74	298231	299010	+
<i>yafE</i>	12	11	1.14	ST4-74	299088	299858	+
<i>dniR</i>	224	296	0.76	ST4-74	299914	301281	-
<i>gloB</i>	8	10	0.79	ST4-74	301353	302108	-
<i>yafS</i>	19	18	1.07	ST4-74	302143	302865	+
<i>rnhA</i>	35	28	1.27	ST4-74	302862	303329	-
<i>dnaQ</i>	49	43	1.13	ST4-74	303393	304124	+
<i>sciA</i>	3	2	1.20	ST4-74	304656	305711	-
<i>sciB</i>	2	1	1.30	ST4-74	305722	306717	-
<i>sciC</i>	2	2	1.22	ST4-74	306714	308597	-
<i>sciD</i>	3	3	1.06	ST4-74	308613	309107	-

<i>Name</i>	Δfur TPM	WT TPM	$\Delta fur/WT$	Chr ^a	Start	End	Strand
<i>sciE</i>	3	3	0.90	ST4-74	309104	309928	-
<i>sciF</i>	4	3	1.24	ST4-74	309915	310817	-
<i>sciG</i>	2	2	0.98	ST4-74	311185	313824	+
<i>sciH</i>	1	1	0.85	ST4-74	313924	314466	+
<i>sciI</i>	2	2	1.15	ST4-74	314490	315983	+
<i>sciJ</i>	4	4	1.25	ST4-74	316169	316615	+
<i>sciK</i>	1	1	0.89	ST4-74	316869	317354	+
STM0277	5	5	1.02	ST4-74	317659	318144	+
STM0278	1	1	1.11	ST4-74	318129	318512	+
<i>sciK1</i>	2	2	1.03	ST4-74	318655	319140	+
<i>sciN</i>	1	0	2.68	ST4-74	319207	319743	+
<i>sciO</i>	2	1	1.19	ST4-74	319747	321090	+
<i>sciP</i>	2	2	0.95	ST4-74	321087	322391	+
<i>sciQ</i>	3	3	1.22	ST4-74	322396	323169	+
<i>sciR</i>	3	2	1.62	ST4-74	323372	323803	+
<i>sciS</i>	3	3	1.05	ST4-74	323837	327706	+
<i>sciT</i>	4	4	1.05	ST4-74	327706	328494	+
<i>sciU</i>	4	5	0.85	ST4-74	328491	328907	+
<i>sciV</i>	9	9	0.99	ST4-74	328931	329452	+
<i>vgrS</i>	2	2	1.27	ST4-74	329849	332038	+
<i>sciW</i>	1	1	0.60	ST4-74	332062	332508	+
STM0291	26	19	1.39	ST4-74	332521	336123	+
SL1344_0286A	71	45	1.56	ST4-74	336117	336380	+
STM0292	101	84	1.20	ST4-74	336396	337313	+
<i>sciX</i>	33	29	1.14	ST4-74	337307	337753	+
<i>sciY</i>	5	3	1.46	ST4-74	338265	338753	+
<i>IsrA</i>	3	2	1.16	ST4-74	338816	339238	+
STM0295	12	12	0.96	ST4-74	339522	339830	+
STM0296	5	4	1.19	ST4-74	339867	340180	-
STM0297	6	7	0.83	ST4-74	340233	340373	+
STM0298	1	2	0.80	ST4-74	340510	340975	+
<i>safA</i>	39	31	1.25	ST4-74	341687	342199	+
<i>safB</i>	5	5	1.03	ST4-74	342307	343020	+
<i>safC</i>	9	8	1.16	ST4-74	343044	345554	+
<i>safD</i>	11	11	1.00	ST4-74	345576	346046	+
<i>ybeJ</i>	6	6	0.99	ST4-74	346452	347273	+
<i>sinR</i>	26	24	1.06	ST4-74	348088	349035	+
STM0305	8	6	1.33	ST4-74	349152	349367	+
<i>pagN</i>	213	139	1.53	ST4-74	349371	350090	-
<i>sciZ</i>	15	18	0.84	ST4-74	350421	350828	-
STnc1030	470	673	0.70	ST4-74	350892	351095	+
STnc1040	480	633	0.76	ST4-74	351053	351100	-
<i>yafV</i>	21	20	1.06	ST4-74	351199	351966	-
<i>fadE</i>	18	17	1.05	ST4-74	352075	354519	-
<i>gmhA</i>	56	54	1.04	ST4-74	354759	355337	+
<i>yafJ</i>	23	24	0.92	ST4-74	355550	356317	+
<i>yafK</i>	51	52	0.98	ST4-74	356288	357028	-
<i>dbh</i>	15	13	1.20	ST4-74	357278	358333	+
STM0314	8	7	1.07	ST4-74	358540	359684	+
<i>prfH</i>	5	5	0.94	ST4-74	359681	360295	+
<i>pepD</i>	47	53	0.89	ST4-74	360451	361908	-

<i>Name</i>	Δ <i>fnr</i> TPM	WT TPM	Δ <i>fnr</i> /WT	<i>Chr</i> ^a	<i>Start</i>	<i>End</i>	<i>Strand</i>
<i>gpt</i>	84	88	0.95	ST4-74	362157	362615	+
<i>frsA</i>	32	25	1.27	ST4-74	362704	363948	+
<i>crl</i>	185	165	1.12	ST4-74	364006	364407	+
<i>phoE</i>	6	5	1.14	ST4-74	364458	365510	-
<i>proB</i>	35	42	0.83	ST4-74	365793	366896	+
<i>proA</i>	22	24	0.90	ST4-74	366908	368158	+
STM0325	5	4	1.27	ST4-74	368675	369475	-
<i>dhaF</i>	2	2	0.85	ST4-74	369393	370107	+
STM0327	330	397	0.83	ST4-74	370217	370540	+
STM0328	4	3	1.44	ST4-74	370836	372119	+
<i>leuC2</i>	2	2	1.07	ST4-74	372251	373465	+
<i>leuD2</i>	2	1	1.46	ST4-74	373674	374300	+
STM0331	8	6	1.29	ST4-74	374315	375193	+
STM0332	8	7	1.15	ST4-74	375193	376107	+
STnc3270	69	50	1.39	ST4-74	376115	376194	+
STM0333	14	11	1.21	ST4-74	376141	377106	+
STM0334	13	13	0.94	ST4-74	377051	377323	-
STM0335	8	6	1.38	ST4-74	378014	378412	+
<i>stbE</i>	9	8	1.10	ST4-74	378459	379217	-
<i>stbD</i>	9	7	1.32	ST4-74	379183	380508	-
<i>stbC</i>	5	5	1.07	ST4-74	380513	383080	-
<i>stbB</i>	1	1	0.81	ST4-74	383064	383825	-
<i>stbA</i>	1	0	4.83	ST4-74	383887	384423	-
STM0341	17	11	1.50	ST4-74	385057	385821	+
STM0342	16	11	1.44	ST4-74	385794	386294	+
STnc1700	46	19	2.50	ST4-74	386381	386476	+
STM0343	11	9	1.19	ST4-74	386594	388168	+
STM0344	40	38	1.04	ST4-74	388268	389011	+
STM0345	23	21	1.07	ST4-74	388984	389472	+
STM0346	4	4	1.06	ST4-74	389874	390398	+
STM0347	3	1	1.78	ST4-74	390542	391183	+
STM0348	3	4	0.92	ST4-74	391194	391418	+
STM0349	7	7	1.05	ST4-74	391476	391835	+
STM0350	2	2	1.10	ST4-74	391905	393362	-
STM0351	2	2	1.40	ST4-74	393379	396546	-
STM0352	1	1	1.28	ST4-74	396543	397553	-
STM0353	3	3	1.03	ST4-74	398046	400334	+
STM0354	4	4	1.02	ST4-74	400346	400810	+
STM0355	23	29	0.78	ST4-74	400888	401082	+
STM0356	8	9	0.89	ST4-74	401375	402628	+
<i>mod</i>	20	20	1.01	ST4-74	402817	404775	+
<i>res</i>	12	11	1.06	ST4-74	404782	407757	+
STM0359	450	169	2.66	ST4-74	408034	408135	+
STM0360	38	22	1.70	ST4-74	408252	409655	+
STM0361	43	29	1.48	ST4-74	409652	410662	+
STM0362	15	10	1.52	ST4-74	410679	410903	+
STM0363	14	11	1.22	ST4-74	410999	412003	+
<i>foxA</i>	6	5	1.24	ST4-74	412149	414257	+
<i>yahN</i>	99	90	1.10	ST4-74	414298	414930	-
<i>yahO</i>	263	201	1.31	ST4-74	415162	415437	+
<i>prpR</i>	7	7	0.97	ST4-74	415573	417198	-

<i>Name</i>	Δ <i>fnr</i> TPM	WT TPM	Δ <i>fnr</i> /WT	<i>Chr</i> ^a	<i>Start</i>	<i>End</i>	<i>Strand</i>
<i>prpB</i>	2	1	1.74	ST4-74	417463	418350	+
STnc3280	42	37	1.14	ST4-74	418391	418463	-
<i>prpC</i>	2	2	1.14	ST4-74	418473	419642	+
<i>prpD</i>	2	2	1.09	ST4-74	419682	421133	+
<i>prpE</i>	2	3	0.88	ST4-74	421174	423060	+
<i>hemB</i>	21	23	0.93	ST4-74	423164	424138	-
<i>yaiU</i>	21	19	1.13	ST4-74	424651	427587	+
<i>yaiV</i>	17	13	1.27	ST4-74	427673	428296	+
<i>ampH</i>	21	20	1.03	ST4-74	428341	429471	-
<i>sbmA</i>	17	14	1.16	ST4-74	429947	431065	+
<i>yaiW</i>	9	9	1.07	ST4-74	431080	432174	+
<i>yaiY</i>	14	7	1.91	ST4-74	432212	432520	-
<i>yaiZ</i>	273	252	1.09	ST4-74	432788	433003	+
<i>ddlA</i>	41	38	1.09	ST4-74	433029	434123	-
STM0381	18	9	2.06	ST4-74	434201	434914	+
STM0382	9	6	1.43	ST4-74	435083	436294	+
<i>yaiB</i>	761	542	1.40	ST4-74	436585	436851	+
STnc4150	43	27	1.61	ST4-74	436953	437082	-
<i>psiF</i>	112	53	2.14	ST4-74	437203	437523	+
<i>adrA</i>	20	14	1.41	ST4-74	437615	438727	+
<i>proC</i>	22	21	1.02	ST4-74	438742	439551	-
<i>yaiI</i>	16	16	1.04	ST4-74	439691	440146	+
<i>aroL</i>	54	78	0.68	ST4-74	440331	440876	+
<i>yaiA</i>	325	301	1.08	ST4-74	440903	441094	+
<i>aroM</i>	56	54	1.03	ST4-74	441345	442022	+
<i>yaiE</i>	113	133	0.85	ST4-74	442093	442377	+
<i>rdgC</i>	24	24	0.99	ST4-74	442415	443326	-
<i>yajF</i>	21	17	1.22	ST4-74	443452	444360	+
<i>araJ</i>	11	11	1.00	ST4-74	444382	445554	-
<i>sbcC</i>	4	5	0.79	ST4-74	445727	448867	-
<i>sbcD</i>	7	8	0.86	ST4-74	448864	450066	-
<i>phoB</i>	67	58	1.14	ST4-74	450281	450970	+
<i>phoR</i>	21	18	1.15	ST4-74	451040	452335	+
<i>brnQ</i>	71	73	0.97	ST4-74	452744	454063	+
<i>proY</i>	22	19	1.16	ST4-74	454138	455508	+
<i>malZ</i>	7	7	1.07	ST4-74	455670	457487	+
<i>tsaA</i>	154	249	0.62	ST4-74	457559	458161	-
<i>yajB</i>	48	50	0.96	ST4-74	458371	458952	-
<i>queA</i>	19	18	1.06	ST4-74	459046	460110	+
<i>tgt</i>	76	91	0.83	ST4-74	460307	461434	+
<i>yajC</i>	206	306	0.67	ST4-74	461457	461789	+
<i>secD</i>	80	100	0.80	ST4-74	461817	463664	+
<i>secF</i>	77	102	0.75	ST4-74	463675	464646	+
STM0409	19	20	0.95	ST4-74	464794	465159	+
STM0410	9	14	0.65	ST4-74	465185	465877	+
<i>yajD</i>	57	67	0.84	ST4-74	466047	466394	+
STnc1060	1413	1468	0.96	ST4-74	466718	466783	-
<i>tsx</i>	19	31	0.62	ST4-74	467023	467886	-
<i>yajI</i>	9	5	1.67	ST4-74	468186	468725	-
<i>nrdR</i>	170	115	1.49	ST4-74	468877	469326	+
<i>ribD</i>	36	32	1.13	ST4-74	469330	470433	+

<i>Name</i>	Δfnr TPM	WT TPM	$\Delta fnr/WT$	Chr ^a	Start	End	Strand
<i>ribH</i>	136	135	1.01	ST4-74	470522	470992	+
<i>nusB</i>	136	143	0.95	ST4-74	471013	471432	+
<i>thiL</i>	16	17	0.91	ST4-74	471511	472488	+
<i>pgpA</i>	20	19	1.03	ST4-74	472466	472981	+
<i>yajO</i>	23	16	1.40	ST4-74	473085	474059	-
<i>dxs</i>	17	21	0.82	ST4-74	474116	475978	-
<i>ispA</i>	26	28	0.95	ST4-74	476002	476901	-
<i>xseB</i>	102	103	0.99	ST4-74	476902	477144	-
<i>thiI</i>	21	19	1.06	ST4-74	477354	478802	+
<i>phnV</i>	5	5	0.99	ST4-74	478846	479643	-
<i>phnU</i>	3	3	0.85	ST4-74	479646	480506	-
<i>phnT</i>	3	3	1.23	ST4-74	480509	481618	-
<i>phnS</i>	3	3	0.92	ST4-74	481624	482568	-
<i>phnR</i>	10	10	0.98	ST4-74	482835	483554	-
<i>phnW</i>	2	2	0.98	ST4-74	483694	484797	+
<i>phnX</i>	2	2	0.76	ST4-74	484804	485616	+
<i>thiJ</i>	13	12	1.06	ST4-74	485713	486303	-
<i>apbA</i>	30	22	1.36	ST4-74	486266	487177	-
<i>yajQ</i>	182	185	0.99	ST4-74	487285	487794	+
<i>yajR</i>	22	19	1.13	ST4-74	487841	489205	-
SL1344_0430A	35	23	1.52	ST4-74	489507	489698	-
STM0437	12	10	1.22	ST4-74	489742	491253	+
STM0438	10	8	1.29	ST4-74	491475	492758	+
<i>cyoE</i>	93	70	1.32	ST4-74	492840	493730	-
<i>cyoD</i>	116	86	1.35	ST4-74	493742	494071	-
<i>cyoC</i>	97	67	1.43	ST4-74	494071	494586	-
<i>cyoB</i>	83	67	1.24	ST4-74	494675	496666	-
<i>cyoA</i>	165	122	1.36	ST4-74	496677	497633	-
<i>ampG</i>	12	13	0.91	ST4-74	498086	499561	-
<i>yajG</i>	41	46	0.88	ST4-74	499605	500237	-
<i>bolA</i>	351	238	1.48	ST4-74	500487	500804	+
<i>tig</i>	129	142	0.91	ST4-74	501151	502449	+
<i>clpP</i>	133	149	0.89	ST4-74	502696	503319	+
<i>clpX</i>	226	207	1.09	ST4-74	503571	504842	+
<i>SraA</i>	13	11	1.20	ST4-74	504870	504976	-
<i>lon</i>	88	80	1.11	ST4-74	505028	507382	+
<i>hupB</i>	1743	2379	0.73	ST4-74	507591	507863	+
<i>cypD</i>	58	64	0.90	ST4-74	508154	510025	+
<i>comE1</i>	12	13	0.87	ST4-74	510175	510549	+
<i>ybaW</i>	12	9	1.25	ST4-74	510653	511051	+
<i>ybaX</i>	44	41	1.06	ST4-74	511157	511852	-
<i>ybaE</i>	5	6	0.89	ST4-74	511917	513617	-
<i>cof</i>	8	6	1.48	ST4-74	513718	514536	+
STnc930	78	59	1.32	ST4-74	514484	514578	+
STM0458	7	6	1.15	ST4-74	514586	515641	-
<i>ybaO</i>	35	32	1.11	ST4-74	515754	516212	+
<i>mdlA</i>	10	9	1.05	ST4-74	516253	518025	+
<i>mdlB</i>	8	10	0.82	ST4-74	518018	519799	+
<i>glnK</i>	17	10	1.68	ST4-74	520012	520350	+
<i>amiB</i>	19	12	1.54	ST4-74	520382	521668	+
<i>tesB</i>	19	16	1.21	ST4-74	521768	522628	-

<i>Name</i>	Δ <i>fnr</i> TPM	WT TPM	Δ <i>fnr</i> /WT	<i>Chr</i> ^a	<i>Start</i>	<i>End</i>	<i>Strand</i>
<i>ybaY</i>	108	48	2.24	ST4-74	522843	523412	+
<i>ybaZ</i>	153	129	1.19	ST4-74	523445	523756	-
<i>ylaB</i>	25	22	1.14	ST4-74	524065	525615	-
<i>rpmE2</i>	114	63	1.81	ST4-74	525840	526100	+
<i>rpmJa</i>	215	145	1.48	ST4-74	526163	526246	+
<i>ylaC</i>	102	92	1.11	ST4-74	526302	526772	-
<i>maa</i>	99	86	1.16	ST4-74	526889	527440	-
<i>hha</i>	114	92	1.24	ST4-74	527619	527837	-
<i>ybaJ</i>	162	110	1.47	ST4-74	527865	528239	-
<i>acrB</i>	42	51	0.82	ST4-74	528735	531884	-
<i>acrA</i>	29	32	0.90	ST4-74	531907	533100	-
<i>acrR</i>	41	45	0.92	ST4-74	533242	533895	+
<i>aefA</i>	21	20	1.08	ST4-74	534014	537376	+
STM0479	23	22	1.04	ST4-74	537418	538353	-
<i>ybaM</i>	24	16	1.55	ST4-74	538423	538590	-
<i>priC</i>	21	15	1.42	ST4-74	538604	539119	-
<i>apt</i>	43	45	0.94	ST4-74	539730	540281	+
<i>dnaX</i>	39	39	1.00	ST4-74	540395	542323	+
<i>ybaB</i>	36	49	0.73	ST4-74	542369	542698	+
<i>recR</i>	20	31	0.62	ST4-74	542698	543303	+
<i>htpG</i>	35	47	0.74	ST4-74	543414	545288	+
STnc3130	120	175	0.69	ST4-74	545302	545385	-
<i>adk</i>	76	85	0.89	ST4-74	545529	546173	+
<i>hemH</i>	27	24	1.14	ST4-74	546402	547364	+
<i>aes</i>	3	3	0.99	ST4-74	547361	548332	-
<i>gsk</i>	19	18	1.04	ST4-74	548485	549789	+
<i>ybaL</i>	40	38	1.03	ST4-74	549838	551514	-
<i>fsr</i>	9	11	0.85	ST4-74	551729	552949	-
<i>ushA</i>	39	46	0.85	ST4-74	553122	554774	+
<i>ybaK</i>	34	35	0.99	ST4-74	554891	555370	-
<i>ChiX</i>	42639	30555	1.40	ST4-74	555450	555566	+
<i>ybaP</i>	19	19	0.96	ST4-74	555572	556366	-
STM0497	12	9	1.39	ST4-74	556452	557279	-
<i>copA</i>	26	33	0.79	ST4-74	557433	559934	-
<i>cueR</i>	88	84	1.05	ST4-74	560044	560460	+
<i>ybbJ</i>	16	14	1.11	ST4-74	560461	560913	-
<i>ybbK</i>	37	32	1.16	ST4-74	560910	561827	-
<i>ybbL</i>	9	9	1.09	ST4-74	561974	562651	+
<i>ybbM</i>	16	13	1.21	ST4-74	562638	563417	+
<i>ybbN</i>	35	40	0.87	ST4-74	563503	564357	-
<i>ybbO</i>	16	18	0.91	ST4-74	564417	565187	-
<i>tesA</i>	28	26	1.07	ST4-74	565342	565956	-
<i>ybbA</i>	13	17	0.78	ST4-74	565927	566613	+
<i>ybbP</i>	23	21	1.11	ST4-74	566610	569024	+
STnc950	14	19	0.77	ST4-74	569023	569074	+
STM0509	13	11	1.13	ST4-74	569210	570343	+
<i>sfbA</i>	83	77	1.08	ST4-74	570600	571430	+
<i>sfbB</i>	41	44	0.95	ST4-74	571467	572483	+
<i>sfbC</i>	72	61	1.17	ST4-74	572476	573135	+
<i>ybbB</i>	18	21	0.86	ST4-74	573174	574268	-
<i>ybbS</i>	5	5	1.12	ST4-74	574338	575264	-

<i>Name</i>	Δ <i>fnr</i> TPM	WT TPM	Δ <i>fnr</i> /WT	<i>Chr</i> ^a	<i>Start</i>	<i>End</i>	<i>Strand</i>
<i>allA</i>	25	21	1.19	ST4-74	575491	575973	+
<i>allR</i>	40	45	0.88	ST4-74	576052	576870	+
<i>gcl</i>	2	2	0.85	ST4-74	576955	578736	+
<i>gip</i>	4	3	1.11	ST4-74	578749	579525	+
<i>garRa</i>	1	2	0.46	ST4-74	579626	580504	+
STM0520	3	2	1.21	ST4-74	580570	581817	+
<i>allP</i>	2	1	1.44	ST4-74	581913	583367	+
<i>allB</i>	3	2	1.36	ST4-74	583446	584807	+
<i>ybbY</i>	3	3	1.06	ST4-74	584866	586164	+
<i>glxK</i>	3	2	1.15	ST4-74	586187	587335	+
STnc480	137	82	1.68	ST4-74	587347	587412	-
<i>ylbA</i>	13	12	1.10	ST4-74	587415	588200	-
<i>allC</i>	3	3	0.84	ST4-74	588211	589446	-
<i>allD</i>	2	3	0.53	ST4-74	589468	590517	-
<i>fdrA</i>	3	4	0.83	ST4-74	590848	592512	+
<i>ylbE</i>	1	1	1.13	ST4-74	592522	593781	+
<i>ylbF</i>	2	2	1.12	ST4-74	593793	594602	+
<i>arcC</i>	3	3	1.12	ST4-74	594606	595499	+
<i>purK</i>	28	38	0.73	ST4-74	595540	596607	-
<i>purE</i>	43	72	0.59	ST4-74	596604	597113	-
<i>lpxH</i>	6	8	0.83	ST4-74	597231	597953	-
<i>ppiB</i>	216	291	0.74	ST4-74	597956	598450	-
<i>cysS</i>	62	54	1.15	ST4-74	598623	600008	+
STM0538	5	4	1.06	ST4-74	600052	600876	-
STM0539	4	6	0.68	ST4-74	600873	601310	-
<i>ybcI</i>	6	6	1.03	ST4-74	601303	601848	-
<i>ybcJ</i>	28	30	0.93	ST4-74	601976	602188	-
<i>folD</i>	42	45	0.93	ST4-74	602190	603056	-
<i>fimA</i>	11	15	0.72	ST4-74	603618	604160	+
<i>fimI</i>	2	4	0.67	ST4-74	604236	604769	+
<i>fimC</i>	1	2	0.34	ST4-74	604813	605505	+
<i>fimD</i>	2	2	1.17	ST4-74	605536	608148	+
<i>fimH</i>	4	4	0.94	ST4-74	608163	609170	+
<i>fimF</i>	10	7	1.47	ST4-74	609180	609698	+
<i>fimZ</i>	8	7	1.16	ST4-74	609744	610376	-
<i>fimY</i>	1	2	0.69	ST4-74	610980	611702	-
STM0551	3	3	0.94	ST4-74	611721	612032	-
<i>fimW</i>	11	11	0.97	ST4-74	612194	612790	-
STM0555	9	7	1.21	ST4-74	613262	613552	-
STM0557	29	10	2.82	ST4-74	614292	615944	-
<i>gtrBa</i>	17	7	2.44	ST4-74	615925	616851	-
<i>gtrAa</i>	73	23	3.25	ST4-74	616848	617210	-
STnc1870	32	13	2.54	ST4-74	617317	617426	+
STM0561	7	7	1.03	ST4-74	618078	618407	-
<i>cusA</i>	14	16	0.85	ST4-74	618456	618692	+
<i>ykgD</i>	6	5	1.21	ST4-74	618746	619600	-
<i>ykgC</i>	7	6	1.15	ST4-74	619816	621141	+
STM0565	4	3	1.28	ST4-74	621298	621534	+
<i>ykgB</i>	4	3	1.51	ST4-74	621547	622107	+
STM0567	16	24	0.66	ST4-74	622186	623361	-
<i>pheP</i>	40	38	1.05	ST4-74	623687	625081	+

<i>Name</i>	Δfnr TPM	WT TPM	$\Delta fnr/WT$	<i>Chr^a</i>	<i>Start</i>	<i>End</i>	<i>Strand</i>
<i>ybdG</i>	13	18	0.74	ST4-74	625123	626253	-
<i>apeE</i>	14	15	0.90	ST4-74	626681	628651	+
STM0571	20	22	0.93	ST4-74	628818	631547	+
STM0572	2	2	0.68	ST4-74	631675	632661	-
STM0573	1	1	0.77	ST4-74	632728	633771	-
<i>manZ</i>	1	1	1.00	ST4-74	633804	634658	-
<i>manY</i>	2	2	1.48	ST4-74	634661	635335	-
<i>manX</i>	1	0	1.75	ST4-74	635419	635889	-
STM0577	1	1	2.31	ST4-74	635867	636316	-
<i>nfnB</i>	26	29	0.91	ST4-74	636516	637169	-
<i>ybdF</i>	9	9	0.98	ST4-74	637266	637634	-
<i>ramR</i>	39	37	1.05	ST4-74	637634	638215	-
<i>ramA</i>	13	12	1.06	ST4-74	638504	638845	+
<i>ybdJ</i>	24	17	1.36	ST4-74	638851	639099	-
<i>ybdK</i>	7	5	1.52	ST4-74	639166	640284	-
<i>entD</i>	11	5	2.11	ST4-74	640296	641000	-
<i>fepA</i>	8	5	1.65	ST4-74	641046	643301	-
<i>fes</i>	8	4	2.15	ST4-74	643490	644704	+
<i>ybdZ</i>	3	2	1.31	ST4-74	644735	644953	+
<i>entF</i>	4	4	1.26	ST4-74	644950	648834	+
<i>fepE</i>	45	43	1.04	ST4-74	649084	650220	+
<i>fepC</i>	4	3	1.14	ST4-74	650273	651067	-
<i>fepG</i>	4	3	1.26	ST4-74	651064	652053	-
<i>fepD</i>	8	4	1.94	ST4-74	652053	653060	-
<i>ybdA</i>	7	6	1.19	ST4-74	653171	654415	+
<i>fepB</i>	7	4	1.65	ST4-74	654478	655434	-
<i>entC</i>	4	3	1.24	ST4-74	655743	656918	+
<i>entE</i>	3	2	1.41	ST4-74	656928	658538	+
<i>entB</i>	3	2	1.51	ST4-74	658552	659409	+
<i>entA</i>	4	3	1.07	ST4-74	659409	660164	+
<i>ybdB</i>	5	3	1.98	ST4-74	660167	660580	+
<i>cstAa</i>	85	121	0.70	ST4-74	660762	662867	+
<i>ybdD</i>	109	122	0.89	ST4-74	662931	663128	+
<i>ybdH</i>	90	78	1.15	ST4-74	663164	664252	-
<i>ybdL</i>	49	51	0.95	ST4-74	664379	665539	+
<i>ybdM</i>	10	10	0.99	ST4-74	665540	666157	-
<i>ybdN</i>	14	13	1.08	ST4-74	666130	667365	-
<i>ybdO</i>	20	20	1.01	ST4-74	667531	668433	-
STnc3180	27	22	1.19	ST4-74	668611	668719	+
<i>dsbG</i>	14	15	0.90	ST4-74	668750	669496	-
STnc070	831	1959	0.42	ST4-74	669642	669793	+
<i>ahpC</i>	208	299	0.70	ST4-74	669937	670500	+
<i>ahpF</i>	24	33	0.75	ST4-74	670742	672307	+
STM0610	2	2	1.22	ST4-74	672639	673199	+
STM0611	3	3	1.20	ST4-74	673192	675471	+
STM0612	6	4	1.42	ST4-74	675468	676025	+
STM0613	22	20	1.08	ST4-74	676025	676792	+
<i>ybdQ</i>	697	505	1.38	ST4-74	676860	677288	-
<i>ybdR</i>	12	7	1.83	ST4-74	677511	678749	+
<i>rnk</i>	43	42	1.03	ST4-74	678832	679242	-
<i>sRNA10</i>	240	160	1.50	ST4-74	679315	679410	-

<i>Name</i>	Δfnr TPM	WT TPM	$\Delta fnr/WT$	<i>Chr</i> ^a	<i>Start</i>	<i>End</i>	<i>Strand</i>
<i>rna</i>	187	132	1.42	ST4-74	679477	680283	-
<i>citT</i>	12	40	0.30	ST4-74	680393	681856	-
<i>citG</i>	4	16	0.25	ST4-74	681894	682790	-
<i>citX</i>	5	26	0.19	ST4-74	682762	683313	-
<i>citF</i>	4	17	0.25	ST4-74	683317	684846	-
<i>citE</i>	3	10	0.27	ST4-74	684856	685764	-
<i>citD</i>	4	14	0.30	ST4-74	685761	686057	-
<i>citC</i>	20	39	0.50	ST4-74	686054	687130	-
<i>citA</i>	27	26	1.04	ST4-74	687515	689176	+
<i>citB</i>	13	19	0.71	ST4-74	689145	689825	+
STnc3550	37	42	0.88	ST4-74	689844	689990	-
<i>dcuC</i>	5	14	0.33	ST4-74	689879	691132	-
<i>pagP</i>	540	424	1.28	ST4-74	691643	692215	+
<i>cspE</i>	9609	8771	1.10	ST4-74	692400	692612	+
<i>ccrB</i>	114	86	1.33	ST4-74	692670	693053	-
STM0631	13	12	1.08	ST4-74	693144	693932	+
<i>tatE</i>	232	316	0.73	ST4-74	694061	694264	+
<i>lipA</i>	31	31	0.99	ST4-74	694350	695315	-
<i>ybeF</i>	55	36	1.55	ST4-74	695521	696474	-
<i>lipB</i>	27	25	1.10	ST4-74	696776	697417	-
<i>ybeD</i>	273	297	0.92	ST4-74	697517	697711	-
<i>dacA</i>	54	49	1.12	ST4-74	697889	699100	-
<i>rlpA</i>	22	25	0.87	ST4-74	699240	700307	-
<i>mrdB</i>	36	34	1.05	ST4-74	700318	701430	-
<i>mrdA</i>	21	23	0.92	ST4-74	701433	703334	-
<i>ybeA</i>	12	17	0.71	ST4-74	703365	703832	-
<i>ybeB</i>	28	34	0.83	ST4-74	703836	704153	-
<i>cobC</i>	14	12	1.16	ST4-74	704482	705090	-
<i>cobD</i>	7	11	0.64	ST4-74	705187	706281	+
<i>nadD</i>	10	12	0.83	ST4-74	706256	706897	-
<i>holA</i>	21	24	0.86	ST4-74	706899	707930	-
<i>rlpB</i>	66	64	1.03	ST4-74	707930	708520	-
<i>leuS</i>	50	48	1.03	ST4-74	708535	711117	-
STM0649	3	2	1.39	ST4-74	711405	711695	+
STM0650	4	4	1.08	ST4-74	711712	712884	+
STM0651	20	21	0.93	ST4-74	713003	713887	+
STM0652	19	20	0.95	ST4-74	713955	715883	+
<i>ybeL</i>	161	123	1.31	ST4-74	715976	716449	+
<i>ybeQ</i>	12	9	1.36	ST4-74	716488	717483	-
<i>ybeR</i>	4	4	1.08	ST4-74	717608	718315	+
<i>ybeS</i>	3	2	1.41	ST4-74	718312	719745	+
<i>ybeU</i>	5	4	1.30	ST4-74	719757	720453	+
<i>ybeV</i>	7	4	1.51	ST4-74	720450	721922	+
<i>hscC</i>	4	8	0.52	ST4-74	721944	723623	-
STM0660	6	6	0.93	ST4-74	723699	724937	-
<i>rihA</i>	9	11	0.84	ST4-74	724969	725904	-
<i>gltL</i>	15	19	0.75	ST4-74	726021	726746	-
<i>gltK</i>	20	24	0.86	ST4-74	726746	727420	-
<i>gltJ</i>	16	18	0.87	ST4-74	727420	728160	-
<i>SroC</i>	228	158	1.44	ST4-74	728172	728324	-
<i>gltI</i>	127	95	1.34	ST4-74	728320	729246	-

<i>Name</i>	Δfnr TPM	WT TPM	$\Delta fnr/WT$	<i>Chr^a</i>	<i>Start</i>	<i>End</i>	<i>Strand</i>
<i>lnt</i>	29	29	1.00	ST4-74	729583	731121	-
<i>ybeX</i>	75	69	1.09	ST4-74	731141	732019	-
<i>ybeY</i>	92	81	1.13	ST4-74	732177	732650	-
<i>phoL</i>	63	56	1.12	ST4-74	732647	733732	-
<i>miaB</i>	25	24	1.05	ST4-74	733898	735322	-
<i>ubiF</i>	24	23	1.04	ST4-74	735466	736641	+
STM0672	24	16	1.56	ST4-74	736708	737283	-
STnc3290	108	99	1.10	ST4-74	738320	738476	+
<i>asnB</i>	19	21	0.92	ST4-74	738350	740014	-
<i>nagD</i>	21	21	1.00	ST4-74	740304	741056	-
<i>nagC</i>	12	14	0.86	ST4-74	741103	742323	-
<i>nagA</i>	27	27	0.99	ST4-74	742328	743482	-
<i>nagB</i>	28	32	0.87	ST4-74	743542	744342	-
<i>nagE</i>	17	30	0.58	ST4-74	744669	746621	+
<i>glnS</i>	50	51	0.98	ST4-74	746832	748499	+
STnc3300	109	77	1.42	ST4-74	748530	748639	-
<i>ybfM</i>	29	39	0.75	ST4-74	748945	750351	+
<i>ybfN</i>	25	41	0.61	ST4-74	750401	750733	+
STM0689	11	8	1.37	ST4-74	750782	752086	-
STM0690	2	2	1.02	ST4-74	752137	753276	-
STM0691	3	3	1.21	ST4-74	753263	754666	-
STM0692	12	13	0.96	ST4-74	754764	755690	-
<i>fur</i>	295	280	1.05	ST4-74	755805	756257	-
<i>sRNA9</i>	337	284	1.19	ST4-74	756377	756436	-
<i>fldA</i>	187	179	1.04	ST4-74	756539	757069	-
<i>ybfE</i>	45	43	1.05	ST4-74	757232	757513	-
<i>ybfF</i>	23	24	0.94	ST4-74	757647	758417	-
<i>seqA</i>	76	77	0.99	ST4-74	758602	759144	+
<i>pgm</i>	40	46	0.86	ST4-74	759169	760809	+
STM0699	6	4	1.32	ST4-74	760924	761409	-
<i>potE</i>	4	4	1.09	ST4-74	761474	762793	-
<i>speF</i>	3	2	1.70	ST4-74	762790	764988	-
<i>kdpE</i>	10	8	1.23	ST4-74	765750	766427	-
<i>kdpD</i>	11	9	1.26	ST4-74	766424	769108	-
<i>kdpC</i>	7	6	1.05	ST4-74	769105	769689	-
<i>kdpB</i>	2	2	1.08	ST4-74	769698	771746	-
<i>kdpA</i>	3	3	1.19	ST4-74	771767	773446	-
<i>kdpF</i>	3	2	1.88	ST4-74	773446	773535	-
<i>ybfA</i>	333	227	1.47	ST4-74	773872	774078	+
<i>phrB</i>	13	8	1.70	ST4-74	774189	775610	+
<i>ybgH</i>	14	17	0.83	ST4-74	775649	777130	-
<i>ybgI</i>	41	41	1.01	ST4-74	777459	778202	+
<i>ybgJ</i>	12	14	0.87	ST4-74	778218	778874	+
<i>ybgK</i>	11	9	1.18	ST4-74	778868	779800	+
<i>ybgL</i>	17	17	0.99	ST4-74	779790	780524	+
STM0715	12	9	1.27	ST4-74	780848	780979	+
<i>fimB</i>	29	22	1.30	ST4-74	781039	781605	+
STM0717	5	5	0.97	ST4-74	782065	782400	+
STM0718	4	2	1.84	ST4-74	782402	783142	+
STM0719	2	2	1.27	ST4-74	783428	784579	+
STM0720	3	1	2.12	ST4-74	784576	785472	+

<i>Name</i>	Δfnr TPM	WT TPM	$\Delta fnr/WT$	Chr ^a	Start	End	Strand
STM0721	3	2	1.62	ST4-74	785485	786618	+
STM0722	5	4	1.33	ST4-74	786747	787517	+
STM0723	3	2	1.43	ST4-74	787521	788231	+
STM0724	3	3	1.31	ST4-74	788325	790103	+
STM0725	3	2	1.30	ST4-74	790296	791129	+
STM0726	3	3	1.22	ST4-74	791187	793082	+
STM0727	59	54	1.09	ST4-74	793150	793287	+
<i>nei</i>	15	18	0.86	ST4-74	793336	794127	+
<i>abrB</i>	9	7	1.33	ST4-74	794182	795144	-
<i>gltA</i>	65	78	0.83	ST4-74	795365	796648	-
STM0731	6	5	1.08	ST4-74	796623	796994	+
<i>sdhC</i>	101	118	0.86	ST4-74	797403	797792	+
<i>sdhD</i>	69	81	0.85	ST4-74	797786	798133	+
<i>sdhA</i>	30	40	0.75	ST4-74	798133	799899	+
<i>sdhB</i>	60	74	0.81	ST4-74	799913	800632	+
<i>sucA</i>	33	42	0.80	ST4-74	801156	803957	+
<i>sucB</i>	39	55	0.70	ST4-74	803972	805180	+
<i>sucC</i>	37	44	0.84	ST4-74	805322	806488	+
<i>sucD</i>	60	69	0.87	ST4-74	806488	807357	+
<i>RybD</i>	122	185	0.66	ST4-74	807346	807429	+
<i>cydA</i>	152	125	1.22	ST4-74	808940	810508	+
<i>cydB</i>	131	102	1.29	ST4-74	810524	811663	+
<i>ybgT</i>	362	226	1.60	ST4-74	811678	811791	+
<i>ybgE</i>	269	209	1.29	ST4-74	811928	812209	+
<i>ybgC</i>	68	60	1.15	ST4-74	812438	812842	+
<i>tolQ</i>	28	33	0.83	ST4-74	812839	813531	+
<i>tolR</i>	25	29	0.86	ST4-74	813535	813963	+
<i>tolA</i>	30	32	0.94	ST4-74	814028	815251	+
<i>tolB</i>	113	123	0.92	ST4-74	815375	816667	+
<i>pal</i>	206	289	0.71	ST4-74	816702	817226	+
<i>ybgF</i>	86	101	0.85	ST4-74	817236	818024	+
<i>nadA</i>	22	24	0.91	ST4-74	819489	820532	+
<i>pnuC</i>	36	39	0.92	ST4-74	820557	821276	+
<i>ybgR</i>	20	17	1.19	ST4-74	821273	822211	-
<i>ybgS</i>	114	53	2.14	ST4-74	822322	822708	-
<i>aroG</i>	127	105	1.21	ST4-74	823028	824080	+
STM0761	29	42	0.70	ST4-74	824174	824719	-
STM0762	22	38	0.58	ST4-74	824734	825579	-
STM0763	27	32	0.84	ST4-74	825709	826599	+
STM0764	10	11	0.93	ST4-74	826600	827526	-
STM0765	3	1	2.10	ST4-74	827806	829074	+
<i>dcoC</i>	4	4	1.16	ST4-74	829124	829369	+
<i>dcoA</i>	2	1	1.07	ST4-74	829385	831160	+
<i>dcoB</i>	3	3	1.04	ST4-74	831173	832474	+
STM0769	5	5	1.00	ST4-74	832593	833291	+
STM0770	6	6	1.13	ST4-74	833671	834750	+
STM0771	7	7	1.00	ST4-74	834750	835526	+
<i>gpmA</i>	309	243	1.27	ST4-74	835617	836369	-
<i>galM</i>	12	13	0.92	ST4-74	836593	837633	-
<i>galK</i>	14	15	0.94	ST4-74	837627	838775	-
<i>galT</i>	5	5	1.18	ST4-74	838778	839824	-

<i>Name</i>	Δ <i>fnr</i> TPM	WT TPM	Δ <i>fnr</i> /WT	Chr ^a	Start	End	Strand
<i>galE</i>	19	15	1.26	ST4-74	839835	840851	-
STM0777	4	5	0.88	ST4-74	841074	841982	-
<i>modF</i>	30	33	0.92	ST4-74	842153	843628	-
<i>modE</i>	18	16	1.09	ST4-74	843696	844484	-
<i>ybhT</i>	813	567	1.43	ST4-74	844613	844762	+
<i>modA</i>	50	105	0.47	ST4-74	844929	845702	+
<i>modB</i>	13	42	0.31	ST4-74	845702	846391	+
<i>modC</i>	10	28	0.37	ST4-74	846394	847452	+
<i>ybhA</i>	20	16	1.21	ST4-74	847453	848271	-
<i>ybhE</i>	26	21	1.22	ST4-74	848435	849430	+
<i>ybhC</i>	22	24	0.93	ST4-74	849574	850857	-
<i>hutI</i>	16	17	0.94	ST4-74	851095	852318	+
<i>hutG</i>	8	10	0.82	ST4-74	852315	853256	+
<i>hutC</i>	11	12	0.84	ST4-74	853349	854026	+
<i>hutU</i>	4	3	1.24	ST4-74	854223	855908	+
<i>hutH</i>	3	3	0.88	ST4-74	855910	857430	+
<i>ybhB</i>	87	67	1.30	ST4-74	857515	857991	-
<i>bioA</i>	69	45	1.52	ST4-74	858049	859338	-
<i>bioB</i>	110	81	1.36	ST4-74	859425	860465	+
<i>bioF</i>	45	41	1.10	ST4-74	860462	861619	+
<i>bioC</i>	31	31	0.99	ST4-74	861603	862358	+
<i>bioDa</i>	29	27	1.06	ST4-74	862351	863037	+
STnc3340	72	63	1.15	ST4-74	863329	863391	-
<i>uvrB</i>	21	21	1.03	ST4-74	863688	865709	+
<i>slrP</i>	23	15	1.49	ST4-74	866199	868496	+
<i>ybhK</i>	13	27	0.49	ST4-74	868588	869496	-
<i>moaA</i>	18	65	0.28	ST4-74	869893	870882	+
<i>moaB</i>	14	30	0.46	ST4-74	870904	871416	+
<i>moaC</i>	8	18	0.47	ST4-74	871419	871904	+
<i>moaD</i>	13	27	0.48	ST4-74	871891	872142	+
<i>moaE</i>	11	21	0.50	ST4-74	872144	872596	+
<i>ybhL</i>	176	164	1.07	ST4-74	872644	873348	+
<i>ybhM</i>	4	3	1.42	ST4-74	873495	874202	+
STM0809	4	6	0.69	ST4-74	874226	874834	+
STM0810	4	2	1.80	ST4-74	874842	875402	+
<i>ybhN</i>	18	11	1.61	ST4-74	875405	876367	-
<i>ybhO</i>	7	5	1.46	ST4-74	876367	877608	-
<i>ybhP</i>	20	8	2.53	ST4-74	877605	878363	-
<i>ybhQ</i>	403	358	1.13	ST4-74	878496	878906	+
<i>ybhR</i>	16	14	1.17	ST4-74	878868	879974	-
<i>ybhS</i>	14	11	1.29	ST4-74	880090	881220	-
<i>ybhF</i>	7	7	1.05	ST4-74	881213	882949	-
STM0818	8	8	0.99	ST4-74	882942	883937	-
<i>ybiH</i>	19	16	1.20	ST4-74	883937	884611	-
<i>rhIE</i>	7	5	1.23	ST4-74	884841	886205	+
<i>dinG</i>	13	11	1.11	ST4-74	886512	888557	+
<i>ybiB</i>	12	12	0.98	ST4-74	888587	889561	+
STnc980	44	18	2.46	ST4-74	889558	889714	-
<i>ybiJ</i>	12	8	1.45	ST4-74	889717	889977	-
<i>ybiI</i>	110	58	1.89	ST4-74	890262	890528	-
<i>ybiN</i>	9	10	0.86	ST4-74	890733	891665	+

<i>Name</i>	Δfnr TPM	WT TPM	$\Delta fnr/WT$	<i>Chr^a</i>	<i>Start</i>	<i>End</i>	<i>Strand</i>
<i>ybiO</i>	11	8	1.29	ST4-74	891662	893884	-
<i>glnQ</i>	36	37	0.96	ST4-74	894003	894725	-
<i>glnP</i>	34	40	0.84	ST4-74	894722	895381	-
<i>glnH</i>	126	134	0.94	ST4-74	895525	896271	-
<i>dps</i>	1063	692	1.54	ST4-74	896748	897251	-
<i>ybiF</i>	11	10	1.05	ST4-74	897554	898441	-
<i>ompX</i>	975	596	1.64	ST4-74	898795	899310	+
<i>ybiP</i>	10	10	0.99	ST4-74	899373	900953	-
<i>RybA</i>	597	429	1.39	ST4-74	901301	901397	-
STM0835	51	49	1.04	ST4-74	901532	902005	+
<i>ybiR</i>	13	12	1.10	ST4-74	902002	903114	+
<i>ybiS</i>	40	35	1.14	ST4-74	903158	904078	-
<i>ybiT</i>	39	33	1.16	ST4-74	904297	905889	+
STM0839	7	6	1.20	ST4-74	906498	907241	+
<i>ybiV(2)</i>	1	1	0.93	ST4-74	907270	907800	-
<i>ybiU</i>	3	2	1.37	ST4-74	908194	909459	-
<i>ybiV(1)</i>	31	22	1.41	ST4-74	909721	910530	+
<i>pflF</i>	1	2	0.79	ST4-74	910608	913040	-
<i>pflE</i>	2	3	0.52	ST4-74	913046	913945	-
<i>moeB</i>	8	10	0.83	ST4-74	914223	914972	-
<i>moeA</i>	12	13	0.96	ST4-74	914972	916213	-
<i>ybiK</i>	65	71	0.91	ST4-74	916410	917351	+
<i>yliA</i>	22	25	0.87	ST4-74	917362	919233	+
<i>yliB</i>	22	27	0.82	ST4-74	919266	920804	+
<i>yliC</i>	18	20	0.89	ST4-74	920865	921785	+
<i>yliD</i>	20	17	1.18	ST4-74	921788	922699	+
<i>rimO</i>	21	20	1.04	ST4-74	922790	924115	-
<i>bssR</i>	531	543	0.98	ST4-74	924346	924729	+
STnc1200	1244	1655	0.75	ST4-74	924769	924838	-
STM0854	3	2	1.42	ST4-74	925442	925957	+
STM0855	5	4	1.25	ST4-74	925875	926729	+
STM0856	3	3	0.92	ST4-74	926740	927687	+
STM0857	19	19	0.98	ST4-74	927981	929144	+
STM0858	6	5	1.24	ST4-74	929593	931278	+
STM0859	18	12	1.53	ST4-74	931284	932174	-
STnc1710	178	117	1.52	ST4-74	932197	932336	+
STM0860	41	28	1.45	ST4-74	932439	932864	-
<i>yliI</i>	5	4	1.17	ST4-74	933211	933891	+
<i>yliJ</i>	27	29	0.93	ST4-74	933888	934514	-
<i>dacC</i>	68	47	1.42	ST4-74	934758	935960	+
<i>deoR</i>	52	50	1.04	ST4-74	936005	936763	-
<i>ybjG</i>	66	71	0.93	ST4-74	936835	937443	-
<i>mdfA</i>	14	15	0.90	ST4-74	937756	938988	+
STM0867	9	12	0.76	ST4-74	939042	939857	-
STM0868	9	9	0.94	ST4-74	939854	941065	-
STM0869	6	5	1.28	ST4-74	941233	941853	+
<i>RybB</i>	1751	1341	1.31	ST4-74	941815	941893	-
STM0870	22	20	1.12	ST4-74	941970	943655	-
<i>ybjM</i>	28	29	0.98	ST4-74	943926	944303	+
<i>grxA</i>	768	870	0.88	ST4-74	944335	944598	-
<i>ybjC</i>	33	25	1.32	ST4-74	944768	945058	+

<i>Name</i>	Δ <i>fnr</i> TPM	WT TPM	Δ <i>fnr</i> /WT	Chr ^a	Start	End	Strand
<i>mdaA</i>	16	14	1.16	ST4-74	945105	945763	+
<i>rimK</i>	53	55	0.97	ST4-74	945821	946723	+
<i>ybjN</i>	35	30	1.19	ST4-74	946820	947296	+
<i>potF</i>	28	32	0.88	ST4-74	947645	948757	+
<i>potG</i>	20	24	0.84	ST4-74	948845	949978	+
<i>potH</i>	21	23	0.91	ST4-74	949988	950941	+
<i>potI</i>	32	36	0.90	ST4-74	950938	951783	+
<i>ybjO</i>	81	70	1.15	ST4-74	951857	952330	+
<i>rumB</i>	10	7	1.37	ST4-74	952373	953503	+
STM0884	5	4	1.19	ST4-74	953786	955129	+
STM0885	9	8	1.14	ST4-74	955159	955479	+
STM0886	7	5	1.33	ST4-74	955489	956976	+
<i>artJ</i>	115	302	0.38	ST4-74	957195	957926	-
<i>artM</i>	79	80	1.00	ST4-74	958163	958831	-
<i>artQ</i>	52	70	0.75	ST4-74	958831	959547	-
<i>artI</i>	65	80	0.81	ST4-74	959554	960285	-
<i>artP</i>	185	178	1.04	ST4-74	960303	961031	-
<i>ybjP</i>	64	57	1.12	ST4-74	961261	961776	-
STM0930	114	87	1.31	ST4-74	961904	962227	+
<i>ybjR</i>	31	29	1.09	ST4-74	962224	963054	+
STM0932	19	19	1.00	ST4-74	963051	964064	-
<i>ybjT</i>	10	11	0.94	ST4-74	964160	965593	-
<i>ltaA</i>	53	45	1.17	ST4-74	965604	966605	-
<i>poxB</i>	15	10	1.55	ST4-74	966644	968362	-
<i>hcr</i>	8	8	1.00	ST4-74	968520	969491	-
<i>hcp</i>	5	6	0.78	ST4-74	969500	971152	-
<i>ybjE</i>	26	35	0.74	ST4-74	971296	972087	-
<i>ybjD</i>	14	14	0.99	ST4-74	972397	974055	+
<i>ybjX</i>	362	307	1.18	ST4-74	974052	975020	-
<i>ybjY</i>	51	43	1.17	ST4-74	975148	976266	+
<i>ybjZ</i>	37	33	1.15	ST4-74	976263	978209	+
<i>cspD</i>	952	1539	0.62	ST4-74	978339	978560	-
<i>clpS</i>	244	248	0.98	ST4-74	978884	979204	+
<i>clpA</i>	54	66	0.82	ST4-74	979235	981511	+
STnc490	24696	33984	0.73	ST4-74	981622	981711	-
<i>tnp</i>	244	250	0.98	ST4-74	981703	982161	+
STM0947	6	5	1.26	ST4-74	982624	983307	-
STM0948	17	9	1.92	ST4-74	983478	983879	-
STM0950	9	8	1.18	ST4-74	984216	984893	-
STM0951	5	4	1.24	ST4-74	984913	985773	-
STM0952	7	7	0.90	ST4-74	985882	986793	+
<i>infA</i>	298	337	0.88	ST4-74	986884	987102	-
STM0954	604	529	1.14	ST4-74	987030	987359	-
<i>aat</i>	33	26	1.25	ST4-74	987414	988118	-
<i>cydC</i>	23	31	0.76	ST4-74	988163	989884	-
<i>cydD</i>	26	34	0.78	ST4-74	989885	991651	-
<i>trxB</i>	88	86	1.02	ST4-74	991765	992733	-
<i>lrp</i>	333	380	0.88	ST4-74	993279	993773	+
<i>fisK</i>	119	136	0.88	ST4-74	993908	997993	+
<i>lolA</i>	82	90	0.91	ST4-74	998133	998747	+
<i>ycaJ</i>	33	37	0.88	ST4-74	998757	1000100	+

<i>Name</i>	Δfnr TPM	WT TPM	$\Delta fnr/WT$	Chr ^a	Start	End	Strand
<i>serS</i>	48	70	0.69	ST4-74	1000359	1001651	+
<i>dmsA</i>	3	52	0.06	ST4-74	1001888	1004332	+
<i>dmsB</i>	3	46	0.06	ST4-74	1004343	1004960	+
<i>dmsC</i>	10	57	0.18	ST4-74	1004962	1005825	+
<i>ycaD</i>	22	19	1.14	ST4-74	1006175	1007323	+
<i>ycaM</i>	16	14	1.14	ST4-74	1007541	1008962	+
STnc3310	108	94	1.15	ST4-74	1009199	1009379	-
<i>pflA</i>	34	31	1.07	ST4-74	1009255	1010079	-
STM0971	109	102	1.07	ST4-74	1010171	1010497	-
<i>sopD2</i>	752	96	7.86	ST4-74	1010628	1011587	+
<i>pflB</i>	76	143	0.53	ST4-74	1011663	1013945	-
<i>focA</i>	126	194	0.65	ST4-74	1014005	1014862	-
<i>ycaO</i>	13	11	1.13	ST4-74	1015267	1017027	-
<i>ycaP</i>	25	16	1.59	ST4-74	1017164	1017856	+
<i>serC</i>	133	126	1.05	ST4-74	1018042	1019130	+
<i>aroA</i>	28	34	0.83	ST4-74	1019201	1020484	+
<i>ycaL</i>	19	19	1.04	ST4-74	1020627	1021388	+
<i>cmk</i>	119	103	1.15	ST4-74	1021561	1022244	+
<i>rpsA</i>	297	358	0.83	ST4-74	1022358	1024031	+
<i>himD</i>	267	272	0.98	ST4-74	1024187	1024471	+
STnc3330	13	11	1.22	ST4-74	1024493	1024591	-
<i>rec2</i>	6	5	1.21	ST4-74	1024701	1026965	+
<i>msbA</i>	48	50	0.95	ST4-74	1027002	1028750	+
<i>lpxK</i>	24	31	0.78	ST4-74	1028747	1029724	+
<i>ycaQ</i>	6	8	0.76	ST4-74	1029768	1031000	+
<i>ycaR</i>	122	111	1.11	ST4-74	1031052	1031234	+
<i>kdsB</i>	13	16	0.79	ST4-74	1031231	1031977	+
STM0989	15	38	0.39	ST4-74	1032188	1033081	+
<i>ycbC</i>	6	7	0.83	ST4-74	1033061	1033837	-
<i>smtA</i>	24	27	0.89	ST4-74	1033973	1034776	+
<i>mukF</i>	14	20	0.73	ST4-74	1034769	1036091	+
<i>mukE</i>	21	28	0.74	ST4-74	1036072	1036776	+
<i>mukB</i>	28	31	0.89	ST4-74	1036776	1041242	+
<i>ycbB</i>	38	34	1.12	ST4-74	1041587	1043428	+
<i>ycbK</i>	87	113	0.77	ST4-74	1043688	1044236	+
<i>ycbL</i>	68	95	0.72	ST4-74	1044264	1044911	+
<i>aspC</i>	72	79	0.92	ST4-74	1044973	1046163	-
<i>ompF</i>	299	372	0.81	ST4-74	1046348	1047439	-
STnc3350	92	48	1.92	ST4-74	1047936	1048028	+
<i>asnCa</i>	99	122	0.81	ST4-74	1048046	1049446	-
STM1001	27	36	0.76	ST4-74	1049647	1050108	-
<i>dpaL</i>	4	4	1.12	ST4-74	1050425	1051639	+
STM1003	3	3	0.95	ST4-74	1051884	1053320	+
<i>pncB</i>	30	29	1.03	ST4-74	1053398	1054600	-
STM1005	53	52	1.03	ST4-74	1054795	1056087	-
STnc4200	308	199	1.55	ST4-74	1055773	1055892	+
STM1006	1	1	0.99	ST4-74	1056132	1056380	-
STM1007	3	2	1.69	ST4-74	1056421	1056660	-
STM1008	3	3	0.82	ST4-74	1056703	1057812	-
<i>recEa</i>	1	1	1.26	ST4-74	1057823	1060708	-
<i>IsrB-2</i>	0	0	-	ST4-74	1060740	1060833	-

<i>Name</i>	Δ <i>fnr</i> TPM	WT TPM	Δ <i>fnr</i> /WT	Chr ^a	Start	End	Strand
<i>IsrB-1</i>	663	1160	0.57	ST4-74	1060741	1060835	+
STM1010	0	1	0.46	ST4-74	1060835	1061134	-
STM2630	0	0	0.00	ST4-74	1061156	1061314	-
STM1011	0	1	0.22	ST4-74	1061307	1061567	-
STM1012	211	178	1.18	ST4-74	1061617	1061958	-
<i>Cl</i>	2	2	0.84	ST4-74	1062352	1062726	+
STnc1080	2025	2577	0.79	ST4-74	1062745	1062806	-
STM2626	2	1	1.35	ST4-74	1062811	1063794	+
STM1015	1	2	0.96	ST4-74	1063797	1064546	+
STM2624	1	2	0.79	ST4-74	1064557	1064904	+
STM2623	22	20	1.06	ST4-74	1064901	1065212	+
STM2622	388	315	1.23	ST4-74	1065290	1065580	+
STM1019	80	85	0.94	ST4-74	1065872	1066105	+
STM1020	28	25	1.10	ST4-74	1066521	1067123	+
<i>ninG</i>	1	2	0.83	ST4-74	1067332	1067943	+
SL1344_0960	0	1	0.00	ST4-74	1067940	1068086	+
STM1022	9	7	1.29	ST4-74	1068076	1068873	+
STM1023	135	125	1.07	ST4-74	1068940	1069257	+
STM1024	3	2	1.27	ST4-74	1069431	1069556	+
STM1025	14	29	0.48	ST4-74	1069692	1070141	-
<i>gtgA</i>	31	25	1.24	ST4-74	1070502	1071188	-
STM2613	6	6	0.97	ST4-74	1071458	1071793	+
<i>nucD</i>	8	6	1.39	ST4-74	1071777	1072229	+
STM1029	1	1	0.93	ST4-74	1072226	1072726	+
STM1030	4	5	0.81	ST4-74	1072934	1073467	+
STM1031	4	3	1.18	ST4-74	1073508	1075562	+
STM1032	3	4	0.93	ST4-74	1075762	1077309	+
STM1033	3	3	0.83	ST4-74	1077233	1079314	+
STM1034	2	1	1.93	ST4-74	1079405	1079728	+
STM1035	2	2	0.98	ST4-74	1079721	1080020	+
STM1036	3	2	1.23	ST4-74	1080001	1080567	+
STM1037	3	3	0.92	ST4-74	1080564	1080965	+
STM1038	3	3	0.87	ST4-74	1081040	1081726	+
STM1039	2	2	0.80	ST4-74	1081772	1082170	+
STM1040	3	2	1.12	ST4-74	1082233	1082496	+
STM1041	4	4	1.04	ST4-74	1082510	1085563	+
STM1042	5	5	1.05	ST4-74	1085560	1085892	+
STM1043	23	19	1.23	ST4-74	1085991	1086488	+
<i>sodCa</i>	222	183	1.22	ST4-74	1086605	1087138	-
STM1045	8	9	0.81	ST4-74	1087228	1087923	+
STM1046	2	3	0.93	ST4-74	1087933	1088670	+
STM1047	3	2	1.10	ST4-74	1088568	1089272	+
STM1048	4	3	1.23	ST4-74	1089344	1092694	+
STM1049	3	2	1.25	ST4-74	1093029	1095236	+
STM1050	4	5	0.93	ST4-74	1095236	1095817	+
SL1344_0990	8	6	1.42	ST4-74	1095821	1096036	-
<i>sseI</i>	14	8	1.83	ST4-74	1096293	1097261	+
STM1052	14	11	1.31	ST4-74	1097359	1097777	+
STM1053	4	2	1.76	ST4-74	1097909	1098535	-
STM1054	346	376	0.92	ST4-74	1098604	1098903	-
<i>gtgE</i>	160	108	1.48	ST4-74	1098888	1099574	-

<i>Name</i>	Δfnr TPM	WT TPM	$\Delta fnr/WT$	<i>Chr^a</i>	<i>Start</i>	<i>End</i>	<i>Strand</i>
<i>gtgF</i>	10	7	1.35	ST4-74	1099845	1100036	-
<i>pepN</i>	23	20	1.13	ST4-74	1100463	1103075	+
<i>pyrD</i>	15	20	0.71	ST4-74	1103256	1104293	+
<i>ycbW</i>	93	92	1.01	ST4-74	1104459	1105001	+
STM1060	15	16	0.94	ST4-74	1104998	1106107	-
<i>rlmL</i>	18	18	1.02	ST4-74	1106206	1108314	+
<i>uup</i>	16	17	0.98	ST4-74	1108327	1110234	+
<i>pqiA</i>	23	22	1.04	ST4-74	1110249	1111502	+
<i>pqiB</i>	21	21	0.99	ST4-74	1111507	1113147	+
<i>ymbA</i>	39	29	1.36	ST4-74	1113144	1113707	+
STnc3390	15	18	0.84	ST4-74	1113731	1113815	-
<i>rmf</i>	4912	6233	0.79	ST4-74	1113963	1114130	+
<i>fabA</i>	149	155	0.96	ST4-74	1114230	1114748	-
<i>lonH</i>	18	18	1.03	ST4-74	1114817	1116403	-
<i>ycbG</i>	78	89	0.88	ST4-74	1116763	1117215	+
<i>ompA</i>	523	496	1.05	ST4-74	1117287	1118339	-
<i>sulA</i>	25	24	1.02	ST4-74	1118696	1119205	-
<i>sxy</i>	11	13	0.81	ST4-74	1119422	1120027	+
<i>yccS</i>	17	19	0.89	ST4-74	1120014	1122167	-
<i>yccF</i>	19	18	1.06	ST4-74	1122186	1122632	-
<i>helD</i>	25	24	1.02	ST4-74	1122756	1124810	+
<i>mgsA</i>	51	87	0.59	ST4-74	1124846	1125304	-
<i>yccT</i>	20	11	1.81	ST4-74	1125399	1126061	-
STM1078	47	43	1.09	ST4-74	1126232	1126648	+
<i>yccV</i>	81	83	0.98	ST4-74	1126693	1127010	-
<i>yccW</i>	15	12	1.21	ST4-74	1127068	1128279	-
STM1081	9	10	0.83	ST4-74	1128494	1129042	+
STM1082	17	16	1.06	ST4-74	1129068	1129847	+
<i>yccX</i>	9	10	0.96	ST4-74	1129896	1130177	+
<i>yccK</i>	63	61	1.04	ST4-74	1130174	1130503	-
<i>yccA</i>	260	288	0.90	ST4-74	1130590	1131168	-
<i>pipA</i>	46	33	1.39	ST4-74	1131870	1132550	-
<i>pipB</i>	89	10	8.47	ST4-74	1132772	1133647	-
STM1089	1	0	3.21	ST4-74	1133859	1134185	+
<i>pipC</i>	56	75	0.75	ST4-74	1134195	1134536	-
<i>sopB</i>	14	18	0.77	ST4-74	1134553	1136238	-
<i>orfX</i>	18	1109	0.02	ST4-74	1136570	1136740	+
STM1093	40	31	1.29	ST4-74	1136741	1136851	-
<i>pipD</i>	66	52	1.27	ST4-74	1136960	1138429	-
<i>copS</i>	6	7	0.93	ST4-74	1138602	1139966	-
<i>copR</i>	28	21	1.33	ST4-74	1139959	1140705	-
STM1097	76	79	0.96	ST4-74	1140775	1141185	+
<i>hpaC</i>	5	4	1.11	ST4-74	1141518	1142030	-
<i>hpaB</i>	4	3	1.05	ST4-74	1142048	1143610	-
<i>hpaR</i>	6	6	1.09	ST4-74	1143828	1144268	-
<i>hpaG</i>	2	2	0.92	ST4-74	1144543	1145832	+
<i>hpaE</i>	2	2	1.14	ST4-74	1145829	1147295	+
<i>hpaD</i>	1	2	0.49	ST4-74	1147297	1148148	+
<i>hpaF</i>	1	3	0.29	ST4-74	1148158	1148538	+
<i>hpaH</i>	1	2	0.77	ST4-74	1148681	1149484	+
<i>hpaI</i>	2	2	0.92	ST4-74	1149495	1150286	+

<i>Name</i>	Δ <i>fnr</i> TPM	WT TPM	Δ <i>fnr</i> /WT	Chr ^a	Start	End	Strand
<i>hpaX</i>	4	4	1.08	ST4-74	1150358	1151734	+
<i>hpaA</i>	2	2	0.98	ST4-74	1151744	1152640	+
STM1109	9	8	1.16	ST4-74	1152675	1153592	+
STnc1880	169	115	1.46	ST4-74	1153745	1153841	+
STM1110	20	7	3.04	ST4-74	1154000	1154362	-
STnc3400	40	31	1.29	ST4-74	1154915	1154976	+
<i>yccD</i>	58	50	1.15	ST4-74	1155016	1155321	-
<i>cbpA</i>	32	36	0.90	ST4-74	1155321	1156241	-
<i>scsA</i>	232	189	1.22	ST4-74	1156476	1156838	+
<i>scsB</i>	3	3	0.92	ST4-74	1156887	1158773	+
<i>scsC</i>	3	3	1.23	ST4-74	1158770	1159393	+
<i>scsD</i>	3	3	1.12	ST4-74	1159383	1159889	+
<i>agp</i>	24	27	0.89	ST4-74	1160022	1161263	+
<i>yccJ</i>	218	229	0.95	ST4-74	1161297	1161524	-
<i>wrbA</i>	128	133	0.96	ST4-74	1161545	1162141	-
<i>ymdF</i>	1005	953	1.05	ST4-74	1162526	1162693	+
<i>ydcC</i>	19	20	0.92	ST4-74	1162830	1163468	+
STM1123	70	63	1.11	ST4-74	1163465	1163860	-
<i>putA</i>	6	12	0.49	ST4-74	1163919	1167881	-
<i>putP</i>	15	23	0.65	ST4-74	1168303	1169811	+
<i>phoH</i>	23	18	1.32	ST4-74	1170638	1171492	+
STM1127	33	31	1.07	ST4-74	1171598	1172479	-
STnc500	724	611	1.19	ST4-74	1172561	1172641	-
STM1128	6	7	0.84	ST4-74	1172764	1174260	-
STM1129	4	6	0.66	ST4-74	1174597	1175277	-
STM1130	6	8	0.75	ST4-74	1175783	1176943	+
STM1131	9	11	0.77	ST4-74	1176989	1177681	+
STM1132	11	10	1.05	ST4-74	1177964	1179244	+
STM1133	22	22	1.00	ST4-74	1179255	1180361	+
<i>ydcW</i>	19	21	0.89	ST4-74	1181205	1182143	+
<i>ydcX</i>	77	71	1.10	ST4-74	1182228	1182965	+
<i>ydcY</i>	21	21	1.00	ST4-74	1182989	1183543	+
<i>ydcZ</i>	31	36	0.87	ST4-74	1183653	1184126	+
<i>csgG</i>	12	8	1.46	ST4-74	1184165	1184911	-
<i>csgF</i>	2	2	1.22	ST4-74	1185025	1185441	-
<i>csgE</i>	5	5	1.06	ST4-74	1185468	1185863	-
<i>csgD</i>	9	8	1.05	ST4-74	1185868	1186518	-
<i>csgB</i>	2	8	0.29	ST4-74	1187273	1187728	+
<i>csgA</i>	3	5	0.50	ST4-74	1187770	1188225	+
<i>csgC</i>	33	57	0.57	ST4-74	1188287	1188613	+
<i>ymdA</i>	10	27	0.37	ST4-74	1188744	1189064	+
STM1147	34	30	1.12	ST4-74	1189154	1189693	+
<i>ymdC</i>	27	22	1.23	ST4-74	1189629	1191116	+
<i>mdoC</i>	16	13	1.24	ST4-74	1191133	1192287	-
<i>mdoG</i>	52	48	1.07	ST4-74	1192559	1194094	+
<i>mdoH</i>	42	45	0.93	ST4-74	1194087	1196630	+
<i>yceK</i>	12	10	1.20	ST4-74	1196704	1196931	+
<i>msyB</i>	180	112	1.61	ST4-74	1196932	1197306	-
<i>yceE</i>	7	6	1.16	ST4-74	1197388	1198602	-
STnc3040	12	13	0.95	ST4-74	1198646	1198752	+
<i>htrB</i>	39	36	1.11	ST4-74	1198757	1199677	-

<i>Name</i>	Δfnr TPM	WT TPM	$\Delta fnr/WT$	Chr ^a	Start	End	Strand
<i>yceA</i>	21	15	1.41	ST4-74	1199897	1200949	+
<i>yceI</i>	19	10	1.84	ST4-74	1201001	1201576	-
<i>yceJ</i>	24	14	1.76	ST4-74	1201573	1202145	-
<i>yceO</i>	24	18	1.34	ST4-74	1202408	1202521	-
<i>solA</i>	17	21	0.85	ST4-74	1202562	1203680	-
<i>bssS</i>	265	233	1.14	ST4-74	1203793	1204050	-
<i>dinI</i>	69	92	0.75	ST4-74	1204337	1204582	-
<i>pyrC</i>	34	44	0.78	ST4-74	1204656	1205702	-
<i>yceB</i>	191	157	1.22	ST4-74	1205807	1206367	-
<i>grxB</i>	167	139	1.20	ST4-74	1206492	1207139	-
<i>yceL</i>	40	41	0.99	ST4-74	1207203	1208411	-
<i>rimJ</i>	72	87	0.83	ST4-74	1208648	1209232	+
<i>yceH</i>	33	46	0.70	ST4-74	1209268	1209915	+
<i>mviM</i>	17	23	0.72	ST4-74	1209917	1210840	+
<i>mviN</i>	17	18	0.95	ST4-74	1211105	1212679	+
<i>flgN</i>	53	236	0.22	ST4-74	1212761	1213183	-
<i>flgM</i>	162	713	0.23	ST4-74	1213188	1213481	-
<i>flgA</i>	21	84	0.24	ST4-74	1213573	1214232	-
<i>flgB</i>	59	251	0.23	ST4-74	1214389	1214805	+
<i>flgC</i>	14	75	0.18	ST4-74	1214809	1215213	+
<i>flgD</i>	15	83	0.18	ST4-74	1215225	1215923	+
<i>flgE</i>	13	71	0.18	ST4-74	1215950	1217161	+
<i>flgF</i>	12	72	0.16	ST4-74	1217182	1217937	+
<i>flgG</i>	12	64	0.19	ST4-74	1217951	1218733	+
<i>flgH</i>	12	57	0.22	ST4-74	1218788	1219486	+
<i>flgI</i>	9	42	0.22	ST4-74	1219498	1220595	+
<i>flgJ</i>	8	35	0.23	ST4-74	1220595	1221545	+
<i>flgK</i>	41	162	0.25	ST4-74	1221610	1223271	+
<i>flgL</i>	37	157	0.24	ST4-74	1223286	1224239	+
STnc840	145	661	0.22	ST4-74	1224244	1224316	+
<i>rne</i>	26	40	0.66	ST4-74	1224496	1227699	-
<i>rhuC</i>	29	23	1.25	ST4-74	1228273	1229232	+
STM1188	24	23	1.03	ST4-74	1229388	1230131	+
SL1344_1125	21	25	0.84	ST4-74	1230337	1230561	+
<i>maf-a</i>	30	32	0.93	ST4-74	1230633	1231217	-
<i>SraB</i>	287	251	1.14	ST4-74	1231270	1231378	+
<i>yceD</i>	668	790	0.85	ST4-74	1231415	1231936	+
<i>rpl32</i>	581	802	0.72	ST4-74	1231988	1232161	+
<i>plsX</i>	67	87	0.77	ST4-74	1232295	1233374	+
<i>fabH</i>	35	39	0.89	ST4-74	1233454	1234407	+
<i>fabD</i>	75	71	1.06	ST4-74	1234423	1235352	+
<i>fabG</i>	206	223	0.92	ST4-74	1235365	1236099	+
<i>acpP</i>	5755	6292	0.91	ST4-74	1236255	1236491	+
<i>fabF</i>	54	77	0.71	ST4-74	1236577	1237818	+
<i>pabC</i>	21	20	1.05	ST4-74	1237942	1238751	+
<i>yceG</i>	27	26	1.05	ST4-74	1238820	1239776	+
<i>tmk</i>	18	19	0.98	ST4-74	1239766	1240407	+
<i>holB</i>	12	14	0.85	ST4-74	1240404	1241408	+
<i>ycfH</i>	70	38	1.82	ST4-74	1241419	1242216	+
<i>ptsG</i>	53	61	0.86	ST4-74	1242511	1243944	+
<i>fhuE</i>	4	3	1.59	ST4-74	1244029	1246203	-

<i>Name</i>	Δ <i>fnr</i> TPM	WT TPM	Δ <i>fnr</i> /WT	Chr ^a	Start	End	Strand
<i>ycfF</i>	152	132	1.15	ST4-74	1246545	1246904	+
<i>ycfL</i>	46	52	0.90	ST4-74	1246907	1247281	+
<i>ycfM</i>	39	39	1.01	ST4-74	1247295	1247933	+
<i>thiK</i>	26	22	1.17	ST4-74	1247914	1248738	+
<i>nagZ</i>	30	48	0.63	ST4-74	1248749	1249774	+
<i>ycfP</i>	56	78	0.72	ST4-74	1249799	1250341	+
<i>ndh</i>	49	27	1.77	ST4-74	1250596	1251900	+
<i>ycfJ</i>	35	18	1.92	ST4-74	1252079	1252618	+
STnc1090	141	103	1.38	ST4-74	1252560	1252626	-
STnc850	123	78	1.58	ST4-74	1252598	1252673	+
<i>ycfQ</i>	83	63	1.33	ST4-74	1252693	1253328	-
<i>ycfR</i>	27	25	1.09	ST4-74	1253570	1253827	+
<i>ycfS</i>	29	35	0.83	ST4-74	1253924	1254889	-
STnc3410	92	115	0.80	ST4-74	1254996	1255077	-
<i>mfd</i>	16	15	1.10	ST4-74	1255037	1258483	-
<i>ycfU</i>	56	55	1.00	ST4-74	1258821	1260020	+
<i>lolD</i>	18	20	0.90	ST4-74	1260013	1260714	+
<i>ycfW</i>	23	28	0.83	ST4-74	1260714	1261958	+
<i>ycfX</i>	35	38	0.92	ST4-74	1261987	1262898	+
<i>cobB</i>	44	49	0.90	ST4-74	1262917	1263738	+
<i>potD</i>	37	42	0.89	ST4-74	1263820	1264866	-
<i>potC</i>	35	35	1.00	ST4-74	1264891	1265670	-
<i>sifA</i>	36	15	2.42	ST4-74	1265986	1266996	-
<i>potB</i>	19	15	1.25	ST4-74	1267325	1268188	-
<i>potA</i>	33	31	1.05	ST4-74	1268172	1269308	-
<i>pepT</i>	18	72	0.25	ST4-74	1269559	1270788	+
STM1228	21	32	0.65	ST4-74	1270792	1272837	+
STM3032	217	230	0.94	ST4-74	1270948	1271457	+
<i>ycfD</i>	39	37	1.05	ST4-74	1272877	1273998	-
<i>phoQ</i>	151	143	1.06	ST4-74	1274079	1275542	-
<i>phoP</i>	618	491	1.26	ST4-74	1275542	1276216	-
<i>purB</i>	22	27	0.81	ST4-74	1276340	1277710	-
<i>ycfC</i>	33	39	0.84	ST4-74	1277714	1278361	-
<i>mmA</i>	71	66	1.07	ST4-74	1278442	1279548	-
<i>ymfB</i>	8	10	0.81	ST4-74	1279602	1280063	-
STM1236	9	10	0.98	ST4-74	1280075	1280404	-
<i>rluB</i>	53	34	1.55	ST4-74	1280401	1281066	-
<i>icdA</i>	176	194	0.91	ST4-74	1281238	1282488	+
STnc150	235	106	2.21	ST4-74	1282521	1282677	-
STM1239	37	21	1.77	ST4-74	1282936	1284060	+
<i>envF</i>	7	4	1.74	ST4-74	1285042	1285830	-
<i>IsrC</i>	11	12	0.94	ST4-74	1285998	1286285	+
<i>msgA</i>	152	142	1.07	ST4-74	1286319	1286558	-
<i>envE</i>	78	51	1.55	ST4-74	1286749	1287270	-
<i>cspH</i>	102	50	2.05	ST4-74	1287685	1287897	-
<i>pagD</i>	180	42	4.26	ST4-74	1288029	1288292	-
<i>pagC</i>	2814	701	4.02	ST4-74	1289191	1289661	+
STnc3420	37	25	1.49	ST4-74	1289667	1289799	-
STnc520	320	368	0.87	ST4-74	1290590	1290674	-
<i>pliC</i>	945	489	1.93	ST4-74	1290898	1291242	-
STM1250	40	29	1.41	ST4-74	1291945	1292217	+

<i>Name</i>	Δ <i>fnr</i> TPM	WT TPM	Δ <i>fnr</i> /WT	<i>Chr</i> ^a	<i>Start</i>	<i>End</i>	<i>Strand</i>
STM1251	334	215	1.55	ST4-74	1292369	1292836	+
STnc1760	76	52	1.48	ST4-74	1292835	1292935	-
STnc1210	296	516	0.57	ST4-74	1292956	1293014	+
STM1252	24	16	1.47	ST4-74	1293175	1294218	+
STM1253	60	68	0.88	ST4-74	1294301	1294831	-
STnc1990	228	156	1.46	ST4-74	1294841	1294974	+
STnc3430	38	37	1.03	ST4-74	1294946	1295057	-
STM1254	102	103	0.99	ST4-74	1294980	1295294	-
STM1255	10	115	0.08	ST4-74	1295976	1297610	+
STM1256	6	48	0.12	ST4-74	1297610	1298584	+
STM1257	5	34	0.16	ST4-74	1298574	1299386	+
STM1258	3	21	0.15	ST4-74	1299380	1300177	+
STM1259	3	28	0.09	ST4-74	1300171	1300761	+
STM1260	32	18	1.76	ST4-74	1300843	1301976	-
STM1261	53	33	1.59	ST4-74	1302170	1302496	+
<i>IsrD</i>	2	2	1.08	ST4-74	1302591	1302641	-
STM1263	58	29	2.01	ST4-74	1302693	1303340	+
STnc3440	22	10	2.11	ST4-74	1303294	1303380	+
<i>aadA</i>	20	21	0.99	ST4-74	1303449	1304237	+
STM1265	25	11	2.27	ST4-74	1304382	1304975	+
STM1266	41	36	1.17	ST4-74	1305044	1305892	+
STM1267	956	311	3.07	ST4-74	1306147	1306395	-
STM1268	80	84	0.96	ST4-74	1306474	1306623	-
<i>aroQ</i>	305	225	1.35	ST4-74	1306706	1307251	+
<i>yeaS</i>	153	130	1.18	ST4-74	1307448	1308086	+
<i>yeaR</i>	29	22	1.30	ST4-74	1308259	1308620	+
<i>yoaG</i>	64	37	1.73	ST4-74	1308623	1308805	+
STM1273	12	9	1.41	ST4-74	1309035	1309676	+
<i>RyhB-2</i>	118	51	2.31	ST4-74	1309727	1309937	-
SL1344_1209	358	219	1.64	ST4-74	1309798	1309983	+
<i>yeaQ</i>	421	268	1.57	ST4-74	1309991	1310239	+
<i>yaoF</i>	135	82	1.65	ST4-74	1310672	1310923	+
STM1276	130	113	1.15	ST4-74	1310992	1311303	+
<i>yeaO</i>	40	38	1.05	ST4-74	1311289	1311636	-
<i>yeaN</i>	5	4	1.15	ST4-74	1311755	1312939	-
<i>yeaM</i>	18	15	1.14	ST4-74	1313040	1313834	+
<i>yeaL</i>	11	12	0.90	ST4-74	1313814	1314260	-
<i>yeaK</i>	14	13	1.05	ST4-74	1314570	1315088	-
<i>yeaJ</i>	28	23	1.25	ST4-74	1315138	1316631	-
STnc1480	833	328	2.54	ST4-74	1316874	1317268	+
<i>yeaH</i>	60	41	1.44	ST4-74	1317272	1318558	-
<i>yeaG</i>	61	33	1.85	ST4-74	1318681	1320465	-
<i>mipA</i>	179	174	1.03	ST4-74	1321042	1321788	+
STM1287	5	4	1.12	ST4-74	1322078	1323274	+
STM1288	16	16	0.99	ST4-74	1323371	1324228	+
<i>yeaD</i>	10	13	0.73	ST4-74	1324327	1325211	-
SL1344_1224A	10	18	0.54	ST4-74	1325211	1325465	-
<i>gapA</i>	223	404	0.55	ST4-74	1325546	1326541	-
<i>yeaA</i>	142	145	0.98	ST4-74	1326853	1327296	+
<i>yeaC</i>	133	153	0.87	ST4-74	1327338	1327616	+
<i>nam</i>	11	11	1.05	ST4-74	1327968	1328624	-

<i>Name</i>	Δ <i>fnr</i> TPM	WT TPM	Δ <i>fnr</i> /WT	Chr ^a	Start	End	Strand
<i>ansA</i>	14	33	0.43	ST4-74	1328651	1329667	-
<i>sppA</i>	22	21	1.02	ST4-74	1329763	1331619	-
<i>ydjA</i>	31	36	0.87	ST4-74	1331793	1332344	+
<i>selD</i>	14	16	0.91	ST4-74	1332462	1333505	+
<i>topB</i>	9	12	0.81	ST4-74	1333510	1335459	+
<i>gdhA</i>	26	62	0.41	ST4-74	1335489	1336832	-
STM1300	122	370	0.33	ST4-74	1337071	1337346	+
STM1301	4	3	1.40	ST4-74	1337306	1337722	-
<i>xthA</i>	20	24	0.84	ST4-74	1337795	1338601	-
<i>argDa</i>	2	2	0.94	ST4-74	1339047	1340273	+
<i>astA</i>	2	2	0.95	ST4-74	1340264	1341298	+
<i>astD</i>	3	2	1.54	ST4-74	1341295	1342773	+
<i>astB</i>	5	3	1.37	ST4-74	1342770	1344113	+
<i>astE</i>	4	3	1.25	ST4-74	1344106	1345074	+
STM1308	42	47	0.89	ST4-74	1345410	1345895	+
STnc1640	358	527	0.68	ST4-74	1345883	1345970	+
STM1309	22	18	1.22	ST4-74	1345970	1346851	-
<i>nadE</i>	43	38	1.12	ST4-74	1346972	1347799	-
<i>osmE</i>	1377	979	1.41	ST4-74	1348018	1348359	+
<i>celA</i>	31	32	0.99	ST4-74	1348660	1348980	+
<i>celB</i>	17	14	1.29	ST4-74	1349063	1350421	+
<i>celC</i>	19	21	0.92	ST4-74	1350472	1350819	+
<i>celD</i>	10	10	0.97	ST4-74	1350908	1351672	+
<i>celF</i>	8	9	0.94	ST4-74	1351797	1353152	+
<i>celG</i>	17	17	1.03	ST4-74	1353165	1353923	+
STnc2010	62	45	1.40	ST4-74	1353832	1353959	+
<i>katE</i>	22	18	1.23	ST4-74	1353967	1356219	-
<i>cedA</i>	56	47	1.20	ST4-74	1356584	1356826	+
<i>ydjN</i>	170	170	1.00	ST4-74	1356928	1358319	-
<i>ydjM</i>	3	2	1.13	ST4-74	1358456	1359055	-
STnc3570	158	130	1.21	ST4-74	1359017	1359183	-
<i>yniC</i>	35	30	1.17	ST4-74	1359193	1359861	-
<i>yniB</i>	77	57	1.34	ST4-74	1360010	1360546	+
STM1324	39	35	1.12	ST4-74	1360589	1361449	-
<i>ydiZ</i>	28	24	1.18	ST4-74	1361556	1361846	-
<i>pfkB</i>	16	20	0.84	ST4-74	1361943	1362875	-
<i>ydiY</i>	37	24	1.54	ST4-74	1363164	1363922	+
STnc3460	236	158	1.50	ST4-74	1363846	1363967	+
STnc4210	175	106	1.65	ST4-74	1363925	1363997	-
STM1328	26	22	1.19	ST4-74	1363971	1364930	-
STM1329	120	58	2.09	ST4-74	1365073	1365387	+
STM1330	80	48	1.67	ST4-74	1365483	1366238	+
STM1331	57	50	1.14	ST4-74	1366411	1366617	+
<i>rfc</i>	41	41	1.00	ST4-74	1366940	1368163	-
<i>thrS</i>	163	176	0.92	ST4-74	1369055	1370983	+
<i>infC</i>	2776	3225	0.86	ST4-74	1370987	1371529	+
<i>rpl35</i>	2531	3010	0.84	ST4-74	1371625	1371822	+
<i>rpl20</i>	1423	1708	0.83	ST4-74	1371873	1372229	+
<i>pheS</i>	26	33	0.81	ST4-74	1372531	1373514	+
<i>pheT</i>	158	131	1.20	ST4-74	1373530	1375917	+

<i>Name</i>	Δfnr TPM	WT TPM	$\Delta fnr/WT$	<i>Chr^a</i>	<i>Start</i>	<i>End</i>	<i>Strand</i>
<i>himA</i>	716	577	1.24	ST4-74	1375910	1376221	+
STnc540	178	180	0.99	ST4-74	1376271	1376364	+
<i>btuC</i>	15	15	1.02	ST4-74	1376424	1377404	+
<i>btuE</i>	35	26	1.35	ST4-74	1377496	1378047	+
<i>btuD</i>	10	9	1.00	ST4-74	1378047	1378796	+
<i>nlpC</i>	102	64	1.58	ST4-74	1378873	1379337	+
<i>ydiV</i>	40	21	1.89	ST4-74	1379651	1380364	+
<i>ydiU</i>	22	16	1.35	ST4-74	1380426	1381868	+
<i>ydiE</i>	98	46	2.16	ST4-74	1381903	1382094	-
<i>aroH</i>	25	25	1.00	ST4-74	1382251	1383297	-
<i>ydiA</i>	20	16	1.26	ST4-74	1383453	1384286	-
<i>pps</i>	84	85	1.00	ST4-74	1384581	1387001	+
<i>ydiD</i>	7	7	1.05	ST4-74	1387043	1388683	-
<i>ydiT</i>	2	2	0.87	ST4-74	1388773	1389066	-
<i>ydiS</i>	3	3	0.96	ST4-74	1389063	1390349	-
<i>ydiR</i>	47	31	1.51	ST4-74	1390406	1391341	-
<i>ydiQ</i>	1	1	0.95	ST4-74	1391363	1392127	-
<i>ydiP</i>	2	2	1.26	ST4-74	1392590	1393480	+
<i>ydiO</i>	22	21	1.02	ST4-74	1393556	1394707	-
<i>ydiF</i>	2	2	1.18	ST4-74	1394721	1396316	-
<i>aroD</i>	11	14	0.81	ST4-74	1396470	1397228	-
<i>aroE</i>	10	8	1.22	ST4-74	1397273	1398139	-
<i>ydiN</i>	1	2	0.79	ST4-74	1398221	1399440	-
<i>ydiM</i>	5	3	1.71	ST4-74	1399804	1401015	-
<i>ydiL</i>	8	10	0.80	ST4-74	1401156	1401515	-
<i>RprA</i>	2345	909	2.58	ST4-74	1401682	1401790	-
<i>ydiK</i>	27	23	1.14	ST4-74	1401973	1403091	-
<i>ydiJ</i>	15	20	0.77	ST4-74	1403356	1406412	+
STM1366	18	26	0.68	ST4-74	1406409	1406819	+
<i>ydiH</i>	351	1003	0.35	ST4-74	1406918	1407106	+
<i>RydB</i>	490	769	0.64	ST4-74	1407278	1407371	+
STM1368	14	17	0.82	ST4-74	1407394	1408740	-
<i>sufA</i>	20	10	1.96	ST4-74	1409167	1409535	+
<i>sufB</i>	11	5	2.12	ST4-74	1409544	1411031	+
<i>sufC</i>	11	7	1.57	ST4-74	1411048	1411794	+
<i>sufD</i>	12	7	1.61	ST4-74	1411769	1413040	+
<i>sufS</i>	10	7	1.42	ST4-74	1413037	1414257	+
<i>ynhA</i>	13	9	1.43	ST4-74	1414270	1414686	+
<i>ynhG</i>	35	26	1.37	ST4-74	1414841	1415842	+
<i>lppB</i>	64	51	1.26	ST4-74	1415909	1416148	-
<i>lpp</i>	27604	27516	1.00	ST4-74	1416231	1416467	-
<i>pykF</i>	39	41	0.96	ST4-74	1416778	1418136	-
<i>orf48</i>	5	7	0.81	ST4-74	1418592	1419935	-
<i>orf32</i>	3	4	0.76	ST4-74	1419957	1420850	-
<i>orf245</i>	10	12	0.84	ST4-74	1420909	1421646	-
<i>orf408</i>	10	10	1.05	ST4-74	1421658	1422884	-
<i>ttrA</i>	2	2	1.11	ST4-74	1423207	1426269	-
<i>ttrC</i>	2	2	0.99	ST4-74	1426262	1427284	-
<i>ttrB</i>	1	2	0.69	ST4-74	1427285	1428037	-
<i>ttrS</i>	20	25	0.79	ST4-74	1428201	1429979	+
<i>ttrR</i>	13	15	0.88	ST4-74	1429936	1430574	+

<i>Name</i>	Δ <i>fnr</i> TPM	WT TPM	Δ <i>fnr</i> /WT	Chr ^a	Start	End	Strand
<i>orf70</i>	133	116	1.15	ST4-74	1430672	1430884	+
<i>orf319</i>	57	45	1.26	ST4-74	1430980	1431939	-
<i>orf242</i>	23	22	1.05	ST4-74	1432112	1432840	-
<i>ssrB</i>	86	44	1.94	ST4-74	1433019	1433657	-
<i>spiR</i>	52	23	2.22	ST4-74	1433688	1436450	-
<i>ssaB</i>	99	11	8.79	ST4-74	1436851	1437252	+
<i>ssaC</i>	37	7	5.61	ST4-74	1437254	1438747	+
<i>ssaD</i>	34	9	3.75	ST4-74	1438728	1439939	+
<i>ssaE</i>	867	84	10.32	ST4-74	1439947	1440189	+
<i>sseA</i>	405	43	9.40	ST4-74	1440510	1440779	+
<i>sseBa</i>	348	50	7.00	ST4-74	1440786	1441376	+
<i>sscA</i>	129	21	6.15	ST4-74	1441373	1441846	+
<i>sseC</i>	211	34	6.13	ST4-74	1441849	1443303	+
<i>sseD</i>	74	14	5.23	ST4-74	1443319	1443906	+
<i>sseE</i>	50	11	4.39	ST4-74	1443909	1444325	+
<i>sscB</i>	75	18	4.20	ST4-74	1444377	1444811	+
<i>sseF</i>	20	7	2.95	ST4-74	1444827	1445609	+
<i>sseG</i>	20	12	1.74	ST4-74	1445606	1446295	+
<i>ssaG</i>	816	93	8.78	ST4-74	1446389	1446604	+
<i>ssaH</i>	500	52	9.57	ST4-74	1446645	1446872	+
<i>ssaI</i>	487	50	9.84	ST4-74	1446884	1447132	+
<i>ssaJ</i>	377	44	8.55	ST4-74	1447129	1447878	+
STM1410	156	29	5.41	ST4-74	1447896	1448444	+
<i>ssaK</i>	112	17	6.61	ST4-74	1448441	1449115	+
STnc1220	50	18	2.75	ST4-74	1448718	1448790	-
<i>ssaL</i>	93	22	4.20	ST4-74	1449081	1450097	+
<i>ssaM</i>	192	26	7.24	ST4-74	1450155	1450523	+
<i>ssaV</i>	54	12	4.33	ST4-74	1450508	1452553	+
<i>ssaN</i>	45	11	4.09	ST4-74	1452543	1453844	+
<i>ssaO</i>	35	12	3.01	ST4-74	1453847	1454224	+
<i>ssaP</i>	46	17	2.69	ST4-74	1454205	1454579	+
<i>ssaQ</i>	36	17	2.09	ST4-74	1454560	1455528	+
<i>ssaR</i>	224	33	6.83	ST4-74	1455596	1456243	+
<i>ssaS</i>	58	10	5.96	ST4-74	1456240	1456506	+
<i>ssaT</i>	67	11	5.84	ST4-74	1456507	1457286	+
<i>ssaU</i>	32	11	2.97	ST4-74	1457283	1458341	+
<i>norM</i>	28	22	1.24	ST4-74	1458814	1460187	-
<i>ribE</i>	64	59	1.09	ST4-74	1460404	1461045	+
<i>cfa</i>	79	60	1.31	ST4-74	1461087	1462235	-
<i>ydhC</i>	6	5	1.15	ST4-74	1462525	1463730	-
<i>ydhB</i>	9	9	1.12	ST4-74	1463843	1464775	+
<i>purR</i>	28	37	0.78	ST4-74	1464772	1465797	-
STnc4220	279	315	0.89	ST4-74	1464776	1464870	-
<i>ynhF</i>	6877	5047	1.36	ST4-74	1466093	1466182	+
<i>sodB</i>	384	547	0.70	ST4-74	1466265	1466846	-
<i>ydhO</i>	51	39	1.31	ST4-74	1466973	1467827	-
<i>ydhD</i>	479	462	1.04	ST4-74	1468129	1468476	+
<i>rnt</i>	51	48	1.06	ST4-74	1468554	1469201	-
<i>gloA</i>	107	118	0.91	ST4-74	1469302	1469709	-
<i>nemA</i>	5	18	0.26	ST4-74	1469778	1470875	-
<i>ydhM</i>	15	36	0.41	ST4-74	1470934	1471533	-

<i>Name</i>	Δfnr TPM	WT TPM	$\Delta fnr/WT$	Chr ^a	Start	End	Strand
<i>ydhL</i>	94	49	1.92	ST4-74	1471636	1471875	+
<i>ydhF</i>	22	24	0.91	ST4-74	1471926	1472822	+
<i>sodCb</i>	68	58	1.18	ST4-74	1472902	1473423	+
STM1441	23	25	0.89	ST4-74	1473399	1475438	-
<i>ydhJ</i>	9	10	0.89	ST4-74	1475438	1476334	-
<i>ydhI</i>	40	33	1.21	ST4-74	1476301	1476537	-
<i>slyA</i>	304	249	1.22	ST4-74	1476732	1477172	+
<i>slyB</i>	646	611	1.06	ST4-74	1477220	1477687	-
<i>anmK</i>	10	11	0.99	ST4-74	1477959	1479080	+
<i>mliC</i>	48	47	1.03	ST4-74	1479168	1479497	+
<i>pdxH</i>	33	40	0.82	ST4-74	1479556	1480212	+
<i>tyrS</i>	85	98	0.87	ST4-74	1480339	1481613	+
<i>pdxY</i>	9	15	0.64	ST4-74	1481673	1482533	+
<i>gst</i>	56	67	0.84	ST4-74	1482592	1483197	-
<i>tppB</i>	38	20	1.93	ST4-74	1483302	1484807	-
<i>nth</i>	21	18	1.15	ST4-74	1485409	1486044	-
<i>rnfE</i>	17	23	0.73	ST4-74	1486044	1486736	-
<i>rnfG</i>	17	16	1.09	ST4-74	1486739	1487359	-
<i>rnfD</i>	13	15	0.91	ST4-74	1487363	1488421	-
<i>rnfC</i>	12	15	0.80	ST4-74	1488422	1490629	-
<i>rnfB</i>	20	26	0.75	ST4-74	1490622	1491200	-
<i>rnfA</i>	50	47	1.08	ST4-74	1491200	1491781	-
<i>ydgK</i>	132	127	1.04	ST4-74	1491858	1492298	-
<i>ydgT</i>	185	148	1.25	ST4-74	1492387	1492617	-
<i>blr</i>	277	229	1.21	ST4-74	1492900	1493025	-
<i>ydgJ</i>	29	28	1.04	ST4-74	1493233	1494273	+
<i>add</i>	26	28	0.93	ST4-74	1494348	1495349	-
STnc3500	47	49	0.96	ST4-74	1495398	1495512	+
<i>ydgA</i>	41	37	1.13	ST4-74	1496053	1497561	-
<i>manA</i>	21	23	0.90	ST4-74	1497664	1498839	-
<i>fumA</i>	25	31	0.81	ST4-74	1499039	1500685	+
<i>fumC</i>	26	28	0.92	ST4-74	1500853	1502256	+
<i>tus</i>	8	8	1.07	ST4-74	1502253	1503182	-
<i>rstB</i>	17	15	1.11	ST4-74	1503258	1504559	-
STM1472	3	2	1.10	ST4-74	1504670	1506376	-
STnc3510	31	20	1.50	ST4-74	1506482	1506596	-
<i>ompN</i>	6	4	1.32	ST4-74	1506529	1507662	-
<i>rstA</i>	355	292	1.22	ST4-74	1508142	1508873	-
<i>ydgC</i>	17	18	0.95	ST4-74	1509000	1509335	+
<i>ydgI</i>	16	10	1.55	ST4-74	1509397	1510779	-
<i>ydgH</i>	53	62	0.85	ST4-74	1511078	1512022	-
<i>pntA</i>	31	57	0.55	ST4-74	1512549	1514078	+
<i>pntB</i>	42	77	0.54	ST4-74	1514089	1515477	+
<i>tqsA</i>	14	17	0.81	ST4-74	1515652	1516686	-
<i>ydgF</i>	19	15	1.28	ST4-74	1517104	1517466	+
<i>ydgE</i>	4	5	0.98	ST4-74	1517453	1517782	+
STM1484	15	12	1.29	ST4-74	1517822	1518643	-
<i>ydgU</i>	16	4	3.52	ST4-74	1518743	1518826	-
<i>asr</i>	119	41	2.87	ST4-74	1518912	1519196	-
STnc3480	18	21	0.86	ST4-74	1519287	1519547	+
<i>ynfM</i>	21	18	1.18	ST4-74	1519555	1520808	-

<i>Name</i>	Δ <i>fnr</i> TPM	WT TPM	Δ <i>fnr</i> /WT	Chr ^a	Start	End	Strand
<i>ynfL</i>	3	4	0.83	ST4-74	1520928	1521827	+
<i>mlc</i>	36	38	0.93	ST4-74	1521955	1523175	+
<i>bioDb</i>	29	199	0.14	ST4-74	1523301	1523996	+
<i>clcB</i>	13	10	1.26	ST4-74	1523952	1525241	-
STM1491	18	8	2.31	ST4-74	1525377	1526525	-
STM1492	17	11	1.52	ST4-74	1526525	1527172	-
STM1493	11	4	2.90	ST4-74	1527182	1528084	-
STM1494	21	7	2.81	ST4-74	1528113	1528823	-
<i>ynfI</i>	26	37	0.70	ST4-74	1529128	1529742	-
STM1496	16	24	0.66	ST4-74	1529785	1530642	-
STM1497	2	14	0.12	ST4-74	1530644	1531261	-
<i>dmsA2</i>	2	8	0.22	ST4-74	1531272	1533707	-
<i>dmsA1</i>	3	21	0.13	ST4-74	1533806	1536247	-
<i>ynfD</i>	67	65	1.03	ST4-74	1536401	1536709	-
<i>ynfC</i>	33	34	0.99	ST4-74	1536804	1537523	+
<i>speG</i>	46	57	0.81	ST4-74	1537564	1538124	-
<i>ynfB</i>	82	84	0.98	ST4-74	1538160	1538501	-
<i>ynfA</i>	16	14	1.11	ST4-74	1538654	1538980	+
<i>rspA</i>	2	3	0.87	ST4-74	1539102	1540316	+
<i>rspB</i>	2	3	0.87	ST4-74	1540327	1541346	+
<i>ydfJ</i>	5	5	0.84	ST4-74	1541400	1542779	+
<i>ydfI</i>	9	10	0.94	ST4-74	1542923	1544389	+
<i>ydfZ</i>	19	386	0.05	ST4-74	1544456	1544659	-
<i>ydfH</i>	37	33	1.11	ST4-74	1544840	1545526	-
<i>ydfG</i>	108	103	1.05	ST4-74	1545656	1546402	-
<i>dcp</i>	11	12	0.89	ST4-74	1546541	1548583	+
STM1513	818	279	2.93	ST4-74	1548928	1549110	+
<i>ydeJ</i>	15	9	1.78	ST4-74	1549230	1549757	-
<i>ydeI</i>	46	29	1.62	ST4-74	1550184	1550576	+
<i>MgrR</i>	10450	8584	1.22	ST4-74	1550746	1550844	+
<i>ydeE</i>	12	11	1.12	ST4-74	1551267	1552454	-
<i>ydeD</i>	15	14	1.08	ST4-74	1552682	1553584	+
STnc2170	24	16	1.48	ST4-74	1553669	1553737	-
<i>marB</i>	8	8	0.99	ST4-74	1553703	1553918	-
<i>marA</i>	6	6	0.93	ST4-74	1553947	1554336	-
<i>marR</i>	6	5	1.09	ST4-74	1554350	1554784	-
<i>marC</i>	78	49	1.60	ST4-74	1555043	1555708	+
<i>sotB</i>	20	16	1.24	ST4-74	1555755	1556945	-
<i>yneJ</i>	5	6	0.78	ST4-74	1557061	1557933	-
<i>yneI</i>	3	4	0.89	ST4-74	1558036	1559424	+
<i>yneH</i>	10	10	1.02	ST4-74	1559497	1560423	+
<i>yneG</i>	17	16	1.07	ST4-74	1560423	1560782	+
STM1527	29	19	1.53	ST4-74	1561039	1561953	+
STM1528	7	5	1.27	ST4-74	1562009	1562551	-
STM1530	14	10	1.48	ST4-74	1563370	1564386	+
STnc3530	132	80	1.64	ST4-74	1564332	1564503	+
<i>hypA</i>	4	4	0.81	ST4-74	1564527	1564868	-
STM1532	4	4	1.07	ST4-74	1564881	1565768	-
<i>hyaF2</i>	10	9	1.14	ST4-74	1565756	1566817	-
<i>hyaE2</i>	4	7	0.66	ST4-74	1566835	1567245	-
STM1535	6	5	1.25	ST4-74	1567242	1567541	-

<i>Name</i>	Δfnr TPM	WT TPM	$\Delta fnr/WT$	<i>Chr</i> ^a	<i>Start</i>	<i>End</i>	<i>Strand</i>
<i>hyaD2</i>	11	12	0.97	ST4-74	1567541	1568149	-
<i>hyaC2</i>	14	13	1.11	ST4-74	1568155	1568898	-
<i>hyaB2</i>	8	9	0.98	ST4-74	1568849	1570651	-
<i>hyaA2</i>	14	13	1.05	ST4-74	1570654	1571757	-
STM1540	17	14	1.21	ST4-74	1572186	1573277	+
STM1541	60	62	0.98	ST4-74	1573443	1574114	+
STM1542	6	4	1.45	ST4-74	1574173	1575198	-
STM1543	8	7	1.21	ST4-74	1575173	1576459	-
<i>pqaA</i>	31	20	1.55	ST4-74	1576636	1578192	-
STM1545	8	6	1.46	ST4-74	1578262	1579503	-
STM1546	2	1	1.33	ST4-74	1579493	1581001	-
STM1547	25	24	1.01	ST4-74	1581046	1581534	+
STM1548	68	34	1.98	ST4-74	1581727	1582806	+
STM1549	18	23	0.77	ST4-74	1582858	1583247	-
STM1550	37	44	0.84	ST4-74	1583418	1583702	-
STM1551	167	142	1.18	ST4-74	1583692	1583940	-
SL1344_1481	11	11	1.03	ST4-74	1584297	1584629	+
STM1552	15	13	1.21	ST4-74	1584772	1585680	+
STM1553	2	2	1.12	ST4-74	1585908	1586495	-
<i>IsrF</i>	21	22	0.98	ST4-74	1586724	1587013	-
STM1554	23	27	0.86	ST4-74	1587258	1588724	-
STM1555	9	9	1.01	ST4-74	1588983	1589990	+
STM1556	7	5	1.21	ST4-74	1590134	1591585	+
STM1557	5	5	1.00	ST4-74	1591598	1592800	+
STM1558	24	15	1.57	ST4-74	1592913	1594988	-
STM1559	10	6	1.63	ST4-74	1595045	1597573	-
STM1560	11	6	1.70	ST4-74	1597570	1599354	-
STM1561	14	8	1.82	ST4-74	1599483	1600268	-
<i>hdeB</i>	33	26	1.27	ST4-74	1600411	1600740	-
<i>osmC</i>	184	117	1.57	ST4-74	1601090	1601521	-
<i>yddX</i>	153	65	2.36	ST4-74	1602034	1602249	+
<i>rpsV</i>	1662	1406	1.18	ST4-74	1602344	1602487	+
<i>sfcA</i>	24	25	0.97	ST4-74	1602664	1604361	+
<i>adhP</i>	26	13	2.07	ST4-74	1604728	1605657	+
STnc3540	161	142	1.14	ST4-74	1605727	1605912	-
<i>fdnI</i>	16	12	1.27	ST4-74	1605748	1606389	-
<i>fdnH</i>	4	7	0.56	ST4-74	1606397	1607281	-
<i>fdnG</i>	4	8	0.51	ST4-74	1607295	1610342	-
<i>yddG</i>	9	11	0.77	ST4-74	1610677	1611501	+
<i>ompD</i>	825	1868	0.44	ST4-74	1611987	1613114	+
STM1573	15	22	0.69	ST4-74	1613198	1613638	+
<i>smvA</i>	8	8	0.92	ST4-74	1613663	1615150	-
STM1575	63	70	0.90	ST4-74	1615267	1615845	+
<i>narU</i>	8	4	1.90	ST4-74	1616060	1617448	+
<i>narZ</i>	4	3	1.24	ST4-74	1617540	1621280	+
<i>narY</i>	3	3	0.89	ST4-74	1621277	1622821	+
<i>narW</i>	4	4	1.08	ST4-74	1622821	1623516	+
<i>narV</i>	13	10	1.30	ST4-74	1623513	1624193	+
<i>yddE</i>	13	12	1.06	ST4-74	1624299	1625192	+
<i>nhoA</i>	12	10	1.17	ST4-74	1625228	1626073	-
<i>steA</i>	326	111	2.93	ST4-74	1626357	1626989	-

<i>Name</i>	Δfnr TPM	WT TPM	$\Delta fnr/WT$	Chr ^a	Start	End	Strand
<i>ansP</i>	13	14	0.96	ST4-74	1627502	1628995	+
STM1585	9	7	1.30	ST4-74	1629072	1629293	-
STM1586	25	16	1.50	ST4-74	1629438	1630499	-
<i>yncD</i>	7	6	1.27	ST4-74	1630763	1632883	+
<i>yncC</i>	12	5	2.53	ST4-74	1632950	1633615	-
<i>yncB</i>	78	47	1.67	ST4-74	1633949	1634986	-
<i>yncA</i>	20	28	0.71	ST4-74	1635198	1635713	+
<i>ydcZ</i>	27	35	0.78	ST4-74	1635713	1636162	+
<i>ydcY</i>	113	111	1.02	ST4-74	1636167	1636400	-
<i>srfA</i>	13	38	0.34	ST4-74	1636624	1637943	+
<i>srfB</i>	4	13	0.34	ST4-74	1637948	1640929	+
<i>srfC</i>	6	15	0.43	ST4-74	1640926	1643070	+
<i>ydcX</i>	38	36	1.07	ST4-74	1643115	1643378	-
STnc1110	744	648	1.15	ST4-74	1643465	1643658	+
<i>ydcW</i>	38	23	1.62	ST4-74	1643687	1645132	-
<i>ydcR</i>	29	20	1.46	ST4-74	1645247	1646671	-
<i>pdgL</i>	70	41	1.71	ST4-74	1646807	1647577	-
STM1600	486	115	4.23	ST4-74	1647836	1648066	-
<i>ugtL</i>	1149	231	4.97	ST4-74	1648099	1648497	-
<i>sifB</i>	268	36	7.54	ST4-74	1649034	1649984	+
<i>yncJ</i>	148	52	2.85	ST4-74	1650258	1650488	+
<i>ydcP</i>	16	14	1.10	ST4-74	1650489	1652453	-
<i>ydcN</i>	19	15	1.27	ST4-74	1652532	1653068	-
STM1606	11	13	0.81	ST4-74	1653159	1654337	+
STM1607	59	69	0.86	ST4-74	1654391	1655059	-
<i>tehB</i>	32	37	0.87	ST4-74	1655215	1655811	-
<i>tehA</i>	29	33	0.86	ST4-74	1655798	1656811	-
<i>ydcK</i>	14	11	1.31	ST4-74	1656918	1657898	+
<i>rimL</i>	17	16	1.04	ST4-74	1657895	1658434	-
STM1612	5	7	0.72	ST4-74	1658651	1659769	+
STM1613	2	5	0.34	ST4-74	1659766	1660047	+
STM1614	5	6	0.96	ST4-74	1660058	1661371	+
STM1615	2	2	0.99	ST4-74	1661385	1662191	+
<i>RyjB</i>	2386	3233	0.74	ST4-74	1662190	1662282	-
STM1616	7	9	0.74	ST4-74	1662323	1662760	+
STM1617	2	4	0.51	ST4-74	1662772	1663404	+
STM1618	9	8	1.13	ST4-74	1663420	1664211	+
<i>aac</i>	25	21	1.18	ST4-74	1664211	1664648	+
STM1620	4	3	1.13	ST4-74	1664695	1665897	-
STM1621	4	4	1.17	ST4-74	1665909	1666484	-
<i>ydcG</i>	15	15	1.03	ST4-74	1666680	1668335	-
STM1623	20	15	1.32	ST4-74	1668555	1670063	-
STM1624	42	27	1.57	ST4-74	1670112	1671455	-
<i>ydcI</i>	33	25	1.34	ST4-74	1671748	1672671	+
<i>trg</i>	14	84	0.17	ST4-74	1672732	1674357	-
<i>adhC</i>	17	22	0.76	ST4-74	1674526	1675644	-
STM1628	21	32	0.65	ST4-74	1675676	1675951	-
<i>steB</i>	45	24	1.92	ST4-74	1676474	1676875	+
STM1630	18	4	4.20	ST4-74	1677004	1677720	-
<i>sseJ</i>	83	8	10.48	ST4-74	1678146	1679372	+
STM1632	17	9	1.97	ST4-74	1679493	1679837	-

<i>Name</i>	Δ <i>fnr</i> TPM	WT TPM	Δ <i>fnr</i> /WT	<i>Chr</i> ^a	<i>Start</i>	<i>End</i>	<i>Strand</i>
STM1633	88	34	2.57	ST4-74	1680744	1681505	+
STM1634	25	14	1.76	ST4-74	1681512	1682159	+
STM1635	7	3	2.15	ST4-74	1682184	1682915	+
STM1636	8	5	1.53	ST4-74	1682912	1683592	+
STM1637	30	19	1.59	ST4-74	1683729	1685279	+
STM1638	135	155	0.87	ST4-74	1685743	1686405	+
<i>RydC</i>	5516	4812	1.15	ST4-74	1686526	1686591	+
<i>cybB</i>	53	52	1.02	ST4-74	1686676	1687206	-
<i>ydcF</i>	12	16	0.76	ST4-74	1687323	1688123	-
<i>hrpA</i>	11	12	0.95	ST4-74	1688187	1692089	-
<i>acpD</i>	10	8	1.27	ST4-74	1692290	1692895	+
STM1643	43	32	1.34	ST4-74	1692892	1693341	-
<i>ydbL</i>	14	12	1.15	ST4-74	1693484	1693807	-
<i>ynbE</i>	19	17	1.14	ST4-74	1693815	1694006	-
<i>ydbH</i>	18	15	1.21	ST4-74	1694006	1696642	-
<i>ldhA</i>	38	31	1.24	ST4-74	1696882	1697871	+
<i>hslJ</i>	17	11	1.58	ST4-74	1697982	1698392	+
STM1649	104	114	0.91	ST4-74	1698436	1698591	-
STM1650	36	16	2.22	ST4-74	1698618	1698917	+
<i>nifJ</i>	10	7	1.44	ST4-74	1698978	1702502	+
<i>MicC</i>	119	111	1.07	ST4-74	1702531	1702639	-
<i>ynaF</i>	418	421	0.99	ST4-74	1702984	1703418	+
STM1653	238	183	1.30	ST4-74	1703468	1703806	-
SL1344_1584	43	35	1.23	ST4-74	1703907	1704110	+
<i>ydaO</i>	20	17	1.14	ST4-74	1704162	1705097	+
<i>dbpA</i>	16	13	1.20	ST4-74	1705141	1706514	-
<i>FnrS</i>	130	4527	0.03	ST4-74	1706784	1706905	-
<i>zntB</i>	33	24	1.35	ST4-74	1707001	1707984	-
STM1657	17	44	0.39	ST4-74	1708130	1709284	-
<i>ydaL</i>	27	35	0.78	ST4-74	1709695	1710258	-
<i>ogt</i>	79	59	1.34	ST4-74	1710516	1711031	+
<i>fnr</i>	1	245	0.00	ST4-74	1711227	1711979	+
<i>ydaA</i>	80	173	0.46	ST4-74	1712130	1713077	+
<i>ynaJ</i>	382	356	1.07	ST4-74	1713132	1713386	-
<i>ynaI</i>	20	20	1.01	ST4-74	1713625	1714656	+
STM1664	20	21	0.94	ST4-74	1714742	1715344	-
STM1665	5	5	0.97	ST4-74	1715388	1716074	+
STM1667	3	2	1.16	ST4-74	1716546	1717103	-
STM1668	4	3	1.50	ST4-74	1717202	1718032	-
STM1669	2	2	1.13	ST4-74	1718053	1720035	-
STM1670	2	2	1.37	ST4-74	1720110	1720955	-
STM1671	4	3	1.48	ST4-74	1721249	1722107	+
STM1672	444	414	1.07	ST4-74	1722495	1723607	+
STM1673	17	17	1.03	ST4-74	1723821	1724075	-
STM1674	7	7	0.91	ST4-74	1724186	1724776	-
STM1675	8	10	0.85	ST4-74	1724854	1725567	+
STM1676	47	39	1.18	ST4-74	1725658	1726527	-
STM1677	9	8	1.05	ST4-74	1726801	1727706	-
STM1678	3	2	1.40	ST4-74	1727825	1728754	+
<i>mppA</i>	32	43	0.74	ST4-74	1728851	1730464	-
<i>ycjI</i>	16	19	0.83	ST4-74	1730654	1731382	+

<i>Name</i>	Δ <i>fnr</i> TPM	WT TPM	Δ <i>fnr</i> /WT	Chr ^a	Start	End	Strand
<i>ycjG</i>	29	21	1.40	ST4-74	1731357	1732322	-
<i>tpx</i>	198	212	0.93	ST4-74	1732438	1732944	+
<i>tyrR</i>	27	24	1.12	ST4-74	1733034	1734575	-
<i>ycjF</i>	11	12	0.90	ST4-74	1734723	1735784	-
<i>ycjX</i>	10	12	0.87	ST4-74	1735781	1737184	-
<i>pspE</i>	179	155	1.15	ST4-74	1737327	1737641	-
<i>pspD</i>	17	17	0.98	ST4-74	1737717	1737935	-
<i>pspC</i>	17	13	1.30	ST4-74	1737958	1738317	-
<i>pspB</i>	26	26	0.99	ST4-74	1738317	1738541	-
<i>pspA</i>	33	38	0.86	ST4-74	1738601	1739269	-
<i>pspF</i>	7	7	0.99	ST4-74	1739440	1740420	+
<i>sapA</i>	23	20	1.11	ST4-74	1740532	1742181	+
<i>sapB</i>	12	15	0.85	ST4-74	1742349	1743143	+
<i>sapC</i>	15	16	0.90	ST4-74	1743130	1744020	+
<i>sapD</i>	12	12	1.00	ST4-74	1744020	1745012	+
<i>sapF</i>	8	9	0.92	ST4-74	1745014	1745820	+
STM1697	48	28	1.70	ST4-74	1745836	1746543	-
<i>steC</i>	88	19	4.71	ST4-74	1747010	1748383	-
STM1698A	64	5	13.29	ST4-74	1748418	1748597	+
<i>ycjE</i>	59	31	1.89	ST4-74	1748572	1748871	+
<i>fabI</i>	146	142	1.03	ST4-74	1748989	1749777	+
<i>yciW</i>	50	49	1.00	ST4-74	1749977	1751110	+
<i>rnb</i>	44	42	1.05	ST4-74	1751199	1753133	+
<i>yciR</i>	13	12	1.10	ST4-74	1753395	1755377	+
SL1344_1635	83	90	0.93	ST4-74	1755466	1755678	+
<i>yciT</i>	21	24	0.87	ST4-74	1755765	1756517	+
<i>osmB</i>	75	58	1.30	ST4-74	1756776	1756994	+
<i>yciH</i>	15	13	1.14	ST4-74	1757114	1757440	-
<i>pyrF</i>	21	19	1.11	ST4-74	1757440	1758177	-
<i>yciM</i>	57	52	1.10	ST4-74	1758368	1759483	-
<i>yciS</i>	179	141	1.27	ST4-74	1759544	1759852	-
<i>pgpB</i>	39	28	1.38	ST4-74	1760002	1760766	-
<i>ribA</i>	42	40	1.05	ST4-74	1760962	1761552	+
<i>acnA</i>	18	14	1.31	ST4-74	1761608	1764283	-
<i>ymiA</i>	730	768	0.95	ST4-74	1764839	1764967	-
<i>cysB</i>	36	38	0.94	ST4-74	1765260	1766234	-
<i>topA</i>	31	34	0.91	ST4-74	1766645	1769242	-
<i>yciN</i>	257	309	0.83	ST4-74	1769645	1769896	+
<i>sohB</i>	54	51	1.07	ST4-74	1769938	1770984	-
<i>yciK</i>	40	58	0.68	ST4-74	1771222	1771983	+
<i>btuR</i>	25	29	0.87	ST4-74	1771980	1772570	+
<i>yciL</i>	31	30	1.03	ST4-74	1772657	1773532	-
<i>yciO</i>	17	20	0.89	ST4-74	1773633	1774253	-
<i>trpH</i>	30	26	1.16	ST4-74	1774261	1775142	-
<i>trpE</i>	12	18	0.65	ST4-74	1775403	1776965	+
<i>trpD</i>	14	18	0.75	ST4-74	1776965	1778560	+
<i>trpC</i>	19	22	0.86	ST4-74	1778564	1779922	+
<i>trpB</i>	17	23	0.76	ST4-74	1779932	1781125	+
<i>trpA</i>	17	20	0.85	ST4-74	1781125	1781931	+
<i>yciG</i>	1187	274	4.34	ST4-74	1782411	1782593	+
<i>yciF</i>	73	21	3.53	ST4-74	1782683	1783186	+

<i>Name</i>	Δ <i>fnr</i> TPM	WT TPM	Δ <i>fnr</i> /WT	<i>Chr</i> ^a	<i>Start</i>	<i>End</i>	<i>Strand</i>
<i>yciE</i>	44	11	3.94	ST4-74	1783260	1783766	+
<i>katN</i>	37	16	2.37	ST4-74	1783786	1784664	+
STnc2030	47	5	8.65	ST4-74	1784673	1784725	+
<i>ompW</i>	28	612	0.05	ST4-74	1784746	1785384	-
STM1733	55	59	0.94	ST4-74	1785722	1786126	+
<i>yciC</i>	110	84	1.31	ST4-74	1786152	1786895	+
<i>ispZ</i>	67	62	1.08	ST4-74	1786952	1787491	+
<i>yciA</i>	59	51	1.17	ST4-74	1787652	1788053	+
<i>tonB</i>	32	19	1.69	ST4-74	1788113	1788841	-
<i>yciI</i>	115	160	0.72	ST4-74	1789065	1789361	+
STnc1270	568	481	1.18	ST4-74	1789368	1789691	-
<i>cls</i>	14	15	0.91	ST4-74	1789721	1791181	+
<i>yciU</i>	106	110	0.97	ST4-74	1791215	1791544	+
STM1741	18	15	1.17	ST4-74	1791592	1792374	-
<i>oppF</i>	32	42	0.75	ST4-74	1792476	1793480	-
<i>oppD</i>	13	20	0.63	ST4-74	1793477	1794484	-
<i>oppC</i>	17	25	0.68	ST4-74	1794496	1795404	-
<i>oppB</i>	15	26	0.57	ST4-74	1795419	1796339	-
<i>oppA</i>	50	70	0.72	ST4-74	1796461	1798092	-
STM1747	11	4	2.56	ST4-74	1798160	1798474	+
STnc3580	33	32	1.04	ST4-74	1798747	1798826	+
<i>ychE</i>	17	16	1.07	ST4-74	1798857	1799504	-
<i>adh</i>	65	74	0.88	ST4-74	1799981	1802659	+
<i>tdk</i>	50	51	0.96	ST4-74	1802856	1803473	-
<i>hns</i>	4183	4711	0.89	ST4-74	1804136	1804549	+
<i>galU</i>	71	57	1.26	ST4-74	1804681	1805589	-
<i>hnr</i>	34	28	1.21	ST4-74	1805792	1806805	-
<i>ychK</i>	60	48	1.23	ST4-74	1806896	1807801	-
<i>ychJ</i>	42	47	0.88	ST4-74	1807912	1808370	+
<i>purU</i>	36	38	0.94	ST4-74	1808421	1809263	+
STM1760	18	14	1.29	ST4-74	1810579	1812054	-
STnc3600	43	46	0.93	ST4-74	1812121	1812328	+
<i>narI</i>	7	7	1.09	ST4-74	1812350	1813027	-
<i>narJ</i>	1	3	0.41	ST4-74	1813027	1813737	-
<i>narH</i>	2	2	0.70	ST4-74	1813734	1815269	-
<i>narG</i>	2	2	0.64	ST4-74	1815266	1819009	-
STnc2040	2	3	0.65	ST4-74	1819352	1819414	-
<i>narK</i>	3	3	0.85	ST4-74	1819397	1820794	-
<i>narX</i>	13	11	1.10	ST4-74	1821135	1822931	+
<i>narL</i>	11	10	1.04	ST4-74	1822924	1823574	+
<i>ychP</i>	28	18	1.54	ST4-74	1823575	1824999	-
<i>ychN</i>	88	93	0.95	ST4-74	1825176	1825529	+
<i>chaB</i>	443	279	1.59	ST4-74	1825609	1825839	-
<i>chaA</i>	61	58	1.06	ST4-74	1826106	1827206	+
<i>kdsA</i>	33	48	0.69	ST4-74	1827260	1828114	-
<i>ychA</i>	27	33	0.82	ST4-74	1828152	1828961	-
<i>sirC</i>	38	38	1.00	ST4-74	1828965	1829354	-
<i>hemK</i>	12	12	0.97	ST4-74	1829351	1830184	-
<i>prfA</i>	16	18	0.93	ST4-74	1830184	1831266	-
<i>hemA</i>	52	55	0.95	ST4-74	1831307	1832563	-
<i>hemM</i>	17	18	0.96	ST4-74	1832877	1833500	+

<i>Name</i>	Δ <i>fnr</i> TPM	WT TPM	Δ <i>fnr</i> /WT	Chr ^a	Start	End	Strand
<i>ipk</i>	78	105	0.74	ST4-74	1833497	1834348	+
<i>prs</i>	67	95	0.70	ST4-74	1834614	1835561	+
<i>ychM</i>	6	8	0.76	ST4-74	1835710	1837371	+
<i>ychH</i>	245	166	1.48	ST4-74	1837416	1837694	-
<i>pth</i>	22	25	0.87	ST4-74	1837970	1838554	+
<i>ychF</i>	44	53	0.83	ST4-74	1838671	1839762	+
STM1785	18	20	0.90	ST4-74	1839921	1841186	-
<i>hyaA</i>	1	1	1.54	ST4-74	1841681	1842799	+
STM1787	2	2	1.14	ST4-74	1842796	1844589	+
<i>hyaC</i>	3	3	1.05	ST4-74	1844608	1845339	+
<i>hyaD</i>	1	1	1.63	ST4-74	1845336	1845932	+
<i>hyaE</i>	2	1	2.45	ST4-74	1845922	1846326	+
<i>hyaF</i>	1	1	0.75	ST4-74	1846323	1847171	+
<i>appC</i>	3	2	1.30	ST4-74	1847246	1848790	+
<i>appB</i>	5	3	1.83	ST4-74	1848802	1849938	+
STM1794	34	27	1.26	ST4-74	1849951	1850040	+
STnc3610	88	82	1.08	ST4-74	1850045	1850400	-
STM1795	9	6	1.59	ST4-74	1850384	1851709	+
<i>treA</i>	33	30	1.11	ST4-74	1851923	1853635	+
<i>ymgE</i>	158	87	1.80	ST4-74	1853698	1853952	-
<i>ycgR</i>	22	67	0.32	ST4-74	1854121	1854855	+
<i>emtA</i>	18	16	1.16	ST4-74	1854869	1855480	-
<i>ldcA</i>	20	15	1.31	ST4-74	1855651	1856565	+
<i>cvrA</i>	59	64	0.93	ST4-74	1856662	1858395	+
<i>alr-a</i>	7	5	1.26	ST4-74	1858458	1859528	-
<i>dadA</i>	11	8	1.32	ST4-74	1859542	1860840	-
<i>ycgB</i>	62	34	1.84	ST4-74	1861169	1862695	+
<i>fadR</i>	143	126	1.14	ST4-74	1862742	1863461	-
<i>nhaB</i>	23	25	0.93	ST4-74	1863681	1865225	+
<i>dsbB</i>	119	126	0.95	ST4-74	1865367	1865897	+
STM1808	3	2	1.15	ST4-74	1866006	1866347	+
STM1809	825	484	1.70	ST4-74	1866419	1866592	-
STnc3620	42	30	1.41	ST4-74	1866668	1866747	+
STM1810	141	90	1.57	ST4-74	1866784	1866921	-
<i>ycgN</i>	82	62	1.32	ST4-74	1867273	1867734	-
<i>ycgM</i>	24	30	0.79	ST4-74	1867812	1868471	-
<i>ycgL</i>	124	94	1.32	ST4-74	1868521	1868853	-
<i>minC</i>	102	114	0.90	ST4-74	1868940	1869647	+
<i>minD</i>	124	131	0.95	ST4-74	1869671	1870483	+
<i>minE</i>	179	182	0.99	ST4-74	1870487	1870753	+
<i>rnd</i>	6	5	1.17	ST4-74	1870875	1872002	-
<i>tmpA_1a</i>	244	250	0.97	ST4-74	1872138	1872596	-
<i>fadD</i>	14	15	0.96	ST4-74	1872787	1874472	-
<i>yeaY</i>	29	27	1.05	ST4-74	1874677	1875258	-
<i>yeaZ</i>	36	34	1.05	ST4-74	1875330	1876025	-
<i>yoaA</i>	10	9	1.07	ST4-74	1876083	1877993	-
<i>yoaB</i>	343	365	0.94	ST4-74	1878124	1878468	+
<i>yoaH</i>	146	125	1.16	ST4-74	1878474	1878653	-
<i>pabB</i>	22	18	1.25	ST4-74	1878734	1880098	+
<i>yeaB</i>	9	8	1.18	ST4-74	1880102	1880680	+
<i>sdaA</i>	17	12	1.40	ST4-74	1880944	1882308	+

<i>Name</i>	Δ <i>fnr</i> TPM	WT TPM	Δ <i>fnr</i> /WT	Chr ^a	Start	End	Strand
STM1827	11	8	1.41	ST4-74	1882446	1884047	+
<i>yoaE</i>	9	8	1.15	ST4-74	1884069	1885628	-
STM1830	69	104	0.66	ST4-74	1886101	1887069	+
STM1831	47	104	0.45	ST4-74	1887122	1887922	+
STM1832	85	120	0.71	ST4-74	1887926	1888786	+
STM1833	11	10	1.14	ST4-74	1888844	1889302	+
<i>yebN</i>	30	32	0.93	ST4-74	1889712	1890278	+
<i>rrmA</i>	16	15	1.09	ST4-74	1890275	1891084	-
<i>ftsI2</i>	7	6	1.21	ST4-74	1891150	1892895	-
<i>cspC</i>	1851	1986	0.93	ST4-74	1893115	1893324	-
<i>yobF</i>	5281	5123	1.03	ST4-74	1893337	1893480	-
STnc3630	302	325	0.93	ST4-74	1894039	1894125	+
STM1839	502	323	1.56	ST4-74	1894129	1894416	-
<i>yobG</i>	4475	2172	2.06	ST4-74	1894487	1894630	-
STM1841	28	15	1.85	ST4-74	1894788	1895027	+
<i>kdgR</i>	96	87	1.11	ST4-74	1895239	1896030	-
STM1843	11	9	1.19	ST4-74	1896206	1897579	+
<i>htpX</i>	125	147	0.85	ST4-74	1897627	1898508	-
<i>prc</i>	60	59	1.02	ST4-74	1898702	1900750	-
<i>proQ</i>	102	117	0.87	ST4-74	1900770	1901456	-
<i>yebR</i>	162	123	1.32	ST4-74	1901554	1902138	-
<i>yebS</i>	58	35	1.65	ST4-74	1902180	1903463	+
STM1849	25	21	1.15	ST4-74	1903426	1906065	+
<i>yebU</i>	10	9	1.08	ST4-74	1906143	1907582	+
STM1851	443	276	1.61	ST4-74	1907697	1907936	+
<i>yebW</i>	126	64	1.98	ST4-74	1908047	1908238	+
<i>pphA</i>	20	10	2.03	ST4-74	1908257	1908907	-
STM1854	897	395	2.27	ST4-74	1909131	1909295	-
<i>sopE2</i>	32	34	0.93	ST4-74	1909580	1910302	-
STM1856	16	19	0.86	ST4-74	1910986	1911381	+
SL1344_1786	89	66	1.34	ST4-74	1911711	1912187	+
STM1857	92	55	1.66	ST4-74	1912575	1912994	-
STM1858	40	26	1.49	ST4-74	1913364	1913633	+
STnc1130	190	104	1.81	ST4-74	1913615	1913755	-
STM1859	93	85	1.09	ST4-74	1913799	1914048	+
STM1860	4	3	1.29	ST4-74	1914085	1915279	-
STM1861	3	3	1.06	ST4-74	1915403	1915771	+
STnc3640	45	27	1.68	ST4-74	1915824	1916082	+
SL1344_1792	7	7	1.05	ST4-74	1916257	1916457	-
<i>pagO</i>	130	49	2.68	ST4-74	1917075	1917989	+
STM1863	222	99	2.25	ST4-74	1918122	1918280	+
STM1864	92	36	2.53	ST4-74	1918290	1918904	+
STM1865	34	18	1.91	ST4-74	1919231	1919377	-
<i>pagM</i>	406	113	3.61	ST4-74	1919657	1919839	-
SL1344_1798	12	6	1.99	ST4-74	1920177	1920299	+
<i>pagK</i>	4535	1482	3.06	ST4-74	1920747	1920947	+
<i>mig-3</i>	3	3	1.04	ST4-74	1921044	1921925	-
SL1344_1801	7	6	1.29	ST4-74	1922080	1922343	-
STM1868A	66	51	1.28	ST4-74	1922651	1922818	+
STM1869	1	1	0.89	ST4-74	1923075	1923608	-
STM1869A	2	1	1.13	ST4-74	1923662	1923892	-

<i>Name</i>	Δ <i>fnr</i> TPM	WT TPM	Δ <i>fnr</i> /WT	Chr ^a	Start	End	Strand
STM1870	3	4	0.77	ST4-74	1923923	1924576	+
STM1871	6	5	1.07	ST4-74	1924594	1925490	+
<i>SraC</i>	434	268	1.62	ST4-74	1925543	1925853	+
<i>SdsR</i>	11807	4767	2.48	ST4-74	1925621	1925723	-
STM1873	26	25	1.02	ST4-74	1925864	1926217	-
STM1874	29	32	0.91	ST4-74	1926234	1927109	-
<i>yobA</i>	48	55	0.86	ST4-74	1927110	1927490	-
<i>holE</i>	69	56	1.25	ST4-74	1927622	1927852	+
STM1877	61	51	1.20	ST4-74	1927960	1928616	+
<i>exoX</i>	82	75	1.09	ST4-74	1928640	1929338	+
<i>opdB</i>	25	22	1.15	ST4-74	1929373	1931424	-
STnc1690	678	966	0.70	ST4-74	1931455	1931546	+
<i>yebE</i>	64	93	0.69	ST4-74	1931637	1932296	-
<i>yebF</i>	198	123	1.62	ST4-74	1932390	1932743	-
<i>yebG</i>	74	73	1.02	ST4-74	1932811	1933101	-
<i>purT</i>	17	29	0.61	ST4-74	1933232	1934410	+
<i>eda</i>	15	20	0.74	ST4-74	1934510	1935151	-
<i>edd</i>	6	10	0.65	ST4-74	1935189	1937000	-
STnc200	23	22	1.04	ST4-74	1937130	1937244	-
<i>zwf</i>	29	32	0.90	ST4-74	1937235	1938710	-
<i>hexR</i>	27	66	0.42	ST4-74	1939052	1939921	+
<i>pykA</i>	29	71	0.40	ST4-74	1940045	1941487	+
<i>msbB</i>	39	31	1.26	ST4-74	1941560	1942531	-
<i>yebA</i>	40	49	0.82	ST4-74	1942648	1943967	-
<i>znuA</i>	85	98	0.86	ST4-74	1943983	1944984	-
<i>znuC</i>	24	18	1.32	ST4-74	1945006	1945761	+
<i>znuB</i>	13	14	0.90	ST4-74	1945758	1946543	+
<i>ruvB</i>	20	18	1.09	ST4-74	1946622	1947551	-
<i>ruvA</i>	41	40	1.01	ST4-74	1947641	1948252	-
STM1896	9	6	1.54	ST4-74	1948585	1949567	+
SL1344_1830A	3	3	1.07	ST4-74	1949628	1950061	-
<i>yebB</i>	8	7	1.20	ST4-74	1950194	1950793	+
<i>ruvC</i>	29	40	0.73	ST4-74	1950795	1951316	-
<i>yebC</i>	54	62	0.88	ST4-74	1951353	1952093	-
<i>ntpA</i>	87	90	0.96	ST4-74	1952123	1952575	-
<i>aspS</i>	49	50	1.00	ST4-74	1952678	1954450	-
<i>yecD</i>	26	21	1.26	ST4-74	1954775	1955341	+
<i>yecE</i>	6	6	0.99	ST4-74	1955338	1956156	+
<i>yecN</i>	101	86	1.17	ST4-74	1956209	1956604	+
<i>yecO</i>	40	34	1.18	ST4-74	1956645	1957388	+
<i>yecP</i>	11	15	0.76	ST4-74	1957385	1958356	+
<i>RyeF</i>	231	188	1.23	ST4-74	1958513	1958819	-
<i>cutC</i>	9	8	1.09	ST4-74	1958592	1959338	-
<i>yecM</i>	27	23	1.19	ST4-74	1959358	1959927	-
<i>argS</i>	27	25	1.06	ST4-74	1960164	1961897	+
STM1910	3	3	1.11	ST4-74	1962086	1963957	+
STM1911	7	9	0.86	ST4-74	1964011	1965150	-
<i>flhE</i>	10	12	0.82	ST4-74	1965387	1965779	-
<i>flhAa</i>	9	30	0.29	ST4-74	1965779	1967857	-
<i>flhB</i>	18	66	0.27	ST4-74	1967850	1969001	-
<i>cheZ</i>	17	71	0.24	ST4-74	1969195	1969839	-

<i>Name</i>	Δfnr TPM	WT TPM	$\Delta fnr/WT$	Chr ^a	Start	End	Strand
<i>cheY</i>	31	117	0.27	ST4-74	1969850	1970239	-
<i>cheB</i>	13	69	0.19	ST4-74	1970257	1971306	-
<i>cheR</i>	17	72	0.23	ST4-74	1971303	1972169	-
<i>cheM</i>	49	204	0.24	ST4-74	1972323	1973984	-
<i>cheW</i>	67	279	0.24	ST4-74	1974221	1974724	-
<i>cheA</i>	28	130	0.21	ST4-74	1974745	1976760	-
<i>motB</i>	49	178	0.28	ST4-74	1976765	1977694	-
<i>motA</i>	53	203	0.26	ST4-74	1977691	1978521	-
<i>flhC</i>	94	189	0.49	ST4-74	1978703	1979281	-
<i>flhD</i>	114	198	0.58	ST4-74	1979284	1979634	-
<i>yecG</i>	53	49	1.08	ST4-74	1980421	1980849	+
<i>otsA</i>	24	16	1.57	ST4-74	1980867	1982288	-
<i>otsB</i>	58	26	2.23	ST4-74	1982263	1983066	-
<i>araH</i>	9	8	1.11	ST4-74	1983700	1984257	-
<i>fnbB</i>	21	40	0.52	ST4-74	1984808	1985311	+
STM1933	8	9	0.98	ST4-74	1985490	1986128	-
STM1934	21	61	0.34	ST4-74	1986384	1986719	+
<i>fnb</i>	158	238	0.66	ST4-74	1986959	1987456	+
<i>yecH</i>	5	110	0.04	ST4-74	1987502	1987741	-
<i>tyrP</i>	11	12	0.91	ST4-74	1987968	1989179	+
<i>yecA</i>	57	59	0.96	ST4-74	1989254	1989919	-
STM1939	201	138	1.45	ST4-74	1990157	1990462	-
STM1940	40	27	1.47	ST4-74	1990696	1992135	-
STM1941	511	221	2.32	ST4-74	1992348	1992680	-
SL1344_1874A	9	7	1.38	ST4-74	1992726	1992853	-
STnc2180	604	643	0.94	ST4-74	1992863	1992913	-
<i>pgsA</i>	97	111	0.87	ST4-74	1993381	1993929	-
<i>uvrC</i>	16	20	0.77	ST4-74	1993986	1995818	-
<i>sirA</i>	154	141	1.09	ST4-74	1995815	1996471	-
<i>yecF</i>	177	179	0.99	ST4-74	1996935	1997159	+
<i>sdiA</i>	25	41	0.62	ST4-74	1997226	1997948	-
<i>yecC</i>	18	23	0.76	ST4-74	1998180	1998932	-
<i>yecS</i>	13	16	0.79	ST4-74	1998929	1999597	-
<i>dcyD</i>	15	19	0.81	ST4-74	1999618	2000604	-
<i>fliY</i>	65	99	0.66	ST4-74	2000758	2001558	-
<i>fliZ</i>	32	124	0.26	ST4-74	2001705	2002256	-
<i>fliA</i>	67	280	0.24	ST4-74	2002315	2003034	-
<i>tnpA_2b</i>	249	288	0.86	ST4-74	2003303	2003812	-
<i>fliB</i>	10	26	0.37	ST4-74	2003942	2005147	-
<i>fliC</i>	279	1324	0.21	ST4-74	2005226	2006713	-
<i>fliD</i>	92	406	0.23	ST4-74	2006970	2008373	+
<i>fliS</i>	39	205	0.19	ST4-74	2008388	2008795	+
<i>fliT</i>	30	153	0.20	ST4-74	2008795	2009163	+
<i>amyA</i>	8	8	0.97	ST4-74	2009235	2010719	+
<i>yedD</i>	42	33	1.26	ST4-74	2010759	2011184	-
<i>yedE</i>	8	11	0.75	ST4-74	2011310	2012575	+
<i>yedF</i>	11	20	0.56	ST4-74	2012572	2012805	+
STM1967	5	7	0.69	ST4-74	2013070	2013456	+
<i>fliE</i>	57	223	0.25	ST4-74	2013576	2013890	-
<i>fliF</i>	15	71	0.21	ST4-74	2014107	2015789	+
<i>fliG</i>	12	60	0.21	ST4-74	2015782	2016777	+

<i>Name</i>	Δfnr TPM	WT TPM	$\Delta fnr/WT$	Chr ^a	Start	End	Strand
<i>fliH</i>	12	53	0.22	ST4-74	2016770	2017477	+
<i>fliI</i>	7	32	0.23	ST4-74	2017477	2018847	+
<i>fliJ</i>	8	48	0.17	ST4-74	2018869	2019312	+
<i>fliK</i>	5	27	0.19	ST4-74	2019309	2020526	+
<i>fliL</i>	23	88	0.26	ST4-74	2020631	2021098	+
<i>fliM</i>	12	55	0.22	ST4-74	2021103	2022107	+
<i>fliN</i>	11	54	0.20	ST4-74	2022104	2022517	+
<i>fliO</i>	10	50	0.20	ST4-74	2022517	2022894	+
<i>fliP</i>	9	34	0.28	ST4-74	2022894	2023631	+
<i>fliQ</i>	5	24	0.20	ST4-74	2023641	2023910	+
<i>fliR</i>	4	9	0.44	ST4-74	2023919	2024713	+
<i>rcsA</i>	9	6	1.60	ST4-74	2024995	2025618	+
<i>dsrB</i>	421	246	1.71	ST4-74	2025657	2025851	-
<i>yodD</i>	199	83	2.39	ST4-74	2025980	2026207	+
<i>DsrA</i>	283	213	1.33	ST4-74	2026216	2026302	-
<i>mngB</i>	8	5	1.52	ST4-74	2026517	2027332	+
<i>gcpA</i>	14	12	1.23	ST4-74	2027311	2029023	-
STM1988	645	427	1.51	ST4-74	2029188	2029373	-
<i>yedI</i>	30	26	1.15	ST4-74	2029450	2030361	-
<i>yedA</i>	5	4	1.03	ST4-74	2030537	2031457	+
<i>vsr</i>	8	10	0.80	ST4-74	2031446	2031916	-
<i>dcm</i>	18	19	0.95	ST4-74	2031897	2033327	-
<i>yedJ</i>	7	7	1.05	ST4-74	2033401	2034096	-
STM1994	9	6	1.40	ST4-74	2034188	2034487	-
<i>RseX</i>	25	19	1.35	ST4-74	2034743	2034837	+
<i>ompS</i>	9	9	1.00	ST4-74	2035137	2036333	+
<i>cspB</i>	40	34	1.15	ST4-74	2036793	2037005	-
<i>umuC</i>	7	5	1.35	ST4-74	2037460	2038728	-
<i>umuD</i>	5	5	1.01	ST4-74	2038731	2039150	-
STM1999	1	1	1.57	ST4-74	2039277	2039438	-
SL1344_1927A	57	32	1.78	ST4-74	2039416	2039658	-
STnc1280	8973	8432	1.06	ST4-74	2039984	2040056	+
SL1344_1927B	197	60	3.31	ST4-74	2040072	2040263	-
SL1344_1928	197	30	6.52	ST4-74	2040503	2041510	+
STM2705	9	9	1.03	ST4-74	2041795	2042394	-
SL1344_1930	3	4	0.80	ST4-74	2042364	2043959	-
SL1344_1931	2	3	0.68	ST4-74	2043913	2044500	-
SL1344_1932	3	2	1.59	ST4-74	2044503	2045024	-
SL1344_1933	4	5	0.82	ST4-74	2045059	2045604	-
SL1344_1934	4	3	1.46	ST4-74	2045576	2045989	-
SL1344_1935	3	4	0.89	ST4-74	2045994	2046527	-
SL1344_1936	4	4	0.93	ST4-74	2046527	2047585	-
SL1344_1937	3	3	0.87	ST4-74	2047582	2048922	-
SL1344_1938	5	5	1.09	ST4-74	2048956	2050884	-
SL1344_1939	5	5	0.89	ST4-74	2050969	2051295	-
SL1344_1940	10	10	0.95	ST4-74	2051292	2051648	-
SL1344_1941	3	3	0.78	ST4-74	2051648	2053144	-
SL1344_1942	2	2	1.16	ST4-74	2053302	2053862	-
SL1344_1943	1	1	0.77	ST4-74	2053859	2054377	-
SL1344_1944	1	2	0.64	ST4-74	2054343	2054747	-
SL1344_1945	2	2	0.72	ST4-74	2054744	2055067	-

<i>Name</i>	Δ <i>fnr</i> TPM	WT TPM	Δ <i>fnr</i> /WT	<i>Chr</i> ^a	<i>Start</i>	<i>End</i>	<i>Strand</i>
SL1344_1946	4	4	0.94	ST4-74	2055070	2055270	-
SL1344_1947	3	4	0.67	ST4-74	2055321	2056526	-
SL1344_1948	2	3	0.61	ST4-74	2056541	2057227	-
SL1344_1949	3	3	0.99	ST4-74	2057169	2058410	-
SL1344_1950	3	3	1.01	ST4-74	2058604	2060337	-
SL1344_1951	5	7	0.68	ST4-74	2060334	2060837	-
SL1344_1952	3	4	0.75	ST4-74	2060954	2061304	-
SL1344_1953	30	25	1.22	ST4-74	2061365	2061667	-
SL1344_1954	4	5	0.73	ST4-74	2061887	2062306	-
<i>rzpR</i>	1	2	0.93	ST4-74	2062519	2063004	-
STM0907	2	2	1.00	ST4-74	2063001	2063615	-
STM0906	4	4	0.93	ST4-74	2063618	2063962	-
SL1344_1958	54	51	1.07	ST4-74	2064488	2064847	-
SL1344_1959	4	5	0.78	ST4-74	2064878	2065501	-
SL1344_1960	4	4	0.98	ST4-74	2065512	2066507	-
SL1344_1961	4	4	1.06	ST4-74	2066509	2067414	-
SL1344_1962	2	2	1.13	ST4-74	2067772	2068665	-
SL1344_1963	1	2	0.74	ST4-74	2068665	2069282	-
SL1344_1964	1	1	1.41	ST4-74	2069149	2069967	-
SL1344_1965	4	4	1.13	ST4-74	2070185	2071393	-
STnc1290	17163	18829	0.91	ST4-74	2070801	2070988	-
STnc1300	5945	8257	0.72	ST4-74	2071271	2071409	+
SL1344_1966	3	3	0.81	ST4-74	2071339	2072049	-
STM0898	222	215	1.03	ST4-74	2072244	2072939	+
STnc1310	81	103	0.79	ST4-74	2073265	2073338	+
SL1344_1968	34	51	0.68	ST4-74	2073535	2074125	+
SL1344_1969	2	4	0.43	ST4-74	2074183	2075010	+
SL1344_1970	2	2	1.16	ST4-74	2075147	2075686	+
SL1344_1971	4	4	0.99	ST4-74	2075984	2076499	+
SL1344_1972	1	3	0.48	ST4-74	2076496	2077113	+
SL1344_1973	5	4	1.40	ST4-74	2077110	2077943	+
SL1344_1974	3	3	0.93	ST4-74	2077947	2078516	+
SL1344_1975	3	4	0.65	ST4-74	2078541	2078783	+
SL1344_1976	9	7	1.27	ST4-74	2078785	2079774	+
<i>yeel</i>	53	60	0.88	ST4-74	2080066	2080863	+
SL1344_1978	4	4	0.99	ST4-74	2081235	2081525	+
STnc2050	297	299	0.99	ST4-74	2082064	2082105	+
STM2005	2	2	1.15	ST4-74	2082173	2082646	+
SL1344_1980	1	3	0.23	ST4-74	2082737	2083009	+
STM2006	3	3	1.32	ST4-74	2083094	2083819	+
STM2007	3	3	1.05	ST4-74	2084162	2086330	+
STM2008	5	4	1.24	ST4-74	2086387	2088117	+
STnc3680	96	98	0.97	ST4-74	2088048	2088167	+
SL1344_1985	11	10	1.03	ST4-74	2088651	2088905	-
<i>amn</i>	17	17	1.02	ST4-74	2089022	2090476	-
STM2011	42	31	1.37	ST4-74	2090672	2090998	-
SL1344_1988	71	55	1.29	ST4-74	2090992	2091378	-
SL1344_1989	115	109	1.05	ST4-74	2091704	2091871	+
<i>yeeO</i>	12	11	1.05	ST4-74	2092092	2093549	-
<i>erfK</i>	46	60	0.76	ST4-74	2094011	2094940	-
<i>cobT</i>	41	78	0.52	ST4-74	2095018	2096088	-

<i>Name</i>	Δ <i>fnr</i> TPM	WT TPM	Δ <i>fnr</i> /WT	Chr ^a	Start	End	Strand
<i>cobS</i>	42	90	0.46	ST4-74	2096115	2096858	-
<i>cobU</i>	39	73	0.54	ST4-74	2096855	2097400	-
<i>cbiP</i>	53	92	0.58	ST4-74	2097397	2098917	-
<i>cbiO</i>	74	129	0.57	ST4-74	2098914	2099729	-
<i>cbiQ</i>	52	115	0.45	ST4-74	2099738	2100415	-
<i>cbiN</i>	55	109	0.50	ST4-74	2100402	2100683	-
<i>cbiM</i>	71	147	0.48	ST4-74	2100685	2101422	-
<i>cbiL</i>	48	113	0.42	ST4-74	2101419	2102132	-
STnc1530	49	27	1.85	ST4-74	2101640	2101718	+
<i>cbiK</i>	48	116	0.41	ST4-74	2102129	2102923	-
<i>cbiJ</i>	47	103	0.46	ST4-74	2102926	2103717	-
<i>cbiH</i>	103	165	0.63	ST4-74	2103714	2104439	-
<i>cbiG</i>	65	124	0.52	ST4-74	2104439	2105494	-
<i>cbiF</i>	44	97	0.45	ST4-74	2105475	2106248	-
<i>cbiT</i>	59	123	0.48	ST4-74	2106232	2106810	-
<i>cbiE</i>	72	126	0.57	ST4-74	2106800	2107405	-
<i>cbiD</i>	85	142	0.60	ST4-74	2107399	2108538	-
<i>cbiC</i>	82	145	0.57	ST4-74	2108538	2109170	-
<i>cbiB</i>	143	215	0.67	ST4-74	2109181	2110140	-
<i>cbiA</i>	94	150	0.63	ST4-74	2110137	2111516	-
<i>pocR</i>	154	195	0.79	ST4-74	2112114	2112878	-
<i>pduF</i>	426	718	0.59	ST4-74	2113242	2114036	-
<i>pduA</i>	566	1125	0.50	ST4-74	2114561	2114845	+
<i>pduB</i>	209	433	0.48	ST4-74	2114953	2115654	+
<i>dhaB</i>	132	257	0.52	ST4-74	2115673	2117337	+
<i>pduD</i>	122	265	0.46	ST4-74	2117348	2118022	+
<i>pduE</i>	158	383	0.41	ST4-74	2118037	2118558	+
<i>pduG</i>	114	243	0.47	ST4-74	2118568	2120400	+
<i>pduH</i>	306	612	0.50	ST4-74	2120390	2120740	+
<i>pduJ</i>	195	436	0.45	ST4-74	2120759	2121034	+
<i>pduK</i>	189	385	0.49	ST4-74	2121038	2121520	+
<i>pduL</i>	152	279	0.55	ST4-74	2121520	2122152	+
<i>pduM</i>	43	105	0.41	ST4-74	2122149	2122640	+
<i>pduN</i>	97	212	0.46	ST4-74	2122644	2122919	+
<i>pduO</i>	70	132	0.53	ST4-74	2122929	2123939	+
<i>pduP</i>	70	128	0.55	ST4-74	2123936	2125330	+
<i>pduQ</i>	48	105	0.45	ST4-74	2125342	2126454	+
<i>pduS</i>	58	119	0.48	ST4-74	2126451	2127806	+
<i>pduT</i>	53	98	0.54	ST4-74	2127809	2128363	+
<i>pduU</i>	58	92	0.62	ST4-74	2128363	2128713	+
<i>pduV</i>	31	67	0.46	ST4-74	2128718	2129170	+
<i>pduW</i>	207	312	0.66	ST4-74	2129155	2130369	+
<i>pduX</i>	87	167	0.52	ST4-74	2130427	2131329	+
<i>yeeX</i>	740	743	1.00	ST4-74	2131363	2131698	-
STnc3700	77	53	1.45	ST4-74	2131885	2131995	+
<i>yeeA</i>	31	30	1.05	ST4-74	2131943	2133001	-
STnc1650	78	49	1.60	ST4-74	2132959	2133102	+
<i>gyrI</i>	254	308	0.82	ST4-74	2133120	2133587	-
<i>dacD</i>	4	4	0.94	ST4-74	2133740	2134912	-
<i>phsC</i>	7	8	0.79	ST4-74	2135036	2135800	-
<i>phsB</i>	8	7	1.15	ST4-74	2135797	2136375	-

<i>Name</i>	Δfnr TPM	WT TPM	$\Delta fnr/WT$	<i>Chr^a</i>	<i>Start</i>	<i>End</i>	<i>Strand</i>
<i>phsA</i>	4	6	0.74	ST4-74	2136390	2138666	-
SL1344_2042	5	4	1.38	ST4-74	2138911	2139018	-
<i>sopA</i>	4	5	0.93	ST4-74	2139285	2141633	+
<i>sbcB</i>	18	17	1.06	ST4-74	2141976	2143406	+
<i>yeeF</i>	36	41	0.89	ST4-74	2143542	2144906	-
<i>yoeI</i>	94	115	0.82	ST4-74	2144890	2144952	-
<i>yeeY</i>	24	13	1.90	ST4-74	2145186	2146100	-
<i>yeeZ</i>	62	41	1.52	ST4-74	2146146	2146970	-
STnc700	3265	2733	1.19	ST4-74	2147102	2147280	+
<i>hisG</i>	50	48	1.03	ST4-74	2147330	2148229	+
<i>hisD</i>	33	28	1.17	ST4-74	2148332	2149636	+
<i>hisC</i>	25	22	1.13	ST4-74	2149633	2150712	+
<i>hisB</i>	30	22	1.35	ST4-74	2150709	2151776	+
<i>hisH</i>	20	19	1.04	ST4-74	2151773	2152366	+
<i>hisA</i>	22	23	0.96	ST4-74	2152366	2153103	+
<i>hisF</i>	44	38	1.16	ST4-74	2153085	2153861	+
<i>hisI</i>	55	42	1.31	ST4-74	2153855	2154466	+
<i>wzzB</i>	120	97	1.24	ST4-74	2154547	2155530	-
<i>udg</i>	163	129	1.27	ST4-74	2155673	2156839	-
<i>gnd</i>	66	60	1.10	ST4-74	2157076	2158482	-
<i>rfbP</i>	110	77	1.42	ST4-74	2158646	2160076	-
<i>rfbK</i>	74	60	1.24	ST4-74	2160148	2161581	-
<i>cpsB2</i>	90	65	1.38	ST4-74	2161568	2163007	-
<i>rfbN</i>	106	85	1.25	ST4-74	2163008	2163952	-
<i>rfbU</i>	111	78	1.42	ST4-74	2163953	2165014	-
<i>rfbV</i>	152	101	1.51	ST4-74	2165334	2166335	-
<i>rfbX</i>	143	97	1.48	ST4-74	2166340	2167632	-
<i>rfbJ</i>	123	99	1.25	ST4-74	2167714	2168613	-
<i>rfbH</i>	203	177	1.14	ST4-74	2168641	2169954	-
<i>rfbG</i>	172	150	1.15	ST4-74	2169981	2171060	-
<i>rfbF</i>	136	118	1.15	ST4-74	2171065	2171838	-
<i>rfbI</i>	143	113	1.27	ST4-74	2171835	2172827	-
<i>rfbC</i>	154	112	1.37	ST4-74	2172833	2173384	-
<i>rfbA</i>	81	61	1.33	ST4-74	2173385	2174263	-
<i>rfbD</i>	36	35	1.03	ST4-74	2174311	2175210	-
STnc1320	80	55	1.45	ST4-74	2174386	2174470	+
<i>rfbB</i>	63	55	1.13	ST4-74	2175210	2176295	-
<i>galF</i>	139	108	1.29	ST4-74	2176672	2177694	-
<i>wcaM</i>	3	2	1.29	ST4-74	2177743	2179146	-
<i>wcaL</i>	2	2	1.45	ST4-74	2179157	2180377	-
<i>wcaK</i>	1	1	1.09	ST4-74	2180374	2181654	-
<i>wzx</i>	3	2	1.36	ST4-74	2181676	2183154	-
<i>wcaJ</i>	2	1	1.19	ST4-74	2183287	2184681	-
<i>cpsG</i>	1	1	0.69	ST4-74	2184735	2186105	-
<i>cpsB</i>	3	4	0.82	ST4-74	2186216	2187652	-
<i>wcaI</i>	1	2	0.66	ST4-74	2187655	2188878	-
<i>gmm</i>	1	2	0.90	ST4-74	2188875	2189348	-
<i>fcl</i>	2	1	1.66	ST4-74	2189351	2190316	-
<i>gmd</i>	2	2	1.02	ST4-74	2190319	2191440	-
<i>wcaF</i>	1	1	1.77	ST4-74	2191464	2192018	-
<i>wcaE</i>	2	1	1.25	ST4-74	2192034	2192780	-

<i>Name</i>	Δ <i>fnr</i> TPM	WT TPM	Δ <i>fnr</i> /WT	Chr ^a	Start	End	Strand
<i>wcaD</i>	3	3	1.11	ST4-74	2192793	2194007	-
<i>wcaC</i>	2	2	1.22	ST4-74	2193982	2195199	-
<i>wcaB</i>	5	4	1.48	ST4-74	2195196	2195684	-
<i>wcaA</i>	2	2	1.07	ST4-74	2195687	2196529	-
<i>wzc</i>	2	1	1.36	ST4-74	2196616	2198775	-
<i>wzb</i>	2	1	1.84	ST4-74	2198772	2199221	-
<i>wza</i>	2	1	1.36	ST4-74	2199227	2200282	-
<i>yegH</i>	23	21	1.11	ST4-74	2201041	2202621	+
<i>asmaA</i>	40	44	0.89	ST4-74	2202707	2204563	-
<i>dcd</i>	27	34	0.79	ST4-74	2204602	2205183	-
<i>udk</i>	34	37	0.92	ST4-74	2205274	2205915	-
<i>yegE</i>	12	11	1.16	ST4-74	2206246	2209236	+
<i>alkA</i>	8	7	1.22	ST4-74	2209204	2210073	-
<i>yegD</i>	5	5	1.00	ST4-74	2210207	2211559	+
<i>RyeC</i>	7136	10986	0.65	ST4-74	2211623	2211760	+
STM2126	4	4	1.04	ST4-74	2212000	2213241	+
<i>yegN</i>	4	3	1.16	ST4-74	2213241	2216363	+
<i>yegO</i>	5	4	1.27	ST4-74	2216364	2219444	+
<i>yegB</i>	11	9	1.24	ST4-74	2219441	2220853	+
<i>baeS</i>	11	10	1.10	ST4-74	2220853	2222256	+
<i>baeR</i>	12	10	1.22	ST4-74	2222253	2222975	+
STnc1150	2434	873	2.79	ST4-74	2222979	2223134	+
STM2133	1	1	1.46	ST4-74	2223562	2224446	+
STM2134	2	2	1.19	ST4-74	2224446	2225162	+
STM2135	4	4	1.16	ST4-74	2225173	2227284	+
<i>yegQ</i>	9	9	0.98	ST4-74	2227400	2228761	+
<i>CyaR</i>	35723	36420	0.98	ST4-74	2228847	2228932	+
<i>sseK2</i>	9	4	2.04	ST4-74	2229212	2230258	+
<i>srcA</i>	80	16	4.87	ST4-74	2230294	2230710	-
STM2139	116	38	3.09	ST4-74	2230832	2231167	-
SL1344_2116	12	12	0.96	ST4-74	2231529	2231645	-
<i>yegS</i>	24	14	1.71	ST4-74	2231729	2232628	+
<i>fbaB</i>	116	72	1.61	ST4-74	2232681	2233733	-
<i>yegT</i>	5	4	1.17	ST4-74	2233987	2235258	+
<i>yegU</i>	7	6	1.21	ST4-74	2235255	2236259	+
<i>yegV</i>	4	4	1.11	ST4-74	2236361	2237221	+
<i>yegW</i>	49	51	0.96	ST4-74	2237195	2237941	-
<i>thiD</i>	32	37	0.86	ST4-74	2237977	2238777	-
<i>thiM</i>	20	22	0.90	ST4-74	2238764	2239561	-
STM2148	34	42	0.81	ST4-74	2239971	2240285	+
STnc740	174	118	1.48	ST4-74	2240283	2240366	-
<i>stcD</i>	7	7	0.95	ST4-74	2240548	2241555	-
<i>stcC</i>	7	6	1.14	ST4-74	2241571	2244060	-
<i>stcB</i>	1	1	1.05	ST4-74	2244074	2244757	-
<i>stcA</i>	3	19	0.15	ST4-74	2244813	2245343	-
<i>yehE</i>	35	40	0.88	ST4-74	2245622	2245903	-
<i>mrp</i>	34	37	0.90	ST4-74	2246181	2247290	-
<i>metG</i>	40	46	0.87	ST4-74	2247455	2249488	+
<i>yehR</i>	11	8	1.32	ST4-74	2249729	2250187	+
STM2156A	13	9	1.48	ST4-74	2250359	2250889	+
STnc1890	26	23	1.12	ST4-74	2250891	2250938	+

<i>Name</i>	Δ <i>fnr</i> TPM	WT TPM	Δ <i>fnr</i> /WT	<i>Chr</i> ^a	<i>Start</i>	<i>End</i>	<i>Strand</i>
<i>yehS</i>	49	43	1.12	ST4-74	2250946	2251413	-
<i>yehT</i>	10	12	0.90	ST4-74	2251460	2252179	-
<i>yehU</i>	18	19	0.95	ST4-74	2252176	2253861	-
<i>yehV</i>	61	42	1.44	ST4-74	2254084	2254815	+
<i>yohO</i>	630	453	1.39	ST4-74	2254875	2254982	+
<i>yehW</i>	13	9	1.39	ST4-74	2254963	2255694	-
<i>yehX</i>	17	11	1.46	ST4-74	2255678	2256625	-
<i>yehY</i>	27	19	1.44	ST4-74	2256618	2257787	-
<i>yehZ</i>	48	36	1.33	ST4-74	2257791	2258708	-
<i>bglX</i>	11	11	0.98	ST4-74	2258889	2261186	-
<i>dld</i>	13	13	0.99	ST4-74	2261453	2263183	+
<i>pbpG</i>	16	15	1.07	ST4-74	2263241	2264149	-
STnc3720	82	58	1.42	ST4-74	2264259	2264328	+
<i>yohC</i>	45	21	2.11	ST4-74	2264354	2264941	-
<i>yohD</i>	15	13	1.18	ST4-74	2265073	2265669	+
<i>yohF</i>	11	8	1.43	ST4-74	2265718	2266479	-
<i>yohG</i>	5	3	1.39	ST4-74	2266545	2267981	-
STnc1330	1078	526	2.05	ST4-74	2268274	2268414	+
<i>yohI</i>	8	7	1.14	ST4-74	2268440	2269378	-
STM2175	11	9	1.16	ST4-74	2269487	2270680	-
STM2176	4	3	1.60	ST4-74	2270695	2271339	-
STM2177	2	2	1.21	ST4-74	2271348	2272049	-
STM2178	1	1	1.09	ST4-74	2272065	2273102	-
STM2179	2	2	0.92	ST4-74	2273114	2274472	-
STM2180	16	14	1.14	ST4-74	2274598	2275506	+
<i>yohJ</i>	60	41	1.48	ST4-74	2275638	2276036	+
<i>yohK</i>	9	9	1.10	ST4-74	2276033	2276728	+
<i>cdd</i>	7	8	0.85	ST4-74	2276882	2277766	+
<i>sanA</i>	62	60	1.03	ST4-74	2277943	2278662	+
<i>b2145</i>	20	18	1.09	ST4-74	2278659	2278904	+
STM2186	17	17	0.96	ST4-74	2279109	2280350	+
<i>yeiA</i>	10	13	0.79	ST4-74	2280344	2281579	+
<i>mglC</i>	10	14	0.74	ST4-74	2281654	2282664	-
<i>mglA</i>	8	12	0.67	ST4-74	2282680	2284200	-
<i>mglB</i>	13	21	0.60	ST4-74	2284334	2285332	-
<i>galS</i>	15	13	1.15	ST4-74	2285831	2286853	-
<i>yeiB</i>	16	17	0.96	ST4-74	2287003	2288145	-
<i>folE</i>	26	25	1.08	ST4-74	2288160	2288828	-
<i>yeiG</i>	78	66	1.20	ST4-74	2289158	2290015	+
STM2195	20	24	0.82	ST4-74	2290004	2290393	-
STM2196	5	6	0.98	ST4-74	2290398	2291765	-
STM2197	1	1	0.77	ST4-74	2291982	2292869	+
STM2198	6	5	1.15	ST4-74	2292902	2294224	+
<i>cirA</i>	4	3	1.27	ST4-74	2294268	2296259	-
<i>lysP</i>	72	77	0.94	ST4-74	2296604	2298073	-
<i>yeiE</i>	25	25	0.98	ST4-74	2298263	2299126	-
<i>yeiH</i>	8	12	0.68	ST4-74	2299247	2300296	+
<i>nfo</i>	15	15	1.01	ST4-74	2300375	2301232	+
<i>fruA</i>	7	9	0.78	ST4-74	2301297	2302985	-
<i>fruK</i>	6	7	0.91	ST4-74	2303002	2303859	-
<i>fruB</i>	5	7	0.64	ST4-74	2303940	2305070	-

<i>Name</i>	Δfnr TPM	WT TPM	$\Delta fnr/WT$	Chr ^a	Start	End	Strand
<i>setB</i>	5	6	0.91	ST4-74	2305439	2306620	+
STM2208	10	7	1.40	ST4-74	2306685	2307350	-
STM2209	19	14	1.37	ST4-74	2307352	2307474	-
SL1344_2187	21	21	0.97	ST4-74	2307862	2308116	-
<i>yeiP</i>	38	42	0.92	ST4-74	2308440	2309012	+
<i>yeiR</i>	25	23	1.11	ST4-74	2309225	2310211	+
<i>yeiU</i>	146	138	1.06	ST4-74	2310241	2310960	+
STnc3010	176	177	1.00	ST4-74	2310959	2311126	-
<i>spr</i>	664	1075	0.62	ST4-74	2311374	2311946	+
<i>rtn</i>	30	29	1.06	ST4-74	2312272	2313828	+
<i>yejA</i>	21	22	0.94	ST4-74	2313935	2315740	+
<i>yejB</i>	25	25	1.00	ST4-74	2315750	2316844	+
<i>yejE</i>	10	12	0.90	ST4-74	2316844	2317869	+
<i>yejF</i>	9	10	0.96	ST4-74	2317871	2319460	+
<i>yejG</i>	162	100	1.62	ST4-74	2319464	2319808	-
STnc1340	126	356	0.35	ST4-74	2319956	2320037	-
<i>bcr</i>	15	16	0.91	ST4-74	2320199	2321389	-
STnc1540	316	530	0.60	ST4-74	2321042	2321137	-
<i>rsuA</i>	39	33	1.20	ST4-74	2321417	2322112	-
<i>yejH</i>	4	4	0.90	ST4-74	2322264	2324024	+
<i>rplY</i>	405	553	0.73	ST4-74	2324149	2324433	+
STM2225	51	46	1.11	ST4-74	2324542	2325162	-
<i>yejK</i>	22	23	0.92	ST4-74	2325190	2326197	-
<i>yejL</i>	209	187	1.12	ST4-74	2326377	2326604	+
<i>yejM</i>	36	35	1.02	ST4-74	2326636	2328396	+
STM2230	3	4	0.69	ST4-74	2328677	2329147	-
STM2231	3	2	1.18	ST4-74	2329208	2329498	+
<i>oafA</i>	69	58	1.20	ST4-74	2329846	2331675	+
STM2233	2	3	0.74	ST4-74	2331729	2332172	-
STM2234	4	4	1.13	ST4-74	2332550	2333077	-
STM2235	4	3	1.19	ST4-74	2333080	2334321	-
STM2236	2	2	1.04	ST4-74	2334382	2334900	-
STM2237	1	1	0.50	ST4-74	2334914	2335243	-
STM2238	54	46	1.17	ST4-74	2335540	2336871	+
STM2239	11	10	1.12	ST4-74	2336900	2337268	-
STM2240	6	5	1.15	ST4-74	2337283	2338272	-
<i>sspH2</i>	12	10	1.18	ST4-74	2338601	2340967	-
STM2242	4	2	1.68	ST4-74	2341136	2341339	-
STM2243	5	4	1.21	ST4-74	2341636	2342463	-
<i>IsrG</i>	6	6	0.98	ST4-74	2342448	2342729	+
STM2244	6	4	1.65	ST4-74	2342730	2342933	+
STM2245	125	17	7.30	ST4-74	2343125	2343688	-
<i>narP</i>	23	24	0.99	ST4-74	2344418	2345065	+
<i>ccmH2</i>	3	7	0.48	ST4-74	2345109	2346152	-
<i>ccmG2</i>	7	13	0.58	ST4-74	2346149	2346706	-
<i>ccmF2</i>	7	14	0.49	ST4-74	2346703	2348634	-
<i>ccmE2</i>	6	13	0.44	ST4-74	2348631	2349110	-
<i>ccmD2</i>	4	10	0.45	ST4-74	2349107	2349280	-
<i>ccmC2</i>	11	29	0.36	ST4-74	2349316	2350062	-
<i>ccmB2</i>	5	10	0.51	ST4-74	2350105	2350761	-
<i>ccmA2</i>	5	15	0.33	ST4-74	2350761	2351378	-

<i>Name</i>	Δfnr TPM	WT TPM	$\Delta fnr/WT$	<i>Chr</i> ^a	<i>Start</i>	<i>End</i>	<i>Strand</i>
<i>napC</i>	5	8	0.70	ST4-74	2351399	2352001	-
<i>napB</i>	2	5	0.38	ST4-74	2352011	2352460	-
<i>napH</i>	5	7	0.72	ST4-74	2352576	2353445	-
<i>napG</i>	2	4	0.48	ST4-74	2353432	2354127	-
<i>napA</i>	3	5	0.70	ST4-74	2354134	2356620	-
<i>napD</i>	1	6	0.24	ST4-74	2356617	2356880	-
<i>napF</i>	2	12	0.19	ST4-74	2356870	2357361	-
<i>eco</i>	6	3	2.28	ST4-74	2357775	2358269	+
<i>yojI</i>	21	17	1.30	ST4-74	2358478	2360121	-
<i>alkB</i>	6	6	1.12	ST4-74	2360197	2360847	-
<i>ada</i>	21	11	1.90	ST4-74	2360850	2361911	-
<i>apbE</i>	7	8	0.81	ST4-74	2361992	2363044	-
<i>ompC</i>	328	443	0.74	ST4-74	2363159	2364127	-
<i>MicF</i>	295	201	1.47	ST4-74	2364629	2364721	+
<i>yojN</i>	35	36	0.99	ST4-74	2365024	2367693	+
<i>rscB</i>	60	60	1.01	ST4-74	2367710	2368360	+
<i>rscC</i>	25	23	1.08	ST4-74	2368463	2371309	-
<i>gyrA</i>	62	63	0.98	ST4-74	2371427	2374063	-
STM2273	11	9	1.20	ST4-74	2374473	2375675	-
STM2274	3	3	1.29	ST4-74	2375690	2377015	-
STM2275	9	11	0.78	ST4-74	2377254	2377949	+
<i>ubiG</i>	72	61	1.17	ST4-74	2378032	2378760	+
<i>nrdA</i>	29	25	1.15	ST4-74	2379116	2381401	+
<i>nrdB</i>	21	22	0.95	ST4-74	2381514	2382644	+
<i>yfaE</i>	15	20	0.72	ST4-74	2382644	2382898	+
STM2280	14	14	0.99	ST4-74	2382900	2384090	-
STM2281	10	10	1.05	ST4-74	2384252	2385130	+
<i>glpQ</i>	315	531	0.59	ST4-74	2385246	2386316	-
<i>glpT</i>	345	527	0.66	ST4-74	2386321	2387679	-
<i>glpA</i>	70	177	0.39	ST4-74	2387952	2389580	+
<i>glpB</i>	40	111	0.36	ST4-74	2389570	2390829	+
<i>glpC</i>	64	144	0.44	ST4-74	2390826	2392016	+
<i>IsrH_1_2</i>	19	6	3.44	ST4-74	2392019	2392469	-
<i>sseL</i>	276	43	6.41	ST4-74	2392511	2393464	+
STM2288	28	24	1.15	ST4-74	2393574	2393750	-
STM2289	7	7	1.02	ST4-74	2393756	2394559	-
<i>yfaV</i>	8	8	1.02	ST4-74	2394585	2395874	-
<i>yfaW</i>	8	6	1.42	ST4-74	2395930	2397147	-
<i>yfaX</i>	4	4	1.07	ST4-74	2397149	2397931	-
STM2293	21	19	1.13	ST4-74	2398181	2399377	-
<i>yfaZ</i>	31	29	1.06	ST4-74	2399492	2400058	-
<i>yfaO</i>	58	70	0.83	ST4-74	2400313	2400738	+
<i>ais</i>	59	69	0.85	ST4-74	2400783	2401388	-
<i>yfbE</i>	162	201	0.80	ST4-74	2401669	2402826	+
<i>pmrF</i>	79	109	0.72	ST4-74	2402829	2403812	+
<i>yfbG</i>	49	74	0.65	ST4-74	2403809	2405791	+
STM2300	43	67	0.65	ST4-74	2405788	2406687	+
<i>arnT</i>	49	67	0.73	ST4-74	2406684	2408330	+
STM2302	33	51	0.64	ST4-74	2408405	2408662	+
STM2303	16	25	0.66	ST4-74	2408662	2409039	+
<i>pmrD</i>	1558	1210	1.29	ST4-74	2409034	2409291	-

<i>Name</i>	Δ <i>fnr</i> TPM	WT TPM	Δ <i>fnr</i> /WT	Chr ^a	Start	End	Strand
<i>menE</i>	8	13	0.61	ST4-74	2409389	2410756	-
<i>menC</i>	7	12	0.61	ST4-74	2410753	2411715	-
<i>menB</i>	9	18	0.50	ST4-74	2411715	2412572	-
<i>yfbB</i>	10	18	0.55	ST4-74	2412587	2413345	-
<i>menD</i>	6	19	0.33	ST4-74	2413342	2415012	-
<i>menF</i>	16	17	0.96	ST4-74	2415098	2416393	-
<i>elaB</i>	332	242	1.37	ST4-74	2416494	2416805	-
<i>elaA</i>	20	19	1.05	ST4-74	2416854	2417315	-
<i>elaC</i>	18	16	1.12	ST4-74	2417376	2418293	+
STM2314	41	119	0.35	ST4-74	2418359	2419360	+
<i>yfbK</i>	6	6	1.11	ST4-74	2419401	2421182	-
<i>nuoN</i>	29	72	0.41	ST4-74	2422070	2423527	-
<i>nuoM</i>	37	93	0.39	ST4-74	2423534	2425063	-
<i>nuoL</i>	43	97	0.44	ST4-74	2425377	2427218	-
<i>nuoK</i>	26	64	0.41	ST4-74	2427215	2427517	-
<i>nuoJ</i>	29	73	0.39	ST4-74	2427514	2428068	-
<i>nuoI</i>	45	100	0.45	ST4-74	2428079	2428621	-
<i>nuoH</i>	34	77	0.44	ST4-74	2428636	2429613	-
<i>nuoG</i>	33	71	0.46	ST4-74	2429610	2432336	-
<i>nuoF</i>	22	47	0.47	ST4-74	2432367	2433704	-
<i>nuoE</i>	31	74	0.43	ST4-74	2433701	2434201	-
<i>nuoC</i>	35	72	0.48	ST4-74	2434204	2436006	-
<i>nuoB</i>	37	74	0.50	ST4-74	2436093	2436755	-
<i>nuoA</i>	84	175	0.48	ST4-74	2436771	2437214	-
STM2329	20	15	1.30	ST4-74	2437609	2437761	-
STnc1550	142	223	0.64	ST4-74	2437665	2437806	+
<i>lrhA</i>	55	48	1.13	ST4-74	2437841	2438779	-
<i>yfbQ</i>	15	19	0.77	ST4-74	2439711	2440925	+
STM2332	14	16	0.90	ST4-74	2441019	2441618	+
<i>yfbS</i>	20	25	0.79	ST4-74	2441710	2443536	-
<i>yfbT</i>	37	49	0.75	ST4-74	2443613	2444290	-
<i>yfbU</i>	85	122	0.69	ST4-74	2444283	2444777	-
STM2336	65	76	0.85	ST4-74	2444860	2445315	-
<i>ackA</i>	45	117	0.39	ST4-74	2445655	2446857	+
<i>pta</i>	14	44	0.33	ST4-74	2446934	2449078	+
STnc1560	69	381	0.18	ST4-74	2449075	2449183	+
STnc3730	122	63	1.93	ST4-74	2449087	2449281	-
<i>yfcC</i>	5	14	0.35	ST4-74	2449296	2450816	+
STM2340	11	12	0.87	ST4-74	2450865	2451818	-
STM2341	4	6	0.67	ST4-74	2451811	2452641	-
STM2342	7	11	0.67	ST4-74	2452638	2454029	-
STM2343	3	7	0.47	ST4-74	2454050	2454322	-
STM2344	19	20	0.93	ST4-74	2454403	2454846	-
STM2345	16	19	0.83	ST4-74	2455099	2456118	+
STM2346	68	66	1.04	ST4-74	2456124	2456678	-
<i>yfcE</i>	87	81	1.07	ST4-74	2456735	2457286	-
<i>yfcF</i>	34	29	1.17	ST4-74	2457342	2457986	-
<i>yfcG</i>	14	7	2.00	ST4-74	2458129	2458776	+
<i>yfcH</i>	24	20	1.25	ST4-74	2458902	2459795	+
STnc3740	176	129	1.37	ST4-74	2459768	2459846	+
<i>hisP</i>	24	27	0.90	ST4-74	2459847	2460623	-

<i>Name</i>	Δfnr TPM	WT TPM	$\Delta fnr/WT$	<i>Chr</i> ^a	<i>Start</i>	<i>End</i>	<i>Strand</i>
<i>hisM</i>	25	30	0.85	ST4-74	2460634	2461341	-
<i>hisQ</i>	34	42	0.82	ST4-74	2461338	2462024	-
<i>hisJ</i>	78	100	0.78	ST4-74	2462207	2462989	-
<i>argT</i>	20	19	1.05	ST4-74	2463227	2464009	-
<i>ubiX</i>	46	37	1.23	ST4-74	2464298	2464867	-
STM2357	22	22	1.00	ST4-74	2464894	2466300	-
STM2358	11	9	1.24	ST4-74	2466364	2467467	-
STM2359	6	6	0.94	ST4-74	2467469	2468890	-
STM2360	4	3	1.22	ST4-74	2468981	2470378	-
STM2361	11	10	1.06	ST4-74	2470589	2472016	+
<i>purF</i>	75	87	0.86	ST4-74	2472052	2473569	-
<i>cvpA</i>	196	270	0.72	ST4-74	2473607	2474095	-
<i>dedD</i>	71	73	0.97	ST4-74	2474406	2475080	-
<i>folC</i>	40	44	0.90	ST4-74	2475070	2476338	-
<i>accD</i>	118	117	1.01	ST4-74	2476406	2477320	-
<i>dedA</i>	33	31	1.06	ST4-74	2477470	2478129	-
<i>truA</i>	49	47	1.04	ST4-74	2478178	2478990	-
<i>usg</i>	20	22	0.90	ST4-74	2478990	2480003	-
<i>pdxB</i>	34	32	1.05	ST4-74	2480071	2481207	-
<i>div</i>	6	6	0.88	ST4-74	2481311	2482312	+
STM2372	16	19	0.81	ST4-74	2482309	2483487	-
STM2373	5	4	1.23	ST4-74	2483667	2484041	-
STM2374	5	4	1.34	ST4-74	2484214	2484462	+
STM2375	2	2	1.10	ST4-74	2484631	2484999	+
STM2376	1	1	0.54	ST4-74	2484999	2485517	+
STM2377	13	12	1.03	ST4-74	2485584	2486240	-
<i>fabB</i>	155	152	1.02	ST4-74	2486338	2487552	-
<i>mnmC</i>	27	30	0.90	ST4-74	2487652	2489712	+
<i>yfcL</i>	77	66	1.16	ST4-74	2489764	2490039	-
<i>yfcM</i>	20	20	1.03	ST4-74	2490072	2490620	-
<i>yfcA</i>	10	12	0.85	ST4-74	2490620	2491429	-
<i>mepA</i>	11	13	0.88	ST4-74	2491429	2492253	-
<i>aroC</i>	18	21	0.89	ST4-74	2492257	2493342	-
<i>yfcB</i>	31	30	1.02	ST4-74	2493378	2494310	-
<i>yfcN</i>	24	20	1.23	ST4-74	2494476	2495027	+
<i>sixA</i>	156	143	1.09	ST4-74	2495127	2495612	-
<i>fadJ</i>	29	20	1.44	ST4-74	2495821	2497968	-
<i>fadI</i>	5	5	0.91	ST4-74	2497968	2499278	-
<i>yfcZ</i>	78	185	0.42	ST4-74	2499456	2499740	-
<i>fadL</i>	22	24	0.93	ST4-74	2500105	2501418	+
<i>vacJ</i>	92	84	1.10	ST4-74	2501479	2502234	-
<i>yfdC</i>	24	13	1.82	ST4-74	2502523	2503464	+
STnc3750	128	54	2.36	ST4-74	2503726	2503803	-
<i>pgtE</i>	47	23	2.00	ST4-74	2503771	2504709	-
<i>pgtA</i>	9	10	0.87	ST4-74	2504977	2506224	-
<i>pgtB</i>	9	12	0.76	ST4-74	2506214	2508220	-
<i>pgtC</i>	12	9	1.30	ST4-74	2508217	2509410	-
<i>pgtP</i>	11	8	1.33	ST4-74	2509846	2511237	+
STM2400	93	85	1.09	ST4-74	2511513	2511755	-
<i>lpxP</i>	7	6	1.24	ST4-74	2512277	2513197	+
<i>tpke70</i>	6	3	2.25	ST4-74	2513324	2513722	-

<i>Name</i>	Δ <i>fnr</i> TPM	WT TPM	Δ <i>fnr</i> /WT	Chr ^a	Start	End	Strand
<i>ypdK</i>	106	85	1.25	ST4-74	2513600	2513671	+
<i>yfdZ</i>	45	36	1.27	ST4-74	2513721	2514959	-
STnc3760	57	55	1.03	ST4-74	2515508	2515633	+
<i>glk</i>	67	66	1.02	ST4-74	2515680	2516645	-
STM2404	8	8	1.04	ST4-74	2516849	2518084	+
STM2405	3	3	1.01	ST4-74	2518104	2519756	-
STM2406	9	6	1.52	ST4-74	2519936	2520934	+
<i>ypeC</i>	20	14	1.42	ST4-74	2521048	2521374	+
<i>mntH</i>	9	9	0.99	ST4-74	2521435	2522676	-
<i>nupC</i>	40	38	1.05	ST4-74	2523019	2524221	+
<i>yfeA</i>	15	17	0.93	ST4-74	2524274	2526463	-
<i>yfeC</i>	151	152	0.99	ST4-74	2527069	2527431	+
<i>yfeD</i>	39	55	0.71	ST4-74	2527433	2527825	+
<i>gltX</i>	40	40	1.00	ST4-74	2527879	2529294	-
<i>xapR</i>	8	6	1.31	ST4-74	2530110	2530994	-
SL1344_2383	7	7	1.02	ST4-74	2531046	2531204	-
<i>xapB</i>	13	10	1.28	ST4-74	2531263	2532519	-
<i>flhAb</i>	4	9	0.47	ST4-74	2532574	2533407	-
<i>yfeN</i>	8	7	1.21	ST4-74	2533663	2534424	+
<i>yfeR</i>	5	5	0.88	ST4-74	2534486	2535412	-
<i>yfeH</i>	19	16	1.15	ST4-74	2535502	2536500	+
STM2426	14	13	1.05	ST4-74	2536497	2536724	-
<i>lig</i>	13	13	0.95	ST4-74	2536717	2538732	-
<i>zipA</i>	148	151	0.98	ST4-74	2538804	2539790	-
<i>cysZ</i>	19	18	1.06	ST4-74	2540022	2540783	+
<i>cysK</i>	280	325	0.86	ST4-74	2540947	2541918	+
<i>ptsH</i>	248	389	0.64	ST4-74	2542302	2542559	+
<i>ptsI</i>	159	212	0.75	ST4-74	2542608	2544335	+
<i>crr</i>	292	322	0.91	ST4-74	2544376	2544885	+
STM2434	5	7	0.79	ST4-74	2545034	2545273	-
<i>pdxK</i>	9	8	1.10	ST4-74	2545270	2546136	-
<i>ptsJ</i>	4	4	1.00	ST4-74	2546219	2547511	+
<i>yfeJ</i>	3	3	0.76	ST4-74	2547526	2548245	+
<i>yfeK</i>	7	9	0.81	ST4-74	2548304	2548684	+
<i>yfeL</i>	42	29	1.47	ST4-74	2548697	2549236	+
<i>cysM</i>	30	32	0.94	ST4-74	2549367	2550278	-
<i>cysA</i>	66	77	0.86	ST4-74	2550346	2551443	-
<i>cysW</i>	108	128	0.84	ST4-74	2551433	2552308	-
<i>cysU</i>	106	121	0.88	ST4-74	2552308	2553141	-
<i>cysP</i>	108	123	0.88	ST4-74	2553141	2554157	-
<i>ucpA</i>	67	82	0.81	ST4-74	2554315	2555106	-
STM2446	18	47	0.37	ST4-74	2555344	2556243	-
<i>yfeY</i>	16	19	0.86	ST4-74	2556338	2556913	-
<i>yfeZ</i>	20	17	1.17	ST4-74	2556975	2557424	-
STM2449	58	64	0.90	ST4-74	2557411	2557836	-
<i>amiA</i>	22	17	1.33	ST4-74	2558049	2558918	+
<i>hemF</i>	6	6	1.04	ST4-74	2558921	2559820	+
STM2452	11	9	1.24	ST4-74	2559841	2560170	+
STM2453	7	6	1.18	ST4-74	2560299	2561576	+
<i>eutR</i>	7	6	1.17	ST4-74	2561776	2562828	-
<i>eutK</i>	4	4	0.82	ST4-74	2562876	2563370	-

<i>Name</i>	Δfnr TPM	WT TPM	$\Delta fnr/WT$	<i>Chr</i> ^a	<i>Start</i>	<i>End</i>	<i>Strand</i>
<i>eutL</i>	11	10	1.12	ST4-74	2563383	2564042	-
<i>eutC</i>	2	2	1.45	ST4-74	2564052	2564948	-
<i>eutB</i>	1	2	0.66	ST4-74	2564967	2566328	-
<i>eutA</i>	26	28	0.93	ST4-74	2566340	2567743	-
<i>eutH</i>	8	8	0.98	ST4-74	2567740	2568966	-
<i>eutG</i>	1	2	0.66	ST4-74	2569086	2570273	-
<i>eutJ</i>	2	1	1.10	ST4-74	2570263	2571102	-
<i>eutE</i>	2	2	1.43	ST4-74	2571113	2572516	-
<i>eutN</i>	3	3	0.97	ST4-74	2572528	2572827	-
<i>eutM</i>	4	2	2.17	ST4-74	2572928	2573218	-
<i>eutD</i>	1	1	0.63	ST4-74	2573259	2574275	-
<i>eutT</i>	1	1	1.50	ST4-74	2574272	2575075	-
<i>eutQ</i>	4	5	0.72	ST4-74	2575072	2575761	-
<i>eutP</i>	1	1	0.49	ST4-74	2575739	2576218	-
<i>eutS</i>	2	1	1.04	ST4-74	2576231	2576566	-
<i>tnpA_1b</i>	244	250	0.97	ST4-74	2577047	2577505	-
<i>maeB</i>	17	26	0.66	ST4-74	2577695	2579974	-
<i>tal</i>	29	19	1.49	ST4-74	2580246	2581196	+
<i>tktB</i>	17	13	1.31	ST4-74	2581216	2583216	+
STM2475	101	108	0.94	ST4-74	2583279	2583509	-
<i>ypfG</i>	9	5	1.78	ST4-74	2583637	2584680	-
<i>yffH</i>	25	20	1.24	ST4-74	2584805	2585380	-
STM2478	17	16	1.03	ST4-74	2585584	2586882	+
<i>aeqA</i>	3	12	0.25	ST4-74	2587331	2589292	-
<i>narQ</i>	6	7	0.86	ST4-74	2589478	2591178	+
<i>acrD</i>	6	6	1.04	ST4-74	2591363	2594476	+
<i>ypfM</i>	1269	780	1.63	ST4-74	2594578	2594637	-
<i>yffB</i>	21	24	0.86	ST4-74	2595050	2595406	+
<i>dapE</i>	25	21	1.20	ST4-74	2595410	2596537	+
STM2484	50	36	1.40	ST4-74	2596565	2596765	+
<i>ypfI</i>	8	8	1.00	ST4-74	2596792	2598810	-
STM2486	39	31	1.26	ST4-74	2598826	2599689	-
<i>purC</i>	40	78	0.52	ST4-74	2599820	2600533	-
<i>nlpB</i>	83	91	0.91	ST4-74	2600708	2601742	-
<i>dapA</i>	168	178	0.94	ST4-74	2601759	2602637	-
<i>gcvR</i>	85	95	0.90	ST4-74	2602783	2603355	+
<i>bcp</i>	70	82	0.85	ST4-74	2603355	2603825	+
STM2492	9	7	1.27	ST4-74	2603872	2604114	-
<i>perM</i>	30	34	0.88	ST4-74	2604412	2605479	-
STM2494	28	27	1.03	ST4-74	2605687	2607150	+
<i>yfgD</i>	31	31	1.00	ST4-74	2607190	2607549	+
<i>yfgE</i>	52	48	1.08	ST4-74	2607576	2608301	-
<i>uraA</i>	11	21	0.53	ST4-74	2608372	2609661	-
<i>upp</i>	54	86	0.62	ST4-74	2609749	2610375	-
<i>purM</i>	76	106	0.72	ST4-74	2610774	2611826	+
<i>purN</i>	53	73	0.72	ST4-74	2611826	2612464	+
<i>ppk</i>	35	32	1.10	ST4-74	2612653	2614719	+
<i>ppx</i>	15	15	0.95	ST4-74	2614724	2616265	+
STM2503	7	18	0.42	ST4-74	2616301	2618514	-
STM2505	4	5	0.82	ST4-74	2618819	2619079	-
STM2506	378	469	0.81	ST4-74	2618927	2619118	+
STM2508	25	20	1.23	ST4-74	2619659	2619988	+

<i>Name</i>	Δ <i>fnr</i> TPM	WT TPM	Δ <i>fnr</i> /WT	Chr ^a	Start	End	Strand
STM2509	3	3	0.81	ST4-74	2620008	2620364	-
<i>guaA</i>	23	30	0.76	ST4-74	2620521	2622098	-
<i>guaB</i>	34	36	0.94	ST4-74	2622168	2623634	-
<i>xseA</i>	32	20	1.62	ST4-74	2623795	2625144	+
<i>shdA</i>	4	3	1.16	ST4-74	2625306	2631425	-
<i>ratB</i>	6	5	1.04	ST4-74	2632119	2639425	-
<i>ratA</i>	10	7	1.39	ST4-74	2639591	2645188	-
<i>sinI</i>	3	3	1.18	ST4-74	2645308	2646267	-
<i>sinH</i>	2	2	1.02	ST4-74	2646325	2648517	-
<i>yfgJ</i>	23	25	0.92	ST4-74	2648863	2649084	-
<i>engA</i>	21	16	1.30	ST4-74	2649173	2650645	-
<i>yfgL</i>	110	96	1.14	ST4-74	2650764	2651942	-
<i>yfgM</i>	51	51	0.99	ST4-74	2651953	2652573	-
<i>hisS</i>	47	48	0.99	ST4-74	2652587	2653861	-
<i>gcpE</i>	40	42	0.94	ST4-74	2653972	2655090	-
<i>yfgA</i>	57	57	1.00	ST4-74	2655117	2656121	-
<i>yfgB</i>	18	20	0.92	ST4-74	2656413	2657579	-
<i>ndk</i>	98	103	0.95	ST4-74	2657786	2658217	-
STM2527	2	5	0.39	ST4-74	2658338	2659201	-
STM2528	5	11	0.43	ST4-74	2659201	2660010	-
STM2529	2	7	0.27	ST4-74	2660003	2660632	-
STM2530	2	8	0.30	ST4-74	2660629	2663007	-
<i>pbpC</i>	4	5	0.71	ST4-74	2663163	2665478	-
STM2532	20	24	0.85	ST4-74	2665479	2670413	-
STM2533	42	35	1.19	ST4-74	2670622	2671464	+
STM2534	12	9	1.26	ST4-74	2671711	2672379	+
STnc2070	1487	1725	0.86	ST4-74	2672469	2672567	-
<i>RyfA</i>	169	315	0.54	ST4-74	2672651	2672944	+
<i>sseBb</i>	7	10	0.65	ST4-74	2672948	2673733	-
<i>pepB</i>	11	15	0.70	ST4-74	2673834	2675117	-
<i>yfhJ</i>	46	57	0.81	ST4-74	2675364	2675564	-
<i>fdx</i>	36	50	0.71	ST4-74	2675576	2675911	-
<i>hscA</i>	18	29	0.61	ST4-74	2675913	2677763	-
<i>hscB</i>	25	32	0.80	ST4-74	2677776	2678291	-
<i>iscA</i>	110	137	0.80	ST4-74	2678487	2678810	-
<i>nifU</i>	70	85	0.82	ST4-74	2678839	2679225	-
<i>iscS</i>	49	69	0.71	ST4-74	2679253	2680467	-
<i>yfhP</i>	72	86	0.84	ST4-74	2680648	2681142	-
STM2545	160	119	1.35	ST4-74	2681302	2682033	-
<i>suhB</i>	132	105	1.25	ST4-74	2682152	2682955	+
STM2547	5	5	1.08	ST4-74	2683100	2683978	+
<i>asrA</i>	4	6	0.67	ST4-74	2684160	2685203	+
<i>asrB</i>	3	3	0.99	ST4-74	2685207	2686025	+
<i>asrC</i>	4	4	0.99	ST4-74	2686036	2687049	+
STM2551	13	14	0.97	ST4-74	2687050	2688036	-
STM2552	13	11	1.21	ST4-74	2688027	2688665	-
<i>csiE</i>	30	19	1.62	ST4-74	2688791	2690068	+
<i>hcaT</i>	19	19	0.97	ST4-74	2690063	2691202	-
<i>glyA</i>	142	178	0.80	ST4-74	2691398	2692651	-
<i>hmpA</i>	6	6	1.06	ST4-74	2692976	2694166	+
<i>cadC</i>	39	28	1.37	ST4-74	2694348	2695892	+

<i>Name</i>	Δfnr TPM	WT TPM	$\Delta fnr/WT$	Chr ^a	Start	End	Strand
<i>cadB</i>	2	2	1.18	ST4-74	2696253	2697584	+
<i>cadA</i>	11	11	1.04	ST4-74	2697730	2699811	+
<i>yjdL</i>	7	7	1.05	ST4-74	2699867	2701327	+
<i>glnB</i>	140	148	0.94	ST4-74	2701376	2701714	-
<i>yfhA</i>	14	18	0.79	ST4-74	2701791	2703128	-
<i>yfhG</i>	26	28	0.91	ST4-74	2703125	2703889	-
<i>yfhK</i>	38	34	1.11	ST4-74	2703891	2705333	-
<i>GlmY</i>	8870	10575	0.84	ST4-74	2705381	2705564	-
<i>purG</i>	19	36	0.52	ST4-74	2705971	2709858	-
<i>yfhD</i>	34	22	1.55	ST4-74	2710114	2711658	+
<i>yfhC</i>	26	23	1.16	ST4-74	2711709	2712260	-
<i>yfhB</i>	25	22	1.11	ST4-74	2712285	2712920	-
STM2570	14	14	0.96	ST4-74	2712924	2714285	-
<i>murQ</i>	6	8	0.77	ST4-74	2714296	2715189	-
<i>yfhH</i>	5	5	0.99	ST4-74	2715305	2716153	+
STM2573	11	11	0.97	ST4-74	2716192	2717058	-
STM2574	4	3	1.46	ST4-74	2717131	2718327	-
STM2575	7	6	1.19	ST4-74	2718443	2719369	+
<i>yfhL</i>	115	69	1.67	ST4-74	2719407	2719667	+
<i>acpS</i>	17	22	0.75	ST4-74	2719779	2720159	-
<i>pdxJ</i>	13	16	0.81	ST4-74	2720159	2720890	-
<i>recO</i>	30	34	0.90	ST4-74	2720902	2721630	-
<i>era</i>	34	39	0.86	ST4-74	2721642	2722547	-
<i>rnc</i>	81	66	1.23	ST4-74	2722544	2723146	-
<i>lepB</i>	53	60	0.89	ST4-74	2723498	2724472	-
<i>lepA</i>	50	46	1.10	ST4-74	2724489	2726288	-
<i>gogB</i>	55	38	1.42	ST4-74	2726744	2728186	+
STM2585	357	85	4.21	ST4-74	2729142	2729588	+
STnc1380	538	842	0.64	ST4-74	2729634	2729701	-
SL1344_2548	28	15	1.85	ST4-74	2730253	2730318	-
STM2585A	1233	401	3.08	ST4-74	2730700	2730927	+
STM2586	1	1	0.63	ST4-74	2731024	2731602	-
STM2587	1	1	1.37	ST4-74	2731592	2732416	-
STM2588	3	3	0.91	ST4-74	2732413	2734785	-
SL1344_2552A	2	2	0.72	ST4-74	2734839	2735081	-
STM2589	3	3	0.96	ST4-74	2735120	2738482	-
STM2590	3	3	1.20	ST4-74	2738544	2739191	-
STM2591	3	3	1.00	ST4-74	2739089	2739826	-
STM2592	7	7	1.15	ST4-74	2739833	2740534	-
STM2593	9	9	1.02	ST4-74	2740541	2740870	-
STM2594	4	3	1.07	ST4-74	2740873	2743968	-
STnc3770	84	66	1.27	ST4-74	2743288	2743373	+
STM2595	3	1	2.05	ST4-74	2743940	2744257	-
STM2596	1	1	0.72	ST4-74	2744275	2744670	-
STM2597	5	5	1.06	ST4-74	2744721	2745467	-
STM2598	5	6	0.77	ST4-74	2745475	2745876	-
<i>gipA</i>	128	169	0.76	ST4-74	2745865	2747115	+
STM2600	3	3	0.91	ST4-74	2747164	2747742	-
STM2601	6	4	1.48	ST4-74	2747770	2748153	-
STM2602	5	6	0.95	ST4-74	2748164	2748523	-
STM2603	5	5	0.98	ST4-74	2748581	2749609	-

<i>Name</i>	Δ <i>fnr</i> TPM	WT TPM	Δ <i>fnr</i> /WT	Chr ^a	Start	End	Strand
STM2604	2	2	0.91	ST4-74	2749664	2750011	-
STM2605	2	1	1.22	ST4-74	2750024	2751472	-
STM2606	3	3	1.11	ST4-74	2751510	2753090	-
STM2607	3	3	1.18	ST4-74	2753087	2753290	-
STM2608	2	2	1.01	ST4-74	2753274	2755205	-
STM2609	2	1	1.20	ST4-74	2755177	2755722	-
STM2610	41	35	1.18	ST4-74	2756009	2756410	+
STnc1920	362	175	2.08	ST4-74	2756549	2756646	+
STM2611	2	2	1.17	ST4-74	2756646	2757119	-
STM2612	8	6	1.47	ST4-74	2757116	2757568	-
STM2614	38	28	1.34	ST4-74	2758157	2758843	+
<i>IsrI</i>	84	36	2.38	ST4-74	2759018	2759265	-
STnc2080	1089	811	1.34	ST4-74	2759410	2759518	-
<i>IsrJ</i>	1020	860	1.19	ST4-74	2759646	2759717	-
STM2616	12	11	1.16	ST4-74	2759753	2760316	-
STnc1160	26385	28610	0.92	ST4-74	2760372	2760451	-
<i>IsrK</i>	604	775	0.78	ST4-74	2760480	2760556	-
STM2617	2	3	0.80	ST4-74	2760589	2761266	-
STM2618	1	1	1.25	ST4-74	2761263	2761403	-
STM2619	2	1	1.11	ST4-74	2761400	2762011	-
STM2620	23	28	0.84	ST4-74	2762220	2762822	-
SL1344_2583	60	53	1.12	ST4-74	2762857	2763105	-
STM2621	53	62	0.85	ST4-74	2763222	2763455	-
SL1344_2585	267	194	1.37	ST4-74	2763714	2763905	-
SL1344_2586	4	4	0.99	ST4-74	2764017	2764298	-
SL1344_2587	3	4	0.68	ST4-74	2764291	2764944	-
SL1344_2588	3	2	1.31	ST4-74	2764947	2765417	-
SL1344_2589	2	2	1.04	ST4-74	2765419	2766084	-
<i>gpP</i>	2	2	1.04	ST4-74	2766099	2766791	-
<i>gpO</i>	1	2	0.81	ST4-74	2766788	2767693	-
STnc1390	919	1156	0.80	ST4-74	2767704	2767767	+
<i>cIIa</i>	2	2	0.73	ST4-74	2767785	2768207	-
SL1344_2593	353	348	1.01	ST4-74	2768450	2768833	+
SL1344_2594	406	393	1.03	ST4-74	2768985	2770070	+
SL1344_2595	134	104	1.29	ST4-74	2770178	2770384	-
STM2629	2	2	0.92	ST4-74	2770636	2770791	+
STnc1400	536	866	0.62	ST4-74	2770951	2771060	-
<i>recEb</i>	2	2	0.93	ST4-74	2771095	2774295	+
STM2633	3	3	0.79	ST4-74	2774306	2775415	+
STM2634	3	2	1.40	ST4-74	2775458	2775697	+
STM2635	1	3	0.33	ST4-74	2775738	2776022	+
STM2636	7	6	1.20	ST4-74	2776000	2777229	-
<i>rseC</i>	17	19	0.89	ST4-74	2777727	2778206	-
<i>rseB</i>	39	39	1.00	ST4-74	2778203	2779159	-
<i>rseA</i>	128	124	1.03	ST4-74	2779159	2779809	-
<i>rpoE</i>	168	148	1.14	ST4-74	2779841	2780416	-
<i>nadB</i>	11	12	0.91	ST4-74	2780841	2782463	+
<i>yfiC</i>	23	22	1.04	ST4-74	2782448	2783185	-
<i>srmB</i>	31	27	1.12	ST4-74	2783316	2784650	+
<i>yfiE</i>	16	13	1.25	ST4-74	2784668	2785567	-
<i>yfiK</i>	10	6	1.75	ST4-74	2785670	2786257	+

<i>Name</i>	Δfnr TPM	WT TPM	$\Delta fnr/WT$	<i>Chr</i> ^a	<i>Start</i>	<i>End</i>	<i>Strand</i>
<i>yfiD</i>	26	905	0.03	ST4-74	2786319	2786702	-
<i>ung</i>	57	54	1.05	ST4-74	2787021	2787710	+
<i>yfiF</i>	13	14	0.91	ST4-74	2787826	2788863	-
<i>trxC</i>	97	90	1.09	ST4-74	2789067	2789486	+
<i>yfiP</i>	26	24	1.09	ST4-74	2789559	2790239	+
<i>yfiQ</i>	45	40	1.13	ST4-74	2790293	2792953	+
<i>pssA</i>	52	48	1.10	ST4-74	2793068	2794423	+
<i>yfiM</i>	12	12	0.96	ST4-74	2794468	2794791	+
<i>kgtP</i>	14	10	1.38	ST4-74	2794788	2796089	-
STM2655	24	11	2.06	ST4-74	2796193	2796648	-
<i>clpB</i>	425	447	0.95	ST4-74	2802529	2805102	-
<i>yfiH</i>	61	45	1.35	ST4-74	2805232	2805963	-
<i>rluD</i>	180	119	1.50	ST4-74	2805960	2806940	-
<i>yfiO</i>	131	123	1.07	ST4-74	2807072	2807809	+
STnc3160	112	133	0.84	ST4-74	2807810	2807900	-
<i>yfiA</i>	4097	4054	1.01	ST4-74	2808081	2808419	+
STnc2090	17527	9266	1.89	ST4-74	2808306	2808464	+
<i>sRNA3</i>	1428	1110	1.29	ST4-74	2808504	2808645	+
<i>pheA</i>	16	23	0.72	ST4-74	2808670	2809830	+
STM2668	14	10	1.39	ST4-74	2809791	2810699	-
STnc3790	53	30	1.80	ST4-74	2810663	2810737	+
<i>tyrA</i>	37	52	0.70	ST4-74	2810757	2811824	-
<i>aroF</i>	72	110	0.66	ST4-74	2811888	2812958	-
<i>yfiR</i>	30	23	1.29	ST4-74	2813398	2813916	+
<i>yfiN</i>	7	8	0.93	ST4-74	2813909	2815129	+
<i>int</i>	55	53	1.04	ST4-74	2815382	2816431	-
SL1344_2632	67	78	0.86	ST4-74	2816456	2816794	-
SL1344_2633	57	54	1.06	ST4-74	2816803	2817648	-
SL1344_2634	1	1	1.20	ST4-74	2817762	2818115	+
<i>cIIb</i>	1	1	1.60	ST4-74	2818166	2818675	+
STM2735	1	1	0.98	ST4-74	2818683	2818883	+
SL1344_2637	0	1	0.41	ST4-74	2818847	2819185	+
STM2732	1	0	2.18	ST4-74	2819253	2819480	+
SL1344_2639	1	2	0.65	ST4-74	2819480	2819704	+
SL1344_2640	1	0	2.00	ST4-74	2819701	2820222	+
SL1344_2641	2	2	1.31	ST4-74	2820291	2823074	+
<i>gpF</i>	13	7	1.69	ST4-74	2823088	2823573	+
<i>gpD</i>	4	5	0.90	ST4-74	2823570	2824736	+
STnc3800	112	68	1.65	ST4-74	2824672	2825000	-
SL1344_2644	62	68	0.90	ST4-74	2824931	2825620	+
<i>gpB</i>	113	91	1.24	ST4-74	2825697	2825915	+
<i>rpl19</i>	351	404	0.87	ST4-74	2826061	2826408	-
<i>trmD</i>	155	227	0.69	ST4-74	2826449	2827216	-
<i>rimM</i>	173	252	0.69	ST4-74	2827261	2827809	-
<i>rps16</i>	964	1129	0.85	ST4-74	2827828	2828076	-
<i>ffh</i>	37	38	0.96	ST4-74	2828390	2829751	-
<i>corE</i>	57	49	1.16	ST4-74	2829917	2830708	+
<i>corB</i>	24	19	1.23	ST4-74	2830773	2832014	+
STnc4230	155	102	1.52	ST4-74	2831934	2832038	+
STM2680	17	17	1.00	ST4-74	2832135	2832740	+
<i>grpE</i>	242	259	0.93	ST4-74	2832775	2833365	-

<i>Name</i>	Δ <i>fnr</i> TPM	WT TPM	Δ <i>fnr</i> /WT	Chr ^a	Start	End	Strand
<i>ppnK</i>	19	18	1.09	ST4-74	2833488	2834366	+
<i>recN</i>	9	8	1.05	ST4-74	2834452	2836113	+
<i>smpA</i>	175	182	0.96	ST4-74	2836262	2836600	+
<i>rnfH</i>	52	44	1.18	ST4-74	2836766	2837056	-
<i>yffG</i>	131	120	1.08	ST4-74	2837046	2837501	-
<i>smpB</i>	125	130	0.96	ST4-74	2837672	2838154	+
<i>bapA</i>	3	2	1.43	ST4-74	2838768	2850242	+
<i>IsrL</i>	31	29	1.07	ST4-74	2850244	2850588	-
STM2690	2	1	1.39	ST4-74	2850307	2851716	+
STnc3070	405	311	1.30	ST4-74	2851166	2851225	-
STM2691	3	2	1.76	ST4-74	2851713	2853893	+
STM2692	3	2	1.54	ST4-74	2853901	2855064	+
STM2694	12	11	1.05	ST4-74	2855616	2855834	-
STM2695	1	1	0.96	ST4-74	2855903	2857003	-
<i>gpU</i>	2	1	1.99	ST4-74	2857000	2857485	-
STM2697	2	2	0.97	ST4-74	2857482	2860289	-
<i>gpE'</i>	1	0	1.85	ST4-74	2860282	2860401	-
<i>gpE</i>	1	1	1.03	ST4-74	2860416	2860718	-
STM2700	2	2	1.21	ST4-74	2860773	2861288	-
STM2701	2	2	0.82	ST4-74	2861298	2862470	-
STM2702	6	5	1.15	ST4-74	2862587	2862790	-
<i>sopE</i>	49	72	0.67	ST4-74	2863004	2863726	+
STM2704	7	6	1.05	ST4-74	2863923	2864330	-
STM2706	3	2	1.14	ST4-74	2864337	2865956	-
<i>gpI</i>	1	2	0.51	ST4-74	2865953	2866558	-
<i>gpJ</i>	2	2	1.26	ST4-74	2866551	2867459	-
<i>gpW</i>	1	2	0.47	ST4-74	2867446	2867805	-
STM2710	3	2	1.21	ST4-74	2867802	2868380	-
STM2711	0	0	0.65	ST4-74	2868449	2868895	-
STM2712	1	1	1.15	ST4-74	2868888	2869319	-
STM2713	1	1	0.75	ST4-74	2869282	2869485	-
STM2714	1	0	1.09	ST4-74	2869415	2869843	-
SL1344_2685	4	3	1.31	ST4-74	2869840	2870214	-
<i>nucD2</i>	1	1	0.87	ST4-74	2870219	2870689	-
<i>nucE2</i>	3	3	0.99	ST4-74	2870709	2870924	-
STM2717	2	2	0.92	ST4-74	2870928	2871131	-
STM2718	2	1	1.54	ST4-74	2871131	2871595	-
STM2719	1	1	0.71	ST4-74	2871689	2872342	-
STM2720	2	1	1.07	ST4-74	2872346	2873428	-
STM2721	0	0	0.77	ST4-74	2873445	2874278	-
STM2722	1	1	1.51	ST4-74	2874421	2876187	+
STM2723	1	1	1.34	ST4-74	2876187	2877218	+
SL1344_2695	49	80	0.61	ST4-74	2877245	2878222	-
SL1344_2696	239	357	0.67	ST4-74	2878212	2878793	-
SL1344_2697	101	221	0.46	ST4-74	2879070	2879447	-
SL1344_2698	79	225	0.35	ST4-74	2879425	2880480	-
STM2727	10	12	0.82	ST4-74	2880640	2880873	-
STM2728	20	20	1.04	ST4-74	2880885	2881073	-
STM2729	3	3	1.11	ST4-74	2881397	2883640	-
STM2730	3	3	0.96	ST4-74	2883631	2884488	-
STM2731	1	1	1.06	ST4-74	2884485	2884712	-

<i>Name</i>	Δ <i>fnr</i> TPM	WT TPM	Δ <i>fnr</i> /WT	Chr ^a	Start	End	Strand
STM2733	1	1	0.64	ST4-74	2885007	2885348	-
SL1344_2705	6	4	1.47	ST4-74	2885312	2885608	-
<i>cIIc</i>	1	1	1.25	ST4-74	2885953	2886462	-
<i>apl</i>	0	2	0.28	ST4-74	2886495	2886743	-
<i>cI</i>	27	28	0.97	ST4-74	2886920	2887495	+
STM2739	8	8	0.93	ST4-74	2887497	2888522	+
SL1344_2710	15	17	0.88	ST4-74	2888519	2889730	+
STM2740	9	8	1.15	ST4-74	2890073	2891269	+
SL1344_2713	35	56	0.63	ST4-74	2891273	2892970	-
SL1344_2714	61	102	0.60	ST4-74	2892957	2893190	-
SL1344_2715	65	92	0.70	ST4-74	2893177	2893725	-
SL1344_2716	0	1	0.56	ST4-74	2894442	2895008	-
SL1344_2717	3	2	1.43	ST4-74	2895025	2895267	-
SL1344_2718	2	2	0.95	ST4-74	2895264	2896067	-
SL1344_2719	3847	5429	0.71	ST4-74	2896802	2897353	+
SL1344_2720	1	2	0.62	ST4-74	2897350	2897577	+
SL1344_2721	1	1	1.36	ST4-74	2897574	2897894	+
SL1344_2722	3	3	0.90	ST4-74	2897858	2900242	+
STM2740	16	14	1.16	ST4-74	2900734	2901979	+
STM2741	8	7	1.14	ST4-74	2901981	2902619	+
STM2742	38	35	1.07	ST4-74	2903009	2904202	+
STM2743	50	48	1.03	ST4-74	2904537	2905364	-
STM2744	3	2	1.43	ST4-74	2905815	2906030	+
STM2745	1	1	1.12	ST4-74	2906066	2908135	+
STM2746	74	73	1.01	ST4-74	2908638	2909921	+
STM2747	28	34	0.81	ST4-74	2909966	2910784	+
STM2748	156	153	1.02	ST4-74	2910939	2911229	-
STM2749	4	4	0.82	ST4-74	2911390	2911674	+
STM2750	2	2	0.95	ST4-74	2911787	2912308	+
STM2751	2	3	0.93	ST4-74	2912305	2912679	+
STM2752	2	2	1.10	ST4-74	2912676	2913656	+
STM2753	3	5	0.56	ST4-74	2913667	2914680	+
STM2754	8	10	0.80	ST4-74	2914975	2916177	+
<i>hxlA</i>	3	3	0.96	ST4-74	2916251	2916886	-
<i>hxlB</i>	2	1	2.37	ST4-74	2916910	2917473	-
STM2757	2	2	0.99	ST4-74	2917473	2918315	-
STM2758	2	2	1.30	ST4-74	2918445	2919986	-
STM2759	3	2	1.16	ST4-74	2920209	2921888	+
STM2760	2	1	1.42	ST4-74	2923005	2923880	+
STM2761	7	5	1.38	ST4-74	2924046	2925920	+
STM2762	16	12	1.38	ST4-74	2926180	2927463	-
<i>IsrM</i>	8	3	2.40	ST4-74	2927616	2927944	+
STM2763	24	23	1.06	ST4-74	2928000	2928911	+
STM2764	7	8	0.87	ST4-74	2928907	2929495	-
<i>IsrN</i>	4	2	2.35	ST4-74	2929501	2929643	+
STM2765	15	18	0.84	ST4-74	2929642	2929908	-
STM2766	34	34	0.99	ST4-74	2930361	2930999	-
STM2767	79	77	1.03	ST4-74	2930996	2932978	-
STM2768	8	8	1.02	ST4-74	2933257	2933556	+
STM2769	11	9	1.20	ST4-74	2933553	2934419	+
<i>fljA</i>	7	7	1.08	ST4-74	2935199	2935738	-

<i>Name</i>	Δ <i>fnr</i> TPM	WT TPM	Δ <i>fnr</i> /WT	Chr ^a	Start	End	Strand
<i>fljB</i>	54	218	0.25	ST4-74	2935806	2937326	-
<i>hin</i>	28	20	1.39	ST4-74	2937418	2937990	+
<i>iroB</i>	3	2	1.31	ST4-74	2938953	2940068	+
<i>iroC</i>	3	3	1.01	ST4-74	2940149	2943802	+
<i>iroD</i>	2	1	1.38	ST4-74	2943912	2945156	+
<i>iroE</i>	4	3	1.44	ST4-74	2945188	2946123	+
<i>iroN</i>	4	4	1.12	ST4-74	2946165	2948345	-
<i>pipB2</i>	343	78	4.40	ST4-74	2949378	2950430	-
<i>virK</i>	1248	691	1.81	ST4-74	2950949	2951878	+
<i>mig-14</i>	857	501	1.71	ST4-74	2952171	2953067	+
<i>nixA</i>	31	29	1.06	ST4-74	2953789	2954802	-
<i>tctE</i>	7	11	0.62	ST4-74	2954935	2956350	-
<i>tctD</i>	12	14	0.86	ST4-74	2956337	2957011	-
STM2786	18	25	0.73	ST4-74	2957166	2958143	+
STM2787	7	9	0.69	ST4-74	2958155	2958589	+
STM2788	11	16	0.67	ST4-74	2958600	2960114	+
<i>csiD</i>	8	5	1.77	ST4-74	2960408	2961394	+
<i>ygaF</i>	5	3	1.60	ST4-74	2961420	2962688	+
<i>gabD</i>	3	2	1.63	ST4-74	2962710	2964158	+
<i>gabT</i>	4	3	1.58	ST4-74	2964173	2965456	+
<i>gabP</i>	9	6	1.52	ST4-74	2965586	2966986	+
<i>ygaE</i>	8	7	1.15	ST4-74	2967028	2967705	+
<i>ygaU</i>	383	176	2.19	ST4-74	2967727	2968176	-
<i>yqaE</i>	749	330	2.27	ST4-74	2968276	2968434	-
STM2797	13	12	1.06	ST4-74	2968677	2968916	+
<i>ygaP</i>	8	9	0.91	ST4-74	2968926	2969453	+
<i>stpA</i>	295	336	0.88	ST4-74	2969801	2970202	-
STM2800	100	19	5.26	ST4-74	2970901	2971350	+
<i>ygaC</i>	35	19	1.80	ST4-74	2971385	2971735	-
<i>ygaM</i>	253	157	1.62	ST4-74	2971885	2972223	+
STM2803	9	7	1.24	ST4-74	2972307	2973641	-
STM2804	3	3	1.00	ST4-74	2973730	2974161	+
SL1344_2789	1	1	0.64	ST4-74	2974158	2974334	+
STnc3080	12	9	1.39	ST4-74	2974260	2974404	-
<i>nrdH</i>	16	11	1.48	ST4-74	2974433	2974678	+
<i>nrdI</i>	4	2	1.93	ST4-74	2974675	2975085	+
<i>nrdE</i>	4	2	1.80	ST4-74	2975058	2977202	+
<i>nrdF</i>	12	8	1.37	ST4-74	2977213	2978172	+
<i>proV</i>	67	91	0.73	ST4-74	2978527	2979729	+
<i>proW</i>	30	60	0.51	ST4-74	2979722	2980786	+
<i>proX</i>	28	59	0.48	ST4-74	2980856	2981851	+
STM2812	7	7	0.97	ST4-74	2982016	2983200	+
<i>emrR</i>	56	65	0.87	ST4-74	2983697	2984227	+
<i>emrA</i>	17	16	1.04	ST4-74	2984354	2985526	+
<i>emrB</i>	9	10	0.86	ST4-74	2985543	2987081	+
STM2816	5	5	1.02	ST4-74	2987130	2988500	-
<i>luxS</i>	84	85	0.98	ST4-74	2988846	2989361	-
<i>MicA</i>	6889	4862	1.42	ST4-74	2989429	2989502	+
<i>gshA</i>	26	23	1.14	ST4-74	2989511	2991067	-
<i>yqaA</i>	34	35	0.98	ST4-74	2991144	2991569	-
<i>yqaB</i>	73	79	0.92	ST4-74	2991566	2992132	-

<i>Name</i>	Δfnr TPM	WT TPM	$\Delta fnr/WT$	<i>Chr</i> ^a	<i>Start</i>	<i>End</i>	<i>Strand</i>
<i>csrA</i>	1495	1166	1.28	ST4-74	2993527	2993712	-
<i>alaS</i>	53	63	0.84	ST4-74	2993947	2996577	-
<i>oraA</i>	21	15	1.36	ST4-74	2996813	2997313	-
<i>recA</i>	55	56	0.97	ST4-74	2997430	2998491	-
<i>ygaD</i>	33	33	0.99	ST4-74	2998576	2999073	-
<i>mltB</i>	30	25	1.21	ST4-74	2999551	3000630	-
<i>srlA</i>	3	4	0.64	ST4-74	3000884	3001447	+
<i>srlE</i>	2	3	0.68	ST4-74	3001444	3002415	+
<i>slrB</i>	1	2	0.66	ST4-74	3002427	3002789	+
<i>gutD</i>	4	5	0.78	ST4-74	3002801	3003580	+
<i>gutM</i>	30	25	1.22	ST4-74	3003656	3004015	+
<i>srlR</i>	15	21	0.74	ST4-74	3004213	3004986	+
<i>gutQ</i>	9	14	0.69	ST4-74	3004979	3005944	+
<i>norR</i>	5	4	1.17	ST4-74	3005941	3007461	-
<i>norV</i>	2	3	0.91	ST4-74	3007647	3009086	+
<i>norW</i>	2	2	1.08	ST4-74	3009083	3010216	+
<i>C0664</i>	2	3	0.74	ST4-74	3010214	3010321	+
<i>hydA</i>	6	7	0.80	ST4-74	3010313	3012553	-
<i>hydN</i>	3	5	0.61	ST4-74	3012699	3013244	-
STM2844	3	5	0.64	ST4-74	3013445	3014254	-
<i>hycI</i>	3	5	0.60	ST4-74	3014281	3014751	-
<i>hycH</i>	3	4	0.91	ST4-74	3014744	3015154	-
<i>hycG</i>	3	3	0.90	ST4-74	3015151	3015918	-
<i>hycF</i>	2	4	0.53	ST4-74	3015918	3016460	-
<i>hycE</i>	3	3	0.97	ST4-74	3016470	3018179	-
<i>hycD</i>	3	3	1.02	ST4-74	3018197	3019120	-
<i>hycC</i>	4	5	0.77	ST4-74	3019123	3020949	-
<i>hycB</i>	2	2	0.83	ST4-74	3020949	3021557	-
<i>hycA</i>	2	5	0.37	ST4-74	3021703	3022164	-
STM2854	20	85	0.23	ST4-74	3022374	3022730	+
<i>hypB</i>	8	26	0.31	ST4-74	3022799	3023671	+
<i>hypC</i>	10	26	0.39	ST4-74	3023662	3023934	+
<i>hypD</i>	4	17	0.22	ST4-74	3023934	3025055	+
<i>hypE</i>	7	24	0.30	ST4-74	3025052	3026062	+
<i>fhlA</i>	7	10	0.69	ST4-74	3026281	3028359	+
<i>ygbA</i>	8	9	0.92	ST4-74	3028421	3028765	-
<i>sitA</i>	11	9	1.30	ST4-74	3028947	3029864	+
<i>sitB</i>	9	6	1.54	ST4-74	3029861	3030682	+
<i>sitC</i>	8	6	1.36	ST4-74	3030679	3031539	+
<i>sitD</i>	15	13	1.13	ST4-74	3031530	3032378	+
<i>avrA</i>	53	46	1.14	ST4-74	3032477	3033382	-
<i>sprB</i>	8	12	0.66	ST4-74	3033543	3034298	-
<i>hilC</i>	35	39	0.91	ST4-74	3034683	3035570	-
<i>orgC</i>	84	69	1.22	ST4-74	3035915	3036367	-
<i>orgB</i>	116	90	1.29	ST4-74	3036364	3037044	-
<i>orgA</i>	67	53	1.27	ST4-74	3037001	3037600	-
STnc4240	192	177	1.08	ST4-74	3037101	3037394	+
<i>prgK</i>	20	38	0.53	ST4-74	3037572	3038330	-
<i>prgJ</i>	20	38	0.52	ST4-74	3038327	3038632	-
<i>prgI</i>	19	34	0.54	ST4-74	3038651	3038893	-
STnc3020	18	14	1.33	ST4-74	3038687	3038786	+

<i>Name</i>	Δ <i>fnr</i> TPM	WT TPM	Δ <i>fnr</i> /WT	Chr ^a	Start	End	Strand
<i>prgH</i>	27	42	0.63	ST4-74	3038918	3040096	-
<i>hilD</i>	97	110	0.88	ST4-74	3040412	3041341	+
<i>hilA</i>	8	13	0.62	ST4-74	3042432	3044093	+
<i>iagB</i>	26	32	0.82	ST4-74	3044111	3044593	+
<i>sptP</i>	58	59	0.98	ST4-74	3044647	3046278	-
<i>sicP</i>	102	100	1.02	ST4-74	3046265	3046657	-
<i>iacP</i>	136	111	1.23	ST4-74	3046988	3047236	-
<i>sipA</i>	11	16	0.69	ST4-74	3047255	3049312	-
STnc1410	142	106	1.35	ST4-74	3048830	3049012	+
<i>sipD</i>	8	12	0.67	ST4-74	3049331	3050362	-
<i>sipC</i>	23	42	0.54	ST4-74	3050433	3051662	-
<i>sipB</i>	12	25	0.47	ST4-74	3051690	3053471	-
<i>sicA</i>	38	61	0.62	ST4-74	3053474	3053971	-
<i>spaS</i>	3	6	0.57	ST4-74	3054109	3055179	-
<i>spaR</i>	7	10	0.69	ST4-74	3055166	3055957	-
<i>spaQ</i>	11	19	0.57	ST4-74	3055961	3056221	-
<i>spaP</i>	7	12	0.60	ST4-74	3056247	3056921	-
<i>spaO</i>	6	11	0.57	ST4-74	3056911	3057822	-
<i>invJ</i>	3	7	0.47	ST4-74	3057822	3058832	-
<i>invI</i>	11	18	0.58	ST4-74	3058832	3059275	-
<i>invC</i>	5	10	0.56	ST4-74	3059253	3060548	-
<i>invB</i>	16	27	0.60	ST4-74	3060545	3060952	-
<i>invA</i>	16	26	0.63	ST4-74	3060976	3063033	-
<i>invE</i>	11	17	0.62	ST4-74	3063058	3064176	-
<i>invG</i>	11	18	0.58	ST4-74	3064173	3065861	-
<i>invF</i>	17	27	0.61	ST4-74	3065858	3066508	-
<i>invH</i>	14	22	0.66	ST4-74	3066965	3067408	+
<i>InvR</i>	1206	1290	0.94	ST4-74	3067500	3067579	+
STM2901	102	109	0.94	ST4-74	3067839	3068288	+
STM2902	21	23	0.91	ST4-74	3068273	3068620	+
STM2903	61	32	1.92	ST4-74	3068893	3069219	-
SL1344_2883	2	1	1.16	ST4-74	3069460	3069567	+
STM2904	98	83	1.19	ST4-74	3069908	3070198	+
STM2905	17	15	1.08	ST4-74	3070195	3070722	+
STM2906	4	3	1.23	ST4-74	3070798	3071012	-
<i>pphB</i>	10	7	1.54	ST4-74	3071347	3072003	+
STM2908	5	3	1.79	ST4-74	3072175	3072696	-
<i>mutS</i>	11	14	0.80	ST4-74	3072897	3075422	+
STM2910	5	4	1.21	ST4-74	3075478	3075858	-
STM2911	3	2	1.34	ST4-74	3075855	3077063	-
STM2912	4	4	0.95	ST4-74	3077151	3078083	+
STM2913	6	6	0.97	ST4-74	3078125	3079621	-
STM2914	4	2	1.68	ST4-74	3079618	3080568	-
<i>hyi</i>	2	2	0.99	ST4-74	3080608	3081369	-
<i>ygbL</i>	2	2	1.02	ST4-74	3081374	3082012	-
<i>ygbK</i>	1	1	1.09	ST4-74	3082009	3083271	-
<i>ygbJ</i>	2	3	0.91	ST4-74	3083265	3084188	-
<i>ygbI</i>	15	15	1.03	ST4-74	3084385	3085149	+
STM2920	33	32	1.03	ST4-74	3085168	3085572	-
STM2921	3	2	1.17	ST4-74	3085743	3086336	+
STM2922	2	1	1.45	ST4-74	3086336	3087763	+

<i>Name</i>	Δfnr TPM	WT TPM	$\Delta fnr/WT$	<i>Chr^a</i>	<i>Start</i>	<i>End</i>	<i>Strand</i>
STM2923	2	3	0.89	ST4-74	3087774	3088010	+
<i>rpoS</i>	372	400	0.93	ST4-74	3088055	3089047	-
<i>nlpD</i>	587	602	0.97	ST4-74	3089110	3090243	-
<i>pcm</i>	26	29	0.90	ST4-74	3090419	3091045	-
<i>surE</i>	28	30	0.94	ST4-74	3091039	3091800	-
<i>truD</i>	23	25	0.93	ST4-74	3091781	3092830	-
<i>ispF</i>	10	12	0.85	ST4-74	3092827	3093306	-
<i>ispD</i>	12	15	0.77	ST4-74	3093306	3094016	-
<i>ftsB</i>	82	77	1.05	ST4-74	3094035	3094346	-
<i>ygbE</i>	44	39	1.14	ST4-74	3094537	3094893	-
<i>cysC</i>	85	88	0.97	ST4-74	3094911	3095516	-
<i>cysN</i>	63	71	0.88	ST4-74	3095503	3096942	-
<i>cysD</i>	212	219	0.97	ST4-74	3096952	3097860	-
<i>iap</i>	8	6	1.31	ST4-74	3098111	3099157	+
<i>ygbF</i>	9	9	0.99	ST4-74	3100256	3100552	-
STM2938	7	6	1.16	ST4-74	3100549	3101469	-
<i>ygcH</i>	4	3	1.12	ST4-74	3101466	3102116	-
STM2940	3	3	0.82	ST4-74	3102098	3102844	-
<i>yghJ</i>	3	4	0.74	ST4-74	3102855	3103913	-
STM2942	3	4	0.75	ST4-74	3103927	3104487	-
STM2943	2	3	0.84	ST4-74	3104484	3106040	-
<i>ygcB</i>	5	6	0.87	ST4-74	3106052	3108715	-
<i>sopD</i>	9	9	1.00	ST4-74	3109160	3110113	+
STnc3140	679	560	1.21	ST4-74	3109885	3109981	-
<i>cysH</i>	52	59	0.89	ST4-74	3110201	3110935	-
<i>cysI</i>	74	84	0.88	ST4-74	3111011	3112723	-
<i>cysJ</i>	58	63	0.92	ST4-74	3112723	3114522	-
<i>ptpS</i>	15	15	0.99	ST4-74	3114946	3115308	+
STM2950	17	18	0.96	ST4-74	3115396	3116193	-
<i>ygcF</i>	86	68	1.28	ST4-74	3118020	3118691	-
<i>eno</i>	193	301	0.64	ST4-74	3118827	3120125	-
<i>pyrG</i>	122	134	0.91	ST4-74	3120208	3121845	-
<i>mazG</i>	21	20	1.08	ST4-74	3122073	3122873	-
SL1344_2934	1	1	1.24	ST4-74	3123527	3123631	+
SL1344_2935	47	35	1.34	ST4-74	3123641	3123898	-
STM2955	247	180	1.38	ST4-74	3123903	3124178	-
<i>relA</i>	53	57	0.93	ST4-74	3124343	3126577	-
<i>rumA</i>	93	74	1.27	ST4-74	3126629	3127924	-
<i>barA</i>	11	15	0.71	ST4-74	3127982	3130738	+
STM2959	9	7	1.32	ST4-74	3130782	3131924	-
<i>gudD</i>	6	5	1.18	ST4-74	3132002	3133342	-
<i>ygcY</i>	7	5	1.42	ST4-74	3133363	3134703	-
<i>gudT</i>	12	7	1.60	ST4-74	3134700	3136058	-
STM2963	50	57	0.88	ST4-74	3136539	3136988	-
<i>yqcB</i>	21	19	1.08	ST4-74	3137007	3137789	-
<i>yqcC</i>	15	19	0.78	ST4-74	3137789	3138118	-
<i>CsrB</i>	24986	23151	1.08	ST4-74	3138160	3138522	-
<i>syd</i>	76	71	1.07	ST4-74	3138730	3139275	-
<i>queF</i>	24	21	1.10	ST4-74	3139344	3140192	+
<i>ygdH</i>	55	64	0.87	ST4-74	3140305	3141669	+
<i>sdaC</i>	26	17	1.50	ST4-74	3142234	3143523	+

<i>Name</i>	Δfnr TPM	WT TPM	$\Delta fnr/WT$	Chr ^a	Start	End	Strand
<i>sdaB</i>	13	10	1.37	ST4-74	3143582	3144949	+
<i>exo</i>	15	14	1.09	ST4-74	3145060	3145875	+
<i>fucO</i>	4	4	0.87	ST4-74	3145967	3147115	-
<i>fucA</i>	3	5	0.68	ST4-74	3147132	3147779	-
<i>fucP</i>	3	3	0.89	ST4-74	3148334	3149650	+
<i>fucI</i>	1	2	0.64	ST4-74	3149682	3151457	+
<i>fucK</i>	2	2	0.81	ST4-74	3151558	3152976	+
<i>fucU</i>	2	3	0.91	ST4-74	3152978	3153400	+
<i>fucR</i>	14	21	0.67	ST4-74	3153458	3154168	+
<i>ygdE</i>	34	37	0.90	ST4-74	3154227	3155327	-
<i>ygdD</i>	22	26	0.83	ST4-74	3155320	3155715	-
<i>gcvA</i>	43	34	1.27	ST4-74	3155734	3156651	-
<i>GcvB</i>	2629	204	12.85	ST4-74	3156779	3156979	+
<i>ygdI</i>	1573	801	1.96	ST4-74	3156998	3157225	-
<i>csdA</i>	12	13	0.87	ST4-74	3157418	3158623	+
<i>ygdK</i>	6	8	0.77	ST4-74	3158623	3159066	+
STM2986	4	30	0.13	ST4-74	3159339	3160253	+
<i>ygdL</i>	50	48	1.06	ST4-74	3160305	3161111	-
<i>mltA</i>	58	58	1.01	ST4-74	3161221	3162318	-
<i>amiC</i>	60	56	1.08	ST4-74	3162818	3164071	-
<i>argA</i>	88	139	0.63	ST4-74	3164304	3165635	+
<i>recD</i>	5	6	0.94	ST4-74	3165738	3167573	-
<i>recB</i>	9	11	0.80	ST4-74	3167570	3171115	-
<i>ptr</i>	12	13	0.91	ST4-74	3171108	3173996	-
<i>recC</i>	9	8	1.10	ST4-74	3174174	3177545	-
<i>comQ</i>	8	8	0.99	ST4-74	3177561	3177881	-
<i>comP</i>	4	3	1.11	ST4-74	3177866	3178273	-
<i>comO</i>	5	5	0.90	ST4-74	3178270	3178833	-
<i>comN</i>	4	5	0.89	ST4-74	3178824	3179294	-
<i>thyA</i>	23	21	1.10	ST4-74	3179479	3180273	-
<i>lgt</i>	42	42	1.01	ST4-74	3180280	3181155	-
<i>ptsP</i>	30	31	0.95	ST4-74	3181371	3183617	-
<i>nudH</i>	168	169	0.99	ST4-74	3183630	3184160	-
<i>mutH</i>	29	36	0.81	ST4-74	3184843	3185538	+
<i>ygdQ</i>	47	41	1.16	ST4-74	3185720	3186433	+
STnc3830	58	61	0.96	ST4-74	3186446	3186537	-
<i>ygdR</i>	260	314	0.83	ST4-74	3186603	3186821	+
<i>tas</i>	21	23	0.93	ST4-74	3187012	3188052	+
<i>ygeD</i>	16	17	0.90	ST4-74	3188139	3189341	-
<i>aas</i>	19	19	1.00	ST4-74	3189334	3191493	-
<i>OmrA</i>	192	109	1.77	ST4-74	3191584	3191670	-
<i>OmrB</i>	248	178	1.39	ST4-74	3191785	3191870	-
<i>galR</i>	30	33	0.91	ST4-74	3192086	3193114	+
STM3012	16	17	0.98	ST4-74	3193125	3194147	+
<i>lysA</i>	27	30	0.90	ST4-74	3194157	3195419	-
<i>lysR</i>	4	5	0.84	ST4-74	3195537	3196472	+
<i>ygeA</i>	41	38	1.08	ST4-74	3196444	3197151	-
<i>araE</i>	6	7	0.78	ST4-74	3197264	3198682	-
<i>kduD</i>	9	10	0.86	ST4-74	3199036	3199797	-
<i>kduI</i>	3	4	0.70	ST4-74	3199854	3200690	-
<i>yqeF</i>	15	16	0.94	ST4-74	3201120	3202298	-

<i>Name</i>	Δ <i>fnr</i> TPM	WT TPM	Δ <i>fnr</i> /WT	<i>Chr</i> ^a	<i>Start</i>	<i>End</i>	<i>Strand</i>
STM3020	17	21	0.81	ST4-74	3202421	3203284	-
STM3021	18	13	1.41	ST4-74	3203361	3203843	+
STM3022	13	11	1.15	ST4-74	3203985	3205214	+
<i>yohL</i>	49	130	0.38	ST4-74	3205245	3205517	-
<i>yohM</i>	5	28	0.20	ST4-74	3205639	3206475	+
STM3025	5	3	1.64	ST4-74	3206685	3207383	-
STM3025.1N	2	2	0.88	ST4-74	3207430	3207942	-
STM3026	4	4	0.91	ST4-74	3208086	3209162	-
<i>stdC</i>	2	1	1.66	ST4-74	3209159	3209902	-
<i>stdB</i>	2	2	1.01	ST4-74	3209943	3212432	-
<i>stdA</i>	3	2	1.28	ST4-74	3212552	3213262	-
STM3030	35	32	1.09	ST4-74	3213855	3214487	-
STM3031	4	3	1.27	ST4-74	3214534	3215070	-
STnc290	460	501	0.92	ST4-74	3215639	3215717	-
STM3033	84	84	1.01	ST4-74	3215876	3216274	-
STM3034	412	365	1.13	ST4-74	3216274	3216501	-
STM3036	21	9	2.28	ST4-74	3217204	3218010	+
STM3038	46	45	1.01	ST4-74	3218295	3219053	-
<i>IsrO</i>	81	48	1.69	ST4-74	3219100	3219300	+
<i>idi</i>	50	36	1.38	ST4-74	3219318	3219863	+
<i>lysS</i>	45	57	0.78	ST4-74	3219939	3221456	-
<i>prfB</i>	67	68	0.99	ST4-74	3221466	3222542	-
<i>recJ</i>	18	20	0.87	ST4-74	3222669	3224402	-
<i>dsbC</i>	29	31	0.92	ST4-74	3224408	3225082	-
<i>xerD</i>	33	33	1.01	ST4-74	3225145	3226041	-
<i>fldB</i>	25	27	0.93	ST4-74	3226154	3226675	+
<i>ygfX</i>	56	58	0.96	ST4-74	3226728	3227141	-
<i>ygfY</i>	110	114	0.96	ST4-74	3227122	3227388	-
<i>ygfZ</i>	29	33	0.89	ST4-74	3227638	3228618	+
<i>yqfA</i>	62	46	1.34	ST4-74	3228734	3229393	-
<i>yqfB</i>	74	98	0.75	ST4-74	3229557	3229868	-
<i>bglA</i>	12	13	0.95	ST4-74	3230027	3231460	+
STM3052	8	7	1.15	ST4-74	3231508	3232401	-
<i>gcvP</i>	10	9	1.13	ST4-74	3232857	3235730	-
<i>gcvH</i>	37	29	1.28	ST4-74	3235893	3236282	-
<i>gcvT</i>	16	12	1.37	ST4-74	3236308	3237402	-
<i>visC</i>	21	22	0.98	ST4-74	3237857	3239059	-
<i>ubiH</i>	23	21	1.09	ST4-74	3239185	3240363	-
<i>pepP</i>	34	32	1.08	ST4-74	3240360	3241502	-
<i>ygfB</i>	58	57	1.01	ST4-74	3241702	3242280	-
<i>ygfE</i>	106	101	1.05	ST4-74	3242447	3242776	+
<i>SsrS</i>	87372	116036	0.75	ST4-74	3242594	3243000	+
<i>ygfA</i>	11	10	1.02	ST4-74	3243142	3243618	+
<i>RygC</i>	7077	8117	0.87	ST4-74	3243669	3243813	+
<i>serA</i>	119	128	0.93	ST4-74	3243999	3245231	-
<i>rpiA</i>	92	99	0.92	ST4-74	3245497	3246156	-
<i>iciA</i>	9	11	0.83	ST4-74	3246310	3247203	+
<i>yggE</i>	59	37	1.60	ST4-74	3247469	3248215	-
<i>yggA</i>	13	8	1.54	ST4-74	3248309	3248944	-
<i>yggB</i>	90	75	1.20	ST4-74	3249144	3250004	-
STnc3030	94	115	0.82	ST4-74	3250106	3250210	+

<i>Name</i>	Δ <i>fnr</i> TPM	WT TPM	Δ <i>fnr</i> /WT	Chr ^a	Start	End	Strand
<i>fb</i>	99	126	0.78	ST4-74	3250231	3251310	-
<i>pgk</i>	56	76	0.73	ST4-74	3251412	3252575	-
<i>epd</i>	74	83	0.88	ST4-74	3252597	3253643	-
STM3071	6	22	0.27	ST4-74	3254017	3254442	+
STM3072	4	15	0.28	ST4-74	3254468	3255046	+
STM3073	6	11	0.53	ST4-74	3255047	3255754	+
STM3074	3	7	0.41	ST4-74	3255742	3256419	+
STM3075	4	8	0.50	ST4-74	3256413	3257069	+
<i>tklA</i>	39	63	0.62	ST4-74	3257113	3259059	-
<i>yggG</i>	21	17	1.25	ST4-74	3259380	3260138	+
<i>speB</i>	11	12	0.89	ST4-74	3260239	3261159	-
STnc750	297	259	1.15	ST4-74	3261185	3261273	-
STM3079	7	6	1.20	ST4-74	3261364	3262254	-
STM3080	4	3	1.10	ST4-74	3262534	3263007	-
STM3081	6	6	1.13	ST4-74	3263046	3264053	-
STM3082	3	3	0.86	ST4-74	3264067	3265083	-
STM3083	2	1	1.35	ST4-74	3265086	3266558	-
STM3084	83	77	1.09	ST4-74	3267800	3268549	-
STM3085	5	5	1.14	ST4-74	3268754	3269485	-
<i>speA</i>	32	23	1.37	ST4-74	3269629	3271542	-
<i>yqgB</i>	239	148	1.62	ST4-74	3271614	3271745	-
<i>yqgD</i>	52	41	1.25	ST4-74	3272040	3272339	-
<i>metK</i>	150	194	0.77	ST4-74	3272395	3273549	+
STnc3150	27	13	2.07	ST4-74	3273499	3273824	-
<i>galP</i>	27	20	1.34	ST4-74	3274081	3275436	+
<i>sprT</i>	22	15	1.46	ST4-74	3275515	3276012	+
STnc3850	26	26	0.98	ST4-74	3275931	3276099	-
<i>endA</i>	9	7	1.19	ST4-74	3276107	3276814	+
<i>yggJ</i>	33	28	1.19	ST4-74	3276843	3277622	+
<i>gshB</i>	19	19	0.98	ST4-74	3277642	3278589	+
<i>yqgE</i>	37	32	1.16	ST4-74	3278805	3279368	+
<i>yqgF</i>	9	10	0.87	ST4-74	3279368	3279784	+
<i>iclR</i>	13	11	1.19	ST4-74	3279831	3280517	-
<i>pilT</i>	4	4	1.00	ST4-74	3280649	3281629	-
<i>yggS</i>	36	44	0.83	ST4-74	3281647	3282351	+
<i>yggT</i>	28	31	0.89	ST4-74	3282370	3282936	+
<i>yggU</i>	27	33	0.82	ST4-74	3282933	3283223	+
<i>yggV</i>	20	25	0.80	ST4-74	3283231	3283824	+
STnc3860	47	46	1.04	ST4-74	3283748	3283844	-
<i>yggW</i>	10	11	0.92	ST4-74	3283817	3284953	+
<i>yggM</i>	10	9	1.14	ST4-74	3285044	3286051	-
<i>ansB</i>	16	45	0.35	ST4-74	3286184	3287230	-
<i>yggN</i>	48	38	1.26	ST4-74	3287419	3288138	-
<i>yggL</i>	182	164	1.11	ST4-74	3288188	3288514	-
<i>trmB</i>	98	87	1.12	ST4-74	3288514	3289233	-
<i>mutY</i>	28	27	1.04	ST4-74	3289388	3290440	+
<i>yggX</i>	50	61	0.82	ST4-74	3290468	3290743	+
<i>mltC</i>	18	18	0.99	ST4-74	3290856	3291941	+
<i>nupG</i>	10	15	0.69	ST4-74	3292158	3293414	+
<i>speC</i>	8	10	0.78	ST4-74	3293476	3295611	-
<i>yqgA</i>	8	6	1.35	ST4-74	3296036	3296743	+

<i>Name</i>	Δ <i>fnr</i> TPM	WT TPM	Δ <i>fnr</i> /WT	<i>Chr</i> ^a	<i>Start</i>	<i>End</i>	<i>Strand</i>
STnc3870	146	125	1.17	ST4-74	3296886	3297024	-
STM3117	13	12	1.03	ST4-74	3297083	3297517	-
STM3118	3	3	1.06	ST4-74	3297528	3298853	-
STM3119	5	4	1.35	ST4-74	3298878	3299405	-
STM3120	9	9	1.07	ST4-74	3299429	3300271	-
STM3121	4	5	0.91	ST4-74	3300513	3301241	+
STM3122	13	9	1.39	ST4-74	3301289	3303028	-
STM3123	2	2	1.19	ST4-74	3303097	3304281	-
STM3124	9	9	0.98	ST4-74	3304793	3305476	+
STnc3880	14	8	1.71	ST4-74	3305410	3305515	+
STM3125	12	12	0.97	ST4-74	3305580	3306137	-
STM3126	12	11	1.11	ST4-74	3306115	3307614	-
STM3127	9	11	0.83	ST4-74	3307823	3308197	-
<i>ordL</i>	21	14	1.53	ST4-74	3308212	3309513	-
STM3129	9	7	1.20	ST4-74	3309675	3311159	+
<i>iraD</i>	5	8	0.65	ST4-74	3311295	3311675	-
STM3131	7	10	0.69	ST4-74	3311675	3312160	-
STnc1170	393	245	1.60	ST4-74	3312429	3312525	-
STM3132	86	33	2.58	ST4-74	3312886	3313809	-
STM3133	120	35	3.46	ST4-74	3313848	3314726	-
<i>exuT</i>	8	8	1.04	ST4-74	3315122	3316426	-
<i>uxuA</i>	8	9	0.82	ST4-74	3316831	3318015	+
<i>uxuB</i>	4	4	0.96	ST4-74	3318126	3319598	+
<i>uxaC</i>	13	10	1.27	ST4-74	3319610	3321022	+
STM3138	203	328	0.62	ST4-74	3321322	3322380	-
STnc3890	73	71	1.03	ST4-74	3322951	3323033	+
<i>gsp</i>	11	10	1.18	ST4-74	3323050	3324906	-
<i>yghU</i>	24	21	1.15	ST4-74	3325133	3325999	+
STM3141	8	9	0.94	ST4-74	3326067	3326777	-
STM3142	3	4	0.79	ST4-74	3326777	3327829	-
<i>hybG</i>	21	77	0.27	ST4-74	3327905	3328153	-
<i>hybF</i>	14	43	0.32	ST4-74	3328181	3328522	-
<i>hybE</i>	11	34	0.34	ST4-74	3328515	3329003	-
<i>hybD</i>	20	58	0.34	ST4-74	3328996	3329490	-
<i>hybC</i>	17	45	0.39	ST4-74	3329490	3331193	-
<i>hybB</i>	19	57	0.33	ST4-74	3331190	3332368	-
<i>hybA</i>	13	44	0.29	ST4-74	3332358	3333344	-
<i>hypO</i>	26	61	0.42	ST4-74	3333347	3334465	-
<i>yghW</i>	5	18	0.26	ST4-74	3334655	3334942	-
STM3152	10	21	0.46	ST4-74	3335027	3336670	-
<i>yqhA</i>	48	65	0.74	ST4-74	3336977	3337471	-
STM3154	111	261	0.43	ST4-74	3337751	3338266	-
STM3155	58	124	0.46	ST4-74	3338358	3338768	+
STM3156	11	36	0.32	ST4-74	3338755	3339159	+
<i>yghA</i>	32	31	1.04	ST4-74	3339283	3340167	+
<i>exbD</i>	72	42	1.69	ST4-74	3340280	3340705	-
<i>exbB</i>	61	38	1.60	ST4-74	3340712	3341446	-
STM3160	139	76	1.84	ST4-74	3341439	3341588	-
<i>metC</i>	25	23	1.09	ST4-74	3341698	3342885	+
<i>yghB</i>	79	79	1.00	ST4-74	3343025	3343684	+
<i>yqhC</i>	22	23	0.93	ST4-74	3343748	3344665	-

<i>Name</i>	Δ <i>fnr</i> TPM	WT TPM	Δ <i>fnr</i> /WT	Chr ^a	Start	End	Strand
<i>yqhD</i>	9	12	0.74	ST4-74	3344840	3346003	+
<i>dkgA</i>	41	30	1.35	ST4-74	3346109	3346936	+
STM3166	7	8	0.91	ST4-74	3347286	3348587	+
STM3167	23	26	0.90	ST4-74	3348632	3349087	+
STnc1820	105	73	1.44	ST4-74	3349037	3349187	-
STnc3920	3	2	1.65	ST4-74	3349508	3349727	+
<i>ygiR</i>	20	15	1.26	ST4-74	3349642	3351813	-
STM3169	2	2	1.27	ST4-74	3352301	3353284	+
STM3170	4	4	0.99	ST4-74	3353326	3353808	+
<i>ygiK</i>	7	6	1.21	ST4-74	3353819	3355126	+
<i>sufI</i>	16	21	0.78	ST4-74	3355171	3356583	-
<i>plsC</i>	33	32	1.01	ST4-74	3356657	3357394	-
<i>parC</i>	27	31	0.88	ST4-74	3357651	3359909	-
STM3175	9	15	0.60	ST4-74	3360020	3360886	-
<i>ygiW</i>	34	52	0.64	ST4-74	3360958	3361350	-
<i>ygiX</i>	13	14	0.93	ST4-74	3361502	3362161	+
<i>ygiY</i>	6	6	0.93	ST4-74	3362158	3363507	+
<i>mdaB</i>	12	16	0.76	ST4-74	3363614	3364195	+
<i>ygiN</i>	60	68	0.89	ST4-74	3364227	3364541	+
<i>parE</i>	24	27	0.90	ST4-74	3364666	3366558	-
<i>yqiA</i>	42	41	1.02	ST4-74	3366586	3367167	-
<i>cpdA</i>	57	56	1.03	ST4-74	3367167	3367994	-
<i>yqiB</i>	145	127	1.14	ST4-74	3368019	3368441	-
<i>nudF</i>	17	20	0.83	ST4-74	3368438	3369070	-
<i>tolC</i>	64	63	1.01	ST4-74	3369271	3370746	+
<i>ygiB</i>	236	218	1.08	ST4-74	3370959	3371630	+
<i>ygiC</i>	58	67	0.87	ST4-74	3371636	3372799	+
<i>ygiD</i>	16	17	0.95	ST4-74	3372861	3373691	-
<i>ygiE</i>	22	22	1.04	ST4-74	3373790	3374563	+
<i>assT</i>	3	3	0.78	ST4-74	3375206	3377002	+
STM3193	4	6	0.71	ST4-74	3377022	3377693	+
STM3194	14	12	1.13	ST4-74	3377708	3378385	+
<i>ribB</i>	39	64	0.61	ST4-74	3378556	3379209	-
<i>SroG</i>	841	1383	0.61	ST4-74	3379312	3379412	-
<i>yqiC</i>	150	119	1.26	ST4-74	3379646	3379945	+
<i>glgS</i>	207	175	1.18	ST4-74	3380019	3380228	-
STM3198	5	5	0.96	ST4-74	3380486	3381106	+
<i>yqiK</i>	7	8	0.94	ST4-74	3381125	3382804	+
STnc1420	447	514	0.87	ST4-74	3382981	3383131	+
<i>RygD</i>	4757	4738	1.00	ST4-74	3383000	3383144	-
<i>ibsC</i>	0	0	-	ST4-74	3383044	3383103	+
<i>rfaE</i>	22	27	0.81	ST4-74	3383264	3384697	-
<i>glnE</i>	14	15	0.93	ST4-74	3384745	3387588	-
<i>ygiF</i>	17	19	0.92	ST4-74	3387706	3389007	-
<i>ygiM</i>	44	48	0.91	ST4-74	3389249	3389863	+
<i>cca</i>	29	24	1.19	ST4-74	3389926	3391167	+
<i>bacA</i>	37	33	1.13	ST4-74	3391272	3392096	-
<i>folB</i>	56	41	1.36	ST4-74	3392191	3392553	-
<i>ygiH</i>	158	154	1.03	ST4-74	3392657	3393268	+
<i>gcp</i>	46	36	1.27	ST4-74	3393519	3394532	-
<i>rpsU</i>	4703	4126	1.14	ST4-74	3394760	3394975	+

<i>Name</i>	Δfnr TPM	WT TPM	$\Delta fnr/WT$	Chr ^a	Start	End	Strand
<i>dnaG</i>	55	57	0.96	ST4-74	3395211	3396956	+
<i>rpoD</i>	50	60	0.83	ST4-74	3397106	3398953	+
<i>mug</i>	60	45	1.34	ST4-74	3399077	3399583	-
<i>yqjH</i>	15	12	1.24	ST4-74	3399864	3400631	-
<i>yqjI</i>	28	31	0.92	ST4-74	3400863	3401510	+
STM3216	20	65	0.30	ST4-74	3401507	3403072	-
<i>aer</i>	12	33	0.38	ST4-74	3403460	3404980	-
<i>oat</i>	16	7	2.39	ST4-74	3405500	3406789	+
<i>fadH</i>	7	6	1.31	ST4-74	3406960	3408978	+
<i>ygjO</i>	12	12	1.04	ST4-74	3409059	3410195	-
<i>ygjP</i>	13	12	1.07	ST4-74	3410419	3410778	+
<i>ygjQ</i>	4	3	1.23	ST4-74	3410930	3411622	+
<i>ygjR</i>	21	26	0.83	ST4-74	3411711	3412709	+
<i>SraF</i>	890	771	1.15	ST4-74	3412774	3412961	+
<i>ygjT</i>	28	20	1.35	ST4-74	3412982	3413950	+
STnc310	14	6	2.26	ST4-74	3413972	3414032	-
<i>ygjU</i>	64	86	0.75	ST4-74	3414205	3415449	+
<i>yqjA</i>	138	121	1.14	ST4-74	3415899	3416561	+
<i>yqjB</i>	79	63	1.26	ST4-74	3416565	3416948	+
<i>yqjC</i>	344	228	1.51	ST4-74	3417093	3417461	+
<i>yqjE</i>	141	133	1.06	ST4-74	3417811	3418209	+
<i>yqjK</i>	54	58	0.94	ST4-74	3418206	3418505	+
<i>yqjF</i>	2	3	0.86	ST4-74	3418650	3419135	+
<i>yqjG</i>	29	16	1.84	ST4-74	3419203	3420189	+
<i>yhaH</i>	59	49	1.22	ST4-74	3420313	3420678	+
<i>yhaJ</i>	22	21	1.06	ST4-74	3420717	3421613	-
<i>yhaK</i>	15	23	0.65	ST4-74	3421718	3422419	+
<i>yhaL</i>	44	71	0.62	ST4-74	3422476	3422607	+
<i>yhaN</i>	9	7	1.34	ST4-74	3422720	3424030	-
<i>yhaO</i>	5	5	1.02	ST4-74	3424056	3425387	-
<i>tdcG</i>	4	5	0.84	ST4-74	3425703	3427067	-
<i>tdcE</i>	2	3	0.88	ST4-74	3427137	3429431	-
<i>tdcD</i>	3	5	0.65	ST4-74	3429465	3430673	-
<i>tdcC</i>	6	7	0.91	ST4-74	3430739	3432070	-
<i>tdcB</i>	3	5	0.60	ST4-74	3432091	3433080	-
<i>tdcA</i>	15	13	1.10	ST4-74	3433178	3434116	-
<i>garK</i>	10	6	1.56	ST4-74	3435915	3437060	-
<i>garRb</i>	9	8	1.12	ST4-74	3437158	3438048	-
<i>garL</i>	49	15	3.29	ST4-74	3438074	3438790	-
<i>garD</i>	5	4	1.14	ST4-74	3439374	3440945	+
STM3251	12	12	0.97	ST4-74	3441185	3442132	-
<i>agaR</i>	35	29	1.19	ST4-74	3442143	3442976	-
<i>gatY</i>	3	2	1.21	ST4-74	3443310	3444164	+
STM3254	1	1	0.48	ST4-74	3444175	3445089	+
STM3255	2	3	0.77	ST4-74	3445116	3446543	+
STM3256	2	2	1.03	ST4-74	3446530	3447336	+
STM3257	2	1	1.37	ST4-74	3447534	3448805	+
<i>gatA</i>	2	1	1.29	ST4-74	3448820	3449284	+
<i>gatB</i>	3	2	1.18	ST4-74	3449315	3449599	+
<i>gatC</i>	5	5	0.90	ST4-74	3449603	3450976	+
<i>gatD</i>	2	1	1.53	ST4-74	3451020	3452063	+

<i>Name</i>	Δfnr TPM	WT TPM	$\Delta fnr/WT$	Chr ^a	Start	End	Strand
<i>gatR</i>	22	25	0.86	ST4-74	3452174	3452947	+
<i>yraL</i>	18	16	1.13	ST4-74	3453105	3453968	-
<i>yraM</i>	31	32	0.96	ST4-74	3454032	3456074	+
<i>yraN</i>	50	54	0.93	ST4-74	3456032	3456427	+
<i>yraO</i>	87	70	1.25	ST4-74	3456449	3457039	+
<i>yraP</i>	37	39	0.94	ST4-74	3457049	3457624	+
<i>yraR</i>	11	7	1.59	ST4-74	3457691	3458359	-
<i>yhbO</i>	42	22	1.91	ST4-74	3458457	3458975	+
<i>yhbP</i>	5	9	0.54	ST4-74	3458955	3459398	-
<i>yhbQ</i>	37	28	1.32	ST4-74	3459436	3459753	+
<i>yhbS</i>	34	67	0.50	ST4-74	3459740	3460243	-
<i>yhbT</i>	76	166	0.46	ST4-74	3460237	3460761	-
<i>yhbU</i>	2	34	0.06	ST4-74	3460978	3461973	+
<i>yhbV</i>	2	12	0.16	ST4-74	3461982	3462860	+
<i>yhbW</i>	7	8	0.81	ST4-74	3463038	3464045	+
STM3277	5	3	1.67	ST4-74	3464023	3464742	-
STM3278	3	2	1.43	ST4-74	3464901	3465431	+
<i>mtr</i>	18	20	0.90	ST4-74	3465492	3466652	-
<i>deaD</i>	17	19	0.88	ST4-74	3466890	3468779	-
<i>yrbN</i>	73	76	0.97	ST4-74	3468772	3468852	-
<i>nlpI</i>	475	478	0.99	ST4-74	3468958	3469842	-
<i>pnp</i>	53	68	0.79	ST4-74	3469952	3472087	-
<i>SraG</i>	562	639	0.88	ST4-74	3472142	3472312	-
<i>rpsO</i>	2177	2346	0.93	ST4-74	3472329	3472598	-
<i>truB</i>	35	35	1.01	ST4-74	3472749	3473693	-
<i>rbfA</i>	18	25	0.74	ST4-74	3473693	3474094	-
<i>infB</i>	46	58	0.80	ST4-74	3474315	3476993	-
<i>nusA</i>	39	49	0.80	ST4-74	3477018	3478520	-
<i>yhbC</i>	54	62	0.88	ST4-74	3478548	3478970	-
<i>argG</i>	37	76	0.49	ST4-74	3479628	3480971	+
STnc3950	28	21	1.34	ST4-74	3480987	3481116	-
STM3291	11	12	0.93	ST4-74	3481057	3482121	-
<i>secG</i>	1077	1119	0.96	ST4-74	3482557	3482889	-
<i>glmM</i>	16	17	0.95	ST4-74	3483112	3484449	-
<i>folP</i>	22	22	0.96	ST4-74	3484442	3485290	-
<i>tnpA_1c</i>	244	250	0.97	ST4-74	3485437	3485895	-
<i>fisH</i>	212	247	0.86	ST4-74	3486106	3488040	-
<i>fisJ</i>	250	236	1.06	ST4-74	3488144	3488770	-
<i>yhbY</i>	165	161	1.03	ST4-74	3488897	3489190	+
STnc1660	231	278	0.83	ST4-74	3489125	3489247	-
<i>greA</i>	87	90	0.97	ST4-74	3489346	3489822	-
<i>dacB</i>	26	25	1.04	ST4-74	3490070	3491503	+
STnc3960	12	10	1.28	ST4-74	3491490	3491592	+
<i>obgE</i>	25	24	1.05	ST4-74	3491635	3492807	-
<i>yhbE</i>	39	27	1.41	ST4-74	3492823	3493833	-
<i>rpmA</i>	481	559	0.86	ST4-74	3493918	3494175	-
<i>rplU</i>	1962	1797	1.09	ST4-74	3494195	3494506	-
<i>ispB</i>	69	63	1.11	ST4-74	3494764	3495735	+
<i>nlp</i>	7	5	1.36	ST4-74	3495967	3496254	+
<i>murA</i>	23	23	0.96	ST4-74	3496312	3497571	-
<i>yrbA</i>	46	49	0.94	ST4-74	3497625	3497918	-

<i>Name</i>	Δ <i>fnr</i> TPM	WT TPM	Δ <i>fnr</i> /WT	<i>Chr</i> ^a	<i>Start</i>	<i>End</i>	<i>Strand</i>
<i>yrbB</i>	41	52	0.78	ST4-74	3498067	3498363	-
<i>yrbC</i>	40	44	0.90	ST4-74	3498363	3498998	-
<i>yrbD</i>	29	31	0.94	ST4-74	3499017	3499568	-
<i>yrbE</i>	14	16	0.88	ST4-74	3499573	3500355	-
<i>yrbF</i>	29	31	0.95	ST4-74	3500363	3501175	-
<i>yrbG</i>	35	39	0.88	ST4-74	3501430	3502365	+
<i>yrbH</i>	34	38	0.89	ST4-74	3502379	3503365	+
<i>yrbI</i>	55	56	0.99	ST4-74	3503386	3503952	+
<i>yrbK</i>	37	38	0.97	ST4-74	3503949	3504524	+
<i>yhbN</i>	29	38	0.75	ST4-74	3504493	3505047	+
<i>yhbG</i>	26	31	0.83	ST4-74	3505054	3505779	+
<i>rpoN</i>	88	109	0.81	ST4-74	3505827	3507260	+
<i>yhbH</i>	365	495	0.74	ST4-74	3507283	3507570	+
STnc3970	160	90	1.78	ST4-74	3507628	3507677	-
<i>ptsN</i>	46	62	0.75	ST4-74	3507688	3508179	+
<i>yhbJ</i>	24	31	0.78	ST4-74	3508225	3509079	+
<i>ptsO</i>	11	13	0.81	ST4-74	3509076	3509348	+
<i>yrbL</i>	20	17	1.18	ST4-74	3509597	3510229	+
<i>mtgA</i>	19	26	0.73	ST4-74	3510304	3511032	-
<i>yhbL</i>	34	51	0.67	ST4-74	3511029	3511682	-
<i>ArcZ</i>	16269	16401	0.99	ST4-74	3511800	3511917	+
<i>arcB</i>	27	33	0.80	ST4-74	3511909	3514245	-
<i>yhcC</i>	5	12	0.40	ST4-74	3514339	3515268	-
<i>gltB</i>	29	54	0.54	ST4-74	3515940	3520400	+
<i>gltD</i>	33	60	0.55	ST4-74	3520410	3521828	+
<i>yhcG</i>	3	2	1.42	ST4-74	3522035	3523138	+
<i>codB</i>	30	41	0.75	ST4-74	3523255	3524508	+
<i>codA</i>	20	30	0.67	ST4-74	3524495	3525775	+
<i>yhcH</i>	11	10	1.06	ST4-74	3525858	3526325	-
<i>nanK</i>	12	9	1.29	ST4-74	3526322	3527197	-
<i>nanE</i>	4	6	0.73	ST4-74	3527194	3527883	-
<i>nanT</i>	12	11	1.10	ST4-74	3527930	3529420	-
<i>nanA</i>	3	4	0.92	ST4-74	3529536	3530429	-
<i>yhcK</i>	30	34	0.89	ST4-74	3530564	3531355	-
<i>sspB</i>	77	80	0.97	ST4-74	3531464	3531964	-
<i>sspA</i>	97	109	0.89	ST4-74	3531970	3532608	-
STM3343	12	12	1.02	ST4-74	3532871	3533623	-
STnc3060	42	40	1.05	ST4-74	3533708	3533783	+
<i>rpsI</i>	239	370	0.64	ST4-74	3533823	3534215	-
<i>rplM</i>	324	456	0.71	ST4-74	3534231	3534659	-
<i>yhcM</i>	16	19	0.89	ST4-74	3534962	3536086	-
<i>yhcB</i>	200	224	0.89	ST4-74	3536273	3536677	+
<i>degQ</i>	20	26	0.77	ST4-74	3536834	3538201	+
<i>degS</i>	28	27	1.02	ST4-74	3538294	3539364	+
STM3350	4	3	1.33	ST4-74	3539398	3540129	-
<i>oadB2</i>	3	2	1.39	ST4-74	3540149	3541450	-
<i>oadA2</i>	1	1	0.72	ST4-74	3541466	3543241	-
STM3353	3	4	0.87	ST4-74	3543257	3543511	-
STnc3050	154	171	0.90	ST4-74	3543529	3543654	-
<i>ttdB</i>	4	3	1.32	ST4-74	3543667	3544284	-
<i>ttdA</i>	4	2	1.54	ST4-74	3544284	3545183	-

<i>Name</i>	Δ <i>fnr</i> TPM	WT TPM	Δ <i>fnr</i> /WT	Chr ^a	Start	End	Strand
STM3356	3	2	1.50	ST4-74	3545216	3546484	-
STM3357	17	18	0.97	ST4-74	3546695	3547360	-
STM3358	52	53	0.99	ST4-74	3547347	3547976	-
<i>mdh</i>	159	233	0.68	ST4-74	3548096	3549034	-
<i>argR</i>	344	300	1.15	ST4-74	3549448	3549918	+
<i>yhcN</i>	9	7	1.22	ST4-74	3550283	3550546	+
STM3362	8	6	1.35	ST4-74	3550650	3550916	+
STnc2100	14	12	1.15	ST4-74	3550903	3550965	+
<i>yhcO</i>	200	83	2.41	ST4-74	3550976	3551248	-
<i>yhcP</i>	7	7	1.11	ST4-74	3551420	3553387	-
<i>yhcQ</i>	6	5	1.22	ST4-74	3553393	3554325	-
<i>yhcR</i>	8	9	0.97	ST4-74	3554333	3554536	-
<i>yhcS</i>	9	10	0.92	ST4-74	3554718	3555647	+
<i>tldD</i>	27	23	1.14	ST4-74	3555770	3557215	-
<i>yhdP</i>	14	17	0.83	ST4-74	3557360	3561073	-
<i>cafA</i>	33	37	0.89	ST4-74	3561267	3562736	-
<i>maf-b</i>	35	34	1.03	ST4-74	3562726	3563319	-
<i>mreD</i>	43	37	1.17	ST4-74	3563328	3563819	-
<i>mreC</i>	28	31	0.93	ST4-74	3563819	3564871	-
<i>mreB</i>	52	63	0.83	ST4-74	3564936	3565979	-
<i>yhdA</i>	22	27	0.81	ST4-74	3566287	3568227	-
<i>yhdH</i>	21	34	0.63	ST4-74	3568431	3569405	+
STM3377	14	20	0.69	ST4-74	3569518	3570522	+
STM3378	30	33	0.90	ST4-74	3570523	3571122	+
<i>accB</i>	70	87	0.80	ST4-74	3571515	3571985	+
<i>accC</i>	66	83	0.79	ST4-74	3572086	3573345	+
<i>yhdT</i>	16	20	0.80	ST4-74	3573454	3573696	+
<i>panF</i>	8	10	0.83	ST4-74	3573686	3575137	+
<i>prmA</i>	8	9	0.85	ST4-74	3575149	3576030	+
<i>yhdG</i>	124	144	0.86	ST4-74	3576691	3577656	+
<i>fis</i>	81	107	0.76	ST4-74	3577682	3577978	+
<i>yhdJ</i>	10	11	0.96	ST4-74	3578064	3578948	+
<i>yhdU</i>	87	78	1.13	ST4-74	3579031	3579195	+
STM3388	8	7	1.15	ST4-74	3579346	3581445	+
<i>envR</i>	2	2	0.82	ST4-74	3581448	3582110	-
<i>acrE</i>	1	1	0.98	ST4-74	3582524	3583681	+
<i>acrF</i>	5	4	1.13	ST4-74	3583693	3586806	+
<i>yhdV</i>	22	23	0.96	ST4-74	3587042	3587263	+
STnc3990	111	61	1.81	ST4-74	3587262	3587429	-
STnc1670	175	98	1.78	ST4-74	3593794	3593896	+
<i>yrdA</i>	43	32	1.32	ST4-74	3593964	3594518	+
<i>yrdB</i>	22	24	0.91	ST4-74	3594494	3594751	-
STM3401	20	18	1.12	ST4-74	3594748	3595566	-
<i>yrdC</i>	16	16	1.01	ST4-74	3595571	3596143	-
<i>yrdD</i>	124	99	1.25	ST4-74	3596148	3596690	-
<i>smg</i>	301	210	1.43	ST4-74	3596717	3597190	-
<i>dprA</i>	51	43	1.20	ST4-74	3597162	3598286	-
<i>def</i>	175	126	1.39	ST4-74	3598418	3598927	+
<i>fnt</i>	36	32	1.15	ST4-74	3598943	3599890	+
<i>fmu</i>	9	9	1.00	ST4-74	3599942	3601231	+
<i>sapG</i>	14	11	1.29	ST4-74	3601253	3602629	+

<i>Name</i>	Δfnr TPM	WT TPM	$\Delta fnr/WT$	<i>Chr</i> ^a	<i>Start</i>	<i>End</i>	<i>Strand</i>
<i>mscL</i>	420	281	1.49	ST4-74	3602771	3603184	+
STM3411	392	266	1.47	ST4-74	3603120	3603389	-
<i>zntR</i>	54	52	1.03	ST4-74	3603447	3603872	-
<i>yhdN</i>	120	95	1.27	ST4-74	3603883	3604251	-
<i>rplQ</i>	412	549	0.75	ST4-74	3604359	3604742	-
<i>pez</i>	436	594	0.73	ST4-74	3604783	3605772	-
<i>rpsD</i>	498	611	0.81	ST4-74	3605798	3606418	-
<i>rpsK</i>	467	607	0.77	ST4-74	3606452	3606784	-
<i>rpsM</i>	951	1015	0.94	ST4-74	3606858	3607214	-
<i>rpmJb</i>	976	1148	0.85	ST4-74	3607361	3607477	-
<i>prlA</i>	605	774	0.78	ST4-74	3607509	3608840	-
<i>rplO</i>	389	540	0.72	ST4-74	3608848	3609282	-
<i>rpmD</i>	386	501	0.77	ST4-74	3609286	3609465	-
<i>rpsE</i>	341	475	0.72	ST4-74	3609469	3609972	-
<i>rl18</i>	362	478	0.76	ST4-74	3609987	3610340	-
<i>rplF</i>	312	421	0.74	ST4-74	3610350	3610883	-
<i>rpsH</i>	399	505	0.79	ST4-74	3610896	3611288	-
<i>rpsN</i>	324	395	0.82	ST4-74	3611322	3611612	-
<i>rplE</i>	553	671	0.82	ST4-74	3611642	3612181	-
<i>rplX</i>	851	999	0.85	ST4-74	3612196	3612510	-
<i>rplN</i>	1084	1337	0.81	ST4-74	3612521	3612892	-
<i>rpsQ</i>	410	543	0.76	ST4-74	3613056	3613310	-
<i>rpmC</i>	607	710	0.86	ST4-74	3613310	3613501	-
<i>rplP</i>	460	515	0.89	ST4-74	3613501	3613911	-
<i>rpsC</i>	330	438	0.75	ST4-74	3613924	3614625	-
<i>rplV</i>	294	365	0.80	ST4-74	3614643	3614975	-
<i>rpsS</i>	525	667	0.79	ST4-74	3614990	3615268	-
<i>rplB</i>	148	208	0.71	ST4-74	3615285	3616106	-
<i>rplW</i>	196	284	0.69	ST4-74	3616124	3616426	-
<i>rplD</i>	206	274	0.75	ST4-74	3616423	3617028	-
<i>rplC</i>	215	279	0.77	ST4-74	3617039	3617668	-
<i>rpsJ</i>	429	543	0.79	ST4-74	3617701	3618012	-
<i>hopD</i>	6	5	1.07	ST4-74	3618392	3618859	+
<i>bfr</i>	481	319	1.51	ST4-74	3618856	3619332	-
<i>bfd</i>	489	163	2.99	ST4-74	3619405	3619599	-
STnc4000	99	28	3.47	ST4-74	3619657	3619755	+
<i>tufA</i>	563	709	0.79	ST4-74	3619784	3620968	-
<i>fusA</i>	173	211	0.82	ST4-74	3621040	3623154	-
<i>rpsG</i>	269	328	0.82	ST4-74	3623251	3623721	-
<i>rpsL</i>	726	723	1.00	ST4-74	3623817	3624191	-
<i>yheL</i>	162	92	1.75	ST4-74	3624317	3624604	-
<i>yheM</i>	28	33	0.85	ST4-74	3624612	3624968	-
<i>yheN</i>	30	38	0.80	ST4-74	3624968	3625354	-
<i>yheO</i>	86	95	0.91	ST4-74	3625354	3626088	-
<i>fkpA</i>	100	111	0.90	ST4-74	3626353	3627171	-
<i>slyX</i>	73	80	0.91	ST4-74	3627391	3627609	+
<i>slyD</i>	119	132	0.90	ST4-74	3627797	3628387	-
<i>yheV</i>	18	17	1.06	ST4-74	3628482	3628682	-
<i>kefB</i>	19	15	1.27	ST4-74	3628693	3630498	-
<i>yheR</i>	17	12	1.40	ST4-74	3630498	3631049	-
<i>yheS</i>	14	16	0.93	ST4-74	3631315	3633222	+

<i>Name</i>	Δfnr TPM	WT TPM	$\Delta fnr/WT$	Chr ^a	Start	End	Strand
STnc1590	1627	2319	0.70	ST4-74	3633247	3633424	-
SL1344_3427	13	12	1.13	ST4-74	3633385	3633606	+
STM3461	78	97	0.80	ST4-74	3633608	3633919	-
<i>yheT</i>	26	23	1.10	ST4-74	3634117	3635184	+
<i>yheU</i>	25	28	0.91	ST4-74	3635181	3635399	+
<i>prkB</i>	23	21	1.07	ST4-74	3635451	3636320	+
<i>yhfA</i>	99	112	0.88	ST4-74	3636416	3636820	-
<i>crp</i>	111	138	0.80	ST4-74	3637128	3637760	+
<i>yhfK</i>	23	31	0.73	ST4-74	3637809	3639896	+
<i>argDb</i>	74	108	0.68	ST4-74	3639939	3641156	-
<i>pabA</i>	13	14	0.98	ST4-74	3641242	3641805	-
<i>fic</i>	19	13	1.53	ST4-74	3641837	3642439	-
<i>yhfG</i>	118	72	1.64	ST4-74	3642429	3642596	-
<i>ppiA</i>	124	129	0.96	ST4-74	3642705	3643277	-
<i>yhfC</i>	6	6	1.01	ST4-74	3643554	3644735	+
<i>nirB</i>	3	6	0.41	ST4-74	3644998	3647541	+
<i>nirD</i>	6	20	0.32	ST4-74	3647538	3647864	+
<i>nirC</i>	13	16	0.83	ST4-74	3648130	3648939	+
<i>cysG</i>	13	17	0.74	ST4-74	3648951	3650324	+
<i>bigA</i>	3	3	1.08	ST4-74	3650653	3656547	+
<i>tnpA_1d</i>	244	250	0.97	ST4-74	3656679	3657137	-
STnc340	10	14	0.73	ST4-74	3657275	3657403	-
<i>yhfL</i>	83	69	1.20	ST4-74	3657451	3657621	+
<i>trpS</i>	48	51	0.94	ST4-74	3657766	3658770	-
<i>gph</i>	40	39	1.03	ST4-74	3658763	3659521	-
<i>rpe</i>	21	21	1.00	ST4-74	3659514	3660191	-
<i>dam</i>	33	39	0.84	ST4-74	3660209	3661045	-
<i>damX</i>	58	73	0.79	ST4-74	3661226	3662503	-
<i>aroB</i>	56	63	0.88	ST4-74	3662601	3663689	-
<i>aroK</i>	135	149	0.91	ST4-74	3663746	3664267	-
<i>comE</i>	6	6	0.97	ST4-74	3664732	3665970	-
<i>comD</i>	6	4	1.52	ST4-74	3665885	3666286	-
<i>comC</i>	3	4	0.92	ST4-74	3666276	3666749	-
<i>comB</i>	3	2	1.28	ST4-74	3666733	3667272	-
<i>comA</i>	4	3	1.40	ST4-74	3667272	3668051	-
<i>mrcA</i>	22	22	1.00	ST4-74	3668148	3670724	+
<i>nudE</i>	37	32	1.16	ST4-74	3670820	3671383	-
<i>igaA</i>	29	36	0.82	ST4-74	3671706	3673838	+
<i>yrfG</i>	49	36	1.34	ST4-74	3673903	3674571	+
<i>hslR</i>	16	16	0.96	ST4-74	3674582	3674983	+
<i>hslO</i>	12	13	0.93	ST4-74	3675002	3675886	+
<i>yhgE</i>	11	11	1.02	ST4-74	3675996	3677705	-
<i>pckA</i>	116	135	0.86	ST4-74	3678085	3679704	+
<i>envZ</i>	20	29	0.69	ST4-74	3679779	3681014	-
<i>ompR</i>	45	50	0.89	ST4-74	3681128	3681847	-
<i>greB</i>	22	21	1.02	ST4-74	3682073	3682546	+
<i>yhgF</i>	13	13	0.96	ST4-74	3682648	3684975	+
STnc760	463	362	1.28	ST4-74	3684975	3685117	-
<i>feoA</i>	43	31	1.38	ST4-74	3685412	3685639	+
<i>feoB</i>	26	23	1.14	ST4-74	3685658	3687976	+
<i>yhgG</i>	58	46	1.26	ST4-74	3687989	3688225	+

<i>Name</i>	Δfnr TPM	WT TPM	$\Delta fnr/WT$	<i>Chr</i> ^a	<i>Start</i>	<i>End</i>	<i>Strand</i>
STM3508	14	15	0.91	ST4-74	3688460	3689374	+
<i>bioH</i>	21	22	0.95	ST4-74	3689410	3690180	-
<i>comF</i>	35	28	1.25	ST4-74	3690218	3690901	+
<i>yhgI</i>	63	70	0.90	ST4-74	3690960	3691535	+
<i>gntT</i>	7	8	0.97	ST4-74	3691960	3693228	+
<i>malQ</i>	11	8	1.36	ST4-74	3693347	3695425	-
<i>malP</i>	11	8	1.27	ST4-74	3695435	3697828	-
<i>malT</i>	36	40	0.91	ST4-74	3698422	3701127	+
STM3516	51	42	1.23	ST4-74	3701215	3701490	-
STM3517	314	229	1.37	ST4-74	3701493	3701753	-
<i>rtcA</i>	5	6	0.83	ST4-74	3701862	3702881	-
<i>rtcB</i>	15	14	1.08	ST4-74	3702885	3704102	-
STM3521	2	2	1.00	ST4-74	3704447	3706000	-
<i>rtcR</i>	5	5	1.05	ST4-74	3706190	3707773	+
<i>glpR</i>	31	32	0.98	ST4-74	3707770	3708528	-
<i>glpG</i>	31	31	1.00	ST4-74	3708622	3709452	-
<i>glpE</i>	98	81	1.20	ST4-74	3709528	3709854	-
<i>glpD</i>	331	313	1.06	ST4-74	3710053	3711561	+
STM3527	7	5	1.37	ST4-74	3711608	3712153	-
STM3528	14	13	1.10	ST4-74	3712163	3713623	-
STM3529	6	5	1.16	ST4-74	3713816	3714925	-
STM3530	4	3	1.35	ST4-74	3715263	3716597	+
STM3531	3	4	0.72	ST4-74	3716594	3718309	+
STM3532	11	8	1.43	ST4-74	3718353	3719258	+
STM3533	37	52	0.72	ST4-74	3719302	3720057	-
<i>glgP</i>	32	33	0.96	ST4-74	3720235	3722682	-
<i>glgA</i>	28	25	1.11	ST4-74	3722702	3724135	-
<i>glgC</i>	27	34	0.78	ST4-74	3724135	3725430	-
<i>glgX</i>	29	24	1.21	ST4-74	3725445	3727421	-
<i>glgB</i>	41	35	1.20	ST4-74	3727418	3729604	-
STnc4010	44	16	2.77	ST4-74	3729766	3729898	+
<i>asd</i>	64	102	0.63	ST4-74	3729951	3731057	-
<i>gntU</i>	7	6	1.17	ST4-74	3731481	3732821	-
<i>gntK</i>	4	3	1.14	ST4-74	3732818	3733351	-
<i>gntR</i>	30	23	1.29	ST4-74	3733490	3734485	-
<i>yhhW</i>	6	6	1.06	ST4-74	3734615	3735310	-
<i>yhhX</i>	16	15	1.10	ST4-74	3735434	3736471	-
<i>RyhB-1</i>	41	31	1.35	ST4-74	3736722	3736817	-
<i>yhhY</i>	21	23	0.93	ST4-74	3736940	3737428	+
STM3547	2	2	0.75	ST4-74	3737960	3738907	+
STM3548	4	3	1.39	ST4-74	3738923	3739684	+
STnc1830	54	44	1.23	ST4-74	3739678	3739897	-
STM3549	3	2	1.19	ST4-74	3739738	3740709	+
STM3550	4	4	1.06	ST4-74	3740706	3741740	+
<i>ggt</i>	17	15	1.16	ST4-74	3741785	3743527	-
<i>yhhA</i>	75	43	1.75	ST4-74	3743653	3744069	+
<i>ugpQ</i>	14	15	0.97	ST4-74	3744082	3744822	-
<i>ugpC</i>	7	7	0.99	ST4-74	3744819	3745889	-
<i>ugpE</i>	7	5	1.39	ST4-74	3745891	3746736	-
<i>ugpA</i>	9	8	1.18	ST4-74	3746733	3747620	-
<i>ugpB</i>	33	27	1.22	ST4-74	3747684	3748976	-

<i>Name</i>	Δfnr TPM	WT TPM	$\Delta fnr/WT$	Chr ^a	Start	End	Strand
<i>kil</i>	12	11	1.13	ST4-74	3749259	3749627	-
<i>phd</i>	61	63	0.96	ST4-74	3749624	3749851	-
<i>livF</i>	16	31	0.54	ST4-74	3749977	3750690	-
<i>livG</i>	14	27	0.52	ST4-74	3750692	3751459	-
<i>livM</i>	18	34	0.53	ST4-74	3751456	3752733	-
<i>livH</i>	20	33	0.59	ST4-74	3752730	3753656	-
<i>livK</i>	29	53	0.56	ST4-74	3753716	3754825	-
<i>sRNA12</i>	19	7	2.78	ST4-74	3755044	3755124	-
<i>yhhK</i>	26	23	1.11	ST4-74	3755247	3755630	+
<i>livJ</i>	37	74	0.50	ST4-74	3755825	3756928	-
<i>rpoH</i>	147	159	0.92	ST4-74	3757250	3758104	-
<i>fisX</i>	36	37	0.97	ST4-74	3758350	3759405	-
<i>ftsE</i>	29	30	0.98	ST4-74	3759398	3760066	-
<i>ftsY</i>	35	36	0.97	ST4-74	3760069	3761544	-
<i>rsmD</i>	22	20	1.09	ST4-74	3761670	3762266	+
<i>yhhL</i>	16	15	1.05	ST4-74	3762253	3762525	+
<i>yhhM</i>	19	20	0.91	ST4-74	3762547	3762789	-
<i>yhhN</i>	38	31	1.20	ST4-74	3763060	3763686	+
<i>zntA</i>	4	5	0.82	ST4-74	3763767	3765965	+
<i>tcp</i>	21	97	0.21	ST4-74	3766165	3767808	+
<i>yhhP</i>	186	109	1.70	ST4-74	3767832	3768077	-
<i>yhhQ</i>	39	24	1.63	ST4-74	3768247	3768912	+
STM3580	98	83	1.19	ST4-74	3768985	3769542	+
<i>yhhS</i>	24	22	1.09	ST4-74	3769546	3770763	-
<i>yhhT</i>	16	10	1.57	ST4-74	3770895	3771944	+
<i>acpT</i>	24	20	1.23	ST4-74	3771996	3772574	+
<i>nikR</i>	30	33	0.91	ST4-74	3772666	3773067	+
<i>yhhJ</i>	11	14	0.78	ST4-74	3773157	3774281	-
<i>yhiH</i>	6	8	0.77	ST4-74	3774281	3777022	-
<i>yhiI</i>	15	18	0.83	ST4-74	3777019	3778086	-
STnc770	592	481	1.23	ST4-74	3778180	3778332	-
<i>yhiN</i>	16	17	0.97	ST4-74	3778392	3779588	-
<i>pitA</i>	30	48	0.64	ST4-74	3779942	3781315	+
<i>uspB</i>	162	112	1.45	ST4-74	3781455	3781790	-
<i>uspA</i>	308	341	0.90	ST4-74	3782178	3782612	+
STnc350	45	12	3.91	ST4-74	3782695	3782856	-
<i>yhiP</i>	7	6	1.32	ST4-74	3782937	3784409	+
<i>yhiQ</i>	7	9	0.86	ST4-74	3784501	3785259	-
<i>prlC</i>	16	19	0.82	ST4-74	3785266	3787308	-
STM3595	37	25	1.50	ST4-74	3787490	3788761	-
<i>yhiR</i>	27	25	1.10	ST4-74	3788972	3789814	+
<i>gor</i>	31	32	0.96	ST4-74	3789919	3791271	+
STM3598	10	11	0.92	ST4-74	3791318	3792361	-
STM3599	8	7	1.00	ST4-74	3792420	3793739	-
STM3600	2	3	0.61	ST4-74	3793793	3794638	-
STM3601	13	12	1.10	ST4-74	3794702	3795679	-
STM3602	20	17	1.21	ST4-74	3795855	3796574	-
<i>treF</i>	16	14	1.19	ST4-74	3796900	3798549	+
STM3604	38	72	0.52	ST4-74	3798562	3800151	-
STM3605	4	4	0.91	ST4-74	3800432	3800788	+
<i>yhjB</i>	4	3	1.18	ST4-74	3800794	3801396	-

<i>Name</i>	Δfnr TPM	WT TPM	$\Delta fnr/WT$	<i>Chr</i> ^a	<i>Start</i>	<i>End</i>	<i>Strand</i>
STnc4020	40	42	0.95	ST4-74	3801174	3801265	+
<i>yhjC</i>	9	8	1.03	ST4-74	3802027	3802926	+
<i>yhjD</i>	20	13	1.48	ST4-74	3802999	3804027	+
<i>yhjE</i>	56	74	0.75	ST4-74	3804378	3805700	+
<i>yhjG</i>	21	19	1.10	ST4-74	3805740	3807800	-
<i>yhjH</i>	27	101	0.26	ST4-74	3807910	3808677	-
<i>kdgK</i>	12	37	0.33	ST4-74	3808906	3809835	+
<i>yhjJ</i>	22	27	0.83	ST4-74	3809889	3811376	-
<i>dctA</i>	44	90	0.48	ST4-74	3811596	3812882	-
<i>yhjK</i>	14	13	1.08	ST4-74	3813040	3814959	-
<i>yhjL</i>	18	18	0.99	ST4-74	3815220	3818762	-
<i>bcsC</i>	20	21	0.95	ST4-74	3818744	3819853	-
<i>yhjN</i>	12	15	0.81	ST4-74	3819857	3822157	-
<i>bcsA</i>	15	17	0.92	ST4-74	3822168	3824792	-
<i>yhjQ</i>	13	14	0.92	ST4-74	3824789	3825541	-
<i>yhjR</i>	81	74	1.09	ST4-74	3825542	3825745	-
<i>yhjS</i>	30	21	1.40	ST4-74	3825990	3827561	+
<i>yhjT</i>	20	17	1.21	ST4-74	3827558	3827749	+
<i>yhjU</i>	20	18	1.14	ST4-74	3827746	3829425	+
STnc1430	648	927	0.70	ST4-74	3829427	3829796	-
STnc710	5219	4839	1.08	ST4-74	3829660	3829727	+
STM3624A	23	18	1.34	ST4-74	3829889	3830139	+
<i>yhjV</i>	11	10	1.12	ST4-74	3830257	3831555	+
<i>dppF</i>	15	34	0.44	ST4-74	3831656	3832669	-
<i>dppD</i>	22	44	0.49	ST4-74	3832666	3833649	-
<i>dppC</i>	26	52	0.49	ST4-74	3833660	3834562	-
<i>dppB</i>	36	68	0.52	ST4-74	3834572	3835591	-
<i>dppA</i>	124	244	0.51	ST4-74	3835748	3837304	-
STM3631	4	3	1.08	ST4-74	3837911	3839236	-
STM3632	4	4	1.04	ST4-74	3839294	3840418	-
STM3633	16	19	0.84	ST4-74	3840568	3841575	+
<i>yhjW</i>	21	24	0.88	ST4-74	3841902	3843593	-
<i>lpfE</i>	5	5	0.91	ST4-74	3843811	3844338	-
<i>lpfD</i>	8	8	0.99	ST4-74	3844344	3845413	-
<i>lpfC</i>	2	3	0.85	ST4-74	3845431	3847959	-
<i>lpfB</i>	2	2	1.09	ST4-74	3847982	3848680	-
<i>lpfA</i>	3	4	0.86	ST4-74	3848765	3849301	-
<i>yhjY</i>	26	15	1.65	ST4-74	3849807	3850511	-
<i>tag</i>	16	21	0.78	ST4-74	3850668	3851249	+
<i>viaC</i>	14	25	0.57	ST4-74	3851227	3851667	+
<i>bisC</i>	15	15	0.97	ST4-74	3851636	3853969	-
<i>viaD</i>	8	9	0.91	ST4-74	3854155	3854784	+
<i>viaE</i>	16	21	0.78	ST4-74	3855003	3855977	+
<i>viaF</i>	129	110	1.17	ST4-74	3856027	3856737	-
<i>viaG</i>	405	183	2.21	ST4-74	3857176	3857466	+
<i>cspA</i>	242	203	1.19	ST4-74	3857767	3857967	+
STM3650	48	92	0.52	ST4-74	3858264	3858680	+
STnc780	264	136	1.94	ST4-74	3858665	3858992	-
STM3651	17	19	0.88	ST4-74	3859052	3859537	-
STM3652	60	58	1.03	ST4-74	3859525	3859812	-
<i>yafP</i>	17	16	1.05	ST4-74	3859990	3860457	-

<i>Name</i>	Δfnr TPM	WT TPM	$\Delta fnr/WT$	Chr ^a	Start	End	Strand
<i>glyS</i>	22	26	0.85	ST4-74	3861086	3863155	-
<i>glyQ</i>	30	35	0.85	ST4-74	3863165	3864076	-
STM3657	56	42	1.35	ST4-74	3864215	3864517	-
<i>yiaH</i>	13	10	1.31	ST4-74	3864683	3865678	+
<i>yiaB</i>	17	13	1.28	ST4-74	3865701	3866054	-
<i>xylB</i>	6	6	1.10	ST4-74	3866229	3867683	-
<i>xylA</i>	10	9	1.11	ST4-74	3867783	3869105	-
<i>xylR</i>	11	12	0.90	ST4-74	3869468	3870646	+
<i>bax</i>	225	301	0.75	ST4-74	3870707	3871531	-
<i>malS</i>	2	2	0.79	ST4-74	3871847	3873874	+
<i>avtA</i>	48	60	0.81	ST4-74	3874048	3875298	+
<i>ysaA</i>	16	61	0.26	ST4-74	3875335	3875808	-
<i>yiaJ</i>	31	26	1.20	ST4-74	3875925	3876725	-
<i>yiaK</i>	2	2	0.84	ST4-74	3876955	3877953	+
<i>yiaL</i>	3	2	1.26	ST4-74	3877965	3878429	+
STM3670	4	5	0.96	ST4-74	3878453	3879385	+
<i>yiaM</i>	3	2	1.73	ST4-74	3879524	3879997	+
<i>yiaN</i>	1	1	1.02	ST4-74	3880000	3881277	+
<i>yiaO</i>	1	0	3.16	ST4-74	3881289	3882275	+
<i>lyxK</i>	1	1	1.08	ST4-74	3882279	3883775	+
<i>sgbH</i>	1	1	1.06	ST4-74	3883772	3884434	+
<i>sgbU</i>	1	1	0.63	ST4-74	3884427	3885287	+
<i>sgbE</i>	3	2	1.30	ST4-74	3885305	3885976	+
STM3678	6	9	0.64	ST4-74	3886137	3886952	-
STM3679	3	3	0.97	ST4-74	3887216	3889171	+
<i>aldB</i>	62	63	0.98	ST4-74	3889289	3890827	-
STM3681	20	13	1.54	ST4-74	3890996	3891877	+
<i>selB</i>	10	14	0.73	ST4-74	3892162	3894012	-
<i>selA</i>	20	27	0.75	ST4-74	3894009	3895400	-
<i>yibF</i>	71	50	1.40	ST4-74	3895499	3896107	-
<i>mltA</i>	26	31	0.84	ST4-74	3896583	3898499	+
<i>mltD</i>	27	28	0.98	ST4-74	3898720	3899868	+
<i>mltR</i>	15	15	0.99	ST4-74	3899865	3900455	+
STM3688	64	32	1.97	ST4-74	3900465	3900674	-
<i>yibL</i>	41	43	0.94	ST4-74	3900965	3901327	+
STM3690	1	0	1.50	ST4-74	3901817	3902500	+
<i>sadA</i>	7	4	1.51	ST4-74	3902544	3906929	+
STnc380	55	22	2.48	ST4-74	3906944	3907051	-
<i>lctP</i>	5	5	0.97	ST4-74	3907228	3908883	+
<i>lctR</i>	3	3	1.04	ST4-74	3908880	3909656	+
<i>lctD</i>	3	2	1.28	ST4-74	3909653	3910843	+
<i>yibK</i>	15	16	0.95	ST4-74	3910907	3911380	+
STM3696	22	22	1.01	ST4-74	3911448	3912452	-
STM3697	3	2	1.60	ST4-74	3912771	3913967	+
STM3698	7	8	0.92	ST4-74	3914041	3915219	+
SL1344_3664	13	6	2.17	ST4-74	3915216	3915350	+
<i>cysE</i>	25	39	0.65	ST4-74	3915433	3916254	-
<i>gpsA</i>	83	88	0.94	ST4-74	3916332	3917351	-
<i>secB</i>	253	256	0.99	ST4-74	3917351	3917818	-
<i>grxC</i>	179	196	0.91	ST4-74	3917862	3918113	-
<i>yibN</i>	187	189	0.99	ST4-74	3918200	3918631	-

<i>Name</i>	Δfnr TPM	WT TPM	$\Delta fnr/WT$	<i>Chr</i> ^a	<i>Start</i>	<i>End</i>	<i>Strand</i>
<i>pmgI</i>	10	41	0.25	ST4-74	3918879	3920423	+
<i>yibP</i>	53	50	1.07	ST4-74	3920433	3921716	+
<i>yigQ</i>	7	8	0.94	ST4-74	3921720	3922682	+
<i>yibD</i>	12	13	0.90	ST4-74	3922669	3923703	-
SL1344_3673A	105	94	1.12	ST4-74	3923989	3924108	-
<i>tdh</i>	35	40	0.87	ST4-74	3924197	3925222	-
<i>kbl</i>	28	31	0.90	ST4-74	3925232	3926428	-
<i>rfaD</i>	70	69	1.01	ST4-74	3926631	3927563	+
<i>rfaF</i>	23	29	0.79	ST4-74	3927566	3928612	+
<i>rfaC</i>	19	20	0.94	ST4-74	3928612	3929565	+
<i>rfaL</i>	48	49	0.98	ST4-74	3929605	3930819	+
<i>rfaK</i>	40	32	1.24	ST4-74	3930876	3931739	-
<i>rfaZ</i>	117	72	1.62	ST4-74	3932122	3932931	-
<i>rfaY</i>	76	60	1.27	ST4-74	3933081	3933635	-
<i>rfaJ</i>	69	59	1.18	ST4-74	3933802	3934812	-
<i>rfaI</i>	83	62	1.33	ST4-74	3934830	3935843	-
<i>rfaB</i>	57	48	1.18	ST4-74	3935849	3936928	-
<i>yibR</i>	43	34	1.27	ST4-74	3936998	3937231	-
<i>rfaP</i>	34	27	1.26	ST4-74	3937263	3938060	-
<i>rfaG</i>	35	32	1.11	ST4-74	3938053	3939177	-
<i>rfaQ</i>	30	29	1.02	ST4-74	3939174	3940208	-
<i>kdtA</i>	38	36	1.04	ST4-74	3940719	3941930	+
<i>coaD</i>	25	34	0.75	ST4-74	3941939	3942418	+
<i>mutM</i>	8	7	1.08	ST4-74	3942446	3943255	-
<i>rpmG</i>	494	600	0.82	ST4-74	3943353	3943520	-
<i>rpmB</i>	1240	1350	0.92	ST4-74	3943541	3943777	-
<i>radC</i>	28	29	0.96	ST4-74	3943995	3944660	-
<i>dfp</i>	31	31	1.01	ST4-74	3944833	3946056	+
<i>dut</i>	28	27	1.01	ST4-74	3946037	3946492	+
<i>slmA</i>	18	24	0.78	ST4-74	3946600	3947196	+
<i>pyrE</i>	11	12	0.86	ST4-74	3947274	3947915	-
<i>rph</i>	50	46	1.09	ST4-74	3947994	3948710	-
<i>yicC</i>	43	38	1.14	ST4-74	3948836	3949699	+
STM3736	10	8	1.26	ST4-74	3949749	3950606	-
STM3737	4	3	1.53	ST4-74	3950725	3951606	+
STM3738	10	8	1.25	ST4-74	3951857	3952474	+
<i>ligB</i>	5	4	1.29	ST4-74	3952471	3954156	-
<i>gmk</i>	101	97	1.04	ST4-74	3954413	3955036	+
<i>rpoZ</i>	175	184	0.95	ST4-74	3955091	3955366	+
<i>spoT</i>	41	46	0.89	ST4-74	3955385	3957496	+
<i>spoU</i>	29	29	1.00	ST4-74	3957501	3958190	+
<i>recG</i>	12	13	0.94	ST4-74	3958196	3960277	+
STM3745	24	30	0.79	ST4-74	3960280	3961131	-
<i>gltS</i>	28	35	0.79	ST4-74	3961134	3962339	-
<i>yicE</i>	35	51	0.68	ST4-74	3962567	3963958	+
<i>yicH</i>	40	44	0.93	ST4-74	3964079	3965788	+
<i>yicI</i>	3	2	1.31	ST4-74	3965891	3968209	-
<i>yicJ</i>	4	4	1.16	ST4-74	3968221	3969603	-
STM3752	23	16	1.42	ST4-74	3970302	3970670	-
<i>sugR</i>	20	20	0.98	ST4-74	3971324	3972861	+
<i>rhuM</i>	14	14	1.01	ST4-74	3973048	3974085	+

<i>Name</i>	Δ <i>fnr</i> TPM	WT TPM	Δ <i>fnr</i> /WT	Chr ^a	Start	End	Strand
<i>rmbA</i>	1	2	0.85	ST4-74	3975384	3976001	+
<i>misL</i>	6	5	1.35	ST4-74	3976076	3978943	+
<i>fidL</i>	16	12	1.28	ST4-74	3979038	3979520	-
<i>marT</i>	8	5	1.47	ST4-74	3979513	3980301	-
<i>slsA</i>	15	13	1.09	ST4-74	3981154	3981834	+
<i>cigR</i>	59	80	0.74	ST4-74	3982063	3982542	-
<i>mgtR</i>	14	15	0.92	ST4-74	3982743	3982835	-
<i>mgtB</i>	10	9	1.09	ST4-74	3982857	3985583	-
<i>AmgR</i>	6	4	1.66	ST4-74	3985659	3986858	+
<i>mgtC</i>	20	12	1.69	ST4-74	3985803	3986498	-
<i>yicL</i>	19	16	1.15	ST4-74	3987007	3987909	+
STM3766	10	9	1.14	ST4-74	3987952	3988893	-
STM3767	6	7	0.83	ST4-74	3989129	3989872	-
STM3768	3	3	0.91	ST4-74	3989859	3990968	-
STM3769	2	3	0.83	ST4-74	3990972	3991829	-
STM3770	4	4	0.97	ST4-74	3991829	3992578	-
STM3771	1	1	1.21	ST4-74	3992724	3993209	-
STM3772	1	1	1.04	ST4-74	3993220	3993645	-
STnc4040	91	62	1.46	ST4-74	3993821	3993944	-
STM3773	19	18	1.06	ST4-74	3993864	3996662	-
STM3774	33	23	1.45	ST4-74	3996859	3997152	+
STM3775	13	9	1.41	ST4-74	3997258	3998640	+
<i>nepI</i>	8	6	1.34	ST4-74	3998700	3999892	-
STM3777	30	26	1.15	ST4-74	4000108	4000467	+
STM3778	13	13	0.97	ST4-74	4000451	4000774	+
STM3779	23	18	1.32	ST4-74	4000865	4001134	-
STM3780	3	3	0.78	ST4-74	4001144	4002004	-
STM3781	6	6	0.97	ST4-74	4002067	4003551	-
STM3782	8	10	0.88	ST4-74	4003544	4004902	-
STM3783	14	16	0.87	ST4-74	4004978	4005265	-
STM3784	27	28	0.98	ST4-74	4005262	4005735	-
STM3785	46	34	1.35	ST4-74	4005753	4006496	-
<i>yicN</i>	36	34	1.05	ST4-74	4006849	4007301	-
<i>uhpT</i>	4	4	1.00	ST4-74	4007493	4008884	-
<i>uhpC</i>	6	6	1.04	ST4-74	4009027	4010355	-
<i>uhpB</i>	7	7	0.92	ST4-74	4010365	4011867	-
<i>uhpA</i>	20	15	1.36	ST4-74	4011867	4012457	-
STM3791	5	7	0.79	ST4-74	4012532	4013545	-
STM3792	4	8	0.50	ST4-74	4013557	4014873	-
STM3793	7	13	0.56	ST4-74	4014904	4015824	-
STM3794	9	9	0.94	ST4-74	4016149	4016934	+
<i>ilvN</i>	15	17	0.90	ST4-74	4016936	4017226	-
<i>ilvB</i>	13	13	0.95	ST4-74	4017230	4018918	-
<i>ivbL</i>	4003	3906	1.02	ST4-74	4019025	4019123	-
<i>IstR-1,2</i>	74	82	0.90	ST4-74	4019328	4019459	-
STM3796A	7	7	0.96	ST4-74	4020012	4020800	+
<i>emrD</i>	3	3	1.22	ST4-74	4021003	4022187	+
STM3799	19	16	1.21	ST4-74	4022114	4023199	-
<i>dsdC</i>	10	11	0.98	ST4-74	4023263	4024186	-
<i>dsdX</i>	6	5	1.12	ST4-74	4024412	4025749	+
<i>dsdA</i>	7	7	1.08	ST4-74	4025767	4027089	+

<i>Name</i>	Δfnr TPM	WT TPM	$\Delta fnr/WT$	<i>Chr</i> ^a	<i>Start</i>	<i>End</i>	<i>Strand</i>
<i>yidF</i>	26	34	0.78	ST4-74	4027171	4027701	-
<i>yidG</i>	70	70	1.00	ST4-74	4027698	4028060	-
<i>yidH</i>	50	34	1.48	ST4-74	4028050	4028397	-
<i>yidE</i>	35	32	1.09	ST4-74	4028841	4030502	-
STnc2110	12	16	0.76	ST4-74	4030645	4030701	-
<i>hslS</i>	46	49	0.94	ST4-74	4030692	4031126	-
<i>hslT</i>	103	94	1.10	ST4-74	4031230	4031649	-
<i>yidQ</i>	119	102	1.17	ST4-74	4031950	4032285	+
<i>yidR</i>	16	18	0.86	ST4-74	4032287	4033513	-
<i>ccmH1</i>	4	10	0.41	ST4-74	4033635	4034678	-
<i>ccmG1</i>	8	13	0.58	ST4-74	4034675	4035232	-
<i>ccmF1</i>	7	14	0.49	ST4-74	4035229	4037160	-
<i>ccmE1</i>	6	14	0.46	ST4-74	4037157	4037636	-
<i>ccmD1</i>	4	8	0.46	ST4-74	4037633	4037845	-
<i>ccmC1</i>	11	29	0.37	ST4-74	4037842	4038579	-
<i>ccmB1</i>	5	10	0.51	ST4-74	4038631	4039287	-
<i>ccmA1</i>	5	15	0.31	ST4-74	4039287	4039913	-
<i>yhjA</i>	22	47	0.47	ST4-74	4039910	4041310	-
<i>torD</i>	39	35	1.10	ST4-74	4041500	4042132	-
<i>torA</i>	31	34	0.91	ST4-74	4042125	4044677	-
<i>torC</i>	123	108	1.14	ST4-74	4044667	4045851	-
<i>torR</i>	39	48	0.81	ST4-74	4045981	4046673	+
<i>torT</i>	24	27	0.89	ST4-74	4046646	4047686	-
<i>torS</i>	6	6	0.93	ST4-74	4047766	4050501	+
<i>dgoT</i>	4	4	1.13	ST4-74	4050527	4051864	-
<i>dgoD</i>	3	2	1.46	ST4-74	4051949	4053097	-
<i>dgoA</i>	2	2	0.83	ST4-74	4053094	4053711	-
<i>dgoK</i>	12	13	0.94	ST4-74	4053695	4054573	-
<i>dgoR</i>	8	9	0.90	ST4-74	4054570	4055259	-
<i>yidA</i>	21	22	0.95	ST4-74	4055520	4056365	-
STM3832	3	3	1.18	ST4-74	4056671	4057933	+
STM3833	8	8	0.99	ST4-74	4057947	4059140	+
STM3834	31	27	1.16	ST4-74	4059255	4060151	+
<i>gyrB</i>	27	29	0.92	ST4-74	4060170	4062584	-
<i>recF</i>	43	35	1.22	ST4-74	4062613	4063686	-
<i>dnaN</i>	19	25	0.76	ST4-74	4063834	4064934	-
<i>dnaA</i>	55	62	0.90	ST4-74	4064939	4066339	-
<i>rpmH</i>	3994	3735	1.07	ST4-74	4067000	4067140	+
<i>rnpA</i>	66	82	0.81	ST4-74	4067157	4067516	+
STM3841	55	61	0.90	ST4-74	4067480	4067737	+
<i>yidC</i>	46	62	0.74	ST4-74	4067740	4069386	+
STnc4250	118	138	0.86	ST4-74	4069296	4069428	+
<i>thdF</i>	6	6	1.05	ST4-74	4069516	4070892	+
STnc3170	182	100	1.83	ST4-74	4070922	4071037	-
<i>intA</i>	8	7	1.25	ST4-74	4071148	4072365	+
STnc400	18109	36392	0.50	ST4-74	4072456	4072529	+
STM3845	83	76	1.08	ST4-74	4072690	4073652	+
STM3846	37	40	0.94	ST4-74	4073652	4074587	+
<i>yidY</i>	7	6	1.21	ST4-74	4075389	4076576	+
<i>yidZ</i>	8	5	1.55	ST4-74	4076545	4077504	+
<i>yieE</i>	35	30	1.18	ST4-74	4077662	4078417	+

<i>Name</i>	Δfnr TPM	WT TPM	$\Delta fnr/WT$	Chr ^a	Start	End	Strand
<i>yieF</i>	76	49	1.54	ST4-74	4078417	4079001	+
<i>yieG</i>	31	38	0.80	ST4-74	4079046	4080383	-
<i>yieH</i>	59	62	0.96	ST4-74	4080552	4081217	+
STnc1860	137	187	0.73	ST4-74	4081218	4081302	-
<i>phoU</i>	14	13	1.07	ST4-74	4081312	4082037	-
<i>pstB</i>	17	20	0.84	ST4-74	4082052	4082825	-
<i>pstA</i>	14	12	1.20	ST4-74	4082912	4083802	-
<i>pstC</i>	15	14	1.06	ST4-74	4083802	4084761	-
<i>pstS</i>	20	20	0.99	ST4-74	4084897	4085937	-
STM3858	7	7	1.02	ST4-74	4086104	4087477	-
STM3859	2	2	0.82	ST4-74	4087526	4088344	-
STM3860	6	7	0.88	ST4-74	4088439	4090196	+
<i>glmS</i>	43	56	0.77	ST4-74	4090347	4092176	-
<i>glmU</i>	119	124	0.96	ST4-74	4092365	4093735	-
STM3863	22	16	1.34	ST4-74	4094055	4094753	-
<i>atpC</i>	126	208	0.61	ST4-74	4094983	4095402	-
<i>atpD</i>	69	111	0.62	ST4-74	4095423	4096805	-
<i>atpG</i>	81	139	0.58	ST4-74	4096832	4097695	-
<i>atpA</i>	86	138	0.63	ST4-74	4097746	4099287	-
<i>atpH</i>	125	194	0.64	ST4-74	4099300	4099833	-
<i>atpF</i>	267	417	0.64	ST4-74	4099848	4100318	-
<i>atpE</i>	398	640	0.62	ST4-74	4100378	4100617	-
<i>atpB</i>	160	218	0.74	ST4-74	4100664	4101479	-
<i>atpI</i>	333	374	0.89	ST4-74	4101488	4101868	-
<i>gidB</i>	19	20	0.95	ST4-74	4102484	4103113	-
<i>gidA</i>	24	26	0.92	ST4-74	4103210	4105099	-
<i>mioC</i>	114	115	0.99	ST4-74	4105478	4105921	-
<i>asnCb</i>	23	20	1.14	ST4-74	4106011	4106469	-
<i>asnA</i>	67	78	0.86	ST4-74	4106620	4107612	+
<i>yieM</i>	8	10	0.83	ST4-74	4107617	4109017	-
<i>yieN</i>	25	23	1.09	ST4-74	4109062	4110558	-
<i>kup</i>	19	21	0.89	ST4-74	4110906	4112774	+
<i>rbsD</i>	34	40	0.85	ST4-74	4112971	4113390	+
<i>rbsA</i>	4	5	0.86	ST4-74	4113398	4114903	+
<i>rbsC</i>	12	14	0.86	ST4-74	4114909	4115874	+
<i>rbsB</i>	337	283	1.19	ST4-74	4115899	4116789	+
<i>rbsK</i>	15	21	0.72	ST4-74	4116923	4117852	+
<i>rbsR</i>	11	17	0.70	ST4-74	4117856	4118854	+
<i>yieO</i>	11	9	1.21	ST4-74	4118820	4120243	-
<i>yieP</i>	16	18	0.93	ST4-74	4120255	4120959	-
<i>yifA</i>	24	27	0.88	ST4-74	4127091	4127939	-
<i>yifE</i>	826	598	1.38	ST4-74	4128046	4128384	+
<i>comM</i>	3	3	1.04	ST4-74	4128409	4129929	-
<i>ilvX</i>	237	232	1.02	ST4-74	4130466	4130516	+
<i>ilvG</i>	32	35	0.92	ST4-74	4130519	4132165	+
<i>ilvM</i>	63	66	0.95	ST4-74	4132165	4132425	+
<i>ilvE</i>	43	47	0.90	ST4-74	4132443	4133372	+
<i>ilvD</i>	28	33	0.84	ST4-74	4133533	4135383	+
<i>ilvA</i>	65	78	0.83	ST4-74	4135386	4136930	+
STM3906	51	48	1.06	ST4-74	4137214	4137531	+
STM3907	48	41	1.16	ST4-74	4137528	4137869	+

<i>Name</i>	Δfnr TPM	WT TPM	$\Delta fnr/WT$	<i>Chr</i> ^a	<i>Start</i>	<i>End</i>	<i>Strand</i>
<i>ilvY</i>	6	7	0.80	ST4-74	4137872	4138759	-
<i>ilvC</i>	200	239	0.84	ST4-74	4138923	4140398	+
<i>ppiC</i>	198	193	1.03	ST4-74	4140490	4140771	-
SL1344_3870A	20	22	0.91	ST4-74	4140776	4141081	+
SL1344_3871	17	17	0.99	ST4-74	4141099	4141209	+
<i>rep</i>	15	13	1.21	ST4-74	4141309	4143333	+
<i>gppA</i>	17	23	0.77	ST4-74	4143373	4144854	-
<i>rhlB</i>	55	63	0.87	ST4-74	4144973	4146238	-
<i>trxA</i>	589	654	0.90	ST4-74	4146382	4146711	+
<i>rho</i>	134	122	1.10	ST4-74	4147130	4148389	+
<i>rfe</i>	79	77	1.02	ST4-74	4148619	4149722	+
<i>wzzE</i>	91	83	1.11	ST4-74	4149734	4150780	+
<i>rffE</i>	26	28	0.93	ST4-74	4150836	4151966	+
<i>rffD</i>	24	27	0.88	ST4-74	4151963	4153225	+
<i>rffG</i>	18	18	0.99	ST4-74	4153240	4154292	+
<i>rffH</i>	21	23	0.92	ST4-74	4154325	4154549	+
<i>rffC</i>	15	16	0.91	ST4-74	4154656	4155204	+
<i>rffA</i>	17	18	0.96	ST4-74	4155209	4156339	+
<i>wzxE</i>	13	14	0.94	ST4-74	4156341	4157591	+
STM3927	9	9	0.94	ST4-74	4157588	4158667	+
<i>rffT</i>	17	18	0.95	ST4-74	4158664	4160022	+
<i>rffM</i>	11	12	0.88	ST4-74	4160019	4160759	+
<i>yifK</i>	48	32	1.51	ST4-74	4160966	4162351	+
<i>GlmZ</i>	3736	3416	1.09	ST4-74	4163192	4163399	+
<i>hemY</i>	34	38	0.90	ST4-74	4163468	4164607	-
<i>hemX</i>	31	35	0.88	ST4-74	4164667	4165836	-
<i>hemD</i>	27	37	0.72	ST4-74	4165858	4166598	-
<i>hemC</i>	73	74	0.99	ST4-74	4166595	4167551	-
<i>cyaA</i>	51	45	1.14	ST4-74	4167913	4170459	+
STM3940	12	9	1.24	ST4-74	4170567	4170920	+
STM3941	5	3	1.82	ST4-74	4171106	4171648	+
STM3942	4	5	0.96	ST4-74	4171660	4172022	+
<i>cyaY</i>	56	76	0.73	ST4-74	4172093	4172413	-
STM3944	3	2	1.26	ST4-74	4172483	4172872	-
STM3945	3	3	1.01	ST4-74	4172860	4173382	-
<i>yifL</i>	52	62	0.84	ST4-74	4173568	4173771	+
<i>dapF</i>	29	35	0.82	ST4-74	4173805	4174632	+
<i>yigA</i>	15	20	0.76	ST4-74	4174629	4175336	+
<i>xerC</i>	12	16	0.70	ST4-74	4175333	4176235	+
<i>yigB</i>	10	12	0.82	ST4-74	4176235	4176951	+
<i>uvrD</i>	18	18	0.98	ST4-74	4177087	4179249	+
<i>corA</i>	21	22	0.98	ST4-74	4179721	4180671	+
<i>yigF</i>	7	4	1.85	ST4-74	4180720	4181100	-
<i>yigG</i>	5	4	1.31	ST4-74	4181116	4181574	-
<i>rarD</i>	23	21	1.11	ST4-74	4181609	4182493	-
<i>yigI</i>	9	6	1.33	ST4-74	4182537	4183022	-
<i>pldA</i>	73	41	1.81	ST4-74	4183292	4184038	+
<i>recQ</i>	28	26	1.09	ST4-74	4184104	4185951	+
<i>rhtC</i>	15	16	0.94	ST4-74	4186015	4186635	+
<i>rhtB</i>	9	10	0.86	ST4-74	4186675	4187295	-
<i>pldB</i>	39	38	1.03	ST4-74	4187406	4188422	+

<i>Name</i>	Δ <i>fnr</i> TPM	WT TPM	Δ <i>fnr</i> /WT	Chr ^a	Start	End	Strand
<i>yigL</i>	20	16	1.21	ST4-74	4188438	4189238	+
<i>yigM</i>	62	64	0.98	ST4-74	4189319	4190218	+
<i>metR</i>	33	38	0.86	ST4-74	4190106	4191059	-
<i>metE</i>	91	115	0.79	ST4-74	4191308	4193572	+
STM3966	5	5	0.94	ST4-74	4193916	4195259	+
<i>dlhH</i>	43	39	1.11	ST4-74	4195339	4196151	-
<i>udp</i>	31	31	1.02	ST4-74	4196410	4197171	+
<i>yigN</i>	14	15	0.93	ST4-74	4197311	4198741	+
<i>ubiE</i>	100	86	1.17	ST4-74	4198837	4199592	+
<i>yigP</i>	34	34	1.00	ST4-74	4199602	4200207	+
<i>aarF</i>	59	54	1.10	ST4-74	4200204	4201844	+
<i>tatA</i>	614	636	0.97	ST4-74	4202050	4202304	+
<i>tatB</i>	109	137	0.80	ST4-74	4202308	4202856	+
<i>tatC</i>	69	77	0.90	ST4-74	4202859	4203638	+
<i>tatD</i>	6	6	0.91	ST4-74	4203668	4204462	+
<i>rfaH</i>	82	72	1.14	ST4-74	4204470	4204958	-
<i>yigC</i>	59	56	1.05	ST4-74	4205144	4206622	+
<i>fre</i>	54	44	1.24	ST4-74	4206708	4207409	+
STM3980	19	14	1.34	ST4-74	4207663	4209486	+
STnc790	44	33	1.32	ST4-74	4209485	4209680	-
<i>fadA</i>	7	7	1.12	ST4-74	4209683	4210846	-
<i>fadB</i>	5	4	1.33	ST4-74	4210856	4213045	-
<i>pepQ</i>	35	36	0.98	ST4-74	4213235	4214566	+
<i>yigZ</i>	34	33	1.05	ST4-74	4214566	4215180	+
<i>trkH</i>	26	26	0.97	ST4-74	4215219	4216670	+
<i>hemG</i>	21	22	0.94	ST4-74	4216682	4217227	+
<i>mobB</i>	19	18	1.09	ST4-74	4223123	4223638	-
<i>mobA</i>	41	34	1.21	ST4-74	4223635	4224219	-
<i>yihD</i>	171	197	0.87	ST4-74	4224289	4224558	+
<i>rodA</i>	99	101	0.98	ST4-74	4224635	4225621	+
<i>dsbA</i>	110	116	0.94	ST4-74	4225638	4226261	+
<i>yihG</i>	22	18	1.23	ST4-74	4226274	4227182	-
<i>polA</i>	20	21	0.94	ST4-74	4227570	4230356	+
<i>Spf</i>	1745	983	1.77	ST4-74	4230504	4230613	+
<i>engB</i>	60	59	1.01	ST4-74	4230691	4231290	-
<i>CsrC</i>	56981	31195	1.83	ST4-74	4231595	4231838	+
<i>yihI</i>	98	79	1.23	ST4-74	4231906	4232421	+
<i>hemN</i>	18	18	1.05	ST4-74	4232610	4233983	+
<i>yshB</i>	737	991	0.74	ST4-74	4234073	4234183	-
<i>glnG</i>	6	6	1.03	ST4-74	4234296	4235705	-
<i>glnL</i>	9	8	1.02	ST4-74	4235714	4236763	-
STnc800	559	331	1.69	ST4-74	4236851	4237035	-
<i>glnA</i>	88	71	1.23	ST4-74	4237038	4238447	-
<i>typA</i>	61	61	1.01	ST4-74	4238823	4240646	+
STM4010	11	9	1.22	ST4-74	4240701	4241435	-
STM4011	6	5	1.18	ST4-74	4241420	4242298	-
STM4012	3	2	1.47	ST4-74	4242295	4243536	-
STM4013	10	6	1.77	ST4-74	4243538	4244401	-
STM4014	2	1	1.47	ST4-74	4244406	4245431	-
STM4015	4	4	0.85	ST4-74	4245444	4246292	-
<i>ompL</i>	2	2	1.00	ST4-74	4246449	4247141	-

<i>Name</i>	Δfnr TPM	WT TPM	$\Delta fnr/WT$	Chr ^a	Start	End	Strand
<i>yihO</i>	9	8	1.12	ST4-74	4247209	4248630	-
<i>yihP</i>	5	6	0.87	ST4-74	4248676	4250058	-
STnc3120	180	89	2.03	ST4-74	4249942	4250100	+
<i>yihQ</i>	4	4	1.19	ST4-74	4250104	4252140	-
<i>yihR</i>	2	1	1.40	ST4-74	4252184	4253035	-
<i>yihS</i>	1	1	1.08	ST4-74	4253045	4254286	-
<i>yihT</i>	1	1	1.25	ST4-74	4254302	4255180	-
<i>yihU</i>	1	1	2.07	ST4-74	4255203	4256099	-
<i>yihV</i>	4	4	0.91	ST4-74	4256258	4257160	+
<i>yihW</i>	23	24	0.94	ST4-74	4257194	4257997	+
<i>yihX</i>	68	58	1.16	ST4-74	4258188	4258787	+
<i>rbn</i>	58	48	1.23	ST4-74	4258781	4259653	+
<i>yihZ</i>	29	29	1.02	ST4-74	4259650	4260087	+
<i>yiiD</i>	21	19	1.13	ST4-74	4260084	4261073	+
STM4030	23	21	1.12	ST4-74	4261088	4261516	-
STM4031	65	55	1.19	ST4-74	4261531	4261842	-
STM4032	5	6	0.95	ST4-74	4261928	4262857	-
SL1344_3979	102	96	1.07	ST4-74	4263075	4263386	+
STM4033	33	27	1.20	ST4-74	4263387	4263677	+
<i>fdhE</i>	9	15	0.64	ST4-74	4263724	4264653	-
<i>fdoI</i>	36	36	1.00	ST4-74	4264650	4265285	-
<i>fdoH</i>	5	8	0.72	ST4-74	4265282	4266184	-
<i>fdoG</i>	15	20	0.74	ST4-74	4266197	4269247	-
<i>fdhD</i>	10	13	0.80	ST4-74	4269442	4270278	+
STM4039	13	11	1.18	ST4-74	4270546	4271523	-
<i>yiiG</i>	2	2	1.04	ST4-74	4271802	4272860	+
STM4041	14	15	0.93	ST4-74	4273215	4273538	-
STM4042	22	33	0.66	ST4-74	4273538	4274197	-
STM4042A	40	38	1.05	ST4-74	4274280	4274846	+
<i>yiiL</i>	16	18	0.89	ST4-74	4274935	4275249	-
STM4044	5	5	1.02	ST4-74	4275246	4276394	-
<i>rhaD</i>	6	4	1.50	ST4-74	4276521	4277348	-
<i>rhaA</i>	1	1	1.06	ST4-74	4277491	4278750	-
<i>rhaB</i>	1	1	1.23	ST4-74	4278747	4280216	-
<i>rhaS</i>	9	10	0.86	ST4-74	4280504	4281340	+
<i>rhaR</i>	12	13	0.91	ST4-74	4281493	4282341	+
<i>rhaT</i>	4	5	0.99	ST4-74	4282338	4283372	-
STM4051	4	3	1.11	ST4-74	4283991	4284674	+
STM4052	5	5	0.88	ST4-74	4284832	4286139	-
STM4053	2	3	0.79	ST4-74	4286132	4286647	-
STM4054	2	2	0.81	ST4-74	4286666	4287649	-
<i>sodA</i>	103	65	1.58	ST4-74	4287978	4288598	+
<i>yiiM</i>	11	16	0.66	ST4-74	4288668	4289357	+
STM4057	18	26	0.68	ST4-74	4289369	4289764	+
<i>cpxA</i>	23	35	0.67	ST4-74	4289815	4291188	-
<i>cpxR</i>	46	58	0.80	ST4-74	4291185	4291883	-
<i>cpxP</i>	2655	2314	1.15	ST4-74	4292034	4292534	+
STnc870	8576	11967	0.72	ST4-74	4292540	4292597	+
<i>fieF</i>	87	64	1.37	ST4-74	4292682	4293584	+
<i>pfkA</i>	49	72	0.68	ST4-74	4293769	4294731	+
<i>sbp</i>	62	113	0.55	ST4-74	4294935	4295924	+

<i>Name</i>	Δfnr TPM	WT TPM	$\Delta fnr/WT$	Chr ^a	Start	End	Strand
<i>cdh-a</i>	159	130	1.23	ST4-74	4296025	4296780	+
STM4065	7	8	0.90	ST4-74	4297043	4298377	+
STM4066	5	5	1.02	ST4-74	4298388	4299347	+
STM4067	46	43	1.07	ST4-74	4299357	4300397	+
STM4068	30	35	0.88	ST4-74	4300460	4301182	+
STM4069	26	17	1.49	ST4-74	4301280	4301444	+
<i>cdh-b</i>	7	5	1.25	ST4-74	4301460	4301591	+
STM4071	12	16	0.75	ST4-74	4301681	4301947	-
<i>ydeV</i>	15	12	1.24	ST4-74	4302045	4303637	-
<i>ydeW</i>	22	20	1.10	ST4-74	4303725	4304684	-
<i>ego</i>	12	15	0.79	ST4-74	4304940	4306475	+
<i>ydeY</i>	11	14	0.79	ST4-74	4306469	4307512	+
<i>ydeZ</i>	16	19	0.87	ST4-74	4307509	4308510	+
<i>yneA</i>	11	18	0.63	ST4-74	4308539	4309561	+
<i>yneB</i>	26	29	0.90	ST4-74	4309590	4310465	+
<i>yneC</i>	26	28	0.91	ST4-74	4310545	4310838	+
STM4080	30	30	1.00	ST4-74	4310848	4311612	+
<i>tpiA</i>	117	169	0.69	ST4-74	4311704	4312471	-
<i>yiiQ</i>	48	38	1.26	ST4-74	4312584	4313180	-
<i>yiiR</i>	35	25	1.37	ST4-74	4313281	4313709	+
<i>fpr</i>	17	18	0.95	ST4-74	4313816	4314562	-
<i>glpX</i>	11	24	0.44	ST4-74	4314659	4315669	-
<i>glpK</i>	161	287	0.56	ST4-74	4315781	4317289	-
<i>glpF</i>	226	417	0.54	ST4-74	4317310	4318155	-
<i>yiiU</i>	1019	918	1.11	ST4-74	4318554	4318793	+
<i>menG</i>	261	319	0.82	ST4-74	4319015	4319500	-
<i>menA</i>	18	17	1.06	ST4-74	4319593	4320522	-
<i>hslU</i>	122	69	1.77	ST4-74	4320589	4321920	-
<i>hslV</i>	53	63	0.84	ST4-74	4321930	4322460	-
<i>fisN</i>	79	77	1.04	ST4-74	4322552	4323526	-
<i>cytR</i>	18	24	0.74	ST4-74	4323620	4324645	-
<i>priA</i>	18	18	1.01	ST4-74	4324800	4326998	-
<i>rpmE</i>	221	329	0.67	ST4-74	4327202	4327414	+
STM4097	6	6	1.07	ST4-74	4327460	4328122	-
<i>IsrP</i>	55	33	1.66	ST4-74	4328157	4328304	+
STM4098	5	3	1.36	ST4-74	4328323	4330113	-
<i>metJ</i>	220	194	1.13	ST4-74	4330570	4330887	-
<i>metB</i>	59	71	0.83	ST4-74	4331152	4332312	+
<i>metL</i>	30	40	0.73	ST4-74	4332315	4334747	+
STnc4070	42	41	1.01	ST4-74	4334757	4334855	-
STM4102	2	3	0.83	ST4-74	4335001	4335720	-
SL1344_4052	2	2	1.24	ST4-74	4335723	4336721	-
STM4103	10	13	0.80	ST4-74	4336956	4338080	-
STM4104	7	6	1.16	ST4-74	4338216	4339772	+
STnc4080	45	33	1.39	ST4-74	4339805	4339929	-
<i>metF</i>	268	273	0.98	ST4-74	4339967	4340857	+
<i>katG</i>	24	33	0.71	ST4-74	4341022	4343202	+
<i>yijF</i>	12	10	1.17	ST4-74	4343260	4343883	-
<i>gldA</i>	11	28	0.40	ST4-74	4344142	4345245	-
<i>talC</i>	14	23	0.61	ST4-74	4345257	4345919	-
<i>ptsA</i>	6	6	1.03	ST4-74	4345930	4348431	-

<i>Name</i>	Δ <i>fnr</i> TPM	WT TPM	Δ <i>fnr</i> /WT	Chr ^a	Start	End	Strand
<i>frwC</i>	13	9	1.40	ST4-74	4348740	4349819	+
<i>frwB</i>	37	25	1.49	ST4-74	4349834	4350154	+
<i>pflD</i>	15	10	1.52	ST4-74	4350253	4352550	+
<i>pflC</i>	25	18	1.42	ST4-74	4352516	4353394	+
<i>frwD</i>	12	8	1.46	ST4-74	4353396	4353749	+
<i>yijO</i>	38	36	1.07	ST4-74	4353736	4354587	-
<i>yijP</i>	48	52	0.91	ST4-74	4354748	4356481	-
STnc1600	285	256	1.12	ST4-74	4356616	4356686	+
<i>ppc</i>	35	49	0.71	ST4-74	4356692	4359343	-
<i>argE</i>	30	45	0.67	ST4-74	4359712	4360863	-
<i>argC</i>	119	184	0.65	ST4-74	4360952	4361956	+
<i>argB</i>	39	77	0.51	ST4-74	4361964	4362740	+
<i>argH</i>	50	89	0.56	ST4-74	4362858	4364234	+
<i>OxyS</i>	27	42	0.63	ST4-74	4364305	4364423	-
<i>oxyR</i>	25	35	0.71	ST4-74	4364519	4365436	+
<i>udhA</i>	24	24	0.98	ST4-74	4365419	4366819	-
<i>yijC</i>	74	79	0.94	ST4-74	4367018	4367653	+
<i>yijD</i>	41	46	0.89	ST4-74	4367669	4368028	+
<i>trmA</i>	18	16	1.11	ST4-74	4368075	4369175	-
<i>btuB</i>	19	23	0.84	ST4-74	4369507	4371393	+
<i>murI</i>	20	22	0.93	ST4-74	4371338	4372189	+
<i>murB</i>	24	20	1.20	ST4-74	4378004	4379032	+
<i>birA</i>	19	19	1.01	ST4-74	4379029	4379991	+
<i>coaA</i>	39	38	1.04	ST4-74	4380026	4380976	-
STM4141	18	11	1.69	ST4-74	4381185	4381358	-
<i>tufB</i>	545	788	0.69	ST4-74	4381935	4383119	+
<i>secE</i>	165	185	0.89	ST4-74	4383349	4383732	+
<i>nusG</i>	72	91	0.80	ST4-74	4383734	4384279	+
<i>rplK</i>	404	406	0.99	ST4-74	4384437	4384865	+
<i>rplA</i>	192	252	0.76	ST4-74	4384869	4385573	+
<i>rplJ</i>	580	731	0.79	ST4-74	4385993	4386490	+
<i>rplL</i>	690	935	0.74	ST4-74	4386557	4386922	+
<i>rpoB</i>	51	72	0.71	ST4-74	4387240	4391268	+
<i>rpoC</i>	53	76	0.69	ST4-74	4391345	4395568	+
STnc3490	21	15	1.40	ST4-74	4395603	4395691	-
STM4155	9	6	1.46	ST4-74	4395610	4395933	+
STM4156	6	5	1.13	ST4-74	4395939	4396283	-
<i>sseK1</i>	59	40	1.48	ST4-74	4396682	4397692	+
STM4158	186	136	1.37	ST4-74	4398015	4398203	+
<i>thiH</i>	32	37	0.85	ST4-74	4398354	4399487	-
<i>thiG</i>	21	27	0.80	ST4-74	4399484	4400254	-
<i>thiS</i>	30	39	0.77	ST4-74	4400256	4400456	-
<i>thiF</i>	23	30	0.76	ST4-74	4400437	4401195	-
<i>thiE</i>	19	23	0.81	ST4-74	4401188	4401823	-
<i>thiC</i>	29	34	0.85	ST4-74	4401823	4403718	-
STnc1460	5179	6313	0.82	ST4-74	4403810	4404049	-
<i>rsd</i>	38	26	1.47	ST4-74	4404082	4404570	-
<i>nudC</i>	13	9	1.33	ST4-74	4404663	4405436	+
<i>hemE</i>	26	20	1.28	ST4-74	4405477	4406541	+
<i>nfi</i>	23	19	1.23	ST4-74	4406551	4407222	+
<i>yjaG</i>	65	66	0.99	ST4-74	4407264	4407854	+

<i>Name</i>	Δ <i>fnr</i> TPM	WT TPM	Δ <i>fnr</i> /WT	Chr ^a	Start	End	Strand
<i>hupA</i>	1467	2155	0.68	ST4-74	4408041	4408313	+
<i>yjaH</i>	17	22	0.75	ST4-74	4408325	4409017	+
<i>zraP</i>	6	7	0.93	ST4-74	4409059	4409514	-
<i>hydH</i>	14	15	0.90	ST4-74	4409768	4411165	+
<i>hydG</i>	11	12	0.95	ST4-74	4411171	4412496	+
<i>purD</i>	10	19	0.52	ST4-74	4412493	4413782	-
<i>purH</i>	16	27	0.61	ST4-74	4413794	4415383	-
<i>yjaB</i>	54	48	1.12	ST4-74	4421537	4421974	-
<i>metA</i>	115	104	1.11	ST4-74	4422131	4423060	+
<i>aceB</i>	5	4	1.15	ST4-74	4423329	4424930	+
<i>aceA</i>	6	5	1.19	ST4-74	4424962	4426266	+
<i>aceK</i>	10	8	1.29	ST4-74	4426368	4428119	+
STM4186	7	7	1.03	ST4-74	4428083	4428517	-
<i>iclR</i>	12	16	0.76	ST4-74	4428501	4429325	-
<i>metH</i>	25	25	1.03	ST4-74	4429629	4433312	+
<i>yjbB</i>	17	17	1.04	ST4-74	4433654	4435210	+
<i>pepE</i>	9	32	0.28	ST4-74	4435286	4435975	-
STM4191	30	24	1.27	ST4-74	4436047	4436148	+
STM4192	74	66	1.13	ST4-74	4436183	4436722	+
<i>yjbC</i>	25	26	0.96	ST4-74	4436769	4437638	+
<i>yjbD</i>	39	44	0.88	ST4-74	4437635	4437907	-
STM4195	16	27	0.60	ST4-74	4438005	4438946	-
STM4196	7	10	0.75	ST4-74	4439208	4439936	-
STM4197	2	3	0.82	ST4-74	4440133	4440423	-
STM4198	5	5	1.02	ST4-74	4440672	4441127	-
STM4199	4	4	0.83	ST4-74	4441124	4441729	-
STM4200	7	7	1.02	ST4-74	4441734	4443479	-
STM4201	1	1	1.06	ST4-74	4443482	4444114	-
STM4202	1	7	0.21	ST4-74	4444107	4445222	-
STM4203	1	0	3.26	ST4-74	4445213	4445572	-
STM4204	11	10	1.08	ST4-74	4445736	4447283	-
<i>gtrBb</i>	9	8	1.08	ST4-74	4447283	4448212	-
<i>gtrAb</i>	53	42	1.25	ST4-74	4448209	4448535	-
STnc4100	97	66	1.47	ST4-74	4448720	4448837	+
STM4207	4	3	1.10	ST4-74	4448899	4449621	-
STM4208	2	1	2.01	ST4-74	4449631	4450674	-
STM4209	5	2	2.53	ST4-74	4450662	4450871	-
STM4210	3	2	1.66	ST4-74	4450871	4451824	-
STM4211	1	1	1.14	ST4-74	4451824	4454178	-
SL1344_4147	3	4	0.83	ST4-74	4454363	4454680	-
STM4212	2	1	1.16	ST4-74	4454732	4455256	-
STM4213	2	2	0.97	ST4-74	4455256	4456683	-
STM4214	1	1	0.63	ST4-74	4456673	4456870	-
STM4215	1	1	1.24	ST4-74	4456867	4457322	-
STM4216	0	0	1.51	ST4-74	4457482	4457796	-
STM4217	1	1	0.64	ST4-74	4457809	4458414	-
STM4218	3	3	0.93	ST4-74	4458417	4458704	-
STM4219	47	43	1.10	ST4-74	4459280	4459627	+
<i>lysC</i>	85	186	0.46	ST4-74	4459760	4461109	-
<i>pgi</i>	52	52	1.00	ST4-74	4461454	4463103	+
<i>yjbE</i>	30	29	1.04	ST4-74	4463547	4463789	+

<i>Name</i>	Δfnr TPM	WT TPM	$\Delta fnr/WT$	<i>Chr</i> ^a	<i>Start</i>	<i>End</i>	<i>Strand</i>
<i>yjbF</i>	2	2	0.95	ST4-74	4463823	4464491	+
<i>yjbG</i>	1	1	1.28	ST4-74	4464488	4465225	+
<i>yjbH</i>	8	8	1.01	ST4-74	4465225	4467321	+
<i>yjbA</i>	169	91	1.87	ST4-74	4467464	4467874	+
STnc810	37	26	1.41	ST4-74	4467934	4467988	-
<i>malG</i>	3	3	1.06	ST4-74	4468040	4468930	-
<i>malF</i>	3	3	0.86	ST4-74	4468945	4470489	-
<i>malE</i>	3	3	0.83	ST4-74	4470621	4471820	-
<i>malK</i>	2	2	0.94	ST4-74	4472173	4473282	+
<i>lamB</i>	6	6	1.10	ST4-74	4473371	4474729	+
<i>malM</i>	8	7	1.13	ST4-74	4474893	4475810	+
STnc2130	96	105	0.91	ST4-74	4475777	4475867	+
<i>ubiC</i>	20	20	1.00	ST4-74	4475991	4476488	+
<i>ubiA</i>	16	17	0.92	ST4-74	4476502	4477374	+
<i>plsB</i>	30	34	0.88	ST4-74	4477473	4479893	-
<i>dgkA</i>	40	39	1.01	ST4-74	4480064	4480432	+
<i>lexA</i>	129	134	0.96	ST4-74	4480541	4481149	+
<i>dinF</i>	11	12	0.93	ST4-74	4481328	4482653	+
<i>yjbJ</i>	381	204	1.87	ST4-74	4482782	4482994	+
<i>zur</i>	34	29	1.15	ST4-74	4483093	4483608	-
STM4242	17	39	0.43	ST4-74	4483855	4485165	+
<i>yjbN</i>	41	37	1.11	ST4-74	4485253	4486251	+
<i>pspG</i>	24	25	0.96	ST4-74	4486464	4486661	+
STnc880	1381	2241	0.62	ST4-74	4486745	4486823	+
<i>qor</i>	22	19	1.18	ST4-74	4486836	4487819	-
<i>dnaB</i>	23	26	0.87	ST4-74	4487884	4489299	+
<i>alr-b</i>	13	14	0.90	ST4-74	4489331	4490410	+
<i>tyrB</i>	24	29	0.80	ST4-74	4490596	4491789	+
<i>aphA</i>	49	66	0.74	ST4-74	4491976	4492689	+
<i>yjbQ</i>	46	46	0.99	ST4-74	4492818	4493234	+
<i>yjbR</i>	19	17	1.12	ST4-74	4493237	4493593	+
STM4252	3	2	1.63	ST4-74	4493594	4493932	-
STM4253	1	1	1.21	ST4-74	4493919	4494374	-
<i>uvrA</i>	12	12	1.07	ST4-74	4494506	4497331	-
STM4255	8	11	0.76	ST4-74	4497296	4497412	+
<i>ssb</i>	93	85	1.09	ST4-74	4497579	4498109	+
<i>siiA</i>	20	12	1.60	ST4-74	4499150	4499782	+
<i>siiB</i>	13	9	1.48	ST4-74	4499779	4501167	+
<i>siiC</i>	12	9	1.45	ST4-74	4501157	4502476	+
<i>siiD</i>	12	8	1.51	ST4-74	4502473	4503750	+
<i>siiE</i>	10	8	1.17	ST4-74	4503767	4520446	+
<i>siiF</i>	11	8	1.48	ST4-74	4520486	4522552	+
<i>yjcB</i>	12	14	0.87	ST4-74	4522830	4523111	-
<i>yjcC</i>	10	8	1.31	ST4-74	4523674	4525275	+
<i>soxS</i>	21	30	0.71	ST4-74	4525263	4525586	-
<i>soxR</i>	12	12	1.00	ST4-74	4525673	4526131	+
<i>SraL</i>	1784	818	2.18	ST4-74	4526162	4526302	-
STM4267	70	45	1.58	ST4-74	4526424	4527092	+
<i>yjcD</i>	30	40	0.74	ST4-74	4527439	4528788	+
<i>yjcE</i>	16	16	0.99	ST4-74	4528938	4530584	+
STM4270	29	24	1.20	ST4-74	4530679	4531566	-

<i>Name</i>	Δfnr TPM	WT TPM	$\Delta fnr/WT$	Chr ^a	Start	End	Strand
STM4271	10	14	0.69	ST4-74	4531670	4532080	+
STM4272	7	7	1.02	ST4-74	4532073	4532762	+
<i>actP</i>	10	8	1.25	ST4-74	4532801	4534450	-
<i>yjcH</i>	5	5	1.12	ST4-74	4534447	4534761	-
<i>acs</i>	17	17	1.06	ST4-74	4535007	4536965	-
STM4276	89	88	1.01	ST4-74	4537152	4537298	+
<i>nrfA</i>	4	19	0.22	ST4-74	4537397	4538833	+
<i>nrfB</i>	6	11	0.51	ST4-74	4538945	4539511	+
<i>nrfC</i>	6	8	0.70	ST4-74	4539508	4540179	+
<i>nrfD</i>	3	5	0.67	ST4-74	4540176	4541132	+
<i>nrfE</i>	6	5	1.21	ST4-74	4541125	4543347	+
<i>nrfG</i>	1	2	0.54	ST4-74	4543344	4543964	+
<i>glpP</i>	37	39	0.97	ST4-74	4544309	4545619	+
<i>yjcO</i>	40	28	1.43	ST4-74	4545777	4546388	-
SC4B5.11c	7	19	0.39	ST4-74	4546643	4548790	-
<i>lpxO</i>	53	30	1.73	ST4-74	4549145	4550053	-
<i>phnO</i>	130	64	2.03	ST4-74	4550311	4550745	-
<i>phnB</i>	20	15	1.31	ST4-74	4550897	4551340	-
<i>phnA</i>	56	91	0.61	ST4-74	4551460	4551795	-
<i>proP</i>	55	41	1.33	ST4-74	4552263	4553765	+
STnc630	2260	1641	1.38	ST4-74	4553813	4553972	+
<i>basS</i>	33	42	0.77	ST4-74	4553932	4555002	-
<i>basR</i>	53	47	1.12	ST4-74	4555012	4555680	-
<i>yjdB</i>	60	69	0.87	ST4-74	4555677	4557320	-
<i>adiC</i>	7	6	1.08	ST4-74	4557454	4558791	-
<i>adiY</i>	3	3	1.08	ST4-74	4558931	4559692	-
STnc1180	18	18	1.01	ST4-74	4559883	4559977	-
<i>adi</i>	4	3	1.20	ST4-74	4559990	4562260	-
STnc4110	29	24	1.22	ST4-74	4562397	4562461	+
<i>melR</i>	13	11	1.10	ST4-74	4562490	4563422	-
<i>melA</i>	3	3	1.22	ST4-74	4563691	4565046	+
<i>melB</i>	6	4	1.43	ST4-74	4565130	4566560	+
<i>fumB</i>	11	78	0.14	ST4-74	4566658	4568304	-
<i>dcuB</i>	15	104	0.15	ST4-74	4568400	4569740	-
STM4302	565	720	0.78	ST4-74	4569887	4570153	-
<i>dcuR</i>	24	42	0.58	ST4-74	4570470	4571189	-
<i>dcuS</i>	23	30	0.79	ST4-74	4571186	4572817	-
STM4305	8	62	0.13	ST4-74	4573173	4575602	+
STM4306	7	37	0.18	ST4-74	4575616	4576242	+
STM4307	8	39	0.20	ST4-74	4576235	4577008	+
STM4308	12	67	0.17	ST4-74	4577024	4577677	+
STM4309	2	3	0.80	ST4-74	4577761	4579161	-
STM4310	7	7	0.97	ST4-74	4579465	4580370	+
STnc440	16639	4653	3.58	ST4-74	4580485	4580565	+
STM4312	2	4	0.57	ST4-74	4580664	4580933	-
STM4313	16	17	0.95	ST4-74	4580941	4581156	-
<i>rtsB</i>	10	17	0.56	ST4-74	4581179	4581466	-
<i>rtsA</i>	29	50	0.58	ST4-74	4581463	4582338	-
STM4316	3	2	1.40	ST4-74	4582603	4582824	-
STM4317	52	57	0.91	ST4-74	4583141	4583434	+
STM4318	14	12	1.10	ST4-74	4583431	4583922	+

<i>Name</i>	Δ <i>fnr</i> TPM	WT TPM	Δ <i>fnr</i> /WT	<i>Chr</i> ^a	<i>Start</i>	<i>End</i>	<i>Strand</i>
<i>phoN</i>	187	101	1.84	ST4-74	4584170	4584922	-
SL1344_4256	2	0	-	ST4-74	4584965	4585099	-
SL1344_4257	4	4	1.01	ST4-74	4586132	4586509	-
STM4320	27	18	1.48	ST4-74	4586581	4586913	+
<i>yjdC</i>	106	65	1.64	ST4-74	4587352	4587927	-
<i>dipZ</i>	13	16	0.77	ST4-74	4587964	4589667	-
<i>cutA</i>	22	22	0.99	ST4-74	4589643	4589990	-
<i>dcuA</i>	36	59	0.60	ST4-74	4590111	4591295	-
STnc3000	9	5	2.02	ST4-74	4591418	4591505	+
<i>aspA</i>	160	225	0.71	ST4-74	4591527	4592963	-
<i>fxsA</i>	76	87	0.88	ST4-74	4593265	4593780	+
<i>yjeH</i>	104	63	1.66	ST4-74	4593839	4595080	-
<i>groES</i>	647	861	0.75	ST4-74	4595356	4595649	+
<i>groEL</i>	150	208	0.72	ST4-74	4595693	4597339	+
<i>yjeI</i>	281	327	0.86	ST4-74	4597565	4597936	+
<i>yjeJ</i>	24	18	1.29	ST4-74	4597984	4598841	-
<i>yjeK</i>	27	21	1.29	ST4-74	4599123	4600151	-
<i>efp</i>	200	223	0.90	ST4-74	4600192	4600758	+
<i>ecnA</i>	22	20	1.09	ST4-74	4600777	4600953	+
<i>ecnB</i>	7018	2863	2.45	ST4-74	4601061	4601207	+
<i>ecnR</i>	16	24	0.69	ST4-74	4601238	4601825	-
<i>sugE</i>	91	72	1.26	ST4-74	4602082	4602399	+
<i>blc</i>	45	23	1.97	ST4-74	4602416	4602949	-
<i>frdD</i>	129	270	0.48	ST4-74	4603061	4603420	-
<i>frdC</i>	40	116	0.35	ST4-74	4603431	4603826	-
<i>frdB</i>	50	147	0.34	ST4-74	4603837	4604571	-
<i>frdA</i>	44	130	0.34	ST4-74	4604564	4606354	-
<i>yjeA</i>	21	17	1.22	ST4-74	4606677	4607654	+
<i>yjeM</i>	6	7	0.96	ST4-74	4607880	4609382	+
<i>yjeO</i>	79	70	1.12	ST4-74	4609434	4609748	+
<i>yjeP</i>	17	19	0.86	ST4-74	4609815	4613117	-
<i>psd</i>	39	44	0.89	ST4-74	4613160	4614128	-
<i>yjeQ</i>	46	40	1.16	ST4-74	4614220	4615296	-
<i>orn</i>	57	57	1.00	ST4-74	4615379	4615924	+
STM4351	14	15	0.91	ST4-74	4615986	4616726	-
<i>yjeV</i>	14	14	1.00	ST4-74	4617775	4617828	+
<i>yjeS</i>	17	14	1.22	ST4-74	4617811	4618950	-
<i>yjeF</i>	21	19	1.16	ST4-74	4618949	4620496	+
<i>yjeE</i>	24	24	0.99	ST4-74	4620468	4620929	+
<i>amiB</i>	31	34	0.92	ST4-74	4620946	4622265	+
<i>mutL</i>	24	30	0.82	ST4-74	4622275	4624131	+
<i>miaA</i>	251	262	0.96	ST4-74	4624124	4625074	+
<i>hfq</i>	680	761	0.89	ST4-74	4625157	4625465	+
<i>hflX</i>	115	132	0.87	ST4-74	4625537	4626817	+
<i>hflK</i>	103	114	0.90	ST4-74	4627032	4628291	+
<i>hflC</i>	119	138	0.87	ST4-74	4628294	4629298	+
<i>purA</i>	230	251	0.91	ST4-74	4629677	4630975	+
<i>nsrR</i>	116	98	1.18	ST4-74	4631182	4631607	+
<i>rnr</i>	28	27	1.02	ST4-74	4631645	4634083	+
<i>yjffH</i>	29	38	0.77	ST4-74	4634174	4634905	+
<i>yjffI</i>	4	3	1.26	ST4-74	4635037	4635441	+

<i>Name</i>	Δ <i>fnr</i> TPM	WT TPM	Δ <i>fnr</i> /WT	Chr ^a	Start	End	Strand
<i>yjfJ</i>	6	5	1.06	ST4-74	4635456	4636154	+
STM4372	3	2	1.30	ST4-74	4636154	4637224	+
<i>yjfK</i>	3	3	1.25	ST4-74	4637197	4637880	+
<i>yjfL</i>	10	9	1.22	ST4-74	4637898	4638296	+
<i>yjfM</i>	4	5	0.94	ST4-74	4638306	4638944	+
<i>yjfC</i>	6	5	1.14	ST4-74	4638947	4640110	+
<i>aidB</i>	13	12	1.13	ST4-74	4640195	4641817	+
<i>yjfN</i>	79	63	1.25	ST4-74	4641862	4642182	-
<i>yjfO</i>	294	222	1.33	ST4-74	4642268	4642570	-
<i>yjfP</i>	13	15	0.81	ST4-74	4642781	4643530	+
<i>yjfQ</i>	20	23	0.86	ST4-74	4643527	4644282	-
<i>yjfR</i>	3	3	0.96	ST4-74	4644387	4645451	-
<i>sgaT</i>	4	3	1.27	ST4-74	4645814	4647211	+
<i>sgaB</i>	1	4	0.34	ST4-74	4647227	4647532	+
<i>ptxA</i>	2	2	0.97	ST4-74	4647542	4648006	+
<i>sgaH</i>	3	3	1.08	ST4-74	4648020	4648670	+
<i>sgaU</i>	4	3	1.28	ST4-74	4648680	4649534	+
<i>sgaE</i>	6	5	1.33	ST4-74	4649534	4650220	+
STnc4120	143	74	1.94	ST4-74	4650287	4650410	-
<i>yjfY</i>	56	30	1.83	ST4-74	4650349	4650624	-
STM4390	355	375	0.95	ST4-74	4650818	4651024	+
<i>rpsF</i>	199	289	0.69	ST4-74	4651095	4651490	+
<i>priB</i>	174	238	0.73	ST4-74	4651497	4651811	+
<i>rpsR</i>	177	262	0.67	ST4-74	4651816	4652043	+
<i>rplI</i>	168	229	0.74	ST4-74	4652085	4652534	+
<i>yifZ</i>	12	9	1.26	ST4-74	4652682	4653608	+
<i>ytfB</i>	62	47	1.33	ST4-74	4653658	4654293	-
<i>fkIB</i>	32	34	0.93	ST4-74	4654471	4655133	+
<i>cycA</i>	27	28	0.95	ST4-74	4655429	4656838	+
<i>ytfE</i>	6	5	1.29	ST4-74	4656950	4657612	-
<i>ytfF</i>	9	7	1.27	ST4-74	4657715	4658680	-
<i>ytfG</i>	3	2	1.33	ST4-74	4658761	4659609	-
<i>ytfH</i>	13	15	0.90	ST4-74	4659697	4660083	+
<i>cpdB</i>	7	10	0.74	ST4-74	4660141	4662084	-
<i>cysQ</i>	33	31	1.08	ST4-74	4662352	4663092	+
<i>ytfJ</i>	26	24	1.08	ST4-74	4663082	4663639	-
<i>ytfK</i>	2510	1102	2.28	ST4-74	4663966	4664172	+
<i>ytfL</i>	35	30	1.17	ST4-74	4664257	4665600	-
<i>msrA</i>	44	28	1.55	ST4-74	4665783	4666421	-
<i>ytfM</i>	45	34	1.34	ST4-74	4666634	4668367	+
<i>ytfN</i>	45	42	1.06	ST4-74	4668364	4672143	+
<i>ytfP</i>	100	101	0.99	ST4-74	4672146	4672490	+
STM4412	6	6	1.01	ST4-74	4672544	4673752	-
STM4413	3	4	0.80	ST4-74	4673749	4674912	-
<i>ppa</i>	274	359	0.76	ST4-74	4675323	4675853	-
<i>fbp</i>	34	36	0.95	ST4-74	4676080	4677078	-
<i>mpl</i>	26	26	0.99	ST4-74	4677253	4678632	+
<i>iolR</i>	22	23	0.94	ST4-74	4679123	4679956	+
<i>iolT1</i>	14	13	1.04	ST4-74	4680007	4681377	-
<i>iolT2</i>	11	7	1.46	ST4-74	4681899	4683335	+
STnc1740	72	56	1.28	ST4-74	4683333	4683512	-

<i>Name</i>	Δfnr TPM	WT TPM	$\Delta fnr/WT$	<i>Chr</i> ^a	<i>Start</i>	<i>End</i>	<i>Strand</i>
STnc2160	50	38	1.31	ST4-74	4683636	4683699	-
<i>iolB</i>	8	7	1.05	ST4-74	4683688	4684497	-
<i>iolA</i>	6	5	1.19	ST4-74	4684522	4686027	-
STM4422	1	1	2.16	ST4-74	4686043	4686345	-
STM4423	3	3	1.04	ST4-74	4686467	4687291	+
<i>iolE</i>	2	2	1.36	ST4-74	4687566	4688471	+
<i>iolG1</i>	7	6	1.15	ST4-74	4688490	4689500	+
<i>srfJ</i>	4	4	1.08	ST4-74	4689597	4690940	+
<i>iolI1</i>	9	8	1.14	ST4-74	4690941	4691774	+
STM4428	4	4	1.11	ST4-74	4691771	4692937	-
<i>iolC</i>	4	4	1.18	ST4-74	4692998	4694935	-
<i>iolD</i>	4	3	1.24	ST4-74	4695343	4697292	+
<i>iolG2</i>	7	6	1.11	ST4-74	4697473	4698495	+
STM4434	8	7	1.17	ST4-74	4698568	4699794	+
<i>iolI2</i>	3	3	1.18	ST4-74	4699955	4700770	+
<i>iolH</i>	7	6	1.23	ST4-74	4700823	4701707	+
<i>yjgA</i>	54	47	1.15	ST4-74	4701763	4702314	-
<i>pmbA</i>	31	27	1.17	ST4-74	4702410	4703762	+
<i>cybC</i>	215	160	1.34	ST4-74	4703861	4704247	+
SL1344_4369A	22	22	1.00	ST4-74	4704251	4704396	+
STM4440	4	5	0.72	ST4-74	4704525	4704863	+
STM4441	3	2	1.56	ST4-74	4704874	4705236	+
STM4442	1	3	0.45	ST4-74	4705236	4705538	+
STM4443	3	2	1.20	ST4-74	4705561	4706337	+
STM4444	4	4	0.97	ST4-74	4706349	4706993	+
STM4445	2	3	0.76	ST4-74	4707052	4708185	+
STM4446	2	3	0.74	ST4-74	4708169	4709287	+
STM4447	4	5	0.77	ST4-74	4709284	4710024	+
STM4448	8	7	1.02	ST4-74	4710041	4711954	+
<i>relB</i>	38	37	1.04	ST4-74	4712032	4712274	+
<i>relE</i>	33	24	1.40	ST4-74	4712264	4712548	+
<i>nrdG</i>	2	6	0.34	ST4-74	4712552	4713016	-
<i>nrdD</i>	9	37	0.24	ST4-74	4713137	4715275	-
SL1344_4383	3	7	0.42	ST4-74	4715480	4715650	+
<i>treC</i>	3	5	0.54	ST4-74	4715684	4717336	-
<i>treB</i>	15	25	0.61	ST4-74	4717386	4718803	-
<i>treR</i>	5	7	0.70	ST4-74	4718941	4719888	-
<i>mgtA</i>	14	14	1.06	ST4-74	4720272	4722980	+
STM4457	23	27	0.83	ST4-74	4723096	4723542	-
<i>yjgF</i>	84	134	0.63	ST4-74	4723617	4724003	-
<i>pyrI</i>	4	7	0.55	ST4-74	4724080	4724541	-
<i>pyrB</i>	4	7	0.59	ST4-74	4724554	4725489	-
<i>pyrL</i>	339	416	0.82	ST4-74	4725525	4725626	-
STM4463	8	6	1.40	ST4-74	4725716	4726204	-
STM4464	4	3	1.20	ST4-74	4726391	4727794	-
STM4465	1	1	0.82	ST4-74	4727850	4728854	-
STM4466	1	1	0.76	ST4-74	4728966	4729898	-
STM4467	1	1	1.15	ST4-74	4729909	4731129	-
<i>yjgK</i>	17	24	0.70	ST4-74	4731805	4732257	+
<i>argI</i>	108	236	0.46	ST4-74	4732331	4733335	-
<i>yjgD</i>	159	137	1.16	ST4-74	4733501	4733917	+

<i>Name</i>	Δfnr TPM	WT TPM	$\Delta fnr/WT$	Chr ^a	Start	End	Strand
<i>miaE</i>	7	7	0.93	ST4-74	4733929	4734741	+
<i>ytgA</i>	11	9	1.20	ST4-74	4734975	4735463	-
<i>yjgM</i>	31	39	0.79	ST4-74	4735570	4736073	-
<i>yjgN</i>	16	16	1.01	ST4-74	4736268	4737455	+
<i>valS</i>	21	28	0.74	ST4-74	4737597	4740452	-
<i>holC</i>	90	96	0.94	ST4-74	4740452	4740895	-
<i>pepA</i>	29	38	0.78	ST4-74	4741032	4742543	-
STM4478	197	199	0.99	ST4-74	4742587	4742706	-
<i>yjgP</i>	50	51	0.99	ST4-74	4742959	4744038	+
<i>yjgQ</i>	36	37	0.98	ST4-74	4744038	4745120	+
<i>idnR</i>	5	5	0.96	ST4-74	4745315	4746313	-
<i>idnT</i>	16	15	1.09	ST4-74	4746377	4747597	-
<i>idnO</i>	3	3	0.92	ST4-74	4747758	4748522	-
<i>idnD</i>	3	2	1.13	ST4-74	4748547	4749578	-
<i>idnK</i>	12	12	0.93	ST4-74	4749795	4750325	+
<i>yjgB</i>	33	17	2.02	ST4-74	4750353	4751372	-
STM4488	2	1	1.94	ST4-74	4751898	4752167	+
STM4489	18	18	1.00	ST4-74	4752547	4756062	+
STM4490	42	40	1.07	ST4-74	4756159	4757148	+
STM4491	19	19	0.98	ST4-74	4757261	4759345	-
STM4492	13	18	0.71	ST4-74	4759356	4761818	-
STM4493	18	23	0.79	ST4-74	4761956	4762777	-
STM4494	26	30	0.87	ST4-74	4762755	4763846	-
STM4495	20	24	0.85	ST4-74	4763846	4767523	-
STM4496	12	16	0.75	ST4-74	4767569	4771210	-
STM4497	18	28	0.63	ST4-74	4771222	4771824	-
STM4498	31	47	0.66	ST4-74	4771821	4772423	-
SL1344_4427A	2	1	2.55	ST4-74	4772932	4773205	+
<i>yeeN</i>	152	129	1.18	ST4-74	4773249	4773974	-
<i>yjhP</i>	4	6	0.71	ST4-74	4774525	4776156	-
STM4501	87	100	0.87	ST4-74	4776161	4776418	-
STM4502	2	16	0.12	ST4-74	4776907	4777515	+
STM4503	142	132	1.07	ST4-74	4778025	4778762	+
STM4504	59	21	2.82	ST4-74	4779038	4779949	+
STM4505	17	14	1.19	ST4-74	4780154	4780615	+
STM4506	12	12	0.99	ST4-74	4780612	4781286	-
<i>uxuR</i>	19	20	0.92	ST4-74	4781636	4782409	+
<i>trpS2</i>	6	5	1.25	ST4-74	4782410	4783423	-
<i>IsrQ</i>	3	2	1.30	ST4-74	4783574	4783741	+
SL1344_4439	4	14	0.26	ST4-74	4783720	4783872	+
STM4509	28	46	0.62	ST4-74	4784225	4784671	+
STM4510	12	17	0.68	ST4-74	4784910	4785644	+
<i>yjiE</i>	9	8	1.05	ST4-74	4785650	4786558	-
<i>iadA</i>	4	6	0.65	ST4-74	4786677	4787849	-
<i>yjiG</i>	4	5	0.78	ST4-74	4787862	4788323	-
<i>yjiH</i>	6	6	0.97	ST4-74	4788320	4788991	-
SL1344_4445A	29	12	2.41	ST4-74	4789349	4789724	-
<i>yjiJ</i>	14	8	1.73	ST4-74	4789864	4791048	-
STnc4260	29	20	1.45	ST4-74	4791124	4791217	+
<i>yjiN</i>	31	18	1.69	ST4-74	4791268	4792539	-
<i>yjiO</i>	7	11	0.62	ST4-74	4792626	4793867	-

<i>Name</i>	Δ <i>fnr</i> TPM	WT TPM	Δ <i>fnr</i> /WT	<i>Chr</i> ^a	<i>Start</i>	<i>End</i>	<i>Strand</i>
STM4518	17	18	0.98	ST4-74	4794346	4794861	+
STM4519	21	11	1.84	ST4-74	4795042	4796412	+
STM4520	29	14	2.14	ST4-74	4796507	4796650	-
<i>yjiS</i>	69	26	2.62	ST4-74	4796617	4796781	+
STnc4130	31	37	0.83	ST4-74	4796788	4796863	-
STM4522	18	15	1.20	ST4-74	4796856	4797557	-
<i>symE</i>	6	8	0.73	ST4-74	4797631	4797963	-
STnc1470	3885	6462	0.60	ST4-74	4797957	4798031	+
<i>hsdS</i>	8	11	0.68	ST4-74	4798190	4799599	-
<i>hsdM</i>	7	10	0.65	ST4-74	4799596	4801185	-
<i>hsdR</i>	5	13	0.36	ST4-74	4801343	4804852	-
<i>mrr</i>	12	10	1.23	ST4-74	4805050	4805964	+
STM4528	40	39	1.04	ST4-74	4806233	4806520	+
STM4529	10	9	1.19	ST4-74	4806507	4806809	+
<i>yjiA</i>	13	18	0.74	ST4-74	4806884	4807840	-
<i>yjiX</i>	42	43	0.97	ST4-74	4807851	4808054	-
<i>cstAb</i>	5	4	1.14	ST4-74	4808149	4810299	-
<i>tsr</i>	40	131	0.30	ST4-74	4810666	4812327	+
STM4534	14	13	1.04	ST4-74	4812651	4815416	+
STM4535	8	9	0.85	ST4-74	4815518	4815940	+
STM4536	2	3	0.78	ST4-74	4815955	4816416	+
STM4537	3	4	0.71	ST4-74	4816442	4817221	+
STM4538	2	3	0.78	ST4-74	4817211	4818047	+
STM4539	4	5	0.73	ST4-74	4818060	4819121	+
STM4540	8	8	0.99	ST4-74	4819139	4820149	+
<i>mdoB</i>	100	85	1.18	ST4-74	4820283	4822475	-
<i>yjiA</i>	10	14	0.75	ST4-74	4822857	4823318	-
<i>dnaC</i>	12	16	0.72	ST4-74	4823376	4824113	-
<i>dnaT</i>	42	42	1.01	ST4-74	4824116	4824655	-
STM4545	9	21	0.43	ST4-74	4824748	4825221	-
<i>yjiP</i>	15	46	0.32	ST4-74	4825212	4826123	-
<i>yjiQ</i>	0	1	0.40	ST4-74	4826701	4827426	+
<i>bglJ</i>	3	2	1.28	ST4-74	4827387	4828061	+
STM4549	43	40	1.08	ST4-74	4828112	4828570	-
<i>fhuF</i>	39	15	2.57	ST4-74	4828721	4829509	-
STM4551	22	21	1.04	ST4-74	4829630	4830694	-
STM4552	17	11	1.50	ST4-74	4830945	4831181	+
<i>rsmC</i>	13	12	1.14	ST4-74	4831722	4832750	-
<i>hold</i>	70	62	1.12	ST4-74	4832853	4833290	+
<i>rimI</i>	15	16	0.94	ST4-74	4833235	4833681	+
<i>yjiG</i>	12	14	0.90	ST4-74	4833703	4834380	+
<i>prfC</i>	17	18	0.93	ST4-74	4834472	4836061	+
<i>osmY</i>	348	132	2.63	ST4-74	4836463	4837080	+
<i>yjiU</i>	25	20	1.24	ST4-74	4837494	4838567	+
<i>yjiV</i>	7	7	0.97	ST4-74	4838564	4839337	+
<i>yjiW</i>	2	11	0.21	ST4-74	4839370	4840233	-
<i>yjiI</i>	2	16	0.12	ST4-74	4840205	4841752	-
<i>deoC</i>	10	9	1.12	ST4-74	4841994	4842791	+
<i>deoA</i>	10	9	1.13	ST4-74	4842915	4844237	+
<i>deoB</i>	28	25	1.12	ST4-74	4844289	4845512	+
<i>deoD</i>	28	29	0.97	ST4-74	4845722	4846441	+

<i>Name</i>	Δ <i>fnr</i> TPM	WT TPM	Δ <i>fnr</i> /WT	Chr ^a	Start	End	Strand
STnc4140	85	54	1.57	ST4-74	4846458	4846540	-
<i>stjA</i>	28	19	1.51	ST4-74	4846479	4847051	-
<i>stjB</i>	9	7	1.35	ST4-74	4847048	4849456	-
<i>stjC</i>	3	1	2.49	ST4-74	4849470	4850090	-
STM4574	8	5	1.60	ST4-74	4850255	4850944	-
STM4575	5	3	1.62	ST4-74	4850992	4851681	-
<i>lplA</i>	10	10	1.01	ST4-74	4851994	4853010	-
<i>smp</i>	15	15	1.01	ST4-74	4853044	4853688	-
<i>serB</i>	19	18	1.04	ST4-74	4853805	4854773	+
<i>radA</i>	11	11	1.00	ST4-74	4854857	4856239	+
<i>nadR</i>	31	30	1.02	ST4-74	4856363	4857622	+
<i>yjjK</i>	44	47	0.94	ST4-74	4857740	4859407	-
<i>slt</i>	26	27	0.98	ST4-74	4859580	4861553	+
<i>trpR</i>	79	87	0.91	ST4-74	4861611	4861937	+
<i>yjjX</i>	19	17	1.09	ST4-74	4862039	4862554	-
<i>gpmB</i>	33	32	1.03	ST4-74	4862603	4863250	+
<i>rob</i>	147	118	1.25	ST4-74	4863247	4864116	-
<i>creA</i>	70	73	0.96	ST4-74	4864328	4864801	+
<i>creB</i>	23	26	0.87	ST4-74	4864814	4865503	+
<i>creC</i>	9	10	0.94	ST4-74	4865701	4866927	+
<i>creD</i>	8	8	1.12	ST4-74	4866985	4868334	+
<i>sthE</i>	4	3	1.24	ST4-74	4868392	4869477	-
<i>sthD</i>	2	2	1.33	ST4-74	4869518	4870075	-
<i>sthB</i>	5	4	1.30	ST4-74	4870093	4872630	-
<i>sthA</i>	2	1	1.20	ST4-74	4872676	4873359	-
STM4595	3	3	1.01	ST4-74	4873430	4873975	-
STM4596	54	45	1.20	ST4-74	4874314	4874985	-
STM4597	22	19	1.16	ST4-74	4875185	4875684	-
<i>arcA</i>	167	204	0.82	ST4-74	4875951	4876667	-
<i>yjjY</i>	18	14	1.30	ST4-74	4876763	4876903	+
<i>lasT</i>	7	7	1.07	ST4-74	4877303	4877989	+

^aChromosome or plasmid

Appendix II

Table S2 A. COG categories.

Amino acid transport and metabolism	Carbohydrate transport and metabolism	Cell envelope biogenesis and outer membrane	Cell motility and secretion	Energy production and conversion	Inorganic iron transport and metabolism	Surface Structures	Transcription	Translation, ribosomal structure and biogenesis
yneH	zwf	yfjM	yfjC	yaaA	zur	stjC	zntR	yjfH
yliD	yjfF	yfjG	tsr	yqhD	zunB	stjB	yfjH	yrdC
yliC	yraO	yfjB	trg	yneI	znuC	stiH	yqjI	yqcB
yliB	yraR	yraR	stjC	yieS	znuA	stiC	yqjC	yohl
yjfc	yneB	yohlK	stjB	yiaK	zntA	stiB	yqgE	yoaB
yjeM	yneA	yohG	stiH	yiaE	yrbG	stiA	yoaA	ymfC
yjeK	yliI	yneA	stiC	yhdH	yqjH	sthE	ynjL	yitG
yjeH	yjiO	yneA	stiB	yhbW	yneD	sthD	yneJ	yjgF
yjeL	yjeP	yieP	stiA	ygrR	yjeE	sthB	yncC	yjfh
yjfk	yigK	yibd	sthE	yfiQ	yjbb	sthA	yjiE	yjeA
yhjV	yihV	yiaD	sthD	yfhL	yitP	stfG	yjgM	yjbn
yhitP	yhitT	yhjG	sthA	yfaE	yibN	stfF	yjfo	yjbc
yhaO	yihS	yhiI	stfG	ydaA	yheN	stfE	yjfi	yihZ
ygiU	yihR	ygsB	stfF	ydtT	yheM	stfD	yjeB	yibK
ygiC	yihQ	ygeA	stfE	ydis	yheL	stfC	yidC	yhdG
yfik	yihP	ygcY	stfD	ydir	ygtT	stfA	yiaB	yhbY
yfthB	yihO	yfhD	stfC	ydtQ	ygtE	stfA	yjio	yhbH
yfdZ	yigM	yfeL	stfA	yqgQ	ygtQ	stfC	yjio	ygo
yfbQ	yjz	yfdH	stfC	ydgP	ygaP	stfA	yitD	ygeA
yjeA	yieO	yfbG	stfB	yqo	yfid	stfD	yihW	yfiF
yehY	yidY	yfbE	stfA	ydgM	yfgD	stfC	yfa	yfa
yehX	yicM	yfaW	stfC	ydcW	yffb	stfB	yieP	yfcb
yehW	yicL	yehZ	stfB	yccX	ybs	stfA	yidZ	yepP
yeeF	yicJ	yeeZ	stfA	yqo	yeaR	stfE	yiaJ	yebU
yeeO	yiaO	yeba	stfE	ugpQ	yean	stfD	yiaG	yctO
yecS	yiaN	ydiY	stfC	udhA	ydiE	stfC	yiaC	yctL
yecC	yiaM	ydhO	stfB	tirA	ydgF	stfB	yhc	yctH
yeeS	yiaL	yecG	stfA	torC	ydgE	stfA	yhhY	yehF
yeeS	yhjE	yefW	ssaN	torA	ydcG	stfD	yhcS	ybfF
ydgR	yehS	yefU	spaS	tdcE	yehN	stfC	yhcO	yadB
ydgl	yhcC	yefN	stfC	tdcD	yehM	stfB	yhcK	yaeJ
yel	yhcH	ybjY	stfC	tas	ygo	stfA	yhaJ	tyrS
yedX	ygiK	ybjT	stfB	sucD	yccK	stfE	ygl	tufB
yedW	ygeD	ybiO	ppdD	sucC	ybiR	stfD	ygaE	tufA
ycaM	ygmM	ybdG	ppdC	sucB	ybgR	stfC	ygaA	tsf
ybiK	ygbL	yajG	ppdA	sfcA	ybeX	stfB	yfe	trub

<i>Amino acid transport and metabolism</i>	<i>Carbohydrate transport and metabolism</i>	<i>Cell envelope biogenesis and outer membrane</i>	<i>Cell motility and secretion</i>	<i>Energy production and conversion</i>	<i>Inorganic iron transport and metabolism</i>	<i>Surface Structures</i>	<i>Transcription</i>	<i>Translation, ribosomal structure and biogenesis</i>
<i>ybhB</i>	<i>yfaV</i>	<i>yaeU</i>	<i>moaB</i>	<i>sdhD</i>	<i>ybdL</i>	<i>lpjA</i>	<i>yfhp</i>	<i>trnA</i>
<i>ybgK</i>	<i>yegV</i>	<i>yaeT</i>	<i>molA</i>	<i>sdhC</i>	<i>yaeE</i>	<i>gfpF</i>	<i>yfhh</i>	<i>tpsS2</i>
<i>ybgL</i>	<i>yegT</i>	<i>yaeL</i>	<i>hchA</i>	<i>sdhB</i>	<i>yaeC</i>	<i>hitT</i>	<i>yfer</i>	<i>tps</i>
<i>ybgH</i>	<i>yegB</i>	<i>yabC</i>	<i>lpjE</i>	<i>sdhA</i>	<i>yadf</i>	<i>fls</i>	<i>yfax</i>	<i>tmU</i>
<i>ybdr</i>	<i>yedA</i>	<i>wzzE</i>	<i>lpjD</i>	<i>gor</i>	<i>yabK</i>	<i>flr</i>	<i>yelh</i>	<i>tmD</i>
<i>ybdL</i>	<i>yead</i>	<i>wzzB</i>	<i>lpjB</i>	<i>putA</i>	<i>trkH</i>	<i>flrQ</i>	<i>yelE</i>	<i>tmA</i>
<i>yahN</i>	<i>ydlN</i>	<i>wz</i>	<i>lpjA</i>	<i>pta</i>	<i>trkA</i>	<i>flp</i>	<i>yehV</i>	<i>hrs</i>
<i>yaeR</i>	<i>ydhC</i>	<i>wza</i>	<i>invC</i>	<i>ppcC</i>	<i>hil</i>	<i>flp</i>	<i>yehT</i>	<i>sun</i>
<i>yadD</i>	<i>ydfU</i>	<i>wecG</i>	<i>hopD</i>	<i>prkB</i>	<i>tehA</i>	<i>flpO</i>	<i>yegW</i>	<i>spoU</i>
<i>yadL</i>	<i>ydfH</i>	<i>wecE</i>	<i>hopC</i>	<i>ppc</i>	<i>sugE</i>	<i>flm</i>	<i>yebK</i>	<i>speG</i>
<i>wcaB</i>	<i>ydeZ</i>	<i>wecC</i>	<i>hojB</i>	<i>ppa</i>	<i>sseA</i>	<i>flL</i>	<i>yeam</i>	<i>smpA</i>
<i>usg</i>	<i>ydeV</i>	<i>wecB</i>	<i>hojB</i>	<i>pntB</i>	<i>sodC</i>	<i>flk</i>	<i>ydlp</i>	<i>serS</i>
<i>hrrP</i>	<i>ydeI</i>	<i>wecL</i>	<i>fljB</i>	<i>pntA</i>	<i>sodB</i>	<i>flU</i>	<i>ydhM</i>	<i>selB</i>
<i>hrrB</i>	<i>ydeD</i>	<i>wcaJ</i>	<i>flr</i>	<i>phsC</i>	<i>sodA</i>	<i>flH</i>	<i>ydhB</i>	<i>rsuA</i>
<i>hrrA</i>	<i>ydeA</i>	<i>wcaI</i>	<i>flrQ</i>	<i>phsB</i>	<i>stlD</i>	<i>flG</i>	<i>ydfH</i>	<i>rsmC</i>
<i>trpE</i>	<i>yddG</i>	<i>wcaG</i>	<i>flp</i>	<i>phsA</i>	<i>sitC</i>	<i>flG</i>	<i>ydeW</i>	<i>rpsU</i>
<i>trpD</i>	<i>yclM</i>	<i>wcaC</i>	<i>flpO</i>	<i>plfE</i>	<i>sitB</i>	<i>flf</i>	<i>ydeR</i>	<i>rpsT</i>
<i>trpC</i>	<i>yceL</i>	<i>wcaJ</i>	<i>fln</i>	<i>pflD</i>	<i>sitA</i>	<i>flE</i>	<i>ydeN</i>	<i>rpsS</i>
<i>trpB</i>	<i>yceE</i>	<i>vacJ</i>	<i>flM</i>	<i>pflB</i>	<i>sfbC</i>	<i>flD</i>	<i>ydel</i>	<i>rpsR</i>
<i>trpA</i>	<i>ycaD</i>	<i>udg</i>	<i>flL</i>	<i>pdwW</i>	<i>sfbB</i>	<i>flC</i>	<i>ydel</i>	<i>rpsQ</i>
<i>thrB</i>	<i>ybhE</i>	<i>isx</i>	<i>flK</i>	<i>pluS</i>	<i>sfbA</i>	<i>flA</i>	<i>yefX</i>	<i>rpsP</i>
<i>thrA</i>	<i>ybhC</i>	<i>tonB</i>	<i>flJ</i>	<i>pluQ</i>	<i>shp</i>	<i>flD</i>	<i>yefQ</i>	<i>rpsO</i>
<i>tesA</i>	<i>ybdJ</i>	<i>tolC</i>	<i>flI</i>	<i>peka</i>	<i>pstC</i>	<i>flc</i>	<i>yedC</i>	<i>rpsN</i>
<i>tdh</i>	<i>ybdA</i>	<i>tolA</i>	<i>flH</i>	<i>peka</i>	<i>pstB</i>	<i>flgN</i>	<i>yecR</i>	<i>rpsM</i>
<i>tdcG</i>	<i>yqjR</i>	<i>spr</i>	<i>flG</i>	<i>oatG</i>	<i>psIA</i>	<i>flgM</i>	<i>yehF</i>	<i>rpsL</i>
<i>tdcC</i>	<i>yadI</i>	<i>skyB</i>	<i>flF</i>	<i>nuoN</i>	<i>pspE</i>	<i>flgI</i>	<i>ybdO</i>	<i>rpsK</i>
<i>tdcB</i>	<i>yadU</i>	<i>sit</i>	<i>flE</i>	<i>nuoM</i>	<i>ppk</i>	<i>flgK</i>	<i>ybdM</i>	<i>rpsJ</i>
<i>suflS</i>	<i>xyfU</i>	<i>slp</i>	<i>flD</i>	<i>nuoL</i>	<i>phoU</i>	<i>flgJ</i>	<i>ybbS</i>	<i>rpsI</i>
<i>speF</i>	<i>xyfA</i>	<i>rspA</i>	<i>flC</i>	<i>nuoK</i>	<i>phnS</i>	<i>flgI</i>	<i>ybaO</i>	<i>rpsH</i>
<i>speE</i>	<i>xapB</i>	<i>rhpB</i>	<i>flgN</i>	<i>nuoJ</i>	<i>phnA</i>	<i>flgH</i>	<i>yqfC</i>	<i>rpsG</i>
<i>speD</i>	<i>uhpT</i>	<i>rffH</i>	<i>flgI</i>	<i>nuoI</i>	<i>pgcC</i>	<i>flgG</i>	<i>xyfR</i>	<i>rpsF</i>
<i>speC</i>	<i>uhpC</i>	<i>rffG</i>	<i>flgK</i>	<i>nuoH</i>	<i>pxiA</i>	<i>flgE</i>	<i>xqjR</i>	<i>rpsE</i>
<i>speB</i>	<i>ugpE</i>	<i>rfe</i>	<i>flgI</i>	<i>nuoG</i>	<i>nrjD</i>	<i>flgE</i>	<i>wecD</i>	<i>rpsD</i>
<i>solA</i>	<i>ugpC</i>	<i>rflV</i>	<i>flgH</i>	<i>nuoF</i>	<i>nrjA</i>	<i>flgC</i>	<i>vacB</i>	<i>rpsC</i>
<i>serB</i>	<i>ugpB</i>	<i>rflU</i>	<i>flgG</i>	<i>nuoE</i>	<i>nrjC</i>	<i>flgB</i>	<i>uxuR</i>	<i>rpsB</i>
<i>serA</i>	<i>ugpA</i>	<i>rflP</i>	<i>flgF</i>	<i>nuoC</i>	<i>nicC</i>	<i>flgA</i>	<i>umuD</i>	<i>rpsA</i>
<i>selD</i>	<i>trfA</i>	<i>rflN</i>	<i>flgE</i>	<i>nuoB</i>	<i>nhab</i>	<i>flgA</i>	<i>tk</i>	<i>rpmJ2</i>
<i>selA</i>	<i>trcC</i>	<i>rflM</i>	<i>flgD</i>	<i>nuoA</i>	<i>nhad</i>	<i>flmZ</i>	<i>trpK</i>	<i>rpmJ</i>
<i>sdaC</i>	<i>trcA</i>	<i>rflJ</i>	<i>flgC</i>	<i>nrjC</i>	<i>naaK</i>	<i>flmY</i>	<i>trrR</i>	<i>rpmI</i>
<i>sdaB</i>	<i>tpiA</i>	<i>rflH</i>	<i>flgB</i>	<i>nrjB</i>	<i>naqD</i>	<i>flmW</i>	<i>tdcA</i>	<i>rpmH</i>
<i>sdaA</i>	<i>torT</i>	<i>rflG</i>	<i>flgA</i>	<i>nrjU</i>	<i>modF</i>	<i>flmI</i>	<i>srL</i>	<i>rpmG</i>
<i>sppA</i>	<i>tkiB</i>	<i>rflF</i>	<i>flmI</i>	<i>nrjA</i>	<i>modC</i>	<i>flmH</i>	<i>sprB</i>	<i>rpmF</i>
<i>rhlB</i>	<i>tkiA</i>	<i>rflD</i>	<i>flmF</i>	<i>nrjB</i>	<i>modC</i>	<i>flmF</i>		<i>rpmE2</i>

Amino acid transport and metabolism	Carbohydrate transport and metabolism	Cell envelope biogenesis and outer membrane	Cell motility and secretion	Energy production and conversion	Inorganic iron transport and metabolism	Surface Structures	Transcription	Translation, ribosomal structure and biogenesis
<i>rspB</i>	<i>talC</i>	<i>rjbC</i>	<i>fimD</i>	<i>nemA</i>	<i>modB</i>	<i>fimD</i>	<i>soxS</i>	<i>rpmE</i>
<i>rhcC</i>	<i>talB</i>	<i>rjfbB</i>	<i>fimC</i>	<i>ndh</i>	<i>modA</i>	<i>fimC</i>	<i>soxR</i>	<i>rpmD</i>
<i>putP</i>	<i>talA</i>	<i>rjfbA</i>	<i>fimA</i>	<i>narZ</i>	<i>nmhH</i>	<i>fimA</i>	<i>slyA</i>	<i>rpmC</i>
<i>putB</i>	<i>subB</i>	<i>rjaQ</i>	<i>cheZ</i>	<i>narW</i>	<i>ngtB</i>	<i>dsbC</i>	<i>simR</i>	<i>rpmB</i>
<i>ptrB</i>	<i>srlE</i>	<i>rjaL</i>	<i>cheW</i>	<i>narV</i>	<i>mdoG</i>	<i>dsbB</i>	<i>sdiA</i>	<i>rpmA</i>
<i>proY</i>	<i>srlA</i>	<i>rjaK</i>	<i>cheR</i>	<i>narJ</i>	<i>kup</i>	<i>csgG</i>	<i>rsd</i>	<i>rplY</i>
<i>proX</i>	<i>smvA</i>	<i>rfaJ</i>	<i>cheB</i>	<i>narI</i>	<i>kefC</i>	<i>csgF</i>	<i>rpoZ</i>	<i>rplX</i>
<i>proW</i>	<i>strB</i>	<i>rfaI</i>	<i>cheA</i>	<i>narH</i>	<i>kefB</i>	<i>csgE</i>	<i>rpoS</i>	<i>rplW</i>
<i>proV</i>	<i>sgbU</i>	<i>rfaG</i>	<i>bcfG</i>	<i>napF</i>	<i>kdpC</i>	<i>csgD</i>	<i>rpoN</i>	<i>rplV</i>
<i>proC</i>	<i>sgaU</i>	<i>rfaF</i>	<i>bcfF</i>	<i>napB</i>	<i>kdpB</i>	<i>csgC</i>	<i>rpoH</i>	<i>rplU</i>
<i>proB</i>	<i>sgaH</i>	<i>rfaE</i>	<i>bcfE</i>	<i>napC</i>	<i>kdpA</i>	<i>csgB</i>	<i>rpoE</i>	<i>rplT</i>
<i>proA</i>	<i>sgaE</i>	<i>rfaD</i>	<i>bcfD</i>	<i>mioC</i>	<i>kaiG</i>	<i>csgA</i>	<i>rpoD</i>	<i>rplR</i>
<i>prlC</i>	<i>sgaB</i>	<i>rfaC</i>	<i>bcfC</i>	<i>mdaA</i>	<i>kaiE</i>	<i>cri</i>	<i>rpoA</i>	<i>rplQ</i>
<i>posB</i>	<i>setB</i>	<i>rfaB</i>	<i>bcfB</i>	<i>maeB</i>	<i>iron</i>	<i>bcfH</i>	<i>rob</i>	<i>rplP</i>
<i>poiI</i>	<i>rpe</i>	<i>pre</i>	<i>bcfA</i>	<i>lpaA</i>	<i>iroD</i>	<i>bcfG</i>	<i>mk</i>	<i>rplO</i>
<i>poiH</i>	<i>rhaT</i>	<i>pqaB</i>	STM3216	<i>lldP</i>	<i>glpE</i>	<i>bcfF</i>	<i>mc</i>	<i>rplN</i>
<i>poiG</i>	<i>rhaD</i>	<i>pmrF</i>	STM3152	<i>lldD</i>	<i>fur</i>	<i>bcfE</i>	<i>mba</i>	<i>rplM</i>
<i>poiF</i>	<i>rhaB</i>	<i>pldA</i>	STM3138	<i>ldhA</i>	<i>finB</i>	<i>bcfD</i>	<i>rho</i>	<i>rplL</i>
<i>poiE</i>	<i>rhaA</i>	<i>phoE</i>	STM1657	<i>icdA</i>	<i>fin</i>	<i>bcfC</i>	<i>rhaS</i>	<i>rplK</i>
<i>poiD</i>	<i>rfaK</i>	<i>pgtE</i>		<i>hypO</i>	<i>foxA</i>	<i>bcfB</i>	<i>rhaR</i>	<i>rplJ</i>
<i>poiC</i>	<i>rbsK</i>	<i>pdgL</i>		<i>hydN</i>	<i>focA</i>	<i>bcfA</i>	<i>rfaH</i>	<i>rplI</i>
<i>poiB</i>	<i>rbsD</i>	<i>pbpG</i>		<i>hycl</i>	<i>fluE</i>		<i>rcaA</i>	<i>rplF</i>
<i>poiA</i>	<i>rbsC</i>	<i>pal</i>		<i>hycG</i>	<i>fluD</i>		<i>rbsR</i>	<i>rplE</i>
<i>pipD</i>	<i>rbsB</i>	<i>pagC</i>		<i>hycF</i>	<i>fluC</i>		<i>purR</i>	<i>rplD</i>
<i>phnW</i>	<i>rbsA</i>	<i>ompX</i>		<i>hycE</i>	<i>fluB</i>		<i>psjJ</i>	<i>rplC</i>
<i>phnV</i>	<i>pykF</i>	<i>ompW</i>		<i>hycD</i>	<i>fluA</i>		<i>pspC</i>	<i>rplB</i>
<i>phnT</i>	<i>pykA</i>	<i>ompN</i>		<i>hycC</i>	<i>fes</i>		<i>pspA</i>	<i>rplA</i>
<i>pheP</i>	<i>pixA</i>	<i>ompC</i>		<i>hycB</i>	<i>fepG</i>		<i>phnR</i>	<i>rph</i>
<i>pepT</i>	<i>pisO</i>	<i>ompA</i>		<i>hybD</i>	<i>fepD</i>		<i>phnO</i>	<i>rnpA</i>
<i>pepQ</i>	<i>pisN</i>	<i>nmpC</i>		<i>hybC</i>	<i>fepC</i>		<i>pdhR</i>	<i>rne</i>
<i>pepP</i>	<i>pisI</i>	<i>nlpD</i>		<i>hybA</i>	<i>fepB</i>		<i>oxyR</i>	<i>rnd</i>
<i>pepH</i>	<i>pisH</i>	<i>nlpC</i>		<i>hmpA</i>	<i>fepA</i>		<i>orf408</i>	<i>rna</i>
<i>pepN</i>	<i>pisG</i>	<i>nlpB</i>		<i>hemG</i>	<i>feoB</i>		<i>orf242</i>	<i>rnf</i>
<i>pepE</i>	<i>pisA</i>	<i>murG</i>		<i>hcr</i>	<i>feoA</i>		<i>nusG</i>	<i>rluD</i>
<i>pepD</i>	<i>prpB</i>	<i>murF</i>		<i>hcp</i>	<i>dps</i>		<i>nusB</i>	<i>rhcC</i>
<i>pepB</i>	<i>proP</i>	<i>murE</i>		<i>gpsA</i>	<i>cysW</i>		<i>nusA</i>	<i>rhuA</i>
<i>pepA</i>	<i>pps</i>	<i>murD</i>		<i>gor</i>	<i>cysQ</i>		<i>nlp</i>	<i>rimM</i>
<i>pdsB</i>	<i>pmgI</i>	<i>murC</i>		<i>glpP</i>	<i>cysP</i>		<i>nikR</i>	<i>rimL</i>
<i>pduV</i>	<i>pgtP</i>	<i>murB</i>		<i>gltA</i>	<i>cysN</i>		<i>nhaR</i>	<i>rimJ</i>
<i>pduU</i>	<i>pgm</i>	<i>murA</i>		<i>glpQ</i>	<i>cysJ</i>		<i>nank</i>	<i>rbaA</i>
<i>pabC</i>	<i>pgk</i>	<i>mitGA</i>		<i>glpD</i>	<i>cysC</i>		<i>nagC</i>	<i>queA</i>
<i>pabb</i>	<i>pgi</i>	<i>mscL</i>		<i>glpC</i>	<i>cysA</i>		<i>nadR</i>	<i>pih</i>

Amino acid transport and metabolism	Carbohydrate transport and metabolism	Cell envelope biogenesis and outer membrane	Cell motility and secretion	Energy production and conversion	Inorganic iron transport and metabolism	Surface Structures	Transcription	Translation, ribosomal structure and biogenesis
<i>pbkA</i>	<i>pkfB</i>	<i>msbB</i>		<i>glpA</i>	<i>cyoY</i>		<i>mLR</i>	<i>proS</i>
<i>orf48</i>	<i>pkfA</i>	<i>mreD</i>		<i>galT</i>	<i>cutC</i>		<i>mle</i>	<i>pmvA</i>
<i>oppF</i>	<i>pdurF</i>	<i>mrdA</i>		<i>gabD</i>	<i>cutA</i>		<i>metR</i>	<i>prfH</i>
<i>oppD</i>	<i>pagO</i>	<i>mrcB</i>		<i>funC</i>	<i>corA</i>		<i>meiR</i>	<i>prfC</i>
<i>oppC</i>	<i>ossB</i>	<i>mraY</i>		<i>fumB</i>	<i>chtT</i>		<i>marT</i>	<i>prfB</i>
<i>oppB</i>	<i>otsA</i>	<i>mpl</i>		<i>funA</i>	<i>cirA</i>		<i>marA</i>	<i>prfA</i>
<i>oppA</i>	<i>mupG</i>	<i>mltC</i>		<i>fucO</i>	<i>chaA</i>		<i>marA</i>	<i>pnp</i>
<i>oat</i>	<i>nanT</i>	<i>mltB</i>		<i>frdD</i>	<i>choQ</i>		<i>malT</i>	<i>pheS</i>
<i>njS</i>	<i>nanE</i>	<i>mltA</i>		<i>frdC</i>	<i>cbiO</i>		<i>hysR</i>	<i>miab</i>
<i>nanA</i>	<i>nazZ</i>	<i>mlsL</i>		<i>frdB</i>	<i>cbiN</i>		<i>hsp</i>	<i>miab</i>
<i>ntr</i>	<i>nagE</i>	<i>mipA</i>		<i>frdA</i>	<i>cbiM</i>		<i>hphA</i>	<i>metG</i>
<i>mppA</i>	<i>nagD</i>	<i>mepA</i>		<i>frdA</i>	<i>bnuf</i>		<i>lhr</i>	<i>metG</i>
<i>meI</i>	<i>nagB</i>	<i>mdoH</i>		<i>fldB</i>	<i>bfr</i>		<i>lldr</i>	<i>map</i>
<i>meIH</i>	<i>nagA</i>	<i>mdoB</i>		<i>fldA</i>	<i>bfd</i>		<i>lexA</i>	<i>hysS</i>
<i>meIF</i>	<i>mild</i>	<i>lspA</i>		<i>fixX</i>	<i>apaG</i>		<i>leuO</i>	<i>lgt</i>
<i>meE</i>	<i>mltA</i>	<i>lpxK</i>		<i>fixC</i>	<i>amtB</i>		<i>kdgR</i>	<i>leuS</i>
<i>meC</i>	<i>mrsA</i>	<i>lpxD</i>		<i>fixB</i>	<i>abc</i>		<i>invF</i>	<i>ksGA</i>
<i>meB</i>	<i>mgsA</i>	<i>lpxC</i>		<i>fixA</i>	<i>STM3820</i>		<i>ivy</i>	<i>ingC</i>
<i>meA</i>	<i>mgfC</i>	<i>lpxB</i>		<i>fixA</i>	<i>STM3528</i>		<i>idnR</i>	<i>infB</i>
<i>hspP</i>	<i>mgfB</i>	<i>lpxA</i>		<i>fixA</i>	<i>STM3528</i>		<i>iclr</i>	<i>infA</i>
<i>hspC</i>	<i>mgfA</i>	<i>lppB</i>		<i>fixA</i>	<i>STM3356</i>		<i>icdA</i>	<i>iles</i>
<i>hspA</i>	<i>meiB</i>	<i>lpp</i>		<i>fixA</i>	<i>STM3166</i>		<i>hucC</i>	<i>henk</i>
<i>hspM</i>	<i>meIA</i>	<i>lolB</i>		<i>fixA</i>	<i>STM3142</i>		<i>hpar</i>	<i>glyS</i>
<i>hspK</i>	<i>meiA</i>	<i>lolA</i>		<i>fixA</i>	<i>STM3141</i>		<i>hpaA</i>	<i>glyO</i>
<i>hspJ</i>	<i>manZ</i>	<i>hnt</i>		<i>fixA</i>	<i>STM122</i>		<i>hilD</i>	<i>glxX</i>
<i>hspH</i>	<i>manY</i>	<i>lgr</i>		<i>fixA</i>	<i>STM3075</i>		<i>hilC</i>	<i>glhS</i>
<i>hspG</i>	<i>manX</i>	<i>kdvA</i>		<i>fixA</i>	<i>STM3074</i>		<i>hila</i>	<i>fusa</i>
<i>hspF</i>	<i>manA</i>	<i>kdsB</i>		<i>fixA</i>	<i>STM3073</i>		<i>greB</i>	<i>fusa</i>
<i>hspE</i>	<i>malZ</i>	<i>kdsA</i>		<i>fixA</i>	<i>STM2446</i>		<i>greA</i>	<i>frr</i>
<i>hspD</i>	<i>malS</i>	<i>imp</i>		<i>fixA</i>	<i>STM2404</i>		<i>gnrR</i>	<i>fnt</i>
<i>hspC</i>	<i>malK</i>	<i>iagB</i>		<i>fixA</i>	<i>STM1874</i>		<i>glpR</i>	<i>efp</i>
<i>hspB</i>	<i>malG</i>	<i>hrrB</i>		<i>fixA</i>	<i>STM1808</i>		<i>gvnA</i>	<i>def</i>
<i>hspA</i>	<i>malF</i>	<i>hrrA</i>		<i>fixA</i>	<i>STM1741</i>		<i>gais</i>	<i>ccsS</i>
<i>hspN</i>	<i>malE</i>	<i>hpaA</i>		<i>fixA</i>	<i>STM1731</i>		<i>gair</i>	<i>cca</i>
<i>hspM</i>	<i>hspK</i>	<i>gnd</i>		<i>fixA</i>	<i>STM1656</i>		<i>gucR</i>	<i>ccgA</i>
<i>hspL</i>	<i>kgfP</i>	<i>glnU</i>		<i>fixA</i>	<i>STM1653</i>		<i>fnuR</i>	<i>aspS</i>
<i>hspG</i>	<i>kgfL</i>	<i>glnS</i>		<i>fixA</i>	<i>STM1490</i>		<i>flaA</i>	<i>argS</i>
<i>hspE</i>	<i>kdgK</i>	<i>gldB</i>		<i>fixA</i>	<i>STM10771</i>		<i>flaM</i>	<i>argS</i>
<i>hspD</i>	<i>iroB</i>	<i>galU</i>		<i>fixA</i>	<i>STM0770</i>		<i>fmfV</i>	<i>alas</i>
<i>hspC</i>	<i>idnT</i>	<i>galF</i>		<i>fixA</i>	<i>STM0765</i>		<i>flaA</i>	<i>STM4450</i>
<i>hspB</i>	<i>idnK</i>	<i>galE</i>		<i>fixA</i>	<i>STM0562</i>		<i>fadR</i>	<i>STM2545</i>
<i>hspA</i>	<i>hpaX</i>	<i>fasQ</i>		<i>fixA</i>	<i>STM0355</i>		<i>eur</i>	<i>STM1550</i>
<i>idnD</i>	<i>hpaI</i>	<i>fstI</i>		<i>fixA</i>	<i>STM0084</i>		<i>emvR</i>	<i>STM1549</i>

Amino acid transport and metabolism	Carbohydrate transport and metabolism	Cell envelope biogenesis and outer membrane	Cell motility and secretion	Energy production and conversion	Inorganic iron transport and metabolism	Surface Structures	Transcription	Translation, ribosomal structure and biogenesis
<i>hutH</i>	<i>hcaT</i>	<i>flgJ</i>		<i>cybC</i>	STM0035		<i>emrR</i>	STM1548
<i>hutG</i>	<i>gudT</i>	<i>jepE</i>		<i>cybB</i>			<i>ecnR</i>	
<i>hpaF</i>	<i>gsk</i>	<i>emiA</i>		<i>citF2</i>			<i>dsdC</i>	
<i>hisQ</i>	<i>gpmB</i>	<i>dniR</i>		<i>citF</i>			<i>dpiA</i>	
<i>hisP</i>	<i>gpmA</i>	<i>dgoA</i>		<i>citD2</i>			<i>dinG</i>	
<i>hisM</i>	<i>gntU</i>	<i>dgkA</i>		<i>citD</i>			<i>dgoR</i>	
<i>hisJ</i>	<i>gntT</i>	<i>dllB</i>		<i>citC2</i>			<i>dcur</i>	
<i>hisI</i>	<i>gntK</i>	<i>dllA</i>		<i>caiB</i>			<i>cyrR</i>	
<i>hisH</i>	<i>gnd</i>	<i>ddg</i>		<i>bisC</i>			<i>cysB</i>	
<i>hisG</i>	<i>gixK</i>	<i>dadX</i>		<i>atpI</i>			<i>cueR</i>	
<i>hisF</i>	<i>gipX</i>	<i>dacD</i>		<i>atpH</i>			<i>cspE</i>	
<i>hisD</i>	<i>gipT</i>	<i>dacC</i>		<i>atpG</i>			<i>cspD</i>	
<i>hisC</i>	<i>gipF</i>	<i>dacB</i>		<i>atpF</i>			<i>cspC</i>	
<i>hisB</i>	<i>gfk</i>	<i>dacA</i>		<i>atpE</i>			<i>cspB</i>	
<i>gsp</i>	<i>gigY</i>	<i>csgG</i>		<i>atpD</i>			<i>csiE</i>	
<i>glyA</i>	<i>gigP</i>	<i>cfa</i>		<i>atpC</i>			<i>csgD</i>	
<i>gltS</i>	<i>gigB</i>	<i>caiT</i>		<i>atpB</i>			<i>cobB</i>	
<i>gltL</i>	<i>gigA</i>	<i>blc</i>		<i>atpA</i>			<i>celD</i>	
<i>gltK</i>	<i>gip</i>	<i>asmA</i>		<i>astD</i>			<i>cdaR</i>	
<i>gltJ</i>	<i>ghmA</i>	<i>amiC</i>		<i>asrC</i>			<i>cadC</i>	
<i>gltI</i>	<i>gcd</i>	<i>amiB</i>		<i>asrA</i>			<i>asnC</i>	
<i>gltD</i>	<i>garL</i>	<i>amiA</i>		<i>alld</i>			<i>araC</i>	
<i>glpB</i>	<i>garK</i>	<i>alr</i>		<i>aldB</i>			<i>allR</i>	
<i>gloA</i>	<i>garD</i>	<i>acrE</i>		<i>adhE</i>			<i>agaR</i>	
<i>glnQ</i>	<i>gapA</i>	<i>acrA</i>		<i>acnB</i>			<i>adiY</i>	
<i>glnP</i>	<i>galP</i>	STM4540		<i>acnA</i>			<i>acrR</i>	
<i>glnK</i>	<i>galM</i>	STM4539		<i>ackA</i>			STM4423	
<i>glnH</i>	<i>fucU</i>	STM4510		<i>aceF</i>			STM4417	
<i>glnB</i>	<i>fucK</i>	STM4272		<i>aceE</i>			STM4320	
<i>glnA</i>	<i>fucI</i>	STM4260		<i>aceB</i>			STM4318	
<i>ggt</i>	<i>fucA</i>	STM4259		<i>aceA</i>			<i>rfsA</i>	
<i>gdhA</i>	<i>fsr</i>	STM4217		STM4519			<i>rfsB</i>	
<i>gevT</i>	<i>frwD</i>	STM4205		STM4421			STM4270	
<i>gevR</i>	<i>frwC</i>	STM4102		STM4306			STM4068	
<i>gevP</i>	<i>frwB</i>	STM3833		STM4305			STM4033	
<i>gevH</i>	<i>fruK</i>	STM3697		STM4044			STM3834	
<i>gabT</i>	<i>fruF</i>	STM3601		STM3529			STM3794	
<i>gabP</i>	<i>fbp</i>	STM3038		STM3355			STM3785	
<i>flhY</i>	<i>fbaB</i>	STM3031		STM3354			STM3778	
<i>eutT</i>	<i>fba</i>	STM2914		STM3129			STM3773	
<i>eutS</i>	<i>eno</i>	STM2756		STM3118			STM3736	
<i>eutQ</i>	<i>emrD</i>	STM2692		STM3081			STM3696	

<i>Amino acid transport and metabolism</i>	<i>Carbohydrate transport and metabolism</i>	<i>Cell envelope biogenesis and outer membrane</i>	<i>Cell motility and secretion</i>	<i>Energy production and conversion</i>	<i>Inorganic iron transport and metabolism</i>	<i>Surface Structures</i>	<i>Transcription</i>	<i>Translation, ribosomal structure and biogenesis</i>
<i>eupP</i>	<i>emrB</i>	STM2690		STM2963			STM3681	
<i>eutL</i>	<i>ego</i>	STM2591		STM2840			STM3678	
<i>eutJ</i>	<i>eda</i>	STM1940		STM2530			STM3653	
<i>eutH</i>	<i>dsdX</i>	STM1910		STM2529			STM3651	
<i>eutC</i>	<i>dgoT</i>	STM1836		STM2527			STM3633	
<i>eutB</i>	<i>dgoK</i>	STM1540		STM2406			STM3602	
<i>eutA</i>	<i>deoB</i>	STM1530		STM1793			STM3533	
<i>dsdA</i>	<i>orr</i>	STM1493		STM1792			STM3358	
<i>dppD</i>	<i>cobC</i>	STM1260		STM1789			STM3357	
<i>dppC</i>	<i>cite2</i>	STM1043		STM1788			STM3262	
<i>dppB</i>	<i>cite</i>	STM0932		STM1787			STM3175	
<i>dppA</i>	<i>citA</i>	STM0818		STM1786			STM3124	
<i>dcp</i>	<i>celF</i>	STM0725		STM1627			STM3121	
<i>dapF</i>	<i>celC</i>	STM0721		STM1620			STM3098	
<i>dapE</i>	<i>celB</i>	STM0719		STM1556			STM3084	
<i>dapB</i>	<i>bglX</i>	STM0573		STM1539			STM3025	
<i>dapA</i>	<i>bglA</i>	STM0572		STM1538			STM3020	
<i>dada</i>	<i>bcsC</i>	STM0509		STM1537			STM3012	
<i>cysZ</i>	<i>ber</i>	STM0352		STM1536			STM2955	
<i>cysM</i>	<i>araJ</i>	STM0350		STM1533			STM2920	
<i>cysK</i>	<i>araE</i>	STM0346		STM1499			STM2912	
<i>cysH</i>	<i>araD</i>	STM0306		STM1498			STM2905	
<i>cysE</i>	<i>ampA</i>	STM0292		STM1459			STM2803	
<i>cysD</i>	<i>ampG</i>			STM1261			STM2797	
<i>cysA</i>		STM4538		STM1253			STM2749	
<i>csdA</i>		STM4537		STM0858			STM2748	
<i>cobD</i>		STM4536		STM0856			STM2744	
<i>carA</i>		STM4535		STM0855			STM2738	
<i>cadB</i>		STM4448		STM0762			STM2575	
<i>cadA</i>		STM4436		STM0761			STM2374	
<i>brnQ</i>		STM4435		STM0691			STM2361	
<i>avfA</i>		STM4434		STM0612			STM2345	
<i>astE</i>	<i>iolH</i>			STM0611			STM2281	
<i>astC</i>	<i>iolI2</i>			STM0564			STM2275	
<i>astB</i>	<i>iolG2</i>			STM0361			STM2230	
<i>astA</i>	<i>iolD</i>			STM0360			STM2180	
<i>aspC</i>	<i>iolC</i>			STM0057			STM1857	
<i>aspA</i>	STM4428			STM0056			STM1677	
<i>asnB</i>	<i>iolI1</i>						STM1674	
<i>asnA</i>	<i>iolG1</i>						STM1671	
<i>asd</i>	<i>iolE</i>						STM1664	
<i>arlQ</i>	<i>iolA</i>						STM1619	
<i>arlP</i>	<i>iolB</i>						STM1618	

<i>Amino acid transport and metabolism</i>	<i>Carbohydrate transport and metabolism</i>	<i>Cell envelope biogenesis and outer membrane</i>	<i>Cell motility and secretion</i>	<i>Energy production and conversion</i>	<i>Inorganic iron transport and metabolism</i>	<i>Surface Structures</i>	<i>Transcription</i>	<i>Translation, ribosomal structure and biogenesis</i>
<i>arlM</i>	<i>tolI2</i>						STM1575	
<i>arlI</i>	<i>tolI1</i>						STM1555	
<i>aroP</i>	STM4412						STM1547	
<i>aroL</i>	STM4080						STM1541	
<i>aroK</i>	STM4066						STM1265	
<i>aroH</i>	STM4065						STM1243	
<i>aroG</i>	STM4054						STM1127	
<i>aroF</i>	STM4053						STM1082	
<i>aroE</i>	STM4052						STM1012	
<i>aroD</i>	STM3858						STM1001	
<i>aroC</i>	STM3832						STM0952	
<i>aroB</i>	STM3793						STM0900	
<i>aroA</i>	STM3792						STM0898A	
<i>argT</i>	STM3784						STM0898	
<i>argR</i>	STM3783						STM0859	
<i>argI</i>	STM3782						STM0835	
<i>argG</i>	STM3781						STM0764	
<i>argE</i>	STM3780						STM0763	
<i>argD</i>	STM3779						STM0692	
<i>argC</i>	STM3775						STM0652	
<i>argB</i>	STM3772						STM0581	
<i>argA</i>	STM3771						STM0580	
<i>arcC</i>	STM3770						STM0571	
<i>ansP</i>	STM3769						STM0410	
<i>ansB</i>	STM3698						STM0363	
<i>ansA</i>	STM3600						STM0354	
<i>allC</i>	STM3547						STM0347	
<i>aegA</i>	STM3260						STM0333	
<i>adi</i>	STM3259						STM0164	
STM4467	STM3258						STM0052	
STM4466	STM3257						STM0031	
STM4465	STM3256						STM0030	
STM4463	STM3255						STM0029	
STM4446	STM3254						STM0017	
STM4431	STM3253						STM0014	
STM4351	STM3251							
STM4042A	STM3170							
STM4042	STM3169							
STM3859	STM3137							
STM3796A	STM3136							
STM3768	STM3134							
STM3598	STM3132							

<i>Amino acid transport and metabolism</i>	<i>Carbohydrate transport and metabolism</i>	<i>Cell envelope biogenesis and outer membrane</i>	<i>Cell motility and secretion</i>	<i>Energy production and conversion</i>	<i>Inorganic ion transport and metabolism</i>	<i>Surface Structures</i>	<i>Transcription</i>	<i>Translation, ribosomal structure and biogenesis</i>
STM3532	STM3120							
STM3261	STM3083							
STM3128	STM2959							
STM3126	STM2913							
STM3117	STM2911							
STM3082	STM2758							
STM3022	STM2757							
STM2360	STM2755							
STM2359	STM2752							
STM2358	STM2751							
STM2357	STM2750							
STM2197	STM2668							
STM2196	STM2574							
STM2186	STM2570							
STM1795	STM2492							
STM1636	STM2405							
STM1635	STM2372							
STM1634	STM2344							
STM1633	STM2343							
STM1557	STM2341							
STM1542	STM2340							
STM1494	STM2303							
STM1492	STM2302							
STM1491	STM2300							
STM1484	STM2289							
STM1269	STM2280							
STM1259	STM2274							
STM1257	STM2198							
STM1256	STM2179							
STM1255	STM1933							
STM1128	STM1843							
STM1003	STM1617							
STM1002	STM1616							
STM0458	STM1614							
STM0330	STM1613							
STM0329	STM1612							
	STM1560							
	STM1559							
	STM1558							
	STM1545							
	STM1543							
	STM1252							
	STM1132							

<i>Amino acid transport and metabolism</i>	<i>Carbohydrate transport and metabolism</i>	<i>Cell envelope biogenesis and outer membrane</i>	<i>Cell motility and secretion</i>	<i>Energy production and conversion</i>	<i>Inorganic ion transport and metabolism</i>	<i>Surface Structures</i>	<i>Transcription</i>	<i>Translation, ribosomal structure and biogenesis</i>
	STM1129							
	STM0885							
	STM0868							
	STM0860							
	STM0854							
	STM0723							
	STM0722							
	STM0650							
	STM0649							
	STM0577							
	STM0576							
	STM0575							
	STM0574							
	STM0520							
	STM0382							
	STM0356							
	STM0257							
	STM0212							
	STM0149							
	STM0042							
	STM0041							
	STM0018							

Table S2 B. COG categories.

<i>Drug analogue and resistance</i>	<i>Aerobic metabolism</i>	<i>Flagella and chemotaxis</i>	<i>Lipid metabolism</i>	<i>Oxidative Phosphorylation</i>	<i>Protein Transport</i>	<i>Nucleotide metabolism</i>	<i>Regulators</i>	<i>Signal transduction</i>
<i>yggT</i>	<i>yglI</i>	<i>yeaJ</i>	<i>yqef</i>	<i>cyoC</i>	<i>secB</i>	<i>yjce</i>	<i>zur</i>	<i>yojN</i>
<i>ygeD</i>	<i>tdcD</i>	<i>isy</i>	<i>yndC</i>	<i>cyoB</i>	<i>secA</i>	<i>yggV</i>	<i>znr</i>	<i>ynaF</i>
<i>ygeA</i>	<i>tdcC</i>	<i>trg</i>	<i>yihU</i>	<i>cyoA</i>	<i>secY</i>	<i>yfhC</i>	<i>yiaJ</i>	<i>yiaB</i>
<i>ybbM</i>	<i>nyfG</i>	<i>tcp</i>	<i>yihG</i>	<i>cydA</i>	<i>secE</i>	<i>yfeJ</i>	<i>xapR</i>	<i>yjiQ</i>
<i>tebB</i>	<i>nyfE</i>	<i>moaB</i>	<i>yhbT</i>	<i>cydB</i>	<i>secG</i>	<i>yelA</i>	<i>wzzE</i>	<i>yjiY</i>
<i>tehA</i>	<i>nyfD</i>	<i>moaA</i>	<i>yebJ</i>	<i>ppk</i>	<i>secD</i>	<i>ybeK</i>	<i>wzzB</i>	<i>yjyC</i>
<i>shnA</i>	<i>nyfC</i>	<i>lhaA</i>	<i>yjfg</i>	<i>ppa</i>	<i>secF</i>	<i>ybbY</i>	<i>uxuR</i>	<i>yjikK</i>
<i>sanA</i>	<i>nyfB</i>	<i>lppB</i>	<i>yfjG</i>	<i>sdhC</i>	<i>secF</i>	<i>xapA</i>	<i>uxuR</i>	<i>yjihH</i>
<i>pmrD</i>	<i>nyfA</i>	<i>fliz</i>	<i>yfjY</i>	<i>sdhD</i>	<i>yqC</i>	<i>uraA</i>	<i>uhpA</i>	<i>yhibB</i>
<i>nyfB</i>	<i>nyfG</i>	<i>fliy</i>	<i>yegS</i>	<i>sdhA</i>	<i>yidC</i>	<i>upp</i>	<i>trpR</i>	<i>yhdaA</i>
<i>marR</i>	<i>nyfD</i>	<i>flit</i>	<i>ydiO</i>	<i>sdhB</i>	<i>lepB</i>	<i>udp</i>	<i>torT</i>	<i>ygiY</i>
<i>marB</i>	<i>narX</i>	<i>flis</i>	<i>ydlr</i>	<i>flil</i>	<i>kspA</i>	<i>udk</i>	<i>torR</i>	<i>ygiX</i>
<i>marA</i>	<i>narL</i>	<i>flir</i>	<i>ydlD</i>	<i>nuoN</i>	<i>fjy</i>	<i>tnk</i>	<i>tdcA</i>	<i>ygiM</i>
<i>ksgA</i>	<i>naph</i>	<i>fliq</i>	<i>yclA</i>	<i>nuoM</i>	<i>ybeC</i>	<i>thyA</i>	<i>sfpA</i>	<i>yfin</i>
<i>emrD</i>	<i>nagG</i>	<i>flip</i>	<i>ybyG</i>	<i>nuoL</i>	<i>tatA</i>	<i>thg</i>	<i>sspA</i>	<i>yfhK</i>
<i>emrB</i>	<i>nagF</i>	<i>flio</i>	<i>ybhO</i>	<i>nuoK</i>	<i>tatB</i>	<i>tdk</i>	<i>soxS</i>	<i>yjfaA</i>
<i>emrA</i>	<i>nagD</i>	<i>flin</i>	<i>yqfH</i>	<i>nuoJ</i>	<i>tatC</i>	<i>rthC</i>	<i>soxR</i>	<i>yfeA</i>
<i>bcr</i>	<i>nagC</i>	<i>flim</i>	<i>ushB</i>	<i>nuoI</i>	<i>tatE</i>	<i>pyrI</i>	<i>sfpA</i>	<i>yehU</i>
<i>bacA</i>	<i>nagB</i>	<i>flil</i>	<i>upps</i>	<i>nuoH</i>		<i>pyrH</i>	<i>sfsA</i>	<i>yecG</i>
<i>ampG</i>	<i>nagA</i>	<i>flik</i>	<i>tesB</i>	<i>nuoG</i>		<i>pyrG</i>	<i>seqA</i>	<i>yebR</i>
<i>ampe</i>	<i>hybG</i>	<i>flj</i>	<i>sseJ</i>	<i>nuoF</i>		<i>pyrF</i>	<i>rslA</i>	<i>yeaJ</i>
<i>acrR</i>	<i>hybF</i>	<i>flj</i>	<i>sbmA</i>	<i>nuoE</i>		<i>pyrE</i>	<i>rsd</i>	<i>yeaG</i>
<i>acrF</i>	<i>hybE</i>	<i>flih</i>	<i>psaA</i>	<i>nuoE</i>		<i>pyrD</i>	<i>rpoS</i>	<i>ydliv</i>
<i>acrA</i>	<i>hybD</i>	<i>flig</i>	<i>psd</i>	<i>nuoA</i>		<i>pyrB</i>	<i>tnk</i>	<i>ydaA</i>
	<i>hybC</i>	<i>flie</i>	<i>prpe</i>	<i>nuoA</i>		<i>purU</i>	<i>rhadR</i>	<i>yelR</i>
	<i>hybB</i>	<i>flie</i>	<i>plsX</i>	<i>nuoA</i>		<i>purT</i>	<i>rfalI</i>	<i>ybil</i>
	<i>hybA</i>	<i>flid</i>	<i>plsC</i>	<i>nuoA</i>		<i>purM</i>	<i>rcsF</i>	<i>ybdQ</i>
	<i>gpcC</i>	<i>flid</i>	<i>plsB</i>	<i>nuoA</i>		<i>purM</i>	<i>rcsB</i>	<i>yatC</i>
	<i>gspb</i>	<i>flia</i>	<i>pldB</i>	<i>nuoA</i>		<i>purK</i>	<i>rcsA</i>	<i>wzb</i>
	<i>gfpA</i>	<i>flie</i>	<i>phoN</i>	<i>nuoA</i>		<i>purH</i>	<i>rbsR</i>	<i>uvrY</i>
	<i>fumB</i>	<i>flhd</i>	<i>pgsA</i>	<i>nuoA</i>		<i>purG</i>	<i>purR</i>	<i>uspA</i>
	<i>frdD</i>	<i>flhc</i>	<i>pgpB</i>	<i>nuoA</i>		<i>purF</i>	<i>phoU</i>	<i>uhpB</i>
	<i>frdC</i>	<i>flhb</i>	<i>oofA</i>	<i>nuoA</i>		<i>purE</i>	<i>phoP</i>	<i>uhpA</i>
	<i>frdB</i>	<i>flhA</i>	<i>menE</i>	<i>nuoA</i>		<i>purD</i>	<i>oxyR</i>	<i>typA</i>
	<i>frdA</i>	<i>flgN</i>	<i>lytB</i>	<i>nuoA</i>		<i>purC</i>	<i>osmE</i>	<i>trS</i>
	<i>fdnI</i>	<i>flgM</i>	<i>ispF</i>	<i>nuoA</i>		<i>purB</i>	<i>oraA</i>	<i>trrR</i>
	<i>fdnI</i>	<i>flgI</i>	<i>ispD</i>	<i>nuoA</i>		<i>purA</i>	<i>nlp</i>	<i>torS</i>
	<i>fdnG</i>	<i>flgK</i>	<i>ipk</i>	<i>nuoA</i>		<i>prxA</i>	<i>nikR</i>	<i>torR</i>
	<i>dnmsC</i>	<i>flgJ</i>	<i>idi</i>	<i>nuoA</i>		<i>pps</i>	<i>nagC</i>	<i>tcle</i>
	<i>dnmsB</i>	<i>flgI</i>	<i>iacP</i>	<i>nuoA</i>		<i>nupC</i>	<i>nadr</i>	<i>tcld</i>
	<i>dnmsA</i>	<i>flgH</i>	<i>glxR</i>	<i>nuoA</i>		<i>mdl</i>	<i>mlr</i>	<i>ssrB</i>
	<i>deuB</i>	<i>flgG</i>	<i>gcpE</i>	<i>nuoA</i>			<i>modE</i>	<i>ssrA</i>

Drug analogue and resistance	Anaerobic metabolism	Flagella and chemotaxis	Lipid metabolism	Oxidative Phosphorylation	Protein Transport	Nucleotide metabolism	Regulators	Signal transduction
<i>dcaA</i>		<i>flgF</i>	<i>garR</i>			<i>nrdF</i>	<i>metR</i>	<i>spoT</i>
<i>cadC</i>		<i>flgE</i>	<i>fadL</i>			<i>nrdD</i>	<i>metJ</i>	<i>sixA</i>
<i>cadB</i>		<i>flgD</i>	<i>fadD</i>			<i>nrdB</i>	<i>marR</i>	<i>rtm</i>
<i>cadA</i>		<i>flgC</i>	<i>fadB</i>			<i>nrdA</i>	<i>marA</i>	<i>rtcR</i>
<i>asrC</i>		<i>flgB</i>	<i>fadA</i>			<i>ndk</i>	<i>lytB</i>	<i>rstB</i>
<i>asrB</i>		<i>flgA</i>	<i>fabZ</i>			<i>miaE</i>	<i>lysR</i>	<i>rstA</i>
<i>asrA</i>		<i>cheZ</i>	<i>fabI</i>			<i>hpt</i>	<i>luxS</i>	<i>rseC</i>
<i>aer</i>		<i>cheY</i>	<i>fabH</i>			<i>guaC</i>	<i>lrp</i>	<i>rseB</i>
STM4307		<i>cheW</i>	<i>fabF</i>			<i>guaA</i>	<i>lthA</i>	<i>rseA</i>
STM4306		<i>cheR</i>	<i>fabD</i>			<i>gpt</i>	<i>lexA</i>	<i>relA</i>
STM4305		<i>cheM</i>	<i>fabB</i>			<i>gmk</i>	<i>ihvY</i>	<i>rscC</i>
STM3599		<i>cheB</i>	<i>fabA</i>			<i>dut</i>	<i>idhR</i>	<i>rscB</i>
STM2530		<i>cheA</i>	<i>dxr</i>			<i>dgt</i>	<i>iclR</i>	<i>pisP</i>
STM2529		<i>aer</i>	<i>cls</i>			<i>deoD</i>	<i>iciA</i>	<i>pspF</i>
STM2528		STM4258	<i>cdsA</i>			<i>deoC</i>	<i>icc</i>	<i>prpR</i>
STM1497		STM4210	<i>caiD</i>			<i>deoA</i>	<i>hycA</i>	<i>prpA</i>
STM0761		STM3670	<i>caiC</i>			<i>dcd</i>	<i>hupB</i>	<i>proQ</i>
STM0612		STM3152	<i>apeE</i>			<i>cyaA</i>	<i>hupA</i>	<i>pphB</i>
		STM3138	<i>aes</i>			<i>cpdB</i>	<i>higA</i>	<i>phoR</i>
		STM2314	<i>acpS</i>			<i>cmk</i>	<i>hms</i>	<i>phoQ</i>
		STM1657	<i>acpD</i>			<i>cdd</i>	<i>himD</i>	<i>phoP</i>
			<i>accD</i>			<i>apt</i>	<i>himA</i>	<i>phoL</i>
			<i>accC</i>			<i>allP</i>	<i>hba</i>	<i>phoH</i>
			<i>accB</i>			<i>allB</i>	<i>hfk</i>	<i>phoB</i>
			<i>accA</i>			<i>allA</i>	<i>hflC</i>	<i>pgtB</i>
			<i>aas</i>			<i>adk</i>	<i>gutM</i>	<i>pgtA</i>
			STM4032			<i>add</i>	<i>gntR</i>	<i>ompR</i>
			STM3595			STM4104	<i>narX</i>	<i>narX</i>
			STM3119			STM3631	<i>glpR</i>	<i>narQ</i>
			STM1623			STM3334	<i>glnK</i>	<i>narQ</i>
			STM0857			STM3333	<i>glnB</i>	<i>narP</i>
			STM0055			STM3167	<i>gcvR</i>	<i>narL</i>
						STM1330	<i>gcvA</i>	<i>luxS</i>
						STM0033	<i>galS</i>	<i>kdpE</i>
							<i>galR</i>	<i>kdpD</i>
							<i>fur</i>	<i>hydH</i>
							<i>fruR</i>	<i>hydG</i>
							<i>fur</i>	<i>hnr</i>
							<i>fliS</i>	<i>glnG</i>
							<i>fliA</i>	<i>fnr</i>
							<i>flhD</i>	<i>fimZ</i>
							<i>flhC</i>	<i>envZ</i>
							<i>fis</i>	<i>dpiB</i>
							<i>fadR</i>	<i>dkxA</i>

<i>Drug analogue and resistance</i>	<i>Anaerobic metabolism</i>	<i>Flagella and chemotaxis</i>	<i>Lipid metabolism</i>	<i>Oxidative Phosphorylation</i>	<i>Protein Transport</i>	<i>Nucleotide metabolism</i>	<i>Regulators</i>	<i>Signal transduction</i>
							<i>envR</i>	<i>dcuS</i>
							<i>emrR</i>	<i>csiA</i>
							<i>eco</i>	<i>csrA</i>
							<i>dsrB</i>	<i>crp</i>
							<i>dgoR</i>	<i>creC</i>
							<i>gyrR</i>	<i>creB</i>
							<i>csrA</i>	<i>cpXR</i>
							<i>cspe</i>	<i>cpxA</i>
							<i>crp</i>	<i>cops</i>
							<i>grl</i>	<i>copr</i>
							<i>creB</i>	<i>chey</i>
							<i>qpXP</i>	<i>bolA</i>
							<i>cheZ</i>	<i>bgIJ</i>
							<i>chey</i>	<i>bass</i>
							<i>cheW</i>	<i>basR</i>
							<i>cheR</i>	<i>barA</i>
							<i>chaB</i>	<i>brcS</i>
							<i>caif</i>	<i>baeR</i>
							<i>bitA</i>	<i>arcB</i>
							<i>bgIJ</i>	<i>arcA</i>
							<i>bass</i>	<i>aer</i>
							<i>basR</i>	<i>aceK</i>
							<i>baeR</i>	STM451
							<i>asnC</i>	STM4534
							<i>argR</i>	STM3388
							<i>allR</i>	STM2731
							<i>agaR</i>	STM2503
							<i>acrR</i>	STM2314
								STM1987
								STM1827
								STM1697
								STM0561
								STM0343
								STM0053

Table S3 A. COG organized DE genes.

<i>Amino acid transport and metabolism</i>	<i>Anaerobic metabolism</i>	<i>Surface structures</i>	<i>Cell motility and secretion</i>	<i>Energy production and conversion</i>	<i>Flagella and chemotaxis</i>	<i>Inorganic iron transport and metabolism</i>
STM1491	STM1497	<i>sfjG</i>	<i>sfjG</i>	STM4305	<i>flgF</i>	<i>fhuA</i>
STM1494	STM4305	<i>stbA</i>	<i>stbA</i>	<i>fumB</i>	<i>trg</i>	<i>fes</i>
STM1633	<i>fumB</i>	<i>sfjC</i>	<i>ssaC</i>	STM4306	<i>fliJ</i>	STM0765
STM1635	<i>dcuB</i>	<i>stcA</i>	<i>ssaN</i>	<i>napF</i>	<i>flgD</i>	<i>ydiE</i>
<i>oat</i>	<i>dmsC</i>	<i>flgF</i>	<i>sfjC</i>	<i>citF</i>	<i>flgE</i>	<i>sseA</i>
STM1256	STM4306	<i>fliJ</i>	<i>stcA</i>	<i>nemA</i>	<i>flgC</i>	<i>bfd</i>
STM1257	<i>napF</i>	<i>flgD</i>	<i>flgF</i>	<i>ysaA</i>	<i>flgG</i>	<i>nrfA</i>
<i>pepI</i>	STM4307	<i>flgE</i>	<i>trg</i>	STM2529	<i>fliS</i>	<i>napD</i>
<i>aegA</i>	<i>nrfA</i>	<i>flgC</i>	<i>fliJ</i>	<i>hybA</i>	<i>cheB</i>	<i>citT</i>
<i>pepE</i>	<i>napD</i>	<i>flgD</i>	<i>flgD</i>	<i>citD</i>	<i>fliK</i>	<i>modB</i>
<i>hpaF</i>	<i>nrdD</i>	<i>flgG</i>	<i>flgE</i>	STM2530	<i>fliO</i>	<i>nirD</i>
<i>ansB</i>	<i>hybG</i>	<i>fliS</i>	<i>flgE</i>	<i>pta</i>	<i>fliT</i>	<i>modC</i>
<i>glpB</i>	STM2529	<i>fliK</i>	<i>flgC</i>	<i>dcuC</i>	<i>fliQ</i>	STM2446
<i>gdhA</i>	<i>hybA</i>	<i>fliT</i>	<i>flgG</i>	<i>frdA</i>	<i>fliQ</i>	STM3074
<i>ansA</i>	STM2530	<i>fliQ</i>	<i>cheB</i>	<i>frdA</i>	<i>fliN</i>	<i>modA</i>
<i>argI</i>	<i>hybF</i>	<i>fliN</i>	<i>fliK</i>	<i>frdA</i>	<i>fliF</i>	<i>cbiM</i>
<i>lysC</i>	STM2530	<i>fliN</i>	<i>fliO</i>	<i>hybD</i>	<i>fliG</i>	
<i>pduI</i>	<i>hybB</i>	<i>fliQ</i>	<i>fliQ</i>	<i>frdC</i>	<i>fliC</i>	
<i>proX</i>	<i>hybE</i>	<i>fliF</i>	<i>fliO</i>	<i>napB</i>	<i>tcp</i>	
<i>eutP</i>	<i>frdB</i>	<i>fliC</i>	<i>fliN</i>	STM2527	<i>cheA</i>	
<i>argG</i>	<i>frdA</i>	<i>flgH</i>	<i>fliG</i>	<i>ackA</i>	<i>flgH</i>	
<i>dppC</i>	<i>hybD</i>	<i>flgI</i>	<i>fliC</i>	<i>ackA</i>	<i>flgI</i>	
<i>dppD</i>	<i>nrdG</i>	<i>fliM</i>	<i>cheA</i>	<i>nuoJ</i>	<i>fliM</i>	
<i>livJ</i>	<i>frdC</i>	<i>flgN</i>	<i>flgH</i>	<i>hybC</i>	<i>flgN</i>	
	<i>glpB</i>	<i>fliH</i>	<i>flgI</i>	<i>nuoM</i>	<i>flgN</i>	
	<i>napB</i>	<i>fliD</i>	<i>fliM</i>	<i>glpA</i>	<i>fliH</i>	
	<i>aer</i>	<i>flgM</i>	<i>fliN</i>	<i>nuoN</i>	<i>fliD</i>	
	<i>hybC</i>	<i>fliI</i>	<i>fliH</i>	<i>narJ</i>	<i>flgM</i>	
	STM2528	<i>flgJ</i>	<i>fliD</i>	<i>nuoK</i>	<i>fliI</i>	
	<i>glpC</i>	<i>flgB</i>	<i>fliI</i>	<i>nirB</i>	<i>cheR</i>	
	<i>frdD</i>	<i>flgL</i>	<i>cheR</i>	<i>hypO</i>	<i>flgJ</i>	
	<i>napG</i>	<i>fliA</i>	<i>flgB</i>	<i>nuoE</i>	<i>flgB</i>	
		<i>flgA</i>	<i>flgL</i>	<i>nuoH</i>	<i>flgL</i>	
		<i>flgK</i>	<i>cheZ</i>	<i>nuoL</i>	<i>cheZ</i>	
		<i>fliE</i>	<i>cheW</i>	<i>glpC</i>	<i>cheM</i>	
		<i>fliL</i>	<i>flgA</i>	<i>nuoI</i>	<i>fliA</i>	
		<i>fliP</i>	<i>flgA</i>	<i>pduQ</i>	<i>cheW</i>	
		<i>csxB</i>	<i>fliB</i>	<i>nuoG</i>	<i>flgA</i>	
		<i>fimC</i>	<i>flgK</i>	<i>nuoF</i>	<i>flgK</i>	
		<i>fliR</i>	<i>fliE</i>	<i>frdD</i>	<i>fliE</i>	
		<i>fliC</i>	<i>fliL</i>	<i>nuoA</i>	<i>fliL</i>	
			<i>motA</i>	<i>pduS</i>	<i>motA</i>	
			<i>fliP</i>	<i>nuoC</i>	<i>fliZ</i>	
			<i>motB</i>	<i>dctA</i>	<i>cheY</i>	

<i>Amino acid transport and metabolism</i>	<i>Anaerobic metabolism</i>	<i>Surface structures</i>	<i>Cell motility and secretion</i>	<i>Energy production and conversion</i>	<i>Flagella and chemotaxis</i>	<i>Inorganic iron transport and metabolism</i>
			STM3216	<i>puuA</i> <i>nuoB</i>	<i>flhB</i> <i>flhP</i> <i>moiB</i>	
			<i>tsr</i> <i>fimC</i> STM1657		<i>tsr</i> STM2314	
			<i>flrR</i> STM3152		<i>aer</i> STM1657	
					<i>flrR</i> STM3152	
					<i>flhC</i>	

Table S3 B. COG organized DE genes.

<i>Oxidative phosphorylation</i>	<i>Regulators</i>	<i>Signal transduction</i>	<i>Transcription</i>	<i>Lipid metabolism</i>	<i>Nucleotide metabolism</i>	<i>Cell envelope biogenesis and outer membrane</i>	<i>Carbohydrate transport and metabolism</i>
<i>flfI</i>	<i>eco</i>	<i>ssrA</i>	STM1265	<i>sscl</i>	<i>nrpD</i>	<i>pagC</i>	STM0577
<i>frdB</i>	<i>fls</i>	<i>yhjH</i>	<i>yncC</i>	<i>yihU</i>		STM1493	<i>pagO</i>
<i>frdA</i>	<i>cheR</i>	<i>cheY</i>	<i>yhcO</i>	<i>yhbT</i>		<i>pgtE</i>	<i>otsB</i>
<i>frdC</i>	<i>cheZ</i>	STM2314	<i>yiaG</i>			<i>figJ</i>	STM3132
<i>nuoJ</i>	<i>flaA</i>	<i>aer</i>	<i>phnO</i>				<i>garL</i>
<i>nuoM</i>	<i>cheW</i>	<i>yjiQ</i>	<i>flgM</i>				<i>yiaO</i>
<i>nuoN</i>	<i>cheY</i>	STM2503	<i>flaA</i>				<i>yadI</i>
<i>nuoK</i>	<i>hycA</i>	<i>ydaA</i>	<i>ydhM</i>				<i>pmgI</i>
<i>nuoE</i>	<i>flhC</i>						<i>ctfE</i>
<i>nuoH</i>							<i>kdgK</i>
<i>nuoL</i>							STM1613
<i>nuoI</i>							<i>sgaB</i>
<i>nuoG</i>							<i>pykA</i>
<i>nuoF</i>							<i>glpX</i>
<i>frdD</i>							STM2343
<i>nuoA</i>							STM3254
<i>nuoB</i>							STM3792

Appendix III

Table S4. ChIP-seq peaks: FNR binding.

<i>Genes associated with peak^a</i>	<i>Chr.^b</i>	<i>Peak</i>	
		<i>Start</i>	<i>End</i>
<i>repY, repZ</i>	pCol1B9SL1344	0	484
<i>yaeA, yaeB, yafA</i>	pCol1B9SL1344	4321	5743
<i>yafB, yagA</i>	pCol1B9SL1344	6037	7620
<i>cib</i>	pCol1B9SL1344	7696	8638
<i>imm, ybaA</i>	pCol1B9SL1344	9141	10730
SLP2_0018, <i>parA</i> , SLP2_0020	pCol1B9SL1344	13879	14877
<i>stbA</i>	pCol1B9SL1344	15184	16230
<i>trbA, pndC, pndA</i>	pCol1B9SL1344	41332	41922
SLP2_0054A, <i>exc</i>	pCol1B9SL1344	42304	46277
<i>traH, traG</i>	pCol1B9SL1344	65594	66734
<i>traF, traE</i>	pCol1B9SL1344	67156	68931
<i>rci, shfB, shfB, shfC</i>	pCol1B9SL1344	69768	71125
<i>pilV, pilU, pilT, pilS, pilR</i>	pCol1B9SL1344	72184	75372
<i>pilQ, pilP</i>	pCol1B9SL1344	76195	77489
<i>pilO</i>	pCol1B9SL1344	78047	78880
<i>pilL, pilK, pilJ</i>	pCol1B9SL1344	81610	82899
<i>trcD</i>	pCol1B9SL1344	83434	84254
<i>traB, traA</i>	pCol1B9SL1344	84936	86908
<i>traT, traS</i>	pSLTSL1344	10573	11429
<i>traV, trbD</i>	pSLTSL1344	26993	27311
<i>traA, traY, traJ, traM</i>	pSLTSL1344	31179	32898
<i>finP</i>	pSLTSL1344	33815	34895
<i>parB, parA, samB</i>	pSLTSL1344	47671	50469
PSLT042, <i>spvR</i>	pSLTSL1344	60927	62144
<i>spvC, spvD</i>	pSLTSL1344	65036	67651
<i>ccdA</i> , PSLT026, PSLT025, <i>repA2</i>	pSLTSL1344	73726	76279
PSLT020, <i>pefB</i>	pSLTSL1344	78271	79352
<i>pefI</i>	pSLTSL1344	85147	85786
<i>repA, tap, repA3, repC</i>	pSLTSL1344	91908	92600
STnc890, STM0014, STM0015, STnc3200	ST4-74	14781	16510
STM0017, <i>chiA</i>	ST4-74	17164	18037
STM0020	ST4-74	23025	23494
<i>bcfA</i>	ST4-74	24008	24437
STM0029, STM0030, STM0031, STM0032	ST4-74	32306	35266
STM0034, STM0035	ST4-74	39372	40230
STM0042	ST4-74	51862	52359
<i>leuA, leuL, leuO</i>	ST4-74	133806	134595
<i>yaeH</i>	ST4-74	247525	247933
<i>sciF, sciG</i>	ST4-74	310765	311287
<i>sciK</i>	ST4-74	316285	316974
STM0277, STM0278, <i>sciK1</i>	ST4-74	317558	318812
SL1344_0286A, STM0292	ST4-74	335838	336360
<i>sciX, sciY, IsrA</i>	ST4-74	337188	338796
STM0295	ST4-74	339416	339923
<i>safA, safB</i>	ST4-74	341032	342393
<i>ybeJ</i>	ST4-74	346063	346501
<i>sinR</i>	ST4-74	347728	349037
<i>pagN</i>	ST4-74	349382	350495
STM0328	ST4-74	370613	371025
STM0334, STM0335	ST4-74	377298	378623
<i>stbA</i> , STM0341, STM0342, STnc1700, STM0343	ST4-74	384214	386526
STM0345, STM0346, STM0347, STM0348, STM0349	ST4-74	388882	391454

<i>Genes associated with peak^a</i>	<i>Chr.^b</i>	<i>Peak</i>	
		<i>Start</i>	<i>End</i>
<i>yaiB</i> , STnc4150	ST4-74	436424	437097
<i>tsx</i>	ST4-74	467672	468094
STM0438	ST4-74	490749	492761
<i>cyoA</i>	ST4-74	497570	498023
<i>rpmE2</i> , <i>rpmJa</i>	ST4-74	525766	526197
<i>maa</i> , <i>hha</i> , <i>ybaJ</i>	ST4-74	527332	528700
STM0497	ST4-74	556592	557400
<i>fimZ</i>	ST4-74	609785	611037
STM0551, <i>fimW</i>	ST4-74	611852	612931
STM0557	ST4-74	614288	616208
<i>gtrBa</i> , <i>gtrAa</i> , STnc1870	ST4-74	616736	617335
<i>ybdN</i> , <i>ybdO</i>	ST4-74	667293	668470
<i>citC</i> , <i>citA</i>	ST4-74	687093	687718
<i>cspE</i>	ST4-74	692120	692617
STM0719, STM0720, STM0721, STM0722, STM0723, STM0724, STM0725, STM0726, STM0727	ST4-74	783417	793157
<i>gltA</i> , STM0731, <i>sdhC</i>	ST4-74	796516	797389
<i>cydA</i>	ST4-74	807541	808981
STM0762, STM0763, STM0764, STM0765	ST4-74	825138	828930
<i>slrP</i>	ST4-74	865818	866532
<i>glnH</i>	ST4-74	896198	896612
STM0854, STM0855, STM0856, STM0857	ST4-74	925176	928619
STM0858	ST4-74	929008	930178
STM0859	ST4-74	931060	932097
<i>pflA</i> , STM0971, <i>sopD2</i>	ST4-74	1010045	1011678
<i>focA</i>	ST4-74	1014575	1015326
<i>ompF</i> , STnc3350	ST4-74	1047357	1048016
STM1001, <i>dpaL</i>	ST4-74	1050149	1050717
STM1003	ST4-74	1051463	1051983
STM1003	ST4-74	1052815	1053283
STM2622, STM1019, STM1020	ST4-74	1065164	1066458
<i>gtgA</i>	ST4-74	1070419	1071256
STM1054, <i>gtgE</i> , <i>gtgF</i>	ST4-74	1098722	1100020
<i>pipA</i> , <i>pipB</i> , STM1089, <i>pipC</i>	ST4-74	1132644	1134847
<i>sopB</i> , <i>orfX</i> , STM1093	ST4-74	1136105	1137136
STnc1880, STM1110	ST4-74	1153672	1154710
<i>phoH</i>	ST4-74	1169962	1170414
STM1130	ST4-74	1175387	1175950
STM1131, STM1132	ST4-74	1176770	1178094
<i>csgF</i> , <i>csgE</i> , <i>csgD</i> , <i>csgB</i>	ST4-74	1185409	1187428
<i>ndh</i>	ST4-74	1250095	1250801
<i>potC</i> , <i>sifA</i>	ST4-74	1265767	1267189
STnc150, SL1344_misc_feature_6, STM1239, <i>envF</i> , <i>IsrC</i>	ST4-74	1282495	1286129
<i>cspH</i> , <i>pagD</i> , <i>pagC</i>	ST4-74	1287849	1289532
STnc520, <i>pliC</i>	ST4-74	1290452	1291651
STM1265, STM1266	ST4-74	1304354	1305232
STM1267, STM1268, <i>aroQ</i>	ST4-74	1306242	1306852
<i>gapA</i> , <i>yeaA</i>	ST4-74	1326449	1326856
STM1331, <i>rfc</i>	ST4-74	1366420	1368646
<i>ydiQ</i> , <i>ydiP</i>	ST4-74	1392171	1392538
<i>ydiN</i>	ST4-74	1399195	1399768
<i>orf408</i>	ST4-74	1422650	1423124
<i>orf70</i>	ST4-74	1430434	1430778
<i>orf242</i> , <i>ssrB</i>	ST4-74	1432932	1434312
<i>ssaH</i> , <i>ssaI</i> , <i>ssaJ</i>	ST4-74	1446497	1447701
<i>ssaU</i>	ST4-74	1457107	1458308
<i>tppB</i>	ST4-74	1484775	1485450
<i>ydgK</i> , <i>ydgT</i> , <i>blr</i>	ST4-74	1492369	1493116

<i>Genes associated with peak^a</i>	<i>Chr.^b</i>	<i>Peak</i>	
		<i>Start</i>	<i>End</i>
STM1527	ST4-74	1560687	1561385
STM1528	ST4-74	1562488	1563261
STM1550, STM1551, SL1344_1481, STM1552	ST4-74	1583358	1585430
STM1554, STM1555	ST4-74	1587253	1588927
<i>steA</i>	ST4-74	1626466	1627272
<i>ydcX</i> , STnc1110	ST4-74	1643054	1643588
<i>pdgL</i> , STM1600, <i>ugtL</i> , <i>sifB</i> , <i>yncJ</i>	ST4-74	1647612	1650271
STM1628, <i>steB</i> , STM1630, <i>sseJ</i> , STM1632, STM1633, STM1634	ST4-74	1676041	1681588
STnc580	ST4-74	1706706	1707160
STM1657	ST4-74	1709097	1709520
<i>fnr</i>	ST4-74	1710839	1711458
STM1670, STM1671, STM1672	ST4-74	1720903	1723651
<i>steC</i> , STM1698A, <i>ycjE</i>	ST4-74	1747101	1748641
<i>ompW</i> , STM1733	ST4-74	1785237	1785803
STM1741	ST4-74	1791930	1792308
STM1747, STnc3580	ST4-74	1798223	1798850
<i>yche</i> , <i>adh</i>	ST4-74	1799396	1800115
STM1785	ST4-74	1839808	1841186
STM1794, STnc3610, STM1795	ST4-74	1850017	1850547
<i>ftsI2</i> , <i>cspC</i> , <i>yobF</i> , STnc3630	ST4-74	1892956	1894056
STM1854	ST4-74	1909338	1909738
<i>sopE2</i> , STM1856, SL1344_1786	ST4-74	1910085	1911622
STnc3640, SL1344_1792, <i>pagO</i> , STM1863, STM1864	ST4-74	1915516	1919190
STM1868A	ST4-74	1922572	1923061
<i>araH</i> , <i>ftnB</i>	ST4-74	1984296	1984864
STM1940, STM1941, SL1344_1874A	ST4-74	1991892	1992807
<i>fliC</i> , <i>fliD</i>	ST4-74	2006714	2007102
SL1344_1927A, STnc1280, SL1344_1927B, SL1344_1928	ST4-74	2039652	2041523
STM2007	ST4-74	2084789	2085479
<i>cbiA</i> , <i>pocR</i>	ST4-74	2111850	2112415
SL1344_2042, <i>sopA</i>	ST4-74	2138880	2140308
<i>wzzB</i>	ST4-74	2155528	2155962
<i>udg</i>	ST4-74	2156399	2157128
<i>rfbP</i>	ST4-74	2158655	2161291
<i>rfbK</i> , <i>cpsB2</i> , <i>rfbN</i> , <i>rfbU</i> , <i>rfbV</i> , <i>rfbX</i> , <i>rfbJ</i>	ST4-74	2161611	2168990
<i>rfbG</i> , <i>rfbF</i> , <i>rfbI</i> , <i>rfbC</i>	ST4-74	2170769	2173903
<i>sseK2</i> , <i>srcA</i>	ST4-74	2229021	2230739
STnc740, <i>stcD</i>	ST4-74	2240321	2241685
<i>stcA</i>	ST4-74	2245041	2245645
STM2186	ST4-74	2278779	2279141
STM2208, STM2209	ST4-74	2306623	2307891
<i>yejG</i> , STnc1340	ST4-74	2319741	2320153
<i>oafA</i>	ST4-74	2329411	2331577
STM2238	ST4-74	2335480	2336899
<i>MicF</i> , <i>yojN</i>	ST4-74	2364341	2364931
STM2274, STM2275	ST4-74	2376859	2377793
<i>yfbK</i>	ST4-74	2421134	2421856
<i>nuoA</i> , STM2329, STnc1550	ST4-74	2437181	2437897
<i>yfbQ</i>	ST4-74	2438908	2439821
STM2360, STM2361	ST4-74	2470310	2470673
<i>yfcZ</i> , <i>fadL</i>	ST4-74	2499678	2500162
<i>upp</i> , <i>purM</i>	ST4-74	2610304	2610723
STM2503, STM2505, STM2506	ST4-74	2618396	2619025
STM2508	ST4-74	2619468	2620057
<i>guaB</i> , <i>xseA</i>	ST4-74	2623538	2623973
<i>cadB</i>	ST4-74	2695797	2696235
<i>lepA</i> , SL1344_misc_feature_12, <i>gogB</i> , STM2585	ST4-74	2726315	2729493

<i>Genes associated with peak^a</i>	<i>Chr.^b</i>	<i>Peak</i>	
		<i>Start</i>	<i>End</i>
STM2585A	ST4-74	2730527	2730972
SL1344_tRNA_44, STnc2080, <i>IsrJ</i>	ST4-74	2759387	2759721
SL1344_2583, STM2621, SL1344_2585	ST4-74	2763106	2764161
SL1344_2594	ST4-74	2768759	2770091
<i>yfiD</i> , <i>ung</i>	ST4-74	2786436	2787186
<i>aroF</i> , <i>yfiR</i>	ST4-74	2812917	2813783
<i>int</i> , SL1344_2632	ST4-74	2816377	2816889
STM2680	ST4-74	2832194	2832785
<i>sopE</i>	ST4-74	2863096	2863454
SL1344_2695, SL1344_2696, SL1344_2697, SL1344_2698	ST4-74	2877180	2880718
<i>cIIc</i> , <i>apl</i> , <i>cl</i>	ST4-74	2886539	2887382
SL1344_2710	ST4-74	2888412	2889786
SL1344_2713, SL1344_2714, SL1344_2715	ST4-74	2890959	2894228
STM2742, STM2743	ST4-74	2902737	2905634
STM2746, STM2747	ST4-74	2908404	2911125
STM2754	ST4-74	2914727	2916052
STM2761, STM2762, <i>IsrM</i> , STM2763	ST4-74	2923895	2928171
STM2766, STM2767, STM2768	ST4-74	2930105	2933192
<i>fljA</i>	ST4-74	2935245	2935655
<i>hin</i> , <i>iroB</i>	ST4-74	2937936	2938401
<i>stpA</i> , STM2800	ST4-74	2970115	2970994
<i>avrA</i>	ST4-74	3032892	3033544
<i>sprB</i> , <i>hilC</i>	ST4-74	3034140	3036066
<i>prgH</i> , <i>hilD</i> , <i>hilA</i>	ST4-74	3040049	3042597
<i>iagB</i>	ST4-74	3043284	3044745
<i>sptP</i> , <i>sicP</i>	ST4-74	3045926	3047129
<i>invB</i>	ST4-74	3060826	3061358
<i>invA</i>	ST4-74	3062836	3063528
<i>invH</i> , <i>InvR</i>	ST4-74	3067025	3067478
STM2902, STM2903	ST4-74	3068163	3069232
<i>ygcB</i> , <i>sopD</i> , STnc3140	ST4-74	3108568	3110081
<i>gcvA</i> , <i>GcvB</i>	ST4-74	3156570	3157077
STM3026	ST4-74	3208296	3209101
STM3079, STM3080	ST4-74	3262296	3263205
STM3083	ST4-74	3266523	3267135
STnc3870, SL1344_misc_feature_126, STM3117	ST4-74	3296996	3297599
STM3123, STM3124	ST4-74	3304249	3304895
STnc1170	ST4-74	3312267	3312920
STM3133	ST4-74	3314354	3314967
<i>exuT</i> , <i>uxuA</i>	ST4-74	3316288	3316949
STM3138, STnc3890	ST4-74	3321791	3322853
<i>assT</i>	ST4-74	3374699	3375163
STM3193	ST4-74	3376907	3377336
<i>yqjH</i> , <i>yqjI</i>	ST4-74	3400564	3400921
STM3216	ST4-74	3402887	3403314
<i>aer</i>	ST4-74	3404904	3405320
<i>garD</i>	ST4-74	3438955	3439404
<i>agaR</i> , <i>gatY</i>	ST4-74	3442922	3443364
STM3257	ST4-74	3447341	3447711
<i>yhbT</i> , <i>yhbU</i>	ST4-74	3460672	3461019
STM3343, STnc3060	ST4-74	3533405	3533758
<i>mdh</i> , <i>argR</i>	ST4-74	3549059	3549604
<i>yhdG</i>	ST4-74	3576305	3576768
<i>yhdU</i>	ST4-74	3578772	3579240
<i>rpsM</i> , <i>rpmJb</i>	ST4-74	3607149	3607568
<i>bfr</i> , <i>bfd</i>	ST4-74	3618952	3619556
<i>nirB</i>	ST4-74	3644686	3645129
STnc760, <i>feoA</i>	ST4-74	3685056	3685447

<i>Genes associated with peak^a</i>	<i>Chr.^b</i>	<i>Peak</i>	
		<i>Start</i>	<i>End</i>
STM3529, STM3530	ST4-74	3714927	3715274
STM3547	ST4-74	3737573	3738211
<i>lpfA</i>	ST4-74	3849010	3849621
STnc780	ST4-74	3858684	3859241
STM3652, <i>yafP</i>	ST4-74	3859848	3861143
STM3690, <i>sadA</i>	ST4-74	3901409	3902504
<i>rfaK, rfaZ, rfaY, rfaJ, rfaI</i>	ST4-74	3931143	3936149
<i>rfaB, yibR</i>	ST4-74	3936491	3937420
<i>rfaQ</i>	ST4-74	3939834	3940571
STM3752, <i>sugR</i>	ST4-74	3970142	3971395
<i>rmbA, misL</i>	ST4-74	3974104	3976057
<i>marT, slsA</i>	ST4-74	3980392	3981119
STM3779, STM3780	ST4-74	4000762	4002180
STM3782, STM3783, STM3784, STM3785	ST4-74	4004820	4006722
<i>yhjA</i>	ST4-74	4041092	4041771
STnc400, STM3845, STM3846	ST4-74	4072267	4074711
<i>atpI</i>	ST4-74	4101840	4102667
<i>yifA, yifE</i>	ST4-74	4127850	4128195
<i>comM, ilvX, ilvG</i>	ST4-74	4129882	4130430
<i>rho</i>	ST4-74	4146784	4147226
<i>tatA</i>	ST4-74	4201127	4201684
STM3980	ST4-74	4207528	4208405
<i>yihG, polA</i>	ST4-74	4227132	4227581
STM4015, <i>ompL</i>	ST4-74	4245984	4247419
SL1344_3979, STM4033	ST4-74	4263008	4263452
STM4051	ST4-74	4283485	4284359
<i>ydeW, ego</i>	ST4-74	4304575	4305108
SL1344_4052	ST4-74	4336272	4337013
<i>coaA</i>	ST4-74	4379995	4380383
SL1344_rRNA_20	ST4-74	4415485	4415924
<i>aceB</i>	ST4-74	4422971	4423548
STM4196, STM4197	ST4-74	4439177	4440672
STM4204	ST4-74	4446447	4447543
STM4218, STM4219	ST4-74	4458715	4459369
SL1344_misc_feature_129, <i>siiA, siiB, siiC, siiD, siiE</i>	ST4-74	4497954	4507001
<i>siiF</i>	ST4-74	4520086	4522699
<i>yjcB, yjcC</i>	ST4-74	4523191	4523870
<i>adiY</i> , STnc1180	ST4-74	4558985	4559993
STM4302	ST4-74	4569882	4570392
STM4313, <i>rtsB, rtsA</i> , STM4316	ST4-74	4581119	4582756
<i>phoN</i> , SL1344_4256	ST4-74	4584700	4586042
<i>aspA, fxsA</i>	ST4-74	4592849	4593368
SL1344_tRNA_82, <i>yjeV</i>	ST4-74	4617550	4617897
STM4413	ST4-74	4674875	4675360
<i>iolT1, iolT2</i>	ST4-74	4681329	4681883
<i>iolE, iolG1</i>	ST4-74	4687026	4688406
<i>nrdD</i> , SL1344_4383	ST4-74	4715206	4715714
STM4467, <i>yjgK</i>	ST4-74	4731066	4731723
<i>ytgA</i>	ST4-74	4734869	4735507
STM4489	ST4-74	4753746	4754156
STM4495	ST4-74	4764531	4766043
SL1344_4427A, <i>yeeN</i>	ST4-74	4773008	4774261
STM4503, STM4504, STM4505	ST4-74	4777524	4780154
<i>IsrQ</i> , SL1344_4439, STM4509	ST4-74	4783586	4784317
<i>yjiH</i>	ST4-74	4789091	4789570
STM4518	ST4-74	4793969	4794278
STM4520, STnc4130, STM4522	ST4-74	4796718	4797610
<i>hsdS</i>	ST4-74	4798610	4799530

Genes associated with peak^a	Chr.^b	Peak	
		Start	End
<i>yjiP, yjiQ</i>	ST4-74	4826026	4827024
<i>yjiI, deoC</i>	ST4-74	4841777	4842074
<i>sthB</i>	ST4-74	4870732	4871229
<i>sthB</i>	ST4-74	4872247	4872645
STM4595, STM4596	ST4-74	4873908	4875191
<i>arcA, yjiY, lasT</i>	ST4-74	4876509	4877354

^aWhen multiple genes are listed a peak was present across the promoter region or TSS of all listed genes

^bChromosome or plasmid

Table S5. ChIP-seq peaks associated with up-regulated DE genes.

Genes associated with peak^a	Chr.^b	Peak	
		Start	End
<i>stbA</i>	pCol1B9SL1344	15184	16230
PSLT042, <i>spvR</i>	pSLTSL1344	60927	62144
<i>spvC, spvD</i>	pSLTSL1344	65036	67651
STnc890, STM0014, STM0015, STnc3200	ST4-74	14781	16510
<i>stbA</i> , STM0341, STM0342, STnc1700, STM0343	ST4-74	384214	386526
STM0557	ST4-74	614288	616208
<i>gtrBa, gtrAa</i> , STnc1870	ST4-74	616736	617335
STM0719, STM0720, STM0721, STM0722, STM0723,	ST4-74	783417	793157
STM0724, STM0725, STM0726, STM0727			
STM0762, STM0763, STM0764, STM0765	ST4-74	825138	828930
<i>pflA</i> , STM0971, <i>sopD2</i>	ST4-74	1010045	1011678
<i>pipA, pipB</i> , STM1089, <i>pipC</i>	ST4-74	1132644	1134847
STnc1880, STM1110	ST4-74	1153672	1154710
<i>potC, sifA</i>	ST4-74	1265767	1267189
STnc150, SL1344_misc_feature_6, STM1239, <i>envF, IsrC</i>	ST4-74	1282495	1286129
<i>cspH, pagD, pagC</i>	ST4-74	1287849	1289532
STM1265, STM1266	ST4-74	1304354	1305232
STM1267, STM1268, <i>aroQ</i>	ST4-74	1306242	1306852
STM1331, <i>rfc</i>	ST4-74	1366420	1368646
<i>orf242, ssrB</i>	ST4-74	1432932	1434312
<i>ssaH, ssaI, ssaJ</i>	ST4-74	1446497	1447701
<i>ssaU</i>	ST4-74	1457107	1458308
<i>steA</i>	ST4-74	1626466	1627272
<i>pdgL</i> , STM1600, <i>ugtL, sifB, yncJ</i>	ST4-74	1647612	1650271
STM1628, <i>steB</i> , STM1630, <i>sseJ</i> , STM1632, STM1633,	ST4-74	1676041	1681588
STM1634			
<i>steC</i> , STM1698A, <i>ycjE</i>	ST4-74	1747101	1748641
STM1747, STnc3580	ST4-74	1798223	1798850
STM1854	ST4-74	1909338	1909738
STnc3640, SL1344_1792, <i>pagO</i> , STM1863, STM1864	ST4-74	1915516	1919190
STM1940, STM1941, SL1344_1874A	ST4-74	1991892	1992807
SL1344_1927A, STnc1280, SL1344_1927B, SL1344_1928	ST4-74	2039652	2041523
<i>sseK2, srcA</i>	ST4-74	2229021	2230739
<i>lepA</i> , SL1344_misc_feature_12, <i>gogB</i> , STM2585	ST4-74	2726315	2729493
STM2585A	ST4-74	2730527	2730972
STM2761, STM2762, <i>IsrM</i> , STM2763	ST4-74	2923895	2928171
<i>stpA</i> , STM2800	ST4-74	2970115	2970994
<i>gcvA, GcvB</i>	ST4-74	3156570	3157077
STM3133	ST4-74	3314354	3314967
<i>bfr, bfd</i>	ST4-74	3618952	3619556
SL1344_4427A, <i>yeaN</i>	ST4-74	4773008	4774261
STM4503, STM4504, STM4505	ST4-74	4777524	4780154
STM4520, STnc4130, STM4522	ST4-74	4796718	4797610

^aWhen multiple genes are listed a peak was present across the promoter region or TSS of all listed genes

^bChromosome or plasmid

Table S6. ChIP-seq peaks associated with down-regulated DE genes.

<i>Genes associated with peak^a</i>	<i>Chr.^b</i>	<i>Peak</i>	
		<i>Start</i>	<i>End</i>
<i>citC, citA</i>	ST4-74	687093	687718
<i>sopB, orfX, STM1093</i>	ST4-74	1136105	1137136
<i>csgF, csgE, csgD, csgB</i>	ST4-74	1185409	1187428
STnc580	ST4-74	1706706	1707160
STM1657	ST4-74	1709097	1709520
<i>fnr</i>	ST4-74	1710839	1711458
<i>ompW, STM1733</i>	ST4-74	1785237	1785803
<i>fliC, fliD</i>	ST4-74	2006714	2007102
<i>stcA</i>	ST4-74	2245041	2245645
<i>yejG, STnc1340</i>	ST4-74	2319741	2320153
<i>nuoA, STM2329, STnc1550</i>	ST4-74	2437181	2437897
<i>yfcZ, fadL</i>	ST4-74	2499678	2500162
STM2503, STM2505, STM2506	ST4-74	2618396	2619025
<i>yfiD, ung</i>	ST4-74	2786436	2787186
SL1344_2695, SL1344_2696, SL1344_2697, SL1344_2698	ST4-74	2877180	2880718
<i>cIIc, apl, cl</i>	ST4-74	2886539	2887382
STM3216	ST4-74	3402887	3403314
<i>aer</i>	ST4-74	3404904	3405320
<i>yhbT, yhbU</i>	ST4-74	3460672	3461019
<i>nirB</i>	ST4-74	3644686	3645129
<i>yhjA</i>	ST4-74	4041092	4041771
STnc400, STM3845, STM3846	ST4-74	4072267	4074711
<i>nrdD, SL1344_4383</i>	ST4-74	4715206	4715714
<i>IsrQ, SL1344_4439, STM4509</i>	ST4-74	4783586	4784317
<i>yjiP, yjiQ</i>	ST4-74	4826026	4827024
<i>yjiL, deoC</i>	ST4-74	4841777	4842074

^aWhen multiple genes are listed a peak was present across the promoter region or TSS of all listed genes

^bChromosome or plasmid

Table S7. Letter-probability matrix of FNR binding motif (TTGATNTRSATCAA)

<i>Position</i>	<i>A</i>	<i>C</i>	<i>G</i>	<i>T</i>
1	0.000000	0.000000	0.250000	0.750000
2	0.000000	0.041667	0.000000	0.958333
3	0.125000	0.000000	0.875000	0.000000
4	1.000000	0.000000	0.000000	0.000000
5	0.000000	0.041667	0.041667	0.916666
6	0.208333	0.250000	0.125000	0.416667
7	0.041667	0.041667	0.083333	0.833333
8	0.333333	0.000000	0.666667	0.000000
9	0.041667	0.458333	0.375000	0.125000
10	0.791666	0.041667	0.125000	0.041667
11	0.000000	0.000000	0.000000	1.000000
12	0.083333	0.916667	0.000000	0.000000
13	1.000000	0.000000	0.000000	0.000000
14	0.750000	0.208333	0.000000	0.041667

Table S8. Top 100 FNR Motif Hits.

<i>Start</i>	<i>Stop</i>	<i>Strand</i>	<i>Score</i>	<i>p-value</i>	<i>Matched Sequence</i>
1430596	1430609	+	22.2036	2.83E-09	TTGATTTGCATCAA
3312562	3312575	+	21.3772	1.13E-08	TTGATTTACATCAA
3644926	3644939	+	21.3772	1.13E-08	TTGATTTACATCAA
2536558	2536571	+	20.5928	2.84E-08	GTGATTTGCATCAA
4715480	4715493	+	20.5928	2.84E-08	GTGATTTGCATCAA
1250446	1250459	-	20.5329	3.43E-08	TTGATGTGCATCAA
2320090	2320103	+	20.4551	3.69E-08	TTGATATACATCAA
1820854	1820867	-	19.8024	5.98E-08	TTGATTTATATCAA
1560987	1561000	+	19.2874	1.13E-07	TTGATCTGGATCAC
1799743	1799756	+	19.2575	1.16E-07	TTGATTTAGATCAC
2437400	2437413	+	18.9042	1.47E-07	TTAATTTACATCAA
3122008	3122021	-	18.8144	1.62E-07	TTGATTTACGTCAA
2478446	2478459	+	18.6826	1.83E-07	TTGATGTGCATCAC
1785488	1785501	-	18.6647	1.86E-07	TTAATCTGGATCAA
2786813	2786826	+	18.6168	2.00E-07	TTGATTTAAATCAA
2786813	2786826	-	18.6168	2.00E-07	TTGATTTAAATCAA
1492609	1492622	-	18.5389	2.17E-07	TTAATATGGATCAA
2320090	2320103	-	18.1317	2.96E-07	TTGATGTATATCAA
2632223	2632236	+	18.0958	3.13E-07	TTGATTTAGATAAA
914001	914014	+	17.9701	3.49E-07	TTGATGTGCGTCAA
1643343	1643356	-	17.9701	3.49E-07	TTGATGTGCGTCAA
1979902	1979915	-	17.9461	3.58E-07	GTGATCTGCATCAC
1183545	1183558	-	17.9162	3.64E-07	GTGATTTACATCAC
2808003	2808016	+	17.9162	3.64E-07	GTGATTTACATCAC
1820854	1820867	+	17.6946	4.34E-07	TTGATATAAATCAA
3439225	3439238	+	17.6766	4.41E-07	GTGATCTGGATCAC
4794134	4794147	-	17.6647	4.44E-07	TTGATTAACATCAA
3554685	3554698	-	17.6467	4.49E-07	GTGATTTAGATCAC
4041407	4041420	+	17.5329	4.96E-07	TTGATTGGTATCAA
2997911	2997924	-	17.4731	5.27E-07	TTGATTTTCATCAA
1808887	1808900	-	17.4371	5.43E-07	TTGATGGGCATCAA
3685208	3685221	-	17.2934	6.13E-07	TTGATATGGCTCAA
3316630	3316643	-	17.2695	6.19E-07	TTGATCTGTGTCAA
2932463	2932476	-	17.2216	6.43E-07	TTGATACGGATCAA
2610465	2610478	+	17.2156	6.53E-07	TTGACCTGGATCAA
1291100	1291113	-	17.2036	6.61E-07	GTGATTTACGTCAA
4783741	4783754	-	17.1856	6.79E-07	ATGATTTGCATCAA
4270771	4270784	-	17.1737	6.81E-07	TTGATATAGATAAA
3021733	3021746	-	17.1677	6.90E-07	TTAATTTGCGTCAA
1253486	1253499	-	17.1198	7.09E-07	GTGATCTACATCAC
73219	73232	+	17.0898	7.29E-07	TTTATTTGCATCAA
1712203	1712216	+	17.0898	7.29E-07	TTTATTTGCATCAA
261574	261587	+	16.9641	8.00E-07	TTGATTTACGTCAA
3715132	3715145	-	16.9521	8.06E-07	GTGATTTGCTTCAA
3312562	3312575	-	16.9461	8.09E-07	TTGATGTAAATCAA
3644926	3644939	-	16.9461	8.09E-07	TTGATGTAAATCAA
2692936	2692949	+	16.8922	8.46E-07	TTGATATAACATCAT
4243812	4243825	+	16.8922	8.46E-07	TTGATATAACATCAT
3224429	3224442	-	16.8204	8.94E-07	TTGATGAGCATCAA
510687	510700	-	16.7425	9.74E-07	TTGATAAACATCAA
527520	527533	-	16.7246	9.87E-07	GTGATATAGATCAC
1992348	1992361	+	16.7186	9.89E-07	TTAATTTGCATAAA
4189176	4189189	+	16.7006	1.01E-06	GTGATCGGCATCAA
2656423	2656436	-	16.6707	1.04E-06	GTGATTGACATCAA
1518635	1518648	-	16.6587	1.05E-06	GTGATATGCATAAA
1014923	1014936	+	16.6228	1.08E-06	TTGATATAGATCAT
4650494	4650507	-	16.497	1.20E-06	GTAATCTACATCAA

Start	Stop	Strand	Score	p-value	Matched Sequence
4639386	4639399	-	16.4611	1.23E-06	TTGATCGGCATCAC
4822711	4822724	+	16.4611	1.23E-06	TTGATCGGCATCAC
76793	76806	-	16.3892	1.31E-06	GTGATATGGATAAA
4876945	4876958	-	16.3174	1.37E-06	TTGATATATGTCAA
585659	585672	+	16.2934	1.39E-06	TTTATCTGCATCAA
3856862	3856875	+	16.2934	1.39E-06	TTTATCTGCATCAA
1799743	1799756	-	16.2096	1.47E-06	GTGATCTAAATCAA
975730	975743	-	16.1796	1.50E-06	GTGATTTGCGTCAC
3896424	3896437	-	16.1796	1.50E-06	GTGATTTGCGTCAC
495837	495850	+	16.1437	1.54E-06	TTGATGTACATCAT
1136494	1136507	-	16.0838	1.62E-06	TTGATCTGAGTCAA
2156517	2156530	-	16.0838	1.62E-06	GTGATCAGCATCAA
2618644	2618657	+	16.0539	1.65E-06	TTGATTTAAGTCAA
1428394	1428407	+	16.0479	1.66E-06	TGGATCTGCATCAA
2932463	2932476	+	16.0419	1.67E-06	TTGATCCGTATCAA
1253486	1253499	+	15.976	1.78E-06	GTGATGTAGATCAC
3147919	3147932	+	15.976	1.78E-06	GTGATTCACATCAA
2786866	2786879	+	15.9581	1.82E-06	TTGTTTTACATCAA
2891426	2891439	+	15.9581	1.82E-06	TTGATTTACATCGA
288281	288294	+	15.9401	1.83E-06	TTAATGTGGATCAC
3147919	3147932	-	15.9222	1.86E-06	TTGATGTGAATCAC
1250446	1250459	+	15.9162	1.87E-06	TTGATGCACATCAA
2165224	2165237	-	15.8683	1.94E-06	TTGATATATATAAA
780800	780813	+	15.8084	2.07E-06	TTGATTTACCTCAC
4241561	4241574	-	15.7186	2.23E-06	GTAATTTATATCAA
1428165	1428178	-	15.6886	2.28E-06	TTGTTTTAGATCAA
765537	765550	-	15.6467	2.33E-06	TTGATCTGGTTCAC
1316146	1316159	-	15.6048	2.40E-06	TTGATTTAAATAAA
4288995	4289008	-	15.6048	2.40E-06	GTGACCTGGATCAA
1486853	1486866	-	15.5928	2.44E-06	GTGATTTTGTATCAA
2672110	2672123	-	15.5629	2.49E-06	GTGATATAGATAAA
527520	527533	+	15.5449	2.52E-06	GTGATCTATATCAC
1977320	1977333	-	15.5449	2.52E-06	GCGATCTGGATCAA
3605056	3605069	-	15.5329	2.55E-06	GTGATGTACGTCAA
4453798	4453811	+	15.521	2.56E-06	TTGATTGAAATCAA
4599472	4599485	+	15.521	2.56E-06	TTGATATGGTTCAC
947547	947560	+	15.515	2.58E-06	TTCATTTGTATCAA
4829078	4829091	-	15.515	2.58E-06	TTGATGTGCATCAG
869629	869642	-	15.3174	2.88E-06	TTGATATATATCAT
4722369	4722382	-	15.2395	3.03E-06	TTGATATATTTCAA
4593105	4593118	+	15.2036	3.12E-06	GTAATCTGGATCAC
2663061	2663074	-	15.1677	3.22E-06	TTGATAAATATCAA
4715511	4715524	-	15.1617	3.25E-06	TTGTTCTACATCAA

Appendix IV

Table S9. Proteomics: Proteins in WT.

<i>Gene Name</i>	<i>Average of Norm. (fmol)</i>	<i>Average of Norm. (ng)</i>
<i>accA</i>	3.70E-02	3.65E-02
<i>accB</i>	7.81E-02	3.65E-02
<i>accC</i>	1.60E-01	2.22E-01
<i>accD</i>	3.43E-02	3.22E-02
<i>aceA</i>	8.66E-03	1.15E-02
<i>aceE</i>	2.29E-01	6.39E-01
<i>aceF</i>	9.10E-02	1.68E-01
<i>ackA</i>	1.09E-01	1.33E-01
<i>acnA</i>	1.88E-02	5.15E-02
<i>acnB</i>	2.16E-01	5.68E-01
<i>acpP</i>	2.67E-01	6.43E-02
<i>acrA</i>	7.20E-02	8.50E-02
<i>acrB</i>	4.91E-02	1.56E-01
<i>acs</i>	1.96E-02	3.96E-02
<i>adhE</i>	3.13E-01	8.47E-01
<i>adhP</i>	3.09E-02	3.10E-02
<i>adk</i>	1.45E-01	9.55E-02
<i>aeiA</i>	4.58E-02	1.62E-01
<i>agp</i>	5.18E-02	6.64E-02
<i>ahpC</i>	1.88E-01	1.10E-01
<i>ahpF</i>	6.64E-02	1.04E-01
<i>alaS</i>	1.33E-01	3.57E-01
<i>aldB</i>	9.25E-02	1.46E-01
<i>allR</i>	1.75E-02	1.45E-02
<i>anmK</i>	1.51E-02	1.69E-02
<i>apbC</i>	2.64E-02	2.97E-02
<i>aphA</i>	2.64E-02	1.94E-02
<i>argA</i>	6.08E-02	8.42E-02
<i>argB</i>	5.42E-02	4.09E-02
<i>argC</i>	2.46E-02	2.48E-02
<i>argD</i>	1.13E-01	1.39E-01
<i>argG</i>	1.14E-01	1.59E-01
<i>argH</i>	1.19E-01	1.70E-01
<i>argI</i>	5.08E-02	5.25E-02
<i>argS</i>	3.16E-02	5.70E-02
<i>argT</i>	3.55E-02	2.80E-02
<i>arnB</i>	2.82E-02	3.31E-02
<i>arnC</i>	5.17E-02	5.31E-02
<i>aroA</i>	4.54E-02	5.93E-02
<i>aroB</i>	5.37E-02	5.83E-02
<i>aroC</i>	3.48E-02	3.85E-02
<i>aroD</i>	1.38E-02	1.05E-02
<i>aroF</i>	8.14E-02	8.86E-02
<i>aroG</i>	2.10E-02	2.24E-02
<i>artI</i>	8.07E-02	6.11E-02
<i>artJ</i>	6.69E-02	5.00E-02
<i>asd</i>	3.25E-01	3.68E-01
<i>asnB</i>	3.30E-02	5.79E-02
<i>asnS</i>	2.41E-01	3.56E-01
<i>aspA</i>	1.00E-01	1.48E-01
<i>aspC</i>	4.99E-02	6.11E-02
<i>aspS</i>	3.31E-02	6.10E-02
<i>astC</i>	3.88E-02	4.77E-02
<i>atpA</i>	3.93E-01	6.07E-01

<i>Gene Name</i>	<i>Average of Norm. (fmol)</i>	<i>Average of Norm. (ng)</i>
<i>atpC</i>	1.92E-02	8.06E-03
<i>atpD</i>	5.40E-01	7.59E-01
<i>atpF</i>	4.11E-02	2.00E-02
<i>atpG</i>	7.96E-02	7.04E-02
<i>atpH</i>	9.15E-02	4.99E-02
<i>bamA</i>	8.13E-02	2.03E-01
<i>bamB</i>	8.66E-02	1.01E-01
<i>bcp</i>	1.04E-01	5.18E-02
<i>bepA</i>	1.14E-02	1.70E-02
<i>bfd</i>	4.92E-03	1.05E-03
<i>bfr</i>	7.73E-02	3.96E-02
<i>bioA</i>	2.08E-02	2.77E-02
<i>bioB</i>	5.10E-02	5.59E-02
<i>bioD1</i>	5.65E-02	3.84E-02
<i>btuB</i>	6.99E-03	1.33E-02
<i>btuE</i>	5.69E-02	3.27E-02
<i>cafA</i>	1.66E-02	2.58E-02
<i>carA</i>	1.54E-01	1.81E-01
<i>carB</i>	1.31E-01	4.34E-01
<i>cbiD</i>	2.60E-02	3.00E-02
<i>cbiF</i>	1.64E-01	1.30E-01
<i>cbiG</i>	1.77E-02	1.89E-02
<i>cbiH</i>	7.06E-02	5.15E-02
<i>cbiJ</i>	2.40E-01	1.93E-01
<i>cbiK</i>	2.11E-01	1.74E-01
<i>cbiL</i>	5.59E-02	4.08E-02
<i>cbiP</i>	2.18E-02	3.36E-02
<i>ccmH</i>	1.23E-02	1.32E-02
<i>cdh</i>	5.70E-02	4.54E-02
<i>celD</i>	3.05E-02	2.82E-02
<i>cheA</i>	4.09E-02	8.38E-02
<i>cheB</i>	1.96E-02	2.06E-02
<i>cheY</i>	1.55E-02	6.10E-03
<i>cheZ</i>	4.17E-02	2.79E-02
<i>citD1</i>	2.08E-02	6.27E-03
<i>citE</i>	3.30E-02	3.04E-02
<i>clpA</i>	2.20E-02	5.15E-02
<i>clpB</i>	1.63E-01	4.34E-01
<i>clpX</i>	3.40E-02	4.45E-02
<i>cmk</i>	2.88E-02	1.99E-02
<i>coaA</i>	1.47E-02	1.48E-02
<i>cobT</i>	4.30E-02	4.43E-02
<i>cpdB</i>	2.04E-02	4.05E-02
<i>cptA</i>	2.38E-02	4.44E-02
<i>cra</i>	1.66E-02	1.78E-02
<i>crp</i>	2.69E-02	1.79E-02
<i>crr</i>	6.73E-01	3.43E-01
<i>cspA</i>	2.99E-01	6.19E-02
<i>cspC</i>	6.04E-01	1.25E-01
<i>cspD</i>	4.83E-01	1.07E-01
<i>cspE</i>	2.63E-01	5.47E-02
<i>cspJ</i>	8.90E-02	1.93E-02
<i>cueO</i>	3.41E-02	5.57E-02
<i>cyoA</i>	3.87E-02	3.82E-02
<i>cypD</i>	1.30E-01	2.47E-01
<i>cysA</i>	6.20E-02	7.12E-02
<i>cysE</i>	3.32E-02	2.72E-02
<i>cysH</i>	5.61E-02	4.38E-02
<i>cysI</i>	4.07E-02	7.31E-02

<i>Gene Name</i>	<i>Average of Norm. (fmol)</i>	<i>Average of Norm. (ng)</i>
<i>cysJ</i>	7.71E-02	1.43E-01
<i>cysK</i>	3.36E-01	3.24E-01
<i>cysM</i>	2.02E-02	1.84E-02
<i>cysN</i>	7.00E-02	1.04E-01
<i>cysP</i>	5.43E-02	5.69E-02
<i>dacA</i>	2.50E-02	3.10E-02
<i>dacC</i>	2.47E-02	3.01E-02
<i>damX</i>	8.83E-02	1.12E-01
<i>dapA</i>	3.52E-02	3.09E-02
<i>dapB</i>	1.14E-01	9.25E-02
<i>dapD</i>	1.14E-01	9.57E-02
<i>dcp</i>	1.95E-02	4.23E-02
<i>degP</i>	1.14E-01	1.57E-01
<i>degQ</i>	1.19E-02	1.57E-02
<i>deoA</i>	2.37E-02	3.12E-02
<i>deoB</i>	5.20E-02	6.45E-02
<i>deoC</i>	1.94E-02	1.50E-02
<i>deoD</i>	9.74E-02	7.13E-02
<i>dgoD</i>	2.26E-02	2.68E-02
<i>dkgA</i>	3.44E-02	3.00E-02
<i>dkgB</i>	1.94E-02	1.59E-02
<i>dksA</i>	9.34E-02	4.63E-02
<i>dlgD</i>	2.04E-02	2.12E-02
<i>dmsA</i>	3.64E-02	9.25E-02
<i>dnaJ</i>	3.68E-02	4.29E-02
<i>dnaK</i>	4.83E-01	9.35E-01
<i>dppA</i>	1.06E-01	1.78E-01
<i>dppD</i>	3.37E-02	3.38E-02
<i>dppF</i>	2.02E-02	2.15E-02
<i>dps</i>	1.79E-01	9.38E-02
<i>dsbA</i>	4.84E-02	3.11E-02
<i>dsbC</i>	6.97E-02	5.11E-02
<i>dut</i>	8.88E-02	3.98E-02
<i>ecnB</i>	3.31E-01	4.49E-02
<i>eda</i>	1.58E-02	9.86E-03
<i>elaA</i>	4.49E-03	2.20E-03
<i>elaB</i>	9.08E-03	2.94E-03
<i>emrR</i>	2.51E-02	1.46E-02
<i>engB</i>	1.29E-02	8.46E-03
<i>eno</i>	1.38E+00	1.77E+00
<i>entB</i>	3.70E-02	3.35E-02
<i>envF</i>	1.91E-02	1.59E-02
<i>erfK</i>	2.78E-02	2.66E-02
<i>erpA</i>	5.26E-02	1.80E-02
<i>exbB</i>	2.21E-02	1.63E-02
<i>fabA</i>	6.37E-02	3.41E-02
<i>fabB</i>	1.58E-01	1.89E-01
<i>fabD</i>	5.58E-02	5.09E-02
<i>fabF</i>	4.76E-02	5.75E-02
<i>fabG</i>	9.48E-02	6.78E-02
<i>fabH</i>	2.13E-02	2.01E-02
<i>fabI</i>	1.27E-01	9.91E-02
<i>fadL</i>	7.27E-02	9.63E-02
<i>fba</i>	7.13E-02	7.83E-02
<i>fbaB</i>	5.85E-01	6.27E-01
<i>fbp</i>	7.30E-02	7.56E-02
<i>fdx</i>	5.76E-02	2.06E-02
<i>feoA</i>	4.52E-03	1.05E-03
<i>fepA</i>	1.41E-02	3.25E-02

<i>Gene Name</i>	<i>Average of Norm. (fmol)</i>	<i>Average of Norm. (ng)</i>
<i>ffh</i>	3.74E-02	5.21E-02
<i>fhuA</i>	7.49E-02	1.69E-01
<i>fimZ</i>	8.31E-03	5.44E-03
<i>flkB</i>	8.33E-02	5.52E-02
<i>fkpA</i>	6.23E-02	5.04E-02
<i>fldA</i>	4.52E-02	2.50E-02
<i>flgC</i>	8.31E-03	3.25E-03
<i>flgJ</i>	1.22E-02	1.17E-02
<i>flgK</i>	3.74E-02	6.22E-02
<i>fliB</i>	1.82E-02	2.33E-02
<i>fliC</i>	5.88E-01	8.49E-01
<i>fliD</i>	2.88E-02	4.00E-02
<i>fliY</i>	3.80E-02	3.05E-02
<i>fljB</i>	9.04E-02	1.32E-01
<i>jolE</i>	2.75E-02	1.90E-02
<i>frdA</i>	1.79E-01	3.31E-01
<i>frdB</i>	2.58E-01	2.01E-01
<i>frr</i>	9.02E-02	5.19E-02
<i>fsa</i>	1.84E-02	1.21E-02
<i>fin</i>	5.23E-02	2.83E-02
<i>ftsA</i>	4.59E-02	5.85E-02
<i>ftsH</i>	5.29E-02	1.05E-01
<i>ftsI</i>	9.36E-03	1.68E-02
<i>ftsN</i>	1.31E-01	1.34E-01
<i>ftsZ</i>	1.49E-01	1.68E-01
<i>fumA</i>	3.11E-02	5.59E-02
<i>fumB</i>	1.20E-01	2.03E-01
<i>fumC</i>	5.35E-02	7.54E-02
<i>fur</i>	6.53E-02	3.13E-02
<i>fusA</i>	7.85E-01	1.70E+00
<i>gabD</i>	9.11E-03	1.32E-02
<i>galF</i>	3.30E-02	3.05E-02
<i>galK</i>	2.16E-02	2.51E-02
<i>galM</i>	2.55E-02	2.76E-02
<i>galU</i>	1.28E-01	1.19E-01
<i>gapA</i>	2.01E+00	2.01E+00
<i>garR</i>	4.35E-02	3.73E-02
<i>gcvH</i>	3.36E-02	1.30E-02
<i>gcvP</i>	2.89E-02	8.48E-02
<i>gdhA</i>	1.70E-01	2.33E-01
<i>ggt</i>	2.08E-02	3.61E-02
<i>glgA</i>	3.07E-02	4.55E-02
<i>glgP</i>	3.64E-02	9.54E-02
<i>glk</i>	4.97E-02	4.87E-02
<i>glmM</i>	2.14E-02	2.86E-02
<i>glmS</i>	3.98E-02	7.48E-02
<i>glmU</i>	2.21E-02	3.07E-02
<i>glnA</i>	1.91E-01	2.78E-01
<i>glnH</i>	6.95E-02	5.28E-02
<i>glnQ</i>	3.65E-02	2.72E-02
<i>glnS</i>	3.14E-02	5.62E-02
<i>glpA</i>	1.52E-01	2.54E-01
<i>glpB</i>	2.92E-02	3.78E-02
<i>glpC</i>	5.94E-02	7.48E-02
<i>glpD</i>	8.45E-02	1.35E-01
<i>glpK</i>	4.29E-01	6.74E-01
<i>glpQ</i>	2.27E-01	2.56E-01
<i>glpR</i>	5.92E-02	4.61E-02
<i>gltA</i>	9.02E-02	1.22E-01

<i>Gene Name</i>	<i>Average of Norm. (fmol)</i>	<i>Average of Norm. (ng)</i>
<i>gltB</i>	1.13E-01	5.20E-01
<i>gltD</i>	2.71E-02	4.02E-02
<i>gltI</i>	7.20E-02	6.72E-02
<i>gltX</i>	3.04E-02	4.59E-02
<i>glyA</i>	2.03E-01	2.59E-01
<i>glyQ</i>	7.27E-02	7.11E-02
<i>glyS</i>	3.84E-02	8.23E-02
<i>gmhA</i>	4.81E-02	2.82E-02
<i>gnd</i>	1.17E-01	1.68E-01
<i>gns</i>	8.42E-02	1.52E-02
<i>gor</i>	2.36E-02	3.26E-02
<i>gpmA</i>	4.40E-02	3.49E-02
<i>gpmI</i>	1.54E-01	2.42E-01
<i>gppA</i>	5.41E-03	8.41E-03
<i>gpsA</i>	2.25E-02	2.29E-02
<i>grcA</i>	1.55E-01	6.25E-02
<i>greA</i>	6.10E-02	3.01E-02
<i>groL</i>	1.90E+00	3.05E+00
<i>groS</i>	1.32E+00	3.82E-01
<i>grpE</i>	3.97E-02	2.42E-02
<i>grxA</i>	8.05E-02	2.27E-02
<i>grxB</i>	2.29E-01	1.57E-01
<i>gst</i>	5.77E-02	3.64E-02
<i>guaA</i>	7.22E-02	1.19E-01
<i>guaB</i>	9.42E-02	1.37E-01
<i>gyrA</i>	3.34E-02	9.09E-02
<i>gyrB</i>	3.56E-02	8.93E-02
<i>hemE</i>	6.83E-03	7.48E-03
<i>hemL</i>	7.06E-02	9.04E-02
<i>hemX</i>	3.10E-02	3.66E-02
<i>hemY</i>	6.36E-02	8.08E-02
<i>hflC</i>	9.23E-02	9.68E-02
<i>hflK</i>	1.40E-01	1.78E-01
<i>hisA</i>	2.00E-02	1.46E-02
<i>hisB</i>	6.11E-02	6.92E-02
<i>hisC</i>	3.80E-02	4.26E-02
<i>hisD</i>	4.76E-02	6.15E-02
<i>hisF</i>	2.82E-02	2.25E-02
<i>hisG</i>	4.61E-02	4.31E-02
<i>hisH</i>	1.78E-02	1.09E-02
<i>hisJ</i>	1.64E-01	1.30E-01
<i>hldD</i>	2.59E-02	2.52E-02
<i>hldE</i>	5.17E-02	7.43E-02
<i>hns</i>	8.54E-01	3.72E-01
<i>holD</i>	4.69E-03	2.14E-03
<i>holE</i>	0.00E+00	0.00E+00
<i>hsdM</i>	2.47E-02	4.10E-02
<i>hslU</i>	8.20E-02	1.14E-01
<i>htpG</i>	3.64E-01	7.26E-01
<i>hupA</i>	2.07E+00	5.52E-01
<i>hupB</i>	1.27E-01	3.27E-02
<i>hybC</i>	2.67E-02	4.68E-02
<i>hypB</i>	2.59E-02	2.32E-02
<i>iadA</i>	2.58E-02	2.94E-02
<i>icdA</i>	1.06E-01	1.36E-01
<i>ihfA</i>	2.69E-01	8.54E-02
<i>ihfB</i>	2.25E-02	6.65E-03
<i>ileS</i>	3.84E-02	1.14E-01
<i>ilvA</i>	5.57E-02	8.82E-02

<i>Gene Name</i>	<i>Average of Norm. (fmol)</i>	<i>Average of Norm. (ng)</i>
<i>ilvC</i>	2.06E-01	3.12E-01
<i>ilvD</i>	1.10E-01	2.04E-01
<i>ilvE</i>	1.06E-01	1.01E-01
<i>ilvH</i>	2.49E-02	1.25E-02
<i>infA</i>	5.27E-02	1.21E-02
<i>infB</i>	9.92E-02	2.71E-01
<i>infC</i>	5.05E-02	2.90E-02
<i>iraP</i>	1.00E-01	2.76E-02
<i>iscR</i>	6.38E-02	3.13E-02
<i>iscS</i>	5.32E-02	6.72E-02
<i>ispG</i>	6.43E-02	7.34E-02
<i>katE</i>	6.90E-02	1.62E-01
<i>katG</i>	2.73E-02	6.09E-02
<i>kbl</i>	2.91E-02	3.51E-02
<i>kdgR</i>	2.96E-02	2.47E-02
<i>kdsA</i>	4.93E-02	4.27E-02
<i>ldhA</i>	7.08E-02	7.28E-02
<i>lepA</i>	2.76E-02	5.15E-02
<i>leuB</i>	8.61E-02	9.56E-02
<i>leuC1</i>	9.06E-02	1.27E-01
<i>leuD1</i>	1.45E-01	9.15E-02
<i>leuS</i>	1.02E-01	2.77E-01
<i>ligA</i>	3.62E-02	7.44E-02
<i>livG</i>	2.22E-02	1.78E-02
<i>livJ</i>	2.31E-01	2.51E-01
<i>livK</i>	2.72E-02	3.01E-02
<i>lolA</i>	2.03E-02	1.27E-02
<i>lolB</i>	3.64E-02	2.41E-02
<i>lolD</i>	6.45E-03	4.64E-03
<i>lon</i>	6.33E-02	1.55E-01
<i>lpdA</i>	8.57E-02	1.22E-01
<i>lpfB</i>	2.57E-02	1.84E-02
<i>lpp1</i>	3.23E-01	7.60E-02
<i>lptD</i>	4.52E-02	1.14E-01
<i>lptE</i>	6.22E-02	3.73E-02
<i>lrp</i>	6.72E-02	3.55E-02
<i>lsrB</i>	4.32E-02	4.45E-02
<i>lsrF</i>	4.49E-02	4.02E-02
<i>ltaA</i>	1.05E-02	1.07E-02
<i>lysC</i>	3.12E-02	4.27E-02
<i>lysS</i>	5.51E-02	8.89E-02
<i>maeA</i>	2.79E-02	4.92E-02
<i>maeB</i>	7.62E-02	1.76E-01
<i>malP</i>	2.97E-02	7.48E-02
<i>manA</i>	4.42E-02	5.27E-02
<i>manX</i>	2.94E-01	2.87E-01
<i>manY</i>	1.00E-01	7.76E-02
<i>mdh</i>	6.80E-01	6.20E-01
<i>mdoD</i>	2.41E-02	4.21E-02
<i>mdoG</i>	3.31E-02	5.35E-02
<i>metA</i>	3.02E-02	3.01E-02
<i>metE</i>	2.89E-01	6.86E-01
<i>metF</i>	2.90E-02	2.70E-02
<i>metG</i>	7.43E-02	1.59E-01
<i>metH</i>	2.77E-02	1.06E-01
<i>metJ</i>	1.60E-02	5.43E-03
<i>metK</i>	5.16E-02	6.08E-02
<i>metL</i>	3.51E-02	8.79E-02
<i>metN1</i>	4.58E-02	4.84E-02

<i>Gene Name</i>	<i>Average of Norm. (fmol)</i>	<i>Average of Norm. (ng)</i>
<i>metQ</i>	6.21E-01	5.11E-01
<i>mgIB</i>	7.77E-02	7.75E-02
<i>mgsA</i>	4.51E-02	2.14E-02
<i>miaB</i>	6.90E-02	1.04E-01
<i>mig-3</i>	1.47E-02	1.30E-02
<i>minC</i>	4.38E-02	3.10E-02
<i>minD</i>	1.80E-01	1.48E-01
<i>mipA</i>	2.55E-01	1.99E-01
<i>moaB</i>	1.01E-01	5.25E-02
<i>modA</i>	2.19E-01	1.69E-01
<i>modF</i>	1.01E-02	1.55E-02
<i>moeA</i>	6.48E-02	8.07E-02
<i>mppA</i>	1.06E-02	1.77E-02
<i>mrcA</i>	1.43E-02	3.77E-02
<i>mrcB</i>	1.04E-02	2.71E-02
<i>mreB</i>	3.97E-02	4.10E-02
<i>msbA</i>	2.95E-02	5.30E-02
<i>msrA</i>	4.18E-02	2.75E-02
<i>mtlA</i>	4.94E-02	9.43E-02
<i>mtnN</i>	2.77E-02	1.91E-02
<i>mukB</i>	2.60E-02	1.23E-01
<i>murA</i>	4.94E-02	6.23E-02
<i>mutM</i>	8.54E-03	7.34E-03
<i>nadE</i>	3.09E-02	2.63E-02
<i>nagB</i>	1.03E-01	8.54E-02
<i>nanE2</i>	1.86E-02	1.26E-02
<i>ndh</i>	3.03E-02	4.04E-02
<i>ndk</i>	5.99E-02	2.61E-02
<i>nemA</i>	4.74E-02	5.22E-02
<i>nfuA</i>	5.40E-02	3.18E-02
<i>nlpB</i>	9.51E-02	9.83E-02
<i>nlpD</i>	5.66E-02	6.28E-02
<i>nrdA</i>	6.38E-02	1.54E-01
<i>nrfC</i>	1.10E-02	7.92E-03
<i>nuoC</i>	3.62E-02	6.96E-02
<i>nuoF</i>	7.08E-02	9.79E-02
<i>nusA</i>	8.67E-02	1.34E-01
<i>nusG</i>	4.36E-02	2.50E-02
<i>ompA</i>	6.47E+00	6.80E+00
<i>ompC</i>	8.01E-01	9.22E-01
<i>ompD</i>	1.60E+00	1.77E+00
<i>ompF</i>	8.36E-01	9.35E-01
<i>ompN</i>	1.27E-02	1.47E-02
<i>ompR</i>	8.69E-02	6.65E-02
<i>ompS</i>	8.98E-02	1.09E-01
<i>ompW</i>	6.61E-02	4.22E-02
<i>ompX</i>	2.90E-01	1.50E-01
<i>oppA</i>	1.04E-01	1.78E-01
<i>oppD</i>	2.09E-02	2.17E-02
<i>oppF</i>	4.35E-02	4.56E-02
<i>osmC</i>	1.08E-01	4.60E-02
<i>osmE</i>	8.32E-02	2.86E-02
<i>osmX</i>	1.05E-02	9.87E-03
<i>osmY</i>	7.82E-01	4.68E-01
<i>oxyR</i>	3.54E-02	3.39E-02
<i>pagC</i>	1.99E-01	1.12E-01
<i>pagN</i>	8.37E-02	6.02E-02
<i>pal</i>	2.51E-01	1.33E-01
<i>parB</i>	2.63E-02	2.71E-02

<i>Gene Name</i>	<i>Average of Norm. (fmol)</i>	<i>Average of Norm. (ng)</i>
<i>pbpG</i>	4.41E-02	4.23E-02
<i>pckA</i>	1.07E-01	1.78E-01
<i>pdgL</i>	4.49E-02	3.67E-02
<i>pduA</i>	5.05E-01	1.35E-01
<i>pduB</i>	1.49E+00	1.00E+00
<i>pduC</i>	1.21E+00	2.05E+00
<i>pduD</i>	9.91E-01	6.71E-01
<i>pduE</i>	1.90E+00	1.02E+00
<i>pduG</i>	1.22E-01	2.19E-01
<i>pduJ</i>	7.92E-01	2.02E-01
<i>pduL</i>	1.05E-01	6.71E-02
<i>pduN</i>	5.51E-02	1.41E-02
<i>pduO</i>	2.54E-01	2.61E-01
<i>pduP</i>	5.30E-01	7.31E-01
<i>pduQ</i>	7.27E-02	8.08E-02
<i>pduS</i>	1.03E-01	1.40E-01
<i>pduT</i>	3.61E-02	1.95E-02
<i>pduU</i>	4.75E-02	1.66E-02
<i>pduW</i>	6.72E-02	8.33E-02
<i>pdxH</i>	9.33E-03	6.63E-03
<i>pepB</i>	2.85E-02	3.71E-02
<i>pepD</i>	1.29E-01	1.90E-01
<i>pepP</i>	1.70E-02	2.33E-02
<i>pepQ</i>	3.97E-02	5.59E-02
<i>pfkA</i>	9.26E-02	9.12E-02
<i>pfkB</i>	6.41E-02	5.87E-02
<i>pflB</i>	2.28E-01	5.43E-01
<i>pflC</i>	3.42E-02	3.18E-02
<i>pgi</i>	8.28E-02	1.42E-01
<i>pgk</i>	6.09E-01	7.03E-01
<i>pgm</i>	9.45E-02	1.54E-01
<i>pheS</i>	2.56E-02	2.65E-02
<i>pheT</i>	6.19E-02	1.51E-01
<i>phnO</i>	2.41E-02	1.22E-02
<i>phoL</i>	1.76E-02	2.02E-02
<i>phoN</i>	1.75E-01	1.39E-01
<i>phoP</i>	3.86E-01	2.76E-01
<i>phsB</i>	1.23E-02	7.66E-03
<i>pmbA</i>	2.99E-02	4.07E-02
<i>pncB</i>	2.75E-02	3.55E-02
<i>pnp</i>	1.18E-01	2.55E-01
<i>pntA</i>	3.79E-02	5.74E-02
<i>pntB</i>	4.18E-02	5.69E-02
<i>polA</i>	2.13E-02	6.12E-02
<i>potD</i>	4.37E-02	4.77E-02
<i>potF</i>	7.07E-02	8.10E-02
<i>ppa</i>	6.67E-02	3.68E-02
<i>ppc</i>	5.10E-02	1.41E-01
<i>ppiB</i>	2.81E-02	1.43E-02
<i>pps</i>	1.29E-01	3.15E-01
<i>pqiB</i>	2.56E-02	4.36E-02
<i>prc</i>	1.39E-02	3.01E-02
<i>prfA</i>	4.02E-02	4.54E-02
<i>prfB</i>	1.65E-02	1.89E-02
<i>prkB</i>	3.83E-02	3.45E-02
<i>prlC</i>	7.80E-02	1.69E-01
<i>proA</i>	4.16E-02	5.23E-02
<i>proB</i>	2.12E-02	2.32E-02
<i>proC</i>	3.83E-02	3.02E-02

<i>Gene Name</i>	<i>Average of Norm. (fmol)</i>	<i>Average of Norm. (ng)</i>
<i>proQ</i>	2.53E-02	1.80E-02
<i>proS</i>	3.93E-02	6.96E-02
<i>proX</i>	9.88E-02	1.01E-01
<i>prp</i>	2.03E-02	2.95E-02
<i>prs</i>	9.17E-02	8.81E-02
<i>psd</i>	8.08E-02	8.10E-02
PSLT034	3.92E-02	2.28E-02
PSLT046	2.46E-02	1.84E-02
<i>pssA</i>	3.52E-02	5.21E-02
<i>pstS</i>	7.24E-02	7.45E-02
<i>pta</i>	2.29E-01	4.97E-01
<i>ptsG</i>	6.04E-02	8.56E-02
<i>ptsH</i>	8.33E-01	2.12E-01
<i>ptsI</i>	3.33E-01	5.91E-01
<i>ptsN</i>	8.29E-02	4.19E-02
<i>purA</i>	4.23E-02	5.61E-02
<i>purB</i>	5.64E-02	8.13E-02
<i>purC</i>	1.13E-01	8.48E-02
<i>purD</i>	2.87E-02	3.67E-02
<i>purE</i>	6.41E-03	3.17E-03
<i>purF</i>	6.19E-02	9.81E-02
<i>purH</i>	8.53E-02	1.38E-01
<i>purL</i>	4.75E-02	1.88E-01
<i>purN</i>	6.50E-02	4.26E-02
<i>purT</i>	3.61E-02	4.28E-02
<i>purU</i>	3.90E-03	3.47E-03
<i>putA</i>	5.37E-02	2.18E-01
<i>pygM</i>	1.01E-01	2.56E-01
<i>pykA</i>	1.67E-01	2.41E-01
<i>pykF</i>	1.90E-01	2.71E-01
<i>pyrB</i>	1.52E-02	1.48E-02
<i>pyrC</i>	2.31E-02	2.51E-02
<i>pyrD</i>	2.46E-02	2.53E-02
<i>qor</i>	7.76E-02	7.66E-02
<i>rbfA</i>	6.98E-02	2.95E-02
<i>rbsB</i>	8.67E-02	7.50E-02
<i>rdgB</i>	2.42E-02	1.42E-02
<i>recA</i>	6.85E-02	7.29E-02
<i>recD</i>	1.40E-02	2.61E-02
<i>recG</i>	1.59E-02	3.42E-02
<i>res</i>	1.46E-02	4.61E-02
<i>rfbC</i>	5.18E-02	3.00E-02
<i>rfbH</i>	3.49E-02	4.71E-02
<i>rhlB</i>	3.51E-02	4.62E-02
<i>rho</i>	1.30E-01	1.71E-01
<i>ribB</i>	1.88E-02	1.23E-02
<i>ribD</i>	2.21E-02	2.48E-02
<i>ribE</i>	6.93E-02	4.56E-02
<i>ridA</i>	2.08E-01	7.94E-02
<i>rlmF</i>	8.47E-03	8.24E-03
<i>rlpA</i>	2.96E-02	3.24E-02
<i>rmuC</i>	3.29E-02	5.02E-02
<i>rnb</i>	1.67E-02	3.38E-02
<i>rne</i>	7.05E-02	2.36E-01
<i>rodZ</i>	2.48E-02	2.47E-02
<i>rpiA</i>	1.54E-01	9.89E-02
<i>rplA</i>	1.44E+00	9.95E-01
<i>rplB</i>	4.38E-01	3.66E-01
<i>rplC</i>	2.23E-01	1.39E-01

<i>Gene Name</i>	<i>Average of Norm. (fmol)</i>	<i>Average of Norm. (ng)</i>
<i>rplD</i>	4.16E-01	2.56E-01
<i>rplE</i>	6.44E-01	3.66E-01
<i>rplF</i>	6.99E-01	3.69E-01
<i>rplI</i>	8.68E-01	3.83E-01
<i>rplJ</i>	5.10E-01	2.54E-01
<i>rplK</i>	5.64E-01	2.35E-01
<i>rplL</i>	6.57E-01	2.26E-01
<i>rplM</i>	8.23E-02	3.68E-02
<i>rplN</i>	5.20E-01	1.99E-01
<i>rplO</i>	3.48E-01	1.45E-01
<i>rplP</i>	1.06E-01	4.47E-02
<i>rplQ</i>	2.05E-01	8.26E-02
<i>rplR</i>	2.01E-02	7.13E-03
<i>rplS</i>	2.39E-01	8.78E-02
<i>rplT</i>	3.27E-02	1.23E-02
<i>rplU</i>	3.63E-01	1.17E-01
<i>rplV</i>	1.50E-01	5.13E-02
<i>rplW</i>	8.33E-02	2.61E-02
<i>rplX</i>	9.71E-02	3.06E-02
<i>rplY</i>	2.32E-02	6.81E-03
<i>rpmA</i>	1.30E-01	3.33E-02
<i>rpmB</i>	8.40E-02	2.13E-02
<i>rpmC</i>	1.12E-01	2.27E-02
<i>rpmD</i>	5.11E-02	9.27E-03
<i>rpmE2</i>	1.06E-01	2.89E-02
<i>rpmF</i>	8.16E-02	1.46E-02
<i>rpmH</i>	2.82E-02	4.22E-03
<i>rpoA</i>	2.08E-01	2.13E-01
<i>rpoB</i>	2.37E-01	1.00E+00
<i>rpoC</i>	3.93E-01	1.71E+00
<i>rpoE</i>	4.40E-02	2.67E-02
<i>rpoZ</i>	6.42E-02	1.84E-02
<i>rpsA</i>	3.24E-01	5.54E-01
<i>rpsB</i>	6.77E-01	5.07E-01
<i>rpsC</i>	6.50E-01	4.71E-01
<i>rpsD</i>	3.10E-01	2.03E-01
<i>rpsE</i>	8.60E-01	4.23E-01
<i>rpsF</i>	1.34E-01	5.70E-02
<i>rpsG</i>	5.87E-02	2.88E-02
<i>rpsH</i>	2.34E-01	9.26E-02
<i>rpsI</i>	1.17E-01	4.84E-02
<i>rpsJ</i>	6.52E-01	2.14E-01
<i>rpsK</i>	1.43E-01	5.58E-02
<i>rpsL</i>	1.55E-01	6.02E-02
<i>rpsM</i>	1.46E-01	5.39E-02
<i>rpsO</i>	5.03E-02	1.43E-02
<i>rpsR</i>	5.32E-02	1.35E-02
<i>rpsT</i>	1.74E-01	4.68E-02
<i>rpsU</i>	1.33E-02	3.17E-03
<i>rraA</i>	2.96E-02	1.45E-02
<i>rseA</i>	2.09E-02	1.41E-02
<i>rsmH</i>	1.07E-02	1.03E-02
<i>rsxG</i>	7.03E-02	4.37E-02
<i>rtcB</i>	1.93E-01	2.43E-01
<i>sbp</i>	1.68E-01	1.72E-01
<i>sdhA</i>	5.47E-02	9.98E-02
<i>secA</i>	1.35E-01	3.84E-01
<i>secB</i>	3.22E-02	1.57E-02
<i>secD</i>	7.69E-02	1.43E-01

<i>Gene Name</i>	<i>Average of Norm. (fmol)</i>	<i>Average of Norm. (ng)</i>
<i>seqA</i>	2.86E-02	1.61E-02
<i>serA</i>	8.59E-02	1.06E-01
<i>serB</i>	1.53E-02	1.50E-02
<i>serC</i>	1.24E-01	1.39E-01
<i>serS</i>	6.26E-02	8.53E-02
<i>sfbA</i>	3.17E-02	2.64E-02
<i>sitA</i>	1.44E-02	1.35E-02
<i>skp</i>	7.28E-02	3.63E-02
<i>slt</i>	7.55E-03	1.55E-02
<i>slyA</i>	6.32E-02	2.90E-02
<i>slyB</i>	6.54E-01	2.85E-01
<i>smp</i>	6.24E-02	4.22E-02
<i>sodB</i>	2.67E-01	1.60E-01
<i>sodC1</i>	4.90E-02	2.53E-02
<i>solA</i>	2.48E-02	2.83E-02
<i>spy</i>	3.98E-02	2.02E-02
<i>sra</i>	2.36E-01	3.54E-02
<i>ssb</i>	2.52E-02	1.34E-02
<i>sspA</i>	3.46E-02	2.34E-02
<i>sthB</i>	7.12E-03	1.84E-02
STM0032	9.74E-02	1.76E-01
STM0034	1.08E-02	8.82E-03
STM0080	5.08E-02	1.17E-02
STM0164	9.50E-03	7.42E-03
STM0276	3.13E-03	1.55E-03
STM0285	3.49E-02	1.41E-01
STM0327	1.25E-02	4.14E-03
STM0363	7.04E-01	7.43E-01
STM0402	1.02E-01	6.38E-02
STM0564	1.08E-02	1.43E-02
STM0896	2.19E-02	9.11E-03
STM0908	1.34E-02	6.81E-03
STM0918	3.89E-02	1.24E-01
STM1041	9.93E-02	3.02E-01
STM1078	2.44E-02	1.01E-02
STM1119	1.61E-01	9.40E-02
STM1133	2.58E-02	2.93E-02
STM1263	2.51E-01	1.73E-01
STM1541	4.73E-03	3.96E-03
STM1547	5.15E-02	2.62E-02
STM1558	1.36E-02	2.99E-02
STM1560	1.56E-02	2.88E-02
STM1607	3.46E-02	2.37E-02
STM1627	2.10E-02	2.34E-02
STM1633	1.13E-01	9.00E-02
STM1638	2.96E-02	1.30E-02
STM1672	2.63E-02	3.05E-02
STM1676	2.16E-02	1.96E-02
STM1731	9.66E-03	8.59E-03
STM1849	2.56E-02	6.79E-02
STM1857	1.48E-02	6.57E-03
STM1940	1.17E-02	1.78E-02
STM2008	1.22E-02	2.26E-02
STM2243	6.49E-02	5.12E-02
STM2341	1.95E-02	1.67E-02
STM2447	3.20E-02	1.85E-02
STM2475	3.57E-02	8.57E-03
STM2506	1.22E-02	2.54E-03
STM2594	1.49E-02	4.70E-02

<i>Gene Name</i>	<i>Average of Norm. (fmol)</i>	<i>Average of Norm. (ng)</i>
STM2605	9.36E-03	1.36E-02
STM2722	3.40E-02	6.45E-02
STM2740	5.63E-03	6.58E-03
STM2744	6.10E-03	1.42E-03
STM2748	8.20E-03	3.05E-03
STM2797	3.54E-02	1.09E-02
STM3030	7.03E-03	4.56E-03
STM3138	2.76E-02	3.08E-02
STM3152	1.80E-02	2.96E-02
STM3154	3.63E-02	2.05E-02
STM3155	5.78E-02	2.49E-02
STM3533	1.20E-02	9.35E-03
STM3580	1.02E-01	5.66E-02
STM3766	4.56E-02	4.60E-02
STM3820	3.56E-02	5.18E-02
STM4208	1.83E-02	1.93E-02
STM4211	3.23E-02	7.66E-02
STM4212	3.47E-02	1.89E-02
STM4255	8.06E-03	9.18E-04
STM4302	1.24E-02	3.61E-03
STM4423	5.25E-03	4.62E-03
STM4489	6.68E-02	2.46E-01
STM4519	3.93E-02	5.52E-02
<i>stpA</i>	1.62E-01	7.02E-02
<i>sucA</i>	3.61E-02	1.06E-01
<i>sucB</i>	7.79E-02	9.54E-02
<i>sucC</i>	7.11E-02	8.27E-02
<i>sucD</i>	3.05E-02	2.56E-02
<i>suhB</i>	3.01E-02	2.45E-02
<i>surA</i>	8.65E-02	1.14E-01
<i>surE</i>	9.47E-03	7.15E-03
<i>talA</i>	4.82E-02	4.81E-02
<i>talB</i>	3.75E-01	3.70E-01
<i>tar</i>	9.16E-02	1.53E-01
<i>tatB</i>	2.36E-02	1.29E-02
<i>tbpA</i>	4.94E-02	5.03E-02
<i>tcp</i>	9.32E-02	1.54E-01
<i>tdcE</i>	4.37E-03	1.05E-02
<i>tesA</i>	1.31E-02	8.52E-03
<i>tgt</i>	1.70E-02	2.03E-02
<i>thiC</i>	5.78E-02	1.15E-01
<i>thiD</i>	4.18E-02	3.36E-02
<i>thiE</i>	2.73E-02	1.75E-02
<i>thiG</i>	1.87E-02	1.41E-02
<i>thiM</i>	4.62E-02	3.58E-02
<i>thrA</i>	2.36E-01	5.89E-01
<i>thrC</i>	2.32E-01	3.06E-01
<i>thrS</i>	1.01E-01	2.09E-01
<i>tig</i>	3.30E-01	4.43E-01
<i>tktA</i>	7.68E-02	1.55E-01
<i>tktB</i>	3.40E-02	6.94E-02
<i>tmk</i>	2.03E-02	1.34E-02
<i>tolB</i>	6.50E-02	8.37E-02
<i>tolC</i>	1.07E-01	1.60E-01
<i>tpx</i>	3.53E-01	1.80E-01
<i>traN</i>	3.17E-02	5.92E-02
<i>traT</i>	3.52E-01	2.58E-01
<i>treA</i>	4.34E-02	7.70E-02
<i>trg</i>	3.85E-02	6.27E-02

<i>Gene Name</i>	<i>Average of Norm. (fmol)</i>	<i>Average of Norm. (ng)</i>
<i>trkA</i>	8.08E-02	1.13E-01
<i>trmJ</i>	4.34E-02	3.25E-02
<i>trpA</i>	2.91E-02	2.35E-02
<i>trpB</i>	4.23E-02	5.08E-02
<i>trpC</i>	1.69E-02	2.33E-02
<i>trxA</i>	4.20E-01	1.40E-01
<i>trxB</i>	2.47E-01	2.41E-01
<i>tsf</i>	4.47E-01	3.80E-01
<i>tsr</i>	4.54E-02	7.63E-02
<i>tufA</i>	5.82E+00	7.07E+00
<i>typA</i>	7.68E-02	1.45E-01
<i>tyrS</i>	3.20E-02	4.26E-02
<i>ubiE</i>	2.57E-02	2.02E-02
<i>ubiG</i>	6.91E-02	5.22E-02
<i>ucpA</i>	3.74E-02	2.93E-02
<i>udp</i>	3.10E-02	2.36E-02
<i>ugpB</i>	3.11E-02	4.21E-02
<i>ung</i>	1.49E-02	1.06E-02
<i>upp</i>	6.60E-02	4.16E-02
<i>uspA</i>	5.76E-02	2.59E-02
<i>uspE</i>	2.17E-02	2.15E-02
<i>uspF</i>	3.25E-01	1.43E-01
<i>uspG</i>	6.03E-02	2.68E-02
<i>uxaC</i>	1.16E-02	1.75E-02
<i>vacB</i>	4.31E-02	1.12E-01
<i>vacJ</i>	2.18E-02	1.73E-02
<i>valS</i>	1.22E-02	3.72E-02
<i>wzzB</i>	3.29E-02	3.33E-02
<i>wzzE</i>	4.11E-02	4.53E-02
<i>xseB</i>	6.51E-02	1.63E-02
<i>yaaA</i>	2.68E-02	2.23E-02
<i>yadF</i>	6.98E-02	4.86E-02
<i>yaeH</i>	1.03E-01	4.36E-02
<i>yahO</i>	2.41E-01	6.68E-02
<i>yajG</i>	2.62E-02	1.67E-02
<i>yajQ</i>	5.26E-02	2.69E-02
<i>ybaB</i>	5.20E-02	1.75E-02
<i>ybaY</i>	1.52E-01	8.27E-02
<i>ybdH</i>	2.84E-02	3.15E-02
<i>ybeL</i>	1.96E-02	1.02E-02
<i>ybgI</i>	6.77E-02	5.12E-02
<i>ybgJ</i>	3.31E-02	2.24E-02
<i>ybhB</i>	4.54E-02	2.16E-02
<i>ybhC</i>	1.65E-02	2.11E-02
<i>ybiS</i>	1.27E-01	1.19E-01
<i>ybiT</i>	2.28E-02	3.82E-02
<i>ybjP</i>	8.78E-02	4.67E-02
<i>ybjY</i>	8.35E-03	9.58E-03
<i>ycbL</i>	4.25E-02	2.87E-02
<i>yceB</i>	3.30E-02	1.92E-02
<i>ycfF</i>	6.89E-02	2.56E-02
<i>ycgQ</i>	3.25E-02	3.05E-02
<i>ychF</i>	6.19E-02	6.92E-02
<i>yciE</i>	4.06E-02	2.15E-02
<i>yciF</i>	4.60E-02	2.41E-02
<i>yciK</i>	6.16E-02	4.84E-02
<i>ydbH</i>	7.08E-03	1.93E-02
<i>ydeI</i>	1.95E-02	7.79E-03
<i>ydfG</i>	1.53E-01	1.16E-01

<i>Gene Name</i>	<i>Average of Norm. (fmol)</i>	<i>Average of Norm. (ng)</i>
<i>ydfZ</i>	1.48E-02	3.03E-03
<i>ydgA</i>	6.25E-02	9.48E-02
<i>ydgH</i>	1.15E-01	1.10E-01
<i>ydgH</i>	3.95E-02	5.65E-02
<i>ydgI</i>	1.89E-01	4.34E-02
<i>ydgJ</i>	3.14E-02	3.60E-02
<i>ydhD</i>	2.48E-02	9.02E-03
<i>ydhJ</i>	2.70E-02	2.48E-02
<i>ydiR</i>	1.70E-02	1.60E-02
<i>ydjA</i>	7.37E-02	4.18E-02
<i>ydjN</i>	2.82E-02	3.83E-02
<i>yeaG</i>	2.89E-02	6.05E-02
<i>yebC</i>	1.84E-02	1.36E-02
<i>yecM</i>	1.14E-01	6.89E-02
<i>yedD</i>	4.31E-02	1.86E-02
<i>yedF</i>	8.80E-03	2.14E-03
<i>yegS</i>	4.25E-03	3.82E-03
<i>yehZ</i>	8.12E-02	7.45E-02
<i>yeiP</i>	1.38E-02	8.27E-03
<i>yejK</i>	1.72E-01	1.82E-01
<i>yfbU</i>	5.42E-02	2.96E-02
<i>yfcZ</i>	6.96E-02	2.07E-02
<i>yfgD</i>	3.41E-02	1.27E-02
<i>yfgM</i>	8.50E-02	5.26E-02
<i>yfiA</i>	8.24E-02	2.91E-02
<i>ygaM</i>	1.14E-01	3.99E-02
<i>ygaP</i>	5.25E-02	2.73E-02
<i>ygaU</i>	1.95E-01	8.78E-02
<i>ygfZ</i>	5.09E-02	5.14E-02
<i>yggE</i>	2.99E-02	2.20E-02
<i>yggN</i>	2.41E-02	1.78E-02
<i>yggX</i>	4.25E-02	1.30E-02
<i>yghA</i>	9.68E-02	8.54E-02
<i>ygiC</i>	3.08E-02	3.88E-02
<i>ygiM</i>	2.65E-02	1.69E-02
<i>ygjR</i>	3.86E-02	4.03E-02
<i>yhbL</i>	4.50E-02	2.90E-02
<i>yhbN</i>	5.43E-02	3.03E-02
<i>yhbS</i>	6.40E-02	3.31E-02
<i>yhbW</i>	6.71E-03	6.93E-03
<i>yhcB</i>	1.51E-01	6.44E-02
<i>yhdH</i>	3.77E-02	3.67E-02
<i>yhgF</i>	1.46E-02	3.50E-02
<i>yhhA</i>	4.11E-02	1.76E-02
<i>yhjG</i>	2.78E-02	5.81E-02
<i>yhjJ</i>	5.07E-02	7.81E-02
<i>viaD</i>	1.54E-02	9.71E-03
<i>viaO</i>	4.73E-03	4.82E-03
<i>yibF</i>	9.34E-02	5.95E-02
<i>yibN</i>	6.04E-02	2.65E-02
<i>yicC</i>	7.09E-02	6.60E-02
<i>ydC</i>	4.15E-02	7.14E-02
<i>yihD</i>	3.38E-02	9.80E-03
<i>yihG</i>	1.02E-02	1.03E-02
<i>yiiG</i>	7.41E-03	8.16E-03
<i>yjeE</i>	3.13E-02	1.48E-02
<i>yjgM</i>	6.29E-03	3.27E-03
<i>yjjK</i>	8.84E-02	1.54E-01
<i>yliJ</i>	1.21E-02	8.02E-03

<i>Gene Name</i>	<i>Average of Norm. (fmol)</i>	<i>Average of Norm. (ng)</i>
<i>ymbA</i>	1.42E-02	8.15E-03
<i>yncB</i>	3.47E-02	3.83E-02
<i>yncE</i>	3.66E-02	3.93E-02
<i>ynhG</i>	1.65E-02	1.66E-02

Table S10. Proteomics: Proteins in Δ *fnr*.

<i>Gene Name</i>	<i>Average of Norm (fmol)</i>	<i>Average of Norm. (ng)</i>
<i>accA</i>	4.61E-02	4.85E-02
<i>accB</i>	8.77E-02	4.29E-02
<i>accC</i>	1.39E-01	2.04E-01
<i>accD</i>	2.90E-02	2.81E-02
<i>aceE</i>	2.06E-01	6.01E-01
<i>aceF</i>	1.26E-01	2.45E-01
<i>ackA</i>	1.37E-01	1.75E-01
<i>acnA</i>	3.98E-02	1.15E-01
<i>acnB</i>	4.46E-02	1.21E-01
<i>acpP</i>	3.34E-01	8.65E-02
<i>acrA</i>	2.04E-01	2.57E-01
<i>acrB</i>	8.67E-02	2.84E-01
<i>acs</i>	4.97E-02	1.08E-01
<i>adhE</i>	3.16E-01	8.94E-01
<i>adhP</i>	1.03E-01	1.09E-01
<i>adk</i>	9.74E-02	6.62E-02
<i>ahpC</i>	1.20E-01	7.32E-02
<i>ahpF</i>	4.51E-02	7.32E-02
<i>alaS</i>	1.65E-01	4.57E-01
<i>aldB</i>	7.27E-02	1.24E-01
<i>apbC</i>	5.07E-02	5.87E-02
<i>argA</i>	7.80E-02	1.12E-01
<i>argB</i>	7.00E-02	5.47E-02
<i>argD</i>	7.26E-02	9.42E-02
<i>argG</i>	7.42E-02	1.08E-01
<i>argH</i>	1.10E-01	1.62E-01
<i>argI</i>	2.66E-02	2.94E-02
<i>argT</i>	4.05E-02	3.39E-02
<i>arnB</i>	4.15E-02	5.03E-02
<i>arnC</i>	5.42E-02	5.86E-02
<i>aroB</i>	5.40E-02	6.32E-02
<i>aroF</i>	1.96E-02	2.21E-02
<i>artI</i>	5.86E-02	4.65E-02
<i>artJ</i>	2.98E-02	2.31E-02
<i>asd</i>	2.01E-01	2.36E-01
<i>asnS</i>	2.11E-01	3.28E-01
<i>aspA</i>	7.34E-02	1.12E-01
<i>aspC</i>	4.59E-02	5.90E-02
<i>aspS</i>	5.27E-02	1.00E-01
<i>atpA</i>	2.32E-01	3.75E-01
<i>atpD</i>	5.32E-01	7.85E-01
<i>atpF</i>	3.57E-02	1.85E-02
<i>atpG</i>	7.65E-02	6.99E-02
<i>atpH</i>	7.78E-02	4.48E-02
<i>bamA</i>	1.29E-01	3.40E-01
<i>bamB</i>	1.30E-01	1.61E-01
<i>befG</i>	3.67E-02	2.90E-02
<i>bcp</i>	2.03E-01	1.06E-01
<i>bfr</i>	1.30E-01	7.01E-02
<i>bioA</i>	3.48E-02	4.82E-02
<i>bioB</i>	4.99E-02	5.66E-02

<i>Gene Name</i>	<i>Average of Norm (fmol)</i>	<i>Average of Norm. (ng)</i>
<i>bioD1</i>	2.04E-01	1.47E-01
<i>btuE</i>	5.26E-02	3.16E-02
<i>carA</i>	9.47E-02	1.17E-01
<i>carB</i>	1.18E-01	4.14E-01
<i>cbiF</i>	8.71E-02	7.16E-02
<i>cbiL</i>	4.57E-02	3.45E-02
<i>cdh</i>	8.69E-02	7.33E-02
<i>clpB</i>	2.15E-01	6.04E-01
<i>clpX</i>	6.65E-02	9.28E-02
<i>coaE</i>	1.31E-02	8.93E-03
<i>copA</i>	2.15E-02	5.49E-02
<i>cra</i>	2.76E-02	3.04E-02
<i>crl</i>	1.05E-02	5.02E-03
<i>crr</i>	9.20E-01	4.96E-01
<i>cspA</i>	2.77E-01	6.04E-02
<i>cspC</i>	9.22E-01	2.02E-01
<i>cspD</i>	5.11E-02	1.22E-02
<i>cspE</i>	2.62E-01	5.74E-02
<i>cspJ</i>	1.08E-01	2.48E-02
<i>cypD</i>	1.67E-01	3.35E-01
<i>cysA</i>	4.34E-02	5.24E-02
<i>cysE</i>	4.61E-02	4.06E-02
<i>cysI</i>	3.89E-02	7.35E-02
<i>cysJ</i>	4.74E-02	9.32E-02
<i>cysK</i>	2.19E-01	2.21E-01
<i>cysM</i>	1.17E-02	1.10E-02
<i>cysN</i>	5.84E-02	9.14E-02
<i>cysP</i>	5.24E-02	5.80E-02
<i>dacC</i>	2.75E-02	3.47E-02
<i>damX</i>	1.32E-01	1.77E-01
<i>dapA</i>	5.31E-02	4.85E-02
<i>dapB</i>	9.11E-01	7.90E-01
<i>dapD</i>	1.04E-01	9.16E-02
<i>def</i>	4.39E-02	2.55E-02
<i>degP</i>	1.79E-01	2.62E-01
<i>degQ</i>	8.45E-02	1.19E-01
<i>deoA</i>	3.28E-02	4.54E-02
<i>deoB</i>	3.62E-02	4.65E-02
<i>deoD</i>	6.41E-02	4.90E-02
<i>dkgA</i>	8.34E-02	7.71E-02
<i>dkgB</i>	2.20E-02	1.85E-02
<i>dksA</i>	1.29E-01	6.72E-02
<i>dmsA</i>	3.77E-02	1.03E-01
<i>dnaB</i>	4.97E-02	7.56E-02
<i>dnaJ</i>	4.38E-02	5.29E-02
<i>dnaK</i>	6.40E-01	1.31E+00
<i>dnaN</i>	3.36E-02	3.96E-02
<i>dppA</i>	9.44E-02	1.68E-01
<i>dppD</i>	1.71E-02	1.78E-02
<i>dps</i>	2.43E-01	1.34E-01
<i>dsbA</i>	5.86E-02	3.94E-02
<i>dsbC</i>	2.75E-02	2.07E-02
<i>ecnB</i>	9.84E-01	1.40E-01
<i>eda</i>	3.92E-02	2.62E-02
<i>elaB</i>	8.25E-02	2.86E-02
<i>eno</i>	9.55E-01	1.27E+00
<i>entB</i>	4.86E-02	4.61E-02
<i>erfK</i>	4.19E-02	4.29E-02
<i>erpA</i>	6.11E-02	2.25E-02

<i>Gene Name</i>	<i>Average of Norm (fmol)</i>	<i>Average of Norm. (ng)</i>
<i>fabA</i>	6.70E-02	3.76E-02
<i>fabB</i>	3.10E-01	3.93E-01
<i>fabD</i>	1.40E-01	1.32E-01
<i>fabF</i>	8.17E-02	1.05E-01
<i>fabG</i>	1.41E-01	1.04E-01
<i>fabH</i>	3.13E-02	3.11E-02
<i>fabI</i>	8.48E-02	6.92E-02
<i>fadL</i>	8.60E-02	1.18E-01
<i>fabA</i>	7.39E-02	8.40E-02
<i>fabB</i>	1.34E+00	1.52E+00
<i>fbp</i>	5.86E-02	6.38E-02
<i>fdhE</i>	8.16E-02	8.28E-02
<i>fdx</i>	6.93E-02	2.56E-02
<i>ffh</i>	4.81E-02	7.01E-02
<i>fhuA</i>	1.86E-01	4.45E-01
<i>fkfB</i>	1.34E-01	9.35E-02
<i>fkpA</i>	6.10E-02	5.19E-02
<i>fldA</i>	5.65E-02	3.35E-02
<i>flgE</i>	1.71E-02	2.16E-02
<i>flgK</i>	7.18E-02	1.23E-01
<i>flgL</i>	5.44E-02	5.56E-02
<i>fliC</i>	8.47E-02	1.29E-01
<i>fliE</i>	1.35E-02	4.47E-03
<i>fliY</i>	3.55E-02	3.01E-02
<i>fljB</i>	3.76E-02	5.91E-02
<i>frdA</i>	6.13E-02	1.17E-01
<i>frdB</i>	3.56E-02	2.85E-02
<i>frr</i>	1.51E-01	9.18E-02
<i>fin</i>	5.53E-02	3.08E-02
<i>ftsH</i>	9.28E-02	1.95E-01
<i>ftsZ</i>	1.94E-01	2.32E-01
<i>fumC</i>	7.48E-02	1.09E-01
<i>fusA</i>	7.47E-01	1.70E+00
<i>gabT</i>	2.59E-02	3.45E-02
<i>galF</i>	7.87E-02	7.53E-02
<i>galK</i>	2.57E-02	3.10E-02
<i>galU</i>	1.25E-01	1.21E-01
<i>gapA</i>	1.36E+00	1.44E+00
<i>gatY</i>	4.91E-02	4.58E-02
<i>gcvH</i>	9.80E-02	4.08E-02
<i>gcvP</i>	5.16E-02	1.60E-01
<i>ggt</i>	2.55E-02	4.54E-02
<i>glgA</i>	4.54E-02	7.09E-02
<i>glk</i>	3.99E-02	4.07E-02
<i>glmM</i>	8.26E-02	1.14E-01
<i>glnA</i>	1.70E-01	2.59E-01
<i>glnH</i>	7.54E-02	6.07E-02
<i>glpA</i>	5.71E-02	9.86E-02
<i>glpD</i>	9.08E-02	1.52E-01
<i>glpK</i>	1.58E-01	2.62E-01
<i>glpQ</i>	1.22E-01	1.47E-01
<i>glpR</i>	6.96E-02	5.62E-02
<i>gltA</i>	6.18E-02	8.78E-02
<i>gltB</i>	7.38E-02	3.50E-01
<i>gltd</i>	4.29E-02	6.79E-02
<i>glfI</i>	7.51E-02	7.54E-02
<i>glyA</i>	2.06E-01	2.77E-01
<i>glyQ</i>	9.50E-02	9.60E-02
<i>glyS</i>	2.12E-01	4.87E-01

<i>Gene Name</i>	<i>Average of Norm (fmol)</i>	<i>Average of Norm. (ng)</i>
<i>gnd</i>	1.05E-01	1.59E-01
<i>gpmA</i>	8.47E-02	7.09E-02
<i>gppA</i>	1.23E-01	1.97E-01
<i>greA</i>	8.22E-02	4.36E-02
<i>groL</i>	2.00E+00	3.38E+00
<i>groS</i>	1.77E+00	5.37E-01
<i>grpE</i>	7.57E-02	4.88E-02
<i>grxA</i>	4.20E-02	1.22E-02
<i>grxB</i>	3.00E-01	2.16E-01
<i>grxC</i>	3.20E-02	8.59E-03
<i>gst</i>	3.57E-02	2.36E-02
<i>guaA</i>	8.78E-02	1.53E-01
<i>guaB</i>	1.10E-01	1.69E-01
<i>gyrB</i>	4.06E-02	1.06E-01
<i>hemL</i>	5.83E-02	7.84E-02
<i>hemX</i>	1.07E-01	1.32E-01
<i>hemY</i>	7.41E-02	9.99E-02
<i>hflC</i>	1.22E-01	1.35E-01
<i>hflK</i>	1.73E-01	2.35E-01
<i>hisA</i>	2.86E-02	2.21E-02
<i>hisB</i>	6.82E-02	8.09E-02
<i>hisC</i>	1.18E-01	1.40E-01
<i>hisD</i>	5.71E-02	7.82E-02
<i>hisG</i>	1.33E-01	1.32E-01
<i>hisH</i>	5.48E-02	3.47E-02
<i>hisJ</i>	2.35E-01	1.98E-01
<i>hldD</i>	1.46E-02	1.48E-02
<i>hldE</i>	5.80E-02	8.75E-02
<i>hns</i>	5.94E-01	2.70E-01
<i>hslU</i>	4.45E-01	6.60E-01
<i>htpG</i>	2.78E-01	5.84E-01
<i>hupA</i>	1.33E+00	3.71E-01
<i>icdA</i>	1.30E-01	1.77E-01
<i>ihfA</i>	2.27E-01	7.54E-02
<i>ileS</i>	4.60E-02	1.41E-01
<i>ilvC</i>	1.55E-01	2.48E-01
<i>ilvD</i>	1.12E-01	2.18E-01
<i>ilvE</i>	1.37E-01	1.39E-01
<i>infB</i>	8.75E-02	2.50E-01
<i>infC</i>	4.98E-02	3.08E-02
<i>iraP</i>	3.61E-02	1.07E-02
<i>iroN</i>	5.06E-02	1.20E-01
<i>iscR</i>	1.24E-01	6.39E-02
<i>ispG</i>	7.57E-02	9.06E-02
<i>katE</i>	8.77E-02	2.12E-01
<i>kdgR</i>	4.15E-02	3.65E-02
<i>kdsA</i>	9.04E-02	8.39E-02
<i>kdsD (yrbH)</i>	2.30E-02	2.35E-02
<i>ldhA</i>	5.42E-02	5.76E-02
<i>leuB</i>	4.80E-02	5.65E-02
<i>leuC1</i>	8.10E-02	1.20E-01
<i>leuD1</i>	1.07E-01	7.07E-02
<i>leuS</i>	6.02E-02	1.74E-01
<i>livJ</i>	2.38E-01	2.72E-01
<i>lolB</i>	3.41E-02	2.34E-02
<i>lolD</i>	6.02E-03	4.45E-03
<i>lon</i>	7.64E-02	1.97E-01
<i>lpdA</i>	8.13E-02	1.22E-01
<i>lpfB</i>	4.61E-02	3.52E-02

<i>Gene Name</i>	<i>Average of Norm (fmol)</i>	<i>Average of Norm. (ng)</i>
<i>lpp1</i>	8.13E-01	2.03E-01
<i>lpp2</i>	3.15E-03	8.07E-04
<i>lptD</i>	7.24E-02	1.92E-01
<i>lptE</i>	4.08E-02	2.53E-02
<i>lsrB</i>	4.26E-02	4.66E-02
<i>lsrF</i>	3.28E-02	3.03E-02
<i>luxS</i>	9.49E-02	5.54E-02
<i>lysS</i>	8.52E-02	1.44E-01
<i>maeB</i>	7.94E-02	1.90E-01
<i>manA</i>	3.16E-02	3.96E-02
<i>manX</i>	1.60E-01	1.65E-01
<i>manY</i>	2.96E-01	2.41E-01
<i>mdh</i>	6.23E-01	5.99E-01
<i>mdoG</i>	3.80E-02	6.35E-02
<i>metA</i>	4.42E-02	4.61E-02
<i>metE</i>	2.33E-01	5.86E-01
<i>metG</i>	1.02E-01	2.30E-01
<i>metH</i>	2.61E-02	1.03E-01
<i>metK</i>	3.85E-02	4.77E-02
<i>metL</i>	5.18E-02	1.39E-01
<i>metN1</i>	1.04E-01	1.18E-01
<i>metQ</i>	5.95E-01	5.17E-01
<i>mglB</i>	3.69E-02	3.81E-02
<i>minD</i>	1.91E-01	1.67E-01
<i>mipA</i>	2.62E-01	2.15E-01
<i>mlc</i>	2.36E-02	3.03E-02
<i>moaB</i>	4.77E-02	2.57E-02
<i>modA</i>	2.63E-02	2.09E-02
<i>moeA</i>	4.74E-02	6.35E-02
<i>mppA</i>	2.60E-02	4.49E-02
<i>mreB</i>	4.90E-02	5.36E-02
<i>msbA</i>	4.58E-02	8.52E-02
<i>msrA</i>	7.15E-02	4.97E-02
<i>mtlA</i>	5.03E-02	1.01E-01
<i>mukB</i>	3.63E-02	1.79E-01
<i>murA</i>	8.02E-02	1.08E-01
<i>murG</i>	1.02E-02	1.12E-02
<i>mutT</i>	1.03E-02	4.67E-03
<i>nanE2</i>	2.62E-02	1.84E-02
<i>ndk</i>	1.01E-01	4.64E-02
<i>nfuA</i>	5.30E-02	3.24E-02
<i>nifU</i>	1.98E-01	8.30E-02
<i>nlpB</i>	1.66E-01	1.81E-01
<i>nlpD</i>	1.00E-01	1.18E-01
<i>nrdA</i>	2.86E-02	7.14E-02
<i>nrdB</i>	2.99E-02	3.79E-02
<i>nrdI</i>	1.90E-02	8.77E-03
<i>nusA</i>	7.28E-02	1.18E-01
<i>nusG</i>	4.95E-02	3.05E-02
<i>ompA</i>	1.15E+01	1.27E+01
<i>ompC</i>	7.89E-01	9.61E-01
<i>ompD</i>	4.85E-01	5.65E-01
<i>ompF</i>	5.59E-01	6.55E-01
<i>ompR</i>	7.44E-02	5.89E-02
<i>ompX</i>	7.53E-01	4.11E-01
<i>oppA</i>	7.32E-02	1.32E-01
<i>oppF</i>	2.07E-02	2.25E-02
<i>osmC</i>	2.19E-01	9.72E-02
<i>osmE</i>	2.37E-01	8.71E-02

<i>Gene Name</i>	<i>Average of Norm (fmol)</i>	<i>Average of Norm. (ng)</i>
<i>osmY</i>	1.34E+00	8.45E-01
<i>pagC</i>	6.15E-01	3.67E-01
<i>pagN</i>	1.54E-01	1.16E-01
<i>pal</i>	3.70E-01	2.06E-01
<i>parB</i>	2.74E-02	2.97E-02
<i>pckA</i>	1.56E-01	2.76E-01
<i>pdgL</i>	8.70E-02	7.50E-02
<i>pduA</i>	2.02E-01	5.63E-02
<i>pduB</i>	4.05E-01	2.87E-01
<i>pduC</i>	2.88E-01	5.13E-01
<i>pduD</i>	2.99E-01	2.13E-01
<i>pduE</i>	3.55E-01	1.99E-01
<i>pduJ</i>	4.78E-01	1.28E-01
<i>pduL</i>	8.78E-02	5.88E-02
<i>pduO</i>	6.67E-02	7.38E-02
<i>pduP</i>	1.29E-01	1.87E-01
<i>pduQ</i>	3.16E-02	3.64E-02
<i>pduS</i>	2.60E-02	3.73E-02
<i>pepA</i>	3.30E-02	5.47E-02
<i>pepD</i>	7.78E-02	1.22E-01
<i>pepQ</i>	5.64E-02	8.50E-02
<i>pfkA</i>	1.67E-01	1.70E-01
<i>pfkB</i>	8.23E-02	7.94E-02
<i>pflB</i>	1.01E-01	2.54E-01
<i>pgi</i>	1.49E-02	2.74E-02
<i>pgk</i>	9.39E-01	1.14E+00
<i>pgl</i>	6.25E-02	6.85E-02
<i>pgm</i>	7.51E-02	1.28E-01
<i>phoN</i>	2.84E-01	2.39E-01
<i>phoP</i>	4.21E-01	3.19E-01
<i>pnp</i>	1.23E-01	2.80E-01
<i>potD</i>	6.69E-02	7.62E-02
<i>potF</i>	9.13E-02	1.10E-01
<i>ppc</i>	3.19E-02	9.15E-02
<i>pphB</i>	1.03E-01	7.78E-02
<i>pps</i>	1.11E-01	2.86E-01
<i>prc</i>	2.51E-02	5.57E-02
<i>prfB</i>	3.81E-02	4.60E-02
<i>prgJ</i>	4.48E-03	1.47E-03
<i>priB</i>	7.03E-02	2.45E-02
<i>priC</i>	8.30E-02	1.85E-01
<i>proA</i>	4.51E-02	6.08E-02
<i>proC</i>	3.54E-02	3.00E-02
<i>proQ</i>	5.51E-02	4.07E-02
<i>proS</i>	4.21E-02	7.86E-02
<i>proX</i>	4.82E-02	5.23E-02
<i>prr</i>	4.23E-02	6.30E-02
<i>prs</i>	1.59E-01	1.62E-01
<i>pspA</i>	3.20E-02	2.44E-02
<i>pssA</i>	3.80E-02	5.81E-02
<i>pstS</i>	1.40E-01	1.54E-01
<i>pta</i>	7.46E-02	1.67E-01
<i>ptsG</i>	6.63E-02	9.69E-02
<i>ptsH</i>	5.59E-01	1.50E-01
<i>ptsI</i>	2.16E-01	4.02E-01
<i>ptsN</i>	1.10E-01	5.90E-02
<i>purA</i>	5.70E-02	7.83E-02
<i>purB</i>	7.49E-02	1.12E-01
<i>purE</i>	2.42E-02	1.29E-02

<i>Gene Name</i>	<i>Average of Norm (fmol)</i>	<i>Average of Norm. (ng)</i>
<i>purH</i>	5.93E-02	9.90E-02
<i>purT</i>	4.90E-02	6.23E-02
<i>purU</i>	4.70E-02	4.50E-02
<i>PYGM</i>	1.91E-01	5.11E-01
<i>pykA</i>	1.21E-01	1.84E-01
<i>pykF</i>	2.85E-01	4.26E-01
<i>pyrC</i>	7.04E-02	8.21E-02
<i>pyrF</i>	5.76E-03	4.57E-03
<i>pyrI</i>	3.67E-02	1.91E-02
<i>qor</i>	1.41E-01	1.45E-01
<i>rbsB</i>	5.16E-02	4.66E-02
<i>rcsB</i>	5.79E-02	4.11E-02
<i>recA</i>	1.17E-01	1.33E-01
<i>rfaQ</i>	2.40E-02	2.70E-02
<i>rfbB</i>	1.66E-02	2.03E-02
<i>rfbC</i>	4.46E-02	2.70E-02
<i>rhaM</i>	1.94E-02	7.18E-03
<i>rho</i>	1.53E-01	2.11E-01
<i>ribE</i>	1.09E-01	7.55E-02
<i>ribH</i>	5.11E-02	2.43E-02
<i>ridA</i>	1.31E-01	5.22E-02
<i>rlmN (yfgB)</i>	3.09E-02	3.92E-02
<i>rne</i>	5.41E-02	1.87E-01
<i>rodZ</i>	4.78E-02	5.04E-02
<i>rof</i>	1.41E-01	4.14E-02
<i>rpiA</i>	1.41E-01	9.49E-02
<i>rplA</i>	1.60E+00	1.17E+00
<i>rplB</i>	5.08E-01	4.50E-01
<i>rplC</i>	3.46E-01	2.27E-01
<i>rplD</i>	4.28E-01	2.77E-01
<i>rplE</i>	7.27E-01	4.36E-01
<i>rplF</i>	7.70E-01	4.29E-01
<i>rplI</i>	8.69E-01	4.03E-01
<i>rplJ</i>	3.52E-01	1.83E-01
<i>rplK</i>	4.76E-01	2.08E-01
<i>rplL</i>	9.12E-01	3.31E-01
<i>rplM</i>	1.15E-01	5.42E-02
<i>rplN</i>	3.83E-01	1.54E-01
<i>rplO</i>	4.47E-01	1.97E-01
<i>rplP</i>	1.37E-01	6.09E-02
<i>rplQ</i>	1.70E-01	7.14E-02
<i>rplS</i>	2.53E-01	9.77E-02
<i>rplU</i>	4.09E-01	1.39E-01
<i>rplV</i>	1.52E-01	5.36E-02
<i>rplW</i>	1.59E-01	5.24E-02
<i>rplX</i>	3.77E-02	1.25E-02
<i>rpmB</i>	6.45E-02	1.70E-02
<i>rpmD</i>	5.29E-02	9.94E-03
<i>rpmE2</i>	5.99E-02	1.70E-02
<i>rpmF</i>	3.51E-02	6.77E-03
<i>rpoA</i>	2.05E-01	2.23E-01
<i>rpoB</i>	3.09E-01	1.37E+00
<i>rpoC</i>	3.67E-01	1.68E+00
<i>rpoD</i>	3.65E-02	7.74E-02
<i>rpoE</i>	5.98E-02	3.76E-02
<i>rpoZ</i>	8.91E-02	2.63E-02
<i>rpsA</i>	4.08E-01	7.36E-01
<i>rpsB</i>	9.60E-01	7.57E-01
<i>rpsC</i>	7.29E-01	5.57E-01

<i>Gene Name</i>	<i>Average of Norm (fmol)</i>	<i>Average of Norm. (ng)</i>
<i>rpsD</i>	3.49E-01	2.41E-01
<i>rpsE</i>	7.77E-01	4.00E-01
<i>rpsF</i>	1.19E-01	5.30E-02
<i>rpsG</i>	1.70E-01	8.85E-02
<i>rpsH</i>	4.23E-01	1.73E-01
<i>rpsI</i>	1.03E-01	4.51E-02
<i>rpsJ</i>	6.92E-01	2.40E-01
<i>rpsK</i>	2.02E-01	8.30E-02
<i>rpsL</i>	1.49E-01	6.24E-02
<i>rpsM</i>	1.12E-01	4.36E-02
<i>rpsR</i>	6.46E-02	1.70E-02
<i>rpsU</i>	2.78E-02	7.13E-03
<i>rraA</i>	5.12E-02	2.68E-02
<i>rseB</i>	1.38E-02	1.49E-02
<i>rsmG (gidB)</i>	2.71E-02	1.82E-02
<i>rtcB</i>	2.52E-02	3.29E-02
<i>secB</i>	9.37E-02	4.85E-02
<i>secD</i>	7.45E-02	1.43E-01
<i>secG</i>	4.50E-02	1.48E-02
<i>serA</i>	9.96E-02	1.30E-01
<i>serC</i>	1.02E-01	1.20E-01
<i>serS</i>	3.32E-02	4.69E-02
<i>sifB</i>	1.74E-02	1.84E-02
<i>sitA</i>	9.96E-02	9.95E-02
<i>sitB</i>	2.37E-02	2.05E-02
<i>skp</i>	7.27E-02	3.89E-02
<i>slyB</i>	1.14E+00	5.15E-01
<i>sodA</i>	7.35E-02	5.08E-02
<i>sodB</i>	2.30E-01	1.43E-01
<i>sohB</i>	4.89E-02	5.51E-02
<i>sopB</i>	2.07E-02	3.71E-02
<i>spy</i>	1.71E+00	9.02E-01
<i>sra</i>	1.05E-01	1.67E-02
<i>ssb</i>	1.20E-02	6.86E-03
<i>sseA</i>	3.64E-02	3.24E-02
<i>sspA</i>	1.88E-02	1.37E-02
<i>sspB</i>	3.88E-02	2.12E-02
STM0080	8.74E-02	2.11E-02
STM0098	2.37E-02	1.61E-02
STM0297	7.14E-02	1.54E-02
STM0402	7.84E-02	5.21E-02
STM0856	4.50E-02	4.34E-02
STM0908	2.07E-02	1.10E-02
STM0951	1.88E-02	1.70E-02
STM1119	3.19E-01	1.96E-01
STM1239	9.49E-03	1.18E-02
STM1263	1.25E-01	9.10E-02
STM1267	2.02E-02	5.72E-03
STM1607	3.14E-02	2.22E-02
STM1633	9.86E-02	8.26E-02
STM1672	3.42E-02	4.10E-02
STM1731	5.90E-02	5.55E-02
STM1858	1.57E-02	4.86E-03
STM2243	1.91E-02	1.55E-02
STM2447	6.14E-02	3.73E-02
STM2475	9.17E-02	2.36E-02
STM2506	7.75E-03	1.67E-03
STM2722	7.82E-02	1.52E-01
STM3256	3.58E-02	3.13E-02

<i>Gene Name</i>	<i>Average of Norm (fmol)</i>	<i>Average of Norm. (ng)</i>
STM3354 (<i>ttdB</i>)	1.62E-02	1.12E-02
STM3580	1.26E+00	7.42E-01
STM3754	7.31E-03	2.96E-03
STM4033	1.46E-02	4.01E-03
STM4057	4.23E-02	1.88E-02
STM4498	2.41E-02	1.58E-02
STM4519	1.01E-01	1.50E-01
STM4520	5.04E-01	7.91E-02
<i>stpA</i>	1.75E-01	7.92E-02
<i>sucA</i>	4.38E-02	1.33E-01
<i>sucB</i>	1.23E-01	1.59E-01
<i>sucC</i>	5.04E-02	6.23E-02
<i>sucD</i>	4.84E-02	4.20E-02
<i>suhB</i>	2.20E-02	1.86E-02
<i>surA</i>	9.40E-02	1.30E-01
<i>surE</i>	1.97E-02	1.54E-02
<i>talA</i>	1.04E-01	1.09E-01
<i>talB</i>	2.44E-01	2.53E-01
<i>tar</i>	2.44E-02	4.20E-02
<i>tbpA</i>	7.83E-02	8.36E-02
<i>tcp</i>	1.47E-02	2.60E-02
<i>thiC</i>	4.89E-02	1.01E-01
<i>thiD</i>	1.98E-02	1.70E-02
<i>thiM</i>	8.70E-02	7.00E-02
<i>thrA</i>	2.84E-01	7.47E-01
<i>thrC</i>	4.49E-01	6.26E-01
<i>tig</i>	4.04E-01	5.72E-01
<i>tktA</i>	1.57E-01	3.40E-01
<i>tktB</i>	9.05E-02	1.98E-01
<i>tolB</i>	1.30E-01	1.77E-01
<i>tolC</i>	1.31E-01	2.07E-01
<i>topA</i>	2.82E-02	7.99E-02
<i>tpx</i>	3.41E-01	1.81E-01
<i>traM</i>	5.98E-02	2.57E-02
<i>traT</i>	2.28E-01	1.75E-01
<i>treA</i>	9.00E-02	1.69E-01
<i>trmJ</i>	2.18E-02	1.69E-02
<i>trpA</i>	4.58E-02	3.81E-02
<i>trxA</i>	3.83E-01	1.35E-01
<i>trxB</i>	2.16E-01	2.21E-01
<i>tsf</i>	4.42E-01	3.95E-01
<i>tufA</i>	4.51E+00	5.73E+00
<i>typA</i>	1.02E-01	2.03E-01
<i>tyrS</i>	5.97E-02	8.41E-02
<i>ubiB (fre)</i>	2.72E-02	4.98E-02
<i>ubiG</i>	7.93E-02	6.29E-02
<i>udp</i>	3.32E-02	2.61E-02
<i>ugpB</i>	4.71E-02	6.71E-02
<i>umuC</i>	2.06E-02	2.88E-02
<i>upp</i>	5.43E-02	3.59E-02
<i>uspF</i>	3.13E-01	1.44E-01
<i>uspG</i>	1.82E-01	8.57E-02
<i>uxaC</i>	1.60E-02	2.49E-02
<i>vacB</i>	3.32E-02	8.88E-02
<i>valS</i>	3.25E-01	1.06E+00
<i>wzzB</i>	5.77E-02	6.15E-02
<i>wzzE</i>	5.89E-02	6.84E-02
<i>yaaA</i>	1.87E-02	1.61E-02
<i>yadF</i>	4.90E-02	3.61E-02

<i>Gene Name</i>	<i>Average of Norm (fmol)</i>	<i>Average of Norm. (ng)</i>
<i>yaeH</i>	9.51E-02	4.25E-02
<i>yahO</i>	3.24E-01	9.42E-02
<i>yajG</i>	4.65E-02	3.07E-02
<i>yajQ</i>	1.08E-01	5.82E-02
<i>ybaB</i>	6.71E-02	2.34E-02
<i>ybaY</i>	5.13E-01	2.95E-01
<i>ybgI</i>	1.52E-01	1.19E-01
<i>ybgJ</i>	2.72E-02	1.90E-02
<i>ybhB</i>	4.56E-02	2.30E-02
<i>ybhG</i>	2.73E-02	2.87E-02
<i>ybiS</i>	4.82E-02	4.70E-02
<i>ybiT</i>	2.61E-02	4.50E-02
<i>ybjP</i>	1.01E-01	5.66E-02
<i>yceI</i>	4.23E-02	2.66E-02
<i>ycfF</i>	6.23E-02	2.42E-02
<i>ycfP</i>	1.21E-01	7.73E-02
<i>ycgL</i>	1.25E-02	4.72E-03
<i>ycgQ</i>	5.66E-02	5.48E-02
<i>yciE</i>	2.83E-02	1.55E-02
<i>yciF</i>	4.39E-01	2.43E-01
<i>yciO</i>	1.33E-02	9.29E-03
<i>ydeI</i>	1.40E-02	5.81E-03
<i>ydfG</i>	1.12E-01	8.85E-02
<i>ydfI</i>	1.07E-02	1.67E-02
<i>ydgA</i>	6.16E-02	9.87E-02
<i>ydgH</i>	8.30E-02	8.27E-02
<i>ydgJ</i>	1.79E-02	2.13E-02
<i>ydhD</i>	8.77E-02	3.31E-02
<i>ydjA</i>	9.25E-02	5.50E-02
<i>ydjN</i>	1.19E-01	1.67E-01
<i>yeaG</i>	5.85E-02	1.26E-01
<i>yebE</i>	5.56E-02	3.95E-02
<i>yedD</i>	3.25E-02	1.47E-02
<i>yedF</i>	6.74E-03	1.76E-03
<i>yedJ</i>	4.32E-02	3.28E-02
<i>yehZ</i>	6.70E-02	6.44E-02
<i>yfcZ</i>	9.33E-02	2.99E-02
<i>yfeR</i>	1.69E+00	1.66E+00
<i>yfgD</i>	5.92E-02	2.38E-02
<i>yfgM</i>	8.87E-02	5.80E-02
<i>yfiA</i>	9.84E-02	3.73E-02
<i>yfiO</i>	5.25E-02	4.38E-02
<i>ygaM</i>	1.41E-01	5.14E-02
<i>ygaU</i>	4.73E-01	2.26E-01
<i>ygdI</i>	2.31E-01	5.58E-02
<i>ygfZ</i>	6.04E-02	6.41E-02
<i>yggE</i>	7.20E-02	5.71E-02
<i>yggN</i>	2.55E-02	1.94E-02
<i>yggX</i>	5.44E-02	1.78E-02
<i>yghA</i>	2.03E-01	1.90E-01
<i>ygiC</i>	4.47E-02	5.84E-02
<i>ygiM</i>	2.22E-02	1.47E-02
<i>yhaK</i>	1.45E-02	1.14E-02
<i>yhbG</i>	9.51E-03	7.38E-03
<i>yhbL</i>	7.49E-02	5.20E-02
<i>yhbO</i>	8.64E-02	4.90E-02
<i>yhbS</i>	9.69E-03	5.39E-03
<i>yhcB</i>	1.36E-01	6.07E-02
<i>yhgF</i>	1.35E-01	3.44E-01

<i>Gene Name</i>	<i>Average of Norm (fmol)</i>	<i>Average of Norm. (ng)</i>
<i>yhhA</i>	3.80E-02	1.68E-02
<i>yhjB</i>	1.66E-02	1.08E-02
<i>yhjG</i>	4.57E-02	9.87E-02
<i>viaD</i>	9.67E-03	6.47E-03
<i>yibF</i>	2.35E-02	1.54E-02
<i>yibL</i>	3.79E-02	1.51E-02
<i>yibN</i>	1.07E-01	4.84E-02
<i>yicC</i>	7.86E-02	7.60E-02
<i>vidC</i>	9.62E-02	1.76E-01
<i>yleF</i>	5.98E-02	3.74E-02
<i>yigI</i>	3.42E-02	1.69E-02
<i>yjeE</i>	3.57E-02	1.78E-02
<i>yjeJ</i>	2.77E-02	2.63E-02
<i>yjgB</i>	2.61E-02	2.87E-02
<i>yjjK</i>	1.26E-01	2.32E-01
<i>ymbA</i>	6.77E-03	4.18E-03
<i>yncB</i>	3.43E-02	3.95E-02
<i>yncE</i>	4.51E-02	5.10E-02
<i>ynfD</i>	4.72E-02	1.45E-02
<i>yniC</i>	3.75E-02	2.65E-02
<i>yqhD</i>	3.66E-02	4.45E-02
<i>yqiC</i>	5.57E-02	2.32E-02
<i>yqiK</i>	1.57E-01	2.79E-01
<i>yqjC</i>	6.64E-02	2.82E-02
<i>yqjD</i>	3.06E-01	1.02E-01
<i>yraM</i>	3.34E-02	7.01E-02
<i>yraP</i>	9.50E-02	5.65E-02
<i>yrbC</i>	6.66E-02	4.78E-02
<i>yrbD</i>	1.77E-02	1.02E-02
<i>yrfE</i>	1.57E-02	1.02E-02
<i>ysgA</i>	2.36E-02	2.06E-02
<i>ytfM</i>	1.27E-01	2.37E-01
<i>ytfN</i>	3.69E-02	1.45E-01
<i>znuA</i>	3.42E-01	3.66E-01
<i>zwf</i>	1.79E-02	2.90E-02